Appendix A

The Standardized Precipitation Index at Hanford

Z. Fred Zhang

Pacific Northwest National Laboratory
Richland, Washington

Abstract

The performance of the Prototype Hanford Barrier (PHB) was evaluated under natural and elevated precipitation conditions. PHB performance was strongly dependent on precipitation condition. Researchers have defined the standardized precipitation index (SPI) based on the transformed standard normal distribution and precipitation classes, i.e., extreme wet, severe wet, moderate wet, near normal, moderate dry, severe dry, and extreme dry. The nature of the SPI allows an anomalously dry or wet event to be quantified at a particular time scale of interest. The use of SPI for a given period (e.g., a year or a season) will help with understanding the hydrological and ecological performance of the PHB. The 67-year precipitation data from water years (WYs) 1948 to 2014 at the Hanford Site were used for statistical analysis. These data were used to determine the SPIs for each year, winter season, and summer season. Regarding the annual precipitation, of the 19 test years, 2 years (WY95 and WY97) were extreme wet, 4 moderate wet, 12 near normal, and 1 (WY05) severe dry. The precipitation classes for the winter and summer seasons were very similar to those for the annual precipitation. This means that the barrier had the most precipitation stress in WY95 and WY97, even in the unirrigated section of the barrier. Under natural conditions, the estimated probability of the enhanced precipitation from WY95 to WY97 is extremely small, less than once in a million years.

A.1 Introduction

The U.S. Department of Energy's Hanford Site has a shrub-steppe climate (Hoitink et al. 2005). Climatological data at Hanford is recorded by the Hanford Meteorological Station (HMS), which was established in 1944 and is located near the center of the Hanford Site between the 200 West and 200 East Areas. The Hanford climate is summarized in Hoitink et al. (2005).

Surface barrier performance is strongly dependent on precipitation. Different methods can be used to describe precipitation and its variation with time. The standardized precipitation index (SPI) developed by McKee et al. (1993) is used here because SPI allows an anomalously dry or wet event to be quantified at a particular time scale for any location, and allows data from different times or locations to be compared. Precipitation classes have been defined using SPI (McKee et al. 1995).

The SPI for a given period (e.g., a year or a season) will help with understanding the hydrological and ecological performance of the barrier. The following describes the method used to determine SPI and how it was applied to the long-term precipitation data at the Hanford Site and during the barrier test period.

A.2 Definition of the Standard Precipitation Index

Thom (1966) found that the gamma distribution fit climatological precipitation time series well. The probability density function of precipitation for a given period is defined as

$$g(x) = \frac{x^{\alpha-1}\exp(-x/\beta)}{\beta^{\alpha}\Gamma(\alpha)} \qquad for\ x > 0 \qquad \text{A.1}$$

where $\alpha > 0$ is a shape parameter, $\beta > 0$ is a scale parameter, $x > 0$ is the precipitation amount, and $\Gamma(\alpha)$ is the gamma function defined as

$$\Gamma(\alpha) = \int_0^{\infty} y^{\alpha-1}\exp(-y)dy \qquad for\ x > 0 \qquad \text{A.2}$$

Calculation of the SPI involves fitting $g(x)$ to a given frequency distribution of precipitation for a station (Thom 1966). The α and β parameters are estimated for the station for the time scale of interest (e.g., a year or a season). From Thom (1966), the maximum likelihood solutions are used to optimally estimate α and β:

$$\hat{\alpha} = \frac{1}{4A}\left(1+\sqrt{1+\frac{4A}{3}}\right)$$
$$\hat{\beta} = \frac{\overline{x}}{\hat{\alpha}} \qquad \text{A.3}$$
$$A = \ln(\overline{x}) - \frac{1}{n}\sum \ln(x)$$

where n is the number of precipitation observations and $\overline{x}$ is the average of x. The above parameters are then used to determine the cumulative probability, $G(x)$, of an observed precipitation event, x:

$$G(x) = \frac{1}{\hat{\beta}^{\hat{\alpha}}\Gamma(\hat{\alpha})}\int_0^x x^{\hat{\alpha}-1}\exp(-x/\hat{\beta})dx \qquad \text{A.4}$$

Because the gamma function is undefined for trace precipitation (x = 0), the cumulative probability of a precipitation distribution that contain zeros is defined as

$$H(x) = q + (1-q)G(x) \qquad \text{A.5}$$

where $q = m/n$ is the probability of zero precipitations, where m is the number of zero precipitations. The SPI value is then calculated using an approximation provided by Abramowitz and Stegun (1965). The approximation converts cumulative probability $G(x)$ to the standard normal random variable (with mean of zero and variance of one), which is defined as the SPI[1]:

$$SPI = \begin{cases} -\left(t - \dfrac{c_0 + c_1 t + c_2 t^2}{1 + d_1 t + d_2 t^2 + d_3 t^3}\right) & for \quad 0 < G(x) \le 0.5 \\ +\left(t - \dfrac{c_0 + c_1 t + c_2 t^2}{1 + d_1 t + d_2 t^2 + d_3 t^3}\right) & for \quad 0.5 < G(x) < 1 \end{cases} \qquad \text{A.6}$$

where

$$t = \begin{cases} \sqrt{\ln\left(\dfrac{1}{H(x)^2}\right)} & for \quad 0 < G(x) \le 0.5 \\ \sqrt{\ln\left(\dfrac{1}{[1-H(x)]^2}\right)} & for \quad 0.5 < G(x) < 1 \end{cases} \qquad \text{A.7}$$

c_0 = 2.515517, c_1 = 0.802853, c_2 = 0.010328, d_1 = 1.432788, d_2 = 0.189269, and d_3 = 0.001308. The SPI is essentially the standard deviation of a unit normal distribution. Hence, all statistical properties for a unit normal distribution apply to SPI (Figure A.1). For example, precipitation with a probability of 95.0% varies between -1.96SPI and +1.96SPI, a probability of 99.0% between -2.58SPI and +2.58SPI, and a

[1] http://ccc.atmos.colostate.edu/pub/spi.pdf. Accessed on 2/13/2015.

probability of 99.9% between -3.29SPI and +3.29SPI. The probability, *P*, greater than or equal to SPI is calculated by[2]

$$P(SPI) = 0.5\left[1 - erf\left(\frac{SPI}{\sqrt{2)}}\right)\right] \qquad \text{A.8}$$

where *erf*() is the error function. Hence, for any given precipitation at the time of interest, the SPI can be calculated with Eq. (A.6) and its probability can be obtained with Eq. (A.8).

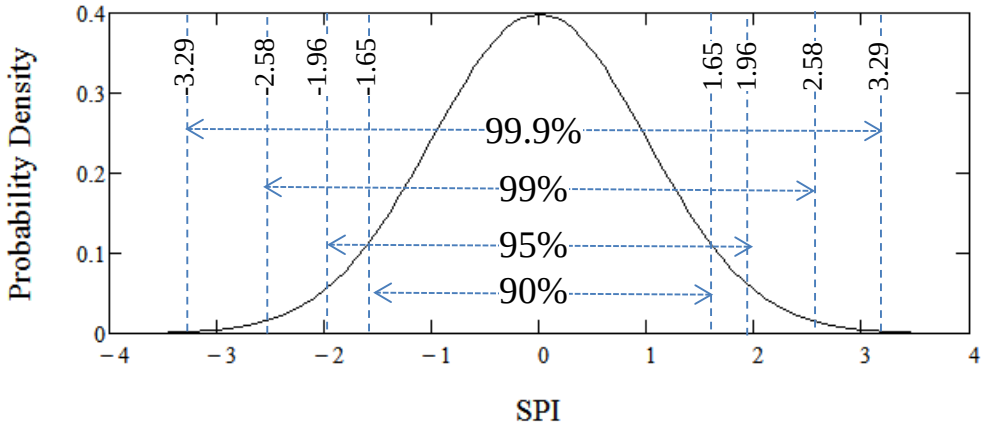

Figure A.1. Standard normal distribution with the SPI having a mean of 0 and a standard deviation of 1. The numbers on the vertical dashed lines indicate the SPI values corresponding to different confidence levels. The horizontal double-arrowed lines with numbers indicate the ranges of the marked confidence levels.

Based on the SPI values, McKee et al. (1995) classified the precipitation of a given period into seven classes: extreme wet, severe wet, moderate wet, near normal, moderate dry, severe dry, and extreme dry (Table A.1). The first three classes may be referred to as the wet classes and the last three as the dry classes. It is noted that the classification of precipitation is not unique and different classifications, e.g., Lloyd-Hughes and Saunders (2002), exist. The McKee et al. (1995) classification is used here.

Table A.1. SPI classification following McKee et al. (1995). [Can also be found in Table 2 of Russo et al. (2013)]

SPI Values	Class	Probability of Event (%)
SPI > 2.0	Extreme wet (EW)	2.3
1.5 < SPI ≤ 2.0	Severe wet (SW)	4.4
1.0 < SPI ≤ 1.5	Moderate wet (MW)	9.2
-1.0 < SPI ≤ 1.0	Near normal (NN)	68.3
-1.5 < SPI ≤ -1.0	Moderate dry (MD)	9.2
-2.0 < SPI ≤ -1.5	Severe dry (SD)	4.4
SPI ≤ -2.0	Extreme dry (ED)	2.3

[2] http://en.m.wikipedia.org/wiki/Standard_deviation#Rules_for_normally_distributed_data. Accessed on 2/13/2015.

A.3 SPI at the Hanford Site

Precipitation data at the HMS are available from 1948 to present (Table A.2). The data were arranged by water year (WY), which is from November of the previous year to October of current year. Each WY is also divided into the winter season (from November to March) and the summer season (from April to October). The 67-year precipitation data from WY 1948 (WY48) to WY 2014 (WY14) at the HMS were used for statistical analysis. These data were used to determine the SPI for the WY, winter season, and summer season. The calculation was conducted with a Mathcad® (PTC Inc., Needham, MA) program and was verified with the NCAR[3] Command Language (Version 6.2.1).[4]

Table A.2. Monthly, seasonal, and water year precipitation at the Hanford Site

Water Year	Nov	Dec	Jan	Feb	Mar	Apr	May	Jun	Jul	Aug	Sep	Oct	Winter Season	Summer Season	WY Annual
WY48	20.57	19.05	34.54	17.53	1.78	24.13	43.43	37.34	10.16	9.91	4.06	11.43	93.47	140.46	233.93
WY49	24.13	28.19	3.30	17.27	28.45	0.51	4.06	0.25	0.25	0.76	5.84	2.54	101.35	14.22	115.57
WY50	37.34	4.06	45.72	26.92	22.10	11.94	6.86	74.17	1.78	0.00	0.25	62.48	136.14	157.48	293.62
WY51	13.97	24.64	21.34	12.95	11.68	13.46	10.92	35.05	9.40	3.81	2.54	18.03	84.58	93.22	177.80
WY52	20.83	17.78	16.51	12.70	1.52	3.30	14.73	27.18	0.00	2.03	2.03	1.02	69.34	50.29	119.63
WY53	5.08	19.56	54.86	6.35	4.32	19.56	7.11	13.97	0.00	24.38	3.30	5.08	90.17	73.41	163.58
WY54	24.38	12.45	37.59	7.11	14.99	1.78	10.41	2.54	5.59	10.67	12.95	10.67	96.52	54.61	151.13
WY55	21.84	8.89	14.22	5.59	4.32	10.16	14.99	7.11	14.48	0.00	19.56	10.16	54.86	76.45	131.32
WY56	39.12	51.56	43.43	14.22	2.54	0.00	5.59	21.84	0.00	9.65	0.25	26.16	150.88	63.50	214.38
WY57	3.81	14.73	12.19	5.84	47.24	9.65	20.83	11.94	1.27	0.51	8.64	69.09	83.82	121.92	205.74
WY58	9.91	13.46	44.20	37.59	11.68	16.26	18.80	20.57	0.51	0.00	1.27	4.83	116.84	62.23	179.07
WY59	19.56	46.74	52.07	29.72	10.16	5.08	12.70	5.84	0.00	0.76	32.00	14.22	158.24	70.61	228.85
WY60	10.41	6.60	12.95	14.73	17.02	13.46	18.03	3.56	0.00	6.60	5.84	5.84	61.72	53.34	115.06
WY61	23.37	16.26	8.38	53.34	25.91	12.19	20.32	10.67	3.81	2.29	0.00	1.78	127.25	51.05	178.31
WY62	12.45	22.61	3.30	22.86	3.56	8.64	34.29	3.05	0.00	12.70	9.65	24.13	64.77	92.46	157.23
WY63	16.51	15.24	24.13	17.53	13.46	29.72	10.92	7.11	7.87	0.25	0.51	1.02	86.87	57.40	144.27
WY64	18.80	28.96	9.40	0.25	0.76	2.79	1.02	22.86	1.02	6.10	2.29	7.11	58.17	43.18	101.35
WY65	23.88	59.44	23.62	3.56	0.76	2.29	3.81	12.45	2.79	0.76	2.79	0.25	111.25	25.15	136.40
WY66	29.72	9.91	17.27	0.76	9.91	0.76	1.27	10.92	20.57	0.00	6.86	9.91	67.56	50.29	117.86
WY67	57.15	15.24	8.13	0.00	3.56	22.86	14.22	14.48	0.00	0.00	1.27	3.30	84.07	56.13	140.21
WY68	4.06	10.92	22.35	14.73	0.51	0.25	1.52	4.83	1.02	12.95	6.35	23.62	52.58	50.55	103.12
WY69	31.24	31.75	31.50	13.72	2.54	30.99	12.95	19.05	0.00	0.00	12.19	2.54	110.74	77.72	188.47
WY70	3.30	32.77	62.74	19.05	6.86	11.43	13.72	6.35	0.25	0.00	0.76	6.10	124.71	38.61	163.32
WY71	18.03	15.49	19.81	2.54	25.91	1.78	14.22	18.03	3.30	2.29	28.70	4.57	81.79	72.90	154.69
WY72	11.68	27.18	4.83	6.86	14.73	2.54	51.56	16.76	4.06	14.22	0.51	0.00	65.28	89.66	154.94
WY73	13.97	32.26	22.86	5.33	2.03	0.00	6.10	0.25	0.00	0.51	10.92	43.69	76.45	61.47	137.92
WY74	67.06	51.31	22.86	10.41	13.21	11.68	7.11	3.05	18.03	0.00	0.25	5.33	164.85	45.47	210.31
WY75	18.03	24.64	36.32	24.89	8.38	10.67	9.65	6.10	8.13	29.46	0.76	22.10	112.27	86.87	199.14
WY76	15.24	17.78	14.22	9.14	5.84	10.41	2.03	2.79	3.30	24.38	0.00	1.02	62.23	43.94	106.17
WY77	0.00	2.79	2.03	14.48	10.41	0.00	16.51	9.40	1.52	34.54	16.76	3.81	29.72	82.55	112.27
WY78	16.00	37.34	43.69	23.37	7.62	11.68	10.41	2.29	13.21	14.48	2.79	0.00	128.02	54.86	182.88

[3] National Center for Atmospheric Research

[4] NCAR Command Language (Version 6.2.1) [Software]. (2014). Boulder, Colorado: UCAR/NCAR/CISL/VETS. http://dx.doi.org/10.5065/D6WD3XH5. Verified on November 25, 2015.

Water Year	Nov	Dec	Jan	Feb	Mar	Apr	May	Jun	Jul	Aug	Sep	Oct	Winter Season	Summer Season	WY Annual
WY79	30.73	6.60	13.72	4.32	13.72	13.21	2.54	0.00	2.29	9.65	5.08	17.02	69.09	49.78	118.87
WY80	34.54	25.15	33.53	33.02	7.62	21.84	35.81	24.38	0.00	0.51	21.59	8.38	133.86	112.52	246.38
WY81	11.18	48.01	14.22	15.24	17.78	0.51	25.15	10.92	4.83	0.76	15.24	9.91	106.43	67.31	173.74
WY82	27.43	36.83	8.38	14.48	7.62	19.05	7.11	19.05	5.59	5.08	13.97	33.78	94.74	103.63	198.37
WY83	23.11	45.47	36.58	34.54	25.40	10.67	13.21	17.27	7.87	3.05	11.68	13.21	165.10	76.96	242.06
WY84	53.85	53.85	5.84	23.88	25.65	15.24	13.97	25.15	1.52	0.00	10.67	1.78	163.07	68.33	231.39
WY85	46.48	14.48	8.64	20.83	9.14	0.25	3.05	3.81	3.05	0.25	16.00	11.68	99.57	38.10	137.67
WY86	31.50	21.34	44.70	34.80	19.30	0.00	7.62	0.00	5.33	0.51	24.38	7.37	151.64	45.21	196.85
WY87	16.51	19.56	20.32	4.83	26.67	3.56	4.32	2.79	12.70	1.78	0.25	0.00	87.88	25.40	113.28
WY88	10.16	41.40	12.19	0.00	9.91	28.45	8.38	2.79	3.30	0.00	9.91	0.25	73.66	53.09	126.75
WY89	20.83	10.16	5.33	42.42	39.62	21.34	14.99	0.25	0.25	6.60	0.51	10.67	118.36	54.61	172.97
WY90	26.42	7.37	19.56	2.29	2.54	10.16	21.84	9.14	3.56	21.08	0.00	19.81	58.17	85.60	143.76
WY91	0.51	18.29	8.38	4.83	28.45	11.43	12.45	36.58	7.37	1.78	0.00	13.46	60.45	83.06	143.51
WY92	36.58	10.16	11.18	23.88	2.29	23.88	0.00	28.96	9.65	5.08	6.86	15.49	84.07	89.92	173.99
WY93	27.18	46.23	33.02	29.72	17.02	18.03	15.24	3.05	44.70	6.10	1.02	2.29	153.16	90.42	243.59
WY94	4.83	23.88	11.18	2.79	0.76	15.49	32.26	9.65	3.81	2.03	2.03	23.62	43.43	88.90	132.33
WY95	17.27	34.54	54.36	17.53	24.13	39.12	20.07	19.56	8.64	1.78	20.07	22.10	147.83	131.32	279.15
WY96	26.42	58.93	36.07	30.99	21.08	10.92	15.75	1.27	3.56	0.51	5.59	22.35	173.48	59.94	233.43
WY97	67.82	93.73	38.35	6.35	17.78	8.38	8.38	11.68	4.83	1.52	8.13	23.37	224.03	66.29	290.32
WY98	25.65	7.87	31.50	29.21	12.70	1.78	13.21	12.19	8.64	1.02	2.54	7.11	106.93	46.48	153.42
WY99	32.77	11.18	22.61	17.78	1.52	0.00	8.64	7.87	1.78	14.48	0.00	12.19	85.85	44.96	130.81
WY00	6.60	1.78	27.69	28.45	23.88	14.48	19.56	6.35	11.68	0.00	14.22	14.48	88.39	80.77	169.16
WY01	27.43	17.02	7.37	10.67	17.02	21.08	2.03	32.26	1.27	2.03	3.30	9.40	79.50	71.37	150.88
WY02	42.42	20.32	10.67	17.02	4.83	7.37	4.06	16.51	4.06	0.25	0.00	3.05	95.25	35.31	130.56
WY03	9.65	59.94	47.50	20.83	6.60	56.64	2.03	0.00	0.00	11.68	6.10	1.78	144.53	78.23	222.76
WY04	3.81	49.78	53.85	23.37	9.14	5.33	22.61	20.83	0.76	24.13	3.56	21.84	139.95	99.06	239.01
WY05	7.37	9.40	23.62	1.02	7.87	6.60	20.07	1.52	2.29	1.52	16.76	7.37	49.28	56.13	105.41
WY06	22.61	51.05	29.97	10.41	6.10	33.02	14.48	33.78	0.00	0.00	5.33	19.30	120.14	105.92	226.06
WY07	18.03	44.45	3.56	19.30	18.80	6.60	7.62	11.43	1.78	8.13	14.48	5.33	104.14	55.37	159.51
WY08	28.70	13.46	32.51	13.97	5.08	2.03	14.22	9.91	0.00	12.19	1.02	5.59	93.73	44.96	138.68
WY09	18.80	24.13	29.21	16.26	20.32	9.91	4.57	4.06	0.00	1.02	1.52	19.81	108.71	40.89	149.61
WY10	14.22	18.03	31.50	14.22	5.08	14.99	33.78	29.21	11.68	3.30	24.13	15.75	83.06	132.84	215.90
WY11	28.96	46.23	13.46	0.76	22.10	6.35	30.99	9.91	3.05	0.00	1.27	19.56	111.51	71.12	182.63
WY12	3.05	2.54	27.69	17.53	16.26	15.49	5.59	38.35	3.81	0.00	0.76	26.67	67.06	90.68	157.73
WY13	20.32	35.81	4.06	2.29	9.91	7.62	40.64	34.54	0.25	6.10	10.67	9.65	72.39	109.47	181.86
WY14	9.14	1.78	9.40	28.45	25.40	9.65	6.10	6.60	1.02	22.35	4.06	19.56	74.17	69.34	143.51
Avg (WY48-WY14)	**21.86**	**26.12**	**23.76**	**15.96**	**12.88**	**11.80**	**13.92**	**13.93**	**4.74**	**5.97**	**7.23**	**13.09**	**100.58**	**70.68**	**171.26**
Avg (WY95-WY13)	**22.20**	**31.59**	**27.659**	**15.681**	**13.168**	**14.09**	**15.173**	**15.855**	**3.5827**	**4.7191**	**7.3393**	**14.037**	**110.30**	**74.80**	**185.10**

Precipitation statistics from WY48 to WY14 and the fitted parameters α and β for Eq. (A.1) are summarized in Table A.3. Note that the average precipitation values were slightly different from the corresponding medians, indicating the probability distribution of precipitation is not normal. The cumulative probability of precipitation is shown in Figure A.2. Although the model can describe the

observed precipitation data well, the estimated precipitation in very low probability (e.g., 0.1%) by extrapolating the 67-year long record would introduce additional uncertainty.

Table A.3. Statistics of precipitation from WY48 to WY14 and the fitted parameters α and β.

	Water Year	Winter Season	Summer Season
Min (mm)	101.4	29.7	14.2
Max (mm)	293.6	224.0	157.5
Average (mm)	171.3	100.6	70.7
Median (mm)	167.1	96.1	66.9
α	13.7	7.5	6.1
β	12.5	13.4	11.5

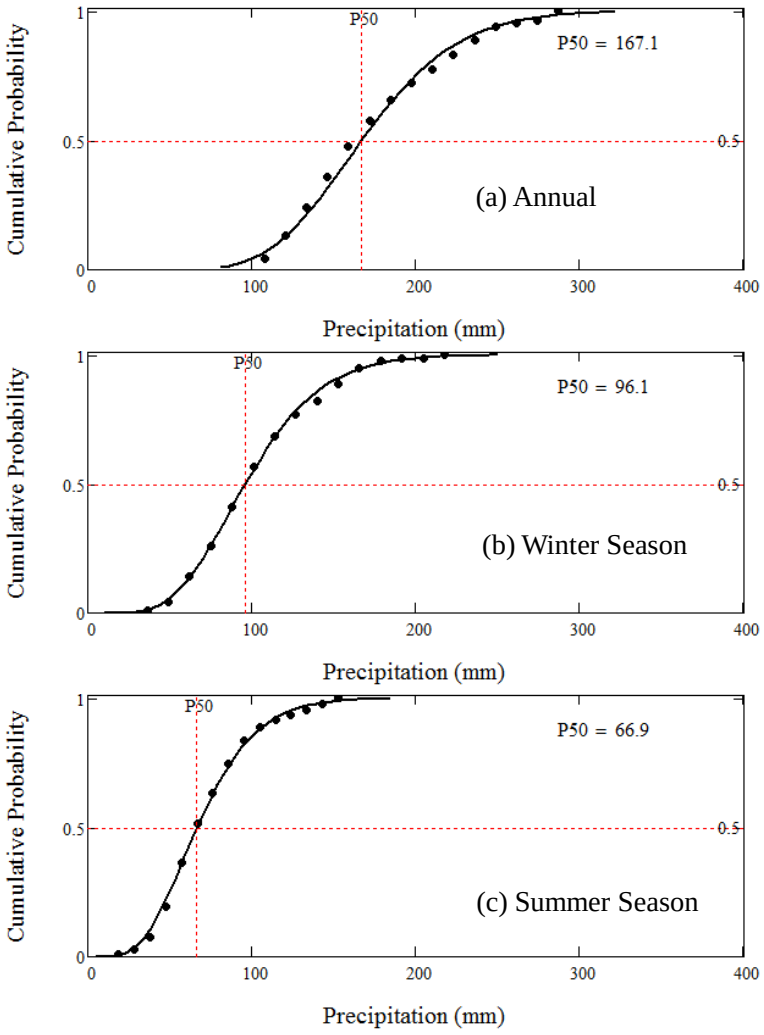

Figure A.2. The cumulative probability of precipitation. The symbols denote data and the curves the best fits of Eq. (A.4). The fitted parameters are summarized in Table A.3. P50 is the median precipitation.

Table A.4 gives the precipitation and SPI at different percentile level. For example, for the 99.9th percentile, there is only 0.1% chance (once in 1000 years) that the annual precipitation will be ≥350.5 mm or the winter precipitation ≥253.0 mm. It is noted that these estimated precipitations were estimated based on the 67-year precipitation record and hence are subjected to extrapolation uncertainty.

Table A.4. Precipitation and SPI at different percentile.

Percentile	SPI	Annual (mm)	Winter Season (mm)	Summer season (mm)
95th	1.645	253.7	167.7	123.1
98th	1.960	273.0	184.4	136.5
99th	2.326	296.6	205.2	153.2
99.9th	3.090	350.5	253.0	191.9

A.4 SPI during the Test Period

The monthly meteoric precipitation during the barrier test period from WY95 to WY13 can be found in Table A.2. The calculated SPI and precipitation classes of the annual, winter, and summer precipitation for each WY are listed in Table A.5. Regarding the annual precipitation, of the 19 test years, 2 years (WY95 and WY97) were extreme wet, 4 moderate wet, 12 near normal, and 1 (WY05) severe dry. This means that the barrier had the most precipitation stress in WY95 and WY97.

To mimic the extreme scenario of precipitation, an irrigation system was used in the northern section of the barrier from WY95 to WY97 such that the total precipitation was about three times (3X) the long-term average. The total annual and winter precipitation and the corresponding SPI for the irrigated section are summarized in Table A.6. The 3X precipitation was considerably more than the precipitation with 0.1% chance (350 mm annually or 253 mm for the winter season). The SPIs for each period were larger than 4.2 except for the winter of WY95, which had an SPI of 3.079 because irrigation was delayed until February 1996. The probability of meteoric WY precipitation at this level is extremely low, only 0.67, 0.68, and 0.47 times every 1 million years for WY95, WY96, and WY97, respectively. The probability of P_w is 9 and 7 times every 1 million years for WY96 and WY97, respectively.

In May 1998, 209.6 mm was applied to the north section of the barrier for instrument calibration, bringing the total WY precipitation to 363.0 mm, which corresponds to a SPI of 3.265. The barrier was exposed to the natural precipitation conditions in WY99 and thereafter.

Table A.5. Precipitation, SPI, and precipitation classes during the test period from WY95 to WY13.

WY	Annual			Winter Season			Summer Season		
	P_a (mm)	SPI	Class	P_w (mm)	SPI	Class	P_s (mm)	SPI	Class
WY95	279.1	2.058	EW	147.8	1.244	MW	131.3	1.84	SW
WY96	233.4	1.298	MW	173.5	1.757	SW	59.9	-0.261	NN
WY97	290.3	2.231	EW	224.0	2.64	EW	66.3	-0.022	NN
WY98	153.4	-0.309	NN	106.9	0.29	NN	46.5	-0.832	NN
WY99	130.8	-0.864	NN	85.9	-0.298	NN	45.0	-0.904	NN
WY00	169.2	0.044	NN	88.4	-0.222	NN	80.8	0.472	NN
WY01	150.9	-0.368	NN	79.5	-0.494	NN	71.4	0.159	NN
WY02	130.6	-0.87	NN	95.3	-0.025	NN	35.3	-1.402	MD
WY03	222.8	1.107	MW	144.5	1.174	MW	78.2	0.389	NN
WY04	239.0	1.396	MW	140.0	1.075	MW	99.1	1.018	MW
WY05	105.4	-1.571	SD	49.3	-1.617	SD	56.1	-0.413	NN
WY06	226.1	1.167	MW	120.1	0.621	NN	105.9	1.206	MW
WY07	159.5	-0.169	NN	104.1	0.217	NN	55.4	-0.444	NN
WY08	138.7	-0.664	NN	93.7	-0.068	NN	45.0	-0.904	NN
WY09	149.6	-0.398	NN	108.7	0.336	NN	40.9	-1.103	MD
WY10	215.9	0.981	NN	83.1	-0.383	NN	132.8	1.876	SW
WY11	182.6	0.33	NN	111.5	0.408	NN	71.1	0.15	NN
WY12	157.7	-0.21	NN	67.1	-0.913	NN	90.7	0.777	NN
WY13	181.9	0.314	NN	72.4	-0.728	NN	109.5	1.3	MW

Table A.6. Statistics of total (meteoric and irrigated) precipitation of the irrigated north section of the barrier from WY95 to WY98.

WY	Annual			Winter Season		
	P (mm)	SPI	Probability of P or higher	P (mm)	SPI	Probability of P or higher
WY95	493.3	4.834	6.68E-07	252.2	3.079	1.04E-03
WY96	493.1	4.832	6.75E-07	339.9	4.277	9.46E-06
WY97	499.7	4.905	4.68E-07	344.2	4.331	7.42E-06
WY98	363.0	3.265	5.46E-04	106.0	0.289	3.86E-01

A.5 Summary

The 67-year precipitation data from WY48 to WY14 at the Hanford Site were used to determine the SPIs for each year, winter season, and summer season. Regarding the annual precipitation, of the 19 test years, 2 years (WY95 and WY97) were extreme wet, 4 moderate wet, 12 near normal, and 1 (WY05) severe dry. The precipitation classes for the winter and summer seasons were very similar to those for the annual precipitation. This means that the barrier had the most precipitation stress in WY95 and WY97, even in the unirrigated section of the barrier. Under natural conditions, the estimated probability of the 3X average precipitation levels from WY95 to WY97 is extremely small, less than once in a million years.

References

Abramowitz, M and IA Stegun. 1965. "Handbook of Mathematical Functions." National Bureau of Standards, Washington, D.C.

Hoitink, DJ, KW Burk, JV Ramsdell (Jr.), and WJ Shaw. 2005. *Hanford Site Climatological Summary 2004 with Historical Data*, PNNL-15160, Pacific Northwest National Laboratory, Richland, Washington.

Lloyd-Hughes, B and MA Saunders. 2002. "A Drought Climatology for Europe," *International Journal of Climatology*, 22(13):1571-1592. doi:10.1002/joc.846.

McKee, TB, NJ Doesken, and J Kleist. 1993. "The Relationship of Drought Frequency and Duration of Time Scales," *Eighth Conference on Applied Climatology, American Meteorological Society,* 179-186 pp. Jan. 17-23, 1993, Anaheim, California.

McKee, TB, NJ Doesken, and J Kleist. 1995. "Drought Monitoring with Multiple Time Scales," *9th Conference on Applied Climatology*, Am. Meteorol. Soc., Dallas, Texas.

Russo, S, A Dosio, A Sterl, P Barbosa, and J Vogt. 2013. "Projection of Occurrence of Extreme Dry-Wet Years and Seasons in Europe with Stationary and Nonstationary Standardized Precipitation Indices," *Journal of Geophysical Research: Atmospheres*, 118:7628-7639. doi:10.1002/jgrd.50571.

Thom, HCS. 1966. *Some Methods of Climatological Analysis*, WMO Technical note 81, Secretariat of the WMO, Geneva, Switzerland.

Appendix B

Prototype Hanford Barrier: Design, Enhanced Precipitation Test, and Controlled Burn Test

Z. Fred Zhang

Pacific Northwest National Laboratory
Richland, Washington

Table of Contents

List of Figures

List of Tables

Executive Summary

The Prototype Hanford Barrier (PHB) consists of an evapotranspiration (ET) barrier, a west 10:1 gentle pit-run gravel (aka clean-fill dike) side slope, and an east 2:1 steep basalt riprap side slope. It was constructed between late 1993 and 1994 over the 216-B-57 Crib in the 200-BP-1 Operable as a mound over the ground surface. The performance of the ET barrier was enhanced by including a coarser layer below a finer storage layer. The texture contrast formed a capillary break (CB) at the interface. The ET barrier with a CB is termed the ETC barrier. This ETC barrier is a 5-m-thick sequence of multiple layers overlying the compacted in situ soil. Each layer serves a distinct purpose. The function of the side slopes is to keep the ETC barrier stable and protect it from damage by natural processes or human activities. After construction, the barrier was revegetated with seedlings of shrubs and seeded with native perennial grasses in November 1994. From 1995 to 1997, an enhanced precipitation test (aka the treatability test) was conducted to test barrier performance under both ambient (natural precipitation) and extreme climate (enhanced precipitation) conditions. A controlled burn was conducted on the north section of the barrier, including the silt loam cover and the gravel side slope, on September 26, 2008, to understand the response of the engineered ecosystems to wildfire. The design of the PHB and the function of each component are described. After presenting details on the revegetation, details of the enhanced precipitation test and controlled burn tests are given. More information about the PHB is presented in other appendices.

This appendix summarizes the design of the Prototype Hanford Barrier (PHB) and the tests carried out between 1994 and 2013.

B.1 Barrier Design

Surface barriers are used to reduce or prevent infiltration water from entering the underlying waste zone and to isolate the waste from plant, animal, and human intrusion. Evapotranspiration (ET) barriers use two natural processes—the soil as a natural water reservoir for precipitation (P) and the ET process to empty the soil water reservoir—to control infiltration into the underlying waste zone.

The description and design of the PHB have been reported in other sources such as Myers and Duranceau (1994), Wing and Gee (1994), Gee et al. (1997), Ward and Gee (1997), and DOE-RL (1999). The PHB (Figure B.1), with an area of 2.5 ha (6.2 acres), was deployed over the 216-B-57 Crib in the 200-BP-1 Operable Unit in Hanford's 200 East Area between late 1993 and 1994. An as built-in drawing for Crib 216-B-57 (Plate 2-5 in DOE-RL 1990) indicates that the crib consists of a 0.305-m corrugated and perforated steel pipe which runs the length of the 61-m long by 4.6-m wide crib. The base of the 3-m deep excavation is at an elevation of 189.3 m and is level. The pipe, which slopes to the north, is 1.1 m above the bottom of the excavation at the south end and 0.85 m above the bottom of the excavation at the north end. The crib bottom is filled with gravel to a depth 1.2 m above the crib bottom. Side slope are 1.5:1. However, Crib 216-B-57 appears to have been constructed from 2 to 3 m deeper than indicated in the as-build drawing for the crib (DOE-RL 1993). More information about the 216-B-57 Crib can be found in DOE-RL (1993).

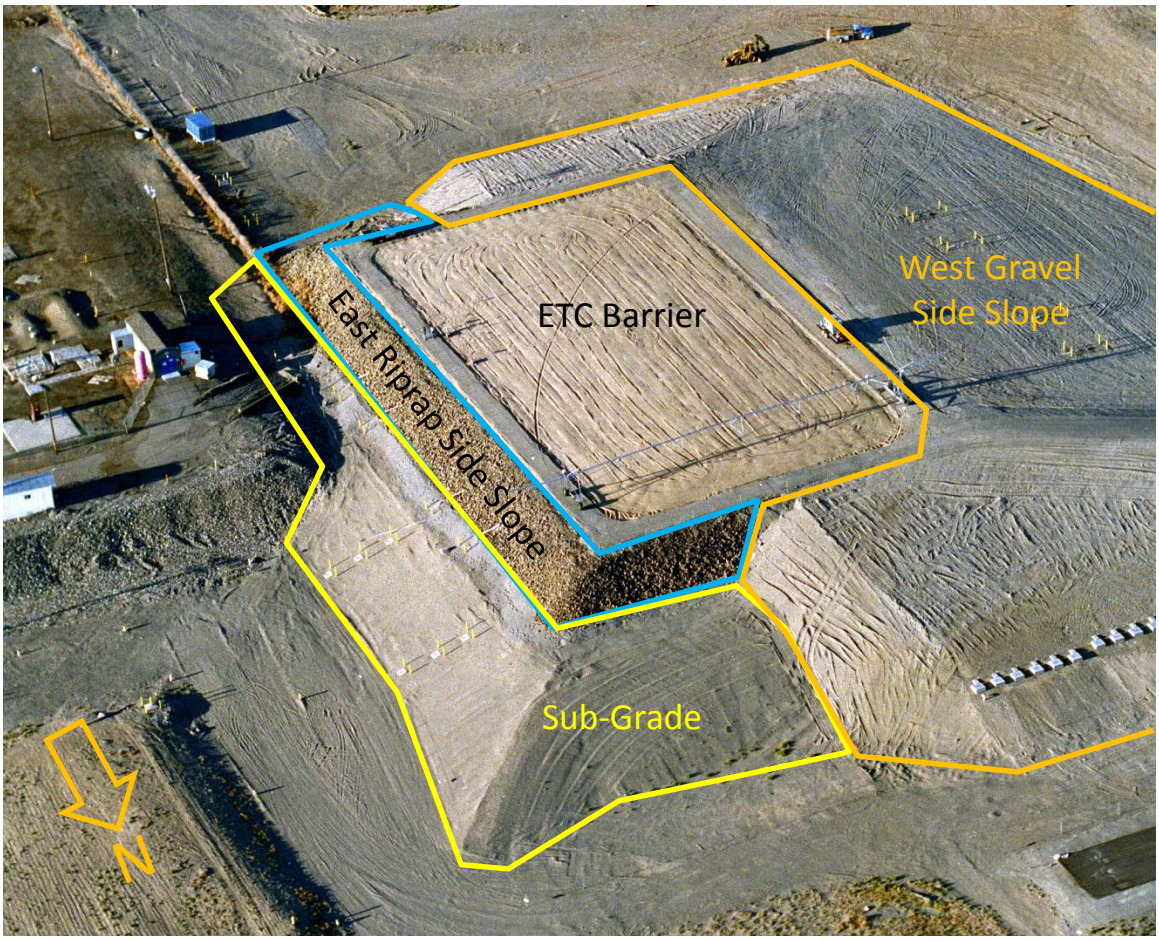

Figure B.1. Plan view of the Prototype Hanford Barrier after completion of construction. (Photo taken on August 9, 1994. Southwest-facing view. The lines show the approximate boundaries of the main barrier components.)

The PHB consists of 4 main components (Figure B.2), which are 1) a silt loam evapotranspiration (ET) layer with an underlying capillary (C) break and an intrusion prevention layer, termed the ETC barrier, in the middle, (2) a gentle pit-run gravel side slope in the west (10:1) and in the west portions of the north and south side slopes (5:1 to 3:1); (3) a 2:1 steep basalt riprap side slope in the east and in the east portion of the north and south side slopes, and 4) an asphalt concrete (AC) barrier with a polymer-modified fluid applied asphalt (FAA) coating and a compacted soil layer at the bottom. The ETC barrier is the center piece of the PHB and sits directly above the waste zone. It stores precipitation and releases the stored water into atmosphere and to deter intrusion by plants, animals, or humans from barrier surface. The two side slopes protect the ETC barrier from damage or intrusion from the sides. The AC barrier is the redundant barrier to divert drainage and to hinder intrusion.

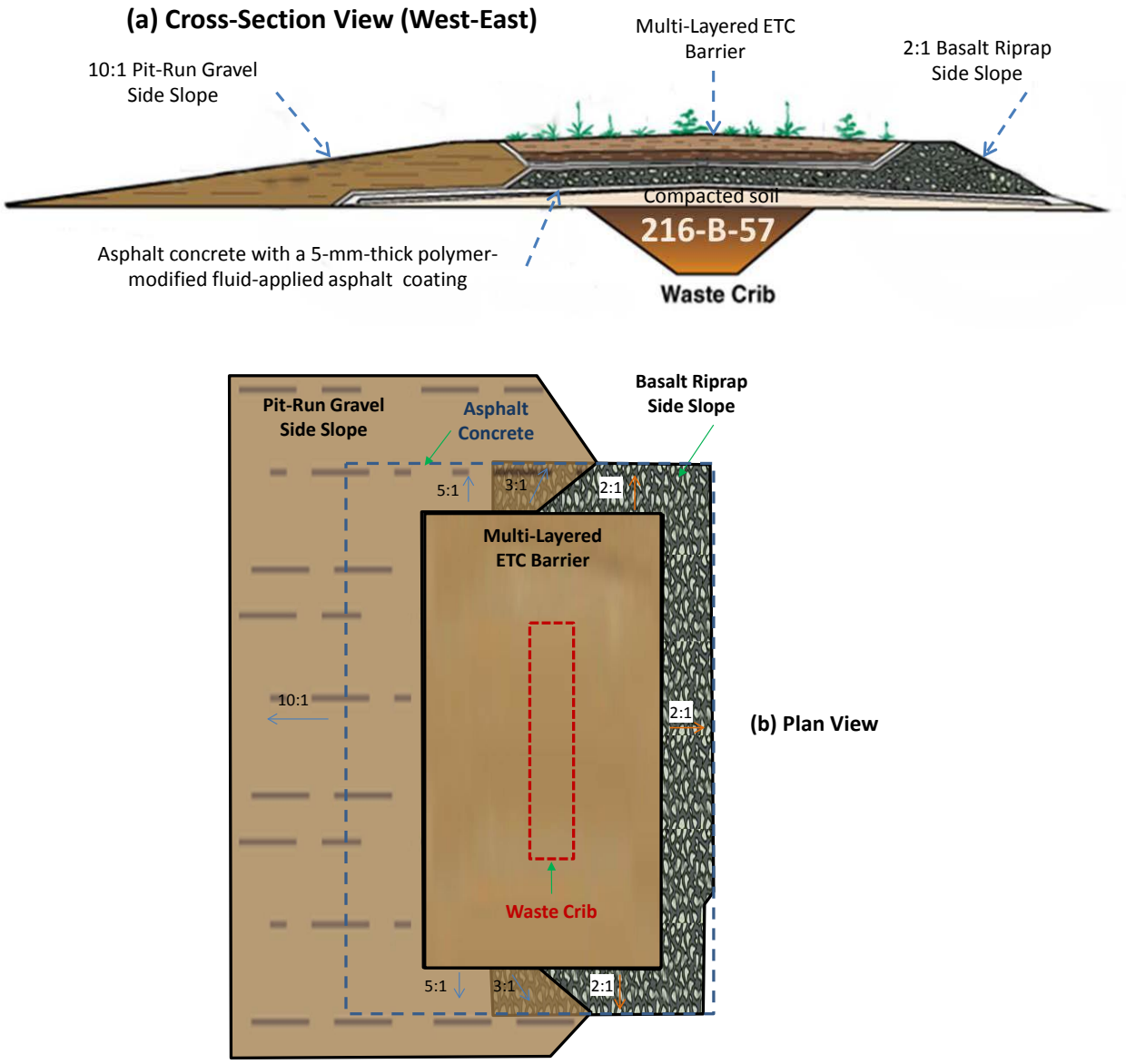

Figure B.2. Schematic of the PHB. (a) cross-section view (west-east) and (b) plan view (approximate scale).

B.1.1 The ETC Barrier

The ETC barrier is composed of multiple layers (Figure B.3) of natural and asphaltic materials and uses a capillary break (CB) to increase the storage capacity of the top ET layer. The silt loam layers were constructed with a 2% slope from the crown (north-to-south center line) to promote the potential runoff of excess precipitation. On August 8, 1994, a series of soil cores were taken from the PHB surface and the dry bulk density of the admix of the ETC barrier after construction was 1380±0.121 kg m^{-3} (Gee et al. 1995). The ETC barrier is a 5-m-thick sequence of multiple layers overlying the compacted in situ soil,

beneath which lies a trench containing nuclear wastes. Each layer serves a distinct purpose as given in Table B.1 and the properties of the materials are summarized in Appendix D.

Table B.1. The layers of the ETC barrier and their functions

Layer No.	Materials	Thickness (m)	Particle Size[a] (m)	Function	Notes
0	Vegetation	NA	NA	Release stored water into the atmosphere by evapotranspiration; protect barrier surface from wind and water erosion	Revegetated native plant species
1	Upper Silt Loam w/ Pea Gravel Admix	1.0	NA for silt loam; 0.002 to 0.01 for pea gravel	Provide a medium for plant growth and water storage; the 15% pea gravel admix is to minimize soil loss by erosion	2% slope from the crown (north-south center line)
2	Lower Silt Loam	1.0	NA	Provide a medium for plant growth and water storage	2% slope from the crown
3	Geotextile	-	NA	Prevent the fine silt loam from entering the underlying coarser sand layer during construction	Non-woven, needle-punched polypropylene geotextile
4	Sand Filter	0.15	< 0.01	Prevent silt loam from falling into the gravel filter; form a capillary break with the overlying silt loam	2% slope from the crown
5	Gravel Filter	0.3	< 0.016	Prevent gravel from falling into the basalt riprap; is a portion of the coarse layer that forms the capillary break	Top course material; 2% slope from the crown
6	Basalt Riprap	1.5	< 0.25	Provide a physical control against digging by humans and burrowing animals; limit root penetration	A layer of shoulder ballast was used at the top of basalt riprap; 2% slope from the crown
7	Drainage Gravel	0.3	<0.025	Protect the underlying layer; provide a medium for lateral water movement	2% slope from the crown
8	Asphalt Concrete	0.15	NA	Divert potential infiltration water away from the waste zone; provide a barrier against noxious gases from the waste zone	AC with 5-mm-thick fluid applied asphalt; the layer is curbed and drainage water is guided out to a designated area; 2% slope from the crown
9	Top Course	0.1	< 0.016	Provide a base for the asphalt concrete	Compacted to 95% of the maximum density;2% slope from the crown
10	Compacted Sandy Soil Fill	0 to 5	NA	Provide a foundation for the barrier	Level north-south; 2% in the west-east direction from crown; compacted to 95% of the maximum density

[a](DOE-RL 1994; KEH 1993)

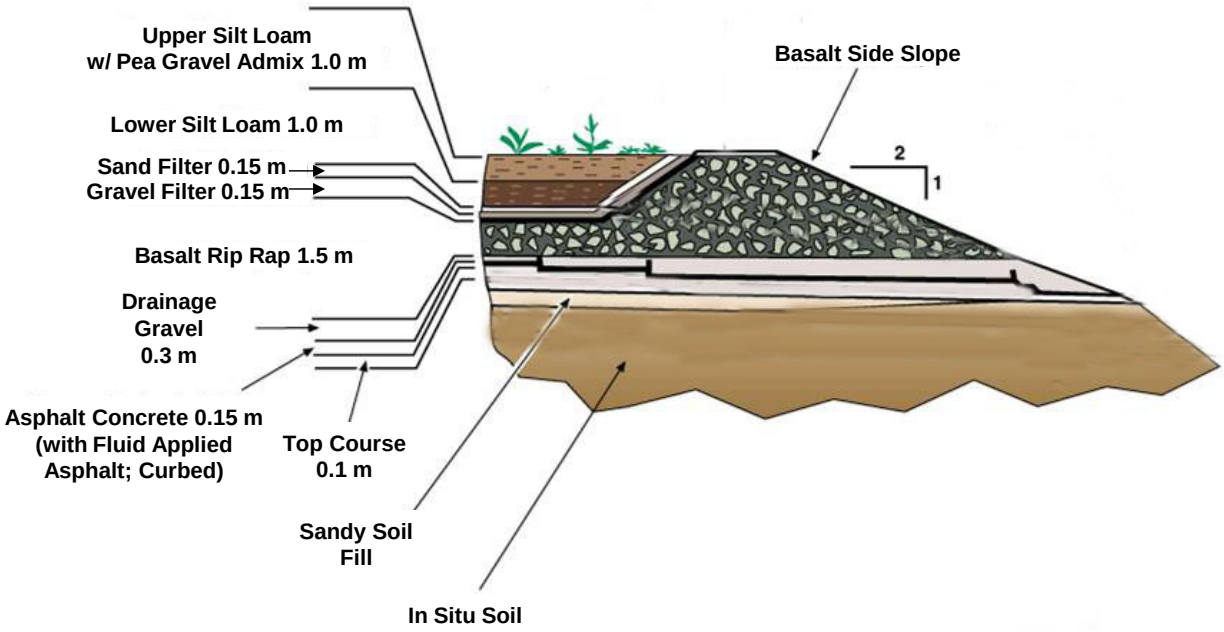

Figure B.3. Prototype Hanford Barrier cross-section – basalt riprap side slope.

The 2-m-thick silt-loam layer acts as the storage layer from which ET processes recycle some or all of the stored water back to the atmosphere. The silt loam also provides a medium for the growth of vegetation, which is necessary for transpiration to take place. In addition, the top 1 m of silt loam was amended with 15% w/w pea gravel to minimize wind and water erosion. Coarser materials (sand overlying gravel) placed directly below the silt-loam layer create a CB that inhibits the downward drainage of water from the silt loam into the coarser material. The 1.5-m-thick layer of basalt riprap helps deter root penetration, animal burrowing, and inadvertent intrusion by humans through the barrier profile. The silt loam (aka Warden silt loam) used for the barrier was from the McGee Ranch, which is about 10 miles west of the PHB. The average particle size distribution of 16 soil samples of the silt loam was 60.6% sand, 31.1% silt, and 8.3% clay.

B.1.2 Asphalt Concrete Barrier

A 65 m by 105 m composite asphalt concrete (AC) barrier covered with 5-mm fluid-applied asphalt (FAA) was placed at the bottom of the barrier to provide a low-permeability hydraulic barrier and redundant biointrusion prevention layer. The drainage layer above the AC helps to promote lateral flow of any water that passes through the ETC barrier.

A conventional paving machine was used to lay approximately 3400 tons of AC. Paving was done in two lifts of approximately 7.5 cm each and the paving was completed in 4 days (DOE-RL 1994). General overlap of the terraces was approximately 1.5 to 1.8 m. A nuclear gauge was used to verify compaction.

Polymer-modified asphalt (or fluid-applied asphalt) was applied by spraying the liquid directly on the AC surface with an asphalt distributor truck. Initially bubbles with the size less than approximately 1 cm developed when the FAA was applied in 100-mil thickness. It was found that thinner layers of FAA tended not to bubble as much. Five to seven thin layers of FAA were applied so that the total depth of

FAA was greater than 200 mils. Bubbles found after FAA application were repaired by heating the material with a propane torch, which allowed the softened FAA to flow into the hole because of the bubble.

B.1.3 West Gravel Side Slope

Enlargement of the cross-section containing the gravel side slope is shown in Figure B.3. The west side slope is a 10:1 (horizontal:vertical) pit-run gravel (aka clean-fill dike) side slope. It contains a small amount of fine (e.g., sand and silt) particles. Sparse vegetation grew on it during the monitoring period.

The clean fill side slope was placed, as designed, to be a rocky, freely draining gravely material. It is produced by mining and screening the Pit 30 material. Pit 30 is located to the west of the 200 East Area, directly northwest of where Route 3 and Route 4N intersect (DOE 2012). It was well graded soil mixtures containing cobbles up to 0.2 m in greatest dimension if uniformly distributed and not constituting more than 40 percent of volume (KEH 1993). It is transported to the PHB site, placed in 30.5-cm lifts, and compacted as common fill by two passes with large rubber-tired vehicles (DOE-RL 1994).

B.1.4 East Riprap Side Slope

An enlargement of the cross-section containing the riprap side slope is shown in Figure B.4. The east side slope is made of basalt riprap with a size up to 0.25 m (KEH 1993). No vegetation grew on it during the monitoring period. The angularity of the riprap provides many interlocking surfaces between adjacent rocks, allowing the creation of a relatively steep yet stable side slope.

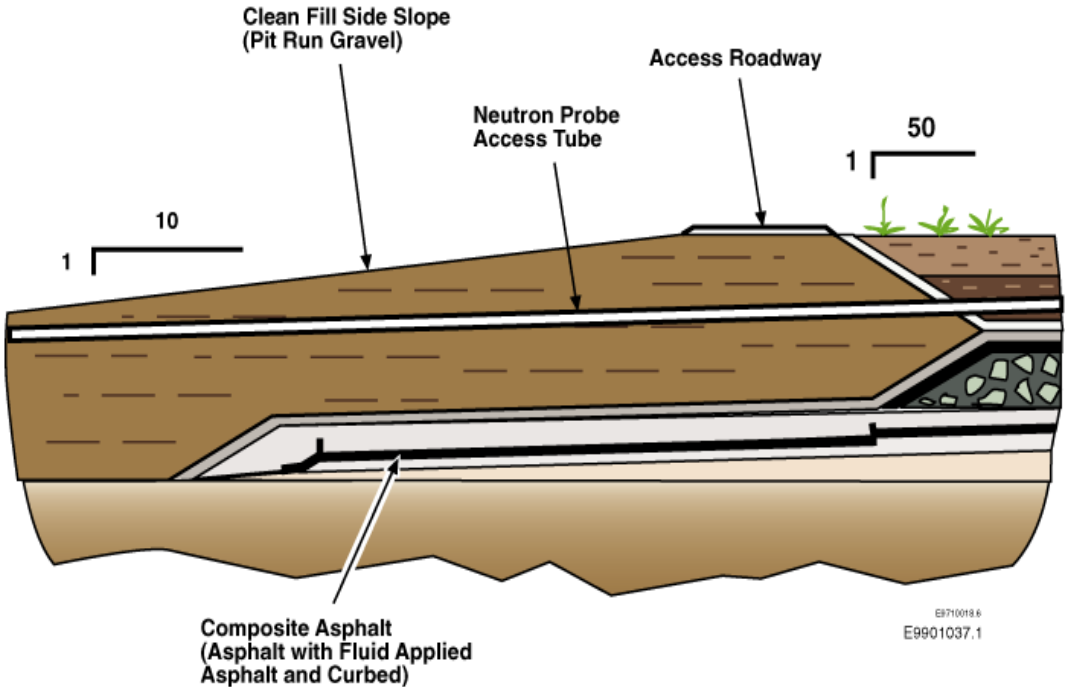

Figure B.4. Prototype Hanford Barrier cross-section – gravel side slope.

B.2 Revegetation of the Barrier

Plants control soil water storage and dynamics and protect the surface from wind and water erosion, but can potentially compromise the barrier by extending roots into the waste zone. The typical vegetation at the PHB is sagebrush (*A. tridentata*) and gray rabbitbrush (*E. nauseosa*) as shown in Figure B.5.

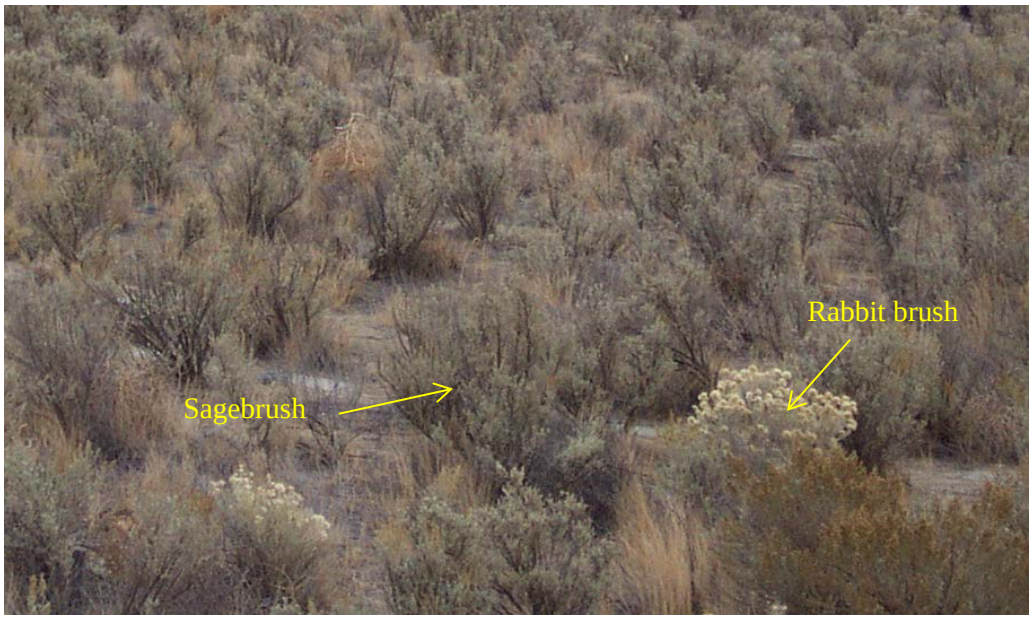

Figure B.5. Vegetation at the Prototype Hanford Barrier (photo taken July 11, 2002).

The PHB surface and the surrounding disturbed areas were planted in the fall of 1994. The perennial shrubs and perennial grasses were planted separately. Perennial shrubs were established by collecting seeds, growing seedlings, and planting them on the surface of the barrier. Seeds of *A. tridentata* and *E. nauseosa* were collected from local populations growing on the silt loam soil used for the upper layer of the barrier. Seeds were collected on December 23, 1993. The entire inflorescence of *A. tridentata* and the fruits of *E. nauseosa* were harvested and stored in plastic bags in the field. The material was transported to a laboratory, removed from the plastic bags, and placed on tabletops to dry. Material was stored in the dark and at room temperature until shipped to a nursery. The seeds were cleaned on April 12 and sown on May 4, 1994. Seedlings were grown in 164-cm^3 tubes until they were approximately 20 cm tall. Planting was initiated on November 7 and completed the next day. A total of 2700 holes were drilled at a density of 1-hole m^{-2} on the prototype surface. Two seedlings were placed in each hole. A total of 1350 *E. nauseosa* and 4050 *A. tridentata* seedlings were planted.

Perennial grasses were established by hydroseeding the barrier surface and surrounding slopes. The hydroseeding mix included seeds, fertilizer, mulch, and a tacking agent. The seven native perennial grass seeds and the fertilizers used in the mixture are listed in Table B.2. Seeds of *E. elymoides* were collected in June 1994 from grasses growing in silt loam soils within 20 km of the barrier. The other perennial grasses originated from sources in the semi-arid West. The mulch was applied as 2240 kg ha^{-1} of Eco-Fibre 100% virgin wood fiber. Degradable glue was added to the mulch as a tackifier at 67 kg ha^{-1}. The hydroseeding done on November 10 with the above material in a slurry form. The material was mixed with water using power augers in a large, truck-mounted tank, then dispersed under pressure from large hoses onto the ground.

Table B.2. Perennial grasses and fertilizers applied by hydroseeding.

Type	Name	Quantity (kg ha^{-1})
Perennial grasses	*Poa secunda* - Sandberg's bluegrass	34
	Elymus lanceolatus	5.6
	Achnatherum hymenoides	22
	Poa ampla	11
	Hesperostipa comata	5.6
	Elymus wawawaiensis	14
	Elymus elymoides	3.4
Fertilizer	Total Nitrogen	67
	P_2O_5	67
	K_2O	67

The status of the seedlings was assessed on December 2, 1994. Plant establishment on the surface was successful with very little loss of perennial shrubs. It is noted that the Russian thistle (*Salsola kali*), also known as tumbleweeds (which possibly came with the silt loam used to construct the surface), overgrew the planted vegetation in 1995, but subsequently died in the fall of 1995. The planted sagebrush and rabbitbrush shrubs grew in rows in 1996 (Figure B.6).

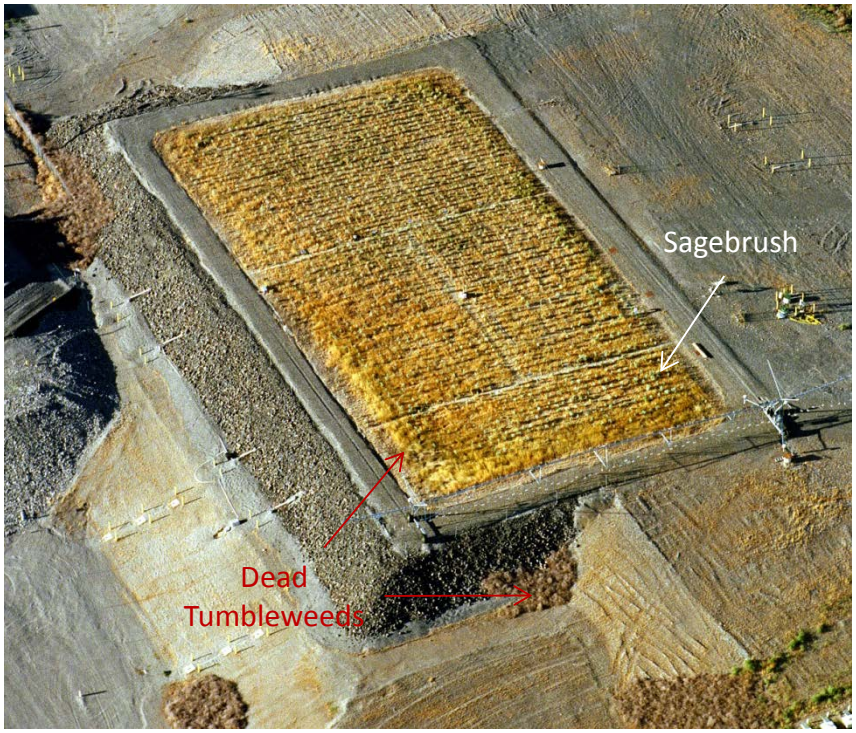

Figure B.6. Plan view of the Prototype Hanford Barrier on September 14, 1996 (southwest-facing view). The barrier was covered by the residual of the dead Russian thistle (or tumbleweeds, *Salsola kali*, in yellowish color). The survived seedlings of sagebrush were still small.

B.3 Enhanced Precipitation Test

An enhanced precipitation test (aka the treatability test) was used to test the barrier under both ambient (natural precipitation) and extreme climate (enhanced precipitation) conditions for a period of 3 years [water year (WY) 1995 (WY95) to WY97, within a time frame of 4 year]. A water year is defined as the 12 months from November of the previous year to October of current year. The enhanced precipitation test was designed to

- evaluate the hydrologic performance of the barrier using approaches of water balance and water processes
- assess the impacts of wind and water erosion on the surface of the barrier
- evaluate plant community dynamics
- evaluate the impacts of biointrusion on the barrier.

Based on the seasonal variation of precipitation and soil water at Hanford, a water year (WY) was used from precipitation calculation. From WY95 to WY97, the barrier surface was divided into two treatments or sections, one to the north (enhanced precipitation) and the other to the south (ambient precipitation). The north section was designated to receive an enhanced amount of precipitation (natural precipitation plus supplemental irrigation) to simulate extremely wet climatic conditions [three times (3X) the long-term annual precipitation], while the south section received only natural precipitation. Figure B.7 is a plan view of the PHB showing the layout of the 2 precipitation treatments, 3 buffer zones, and 12 monitoring plots (lW through 6W and lE through 6E). Plots 1W and 4W started from middle of the west boundary of the silt loam and extended to the west side slope; plots 1E and 4E started from the middle of the east boundary of the silt loam layer and extended to the riprap side slope; plots 3W, 3E, 6W, and 6E in the middle were beneath the ETC barrier; and 2W, 2E, 5W, and 5E transitioned from silt loam to side slopes, covering a 2-m-wide area of silt loam and a 2-m-wide area of the slanted silt loam boundaries. To minimize the impact of the edges, the north plots were separated from the northern edge by an 18-m buffer zone, whereas a 31-m zone separated the south plots from the southern edge. The north and south sections were separated by a 10-m-wide buffer zone.

Irrigation water was applied with a Lockwood® linear-move sprinkler irrigation system by the Petty Irrigation (Toppenish, WA) (Gee et al. 1994). The irrigation system spanned 43.9 m from west to east between road centers and had 10.4-m extension booms beyond the wheels to facilitate irrigation of the side slopes (Figure B.8a). The irrigation system travel speed was a maximum of 1.8 m per minute. Between roadways, the irrigation system was designed to deliver water to outlets spaced 0.76 m (2.5 ft) apart along the distribution pipe (Figure B.8b). Each outlet was equipped with a 1.9 cm (0.75 in.) ball valve, a rocker arm lever and drop cords, a pressure regulator, a metal U-tube, and a drop tube that reached within 0.91 m of the soil surface, to which a Wobbler nozzle was attached (Figure B.8b). The irrigation system was capable of gravity drainage at the roadways at both ends.

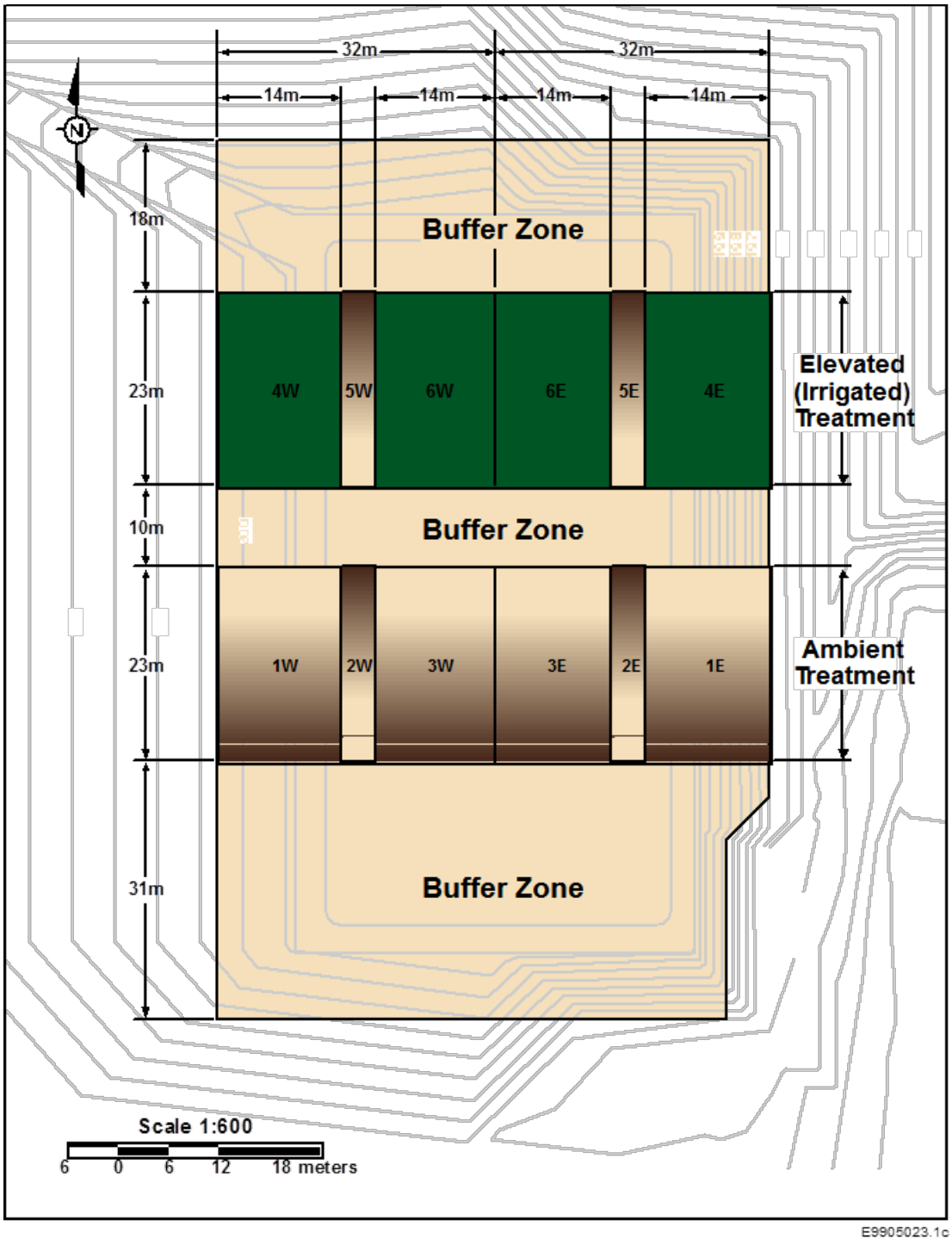

Figure B.7. Plan view of the Prototype Hanford Barrier showing layout of the 2 precipitation treatments, 3 buffer zones, and 12 soil plots (lW - 6W and lE - 6E).

(a)

(b)

Figure B.8. The Lockwood linear-move sprinkler irrigation system. (a) The irrigation system spanned 43.9 m between road centers and had 10.4-m extension booms beyond the wheels to facilitate irrigation of the side slopes. (b) Water was delivered to outlets spaced 0.76 m apart along the distribution pipe. The Wobbler nozzles were within 0.91 m of the soil surface.

During irrigation events, the system traveled in a north-to-south direction and back. To avoid compaction of the soil surface, movement of the irrigation system was limited to the roadway. The system delivered water on the north section of the barrier at a mean rate of about 10 mm hr^{-1} with a coefficient of variation of 6.7% (Appendix F). It took 15 to 17 minutes for the sprinkler system to complete a full pass and the water applied was equivalent to about 2 to 3 mm of precipitation depending on the water pressure. Consequently, there was a significant amount of time during the test when there was no application of irrigation on the test plot. This uneven application of water allowed infiltration of greater amounts of water stored on the surface in localized ponds (depression storage) than would normally occur during a natural rainstorm.

Irrigation was initially scheduled to start on November 1, 1994, but was delayed until February 1995 because of water supply problems. Water was usually applied at biweekly intervals, except in winter and depending on the weather. The amount of water applied in each irrigation event was usually calculated

based on the precipitation since the last irrigation cycle and a 10.0-mm margin to allow for natural precipitation events. In late March of each year from 1995 to 1997, a 1000-year return 24-hour rainstorm was simulated on the north section. Although the simulated rainstorm was 68 mm over a 24-hour period, in practice, 69.4, 69.5, and 69.7 mm of water was applied over 8-hour periods on March 25 of 1995, March 26 of 1996, and March 27 of 1997, respectively. In May 1998, 209.6 mm was applied to the north section for instrument calibration. The barrier was exposed to the natural precipitation conditions in WY99 and after.

Table B.3 tabulates the monthly irrigation on the north section of the barrier and natural precipitation during the enhanced precipitation period. The total amount of water applied on the north section of the barrier was 493.3, 493.1, and 499.7 mm—about three times the multi-year average of natural precipitation—in WY95, WY96, and WY97, respectively.

Table B.3. Monthly irrigation (P_i) and meteoric precipitation (P_m) from WY95 to WY98 (mm)

	WY95			WY96			WY97			WY98		
	P_i	P_m	$P_i + P_m$	P_i	P_m	$P_i + P_m$	P_i	P_m	$P_i + P_m$	P_i	P_m	$P_i + P_m$
Nov	0.0	17.3	17.3	8.9	26.4	35.3	20.6	67.8	88.4	0.0	25.7	25.7
Dec	0.0	34.5	34.5	49.1	58.9	108.0	0.0	93.7	93.7	0.0	7.9	7.9
Jan	0.0	54.4	54.4	13.2	36.1	49.3	30.0	38.4	68.3	0.0	31.5	31.5
Feb	17.0	17.5	34.5	21.6	31.0	52.6	0.0	6.4	6.4	0.0	29.2	29.2
Mar	87.4	24.1	111.5	73.7	21.1	94.7	69.7	17.8	87.4	0.0	12.7	12.7
Apr	62.2	39.1	101.3	0.0	10.9	10.9	0.0	8.4	8.4	0.0	1.8	1.8
May	36.2	20.1	56.3	19.1	15.7	34.8	22.8	8.4	31.2	209.6	13.2	222.8
Jun	11.4	19.6	30.9	40.9	1.3	42.2	11.5	11.7	23.2	0.0	12.2	12.2
Jul	0.0	8.6	8.6	0.0	3.6	3.6	11.3	4.8	16.2	0.0	8.6	8.6
Aug	0.0	1.8	1.8	8.4	0.5	8.9	12.1	1.5	13.7	0.0	1.0	1.0
Sep	0.0	20.1	20.1	12.5	5.6	18.1	31.4	8.1	39.5	0.0	2.5	2.5
Oct	0.0	22.1	22.1	12.4	22.4	34.7	0.0	23.4	23.4	0.0	7.1	7.1
Sum	**214.1**	**279.1**	**493.3**	**259.7**	**233.4**	**493.1**	**209.3**	**290.3**	**499.7**	**209.6**	**153.4**	**363.0**
Sum_w	**104.3**	**147.8**	**252.2**	**166.4**	**173.5**	**339.9**	**120.2**	**224.0**	**344.2**	**0.0**	**106.9**	**106.9**
Sum_s	**109.8**	**131.3**	**241.1**	**93.2**	**59.9**	**153.2**	**89.2**	**66.3**	**155.5**	**209.6**	**46.5**	**256.0**

Sum: WY total; Sum_w: total precipitation of the winter season (from Nov. to Mar.); Sum_s: total precipitation of the summer season (from April to October).

B.4 Controlled Burn Test

On September 26, 2008, a controlled burn was conducted on the north section of the barrier, including the silt loam cover and the gravel side slope (Figure B.9), to understand the response of the engineered ecosystems to wildfire. The test was used primarily to quantify the effects of wildfire on the ecological and hydrological performance of the cover. More details can be found in Ward et al. (2009).

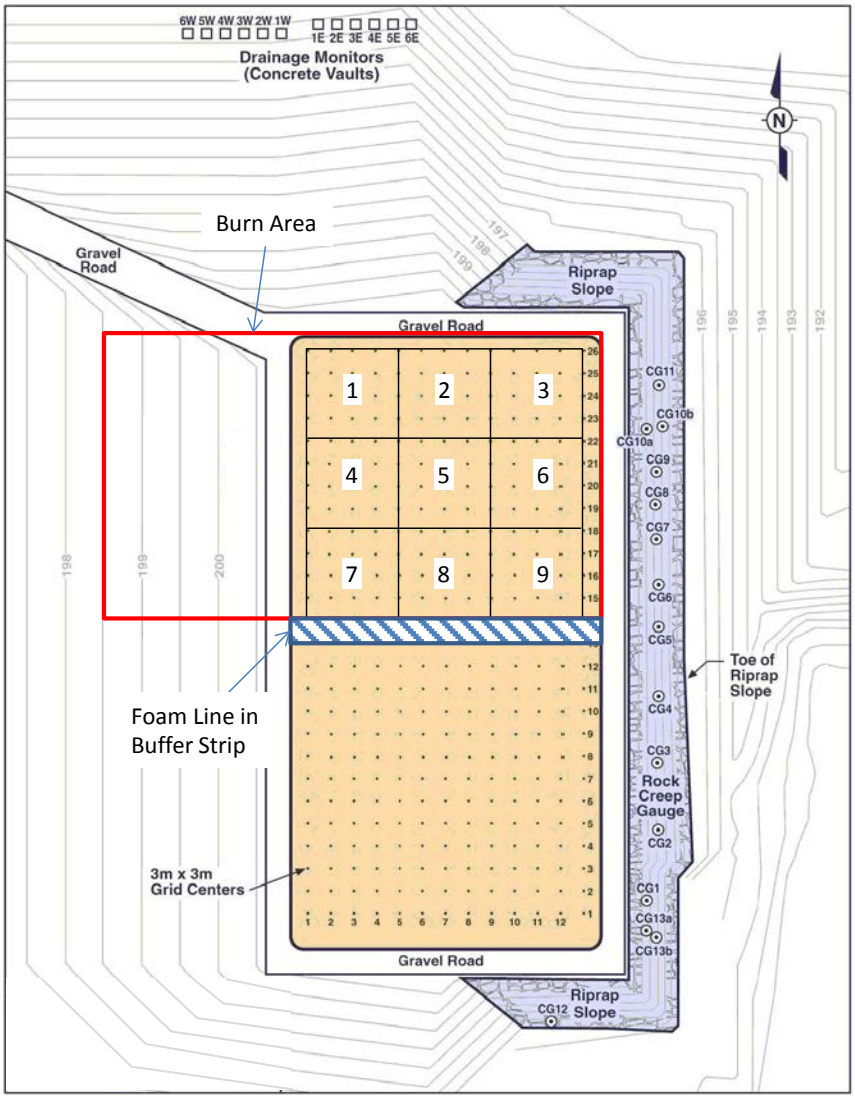

Figure B.9. Schematic plan view of the barrier's surface showing the burn area on the gravel side slope and the silt-loam surface, the 3-m-wide line of fire retardant foam, and the nine 12 × 12 m plots (marked as 1 through 9) used to compare the effects of fuel loads on fire intensity.

B.4.1 Protection of the Existing Monitoring System

Preparing for the controlled fire included protecting monitoring systems, e.g., the polyethylene boxes housing the dataloggers (Figure B.10a) and the polyvinyl chloride conduit (Figure B.10b) for the anticipated temperature increases. To protect the monitoring system, instrument boxes were packed with fiberglass insulation, properly closed, and covered with fire blankets. Exposed conduit and cables were buried in trenches, where soil disturbance could be tolerated, or covered with an appropriate layer of dry soil or aluminum fire shelters. Six mini-rhizotrons, constructed of clear acrylic tube with outer PVC sleeves, were wrapped with a layer of fiberglass insulation and covered with an inverted galvanized pail.

(a) (b)

Figure B.10. Photographs of the barrier surface and gravel side slope showing examples of monitoring infrastructure, (a) instrument boxes containing dataloggers, and (b) conduits carrying communication cables for instruments, that needed protection during the controlled fire.

B.4.2 Fuel-Load Characterization and Modification

Fuel-load plays an important role in the extent of combustion of vegetation and the long-term changes in soil organic matter as well as total and available fractions of nutrients and trace elements. Thus, pre-burn site characterization included assessing the available fuel load. Significant differences in plant density and fuel load were observed on the surface. Ground cover was particularly low in the northeast quadrant. This quadrant has traditionally shown a low shrub density and high grass cover, but at the time of sampling, grasses were also mostly absent.

Shrub biomass that could serve as fuel was determined by measuring the canopy characteristics, including height, greatest width, and greatest diameter at right angles to the greatest width on the shrubs. Measurements were made on 10 individual shrubs off the barrier surface that spanned the range of shrub sizes on the barrier surface. These shrubs were then harvested, weighed, dried, and weighed again to determine the fuel moisture content. Canopy characteristics were then measured on at least 30 individual sagebrush shrubs on the barrier surface to estimate shrub fuel density. The biomasses of other fuel components on the surface were also estimated. Some areas of the barrier surface were quite sparse in vegetative cover and required an increase in biomass to reach representative fire intensities and severities. Other fuel components included tumbleweed. Although some tumbleweed was found near the barrier, it was still necessary to import tumbleweed from other areas. Over 2 tonnes of clean tumbleweeds were brought to the barrier from the 200 East Area. Subsamples of the imported fuel were weighed and dried to determine the moisture content. The dry tumbleweeds were spread across the surface of the barrier by hand to achieve the randomly assigned fuel loads. Approximately 10.5 and 12.8 tonnes ha^{-1} were assigned to the nine 12 × 12 m plots (Figure B.9).

B.4.3 Controlled Burn

Before starting the fire, a 3-m-wide line of fire retardant foam was applied to the buffer strip between the north and south sections of the barrier to protect the south portion of the barrier during the burn. The fire was set up with drip torches to ignite the fire at 3:15 PM on September 26, 2008. The fire lasted approximately 7 minutes, by which time all of the imported fuel and most of the natural biomass had been consumed. After the main fire, plots with incomplete combustion were burned off using a drip torch.

B.5 Barrier Maintenance

After the completion of the PHB construction and revegetation in 1994, there was no significant maintenance of the PHB, other than instrumentation, except to fill a badger hole that was about 0.6-m deep with a 0.3-m diameter.[1] However, there was a major repair away from the southeast side of the PHB riprap side slope. In May 2004, after severe thunderstorms, runoff water from the elevated BY-BX Tank Farm surface (southeast to PHB) flowed down-gradient to the region between the tank farm and the PHB, eroding a channel about 1.1 m deep at the base of the east side of barrier side slope (Figure B.11). The channel extended into the sandy subgrade fill layer of the riprap toe slope. All repairs were completed in fiscal year 2005 (Figure B.12b).

Figure B.11. North-facing photograph taken on June 16, 2004. The orange lines indicate the path and direction of the runoff.

[1] Personal communication with Chris Strickland and Ray Clayton.

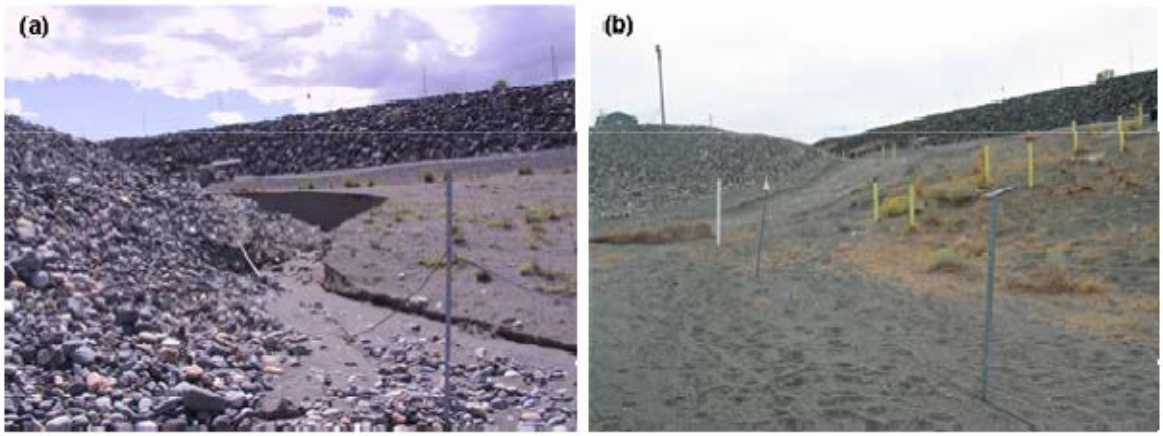

Figure B.12. Erosion near the Prototype Hanford Barrier resulting from a thunderstorm in May 2004. (a) Erosion channel formed between BY-BX Tank Farm and the Prototype Hanford Barrier; (b) repaired toe of the side slope in September 2005.

References

DOE-RL. 1990. *Remedial Investigation/Feasibility Study Work Plan for Hte 200-BP-1 Operable Unit Hanford Site,* DOE/RL-88-32, U.S. Department of Energy Richland Operations Office, Richland, Washington.

DOE-RL. 1993. *Phase I Remedial Investigation Report for the 200-BP-1 Operable Unit,* DOE/RL-92-70, Rev. 0, U.S. Department of Energy Richland Operations Office, Richland, Washington.

DOE-RL. 1994. *Constructability Report for the 200-BP-1 Prototype Surface Barrier*, DOE/RL- 94-76, U.S. Department of Energy Richland Operations Office, Richland, Washington.

DOE-RL. 1999. *200-BP-1 Prototype Barrier Treatability Test Report,* DOE/RL-99-11 Rev. 0, U.S. Department of Energy Richland Operations Office, Richland, Washington.

DOE. 2012. *Environmental Assessment for Expansion of Borrow Areas on the Hanford Site,* DOE/EA-1934 Draft, U.S. Department of Energy, Richland, Washington.

Gee, GW, HD Freeman, WHJ Walters, MW Ligotke, MD Campbell, AL Ward, SO Link, SK Smith, BG Gilmore, and RA Romine. 1994. *Hanford Protoype Surface Barrier Status Report: FY 1994,* PNL-10275, Pacific Northwest Laboratory, Richland, Washington. Available at http://www.osti.gov/energycitations/servlets/purl/10113304-5D9ZgI/webviewable/.

Gee, GW, AL Ward, and MJ Fayer. 1997. "Surface Barrier Research at the Hanford Site," *Land Contamination & Reclamation*, 5(3):233-238.

Gee, GW, AL Ward, BG Gilmore, MW Ligotke, and SO Link. 1995. *Hanford Prototype-Barrier Status Report: FY 1995*, PNL-10872, Pacific Northwest National Laboratory, Richland, Washington. Available at http://www.osti.gov/energycitations/servlets/purl/177965-nd9isN/webviewable/.

KEH. 1993. *Prototype Surface Barrier at 200-BP-1 Operable Unit*, W-263-C2 Rev. 0, Kaiser Engineers Hanford Company, Richland, Washington.

Myers, DR and DA Duranceau. 1994. *Prototype Hanford Surface Barrier: Design Basis Document*, BHI-00007 Rev.0, Bechtel Hanford, Inc., Richland, Washington.

Ward, AL and GW Gee. 1997. "Performance Evaluation of a Field-Scale Surface Barrier," *Journal of Environmental Quality*, 26(3):694-705.

Ward, AL, N Hasan, SO Link, and KE Draper. 2009. *The Effects of Fire on the Function of the 200-BP-1 Engineered Surface Barrier*, PNNL-18934, Pacific Northwest National Laboratory, Richland, Washington.

Wing, NR and GW Gee. 1994. "Quest for the Perfect Cap," *Civil Engineering*, 64(10):38-41.

Appendix C

Prototype Hanford Barrier Monitoring

Z. Fred Zhang, Chris E. Strickland, Ray E. Clayton

Pacific Northwest National Laboratory
Richland, Washington

Table Contents

List of Figures

List of Tables

Executive Summary

The Prototype Hanford Barrier (PHB) was constructed between late 1993 and 1994 over an existing waste site to demonstrate its constructability and long-term performance for a design period of 1000 years. The central component of the PHB is a field-scale evapotranspiration (ET) barrier atop a capillary break denoted as the ETC barrier. The basic concept of an ETC barrier is to store all precipitation in the ET barrier (or layer), where it can be released later via soil evaporation and plant transpiration such that drainage is always less than the design criterion of 0.5 mm yr^{-1}. A comprehensive system was used to monitor the hydrology, stability, and ecology of the PHB from 1994 to 2013. The primary water-balance components monitored for hydrologic performance evaluation of the PHB included precipitation, runoff, water storage in the silt loam, drainage, and percolation. Secondary confirmatory components monitored included soil water content at the bottom of the silt loam and beneath the asphalt concrete (AC) pad, soil water pressure within the silt-loam barrier, and soil water pressure below the AC. The structural stability of the PHB was evaluated by measuring settlement of the barrier below the AC, elevation change of the barrier surface, displacement in the riprap side slope, and soil and water erosion from barrier surface. The ecology monitoring included survivorship and reproduction, the characteristics of vegetation, and animal activities. The vegetation characteristics included species composition, plant cover, canopy structure, seed bank, transpiration and photosynthesis, root density and distribution, xylem pressure, and post-burn soil respiration. Animal activities included the use and intrusion (burrowing) by insects and small mammals, hole size, insect gall formation on plants, and other evidence such as droppings, tracks, nests, and burrows. The air temperature within the flame of the controlled fire was measured in multiple locations. Details of these measurements are described in this appendix.

The design and tests of the Prototype Hanford Barrier (PHB) are described in Appendix B. Briefly, the PHB consists of an evapotranspiration (ET) barrier, a 10:1 gentle pit-run gravel (aka clean-fill dike) side slope on the west, and a 2:1 steep basalt riprap side slope on the east. The PHB was constructed between late 1993 and 1994 over the 216-B-57 Crib in the 200-BP-1 Operable Unit as a mound over the ground surface to demonstrate its constructability and long-term performance for a design life of 1000 years. The performance of the ET barrier was enhanced by including a coarser layer below a finer storage layer. The texture contrast formed a capillary break (CB) at the interface. The ET barrier with a CB is termed the ETC barrier. This ETC barrier is a 5-m-thick sequence of multiple layers overlying the compacted in situ soil. Each layer serves a distinct purpose. The side slopes keep the ETC barrier stable and protect it from damage from natural processes or human activities. After construction, the barrier was revegetated with seedlings of shrubs and seeded with native perennial grasses in November 1994. From 1995 to 1997, an enhanced precipitation test (aka the treatability test) was conducted to evaluate barrier performance under both ambient (natural precipitation) and extreme climate (elevated precipitation) conditions. A controlled burn was conducted on the north section of the barrier, including the silt loam cover and the gravel side slope, on September 26, 2008, to understand the response of the engineered ecosystems to wildfire.

This appendix provides a complete summary of the monitoring system of the PHB. This system monitored the hydrology, stability, and ecology of the PHB.

C.1 Hydrology Monitoring

The primary function of the PHB is to minimize infiltration of water through the buried waste and contaminated soil. Successful performance of the primary function depends on the operation of a series of interactive and dynamic processes that control precipitation, infiltration and redistribution, water storage in the silt loam barrier, and loss of water. The interactive processes therefore depend on the upper 2-m-thick silt-loam layer of the ETC barrier, which is designed to facilitate plant growth and retain water deposited by precipitation until it is recycled, by ET, to the atmosphere.

Because all these processes affect water balance, the primary water-balance components monitored for hydrologic performance evaluation of the PHB include:

- precipitation and irrigation
- surface runoff
- changes in water storage (i.e., water content multiplied by the thickness of the soil layer) within the silt loam
- drainage through the silt loam and side slopes
- deep percolation through the asphalt concrete (AC) with a fluid-applied asphalt (FAA) coating.

Secondary confirmative components monitored include:

- soil water content at the bottom of the silt loam and beneath the AC
- soil water pressure within the silt-loam
- soil water pressure below the AC.

C.1.1 Monitoring Zones and Stations

It was expected that water balance and processes of the PHB would vary spatially. Hence, the PHB was divided into 12 zones or plots (Figure C.1) denoted as 1W through 6W for those located in the west half and 1E through 6E in the east half. These 12 plots represent three main types of barrier structure:

1. Silt loam plots: 3W, 3E, 6W, and 6E
2. Side slope plots:
    a. 1W and 4W for the west gravel side slope
    b. 1E and 4E for the east riprap side slope
3. Transitional or silt loam boundary plots: 2W, 2E, 5W, and 5E

Not all the components were monitored in all of the plots, depending on the primary hydrological processes and the function of the components. Drainage through all 12 plots was monitored with 12 drainage vaults. For water balance, the focus was on the silt loam, which serves as the media for water storage and vegetation growth. The riprap side slope has very little water storage capacity while the gravel side slope has some level of water storage. In addition to the 12 drainage monitoring plots, 14 monitoring stations, denoted as S1 through S14, were established. Each monitoring station (Figure C.2) was equipped with a mini-lysimeter (precipitation meter) to record precipitation events, a vertical aluminum access tube for measurements with a neutron probe (NP), a polyvinyl chloride (PVC) access tube for capacitance probe, and a 1.85-m segmented time domain reflectometry (TDR) probe to measure water content profile. Twelve of the fourteen monitoring stations were installed in the four silt loam plots (Figure C.1)—three stations each in 6W and 6E in the north section and 3W and 3E in the south section—to allow the water processes and balance of these plots to be thoroughly evaluated. Two stations were installed in the two gravel plots, i.e., 1W and 4W, respectively, at the west side slope. There was no water balance monitoring of the east riprap side slope or the four small transition plots because the riprap has little water holding capacity and the transition plots are less important than others.

Only one runoff flume (Figure C.1) was established for runoff monitoring because runoff was not expected to be a major component of the water balance. For the same reason, only one lysimeter was used to monitor percolation through the AC. For confirmative purposes, water content at the bottom of the silt loam and beneath the AC was monitored with multiple horizontal neutron tubes. Methods, instruments, monitoring locations, and monitoring frequency are given in sections below.

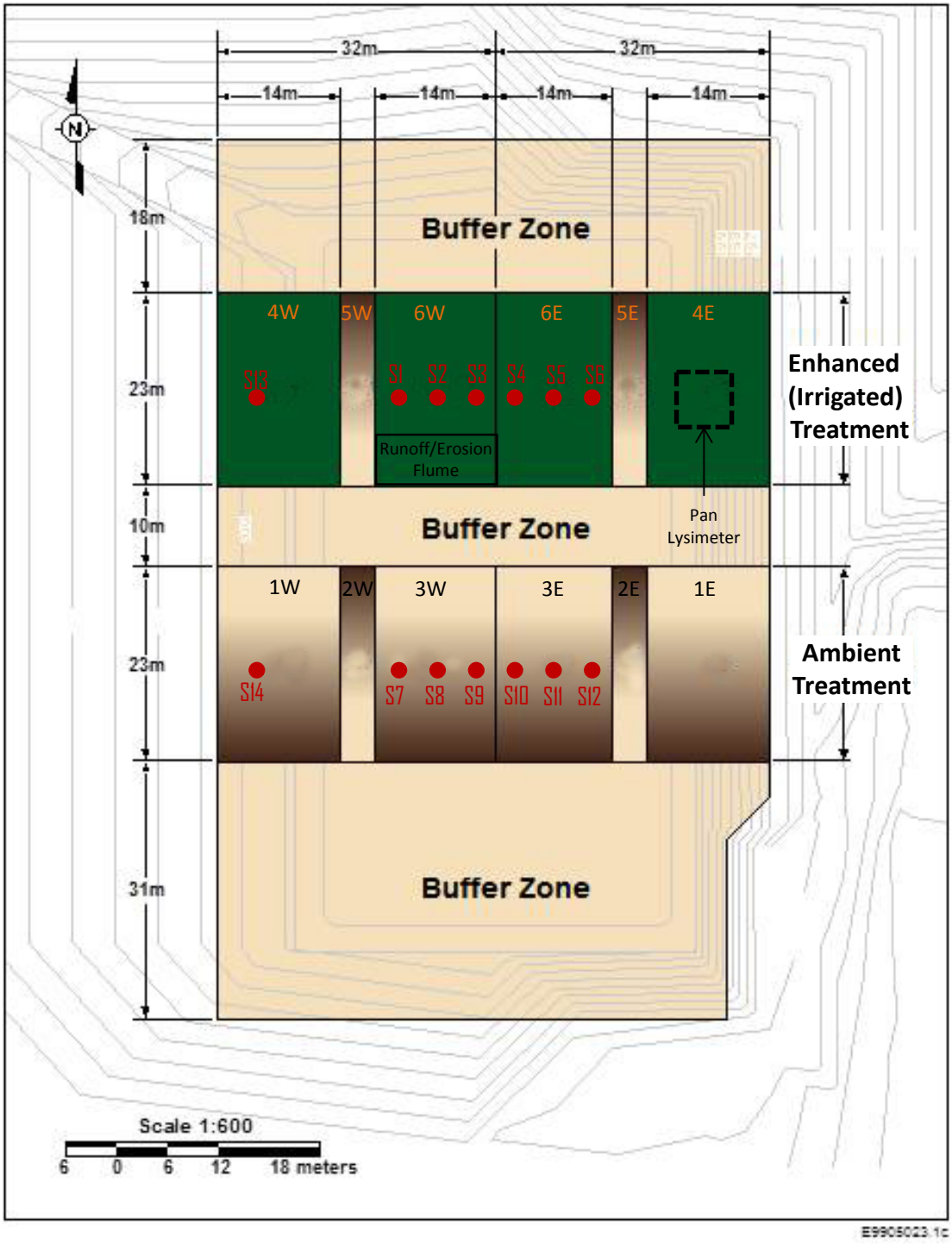

Figure C.1. Plan view of the Prototype Hanford Barrier showing the 14 water balance monitoring stations (marked as S1 through S14), 12 plots for drainage monitoring (marked as 1W through 6W and 1E through 6W), and the runoff/erosion flume.

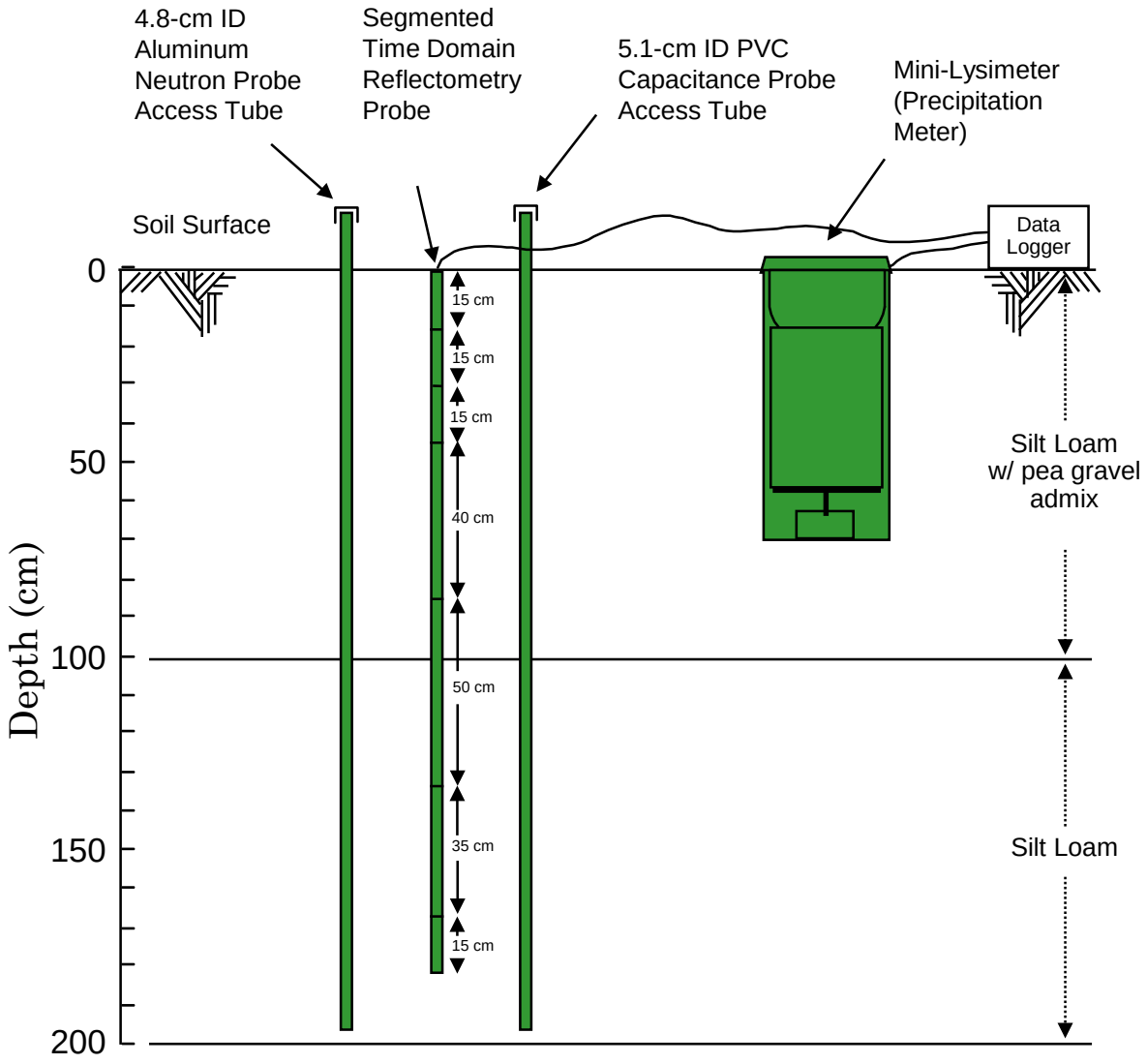

Figure C.2. Schematic cross-section of a typical monitoring station.

C.1.2 Primary Monitoring Components

C.1.2.1 Precipitation and Irrigation Monitoring

Water received by the barrier was measured by specially constructed mini-lysimeters (Figure C.2). The lysimeters used a load cell and a collection system that allowed them to act as a rain gauge/snow pillow combination. Thus, rainfall, irrigation, and snow were measured with a single instrument. Fourteen units were installed on the barrier to measure the spatial distribution of precipitation over the surface. These mini-lysimeters, which were controlled and recorded by a CR-7 datalogger manufactured by Campbell Scientific, Inc. (Logan, UT), took measurements once every hour. Automated measurements of rainfall were supplemented by periodic manual precipitation-gauge measurements at the barrier and data from the Hanford Meteorological Station.

The mini-lysimeters were constructed by placing 20-L plastic containers on electronic Model 6762 Load Cells by Revere Transducers (Cerrittos, CA) and lowering them into the ground inside heavy-walled plastic tube with a slightly larger diameter (Gee et al. 1994). The tube acted as the outer wall of the lysimeter. A round-bottomed, plastic flowerpot sat inside each 20-L container and was positioned so that it rode freely in the 20-L container and was recessed below the top of the outer wall. The pot was filled with white marbles that had low water storage, allowing rapid drainage of water during and after precipitation events and simultaneously minimizing evaporation from the collection containers. The top of the lysimeter was covered with a grill that had about 5-cm horizontal spacing to allow water and snow to readily enter the lysimeter. The open-surface cover was designed to allow the mini-lysimeter to capture and weigh snow directly. This allowed the measurement of rainfall, irrigation, and snow with one instrument. The collected water in the load cells was manually dumped and the marbles/containers were cleaned periodically (roughly once every 6 months).

The actual water applied was measured by six rain gauges located within plots 6W and 6E (Figure C.1), respectively. In fiscal year (FY) 1996, two more rain gauges were added to measure the amount of water applied to the gravel and basalt side slopes.

C.1.2.2Surface Runoff and Erosion Monitoring

The dominant erosional processes are rainsplash coupled with overland runoff in which rainsplash loosens soil particles and makes them available for transport by runoff. Another factor contributing to erosion is runoff volume. For a given rainfall event, the volume of runoff increases as the slope length and surface area increases.

The runoff and erosion were monitored by measuring runoff and sediment yield from a 6-m-wide by 15-m-long flume installed on the soil surface (Figure C.1). The flume was constructed of timber with an opening at the downslope end. A galvanized metal collector system received the water-sediment runoff for measurement by the automated ISCO (ISCO, Inc., Lincoln, NE) monitoring system. The ISCO system used a flume to measure flow and employed the bubbler method to measure water level. The flow meter was used with an open channel. The ISCO had built-in standard level-to-flow conversions. The automatic ISCO system was installed on the west side of the gravel road and connected to the flume by a buried plastic pipe. The automated system consisted of a sediment collector to accumulate runoff and sediment. The ISCO system needed a large enough flow to be activated. The runoff monitoring flume was refurbished in June 2004, after site inspection showed that a pipe leading from the runoff plot to the flume had become disconnected (Ward et al. 2005), and again in May 2012.

A temporary test plot was constructed in the northwest quadrant of the barrier to quantify the amounts of overland runoff, infiltration, and sediment yield from the top surface during the application of a total rainfall amount equivalent to the projected 1000-year storm in March 1995. The temporary test plot had a size of 3.05-m by 15.25-m oriented west-to-east and started from the crown (i.e., the north-to-south centerline) of the barrier. The test plot was constructed with plastic lawn edging around the perimeter of the plot. Using plastic lawn edging allowed for minimal disturbance of the surface and aided in the removal of the test plot after testing. The temporary flume was made of 12-in. PVC with a slot cut into it and a reducer at one end to allow collection of the runoff samples in 1-L sample bottles. Samples of runoff and sediment yield data were collected manually during the test from a pit dug at the south end of the collection flume. Rain gauges were placed every 3 m along the north side of the test plot and read

after every series of passes of the rainfall applicator. Refer to Appendix B for a detailed description of the irrigation system and design.

C.1.2.3Water Content Profile

Soil water content (θ) was measured using a variety of techniques (Table C.1), including methods of neutron moderation, TDR, and capacitance probes. These three techniques are indirect methods in that they are based on measuring a soil physical property that depends on soil water content. All three methods are nondestructive and, except for the TDR method, require manual operation. The three methods are briefly reviewed in the following paragraphs.

Table C.1. Instrument used for silt loam water content and soil water pressure monitoring.

Measured Variable	Instrument Name and Model	Resolution	Time of Service	Manufacturer
Soil Water Content	Neutron Probe, Model 503 DR Hydroprobe	±0.005[(a)] m^3m^{-3}	1994 to present	CPN Corporation, 2830 Howe Road, Martinez, CA 94553
Soil Water Content	Capacitance Probe, Sentry 200-AP	±0.010[(a)] m^3m^{-3}	1994 to 1995	Troxler Electronic Lab, Inc., P.O. Box 12057, Research Triangle Park, NC 26609
Soil Water Content	TDR Probe System, MP-917 DM Meter	±0.005[(a)] m^3m^{-3}	1994 to 2005	Environmental Sensors, 100-4234 Glanford Ave., Victoria, BC V8Z 4B9, Canada
Soil Water Pressure	Model 229L Heat Dissipation Units	±20%[(b)]	1994 to 2013	Campbell Scientific, Inc., 815 W. 1800 N., P.O. Box 551, Logan, UT 84321
Soil Water Pressure	MC-314 Soil Moisture Cells (Fiberglass Blocks)	-	1995 to 2007	ELE International, Inc., Soil Test Products Division, 86 Albrecht Dr., Lake Bluff, IL 6004

[(a)] DOE-RL (1999)
[(b)] Reece (1996)

Neutron Moderation Method

The neutron method is an indirect method that uses a source of fast neutrons that are slowed down when they interact with the medium surrounding the source. Small atoms are the best for attenuating fast neutrons, and the most efficient is the hydrogen atom. In soils, it is assumed that all of the hydrogen that leads to changes in thermalization of the fast neutrons is due to changes in water molecules present in the soil. Thus, the number of slow neutrons is greater when the soil is wetter. The equipment used in this test was a Campbell Pacific Nuclear Hydroprobe model 503DR with a 50 mCi americium-241/beryllium neutron source (CPN International Inc.,[1] Martinez, CA) (Figure C.3). This hydroprobe consists of a protective shield that houses the nuclear source and the electronic counting system. The probe was deployed in 14 vertical (4.8-cm inner diameter [ID]) aluminum access tubes extending down to 1.9 m from the barrier's surface (Figure C.2). The NP was calibrated on April 5, 1995, in the vertical access tubes:

$$\theta = a_0 + a_1 N + a_2 N^2 \qquad \text{(C.1)}$$

[1] http://www.instrotek.com/pdfs/brochure%20503dr.pdf (verified on March 6, 2015)

where N is the 16-sec. neutron count, a_0 = -0.01649, $a_1 = 1.449 \times 10^{-5}$, and $a_2 = 3.234 \times 10^{-10}$. On April 20, 2003, the NP received a new neutron counter that slightly underestimated the neutron count based on the cross-calibration with another NP before and after the use of the new neutron counter. Hence, after this date, the N values needed to be scaled by a factor of 1.041 for vertical logging based on the cross-calibration with another NP before and after the use of the new neutron counter.

As the test progressed, the other water content monitoring methods were eliminated because of technical difficulties, described later in this appendix. Hence, the neutron method remained as the only source of water content data during the entire testing period from 1994 to present.

Figure C.3. A 503DR Hydroprobe for soil moisture logging.

Time Domain Reflectometry Method.

The TDR method is an indirect method based on the dependence of the soil's dielectric constant, κ, on volumetric water content. The velocity of a voltage pulse generated along a probe by a TDR unit is used to calculate κ. The dielectric constant for water is 80, while it is between 4 and 8 for the solid phase (e.g., the silt-loam used to construct the surface layer of the barrier), and 1 for air. Because the soil is a mixture of solid, water, and air, with a fixed amount of the solid phase, the value of κ is strongly dependent on the amount of water present. Thus, different combinations of water, air, and soil will lead to different effective values of κ, from which θ can be determined with the appropriate calibration relationship. A major advantage of TDR is its insensitivity to textural differences, allowing measurement of θ over a range of soils without the need for extensive calibration.

The main components of the TDR system are a signal generator that produces the voltage pulse and measures the return signal and transit time, transmission lines or probes, and coaxial cable. In the test, θ was measured using specially designed shorting diodes Moisture Point® system MP-917[2] TDR probes supplied by Environmental Sensors, Inc. (Sidney, BC, Canada). These probes are of the remote-shorting diode design described by Hook et al. (1992) and were customized to 1.85 m in length (Figure C.2). These probes are referred to herein as long probes or long TDR probes. The unique feature of the shorting diode probe is its ability to measure θ profiles at a given location with a single probe. The shorting diode probe was reported to not require a site-specific calibration and as having a linear relationship between θ and $\kappa^{½}$ for all soils (Hook and Livingston 1996). The system is fully automated and does not require the use of access tubes or additional calibration. The probes were connected via 50-m cables to a central multiplexing system and controlled by a Campbell Scientific CR10 datalogger.

A series of 12 long TDR probes were installed in the surface of the prototype barrier in September 1994 (Gee et al. 1994). Two additional probes were installed in the gravel side slope in October 1994. These units were specially constructed probes configured with eight remote shorting diodes (Figure C.2). This design allowed the measurement of water content across seven segments of a 1.85-m-long probe, buried vertically in the ground. The probes were connected, via two 8-channel multiplexers, to a TDR controller and readout unit. Measurements commenced in March 1995 and were generally taken at 1-hr intervals. Measurement frequency was higher during and after the irrigation of the 1000-year 24-hour rainstorm events.

In FY01, each of the long TDR probes was replaced with three short probes installed at different depths (Figure C.4) in an attempt to improve the accuracy of measurements in the silt-loam soil (Ward et al. 2005). These probes are referred to herein as the short probes or short TDR probes. The intermediate and deepest probes used were the Type K probe of Environmental Sensors, Inc., which is 0.6-m long and consists of four 0.15-m segments. The shallowest probe used was the 0.75-m Type H probe, which consists of five 0.15-m segments. The short TDR measurements showed a large amount of noise, which led to significant uncertainty in water storage calculation. By late 2005, part of the TDR system had failed (Ward et al. 2007). The system had been plagued with problems since FY07 (Ward et al. 2007) and became nonfunctional in late FY08 (Ward et al. 2011).

[2] http://www.esica.com/_docs/tb01.pdf (verified on March 6, 2015)

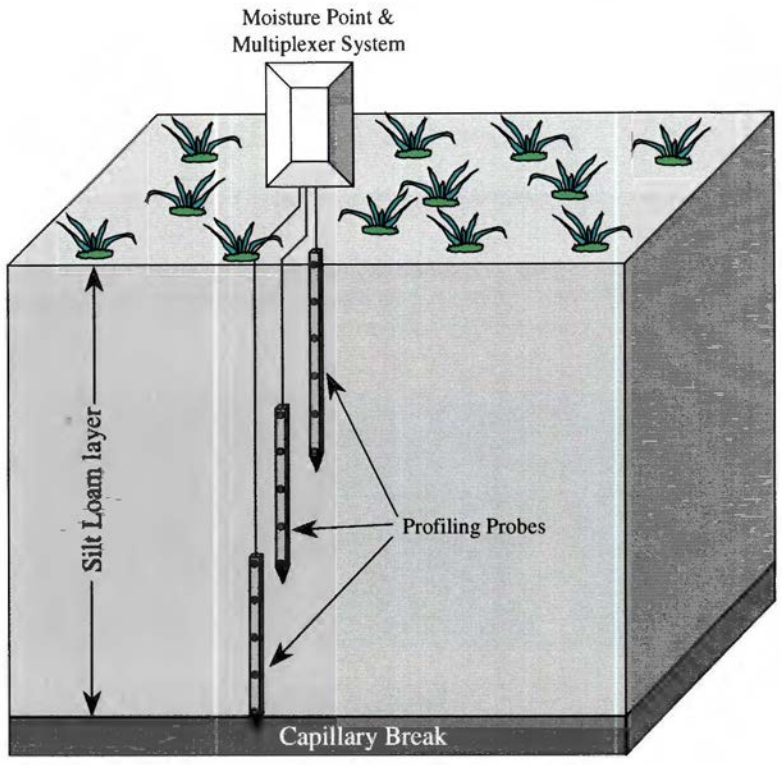

Figure C.4. Schematic of the TDR probe installed in FY01.

Frequency Domain (Capacitance) Method.

Similar to TDR, the capacitance method is an indirect method based on the dependence of the soil's dielectric constant, κ, on volumetric water content. However, the principle of operation is somewhat different. A Sentry 200 probe (Figure C.5) manufactured by Troxler Canada, Inc. (Laval, QC, Canada) was used in this test. This probe consists of a cylindrical form that houses the electronics, and two metal bands on the periphery of the cylinder that act as electrodes. An electric field is formed in the soil around the electrodes, and energy is adsorbed by the soil. The amount of energy adsorbed is dependent on κ and causes a shift in the frequency of the system. The frequency shift can then be converted to θ using the appropriate calibration relationship.

$$\theta = -\frac{\ln[(A-F)/B]}{100C} \qquad \text{(C.2)}$$

where θ is soil moisture content, F is frequency from the capacitance probe, A = 4961.2, B = 2159.8, and C = 0.060544. The probe was deployed in 14 vertical PVC access tubes extending down to 1.9 m from the barrier's surface (Figure C.2).

Use of the capacitance probe method for the test was discontinued in FY96 because it consistently overestimated θ relative to the NP and appeared relatively insensitive to changes in θ at the wetter end of the moisture range (Gee et al. 1995).

Figure C.5. The surface unit of the Troxler Sentry 200 capacitance probe.

C.1.2.4Drainage off the Asphalt Concrete

Because the PHB was designed with a recharge limit of 0.5 mm yr^{-1} or less, measurement of drainage off the FAA-coated AC is critical for performance assessment. In the context of this PHB demonstration, drainage refers to the water that moved through the ETC barrier onto the AC. Therefore, the drainage measurements did not reflect water movement *through* the AC, but only water *diverted* by the AC. The low-permeability FAA-coated AC was built with a 2% slope, parallel to the ground surface, to the east and west of the barrier crown. The entire surface of the AC was covered with a 0.3-m-thick layer of gravel to facilitate lateral water movement toward the lower slope positions of each collection zone. A series of curbs divided a portion of the AC surface into 12 water collection zones, aligned with the 12 plots denoted by 1W through 6W and 1E through 6E (Figure C.1). Most of the area of plots 1W and 4W was below the gravel side slope, while most of the area of plots 1E and 4E was below the riprap side slope. These four plots are referred to as the side slope plots. Plots 2W and 5W were primarily below the west boundary of the ETC barrier and 2E and 5E below the east boundary. These four plots are referred to as the transition plots. The remaining four plots (i.e., 3W, 6W, 3E and 6E) were below the ETC barrier and are referred to as the silt loam plots. The silt loam and side slope zones have the size of 14m×23m and the transition zones have the size of 23m×4m. The water intercepted by the curbed AC corresponding to each of the plots was conveyed through a network of PVC pipes to collection vaults for measurement. In other words, each of the curbed zones behaves like a lysimeter. For the un-curbed AC surface area, the intercepted water flowed off the surface at the AC edge.

The diverted water was conveyed through a network of PVC pipes to collection vaults for measurement. This water would likely be discharged along the edge of the AC and could contribute to recharge unless collected. The drainage monitoring system was composed of 12 concrete vaults (Figure C.6) for the 12 plots, respectively. The vaults were installed to the north and downgradient from the AC to allow the movement of water by gravity. Each vault contained an Orenco® dosing siphon system (Orenco Systems, Inc., Sutherlin, OR) to discharge the collected water once the maximum water level was reached. The average dosing volume was 0.591 m^3, which is equivalent to 1.8 mm of drainage through the side slope or silt loam plots and 6.3 mm of drainage through the smaller transition plots. The drainage rate from each plot was also measured with a tipping bucket and a pressure transducer. Drainage water from the PVC pipe flowed into each vault via a tipping bucket, which allowed monitoring of low flows, e.g., through the silt loam or transition plots. The tipping buckets might not have responded fast enough to high flow rates through the side slope plots. A submersed Druck® pressure transducer (Instrumart, South Burlington, VT) monitored the intermediate-to-high flow rates by recording hydrostatic pressure at intervals ranging from 10 minutes to 1 hour. Each vault was equipped with a lid to prevent precipitation from entering it and was covered with a thick tarp to prevent the water in the vault from freezing in the winter or evaporating in the summer. A thermometer was installed in each vault to monitor the temperature. The instruments and their precision used for drainage monitoring are given in Table C.2. This monitoring was conducted from water year (WY) 1995 to WY13, with some data gaps in WY99, WY05, and WY06.

Table C.2. Instruments and their precision used for drainage monitoring

Instrument Name and Model	Instrument Resolution	Plot-Scale Precision	Time of service	Manufacturer
Druck PDCR 950/TI-0855-1 Pressure Transducer	±0.25%	±0.26 mm yr^{-1}; controlled by evaporation and seepage through vault walls	1994 - 2013	Instrumart, South Burlington, VT
Orenco dosing siphon	±591 L	Main plots: ±1.8 mm Transition plots: ±6.4 mm	1994 - 2013	Orenco Systems, Inc., Sutherlin, OR
RainWise tipping bucket	±11.0 mL	Main plots: $\pm 4.4\times10^{-5}$ mm Transition plots: $\pm 1.5\times10^{-4}$ mm	1994–2013 or Aug. 2012	RainWise, Inc., Trenton, ME
Rain-O-Matic Small tipping bucket, item 100-43	±5.0 mL	Main plots: $\pm 2.0\times10^{-5}$ mm Transition plots: $\pm 6.9\times10^{-5}$ mm	Aug. 2012 - 2013	Pronamic, Denmark

The pressure transducers were calibrated in 1995. The outputs in millivolts were determined at the maximum water level ($Volt_{max}$) right before a siphon and the minimum water level ($Volt_{min}$) right after a siphon. During each siphon, the average low outputs were 1.772±0.166 mV and the high values were 3.597±0.140 mV, with a voltage change ($\Delta Volt$) of 1.825 mV. Additional measurements were taken between the two water levels. Results indicated a strong linear relationship between the pressure transducer outputs and the water level. Hence, the drainage rate was determined according to the variation of water level; the number of siphons was determined based on the sudden change of voltage from a high value to a low value. The pressure transducers were recalibrated in December 2000. The values of $\Delta Volt$ varied between -18.5% and 18.6% (with an average of 4.0%) relative to the previous calibration, which is equivalent to ±0.33 mm of drainage for the main plots and ±1.2 mm for the transition plots.

The siphon was fitted with a dose counter connected to a datalogger to record dosing events. Each dose was equivalent to 591±40 L of water, or 1.8 mm from the main plots and 6.4 mm from the transition plots.

This indicates that the drainage measurement based on siphon counts may not have sufficient precision for drainage lower than 0.5 mm yr^{-1}.

The 12 tipping buckets were initially calibrated in 1995. Overall, the minimum, average, and maximum volume per tip (V_0) were 9.3±0.9, 10.2±0.9, and 11.0±0.9 ml, corresponding to the low, medium, and high flow rates, respectively. The volume of water per tip was about 10 ml but slightly larger for a faster flow rate. The tipping buckets may not function properly if the tipping rate is higher than about 40 counts per minute, which translates to approximately 0.4 L min^{-1}. This indicates that the response of a tipping bucket may not be fast enough for the high flow rate that may happen after a rainstorm, especially through the side slopes.

The tipping buckets were recalibrated in August 2012. The volume per tip varied from -8% to 59% relative to the previous calibration, with an average of 27%. In August 2012, two malfunctioning tipping buckets for 1W and 3W were replaced by two new Rain-O-Matic Small tipping buckets (Pronamic, Denmark), which had a tipping volume of 4.6 ml.

The designed drainage rate for the ETC barrier was 0.5 mm yr^{-1}. In reality, the drainage through the silt loam can be much (by an order of magnitude or more) smaller than 0.5 mm yr^{-1}, and drainage through the side slopes can be as high as hundreds of mm yr^{-1}. Hence, the resolution of a dosing siphon is too low to detect very small drainage such as that from the silt loam plots; the resolution of the tipping bucket is sufficient for measuring very low drainage rates, such as those from the silt loam plots, but may underestimate the drainage from the side slopes; the pressure transducer can serve both the high and low drainage but may still not have sufficient resolution for the silt loam plots. Both the dosing counter and the pressure transducer methods experience the error caused by the water loss due to evaporation and seepage through the vault wall, as discussed below, while the tipping buckets do not have this problem.

Potential Water Loss from the Vaults

The potential loss of water in the vaults was determined for vaults 3W, 3E, 6W, and 6E from March 1995 to August 1996 using three different methods: the monthly manual steel tape measurement, the hourly pressure transducer measurement, and the monthly evaporometer measurement [Section 2.4.3 of Gee et al. (1996)]. The evaporometer was made with a graduated cylinder with a 22.2-mm ID. The results showed that evaporation from the closed vaults is non-zero. Evaporation estimated from steel tape and pressure transducer measurements is quite similar, with rates of 0.26±0.06 mm yr^{-1} and 0.27±0.06 mm yr^{-1}, respectively. However, the rate estimated from evaporometer measurements was only 0.07±0.06 mm yr^{-1}, or about 25% of the rates based the steel tape and pressure transducer measurements. The disparity in calculated evaporation rates may be due to a combination of factors. The evaporometer may underestimate the evaporation because of very small cross-section area relative to that of the vault and limited diffusion of water vapor out of the evaporometer. Another potential source of water loss is through the walls of the vaults, which were constructed of precast concrete with a fluid asphalt coating on the inside.

To reduce evaporation from the drainage vaults, the dosing siphons were covered on November 23, 1996, with a triple folded 0.5-in.-thick concrete blanket and a plastic haystack cover with the reflective side up. The cover also prevented potential ice formation within the vaults.

In the monitoring of drainage using three different methods, the evaporation loss may affect the measurements of the dosing siphons and pressure transducers. However, the measurement using tipping buckets is not impacted by the evaporation from the vaults because this measurement was taken before water entered into the vault.

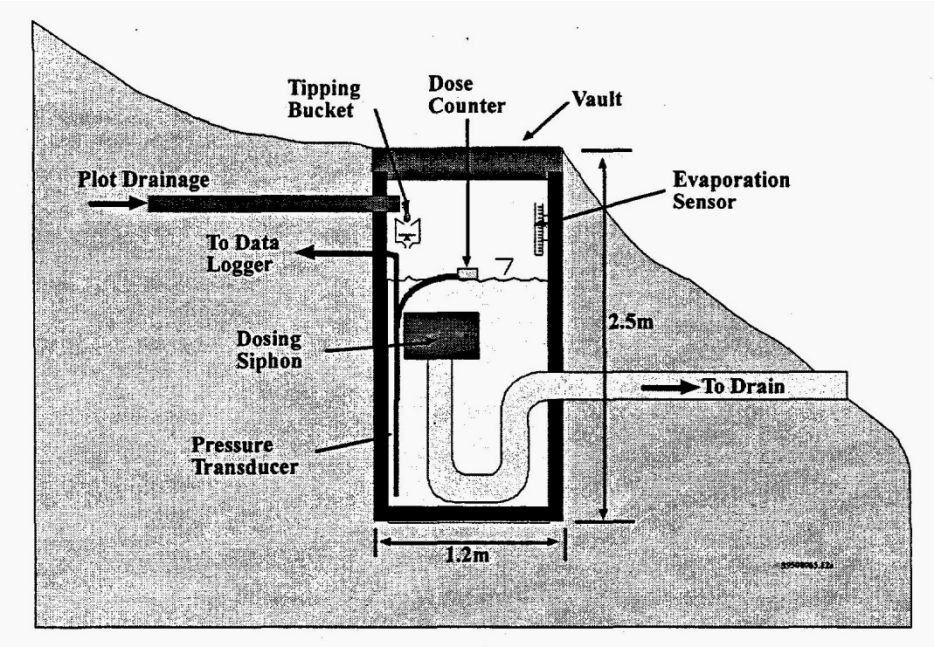

Figure C.6. Schematic of a drainage vault and associated sensors and components (not to scale) (After Figure 2.15 of Gee et al. 1995).

C.1.2.5Deep Percolation through the Asphalt Concrete Layer

Although percolation through the AC was expected to be very small, it was monitored using a pan lysimeter (6.5 m wide, 0.3 m deep) installed under the northeast section of the AC beneath plot 4E on the riprap side slope (Figure C.1)—the section considered most likely to be stressed by infiltration water. This area was irrigated at three times the annual average precipitation from WY95 to WY97 and the drainage through the riprap slope is expected to be high. The pan lysimeter, which is shaped like an inverted pyramid, was filled by 0.1-m-thick drainage gravel and 0.2-m-thick top course gravel with a geotextile in between (DOE-RL 1994). The perimeter of the lysimeter was sealed to the underside of the AC and paired 1.65-mm-diameter stainless steel tubes were used for venting and siphoning water from the bottom of the lysimeter (Myers and Duranceau 1994). The siphon tube was connected to a monitoring system, which consisted of a pump and tipping-bucket rain gauge controlled by a datalogger. This monitoring was discontinued in 2007 because of a system malfunction.

C.1.3 Secondary Monitoring Components

In addition to the water balance monitoring, more instruments were installed to measure water content at the bottom of the silt loam and in the soil below the AC, soil temperature and soil water pressure in the silt loam, and drainage below the AC using a variety of methods as described below.

C.1.3.1Water Content at the Bottom of the Silt Loam and beneath the Asphalt Layer

Water content, θ (m^3m^{-3}) of the soil 0.15 m (DOE-RL 1994) above the bottom of the silt loam storage zone was monitored with eight horizontally oriented NP access tubes to examine how the side boundaries and the CB at the bottom affected water movement. Water content beneath the AC was monitored with six horizontally oriented NP access tubes installed at the depths of 1, 2, and 3 m below the AC. The layout of the access tubes is shown in Figure C.8. To monitor the flow under different treatment, four of the NP access tubes in the silt loam zone (i.e., AA1, AA2, AA5, and AA6) were laid in the north section and the other four (i.e., AA3, AA4, AA7, and AA8) in the south section. All the NP horizontal access tubes below the AC (BA1 through BA6 in Figure C.8) were placed at the north section, where there was a higher chance of percolation through the AC. Water content was monitored at a horizontal interval of 1.0 m using an NP (Hydroprobe Model 503, CPN International, Inc., Martinez, CA) in 76-mm ID aluminum tubes. A sleeve was placed around the NP to keep the NP in the center of the access tubes during each horizontal logging. Water content at the gravel slope was monitored at two locations, i.e., S13 and S14 in Figure C.8, at a vertical interval of 0.15 m using an NP deployed in a vertical (48-mm ID) aluminum access tube extending 1.9 m below the barrier surface. Two separate calibrations were conducted for NP H33115140 in 1995 for the different soil/access tube combination:

Horizontal 76-mm tube in silt loam $$\theta = \exp(b_0 + b_1 N) \quad \text{(C.3)}$$

Horizontal 76-mm tube in sand $$\theta = c_0 + c_1 N \quad \text{(C.4)}$$

where b_0 = -2.9328, $b_1 = 8.869\times10^{-5}$, c_0 = -0.02822, and $c_1 = 1.83\times10^{-5}$. On April 20, 2003, the NP received a new neutron counter and a new sleeve. Hence, after this date, the N values needed to be scaled by a factor 0.988 for horizontal loggings. The NP monitoring was conducted from WY95 to WY13, with some data gaps in WY99, WY05, and WY06.

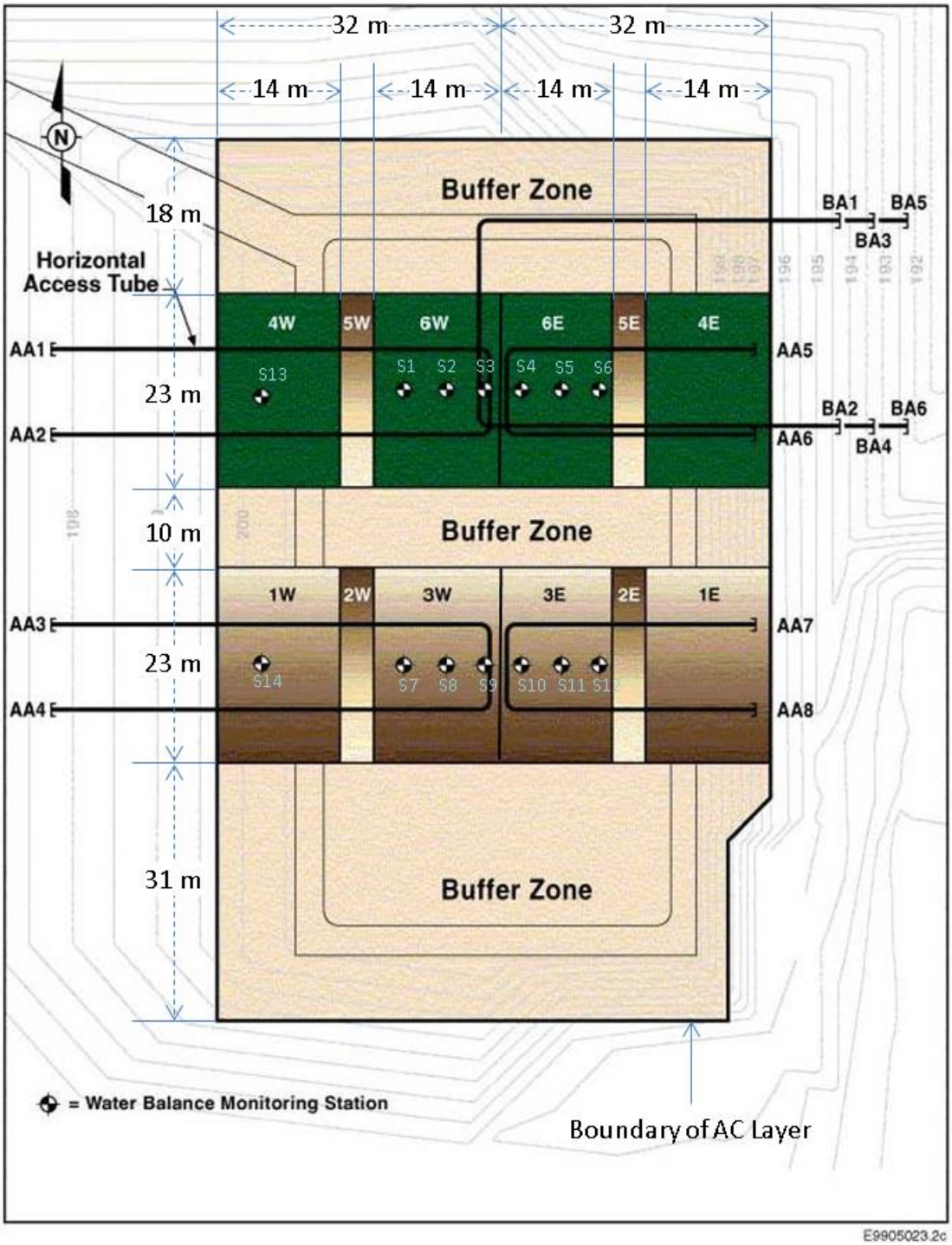

Figure C.7. The horizontal neutron access tubes shown by the U-shaped lines. Tubes AA1 through AA8 are located near the bottom of the silt loam, slightly above the silt-sand interface. Tubes BA1 and BA2 are 1 m below the asphalt concrete, BA3 and BA4 are 2 m below, and BA5 and BA6 are 3 m below.

C.1.3.2Soil Water Pressure and Temperature Using Heat Dissipation Units

Strings of heat dissipation units (HDUs) (Model 229L, Campbell Scientific Inc., Logan, UT) were installed in September 1994 to monitor soil water pressure at depths of 0.075, 0.225, 0.45, 0.80, 1.25, and 1.75 m below ground surface. Before each measurement, the HDU was heated for a fixed period with a needle-type heater inside the HDU. The rate of heat dissipation was controlled by the water content of the porous matrix of the HDU because water conducts heat much faster than air. The temperature increase caused a voltage change in the thermocouple in the HDU, and the voltage was measured. The heat dissipation was determined as the difference between two voltages (ΔV), one measured after 1 sec. of heating and the other measured after a 30-sec. heating time. The relationships between the HDU-measured temperature and output voltage indicated that the variation among the HDUs was very small. Selected HDUs were calibrated in Tempe cells in the laboratory and the general calibration curve (Figure C.7) was used to convert the voltage change to soil water pressure:

$$h = \begin{cases} a\exp(b\Delta V) & if \quad \Delta V \geq 1000 \\ c(1000-\Delta V)^2 + d(1000-\Delta V) - 1 & if \quad \Delta V < 1000 \end{cases} \tag{C.5}$$

where a = -1.514 × 10^{-3}, b = 6.556 × 10^{-3}, c = -1.338 × 10^{-5}, d = 7.331 × 10^{-3}, h is soil water pressure in meters and is negative under unsaturated condition, and ΔV is voltage change in millivolts. It is noted that the upper limit of soil water pressure measured by the HDU generally is considered to be approximately -1 m (CSI 2009; Flint et al. 2002; Reece 1996). However, the HDUs used at the PHB were first generation and seemed to lack clear air entry pressure because of the existence of large pores. The HDUs still responded to soil water pressure when h was higher than -1 m (Figure C.7). Hence, these HDUs were calibrated to near saturation but a different expression was used to describe this part of the curve [Eq. (C.5)]. The HDUs in Flint et al. (2002) also seemed to respond to pressure higher than -1 m. In manufacturing the ceramic for the new generations of HDUs, large pores were removed.[3] Consequently, the newer HDUs generally do not respond to soil water pressure higher than about -1 m. Considering the relatively low sensitivity of HDUs when soil wetness is high, the calculated soil water pressure larger than -0.1 m is not considered in the following analysis.

HDU logging was performed hourly to daily using an automated system. After 2003, most HDUs did not function properly, generally because of malfunctioning peripherals (e.g., power supply, data loggers, or wires).

The HDUs were calibrated before installation to convert the HDU output, V, in millivolts into temperature:

$$T = a + bV \tag{C.6}$$

where a and b are HDU-dependent constants tabulated in Table C.3.

[3] Ritter, J., Campbell Scientific, Inc. Personal communication.

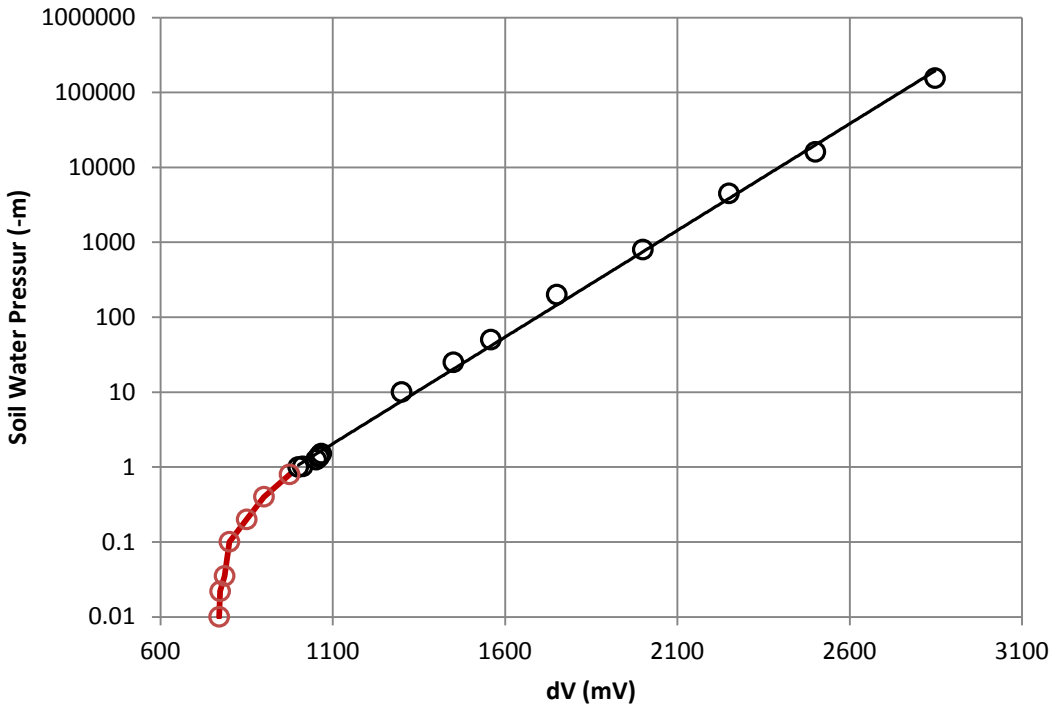

Figure C.8. General calibration curve for heat dissipation units used for soil water pressure monitoring.

Table C.3. Calibration constants for the heat dissipation units.

Station Name[a]	Depth (m)											
	0.075		0.225		0.45		0.80		1.25		1.75	
	a	b	a	b	a	b	a	b	a	b	a	b
S1	0.1868	NA[b]	0.2125	0.9937	0.2034	0.9932	0.2354	0.9929	0.2093	0.9933	0.1943	0.9938
S2	NA	NA	NA	NA	NA	NA	NA	NA	NA	NA	NA	NA
S3	0.1457	0.9940	-0.0381	1.0004	0.0672	0.9954	-0.0136	1.0004	0.1231	0.9935	0.0755	0.9939
S4	0.1260	0.9935	0.1360	0.9935	0.0105	0.9988	0.1392	0.9936	0.0271	0.9983	0.0295	0.9982
S5	0.1386	0.9932	0.1403	0.9932	0.1378	0.9933	0.1438	0.9932	0.1438	0.9932	0.1454	0.9931
S6	0.1548	0.9933	0.1597	0.9933	0.1771	0.9928	0.0463	0.9939	-0.0534	0.9988	0.0878	0.9935
S7	0.1350	0.9931	0.0902	0.9937	0.1011	0.9936	0.1027	0.9936	-0.0136	0.9987	0.1135	0.9935
S8	0.2027	0.9913	0.1875	0.9911	0.1383	0.9930	0.1448	0.9928	0.1350	0.9931	0.1945	0.9916
S9	0.2062	0.9931	0.1468	0.9930	0.1947	0.9935	0.1988	0.9933	0.0487	0.9998	0.0735	0.9990
S10	0.1560	0.9930	0.1759	0.9922	0.1884	0.9919	0.1628	0.9926	0.1495	0.9932	0.1538	0.9929
S11	-0.0619	0.9999	-0.0678	1.0002	0.7631	0.9685	-0.0728	1.0004	-0.0470	0.9997	-0.0545	0.9999
S12	NA	NA	NA	NA	0.2161	0.9925	0.1919	0.9934	0.0445	0.9998	0.2052	0.9928

[a] The stations may also be named as ST501 through ST512 in some past publications or files.
[b] NA: No results available.

The HDU system operation started operation in February 1995 and was halted in August 2007. However, the module for Stations S1, S2, and S3 was reprogrammed and restarted in late August 2007 and is still in operation.

C.1.3.3Soil Water Pressure Using Fiberglass Blocks

Fiberglass blocks (FGBs, MC-314 Soil Moisture Cells, ELE International, Inc., Lake Bluff, IL) were installed to monitor horizontal profiles of soil water pressure at the 1.9-m soil depth and also below the asphalt concrete (Gee et al. 1994). There were 18 FGB sensors in all:

- 6 (FGB1 through FGB6) located at the 1.9-m depth beside a horizontal access tube in the northeast (NE) section of the silt loam
- 6 (FGB7 through FGB12) located at the northeast section under the asphalt concrete
- 6 (FGB13 through FGB18) at the 1.9-m depth in the southeast section of the silt loam

A single calibration was used for all the FGBs to convert the measured electrical resistance, R (k ohm), into soil water pressure, h (m):

$$h = -3.1696R^{1.4317} \tag{C.7}$$

The FGB monitoring was discontinued in FY07 because of a system malfunction.

C.2 Barrier Structural Stability Monitoring

The stability of the PHB as the barrier ages was evaluated by measuring the:

- settlement of the barrier below the AC pad
- elevation change of the barrier surface
- displacement in the riprap side slope
- soil and water erosion from barrier surface.

Figure C.9 is a plan view schematic showing the monitoring stations, settlement and elevation markers, creep gauges (CGs), and erosion flume. The measurement methodology and the results are presented below.

C.2.1 Elevation and Location Monitoring

C.2.1.1Elevation and Location Survey Systems

From the start of monitoring in 1994 through 2003, elevation measurements were made by an electronic distance measurement (EDM) system. From 2004 to 2013, a real-time-kinematic (RTK) global positioning system (Trimble Navigation Ltd., Sunnyvale, CA) was used because of a malfunction in the EDM system.

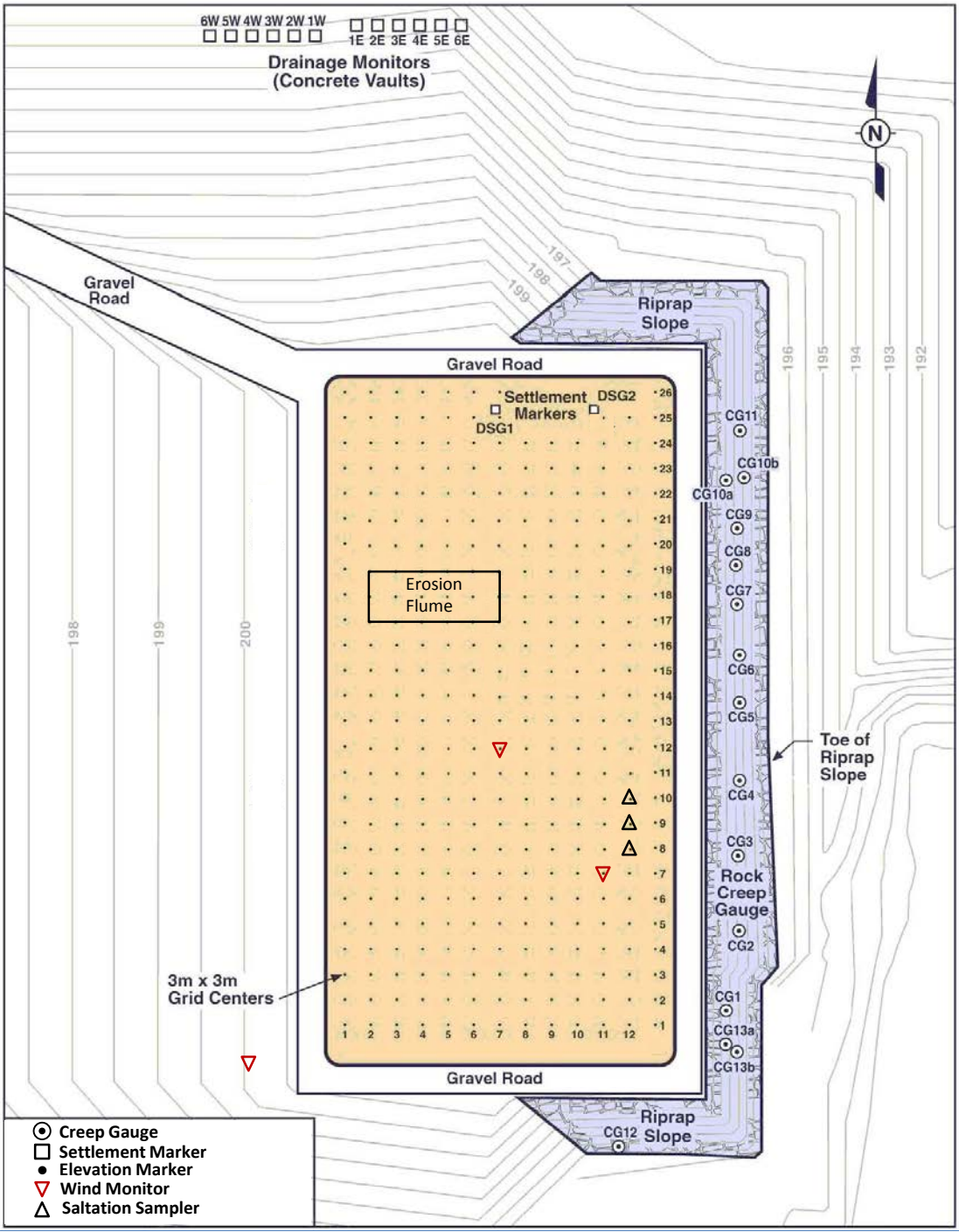

Figure C.9. Plan view schematic showing the 338 elevation stakes, 2 settlement markers, 3 wind monitors, 3 saltation samplers, 15 creep gauges, and the erosion flume.

The GPS surveying equipment consisted of a Trimble RTK 5700 base station with an RTK 5800 rover and a Trimmark 3 base station radio with a 6-ft whip antenna (Figure C.10), all manufactured by Trimble Navigation Limited (Sunnyvale, CA). For the survey, the base station was placed over a known point, benchmark 2E-122 (Hanford well 299-E-122). Using its known position, the base station continually determines the signal travel times from the GPS satellites to the base station and then compares this to the actual travel times. Using this information, the base station then calculates a satellite-specific correction factor, which is then broadcasted to the rover unit using the base-station radio. The rover unit uses the correction factors for dynamic corrections of the rover's GPS measurements. This process allows the accuracy of the GPS system to be improved from meters to less than a centimeter.

From investigations of the optimum measurement times, it was determined that a 10-sec. reading provided the most accuracy with no appreciable accuracy gain after 10 sec. Hence, at each survey point, a 10-sec. reading was taken with the rover unit. All data were stored in the rover unit and later downloaded to a computer.

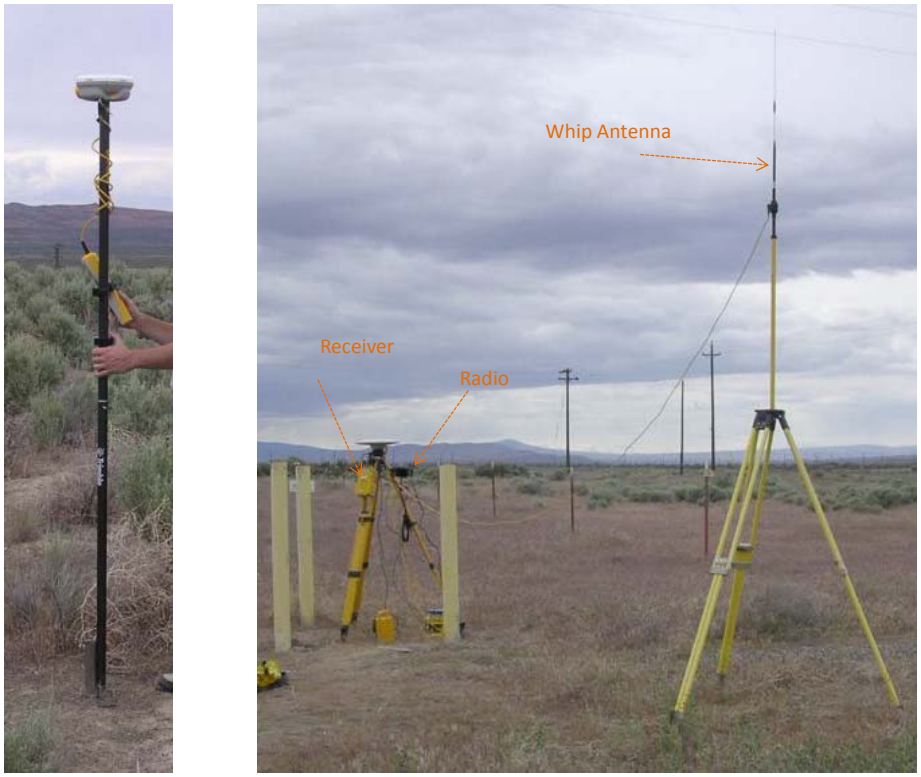

(a) (b)

Figure C.10. Real-time kinematic GPS surveying system. (a) The RTK 5800 Rover unit and (b) the 5700 receiver and Trimmark 3 base station radio with a 6-ft whip antenna.

C.2.1.2Settlement Markers

Movement of the AC surface is an indicator of subgrade settlements and was quantified by measuring the change in the elevation of settlement markers, DSG1 and DSG2 (Figure C.9), attached to the upper surface of the AC. The two settlement markers, 14 m apart, were installed at the north end of the PHB during construction. Each marker consisted of a 4.2-m-long galvanized steel rod (0.025-m diameter) welded to a 0.6-m square plate, which was set on the surface of the AC. The markers were protected by

cast iron monument cases whose tops were set 0.025±0.01 m above the ground surface (Myers and Duranceau 1994). The lower 1.95-m portion of each rod that extended downward from the gravel filter to the plate was encased in a 0.1-m-diameter galvanized steel pipe to prevent binding between the rod and the riprap material. Changes in rod elevations were measured using the EDM or RTK system.

C.2.1.3Barrier Elevation

Elevation changes of the silt loam surface indicate the inflation or deflation of the ETC barrier. To facilitate monitoring of elevation changes, the surface of the ETC barrier was demarcated into 338 3-m by 3-m squares (Figure C.9). This grid was established by setting four corner markers to define a 36-m by 75-m rectangle centered within the perimeter of the compacted gravel roadway. Each interior grid point was marked with a wooden survey stake numbered to identify the grid location. After the controlled fire in 2008, the tops of some of the wooden stakes were charred and hence were replaced by metal stakes. Elevation measurements were taken at the location of each stake using the EDM or RTK system. When combined with barrier settlement measurements, changes to the thickness of the barrier can be assessed.

Before the measurement at each location, to reduce the measurement error because of possible soil compaction, an approximate 2×4×1 inch plastic plate, with a hole in the middle, was placed on the ground in such a way that the stake went through the hole of the plate. The plate was oriented north-to-south and the elevation of the south portion was measured. This method was carried out consistently throughout the monitoring period. In this way, any elevation variation because of the micro-scale relief or vegetation residual near the stakes was averaged out.

C.2.1.4Riprap Side Slope Stability

Because of the steepness of the riprap side slope (2:1), this slope was considered to have the greatest potential for movement. A total of 15 CGs were installed at 13 locations (Figure C.9) in the riprap slope during or after barrier construction to monitor slope displacement. Each CG consisted of a 3-m-long steel rebar encased in a mortar-filled, 0.3-m-long by 0.076-m-diameter PVC tube (Figure C.11). The 0.013-m-diameter head of a large nail embedded in the mortar was used as the benchmark for monitoring CG movement. A CG was installed at the mid-slope on the riprap slope at 11 of the 13 locations. Two CGs were installed at the upper (CG10a and CG13a) and lower (CG10b and CG13b) at positions 10 and 13, respectively.

In total, 18 surveys were conducted at the elevation stakes, 19 at settlement markers, and 19 at the CGs. The survey in May 2004 was the first to use the RTK system at the PHB. The apparent departure from the relatively small changes in the previous years was considered invalid (Ward et al. 2005). A partial EDM elevation survey was also conducted in 2004 and was used to correct the RTK survey in 2004.

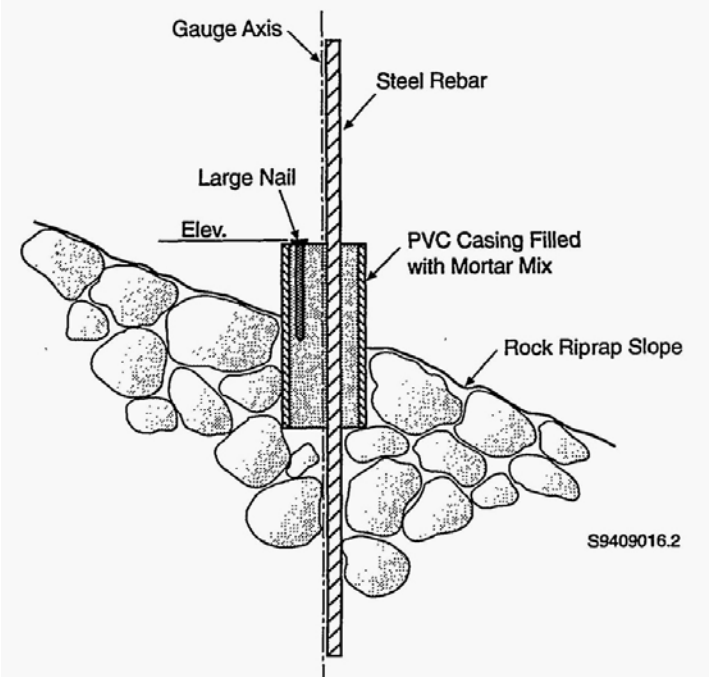

Figure C.11. Schematic of a creep gauge (After Figure 3.2 of Gee et al. 1994).

C.2.2 Wind and Water Erosion

The loss of soil by erosion from the silt loam surface can reduce the thickness of the ETC cover and compromise its ability to control infiltration by reducing the designed water storage capacity. The primary agents of soil loss in arid environments are water and wind erosion. Understanding the effect of erosion on barriers requires knowledge of how it is affected by different kinds of rain and wind and how erosional processes vary for different soil surface conditions.

To reduce soil erosion of the silt loam, the PHB uses both a pea-gravel admix and vegetation to reduce water and wind erosion. The gravel admix was blended with the silt loam during construction and vegetation was planted after construction. The top 1 m of silt loam was amended by adding about 15 wt% (dry weight) pea gravel. The gravel was added to act as an agent against eolian stresses during periods following construction, wildfires, droughts, or other periods of susceptibility. The decision to use 15 wt% pea gravel was based in part on the results of wind tunnel tests (Ligotke 1993; Ligotke and Klopfer 1990), and was also a compromise with the needs of water storage in the silt loam zone.

The preparation and placement of the l-m-thick pea gravel admixture did not pose unusual construction difficulties. A pug-mill operation was set up at the construction site to mix clean pea gravel with silt loam from the same source used to construct the lower soil layer. The material was dumped on the surface and then shaped using a tracked Caterpillar. The final surface was ripped to provide a surface density within specifications. The concentration of pea gravel near the surface appeared to be fairly uniform.

The same system used to monitor runoff (as described in Section C.1.2.2) was used to monitor water erosion of soil. To estimate water erosion, the collected sediment in the runoff was measured. The following methods were used to monitor wind erosion.

- *Gravel Concentration.* The condition of the surface under both deflationary and inflationary influences was monitored to evaluate performance of the admixture. Testing and monitoring activities were initiated in August 28, 1994, and included the collection of 24 evenly spaced samples of the admixture (Gee et al. 1994). The samples were obtained immediately after construction and before redistribution by erosion had occurred. The samples were scooped from the surface to a maximum depth of about 8 cm and contained bulk masses between 1.5 and 2.0 kg. Pea gravel concentration was determined after sieving (0.33-cm sieve) as the mass of pea gravel per the combined mass of dried soil and pea gravel. 6 of the 24 samples were analyzed for gravel concentration in 1994. In 1996 and 1997, soil samples were obtained by coring the soil column from 0 to 2 cm (surface samples) and from 2 to 10 cm (bulk samples).

- *Wind Stress Monitoring at Three Wind Stations.* Wind stress monitoring was initiated in FY94 to provide information on the stresses imparted by wind on the surface of the ETC barrier (Gee et al. 1994). This was accomplished by installing three wind boundary layer stations. Two of the wind stations were located at the ETC barrier (Figure C.9) and were installed in late August 1994. The third station was located at the gravel side slope the southwest of the ETC barrier (Figure C.9). Wind speed sensors were installed at each station at elevations of 0.25, 0.50, 1.0, and 2.0 m above ground surface. Wind direction sensors were installed at each station. The direction sensors were aligned to read 0° when directed true north (18° declination). A solar radiometer was installed at the ETC barrier. The monitoring was carried out from FY94 through FY97.

- *Sand Drift Monitoring at Three Saltation Stations.* The movement of wind-driven sand over the surface of the barrier is expected to be the mechanism by which loss of surface soil occurs. Monitoring of saltation and sand drift was initiated in FY94 by installing three multisensory saltation stations near the eastern side of the southeast quadrant of the ETC barrier. Two of the saltation stations consisted of co-located dust traps and piezoelectric saltation sensors, each set 2 m above ground surface. The third station included multiple co-located sensors at 0.25, 0.50, and 1.0 m elevations and dust traps at 0.125, 0.25, 0.50, and 1.0 m above ground surface. The third station was included to provide information on the vertical distribution of wind-driven sand and soil particles, which was used in evaluating total soil and sand mass flow rates over the ETC barrier surface. The dust trap sensors were Model H7 (Sensit Company, Portland, ND) (Gee et al. 1995). Data acquisition was initiated only during windstorms based on feedback from a wind speed sensor with a threshold of 7.5 m s^{-1}. Dust traps were sampled manually after significant windstorm events. The dust traps were removed in December 1995 because of a lack of a saltation source caused by the rapid growth vegetation and the high moisture content of the silt loam at the ETC barrier.

C.3 Ecology Monitoring

The ecology monitoring included the characteristics of vegetation and animal activities.

C.3.1 Vegetation Characteristics

Vegetation characteristics were monitored in the enhanced precipitation test. The floristics composition, plant cover and spatial distribution, plant height, and canopy characteristics were monitored from 1995 to 2012 generally annually except in FY99, FY05, and FY06. The gas exchange rate, roots, shrub survivorship, reproduction, and xylem pressure potential were measured from FY95 to FY97. Specific dates for these observations are given in the corresponding sections below.

C.3.1.1Survivorship and Reproduction

A census of live and dead shrubs was conducted in all 300 (12 easting and 25 northing) 3 m by 3 m quadrants. These observations were made between April 7 and April 13, 1995. Additional observations were made in1996 and 1997.

In 1997, data were collected to test the hypothesis that irrigation reduces the percentage of sagebrush (*A. Tridentata*) shrubs with mature seed heads, compared to the non-irrigated treatment. For the north irrigated section, sampling was done by selecting the 3rd row and 6th through 15th rows starting from the north border. For the non-irrigated section in the south, sampling was done by selecting the 3rd and 6th through the 15th rows from the south border. In each row, the number of individual shrubs with mature floral heads present and absent was recorded. The percentage of shrubs with mature seed heads (P) was calculated as:

$$P = 100N / T \qquad \text{(C.8)}$$

where N is the number of shrubs in each row with mature seed heads and T is the total number of shrubs in the row. Each row is considered an experimental unit where P is the observation. Five replicate experimental units were observed in each treatment.

C.3.1.2Species Composition, Plant Cover, and Spatial Distribution

Species composition, plant cover, and spatial distribution estimates of grasses, shrubs, herbaceous forbs, litter, and bare soil were made on 300 9-m^2 quadrants patterned after Daubenmire (1959) and DOE-RL (1999). Cover was estimated by visual inspection of each quadrant. The work of Hitchcock and Cronquist (1973) was consulted to assist in plant species identification. Cover was assigned values for percentage ranges as 0%, 0%-5%, 5%-25%, 25%-50%, 50%-75%, 75%-95%, and 95%-100%, and percent cover was assigned the value of the mid-point of each cover range after Rebele and Lehmann (2002).

The resulting data are essentially nonparametric, and statistical analysis is based on the techniques of Seigal (1956). Measures of central tendency for these data are given as the median and the mode. The median is the cover class value where half the values are greater; the mode is the cover class with the greatest frequency. Arithmetic means and parametric statistics are invalid for ordinal data because the distance between classes is not equal (Seigal 1956). Note the distance between the midpoints of classes 1 and 2 is 12.5%, and the difference between the midpoints of classes 2 and 3 is 22.5%. Differences between treatments and years for cover data in this study were assessed using the Mann-Whitney test (Seigal 1956). This test ranks values upon which parametric statistics are valid. The Z values given indicate the direction of change, with the larger values indicating the greatest change. Negative values

indicate decreases. For ease of interpretation, mapping data were converted to the midpoint of the percentage cover ranges.

To use proportion (%Live) data as a dependent variable in a regression, it is necessary to transform the data to confine the projected value within 0-1 and to make the data distribution closer to normal. Prior to statistical analysis, percent survival data were transformed (normalized) using the arcsine transform with radian units (Steele and Torrie 1960) as follows:

$$\arcsin\sqrt{\frac{\%Live}{100}} \qquad \text{C.9}$$

Density data were also normalized by using the square root transformation (Steele and Torrie 1960). Means are presented using untransformed data with error bars based on untransformed data for interpretation. Multiple range comparisons were done using the Tukey-Kramer honestly significant difference (HSD) test. Error terms are 1 standard error of the mean (1 SEM). Significance was tested at the $\alpha = 0.05$ level. Analyses were done using JMP version 5.0 software (SAS Institute 2002).

C.3.1.3Plant Canopy Dimensions, Leaf Area, and Leaf Area Index

Plant height of *A. tridentata* and *Ericameria nauseosa* (gray rabbitbrush) was measured with a meter stick in the irrigated and non-irrigated portions of the barrier in 1995, 1996, and 1997. Observations were made on the height of *Salsola kali* (Russian thistle) and *Elymus lanceolatus* (thickspike wheatgrass) in each treatment. Observations were made of at least 9 individual plants of *S. kali, A. tridentata,* and *E. nauseosa* in each of the treatments on July 26, 1995, on *E. lanceolatus* in each treatment on May 23, 1996, and again on *S. kali, A. tridentata, and E. lanceolatus* in each treatment on August 1, 1996. Height of *A. tridentata* and *E. nauseosa* was measured in each treatment in 2003, 2004, and between June 14 and August 18, 2007. In 2008, plant height was measured on all sagebrush plants in 84 of the 9-m^2 quadrants in the unburned portion of the surface.

Differences between treatments for height data in 1995, 1996, and 1997 were assessed by comparing regression relationships in time using a linear test approach (Neter and Wasserman 1974). Observations were made on April 15, May 15, and June 15 in 1997 to describe canopy characteristics, leaf area, and leaf area index dynamics. Canopy characteristics were measured to estimate leaf area, as described in Link et al. (1990). Canopy characteristics of the same individual shrubs were measured on the three dates. Shrubs were randomly chosen (20 from the non-irrigated treatment and 20 from the irrigated treatment), then labeled with metal tags numbered 1 through 40.

The leaf area of *A. tridentata* was measured by double sampling, using a model relating leaf area to canopy measures. This model was developed by measuring the height, the greatest projected canopy diameter, and the diameter perpendicular to the greatest diameter, then relating these measures to harvested leaf area. These measurements were taken on five shrubs in April and seven shrubs in May and June in both treatment areas. Plants were chosen to represent all possible shrub sizes found in both treatments. The shrubs were measured and then harvested to determine leaf area.

Harvested shrubs were placed in plastic bags and taken to a laboratory for measurement of mass and leaf area. Because the shrubs were large, each one was broken into pieces of similar size for sampling. The

entire shrub was weighed and about 10% taken to measure leaf area. The mass of the sample piece was recorded. Leaves were then stripped from stems and single-sided green leaf area was determined with a Li-Cor® 3100 Leaf Area Meter (Li-Cor, Inc., Lincoln, NE). The leaf area (LA_t) of the entire shrub was determined as:

$$LA_t = LA_s \frac{M_t}{M_s} \quad \text{(C.10)}$$

where LA_s is the leaf area of a sample, M_t the mass of a shrub, and M_s the mass of a leaf sample.

C.3.1.4Seed Bank Assessment

Seedling emergence tests (Roberts 1981) were used to quantify the impact of fire on the seed content of the barrier soils and for comparison with the McGee Ranch sites. Soil samples were collected from the various sites just before the fire (September 17 and 18, 2008) and just after the fire (September 30, 2008). Samples were physically paired on the surface for the before and after comparison. Samples were collected along the west, north, and east edges and randomly chosen under the canopy and between canopy pairs throughout the center of the burned area. Samples were collected at the old-burn McGee Ranch site, which is about 10 miles west of the PHB, between December 9 and 11, 2008, and at the undisturbed mature plant community at the McGee Ranch site on November 18 and December 1, 2008. The old-burn McGee Ranch site burned in 1996 (Easterly and Salstrom 2003). The depth of the sample (about 3 cm) captured the majority of seeds in these soils (Boudell et al. 2002). Samples were placed in paper bags and stored dry at room temperature until placed in a greenhouse in flats.

Soil samples were spread in trays in the climate-controlled Native Plant Greenhouse at Washington State University Tri-Cities. The greenhouse conditions were ambient light, temperatures above 20°C, and daily watering. Generally, the samples were spread in a layer 1 cm thick on top of potting soil in a flat (0.142 m^2). Samples were placed in the greenhouse in flats between February 23 and March 5, 2009, for the barrier samples. McGee Ranch samples were placed in the greenhouse in flats between August 6 and 11, 2009. Observations were made for approximately 1 year for each set.

Germinated seedlings were identified and counted. The seed banks of the barrier before (n = 36) and after the fire (n = 36), the old burn community at McGee Ranch (n = 36), and the unburned mature community at McGee Ranch (n = 36), were compared.

C.3.1.5Transpiration and Photosynthesis

Plant gas exchange data were collected in 1995 and 1996. Transpiration and net photosynthetic data are presented in this section. Such data are a useful indicator of the ability of shrubs to remove water from the surface. Comparisons are made for the effect of the irrigation treatment on gas exchange rates for *A. tridentata.* Previous gas exchange data collected for *E. nauseosa* indicate similar rates as for *A. tridentata* (Gee et al. 1996). Because of the similarity and the decreasing importance of *E. nauseosa* on the surface, only data for *A. tridentata* are presented in this report. These data are graphically presented with earlier data, as in (Gee et al. 1996), to interpret long-term trends in plant gas exchange.

Gas exchange data were gathered with a Li-Cor 6200 gas exchange system. Such data are collected by placing a chamber over plant stem tips and allowing water vapor and CO_2 to change over a few minutes. In 1997, a 10-cm length of stem was placed in the chamber for plants in the non-irrigated area and a shorter piece (less than 5 cm long) was used in the irrigated area. The varying amounts of exposed leaf area were used to maintain similar vapor pressures for the two treatment samples in the chamber. After observations were made, the stem was cut and a single-sided leaf area was measured using a Li-Cor 3100 Leaf Area Meter. All gas exchange observations were made at midday and in full sun.

C.3.1.6Root Density and Distribution

To monitor root intrusion, density, and distribution with depth, 12 clear tubes (mini-rhizotrons) were installed in the silt-loam, extending to a depth of 1.9 m at a 45° angle. Six tubes were placed in the irrigated north section and six in the non-irrigated south section. The mini-rhizotrons were installed near the neutron access tubes so that the correlation between root characteristics and soil water dynamics could be investigated. Root characteristics were observed with a down-well video camera (Circon Agricultural Camera) inserted into the clear tubes. Videos from each root tube were examined to determine root demographics and the number of roots in contact with the rhizotron. Although the root number indicates the mechanical state of the soil, root length density provides more information on how efficiently the root systems remove water from the silt loam. Root length density is normally calculated by dividing the total root length in contact with the glass tube, determined from root number, by the area of the observation window (1.55 cm wide and 10 cm long) (Buckland et al. 1993).

Observations were made from July 13 to July 21 in 1995, in June 1996, and on September 18, 1997. In WY97, only three tubes were examined in each treatment. In 1995 and 1996, all roots observed were considered to be alive. In 1997, live and dead roots were counted separately. Live roots are white to brown and turgid, with some roots having root hairs. Dead roots are dark in color and contracted within root channels in the soil. Differentiating live from dead roots is subjective. Root counts were taken in an area the width of the viewing area (1.55 cm) and 10 cm long. Count data were then divided by the observation area to yield a root length density value.

C.3.1.7Xylem Pressure Potential

Predawn xylem pressure potential data were gathered on August 1,1996, with a pressure chamber (Soil Water Equipment Co.), after Scholander et al. (1965). Data were gathered on *A. tridentata* and *E. nauseosa* in both irrigated and ambient precipitation treatments. Xylem pressure potential data were obtained by placing cut stems (about 10 cm long) in the pressure chamber and slowly pressurizing with nitrogen gas until the tip of the stem showed evidence of a color change due to expressed water. A wet paper towel was placed in the chamber to maintain a humid atmosphere around the stem and leaf material during pressurization. Treatment effects on xylem pressure potential were compared using Student's t-test (Steele and Torrie 1960) within species.

Measurements of water potential of plant leaves, or more exactly, the plant xylem pressure potential, are useful for comparing plant activity and soil water status. Xylem pressure potential was measured on plants with a Model 1005 Pressure Chamber Instrument (PMS Instrument Company, Albany, OR) in the burned and unburned areas of the barrier. In 2009, measurements were made just before dawn to assess maximal xylem pressure potential. Measurements were taken on *A. tridentata*, *S. kali*, and *M. officinalis*

in the west, central, and east sides of the surface. In addition, measurements were taken on *A. tridentata* in the unburned area in late afternoon to determine the lowest possible values. Data were collected on September 5. In 2010, measurements were taken on *A. tridentata* and *M. canescens* in the west, central, and east sides of the surface. Data were collected on August 27.

C.3.2 Animal Activity

Animal activity was observed during 8 years of the monitoring period (i.e., 1995-1997 and 2007-2011) using methods such as surface inspection (e.g., the presence of droppings, tracks, nests, burrows, holes, and gall formation), measurement of the counts and dimension of animal burrows, and direct observation using traps.

Animal evidence on the surface was casually noted in 1995 and measured in 1996. In 1996 and 1997, evidence of animal presence (feces, burrows) was noted by inspecting the surface in all 300 quadrants. Observations in 1996 were made between May 24 and June 7. In 1997, observations were made on April 25; the depths of selected holes were measured on September 12. Hole sizes were not classed into small and large holes for measurements before 2007.

On August 18, 2007, the barrier surface was examined for evidence of use and intrusion (burrowing) by insects and small mammals. This was done by carefully inspecting 20 of 300 sample squares on the surface. Indications of animal use included direct observation and presence of droppings, tracks, nests, burrows, or holes. The greatest width, the width at 90° to the greatest width, and the depths of 11 holes and burrows were measured. Hole depth and volume were analyzed. The side slopes were examined for evidence of animal activity.

In 2008, pre-burn surveys were conducted across the entire surface to document evidence of use and intrusion (burrowing) by insects and small mammals. Small mammal traps were used to positively identify vertebrates on the surface. Evidence of animal use included direct observation (traps) as well as the presence of droppings, tracks, nests, burrows, holes, and resting spots. A small mammal trapping event and reconnaissance of indirect evidence of animal activity was performed in September 2008, just before the controlled burn of the north section of the surface barrier area on September 28.

After the burn, two small mammal arrays, containing nine traps each, of Sherman live traps were placed on the surface; one array was located in the burned section, and the other in the unburned section. Each array consisted of three trap lines, each with three traps spaced 10 m apart (30 m by 30 m area). The traps were placed in the field on September 15, 2008, and left for 1 day before baiting and opening to allow small mammals to acclimate to the new objects. Both small mammal arrays were opened the evening of September 16, 2008, and then checked and re-baited with a mixture of peanut butter and oatmeal each morning until the survey was completed. Species, age, and sex were determined for all small mammals captured, and each animal was marked to identify the occurrence of re-captured specimens. The relative abundance of small mammals was estimated for two areas by dividing the total number of traps and number of nights by the total number of new captures and then multiplying that value by 100. Evidence of animal activity such as scat, tracks, and burrows was noted in each area while field crews were mobilizing/demobilizing and performing daily trap checks.

On September 13, 2009, the barrier surface was examined for evidence of use and intrusion (burrowing) by insects and small mammals. This was done by carefully inspecting 288 of 300 sample squares on the surface. The row between the burned and unburned portions of the surface was not assessed. Indications of animal use included direct observation and the presence of droppings, tracks, nests, burrows, or holes, and gall formation on *A. tridentata*. Hole size was classed as large (greater than ~2 cm in diameter) or small. Holes in each class were counted in each plot. The degree of gall formation and amount of feces were classed into high and low groups. A high degree of gall formation was noted when any shrub had numerous (more than ~50) galls. A large amount of rabbit feces was noted when feces were concentrated in patches, while a plot with few feces that were widely distributed was classed as low. The Van der Waerden non-parametric test (van Der Waerden 1952) was used when data were not normally distributed to compare responses in the burned and unburned sections. The relationship between rabbit (*Sylvilagus nuttallii*) feces and cover of *Elymus wawawaiensis* was determined by relating the percentage of plots in each of 25 rows that had feces with mean percent cover of *E. wawawaiensis* in each row. Each of the 25 rows had 12 plots. The relationship was determined using linear regression.

Between June 3 and July 13, 2010, and in early August 2011, the barrier surface was examined for evidence of use and intrusion (burrowing) by insects and small mammals. This was done by inspecting 300 sample squares on the surface. In 2010, all holes were recognized, whether new or old and regardless of whether they were covered in litter. In 2011, as in earlier years, only well-formed, new holes were counted and no effort was made to count holes under litter. Holes that were counted were about 1 cm diameter or larger. Animal activity on the side slopes was noted by inspection. Indications of animal use included direct observation and presence of droppings, tracks, nests, burrows, or holes, and gall formation on *A. tridentata*. The greatest width, the width at 90° to the greatest width, and the depths of burrows were measured.

C.3.3 Fire and Air Temperature

A controlled burn was conducted on the north section of the barrier, including the silt loam cover and the gravel side slope, on September 26, 2008, to understand the response of the engineered ecosystems to wildfire. Responses to the fire potentially vary according to the intensity of the fire, and the site was configured and instrumented to permit monitoring. Details of the methods can be found in Ward et al. (2009a), Ward et al. (2009b), and Ward et al. (2010). A brief summary is given below.

C.3.3.1Flame Height and Air Temperature

The simulated fire was limited to the north section of the barrier. Nine flame-height poles equipped with thermocouples (Figure C.12a) were installed at the center of each plot for visual observation of flame height and to quantify fire intensity. Flame height was used to estimate radiation intensity of flames, which was related to the rate of spread of a fire. The flame-height poles were constructed of galvanized pipe with alternating colors to allow easy determination of scorch height. The poles were painted in 10-cm sections from 57 cm to a height of 297 cm above ground.

During the fire, the flame height was determined using decimeter-scale flame height rods (black and white metal rods) installed outside at the edge of plots. This was accomplished by peering through the flames to the flame height rods and recording the elevation of the flame.

At each plot, seven Type-K thermocouples (ThermoWorks, Lindon, UT) were installed at 1.5 cm deep, at the ground surface (0 cm), and at heights of 1, 10, 30, 100, and 200 cm (Figure C.12b and c), respectively. Each of the 63 thermocouples was attached to a HOBO datalogger (Onset, Bourne, MA) to record temperatures once per second starting 3 hours before the fire until about 9 hours after the fire. The resulting data were used to map the relative intensity of the fire across the burned surface.

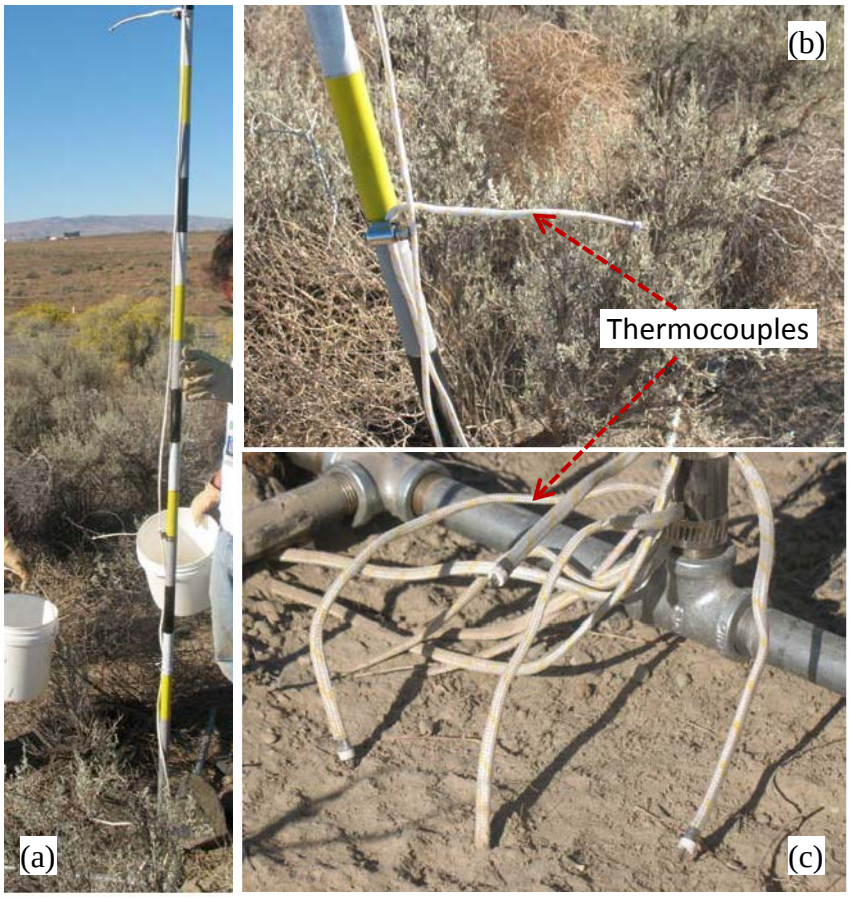

Figure C.12. Temperature monitoring system of the controlled fire. (a) A fire pole was used to measure flame characteristics and to secure thermocouples; (b) thermocouples were installed 1.5 cm deep, at the ground surface (0 cm), and at heights of 1, 10, and 30 cm; and (c) thermocouples were installed at heights of 100 and 200 cm.

C.3.3.2Soil Properties

Soil properties were measured before the fire and at one week, 6 months, and 1 year after the fire. The field-saturated hydraulic conductivity was measured using a Guelph Permeameter (Reynolds and Elrick 1985) and the unsaturated hydraulic conductivity was measured using a Guelph Tension Infiltrometer (Reynolds 1993) at each of the nine 12 m × 12 m plots. Within each plot, measurements were taken, one on each 3 m × 3 m quadrant. Soil samples were collected for the particle size distribution analysis from 0 to 2 and 2 to 10 cm depths on a 3 m × 3 m grid.

Soil water repellency was measured in situ on pre-burn and post-burn soil samples using the water-drop penetration time (WDPT) test (Dekker and Ritsema 1994). After the initial measurement before the fire, three measurements were made after the fire with the last measurement at about 1 year. The soil (< 2 mm thickness) was placed on a Petri dish. Three drops of de-ionized water, each containing 36 μL, were randomly placed on the air-dry sample and the penetration time was measured. The median value of the infiltration time of the three drops was considered as the drop penetration time at the analyzed depth. The soil was considered hydrophobic if the WDPT was greater than 5 seconds (Debano 1981).

Soil macro-nutrients (i.e., N, P, and K) and selected micro-nutrients (i.e., Ca, Mg, and Na) were measured before and 1 week and 1 year after the fire by Northwest Agricultural Consultants (Kennewick, WA) using standard methods (Gavlak et al. 2003). Additionally, soil pH, electric conductivity, organic matter, cation exchange capacity, and specific surface area were measured. Soil mineralogy was analyzed using the X-ray diffraction method for selected samples.

C.3.3.3Barrier Inflation and Deflation

Soil inflation and deflation are likely to occur after a fire with the loss of plant cover. The pattern of inflation and deflation was mapped using 66 stainless steel erosion pins on the burned section of the barrier. Measurements were taken before and nearly 1 year after the fire. These data were used to reveal the ability of the surface to resist erosive stresses after fire and provide insight into changes in surface composition relative to the bulk composition of the top 1 m of admix. The height above the soil surface at the 66 erosion pins was measured with a meter stick. The 66 erosion pins were distributed around the edges and throughout the central region of the burned section of the ETC barrier (Figure C.13). A metal washer was placed on the west side of each pin and used as a measuring base. The measuring technique was used before the fire on September 22, 2008, and repeated on August 13, 2009 and August 21, 2010. Measurements were taken by viewing the interception of the top of the metal erosion pin with the millimeter-ruled meter stick. This was done in the same manner before and after the fire to minimize bias and parallax.

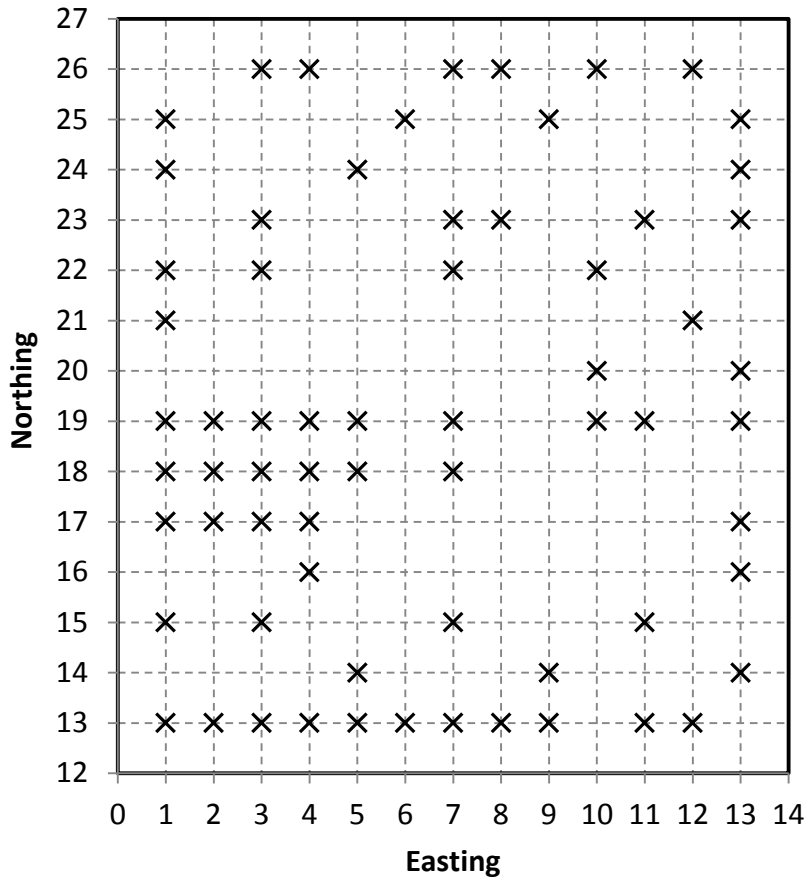

Figure C.13.Locations of the Erosion Pins. The distance between coordinate values is 3 meters.

C.3.3.4Post-Burn Soil Respiration

Soil respiration after fire generally decreases with reductions in biological activity and organic carbon. Biological activity was assessed nearly 1 year after the fire by comparing activity on the unburned and burned sections of the ETC barrier. Respiration rates were compared under very dry surface soil conditions and after a rain that wetted the top 33 mm of the soil profile. Measurements of soil CO_2 were made in situ with a Vaisala CARBOCAP® Model GMP343 hand-held carbon dioxide probe (Vaisala Inc., Boulder, CO) and a Model G70 CARBOCAP hand-held carbon dioxide meter. Measurements were taken in a static diffusion chamber made of glass. Before each measurement, the edges were sealed with a small berm of dry soil placed along the bottom edge. The chamber then was covered with a black cloth that allowed essentially no photosythetically active radiation to enter the chamber. This was measured with an AccuPAR LP-80 Ceptometer (Decagon Devices, Pullman, WA). Measurements were taken for 15 minutes. Steady-state respiration rates were achieved within a few minutes before data were recorded. Six replicates were taken for each condition. The depth to the bottom of the wetting front was measured with a meter stick for wetted soil tests.

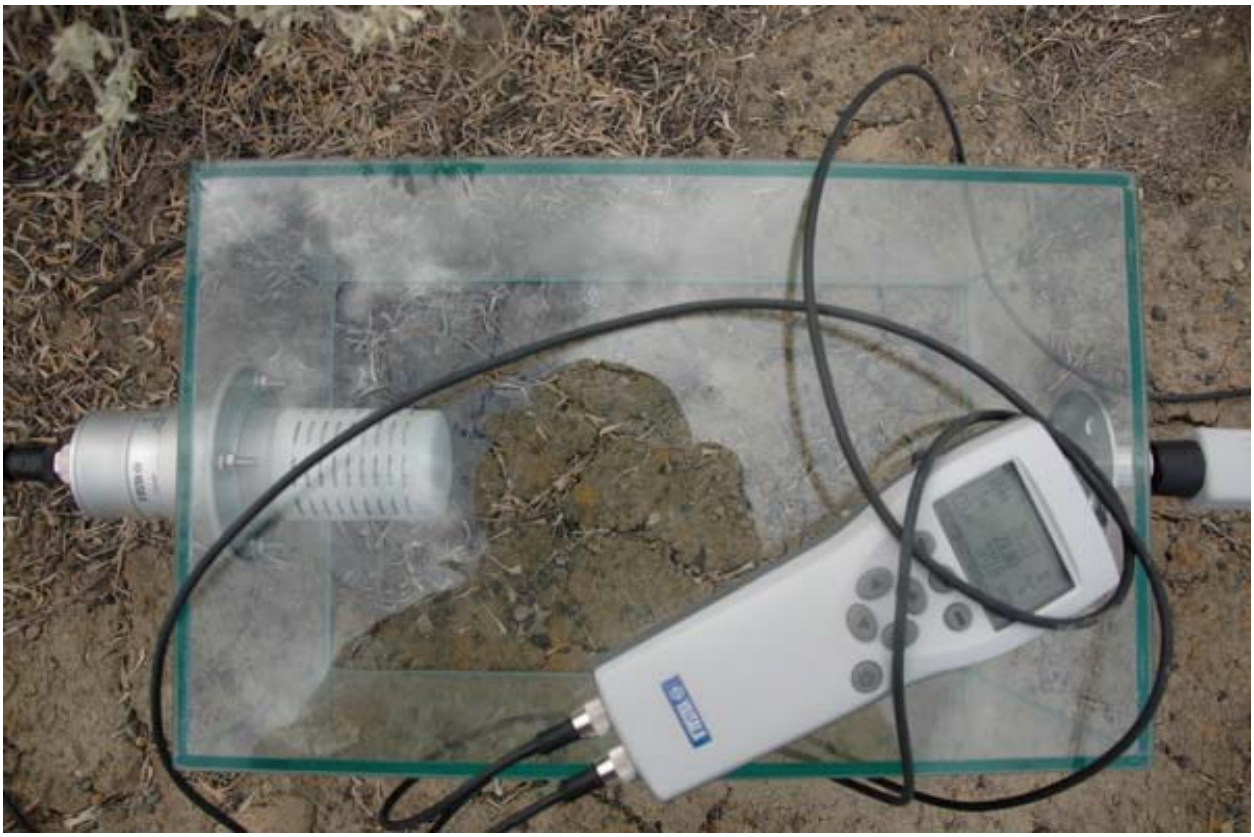

Figure C.14. Static diffusion chamber with sensors and readout device.

C.4 Data Acquisition System

The data for neutron logging, barrier structure stability monitoring, and ecology monitoring were collected manually. The data from the automated system were collected with data loggers powered by 12-V batteries, which were charged by solar panels. The data collected by each datalogger are described in Table C.4. Additionally, the battery voltage and datalogger temperature were recorded.

The wires at ground surface between the sensors and dataloggers were kept in conduits. The dataloggers and batteries were kept in enclosures above ground surface to protect them from being damaged by the weather (Figure C.15).

Additionally, a 12-V DC powered diaphragm pump was used to extract the drainage collected in the pan lysimeter. Extracted drainage water was discharged through a RainWise (RainWise, Inc., Trenton, ME) tipping-bucket style rain gauge and recorded on a Campbell Scientific CR-10 datalogger. The datalogger was located within about 30 m of the pump and tipping bucket in order to minimize signal degradation.

The instrument boxes were intentionally not mounted flush with the ground surface to prevent water or snowmelt from running into the boxes. Consequently, most of the cables were exposed near the entry point to the boxes.

Figure C.15. The conduits for wires and enclosure for the dataloggers and barreries.

Table C.4. Dataloggers and data collected.

Datalogger Number	Data or Sensors
201	From 1994 to 2000: Data from 98 TDR segments at the 14 monitoring stations (S1 through S14; 7 TDR segments at each station). From 2001 to 2007: Data from 104 TDR segments at 8 monitoring stations (S1, S3, S4, S6, S7, S9, S10, and S12; 13 segments at each station).
202	Temperature data from the thermal couples; drainage data from the tipping buckets, dosing siphon counters, and pressure transducers for the 12 drainage vaults.
203	Soil water pressure data from 72 HDUs at the 12 monitoring stations (6 HDUs at each station), precipitation from 14 mini-lysimeters at the 14 stations. There were four remotely located data-acquisition modules (#1 through #4) connected to the main logger. Each of the modules was powered by a battery that was charged by a solar battery and collected data from three stations: Module #1: data from S10, S11, and S12; Module #2: data from S7, S8, and S9; Module #3: data from S4, S5, and S6; Module #4: data from S1, S2, and S3
204	Drainage data from the pan lysimeter and soil water pressure data from 18 fiberglass blocks.
205	Data from the run-off flume. The data include temperature from six thermocouples, soil water pressure from four fiberglass blocks, and precipitation from a rain gauge.

References

Boudell, JA, SO Link, and JR Johansen. 2002. "Effect of Soil Microtopography on Seed Bank Distribution in the Shrub-Steppe," *Western North American Naturalist*, 62:14-24.

Buckland, ST, CD Campbell, LA Mackie-Dawson, GW Horgan, and EI Duff. 1993. "A Method for Counting Roots Observed in Minirhizotrons and Their Theoretical Conversion to Root Length Density," *Plant and Soil*, 153:1-9.

CSI. 2009. *229 Heat Dissipation Matric Water Potential Sensor*, Campbell Scientisic, Inc., Logan, Utah.

Daubenmire, R. 1959. "A Canopy-Coverage Method of Vegetational Analysis," *Northwest Science*, 33:43-64.

Debano, LF. 1981. *Water Repellent Soils: A State of the Art*, General Technical Report PSW-46, Pacific Southwest Forest and Range Exp. Sta., U.S. Department of Agriculture Forest Service, Berkeley, California.

Dekker, LW and CJ Ritsema. 1994. "How Water Moves in a Water-Repellent Sandy Soil: I. Potential and Actual Water Repellency," *Water Resources Research*, 30:2507-2517.

DOE-RL. 1994. *Constructability Report for the 200-BP-1 Prototype Surface Barrier*, DOE/RL- 94-76, U.S. Department of Energy Richland Operations Office, Richland, Washington.

DOE-RL. 1999. *200-BP-1 Prototype Barrier Treatability Test Report*, DOE/RL-99-11 Rev. 0, U.S. Department of Energy Richland Operations Office, Richland, Washington.

Easterly, R and D Salstrom. 2003. *Current Vegetation Map of Mcgee-Riverland Unit, Hanford Reach National Monument*. Accessed on Feb. 20, 2015, at http://Nerp.Pnnl.Gov/Docs/Ecology/Biodiversity/Easterly2003.Pdf.

Flint, AL, GS Campbell, KM Ellett, and C Calissendorff. 2002. "Calibration and Temperature Correction of Heat Dissipation Matric Potential Sensors," *Soil Sci. Soc. Am. J.*, 66:1439-1445.

Gavlak, R, D Horneck, RO Miller, and J Kotuby-Amacher. 2003. *Soil, Plant and Water Reference Methods for the Western Region*, WCC 103 publication WREP 125, 2nd edition, Oregon State University, Corvallis, OR.

Gee, GW, HD Freeman, WHJ Walters, MW Ligotke, MD Campbell, AL Ward, SO Link, SK Smith, BG Gilmore, and RA Romine. 1994. *Hanford Protoype Surface Barrier Status Report: FY 1994*, PNL-10275, Pacific Northwest Laboratory, Richland, Washington. Available at http://www.osti.gov/energycitations/servlets/purl/10113304-5D9ZgI/webviewable/.

Gee, GW, AL Ward, BG Gilmore, MW Ligotke, and SO Link. 1995. *Hanford Prototype-Barrier Status Report: FY 1995*, PNL-10872, Pacific Northwest National Laboratory, Richland, Washington. Available at http://www.osti.gov/energycitations/servlets/purl/177965-nd9isN/webviewable/.

Gee, GW, AL Ward, BG Gilmore, SO Link, GW Dennis, and TK O`Neil. 1996. *Hanford Prototype-Barrier Status Report FY 1996*, PNNL-11367, Pacific Northwest National Laboratory, Richland, Washington. Available at http://www.osti.gov/energycitations/servlets/purl/444009-twIbfZ/webviewable/.

Hitchcock, CL and A Cronquist. 1973. *Flora of the Pacific Northwest*. University of Washington Press, Seattle, Washisngton.

Ligotke, MW. 1993. *Soil Erosion Rates Caused by Wind and Saltating Sand Stresses in a Wind Tunnel,* PNL-8478, Pacific Northwest Laboratory, Richland, Washington. Available at http://www.osti.gov/energycitations/servlets/purl/6377761/.

Ligotke, MW and DC Klopfer. 1990. *Soil Erosion Rates from Mixed Soil and Gravel Surfaces in a Wind Tunnel,* PNL-7435, Pacific Northwest Laboratory, Richland, Washington.

Link, SO, GW Gee, ME Thiede, and PA Beedlow. 1990. "Response of a Shrub-Steppe Ecosystem to Fire: Soil Water and Vegetational Change," *Arid Soils Research and Rehabilitation,* 4:163-172.

Myers, DR and DA Duranceau. 1994. *Prototype Hanford Surface Barrier: Design Basis Document,* BHI-00007 Rev.0, Bechtel Hanford, Inc., Richland, Washington.

Neter, J and W Wasserman. 1974. *Applied Linear Statistical Models: Regression, Analysis of Variance, and Experimental Designs*. Richard D. Irwin, Inc., Homewood, Ill.

Rebele, F and C Lehmann. 2002. "Restoration of a Landfill Site in Berlin, Germany by Spontaneous and Directed Succession," *Restoration Ecology*, 10:340-347.

Reece, CF. 1996. "Evaluation of Line Heat Dissipation Sensor for Measuring Soil Matic Potential," *Soil Sci. Soc. Am. J.*, 60:1022-1028.

Reynolds, WD. 1993. "Unsaturated Hydraulic Conductivity: Field Measurement." In *Soil Sampling and Methods of Analysis,* ed. MR Carter, Canadian Society of Soil Science, pp. 633-644. Lewis Publishers, Boca Raton, Florida.

Reynolds, WD and DE Elrick. 1985. "In Situ Measurement of Field-Saturated Hydraulic Conductivity, Sorptivity and the A-Parameter Using the Guelph Permeameter," *Soil Science*, 140(4):292-302.

Roberts, HA. 1981. *Seed Banks in the Soil - Advances in Applied Biology*. 6, Academic Press, Cambridge.

SAS Institute. 2002. *JMP Statistics and Graphics Guide, Version 5*. SAS Institute Inc, Cary.

Scholander, TF, HT Hammel, ED Bradstreet, and EA Hemmingsen. 1965. "Sap Pressure in Vascular Plants," *Science*, 148:339-346.

Seigal, S. 1956. *Nonparametric Statistics for the Behavioral Sciences*. McGraw-Hill Book Company, New York, New York.

Steele, RBD and JH Torrie. 1960. *Principals and Procedures of Statistics*. McGraw-Hill, New York.

van Der Waerden, BL. 1952. "Order Tests for the Two-Sample Problem and Their Power," *Indagationes Mathematicae*, 14:453-458.

Ward, AL, N Hasan, SO Link, and KE Draper. 2009a. *The Effects of Fire on the Function of the 200-BP-1 Engineered Surface Barrier,* PNNL-18934, Pacific Northwest National Laboratory, Richland, Washington.

Ward, AL, KD Leary, SO Link, GT Berlin, JW Cammann, ML Mandis, and LC Buelow. 2009b. "Short and Long-Term Fire Impacts on Hanford Barrier Performance," *Waste Management Symposium 09*, Phoenix, Arizona.

Ward, AL, SO Link, KE Draper, and RE Clayton. 2011. *200-BP-1 Prototype Hanford Barrier -- 15 Years of Performance Monitoring*, PNNL-18845 Revision 1, Pacific Northwest National Laboratory, Richland, Washington. Available at http://www.osti.gov/energycitations/servlets/purl/1027194/. (Accessed on Aug. 21, 2015).

Ward, AL, SO Link, KD Leary, and GT Berlin. 2010. "Fire Impacts on an Engineered Barrier's Performance: The Hanford Barrier One Year after a Controlled Burn," *WM 2010 conference*, March 7-11, 2010, Phoenix, Arizona. Available at http://www.wmsym.org/app/2010cd/wm2010/pdfs/10472.pdf

Ward, AL, SO Link, CE Strickland, KE Draper, and RE Clayton. 2007. *200-BP-1 Prototype Hanford Barrier Annual Monitoring Report for Fiscal Years 2005 through 2007*, PNNL-17176, Pacific Northwest National Laboratory, Richland, Washington. Available at http://www.osti.gov/energycitations/servlets/purl/927493-58wmF0/.

Ward, AL, JK Linville, JM Keller, and GH Seedahmed. 2005. *200-BP-1 Prototype Hanford Barrier Annual Monitoring Report for Fiscal Year 2004*, PNNL-14960, Pacific Northwest National Laboratory, Richland, Washington. Available at http://www.osti.gov/energycitations/servlets/purl/15020831-RBQnP9/.

Appendix D

Properties of Materials for Barrier Construction

Z. Fred Zhang

Pacific Northwest National Laboratory
Richland, Washington

Content

List of Tables

This appendix summarizes the physical properties of the Warden silt loam, saturated hydraulic conductivity (K_s) of the asphalt concrete (AC), and the particle size distribution of other materials used for constructing the Prototype Hanford Barrier (PHB).

D.1 Warden Silt Loam

The Warden silt loam used to construct the PHB was taken from the McGee Ranch (DOE-RL 1994), which is about 10 miles west to the PHB. The hydraulic properties of the Warden silt loam have been measured in the field, in the laboratory, and using a lysimeter at the Field Lysimeter Test Facility (FLTF). The water retention curve (WRC) is described using the van Genuchten (1980) model:

$$\theta(h) = \theta_r + [\theta_s - \theta_r]\left[1 + (\alpha \mid h \mid)^n\right]^{-m} \quad \text{D.1}$$

where θ_s and θ_r are the saturated and the residual water contents, α is a fitting parameter that is generally inversely proportional to the air-entry pressure, n is the fitting parameter related to particle size distribution, and m = 1-1/n is a constant (van Genuchten 1980).

D.1.1 Hydraulic Properties

D.1.1.1 Field Measurement

Zhang (2015) estimated the retention properties of the silt loam, with and without gravel, using valid monitoring data of water content measured using a neutron probe and water pressure measured using heat-dissipation units from 1995 to 2003 for four depths at 12 monitoring stations (Table D.1). It was found that the spatial variations of parameters θ_s, θ_r, and n were relatively small, with the coefficient of variation being no more than 18%. However, parameter α varied by a factor of 2.33 and the range of one standard deviation was from 2.34 to 12.7 m^{-1}. The spatial variability of the retention properties appeared to be larger than the effects of added 15% w/w pea gravel on the properties.

Additionally, the potential existence of hysteresis of water retention was evaluated by grouping the data by the discharge period (from April to October) and the recharge period (from November to March); the temporal variation of the WRC was evaluated by dividing the data into three periods: 1995 to 1996, 1997 to 1998, and 2000 to 2003. The mean of difference between the observations and the predictions by the corresponding non-hysteric WRCs was used to quantify the effects of hysteresis and time. The results show that neither hysteresis nor time had a detectible effect on the WRCs. These results are also re-captured in Appendix E.

Table D.1. The mean and the range of one standard deviation for the non-hysteric retention parameters at four depths and their average values.

	0.45 m	0.775 m	1.225 m	1.775 m	Average
θ_s (m^3m^{-3})	0.353±0.052	0.315±0.066	0.369±0.051	0.342±0.041	0.344±0.056
θ_r (m^3m^{-3})	0.075±0.012	0.064±0.013	0.068±0.012	0.063±0.009	0.068±0.012
α (m^{-1})	3.92x/2.68	6.27x/1.85	4.27x/2.72	8.80x/1.77	5.46x/2.33
n (-)	1.59±0.14	1.47±0.13	1.53±0.14	1.46±0.06	1.51±0.13
RMSE† (m^3m^{-3})	0.020	0.017	0.014	0.013	0.016

†RMSE: Root of mean squared error.

D.1.1.2 Laboratory Measurement

During the construction of the barrier, the retention property and the saturated hydraulic conductivity of the Warden silt loam were characterized in the laboratory with 16 samples (Table D.2); the mean retention parameters were θ_s = 0.449 m^3m^{-3}, θ_r = 0.082 m^3m^{-3}, α = 0.621 m^{-1}, and n = 1.847, and the mean K_s was 1.42×10^{-6} m s^{-1}.

Table D.2. Laboratory measured physical properties of the Warden silt loam.

	gravel (%)	cs (%)	fs (%)	silt (%)	clay (%)	θ_s (m^3m^{-3})	θ_r (m^3m^{-3})	α (m^{-1})	n (-)	K_s (m s^{-1})
1	0	2	54	34	10	0.453	0.078	0.49	1.977	1.20E-06
2	0	2	63	25	10	0.463	0.082	0.35	2.463	1.20E-06
3	0	4	58	28	10	0.451	0.070	0.72	1.650	1.20E-06
4	0	3	58	30	9	0.443	0.080	0.66	1.757	2.90E-06
5	0	4	63	23	10	0.433	0.086	0.55	1.865	2.90E-06
6	0	3	58	30	9	0.444	0.082	0.51	1.942	1.20E-06
7	0	2	57	31	10	0.454	0.085	0.59	1.853	1.20E-06
8	0	3	51	37	9	0.454	0.080	0.66	1.768	1.20E-06
9	0	2	57	31	10	0.456	0.083	0.69	1.850	1.20E-06
10	0	7	60	29	4	0.446	0.068	0.88	1.618	2.90E-06
11	0	6	59	30	5	0.448	0.085	0.64	1.790	1.20E-06
12	0	4	57	33	6	0.431	0.085	0.61	1.858	1.20E-06
13	0	5	58	32	5	0.431	0.085	0.61	1.757	1.20E-06
14	0	3	52	34	11	0.469	0.098	0.63	1.758	1.20E-06
15	0	4	52	35	9	0.451	0.082	0.7	1.788	1.20E-06
16	0	3	56	36	5	0.459	0.084	0.65	1.855	1.20E-06
Avg	0	3.6	57.1	31.1	8.3	0.449	0.082	0.621	1.847	1.42E-06

cs: coarse sand; fs: fine sand; avg: geometric mean for K_s and arithmetic mean for other variables.

D.1.1.3 Lysimeter Measurement

The retention properties were also measured in the FLTF, where some of the lysimeters were filled with Warden silt loam, as reported in Fayer et al. (1992) (θ_s = 0.411 m^3m^{-3}, θ_r = 0.0 m^3m^{-3}, α = 4.19 m^{-1}, and n = 1.29).

D.1.2 Storage Capacity

Theoretically, all water in the barrier always moves, regardless of how slow the movement is. Practically, the upper bound of a soil's storage capacity is considered as the field capacity, which is often estimated based on the water retention properties of a soil at the pressure head of -3.3 m (e.g., Albright et al. 2010). Based on the average non-hysteretic water retention, the field capacity of the silt loam storage layer is 0.131±0.016 m^3m^{-3}, which translates to 262±32 mm of water in the 2-m storage layer. The lower bound of storage capacity is considered as the wilt point, i.e., the water content that vegetation cannot use. In the case without measurement, the wilt point is often approximated by the water content corresponding to a capillary pressure of 15 bar (Or and Wraith 2001; Romano and Santini 2002). Here, the lower bound of storage capacity is estimated by the observed minimum water content, which was 0.058±0.004 m^3m^{-3} (Table D.1). This is equivalent to 116±8 mm of water in the 2-m storage layer. Hence, the available storage capacity of the 2-m storage layer is 146±40 mm if no capillary break is used below the silt loam layer.

When the silt loam is underlain by a layer of coarse sand and gravel, a strong capillary break is formed. Based on neutron logging during the 3-year enhanced precipitation test from water year (WY) 1995 to WY1997, the observed maximum storage was 517.5±85.8 mm (Appendix F, Table F.3), with negligible drainage (≤ 0.18 mm yr^{-1}). Hence, the storage of 517.5±85.8 mm may be considered as the storage capacity of the 2-m silt loam storage layer with a capillary break. The corresponding available storage capacity is 402±94 mm, which is 256±126 mm more than the case without a capillary break. The above results are summarized in Table D.3.

Table D.3. Estimated storage capacity of the 2-m-thick Warden silt loam layer.

Capillary condition	Item	Value (mm)
Without a capillary break	Total storage capacity	262±32
	Unavailable storage capacity	116±8
	Available storage capacity	146±40
With a capillary break	Total storage capacity	518±86
	Unavailable storage capacity	116±8
	Available storage capacity	402±94

D.2 Asphalt Concrete

The AC covered with fluid-applied asphalt (FAA) was placed at the bottom of the barrier to provide a low-permeability hydraulic barrier and redundant biointrusion prevention layer. Measurements of the K_s of the AC were made in the field and also on cores removed from the field and taken to the laboratory.

D.2.1 Laboratory Test

The K_s of the AC cores (Samples 1A through 5A) from the barrier was measured in the laboratory using the falling head method with 2.5-m head of water (Gee et al. 1994). The cores were obtained from the "non-functional" area of the PHB, at the north end. Table D.4 presents laboratory data from barrier testing. The K_s of cores of FAA-coated AC (Samples 1 through 4) was also measured. The average K_s of AC

without FAA-coating was 3.16×10^{-10} cm s^{-1} (0.11 mm yr^{-1}) and the average K_s of AC with FAA-coating was 1.78×10^{-11} cm s^{-1} (0.0056 mm yr^{-1}), with the former being 18.9 times the latter.

Table D.4. Laboratory-measured saturated hydraulic conductivity of the asphaltic concrete (DOE-RL 1994, Table 1; Gee et al. 1994, Table 3.2).

Sample	Thickness (cm)	Hydraulic Conductivity (cm s^{-1})	Note
1A	15.3	1.32E-09	Without FAA
2A	14.8	3.45E-10	Without FAA
3A	16.7	2.42E-10	Without FAA
4A	17.1	1.24E-10	Without FAA
5A	14.1	3.16E-10	Without FAA
Geometric Mean	**-**	**3.16E-10**	**Without FAA**
1	0.16	1.36E-11	With FAA
2	0.265	1.18E-11	With FAA
3	0.275	2.49E-11	With FAA
4	0.5	2.51E-11	With FAA
Geometric Mean	**-**	**1.78E-11**	**With FAA**

D.2.2 Field Tests

Field hydraulic conductivity measurements of AC without FAA coating were made at the north end of the PHB using a specially constructed field falling head permeameter (Table D.5). The average value was 1.82×10^{-8} cm s^{-1} (5.7 mm yr^{-1}), which is about two orders of magnitude larger than the value measured in the laboratory.

Table D.5. The saturated hydraulic conductivity (cm s^{-1}) of the AC measured with a field falling head permeameter (after DOE-RL 1994, Table 2).

Location	Hydraulic Conductivity (cm s^{-1})
1 NW Corner	1.91E-09
2 NW Corner, seam	1.08E-07
3 N Center	1.47E-08
4 NE Center	4.33E-08
5 NE Corner	1.51E-08
Geometric Mean	**1.82E-08**

D.3 Particle Size of Other Materials

Neither the retention properties nor the K_s were measured for other materials. The particle size distributions for these materials used in constructing the PHB are summarized below.

D.3.1 Subgrade Fill

The subgrade was constructed of sand soil, containing cobbles less than 75 mm (3 in.) in their greatest dimension with a constitution no more than 20% of the volume of the fill (DOE-RL 1994, Section 2.2).

The depth of the subgrade fill varied from 0 to 5 m as required by the original topology of the soil surface in the crib area. The subgrade fill was placed level in the north-south direction and sloped down at 2% in the east-west direction. The subgrade was compacted to 95% of the maximum density.

D.3.2 Basalt Riprap

The riprap was used to construct the east side slope and the intrusion control layer below the silt loam barrier. The riprap used was from the Vernita Quarry, uncleaned, well-blasted (overshot) basalt passing through 25.4-cm-spaced grizzly bars (DOE-RL 1994, Section 2.10). The particle size distribution is given in Table D.6.

Table D.6. Particle size distribution of basalt riprap (KEH 1993, Section 2.1.4).

Sieve Size	Percent Passing
250 mm (10 in.)	100
125 mm (5 in.)	50 to 70
75 mm (3 in.)	30 to 50
15 mm (5/8 in.)	0 to 5

D.3.3 Shoulder Ballast

Railroad shoulder ballast was designed to act as a transition between the large basalt particle sizes and the small gravel to prevent the gravel filter from falling between large basalt pieces (DOE-RL 1994, Section 2.11). The particle size distribution is given in Table D.7.

Table D.7. Particle size distribution of shoulder ballast (KEH 1993, Section 2.1.5).

Sieve Size	Percent Passing
64 mm (2.5 in.)	100
20 mm (3/4 in.)	40 to 80
6.3 mm (1/4 in.)	5 max
0.15 mm (No. 100)	0 to 2

D.3.4 Top Course

The top course material was used as the basis for the AC and gravel filter to form the graded capillary break. The top course material is crushed material, small enough to pass through a 16-mm (5/8 in.) mesh (DOE-RL 1994, Section 2.12). The particle size distribution is given in Table D.8.

Table D.8. Particle size distribution of gravel filter (KEH 1993, Section 2.1.7).

Sieve Size	Percent Passing
16 mm (5/8 in.)	100
6.3 mm (1/4 in.)	55 to 75
0.42 mm (No. 40)	8 to 24
0.074 mm (No. 200)	0 to 10

D.3.5 Drainage Gravel

Drainage gravel was used to protect the underlying AC and as medium for lateral water movement. Drainage gravel consisted of screened, cleaned, round river rock (DOE-RL 1994, Section 2.9). The gravel was placed and consolidated by two passes of a vibratory roller. The particle size distribution is given in Table D.9.

Table D.9. Particle size distribution of drainage gravel (KEH 1993, Section 2.1.6).

Sieve Size	Percent Passing
25 mm (1 in.)	100
20 mm (3/4 in.)	80 to 100
10 mm (3/8 in.)	10 to 40
4.76 mm (No. 4)	0 to 4
0.074 mm (No. 200)	0 to 0.5

D.3.6 Sand Filter

The sand filter was used to form the graded capillary break below the silt loam storage layer. Naturally occurring sands were used (DOE-RL 1994, Section 2.15). The particle size distribution is given in Table D.10.

Table D.10. Particle size distribution of sand filter (KEH 1993, Section 2.1.9).

Sieve Size	Percent Passing
10 mm (3/8 in.)	100
4.76 mm (No. 4)	95 to 100
2 mm (No. 10)	85 to 100
0.84 mm (No. 20)	40 to 95
0.42 mm (No. 40)	17 to 80
0.15 mm (No. 100)	5 to 35
0.074 mm (No. 200)	1 to 25

D.3.7 Clean Fill

The clean fill was used to construct the west side slope of the PHB. The gravely clean fill dike (aka pit-run gravel, common fill) material from Pit 30 was used as is (DOE-RL 1994, Section 2.13). It consisted of well-graded soil mixtures containing up to 200 mm (8 in.) in the greatest dimension and constituting no more than 40% of the volume of fill.

D.3.8 Pea Gravel

Peal gravel consisted of screened gravel, 100% passing a 10-mm (3/8 in.) sieve and 98% retained on a 2-mm (No. 10) sieve (KEH 1993, Section 2.1.10).

D.4 References

Albright, WH, CH Benson, and WJ Waugh. 2010. *Water Balance Covers for Waste Containment Principles and Practices*. ASCE Press, Reston, Virginia.

DOE-RL. 1994. *Constructability Report for the 200-BP-1 Prototype Surface Barrier*, DOE/RL- 94-76, U.S. Department of Energy Richland Operations Office, Richland, Washington.

Fayer, MJ, ML Rockhold, and MD Campbell. 1992. "Hydrologic Modeling of Protective Barriers: Comparison of Field Data and Simulation Results," *Soil Sci. Soc. Am. J.*, 56:690-700.

Gee, GW, HD Freeman, WHJ Walters, MW Ligotke, MD Campbell, AL Ward, SO Link, SK Smith, BG Gilmore, and RA Romine. 1994. *Hanford Protoype Surface Barrier Status Report: FY 1994*, PNL-10275, Pacific Northwest Laboratory, Richland, Washington. Available at http://www.osti.gov/energycitations/servlets/purl/10113304-5D9ZgI/webviewable/.

KEH. 1993. *Prototype Surface Barrier at 200-BP-1 Operable Unit*, W-263-C2 Rev. 0, Kaiser Engineers Hanford Company, Richland, Washington.

Or, D and JM Wraith. 2001. "Soil Water Content and Water Potential Relationships." In *Soil Physics Companion*, ed. AW Warrick, pp. 49-84. CRC Press, Boca Raton.

Romano, N and A Santini. 2002. "Field." In *Methods of Soil Analysis Part 4 Physical Methods*, eds. JH Dane and CT Topp, pp. 721-738. Soil Science Society of America, Inc., Madison, Wisconsin USA.

van Genuchten, MT. 1980. "A Closed-Form Equation for Predicting the Hydraulic Conductivity of Unsaturated Soils," *Soil Science Society of America Journal*, 44:892-898.

Zhang, ZF. 2015. "Field Soil Water Retention of the Prototype Hanford Barrier and Its Variability with Space and Time," *Vadose Zone Journal*, 14(8):1-10. doi:10.2136/vzj2015.01.0011.

Appendix E

Field Soil Water Retention of the Prototype Hanford Barrier and Its Variability with Space and Time

Z. Fred Zhang

Pacific Northwest National Laboratory
Richland, Washington

Content

List of Figures

List of Tables

Abstract

Engineered surface barriers (or covers) are used to isolate underlying contaminants from water, plants, animals, and humans. To understand the flow processes within a barrier and the barrier's ability to store and release water, the field hydraulic properties of the barrier need to be known. A multiyear test of the evapotranspiration (ET) barrier at the U.S. Department of Energy Hanford Site in southeastern Washington State has yielded *in situ* soil water content and pressure data from multiple locations for a 9-year period, offering the opportunity to estimate soil water retention properties at different locations and times. The upper 2 m layer of the ET barrier is a silt loam and the top 1 m also contains 15% w/w pea gravel. Within this layer, valid monitoring data from 1995 to 2003 for four depths at 12 monitoring stations were used to determine the field water retention of the silt loam, with and without gravel. The data covered a wide range of wetness, from near saturation to the permanent wilt point, and each retention curve contained 51 to 96 data points. The data were described well with the commonly used van Genuchten water retention model. It was found that the spatial variation of the saturated and residual water content and the pore size distribution parameter was relatively small, while that of the van Genuchten α was relatively large. The effects of spatial variability of the retention properties appeared to be larger than the combined effects of added 15% w/w pea gravel and plant roots on the properties. Neither the primary wetting process in the winter season nor drying process in the summer season nor time had a detectable effect on the water retention of the silt loam barrier.

E.1 Introduction

Since the 1980s, the U.S. Department of Energy has considered engineered surface barriers (aka surface covers) to be an important option for remediation and closure of Hanford waste sites (e.g., DOE, 1987) . Surface barriers are an integral part of waste site remediation. They minimize the further spread of contamination, allow time for additional radionuclide decay, and reduce worker and environmental risks (DOE-RL 2013). Surface barriers with appropriate side slopes serve many functions, such as minimizing plant and animal intrusion, but generally their most important function is to significantly reduce the deep drainage flux and thus reduce the mobilization and transport of vadose zone contaminants. Accurate knowledge of the field retention properties and their spatial and temporal variation is very important for understanding the flow processes within the storage layer of an evapotranspiration (ET) barrier and its ability to store and release water. Any change in the barrier's retention properties will affect barrier performance.

Investigators have found that, as time passes, large pores may form in surface barriers as a result of biological processes such as ingress of plant roots and burrowing of worms and insects. Other factors that may affect barrier properties include wetting and drying, freezing and thawing, biota intrusion, and weathering. The temporal impacts can be significant for a compacted barrier. Often when a compacted clay liner becomes drier, it cracks and its hydraulic conductivity can increase by several orders of magnitude (Benson et al. 1994; Benson and Othman 1993; Henken-Mellies and Schweizer 2011; Meer and Benson 2007; Meerdink et al. 1997; Melchior et al. 2010). Benson et al. (2010) reported the properties of geosynthetics that had been in service for about 6 years by removing the geosynthetics from the cover. They found that the hydraulic conductivity of the geosynthetic clay liner (GCL) was four orders of magnitude higher than that of the new GCL. Benson et al. (2007) compared the soil hydraulic properties of 10 ET covers in the Alternative Cover Assessment Program at the time of construction and 1 to 4 years after construction with laboratory measurements from core samples. They found significant variations in the saturated hydraulic conductivity, saturated water content, van Genuchten α, and van Genuchten n parameter. They also pointed out that more-compacted barriers with lower as-built porosity had larger changes in properties. However, the focus of this investigation is on the water retention properties based on *in situ* measurements.

Numerous experiments have confirmed the existence of hysteresis in the soil water retention curve (WRC) (e.g., (Gillham et al. 1979; Hillel 1980; Jaynes 1992; Kaluarachchi and Parker 1987; Royer and Vachaud 1975; Vachaud and Thony 1971). Potential causes of the hysteresis include irregularities in the cross-sections of the void passages, the contact angle being greater in an advancing meniscus than in a receding meniscus, and entrapped air (Klausner 1991). The hysteretic nature of soil water retention has long been known, but often in routine engineering and agriculture applications the soil water retention is assumed to be non-hysteretic (NH) (Khire et al. 1999). Several researchers have discussed the potential effects of hysteresis on barrier performance (Khire et al. 1999; Stormont and Anderson 1999). Numerical investigations of flow in surface barriers have generally emphasized the importance of hysteresis (Fayer and Gee 1997; Iryo and Rowe 2004; Lee 2007; Tami et al. 2004; Yang et al. 2011; Zhang et al. 2009). Canone et al. (2008) presented the theory and models to describe hysteresis and applied them to experiments. They pointed out that the negligence of hysteresis may lead to the incorrect interpretation of field data.

The drainage curve of soil retention is usually measured in the laboratory using small (at the scale of several centimeters) intact soil cores (e.g., in a pressure chamber) after the completion of barrier construction, but the lab-measured core-scale property may differ significantly from the field-scale property (Wierenga et al. 1991; Zhang et al. 2004). Drainage curves can also be measured with the

instantaneous profile method in the field (Vachaud and Dane 2002). During the service of a surface barrier, either the destructive coring method or the instantaneous method may not be allowed because they either damage the integrity of the barrier or add water to the barrier system. Further, the absorption curve of the retention is usually not measured because of the lack of a sophisticated method.

The Prototype Hanford Barrier (PHB), constructed in 1994, is an ET barrier and comprises multiple layers of natural and asphaltic materials (Gee et al. 1997; Wing and Gee 1994). The top layer consists of 2-m-thick Warden silt loam, acting as a medium for water storage and plant growth and allowing the stored water to be released to the atmosphere by ET. To prevent wind or water erosion, the top 1-m silt loam contained 15% w/w pea gravel. The silt loam layer has the length of 80 m and width of 40 m with the long sides oriented in the north-to-south direction. From 1994 to 1997, the north section of the barrier was irrigated so that the total precipitation was about 495 mm yr^{-1}. In March of each year, about 69 mm of water was applied over an 8-hour period to simulate a 1000-year return 24-hour rainstorm. Soil water content (θ) and pressure (h) of the barrier were monitored at 12 water balance stations. Water content of the barrier profile at each station was monitored routinely with a neutron probe (NP) and the soil water pressure with heat dissipation units (HDUs).

The monitoring data of water content and pressure covered a relatively long period (e.g., nearly a decade or longer), a wide range of wetness from near saturation to about the residual water content, and multiple horizontal and vertical locations. Although the primary purpose of monitoring was to verify surface barrier performance, the monitoring data can also be used to infer the barrier's retention properties at different locations and times. When data collected during different time periods are processed separately, the temporal variation of the WRC can also be evaluated. An advantage of using the field data is that there was sufficient time for the HDUs to reach equilibrium with the surrounding soil, especially when the soil wetness was near the dry end.

The purpose of this investigation is to determine the field water retention properties using monitoring data such as water content and pressure over a period of 9 years (from 1995 to 2003). It is expected these results can represent the barrier properties better than the laboratory-measured values. The spatial variability of the barrier retention was studied by developing the retention curves for 4 depths at 12 locations as sufficient valid data were available. The temporal stability and the hysteretic nature of the retention curves were evaluated by grouping the data by primary hydrological processes or by time.

E.2 Material and Method

E.2.1 Water Content and Pressure Monitoring

Soil water content and pressure in the silt loam layer were monitored at 12 stations (S1 through S12). Six of the stations were located in the north section and were spaced 5 m apart. The other six stations were in the south section and were also spaced 5 m apart. Each station consisted of an NP access tube and, 0.3 m away, a string of six HDUs arrayed vertically. Water content was monitored at a vertical interval of 0.15 m using an NP (Hydroprobe Model 503DR, CPN International, Inc., Martinez, CA) deployed in a vertical (4.8-cm inner diameter) aluminum access tube extending 1.9 m below the barrier surface. The NP was calibrated on April 5, 1995, in the vertical access tube:

$$\theta = a_0 + a_1 N + a_2 N^2 \qquad \text{E.1}$$

where N is the 16-sec. neutron count, a_0 = -0.01649, $a_1 = 1.449 \times 10^{-5}$, and $a_2 = 3.234 \times 10^{-10}$. On April 20, 2003, the NP received a new neutron counter that slightly underestimated the neutron count based on the cross-calibration with another NP before and after the use of the new neutron counter. Hence, after

this date, the N values needed to be scaled by a factor of 1.041 for vertical logging so that Eq. E.1 could be used to calculate water content. Radioactive decay was corrected for all the measurements before data analysis.

Strings of HDUs (Model 229L, Campbell Scientific Inc., Logan, Utah) were installed in September 1994 to monitor soil water pressure at depths of 0.075, 0.225, 0.45, 0.80, 1.25, and 1.75 m below ground surface. Before each measurement, the HDU was heated for a fixed period with a needle-type heater inside the HDU. The rate of heat dissipation was controlled by the water content of the porous matrix of the HDU because water conducts heat much faster than air. The temperature increase caused a voltage change in the thermocouple in the HDU, and the voltage was measured. The heat dissipation was determined as the difference between two voltages (ΔV), one measured after 1 sec. of heating and the other measured after a 30-sec. heating time. The relationships between the HDU-measured temperature and output voltage indicated that the variation among the HDUs was very small. Selected HDUs were calibrated in Tempe cells in the laboratory and the general calibration curve (Figure E.1) was used to convert the voltage change to soil-water pressure:

$$h = \begin{cases} a\exp(b\Delta V) & if \quad \Delta V \geq 1000 \\ c(1000-\Delta V)^2 + d(1000-\Delta V) - 1 & if \quad \Delta V < 1000 \end{cases} \qquad \text{E.2}$$

where $a = -1.514 \times 10^{-3}$, $b = 6.556 \times 10^{-3}$, $c = -1.338 \times 10^{-5}$, $d = 7.331 \times 10^{-3}$, h is soil-water pressure in meters and is negative under unsaturated condition, and ΔV is voltage change in millivolts. It is noted that the upper limit of water pressure measured by the HDU generally is considered to be approximately -1 m (CSI 2009; Flint et al. 2002; Reece 1996). However, the HDUs used at the PHB were first generation and seemed to lack clear air entry pressure because of the existence of large pores. The HDUs still responded to soil water pressure when h was higher than -1 m (Figure E.1). Hence, these HDUs were calibrated to near saturation but a different expression was used to describe this part of the curve (Eq. E.2). The HDUs in Flint et al. (2002) also seemed to respond to pressure higher than -1 m. In manufacturing the ceramic for the new generations of HDUs, large pores were removed.[2] Consequently, the newer HDUs generally do not respond to soil water pressure higher than about -1 m. Although the lower limit of HDUs is stated to be approximately -250 m by the vendor (CSI, 2009), HDUs continue functioning at h lower than -250 m. For example, Truex et al. (2012) observed h as low as about -450 m in a field experiment of soil desiccation. Oostrom et al. (2012) measured h as low as about -900 m in a laboratory experiment. Considering the relatively low sensitivity of HDUs when h is high and relatively large error when h is very low, the calculated h larger than -0.1 m or less than -1000 m is not considered in the following analysis.

[2] Ritter, J., Campbell Scientific, Inc. Personal communication, 2014.

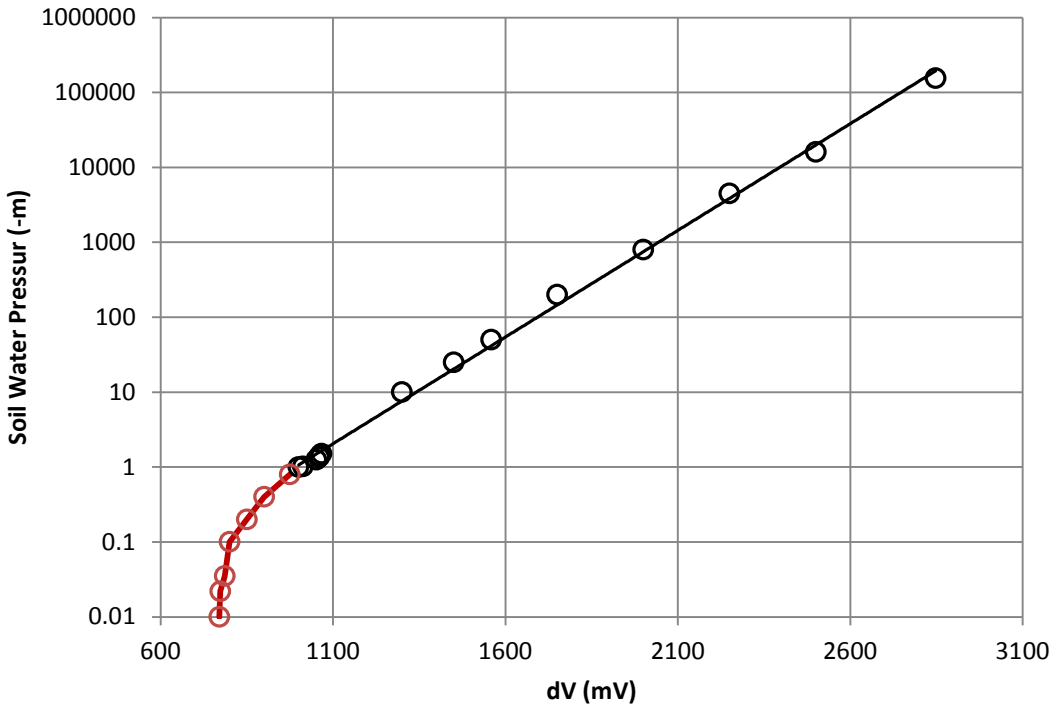

Figure E.1. General calibration curve for heat dissipation units used for soil water pressure monitoring.

E.2.2 Field Water Retention

Water content was monitored with an NP and water pressure using HDUs from 1994 and 2013. Neutron logging was performed roughly weekly to monthly from 1994 to 1997. After 1997, neutron logging was performed less frequently (roughly monthly to quarterly), and there were logging gaps in 1999, 2005, and 2006. HDU logging was performed hourly to daily using an automated system. This analysis only used the data from 1995 to 2003, after which most HDUs did not function properly, generally because of malfunctioning peripherals (e.g., power supply, data loggers, or wires).

To determine the field water retention, the NP-measured water content and the HDU-measured water pressure at the same monitoring station, similar depths, and the same day were paired up. Because not all of the HDUs provided valid data on the days that neutron loggings were performed, the number of valid data pairs for each location varied between 51 and 96. Some of the HDU monitoring systems malfunctioned during the monitoring period and hence their results were not considered in this analysis.

At each water balance station, HDU data were available at 6 depths and NP data at 15 depths. Considering an HDU detects water pressure in a region of several centimeters and an NP detects water content in a region of tens of centimeter, we matched the depths of the two sets of measurements if the depth difference was no more than 0.05 m. The representative depth was the average of the two, and the depths were 0.45, 0.775, 1.225, and 1.775 m, of which the first two were in the silt loam with 15% w/w pea gravel and the last two in the silt loam without pea gravel. The van Genuchten (1980) models were used to describe the water retention:

$$\theta(h) = \theta_r + [\theta_s - \theta_r]\left[1 + (\alpha\,|\,h\,|)^n\right]^{-m} \qquad \text{E.3}$$

where θ_s and θ_r are the saturated and the residual water contents, α is a fitting parameter that is generally inversely proportional to the air-entry pressure, n is fitting parameters related to particle size distribution, and m = 1-1/n is a constant (van Genuchten 1980).

Assuming the soil was NH, parameters θ_s, θ_r, α, and n were fitted to all the data at each of the 36 locations using Mathcad 15 (Parametric Technology Corporation, Needham, MA). To constrain the estimation of θ_s, the field measured θ_s was used as an observation but with only 1/10 of the weight of a true field observation. The objective function was defined as the square root of the mean squared error (RMSE) of water content:

$$RMSE = \left\{ \frac{1}{N+1} \left[\sum_{1}^{N} \left(\theta - \hat{\theta} \right)^2 + w \left(\theta_{sp} - \hat{\theta}_s \right)^2 \right] \right\}^{1/2} \qquad \text{E.4}$$

where N is the number of observations, $\hat{\theta}$ is the predicted water content, $\hat{\theta}_s$ is the estimated θ_s, θ_{sp} = 0.411 m^3m^{-3} is the prior information, and w = 0.1 is the weight.

E.3 Results and Discussion

E.3.1 Observed Water Content and Pressure Head

Figure E.2 demonstrates the NP-measured water content and HDU-measured water pressure at the 0.45-m depth at the water balance station S1. The two plots have remarkable similarity and show the temporal variation of soil wetness. Both plots show clear seasonal variation of soil wetness. During the period of 9 years, water content varied between 0.06 and 0.40 m^3m^{-3}, while water pressure between -0.1 and about -800 m.

Using the NP-measured water content and HDU-measured water pressure, water retention curves were constructed for 36 locations: 9 at the 0.45-m depth, 10 at the 0.775-m depth, 9 at the 1.225-m depth, and 8 at the 1.775-m depth. To demonstrate the results, the measurements of the 9 water retention curves at the 0.45-m depth are shown as points in Figure E.3. The absolute values of h covered a wide range, from nearly 0.01 m (near saturation) to hundreds of meters or more. At each location, most of the data, especially data in the relatively wet range (e.g., roughly wetter than 0.2 m^3m^{-3}), fell very closely on the trend lines, indicating a very consistent θ-h relationship regardless of soil water processes and measurement time. However, the data in the relatively dry range were more scattered. (Please note that, because the symbols of many data points are shadowed by others, there appear to be more scattered points in the plots than there actually are.) One possible cause for the scattering could be the non-uniform distribution of soil water at the points of NP and HDU measurements because of the large change in water content within and beyond a wetting front or the non-uniform water use by plant roots.

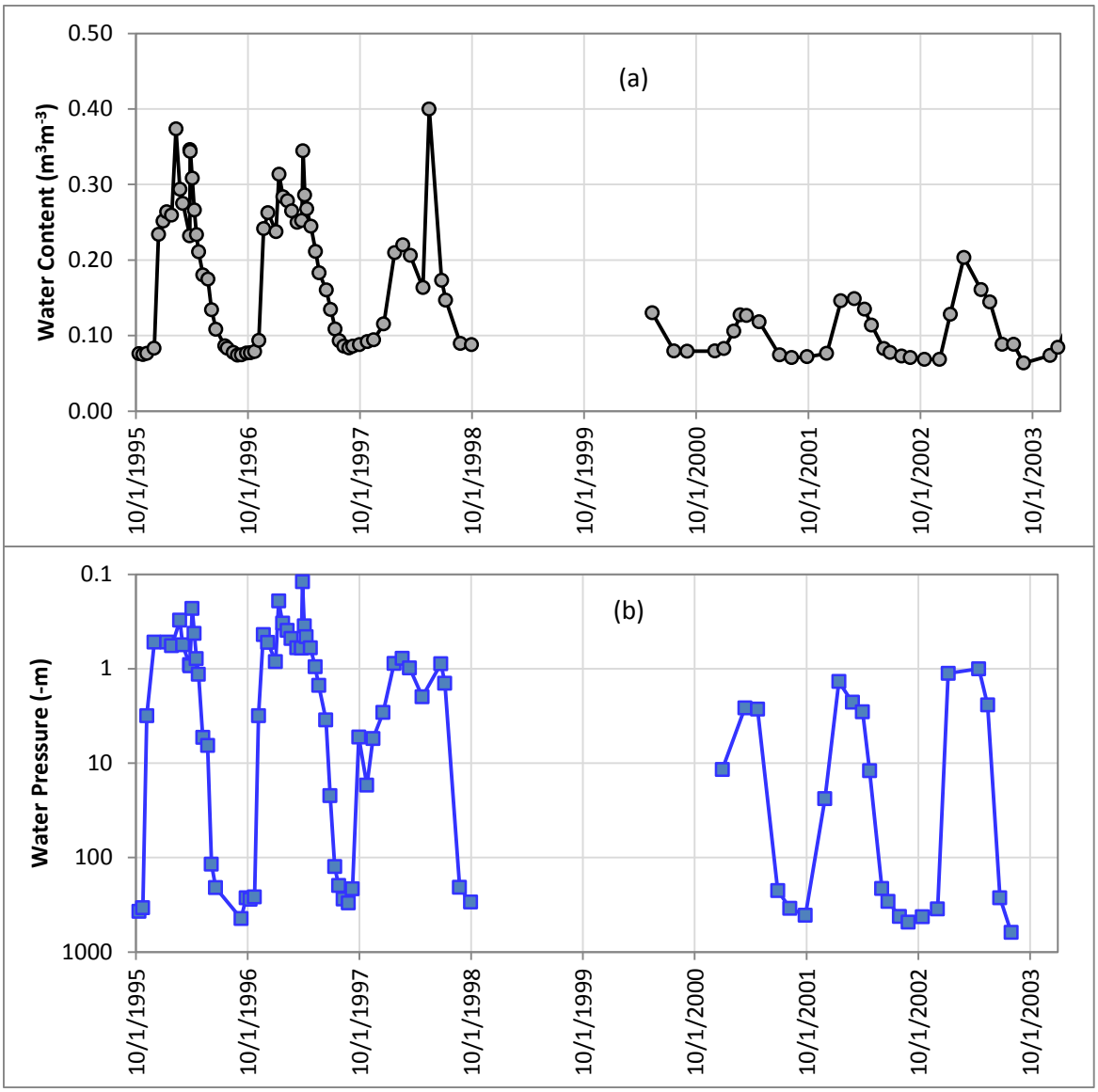

Figure E.2. An example of the field-measured (a) water content and (b) water pressure at 0.45-m depth at the water balance station S1.

Table E.1. Observed minimum water content and pressure at the selected depths of each of the monitoring stations

Station No.	0.45 m		0.775 m		1.225 m		1.775 m		All Depths	
	θ (m^3m^{-3})	h (m)	θ (m^3m^{-3})	h (m)	θ (m^3m^{-3})	h (m)	θ (m^3m^{-3})	h (m)	θ (m^3m^{-3})	h (m)
S1	0.064	-619	0.061	-501	0.066	-804	0.059	-161	0.063	-448
S2	0.064	-384	0.057	-589	0.061	-176	0.061	-46	0.061	-207
S3	0.060	-436	0.056	-546	0.063	-215	0.054	-486	0.058	-397
S4	0.064	-598	0.058	-641	0.062	-448	0.058	-198	0.060	-430
S5	0.064	-180	0.057	-409	0.058	-252	0.054	-258	0.058	-263

S6	0.057	#N/A	0.058	-305	0.064	-214	0.058	-456	0.059	#N/A
S7	0.057	-975	0.054	-810	0.059	-865	0.062	#N/A	0.058	-881
S8	0.057	-223	0.050	-961	0.057	-988	0.058	-985	0.055	-676
S9	0.061	-807	0.053	-942	0.053	-671	0.057	-994	0.056	-911
S10	0.063	#N/A	0.055	#N/A	0.057	#N/A	0.058	#N/A	0.058	#N/A
S11	0.062	#N/A	0.057	#N/A	0.060	#N/A	0.057	#N/A	0.059	#N/A
S12	0.057	-499	0.049	-842	0.052	#N/A	0.056	#N/A	0.053	#N/A
Average	0.061	-463	0.056	-667	0.059	-422	0.058	-309	0.058	-448

#N/A: This HDU was not functioning properly.

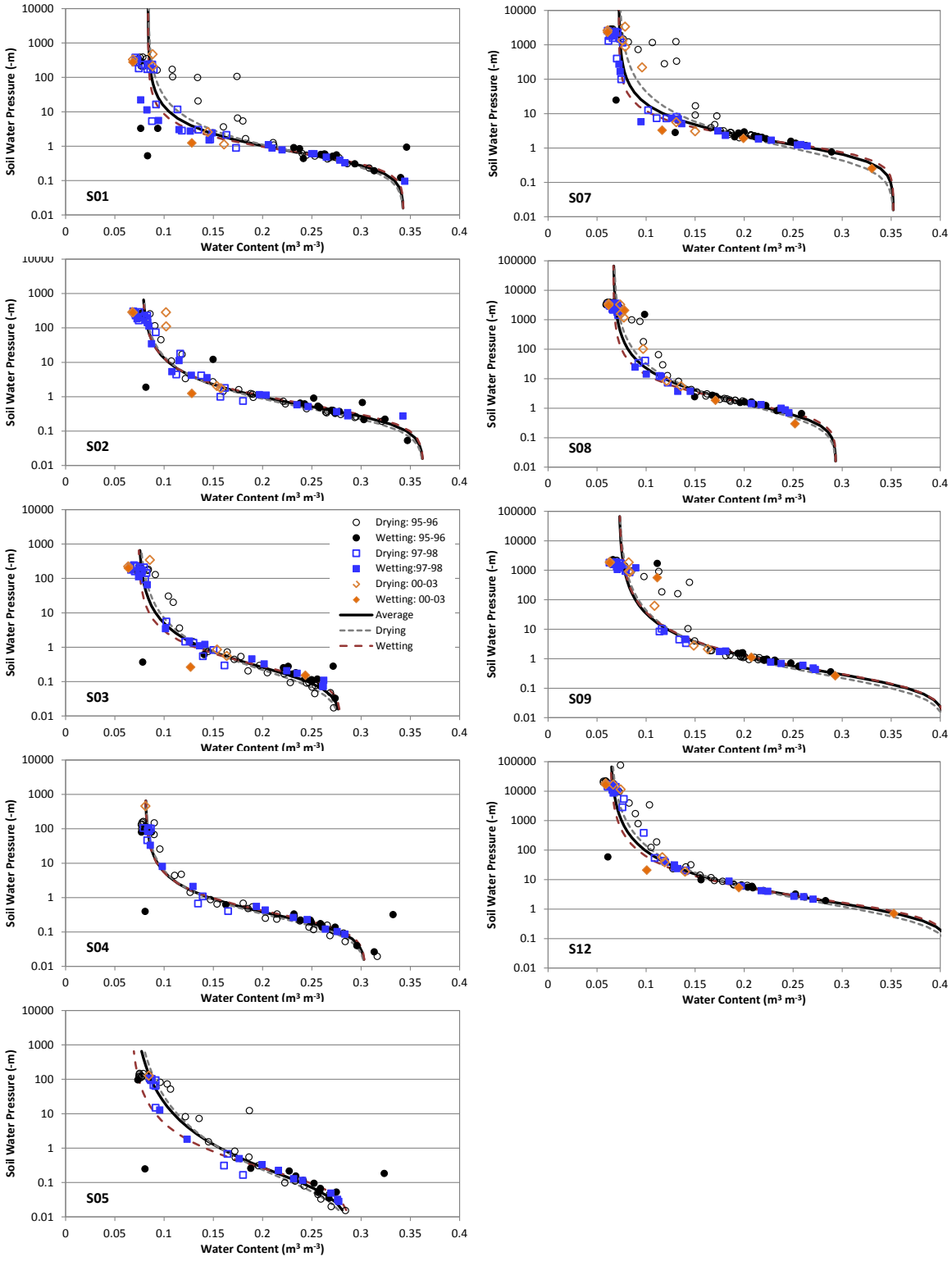

Figure E.3. Soil water retention at the 0.45-m depth for 9 of the 12 monitoring stations. The HDUs at the other 3 stations were not functioning properly.

An ET barrier relies on vegetation to absorb stored water in the storage layer and then release the water into the atmosphere. When the barrier soil is drier than the permanent wilting point, the plant cannot use the remaining stored water because the water is absorbed by the soil particle very tightly. This phenomenon was confirmed by the monitoring data at the PHB. A minimum water content and pressure were observed in each location (Table E.1). The observed minimum water content with standard deviation (σ) was 0.058±0.004 m^3m^{-3}. This water can be considered unavailable to plants at the silt loam layer. This water translates to 116±8 mm of storage of the 2-m-thick silt loam and is unavailable for storing infiltration in the wetting season. The minimum soil water pressure was more variable because *h* tended to be log-normally distributed. The geometric mean of *h* over all the stations at the four depths ranged from -309 to -667 m with an overall mean of -448 m. These values are much lower than the often-assumed permanent wilting point of -150 m (-15 bar) (Or and Wraith 2001; Romano and Santini 2002). The reason for the lower minimum soil water pressure is probably that native plants under the desert environment are more tolerant of water stress and hence could use some water below the *h* of -150 m (Albright et al. 2010; Romano and Santini 2002). At relatively shallow soil, evaporation is another cause for the low-pressure head. A systematic error caused by the extrapolation of the HDU calibration curve might also contribute to the small values of *h*.

E.3.2 Spatial Variability of Water Retention

To examine the spatial variability of the retention properties, the van Genuchten (1980) model (Eq. **E.3**) was used to describe the WRCs. Assuming the soil was NH, parameters θ_s, θ_r, α, and *n* were fitted to all the data at each of the 36 locations using Mathcad 15 (Parametric Technology Corporation, Needham, MA, USA). The mean and the range of one standard deviation for the retention parameters along with the root of mean squared error (RMSE) at the four depths are summarized in Table E.2, while the fitted curves are shown as the solid lines in Figure E.3. The model can generally describe the data at a given location very well (Figure E.3), as shown by the small RMSE values ranging between 0.013 and 0.020 m^3m^{-3}.

The mean parameter values with standard deviation were 0.344±0.056 m^3m^{-3} for θ_s, 0.068±0.012 m^3m^{-3} for θ_r, and 1.51±0.13 for *n* for the four depths. Note that the fitted θ_r is slightly larger than the measured minimum of θ (0.058 m^3m^{-3}), indicating some water below θ_r can be used by plants. The coefficient of variation for these three parameters was no more than 18%. However, parameter α varied considerably across the locations. It had a geometric mean of 5.46 m^{-1} and varied by a factor of 2.33. Namely, the range of one standard deviation was from 2.34 to 12.7 m^{-1}. For an engineered and relatively uniform surface barrier, the spatial variability of hydraulic properties was expected to be relatively small because the barrier was constructed with the same material using a consistent method. The cause of the large variation of α may be the measurement error in soil water pressure. Because parameter α simply scales *h* in the van Genuchten (1980) model, the error in *h* measurements would lead to an estimation error in α. Other factors such as the soil forming processing might also affect soil properties and parameters such as α.

Recall that the top 1 m of the silt loam barrier contained 15% w/w pea gravel, which potentially could reduce the porosity because these gravel were embedded in the silt loam. An opposite soil forming mechanism because of, e.g., the growth of plant roots and the alternation of freezing and thawing, tended to increase the porosity especially in the top soils. The soil forming processing may compensate some of the porosity loss because of the added gravel. The results in Table E.2 show a slight difference in the θ_s but not in other retention parameters between the top 1 m silt loam and those for the bottom 1 m silt loam. This result suggests that the added gravel and the soil forming factors affect soil water retention less than the spatial variability of the retention properties, and hence the effect of these factors on the retention property may be considered negligible.

Table E.2. The mean and the range of one standard deviation for the retention parameters at four depths and their average values.

		0.45 m	0.775 m	1.225 m	1.775 m	Average
Non-Hysteretic	θ_s (m^3m^{-3})	0.353±0.052	0.315±0.066	0.369±0.051	0.342±0.041	0.344±0.056
	θ_r (m^3m^{-3})	0.075±0.012	0.064±0.013	0.068±0.012	0.063±0.009	0.068±0.012
	α (m^{-1})	3.92x/2.68	6.27x/1.85	4.27x/2.72	8.80x/1.77	5.46x/2.33
	n (-)	1.59±0.14	1.47±0.13	1.53±0.14	1.46±0.06	1.51±0.13
	RMSE†† (m^3m^{-3})	0.020	0.017	0.014	0.013	0.016
Dry Seasons	α_d (m^{-1})	5.91x/2.59	8.01x/2.41	4.89x/2.79	8.87x/1.69	6.71x/2.39
	n_d (-)	1.49±0.13	1.45±0.17	1.48±0.10	1.46±0.06	1.47±0.12
	RMSD†† (m^3m^{-3})	0.013	0.016	0.010	0.012	0.013
	MoD†† (m^3m^{-3})	0.0025	-0.0003	0.0015	0.0005	0.0011
	f_{pos}††	58.1%	43.3%	57.4%	53.5%	53.1%
Wet Seasons	α_w (m^{-1})	3.23x/2.61	5.70x/1.74	3.91x/2.72	13.10x/2.71	5.42x/2.71
	n_w (-)	1.69±0.15	1.52±0.27	1.60±0.23	1.43±0.09	1.56±0.22
	RMSD†† (m^3 m^{-3})	0.024	0.012	0.016	0.011	0.016
	MoD†† (m^3m^{-3})	-0.0002	0.0018	-0.0004	0.0006	0.0005
	f_{pos}††	58.8%	59.0%	59.0%	60.5%	59.3%
Dry/Wet Ratios	α_d/α_w	1.83	1.40	1.25	0.68	1.24
	n_d/n_w	0.88	0.96	0.93	1.03	0.94

† ×/ means "by a factor of" for log-normally distributed parameters α, α_d, and α_w.
†† The value here was the average of those of all the water balance stations at the corresponding depth.

E.3.3 Evaluation of Hysteresis in Water Retention

The water content versus water pressure relationship generally also depends on the history of the wetting or drying process (Gillham et al. 1979; Hillel 1980; Jaynes 1992; Likos et al. 2014; Lu et al. 2013; Royer and Vachaud 1975; Simunek et al. 1999; Vachaud and Thony 1971). For a hysteretic soil, the water content is higher in a drying process than in a wetting process for a given water pressure (Hillel 1980). Under the Hanford semi-arid climate condition, the barrier soil generally gains infiltration water and becomes wetter in the wet season from November to March, and loses water and becomes drier in the dry season from April to October (Gee et al. 1992; Gee et al. 2005). Short-term drying events did occur during the wet season and short-term wetting events occurred during the dry season. For a soil with stronger hysteresis, the main drying and wetting curves would be farther apart and the scanning loops would be larger. The effects of the short-term processes on hysteresis were considered secondary relative to the primary wetting or drying process. To investigate the hysteresis in the primary processes, we divided the observations into two groups: one for the wet seasons and the other for the dry seasons. The observations at the 0.45-m depth during the wet seasons are shown as filled symbols and those during the dry seasons as open symbols in Figure E.3. For some of the stations (e.g., S2, S4, and S9), the wetting

and drying water retentions followed nearly the same curve. Slight hysteresis can be seen at other stations, especially when the water content is relative low (e.g., <0.20 m^3m^{-3}).

To quantify the primary hysteresis, parameters α and n for the dry seasons (α_d and n_d) and the wet seasons (α_w and n_w) were fitted to the data for corresponding seasons, respectively, while θ_s and θ_r were fixed as their corresponding NH values. The degree of hysteresis was also quantified with the mean of difference (MoD) in water content between the observations and the predictions with the NH-WRC. A positive value of MoD indicates the observed average is higher than the predicted average. Additionally, the fraction (f_{pos}) of the count of the observations larger than the corresponding predictions was calculated. A value of f_{pos} > 50% means more observations were larger than the corresponding predictions.

The geometric average of α_d for the dry seasons was larger than that of α_w for the recharge period at three of the four depths, while parameter n_d behaved in the opposite way and was less than n_w for the same three depths (Table E.2). On average, the α_d/α_w ratio was 1.24 and the n_d/n_w ratio was 0.94. The average MoD ranged between -0.0004 and 0.0025 m^3m^{-3} for the observation in both the summer and winter seasons. Considering the measurement resolution of an NP is about 0.01 m^3m^{-3}, these average MoD values were all near zero. On average, 53.1% of the observations in the summer seasons and 59.3% in the winter seasons were greater than the corresponding NH-WRC predictions. The near unity values of α_d/α_w and the n_d/n_w ratios, near-zero MoD values, and near 50% f_d values all indicate negligible hysteresis of the WRC for the silt loam storage layer of the barrier.

The lack of hysteresis is surprising, especially when the soil was relatively wet (e.g., >0.2 m^3m^{-3}). It is possible that air entrapment was very minor because often the infiltration rate was generally small and there was often sufficient time for air to migrate or to be dissolved. Another reason may be that water is a strong wetting fluid in the barrier soil and there was no strong advancing or receding meniscus under the field condition. The weak hysteresis especially when the soil was relatively wet is surprising. Fayer and Gee (1997) tested the hydrological processes in an ET barrier constructed also with the Warden silt loam in a 2-m diameter lysimeter using computer simulations. They found that the simulation that considered hysteresis predicted the water content and water pressure the best. A significant difference between a lysimeter and a field is that a lysimeter has an impermeable wall. More air tends to be trapped in a lysimeter than in the field during the infiltration process. Hence, the hysteresis in a lysimeter could be enhanced and part of it might be due to air entrapment.

E.3.4 Temporal Variation of Water Retention

To examine the change of water retention with time, the observations were divided into three periods representing the years 1995 to 1996, 1997 to1998, and 2000 to 2003. All data for the 0.45-m depth for the three periods are shown in different colors in Figure E.3. Visually, the data for the three periods are mingled together, indicating no obvious change in soil water retention with time for all the locations. The potential temporal variation of the WRC was also quantified with the MoD between the observations and the predictions with the corresponding NH retention curves. The average MoD values were -0.0006, -0.0039, and -0.0078 m^3m^{-3} for the 1995 to 1996, 1997 to 1998, and 2000 to 2003 periods, respectively, and were considered very small comparing with the detection resolution of an NP. These results demonstrate no detectable temporal variation of the WRC of the Warden silt loam during the 9-year monitoring period.

This result contradicts the findings of many investigators, such as those of Benson et al. (2007) for 10 alternative covers. Most of the soils in Benson et al. (2007) for barrier construction seem finer than the Warden silt loam used for the PHB storage layer. For example, the Warden silt loam contained about 8% clay particles, while only two soils in Benson et al. (2007) contained ≤8% clay particles. One of the two

soils (i.e., at Apple Valley, CA) did not show a measurable change in soil hydraulic properties. Benson et al. (2007) pointed out that the hydraulic properties of cover soils converge to common values over time. Hence, higher content of clay or initial compaction could be the cause of large change in hydraulic properties of the cover soils in Benson et al. (2007).

During the construction of the barrier, the retention properties of the Warden silt loam were characterized in the laboratory with 16 samples, and the mean retention parameters were θ_s = 0.449 m^3m^{-3}, θ_r = 0.082 m^3m^{-3}, α = 0.621 m^{-1}, and n = 1.847. The retention properties were also measured in the Field Lysimeter Test Facility (FLTF), where some of the lysimeters was filled with Warden silt loam, as reported in Fayer et al. (1992) (θ_s = 0.411 m^3m^{-3}, θ_r = 0.0 m^3m^{-3}, α = 4.19 m^{-1}, and n = 1.29). Figure E.4 compares the predicted retention curves using these parameters and the mean NH parameters with the field-observed data at the PHB at the 0.45-m depth (Table E.2). Comparing with the field retention at the PHB, the laboratory-measured retention significantly overestimates water content especially when water content is high. The main reason is the much higher laboratory-measured θ_s (0.449 m^3m^{-3}) than the field value (0.344 m^3m^{-3}). The FLTF retention also overestimated water content especially when θ is high (roughly > 0.15 m^3m^{-3}) but it underestimates water content when the soil is relatively dry. The main reason is the zero value of θ_r estimated at the FLTF. The prediction RMSEs were 0.055 m^3m^{-3} using the NH average retention, 0.078 m^3m^{-3} using the FLTF retention, and 0.145 m^3m^{-3} using the laboratory-measured retention. However, these differences should not be considered as the temporal impacts on the retention properties. Instead, the differences were caused by the uncertainty of measurement methods or samples. The results based on the 9-year field data are expected to better represent the retention properties of the silt loam storage layer of the PHB.

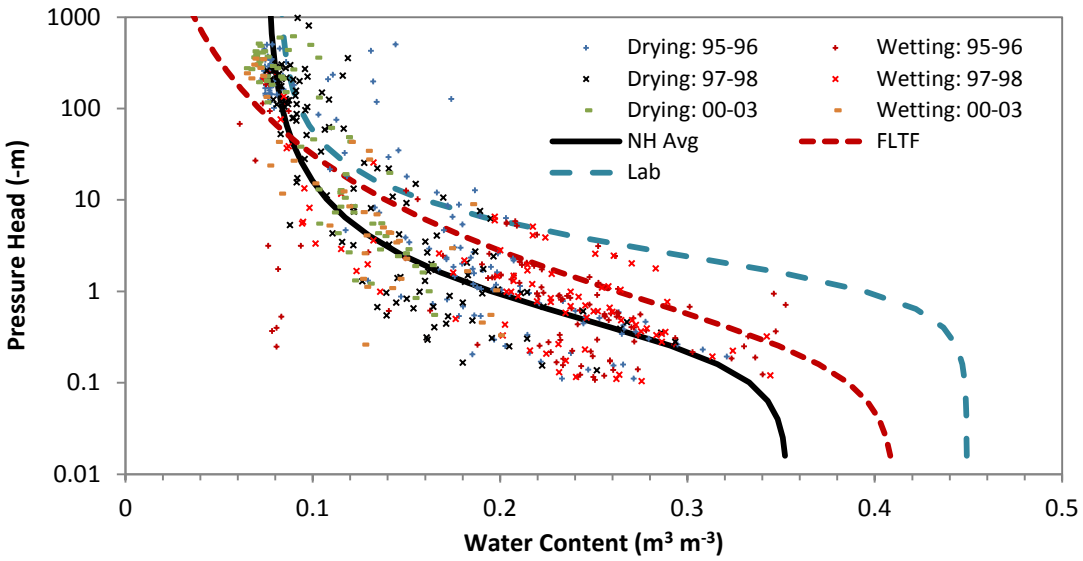

Figure E.4. Comparison of observed soil water retention at the 0.45-m depth and model predictions. There were 583 observations in the plot.

E.4 Conclusions

The *in situ* water content measured by a neutron probe and water pressure by the heat dissipation units from 1995 to 2003 were matched up at four depths and 12 monitoring stations. These data covered a very wide range of water content, from near saturation to the values beyond the wilting point (i.e., -150 m). The geometric mean of the measured minimum *h* over all the stations at the four depths ranged between -

309 and -667 m with an overall mean of -448 m. These very low pressure values imply that the vegetation at the PHB under a semi-arid climate can tolerate higher water stress and could use some water beyond the commonly assumed wilting point. The minimum water content observed across the field was 0.058±0.004 m^3m^{-3}, which could not be used by the vegetation.

The field WRCs of local soils at 36 locations were determined based on the field-measured water content and pressure, and each curve contained 51 to 96 points. The curves were described with the van Genuchten (1980) model. It was found that the spatial variations of parameters θ_s, θ_r, and n were relative small, with the coefficient of variation being no more than 18%. However, parameter α varied by a factor of 2.33 and the range of one standard deviation was from 2.34 to 12.7 m^{-1}. The spatial variability of the retention properties appeared to be larger than the effects of added 15% w/w pea gravel on the properties.

Additionally, the potential existence of hysteresis of water retention was evaluated by grouping the data by the discharge period (from April to October) and the recharge period (from November to March); the temporal variation of the WRC was evaluated by dividing the data into three periods: 1995 to 1996, 1997 to 1998, and 2000 to 2003. The mean of difference between the observations and the predictions by the corresponding NH-WRCs was used to quantify the effects of hysteresis and time. The results show that neither hysteresis nor time had a detectible effect on the WRCs.

References

Albright, WH, CH Benson, and WJ Waugh. 2010. *Water Balance Covers for Waste Containment Principles and Practices*. ASCE Press, Reston, Virginia.

Benson, CH, PJ Bosscher, DT Lane, and RJ Pliska. 1994. "Monitoring-System for Hydrologic Evaluation of Landfill Covers," *Geotechnical Testing Journal*, 17(2):138-149.

Benson, CH, IE Kucukkirca, and J Scalia. 2010. "Properties of Geosynthetics Exhumed from a Final Cover at a Solid Waste Landfill," *Geotextiles and Geomembranes*, 28(6):536-546. doi:10.1016/j.geotexmem.2010.03.001.

Benson, CH and MA Othman. 1993. "Hydraulic and Mechanical Characteristics of a Compacted Municipal Solid-Waste Compost," *Waste Management & Research*, 11(2):127-142. doi:10.1177/0734242x9301100205.

Benson, CH, A Sawangsuriya, B Trzebiatowski, and W Albright. 2007. "Post-Construction Changes in the Hydraulic Properties of Water Balance Cover Soils," *J. of Geotech. and Geoenv. Engr*, 133(4):349-359.

Canone, D, S Ferraris, G Sander, and R Haverkamp. 2008. "Interpretation of Water Retention Field Measurements in Relation to Hysteresis Phenomena," *Water Resources Research*, 44(4):1-14. doi:10.1029/2008wr007068.

CSI. 2009. *229 Heat Dissipation Matric Water Potential Sensor*, Campbell Scientisic, Inc., Logan, Utah.

DOE-RL. 2013. *Hanford Site Cleanup Completion Framework*, DOE/RL-2009-10, Rev. 1, U.S. Department of Energy Richland Operations Office, Richland, Washington. Available at http://www.hanford.gov/files.cfm/Comp_Framework_Jan_%201-23-13-lfm.pdf

DOE. 1987. *Final Environmental Impact Statement - Disposal of Hanford Defense High-Level, Transuranic and Tank Wastes,* DE/EIS-0113, U.S. Department of Energy, Richland, Washington.

Fayer, MJ and GW Gee. 1997. Hydrologic Model Tests for Landfill Covers Using Field Data. In TD Reynolds and RC Morris *Proceedings of Landfill Capping in the Semi-Arid West: Problems, Perspectives, and Solutions,* Environmental Science and Research Foundation, Idaho Falls, ID.

Fayer, MJ, ML Rockhold, and MD Campbell. 1992. "Hydrologic Modeling of Protective Barriers: Comparison of Field Data and Simulation Results," *Soil Sci. Soc. Am. J.*, 56:690-700.

Flint, AL, GS Campbell, KM Ellett, and C Calissendorff. 2002. "Calibration and Temperature Correction of Heat Dissipation Matric Potential Sensors," *Soil Sci. Soc. Am. J.*, 66:1439-1445.

Gee, GW, MJ Fayer, ML Rockhold, and MD Campbell. 1992. "Variations in Recharge at the Hanford Site," *Northwest Science*, 66(4):237-250.

Gee, GW, JM Keller, and AL Ward. 2005. "Measurement and Prediction of Deep Drainage from Bare Sediments at a Semiarid Site," *Vadose Zone Journal*, 4:32-40.

Gee, GW, AL Ward, and MJ Fayer. 1997. "Surface Barrier Research at the Hanford Site," *Land Contamination & Reclamation*, 5(3):233-238.

Gillham, RW, A Klute, and DF Heermann. 1979. "Measurement and Numerical Simulation of Hysteretic Flow in a Heterogeneous Porous Medium," *Soil Sci. Soc. Am. J.*, 43(6):1061-1067.

Henken-Mellies, WU and A Schweizer. 2011. "Long-Term Performance of Landfill Covers - Results of Lysimeter Test Fields in Bavaria (Germany)," *Waste Manag Res*, 29(1):59-68. doi:10.1177/0734242X10385748.

Hillel, D. 1980. *Fundamentals of Soil Physics*. Academic Press, New York.

Iryo, T and RK Rowe. 2004. "Numerical Study of Infiltration into a Soilgeotextile Column," *Geosynthetics International*, 11(5):377-389.

Jaynes, DB. 1992. "Estimating Hysteresis in the Soil Water Retention Function," *the International Workshop on Indirect Methods for Estimating the Hydraulic Properties of Unsaturated Soils*, 219-232 pp. University of California, Riverside.

Kaluarachchi, JJ and JC Parker. 1987. "Effects of Hysteresis with Air Entrapment on Water Flow in the Unsaturated Zone," *Water Resources Research*, 23(10):1967-1976.

Khire, MV, CH Benson, and PJ Bosscher. 1999. "Field Data from a Capillary Barrier and Model Predictions with UNSAT-H," *Journal of Geotechnical and Geoenvironmental Engineering*, 125(6):518-527.

Klausner, Y. 1991. *Fundamentals of Continuum Mechanics of Soils*. Springer-Verlag, New York.

Lee, KS. 2007. "Effects of Hysteresis in K-S-P Relationships on the Performance of Mine-Waste Soil Covers," *Geoscience Journal*, 11(3):241-247.

Likos, WJ, N Lu, and JW Godt. 2014. "Hysteresis and Uncertainty in Soil Water-Retention Curve Parameters," *Journal of Geotechnical and Geoenvironmental Engineering*, 140(4):04013050. doi:10.1061/(ASCE)GT.1943-5606.0001071.

Lu, N, M Kaya, BD Collins, and JW Godt. 2013. "Hysteresis of Unsaturated Hydromechanical Properties of a Silty Soil," *Journal of Geotechnical and Geoenvironmental Engineering*, 139(3):507-510. doi:10.1061/(ASCE)GT.1943-5606.0000786.

Meer, SR and CH Benson. 2007. "Hydraulic Conductivity of Geosynthetic Clay Liners Exhumed from Landfill Final Covers," *Journal of Geotechnical and Geoenvironmental Engineering*, 133(5):550-563. doi:10.1061/(asce)1090-0241(2007)133:5(550).

Meerdink, JS, CH Benson, and MV Khire. 1997. "Unsaturated Hydraulic Conductivity of Two Compacted Barrier Soils - Closure," *Journal of Geotechnical and Geoenvironmental Engineering*, 123(12):1187-1188. doi:10.1061/(ASCE)1090-0241(1997)123:12(1187).

Melchior, S, V Sokollek, K Berger, B Vielhaber, and B Steinert. 2010. "Results from 18 Years of in Situ Performance Testing of Landfill Cover Systems in Germany," *J. Environ. Eng.*, 136:815-823. doi:10.1061/ASCE/EE.1943-7870.0000200.

Oostrom, M, TW Wietsma, CE Strickland, VL Freedman, and MJ Truex. 2012. "Sensor and Numerical Simulator Evaluation for Porous Medium Desiccation and Rewetting at the Intermediate Laboratory Scale," *Vadose Zone Journal*, 11(1):0. doi:10.2136/vzj2011.0089.

Or, D and JM Wraith. 2001. "Soil Water Content and Water Potential Relationships." In *Soil Physics Companion*, ed. AW Warrick, pp. 49-84. CRC Press, Boca Raton.

Reece, CF. 1996. "Evaluation of Line Heat Dissipation Sensor for Measuring Soil Matic Potential," *Soil Sci. Soc. Am. J.*, 60:1022-1028.

Romano, N and A Santini. 2002. "Field." In *Methods of Soil Analysis Part 4 Physical Methods*, eds. JH Dane and CT Topp, pp. 721-738. Soil Science Society of America, Inc., Madison, Wisconsin USA.

Royer, JM and G Vachaud. 1975. "Field Determination of Hysteresis in Soil-Water Characteristics," *Soil Sci. Soc. Am. J.*, 39(2):221-223.

Simunek, J, R Kodesova, M Gribb, and MT van Genuchten. 1999. "Estimating Hysteresis in the Soil Water Retention Function from Cone Permeameter Experiments," *Water Resources Research*, 35(5):1329-1345.

Stormont, JC and CE Anderson. 1999. "Capillary Barrier Effect from Underlying Coarser Soil Layer," *J. of Geotechnical and Geoenvironmental Engineering*, 125(8):641-648.

Tami, D, H Rahardjo, and EC Leong. 2004. "Effects of Hysteresis on Steady-State Infiltration in Unsaturated Slopes," *Journal of Geotechnical and Geoenvironmental Engineering*, 130(9):956-966.

Truex, MJ, M Oostrom, CE Strickland, GB Chronister, MW Benecke, and CD Johnson. 2012. "Field-Scale Assessment of Desiccation Implementation for Deep Vadose Zone Contaminants," *Vadose Zone Journal*, 11(4):0. doi:10.2136/vzj2011.0144.

Vachaud, G and JH Dane. 2002. "Instantaneous Profile." In *Methods of Soil Analysis Part 4 Physical Methods*, eds. JH Dane and CT Topp, pp. 937-944. Soil Science Society of America, Inc., Madison, Wisconsin USA.

Vachaud, G and J-L Thony. 1971. "Hysteresis During Infiltration and Redistribution in a Soil Column at Different Initial Water Contents," *Water Resources Research*, 7(1):111-127.

van Genuchten, MT. 1980. "A Closed-Form Equation for Predicting the Hydraulic Conductivity of Unsaturated Soils," *Soil Science Society of America Journal*, 44:892-898.

Wierenga, PJ, RG Hills, and DB Hudson. 1991. "The Las Cruces Trench Site: Characterization, Experimental Results, and One-Dimensional Flow Predictions," *Water Resources Research*, 27(10):2695-2705.

Wing, NR and GW Gee. 1994. "Quest for the Perfect Cap," *Civil Engineering*, 64(10):38-41.

Yang, C, D Sheng, and JP Carter. 2011. "Hysteretic Seepage Analysis in Unsaturated Soil Covers." In *Unsaturated Soils: Theory and Practice*, eds. Jotisankasa, Sawangsuriya, Soralump, and Mairaing. Kasetsart University, Thailand.

Zhang, Q, AD Werner, RF Aviyanto, and JL Hutson. 2009. "Influence of Soil Moisture Hysteresis on the Functioning of Capillary Barriers," *Hydrological Processes*, 23(9):1369-1375. doi:10.1002/hyp.7261.

Zhang, ZF, AL Ward, and GW Gee. 2004. "A Combined Parameter Scaling and Inverse Technique to Upscale the Unsaturated Hydraulic Parameters for Heterogeneous Soils," *Water Resources Research*, 40(8):1-13. doi:10.1029/2003wr002925.

Appendix F

Evaluating of the Hydrological Monitoring Systems at the Prototype Hanford Barrier

Z. Fred Zhang

Pacific Northwest National Laboratory
Richland, Washington

Content

List of Figures

List of Tables

Abstract

Monitoring data have errors because of the limitations of the instruments or methods used, and the level of error may change with time for a given instrument. The performance of the Prototype Hanford Barrier (PHB), which was constructed in 1994 to isolate the underlying waste, was evaluated using data from monitoring instruments. It is important to examine the performance of the monitoring systems at PHB so that the monitoring data can be used properly in evaluating the PHB performance. At the PHB, the systems for monitoring hydrological variables include the neutron probe (NP) and two types of MP-917 time-domain reflectometry (TDR) probes for measuring water content; concrete vaults equipped with dosing siphons, pressure transducers, and tipping buckets for drainage; heat dissipation units (HDUs) and fiberglass blocks (FGBs) for soil-water pressure; pan lysimeter for percolation through the asphalt layer; rain gauges for irrigation; and load cells for precipitation. Except for the NP and rain gauges, data collection from the instruments was controlled by data loggers connected to peripherals such as batteries, solar panels, and multiplexers. The monitoring data from 1994 to 2013 were used to evaluate the monitoring systems. The monitoring systems were evaluated in three tiers: (1) system performance based on indicators of duration of service, data completeness, and fraction of valid data; (2) sensor performance based on indicators of data instability and measurement uncertainty; and (3) data representativeness based on variation in replicates. The performance indicators were graded as *A* for good performance, *B* for intermediate performance, and *C* for poor performance. After a comprehensive evaluation, the *A*-grade systems were those for the NP, tipping buckets, and rain gauges. The *B*-grade systems were those for MP-917 TDR with long probes, the HDUs, and the pan lysimeter. The C-grade systems were those for MP-917 TDR with short probes, the FGBs, and load cells. Among the three evaluation tiers, data representativeness for most systems had the lowest grade, *C*. The results of this investigation are useful for the selection and installation/layout of sensors, the design of the system, and data collection methods for subsurface hydrological monitoring.

Because of the limitation of instruments or the methods used, monitoring data have errors and some monitoring instruments may fail during the monitoring period for many reasons. Hence, it is important to examine the performance of the monitoring systems at the Prototype Hanford Barrier (PHB) so that the monitoring data can be used properly in evaluating PHB performance. This appendix evaluates the instruments and associated peripherals for monitoring hydrological variables at the PHB.

F.1 Introduction

Surface barriers (also known as surface covers) are used to isolate underlying waste from intrusion and to reduce or eliminate the movement of meteoric precipitation into the waste zone. The design life of surface barriers usually varies from decades to hundreds of years or longer depending on the barrier's purpose. To evaluate the performance of a surface barrier, the static hydrological characteristics (i.e., soil water content, θ, and soil water pressure head, *h*) and dynamic hydrological characteristics (i.e., flow rate, *q*) of the barrier need to be monitored. In the past few decades, a variety of methodologies for measuring θ and *h* at the field conditions has been developed, while the methods for measuring *q* in situ remain limited. The majority of these methods measure θ and *h* indirectly, meaning the measurement is related with θ or *h* by a calibration function. The representative spatial extent of each measurement also varies considerably, ranging from local scale (several centimeters to tens of centimeters), to field scale (several meters to hundreds of meters), to watershed scale (~1 km and larger). For a field scale surface barrier, the measurements of θ and *h* are generally at the local scale and those of *q* is often at field scale.

Soil water content indicates how much water is in the barrier or other media. A few reviews of methods for measuring θ at different spatial scales are available (e.g., Bittelli 2011; Dobriyal et al. 2012; IAEA 2008; Imhoff et al. 2007; Ochsner et al. 2013; Robinson et al. 2008; Topp and Ferre 2002). The gravimetric method measures θ directly by taking a soil sample and drying it at 105°C (Topp and Ferre 2002) or 110°C (ASTM 2010) in an oven and is the reference method to measure θ. The neutron scattering method uses a neutron probe (NP) to measure θ by emitting fast neutron and counting the number of slow neutrons (Gardner and Kirkham 1952). The density of slow neutrons is proportional primarily to θ. By far, the NP is the most accurate indirect method for measuring θ (Evett 2008). Soil permittivity can be derived by measuring the travel time of an electromagnetic (EM) wave traveling back and forth with instruments such as a time domain reflectometry (TDR) (Topp et al. 1980) or a ground-penetrating radar, or by measuring the one way travel time using a time domain transmissometry (Young et al. 2000), or by measuring the frequency of the EM wave on probes such as a frequency domain reflectometry (FDR) or capacitance probe (Campbell and Anderson 1998). A variety of EM-based probes are available commercially (Blonquist Jr. et al. 2005; Robinson et al. 2008).

Soil water pressure (aka soil water potential, matric potential) indicates how tightly soil water is attached to soil particles because of capillary and adsorptive forces. Water retained in smaller soil pores is absorbed by larger capillary forces. The relationship between θ and *h* is called the soil water retention (or characteristic) curve and is dependent on the texture of the soil. The sum of *h* and gravity head makes the hydraulic head, which is the driving force of water flow in most soils with low salt concentration. Some important properties of a soil can be defined based on *h*. For example, the field water capacity of a soil may be approximated by water content at $h = -1$ m or $h = -3.3$ m (Hillel 1980) and the wilting point by $h = -150$ m (Or and Wraith 2001; Romano and Santini 2002).

From the monitoring point of view, *h* has a much larger range of variation than θ, especially when θ is relatively low. Hence, monitoring *h* provides another line of evidence of soil water condition at a given time and location. Methods for measuring *h* were reviewed by, e.g., Scanlon et al. (2002) and Durner and Or (2005). The tensiometry method measures soil water pressure based on the equilibrium of water pressure in the soil and water in the tensiometer through a porous cup (Buckingham 1907). Although it is the most widely used technology for measuring soil water pressure, the *h* measurement range of a

tensiometer is between 0 and -10 m. The reference media method determines *h* based on measuring θ or θ-related properties in well-characterized reference porous media that are in hydrostatic equilibrium with the surrounding soil. Reference porous materials can be blocks of gypsum, fiberglass, nylon, or granular matrix (Durner and Or 2005; Scanlon et al. 2002). Measurement of *h* is obtained by measuring electrical resistance, heat dissipation, or electromagnetic properties of the reference porous medium. The reference porous medium method is best for the condition of intermediate wetness roughly between -1 m and -10^4 m (Durner and Or 2005). The thermocouple psychrometry measures *h* based on equilibrium between liquid soil water and water vapor in the ambient soil atmosphere. It suits very dry conditions, with the measurement of *h* ranging between roughly -10^4 and -10^7 m (Durner and Or 2005). Different from soil water content sensors, water pressure sensors are all for point measurement and no single sensor is currently capable of covering the entire range of interest. A list of soil water pressure instruments is given in Durner and Or (2005).

Soil water flux indicates how fast water migrates in the soil. A commonly used field method to determine soil water flux is to measure drainage using the lysimetry technique (e.g., Allen et al. 1991), which has been used to monitor drainage through surface barriers (e.g.,Albright et al. 2004). Heat pulse probes (e.g.,Kamai et al. 2008) have been used to measure relatively high soil water flux (e.g., during a storm or irrigation) but are not sensitive enough to the low water flux, e.g., below a surface barrier.

One of the challenges of hydrological monitoring is the performance of the monitoring instruments because most instruments are designed to function for only a few years and the test duration of these instruments often is even shorter, e.g., from days to several years. Chow et al. (2009) compared nine commonly used soil water sensors in a sandy loam soil located in Fredericton, NB, Canada, in the summer of 1999 for about 3 months. They found that the CS615 (FDR), Trase (TDR), and Troxler (NP) performed the best with the factory calibrations; TRIME (quasi-TDR based), Moisture Point (MP-917 TDR), and Gopher (capacitance probe) performed slightly worse; and the Gypsum (resistance block), WaterMark (resistance block), and Netafim (capacitance) showed a need for careful calibration before application.

Paige and Keefer (2008) compared the field performance of the ML2x Theta Probes, the Hydra Probe 1 sensors, and the TDR100 system, all using either the TDR or the capacitance technique for measuring water content, for about 9 months. The sensors detected an inconsistent trend when comparing the responses from the sensors to individual precipitation events. Evett et al. (2009) evaluated the field performance of four EM sensors (EnviroSCAN, Diviner, PR1/6, and Trime) against the NP over a period of 3 years. The three capacitance EM sensors produced water content readings for which the standard deviation (σ) values were up to an order of magnitude larger than those from the NP; the EM sensor based on travel time (waveguide) principles produced σ values up to six times larger than those of the NP or gravimetric sampling.

Most instruments or sensors for hydrological monitoring are controlled and data are collected by an automated system. Additional components needed may include a data logger, a battery often powered by a solar panel, and different types of wires of variable lengths. Some monitoring systems also include other components such as multiplexers for a TDR system or an excitation module for a heat dissipation unit (HDU) system. To our knowledge, no evaluation was conducted for the entire system for hydrological monitoring to the life of the instruments or in a relatively long (e.g., a decade or longer) period.

A surface barrier, termed the Prototype Hanford Barrier (PHB), was constructed from late 1993 to 1994 at the U.S. Department of Energy's Hanford Site near Richland, Washington. The primary function of the PHB is to minimize infiltration of water through the buried waste and contaminated soil. Successful performance of the primary function depends on the operation of a series of interactive and dynamic processes that control precipitation, infiltration, redistribution, water storage in the silt loam barrier, and loss of water. Barrier performance has been monitored since 1994 to present. The systems for monitoring hydrological variables include the NP and two types TDR probes for measuring water content; concrete

vaults (similar to pan lysimeters) equipped with dosing siphons, pressure transducers, and tipping buckets for drainage; HDUs and fiberglass blocks (FGBs) for soil-water pressure; pan lysimeter for percolation through the asphalt concrete; rain gauges for irrigation; load cells for precipitation; and a flow meter for runoff. Except for the NP and rain gauges, data collection from the instruments was controlled by data loggers connected to peripherals such as batteries, solar panels, multiplexers, and surface units as applicable.

The monitoring data between 1994 and 2013 were used to evaluate these monitoring systems. The 19-year monitoring duration is longer than the life of many sensors or instruments. The purpose of this paper is to evaluate the monitoring systems by the system performance, instrument/sensor performance, and data representativeness with six indicators, as applicable. The performance of each monitoring system is then graded based on the average or cumulative values of these indicators. The performance of the monitoring systems is important not only for evaluating the performance of the PHB, but also in guiding the design of future long-term monitoring system for a surface barrier or other purpose. The evaluation concept may be used to assess the performance of other monitoring systems.

F.2 Surface Barrier Design and Hydrological Monitoring

The PHB was constructed between late 1993 and 1994 over the 216-B-57 Crib in the 200-BP-1 Operable as a mound over the ground surface to demonstrate its constructability and long-term performance for a design period of 1000 years. The description and design of the PHB are reported in other sources (e.g., DOE-RL 1994, 1999; Gee et al. 1997; KEH 1993; Ward and Gee 1997; Ward et al. 2011 ; Wing and Gee 1994). Details of the design of the PHB and tests at the PHB are also summarized in Appendix B. The PHB consists of four main components (Figure F.1): (1) a silt loam evapotranspiration (ET) layer with an underlying capillary break and an intrusion prevention layer, termed the evapotranspiration-capillary (ETC) barrier, in the middle; a gentle pit-run gravel side slope in the west (10:1) and in the west portions of the north and south side slopes (5:1 to 3:1); (3) a 2:1 steep basalt riprap side slope in the east and in the east portion of the north and south side slopes; and (4) an asphalt concrete (AC) barrier with a polymer-modified fluid applied asphalt coating and a compacted soil layer at the bottom. The ETC barrier is the centerpiece of the PHB and sits directly above the waste zone. It is designed to store precipitation and release the stored water into the atmosphere and to deter intrusion by plants, animals, or humans from barrier surface. The retention properties of the silt loam for constructing the ETC barrier is reported in Appendix E and Zhang (2015). The two side slopes protect the ETC barrier from damage or intrusion. The AC barrier is the redundant barrier to divert drainage and to hinder intrusion.

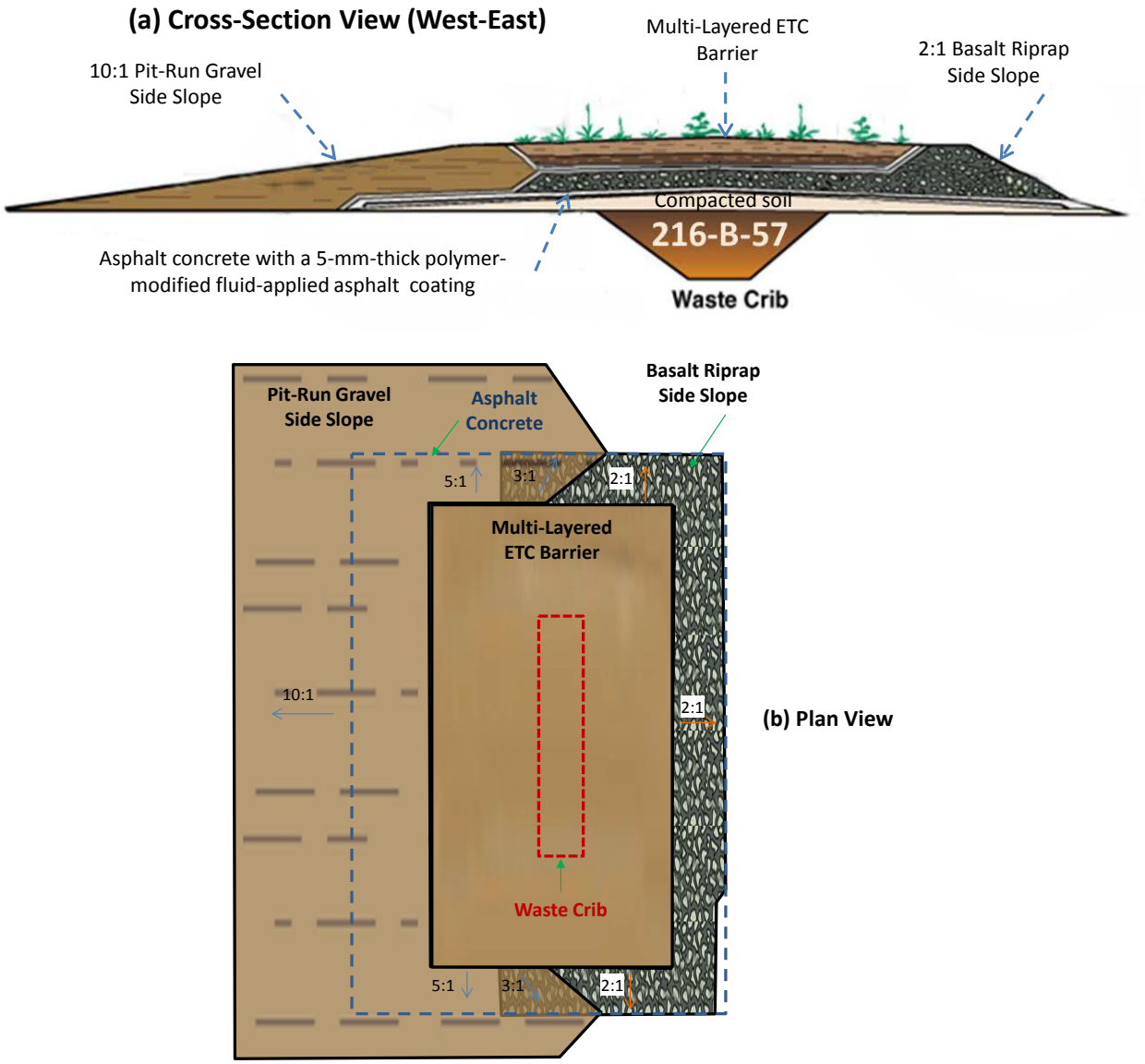

Figure F.1. Schematic of the Prototype Hanford Barrier: (a) cross-section view (west-east) and (b) plan view (approximate scale).

The systems for monitoring hydrological variables at the PHB are summarized in Table F.1 and details of the monitoring systems are described in Appendix C. The primary water-balance components monitored for hydrologic performance evaluation of the PHB included precipitation and irrigation, surface runoff, water storage within the ETC barrier, drainage from the ETC barrier and side slopes, and deep percolation through the AC. Secondary confirmative components monitored include θ at the bottom of the silt loam and beneath the AC, *h* within the silt loam, and *h* below the AC barrier.

Table F.1. The monitoring systems and the hydrological variables monitored.

Monitored Variable	Name of Instrument or Sensor	Manufacturer	Peripherals
Soil water content	503 DR hydroprobe	CPN Corporation, Martinez, CA	NA (manual operation)
Soil water content	MP-917 TDR with long or short probes	Environmental Sensors, Inc., Victoria, BC, Canada	1 surface unit, 1 solar panel, 1 battery, 1 data logger†, 1 multiplexers
Soil water pressure	229L HDUs	Campbell Scientific, Inc., Logan, UT	4 solar panels, 4 batteries, shared data logger
Soil water pressure	MC-314 soil moisture cells (FGBs)	ELE International, Inc., Lake Bluff, IL	1 solar panel, 1 battery, 1 data logger
Drainage	Orenco dosing siphons; Druck PDCR 950/TI-0855-1 pressure transducers; and RainWise tipping buckets	Orenco Systems, Inc., Sutherlin, OR; Instrumart, South Burlington, VT; RainWise, Inc., Trenton, ME	1 solar panel, 1 battery, 1 data logger
Percolation	Pan lysimeter	NA	1 solar panel, 1 battery, 1 data logger, 1 pump, 1 tipping bucket
Irrigation	Rain gauges	NA	NA (manual operation)
Precipitation	6762 load cells	Revere Transducers, Cerritos, CA	1 solar panel, 1 battery, shared data logger
Runoff	ISCO flowmeter	Lincoln, NE	1 surface unit, 1 battery, 1 solar panel
NA: not available; †Data logger: CR7 by Campbell Scientific, Inc.			

F.3 Evaluation Methods

There are no standard criteria for evaluating the performance of an instrument or a monitoring system because the criteria vary depending on the purpose of the monitoring. For example, Yoder et al. (1997) evaluated 23 soil water sensors based on the criteria of accuracy, reliability, durability, and installation factors. Imhoff et al. (2007) used criteria such as the accuracy of measurement, ability to track infiltration front, reliability in the landfill environment, and cost to evaluate the instruments for measuring water in landfills. Evett et al. (2009) examined the spaiotemporal variability of EM and NP sensors in access tubes by their accuracy, variability among sensors, and the volume of sensing. Vaz et al. (2013) evaluated the factory-supplied calibration functions of eight EM moisture sensors by their accuracy. Davis et al. (2012) analyzed the power characteristics of sensors in wireless sensor networking systems based on data sampling and transmission rates in order to achieve extended battery life. Here the purpose of evaluating the monitoring systems is for the best assessment of the long-term hydrological performance of the surface barrier.

Instrument Performace Tiers and Indicators

The monitoring systems at the PHB were evaluated in three tiers: (1) *system performance* based on three indicators: duration of service, data completeness, and fraction of valid data; (2) *sensor performance* based on two indicators: data instability and measurement uncertainty; and (3) *data representativeness* based on the variation among replicates. A robust system for long-term monitoring is expected to have long duration of service, high completeness of data, high fraction of valid data, low instability in data, low uncertainty, and good data representativeness. These six indicators are described below.

Tier 1: System Performance

An amount of problem is caused by the malfunction a monitoring system component, including both the sensors and the peripherals. The system performance is evaluated based on the following three indicators.

Duration of service: When a monitoring system cannot produce acceptable data and it is not or cannot be repaired, the service of the system terminates. The duration of service is the period from when the system started in service to the time service was terminated. For some sensors, this reflects the life of the monitoring system associated with a group of sensors. Exceptions exist when a monitoring system (e.g., the rain gauges for measuring irrigation) is terminated after completing the planned measurement. There may be data gaps during the service period for reasons either related or not related to the monitoring system, e.g., because the monitoring activity is discontinued.

Data completeness: A data logging system may be shut down because of a system malfunction or planned system maintenance. System malfunctions include (but are not limited to) sensor problems, low battery voltage, and problems related to data loggers, solar panels, and wires. System malfunction may lead to the loss of data or bad data. Data completeness is quantified as the ratio of the count of data logged per fiscal year (FY) to that planned. Because of the large data sets collected at the PHB and for the ease of data processing using Excel, when data logging was more frequent than daily, data completeness was calculated based on daily average values for the monitoring systems (e.g., TDR, drainage). Higher data completeness means fewer problems with the system and hence possible less system maintenance.

Fraction of valid data: Invalid data may be collected when one or more components malfunction while the system is still in operation. Invalid data consist of unreasonable values (e.g., negative water content), error codes, and missing data. A higher fraction of valid data indicates better performance of the monitoring system.

Tier 2: Sensor Performance

Sensors are the cores of a monitoring system. Sensor malfunctions may lead to incorrect data, large instability, or large uncertainty even when the rest of the monitoring system functions normally. Sensor performance was evaluated based on the following two indicators.

Data instability: This indicator evaluates the temporal impacts on data quality. Data instability is evaluated either by data noise is the fluctuation of data during a period of hours to days or by the change of sensor properties or a sudden shift of a data trend in months or years.

Measurement uncertainty: This indicator evaluates the measurement error of a specific method or sensor. For NP and TDR, the uncertainty of water content measurements was evaluated by comparing the calculated soil water storage changes before and after the simulated 1000-year rainstorms, each of which added about 69 mm of water to the storage layer of the ETC barrier. The uncertainty of the load cells was assessed by comparing the measured precipitation results with the data from the nearby Hanford Meteorological Station (HMS), about 3 miles west of the PHB. The uncertainty of other instruments could not be assessed because there were no reliable measurements available. Thus, other instruments were evaluated by their resolution of detection.

Tier 3: Data Representativeness

Even when a sensor and the peripherals function normally, the data may not represent the field condition well. For example, if a sensor is installed incorrectly or in an unrepresentative location, the data representativeness can be poor. Data representativeness was generally assessed by the standard deviation (σ), coefficient of variation (CV), or the range of variation of the same measurement among replicates of the same treatment, depending on the nature of the data. The variation might be caused by instrument error or spatial variability in the field.

Although the six indicators were assigned to three different tiers, the indicators in one tier may reflect issues in another. For example, invalid data may be caused by the malfunction of either peripherals or sensors. Although it is impossible to strictly distinguish performance at each of these three tiers because they often are intertwined, this does not affect the evaluation of monitoring systems. These six indicators are expected to cover most issues related to monitoring system performance.

Because of the drastically different types of monitoring systems, not all of the above criteria were applied to all the monitoring systems. For example, the representativeness of the pan lysimeter could not be evaluated because there was only one pan lysimeter installed. Additionally, the sensor performance was conducted for a group sensors of the same type rather than for individual sensors.

Performance Grades

Each of the performance indicator was further graded qualitatively as *A* for good performance, *B* for intermediate performance, and *C* for poor performance. Although these grading criteria for the variables used in monitoring evaluation (Table F.2) are empirical and subjective, they can indicate the relative performance of the monitoring systems. In order to calculate the average within each tier, numerical values are assigned to each grade: 0 to 1 for grade *C*, 1 to 2 for grade *B*, and 2 to 3 for grade *A*. The mid-values (i.e., 0.5, 1.5, and 2.5 for *C*, *B*, and *A*, respectively) are used in calculating the averages. After taking the average within each tier, an average among the three tiers was taken for the overall performance of each monitoring system. The numerical values were than remapped into the letter grades.

Table F.2. Performance grades and grading criteria for the variables used in monitoring evaluation.

Variable Used in Asessment	Performance Grades		
	A (Good Performance)	B (Intermediate Performance)	C (Poor Performance)
Duration of service (yr)	≥10	5 to 10	<5
Data completeness	≥90%	70% to 90%	<70%
Fraction of valid data	≥90%	70% to 90%	<70%
Assessment based on water content (m^3m^{-3})	<0.01	0.01 to 0.03	≥0.03
Assessment based on 2-m water storage (mm)	<20	20 to 60	≥60
Soil water pressure	< a factor[†] of 1.5	A factor of 1.5 to 3	≥ a factor of 3
Drainage volume (m^3)	<0.0001	0.0001 to 0.1	≥0.1
Monthly precipitation (mm)	<2	2 to 6	≥6
Drainage rate (mm yr^{-1})	<0.1	0.1 to 1	≥1
[†] Relative to the geometric mean			

F.4 Results

The following sections present the evaluation sequentially for the monitoring systems NP, 917-MP TDR, drainage measuring instruments (i.e., dosing siphons, pressure transducers, and tipping buckets), HDU, pan lysimeter, FGB, rain gauge, and load cell. For each monitoring system, the system performance is presented first to give the "big picture," followed by a description of sensor performance and data representativeness.

F.4.1 Neutron Probe

System Performance

The NP used was purchased in 1987 and used initially at the Hanford Field Lysimeter Test Facility to support the design of the surface barrier. The same NP was used throughout the monitoring period at the PHB. Hence, the duration of service for the NP was 26 years, longer than the monitoring period at the PHB.

There were missed NP loggings at the larger depths of water balance stations. .The two neutron access tubes installed in the gravel side slope were deformed slightly at depths of about 1.8 and 1.5 m, respectively. As a result, the NP was inaccessible at these depths and below until the deformation was corrected in October 1996. Logging was unintentionally missed on occasion at the lowest one or two depths. Sometimes logging was skipped intentionally at some stations or at some depths. Regardless of

the reason, the data completeness was 97.6%. Nearly all the NP data were valid and hence the fraction of valid data was 100%.

Sensor Performance

The instability in the NP-logged data was evaluated using the shield counts, N_s, which are the counts from the time when the neutron detector was placed in the shield and the probe was positioned on top of the access tube. The mean and standard deviations of N_s among the 14 monitoring stations from 1995 to 2013 were calculated. Considering the radioactive decay and the change to a new neutron detector in 2003, the measured N_s was scaled to the counts in 1995 before conducting further analysis. The variation of μ and σ of the scaled shield counts with time is shown in Figure F.2. The mean scaled shield counts were generally stable during the 19-year monitoring period. The CV for N_s ranged from 0.8% to 14.3%, with an average of 2.3%.

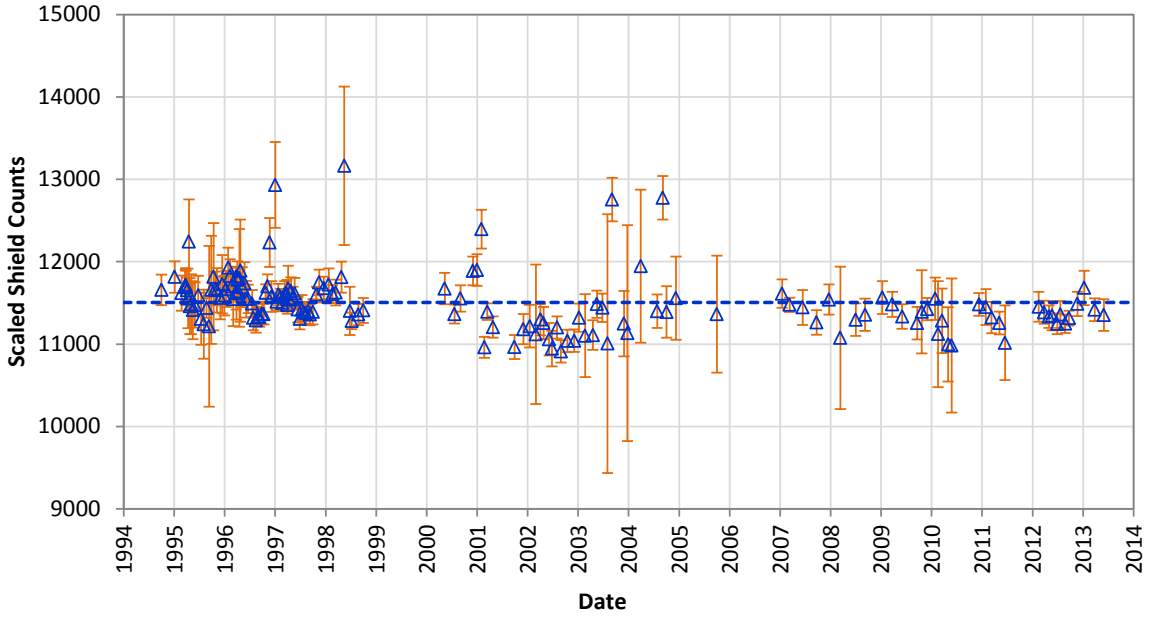

Figure F.2. Scaled shield counts from 1994 to 2013. The vertical bars indicate the range of one standard deviation. The dashed lines indicate the mean of all observations.

The uncertainty of the NP was assessed by comparing the changes in the measured soil water storage before and after the simulated 1000-year, 24-hour rainstorms in 1995, 1996, and 1997 against the amount of water applied during an 8-hour storm period. The water loss by ET between the two NP loggings was considered negligible compared with the large amount of water (about 69 mm) applied. Water storage in the 2-m-thick storage layer was calculated based on the water content measured with the NP. The top-most NP measurements were extrapolated to the ground surface and the bottom-most measurements to the 2-m depth when calculating storage.

The water applied was measured with six rain gauges and soil water content in the irrigated area was measured at six monitoring stations. Comparison of the NP-measured water storage change with the applied amount of water indicates that the NP overestimated the amount of water by 4.3, 14.2, and 12.3 mm in 1995, 1996, and 1997, respectively, with an average overestimation of 10.3 mm (Figure F.3), which is 14.8% of the applied water.

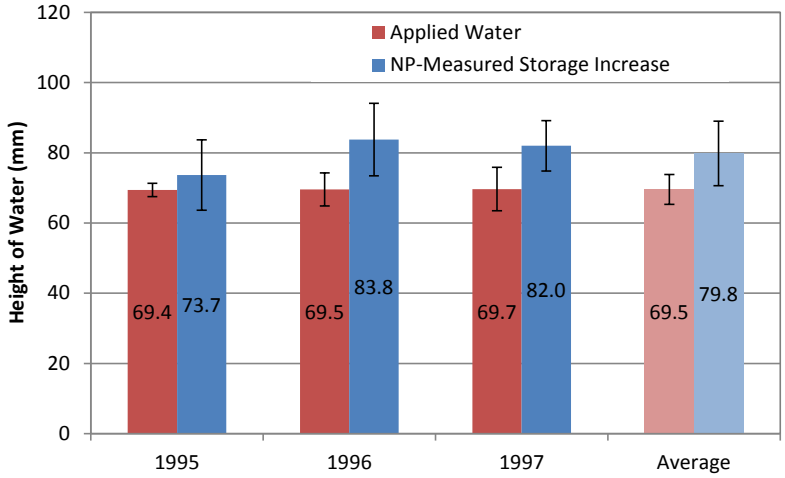

Figure F.3. Comparison of the amount of water applied and computed water storage change based on neutron probe measurements before and after the three simulated 1000-year storms.

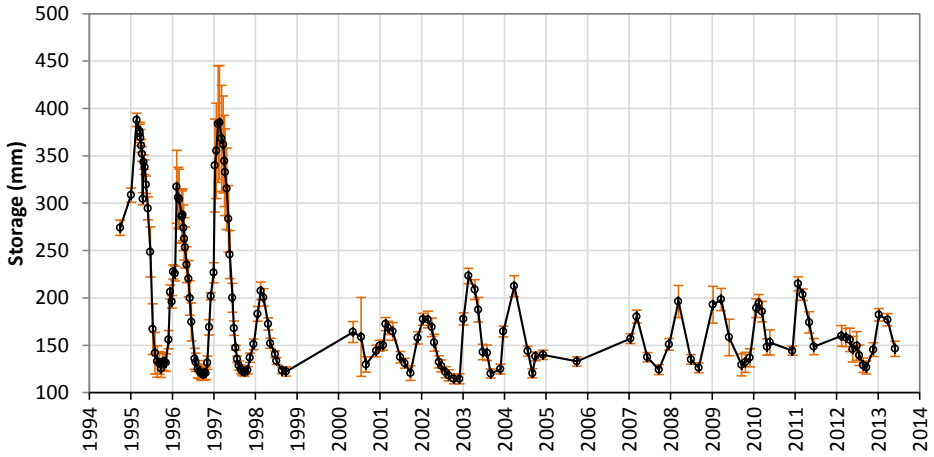

Figure F.4. Average 2-m water storage measured with a neutron probe among the six (from FY95 to FY99) or 12 (from FY00 to FY13) monitoring stations under the natural precipitation condition. The vertical lines indicate the range of one standard deviation.

Data Representativeness

NP data representativeness was evaluated by the standard deviation of the 2-m water storage for silt loam among the monitoring stations under the natural precipitation condition. These included the 6 stations for the south section of the PHB from FY95 to FY99 and the 12 stations on the barrier surface in FY00 and after. The μ and σ of the water storage in the 2-m-thick silt loam are plotted in Figure F.4. The difference among the stations was considered small, as indicated by the small standard deviation of 12.5 mm and the coefficient of variation of 6.2% on average. This difference was comparable with the approximate ±10.3-mm measurement uncertainty of the NP, indicating the NP data could represent the field condition well.

The performance of the NP is summarized in Table F.3. The NP performance was graded *A* for all six indicators in all three tiers. Hence, the overall system performance was also high, indicating the very high reliability of NP. The excellent performance of NP has also been demonstrated elsewhere (Evett et al. 2009; Staub et al. 2010). For example, the monitoring of a sanitary landfill at Karlsruhe, Germany, using neutron probes continued for 17 years (Augenstein et al. 2010).

Table F.3. Performance of the neutron probe.

Performance Type	Indicator	Evaluation Result	Performance Grade
System Performance	Duration of service (yr)	26	A
	Data completeness	97.6%	A
	Fraction of valid data	100%	A
Sensor Performance	Data instability	±2.3%	A
	Data uncertainty‡	10.3 mm average	A
Data Representativeness†	Standard deviation	±12.5 mm average	A

†2-m water storage from 1994 to 2013
‡2-m soil water storage change before and after the simulated 1000-year storms in March of 1995, 1996, and 1997.

F.4.2 MP-917 Time Domain Reflectometry

System Performance

Customized 1.85-m-long MP-917 TDR (Environmental Sensors, BC Canada) probes, referred to as the long probes, were used to monitor water content from 1995 to early 2001 at all 14 monitoring stations. The 0.75-m-long type H and the 0.6-m-long type K TDR probes, referred to as the short probes, were used from late 2001 to 2005 at 8 of the 14 monitoring stations as replacements for the long probes. The TDR controller and readout unit remained unchanged when the probes were replaced. The TDR system was not under maintenance in FY05 and FY06 and hence no data were collected during this period. The TDR system was reactivated in FY07 but the data were very poor and considered unqualified. The system was shut down in FY08. Hence, the duration of service was 6 years for the long TDR probes and 5 years for the short probes.

The TDR system needed regular or even intensive maintenance when in service. The systems were shut down during maintenance, causing data loss. The data completeness of the two TDR systems is shown in Figure F.5. The results indicate that the TDR system needed frequent maintenance in the first year or two, then appeared to perform relatively well in the next 2 to 3 years. After that, the system started performing poorly and eventually reached a condition that was not maintainable. The data completeness varied between 25% and 98% with an average of 74% for the long probes and between 11% and 99% with an average of 57% for the short probes.

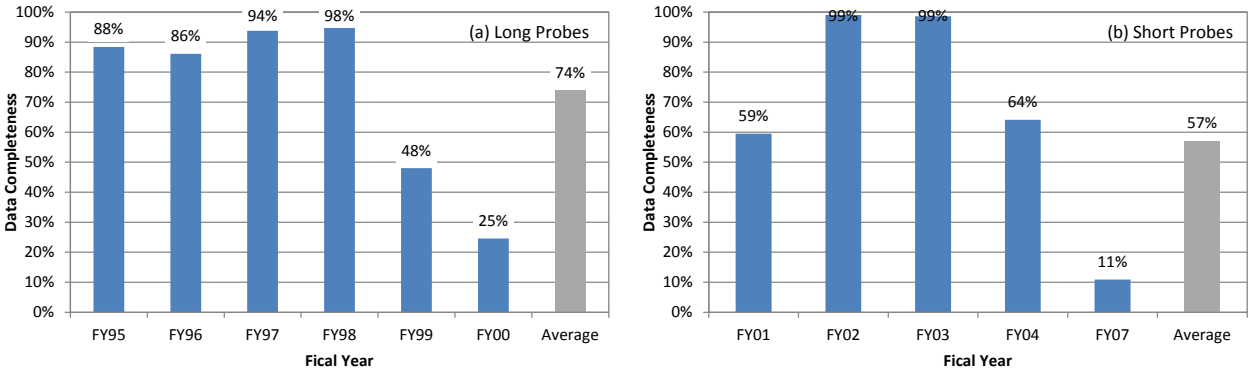

Figure F.5. TDR data completeness of the (a) long probes from FY95 to FY00 and (b) the short probes from FY01 to FY07.

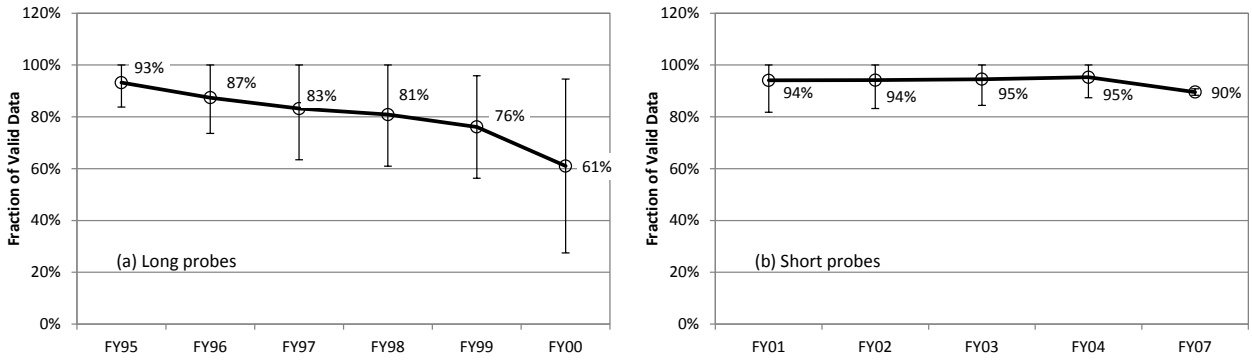

Figure F.6. Fraction of valid data of (a) the long TDR probes and (b) the short (Types H and K) TDR probes. The vertical bars indicate the standard deviation among the 14 long probes or 24 short probes.

The invalid TDR observations were those that were either denoted by an error code, had a value of less than zero, or had a value greater than 0.5 m^3m^{-3}, which is substantially greater than 0.344±0.056 m^3m^{-3}, the porosity of the soil (Zhang 2015). Causes of the invalid data included probe and surface component malfunctions. In the first year of monitoring (FY95), 11 of the 14 long TDR probes produced a minimum of 97.0% of valid data; the probes in stations S02, S05, and S11 performed poorly from the time they were installed. As time went on, the probes generally produced less valid data. The performance of the TDR probes decreased considerably just 1 year later from 93% to 87% valid data (Figure F.6a). Five years later, the fraction of valid data decreased to a mere 61% in FY00 (Figure F.6a), when nearly half of the probes produced more invalid data than valid data. As the fraction of valid data from the long TDR probes decreased with time, the standard deviation increased (Figure F.6a), indicating poorer performance with time. On average, the fraction of valid data over the 6-year monitoring period was 80%.

The fraction of valid data from FY01—when the long probes were replaced by the short probes—through FY04 is shown in Figure F.6b. Note there were no data for FY05 and FY06 because of monitoring discontinuity, while the data collected in FY07 were considered unqualified. With the exception of 5 (S03-2, S06-2, S09-2, S10-3 and S12-2) of the 24 probes, the probes produced a high percentage (97% or higher) of valid data from FY01 to FY04, indicating improved sensor property. On average, the fraction of valid data for the short probes over the 5 monitoring years was 93.5%.

Sensor Performance

The data instability of TDR probes was evaluated by the noise in the data. In contrast to the NP-measured data, the TDR data generally suffered from high noise, although the data were within the valid range. The noise existed at different time scales (e.g., hourly or daily). In this evaluation, the level of noise in the observations was obtained by computing the deviation ($\Delta\theta$) of the daily average from the 5-day moving average. Then the root of mean squares of $\Delta\theta$ for each fiscal year was calculated (Figure F.7). A smaller deviation indicates less noise in the data. The degree of noise in the data is categorized as low ($\Delta\theta < 0.01$ m^3m^{-3}), intermediate ($\Delta\theta$ between 0.01 and 0.03 m^3m^{-3}), or high ($\Delta\theta > 0.03$ m^3m^{-3}).

In the first monitoring year (FY95) using the long TDR probes, 10 of the 14 probes showed low noise, 3 intermediate noise, and 1 high noise. The noise level generally increased with time. The average noise level almost doubled in the second year (Figure F.7a). Five years later (in FY00), the average noise level was more than four times that of the first year. With a low data completeness of 25% (Figure F.5), a low fraction of valid data of 61% (Figure F.6), and high noise in the valid data (Figure F.7), the performance of the TDR system was considered unacceptable in FY00. On average, the noise was 0.023 m^3m^{-3} over the 6 years of monitoring.

The noise level in the data from the short probes was also very low in their first year of service, with 20 of the 24 probes having low noise, 2 intermediate noise, and 2 high noise (Figure F.7b). The noise level increased in the following years from 0.01 in FY01 to 0.016 m^3m^{-3} in FY02, but remained relatively stable in FY03 and FY04. On average, the noise was 0.012 m^3m^{-3} over the 4 years of monitoring.

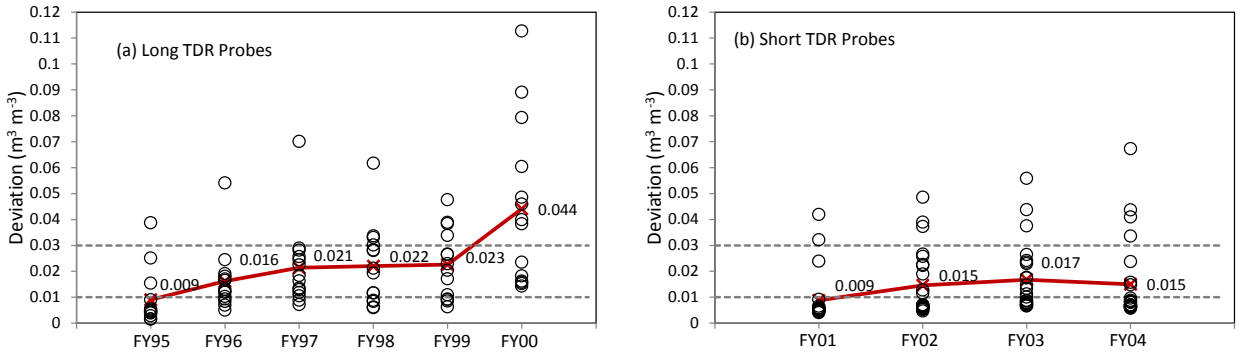

Figure F.7. Deviation of soil water content from the 5-day moving average as measured by (a) the long-TDR probes and (b) the short TDR probes. The circles show the values for individual probes and the red lines show the average values.

To examine the uncertainty of the measurements, the changes in the measured daily average soil water storage between the day before and the day after the simulated 1000-year, 24-hour rainstorms in 1996 and 1997 were compared to the amount of water applied. Note there were no TDR data at the time of the simulated rainstorm in 1995. The ET over the 2-day period was not considered. Comparison of TDR-measured and applied amount of water (Figure F.9) indicates that the TDR underestimated the amount of water by 37.6 mm in 1996 and 10.3 mm in 1997, with an average underestimation of 23.9 mm. The difference in 1996 was very large and possibly due to high noise in the TDR system. Furthermore, there was a very large variation among the TDR measurements, as shown by the vertical bars in Figure F.9.

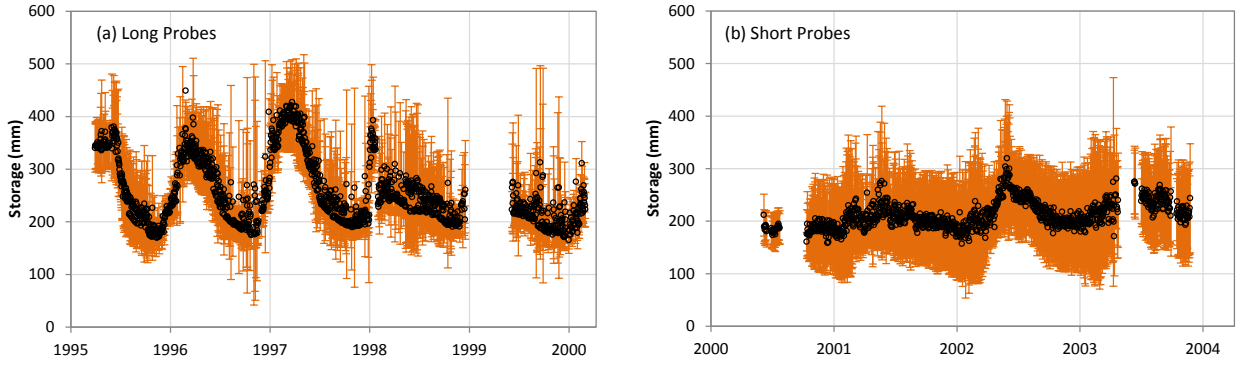

Figure F.8. Average water storage measured with the time-domain reflectometry among the 6 (from FY95 to FY99), or 12 (for FY00), or 8 (from FY00 to FY04) monitoring stations under the natural precipitation condition. The vertical lines indicate the range of one standard deviation. The data shown are daily average values. Data for FY95 through FY00 are from the long probes and data for FY01 through FY04 are from the short probes.

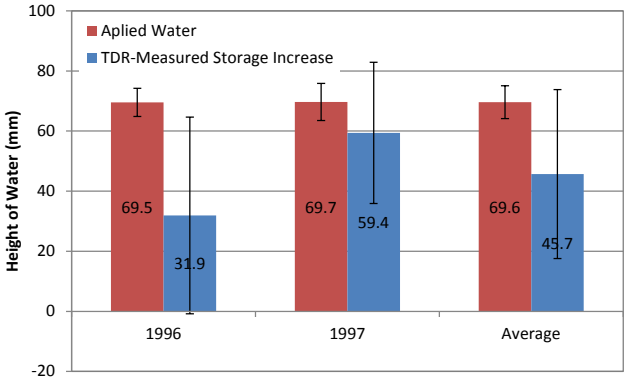

Figure F.9. Comparison of the amount of water applied and the computed water storage change based on TDR measurement before and after the two simulated 1000-year storms in 1996 and 1997.

Data Representativeness

The data representativeness of TDR probes was evaluated by the standard deviation of 2-m water storage for silt loam among the monitoring stations under the natural precipitation condition. These include the 6 observations for the south section from FY95 to FY99, all the 12 monitoring stations for FY00, all the 8 monitoring stations from FY01 to FY04. The time course for the water storage in the 2-m-thick silt loam based on these observations is plotted in Figure F.8. There were relatively large differences among the stations, as indicated by the σ values of 49.4 mm for the long probes and 77.9 mm for the short probes. The relatively large σ values are partially attributed to the very small (several centimeters) sensing range (Evett et al. 2009), noise in the signal as described above, temperature impacts on the sensor and cable (Evett et al. 2005; Olmanson and Ochsner 2006; Pepin et al. 1995), and potential air gap between the probes and the surrounding soil.

The overall performance of the MP-917 TDR systems with the long and short probes is briefly summarized in Table F.4. The short probes indeed show some improvement in the fraction of valid data and data noise, but poor data representativeness was a critical problem. The overall performance of the TDR system with the long probes was graded as *B* for intermediate performance and that of the system with short probes was graded as *C* for poor performance.

Cichota et al. (2008) examined performance of the MP-917 probes from internal drainage experiments in 2 consecutive years by comparing the spatial and temporal variation patterns of water content with that of soil water pressure. The results showed consistency in the variation pattern for the tensiometry data, where the MP-917 estimates were inconsistent, with decreasing sensitivity over time. Chow et al. (2009) compared nine soil water content sensors on a sandy loam soil in New Brunswick, Canada, for about 3 months. They found that the MP-917 probe could not capture the correct pattern of soil water content.

Hence, the data from 917-MP TDR with long probes at the PHB may be used only as a confirmation of field hydrological processes for a relatively short period of about 3 to 4 years. The data from the system with short probes may not be used for barrier performance assessment. Neither of the TDR systems is suitable for long-term (i.e., a decade or longer) monitoring.

However, the performance of MP-917 may not represent other types of TDR probes because the design of the MP-917 TDR probes is different from other TDR probes in that it includes diode switches to profile water content (Hook et al. 1992). For example, TDR probes (model CS615, Campbell Scientific Inc., Logan, UT) were used to monitor the ET cover over the contaminated site at Technical Area 49 at Las Alamos National Laboratory, and the 4-year results appeared to be reasonable (Levitt et al. 2005). Reasonable results were also obtained from TDR probes (type not specified) in monitoring a municipal

solid waste landfill in Michigan (Khire and Haydar 2005). A review of advances using TDR probes can be found in Robinson et al. (2003).

To further examine the long-term performance of the MP-917 TDR system, 2-m soil water storage based on TDR measurements was compared with water storage based on NP readings. Figure F.10 compares the average water storage in the 2-m soil from 1995 to 2000. Figure F.11 compares the average 2-m water storage based on the water content measured by the short TDR probes from 2001 to 2004. Although results from the two methods correctly reflect the seasonal variation, there are substantial differences between the two. Compared with the NP, the TDR probes appear to have considerably overestimated water storage when soil was relatively dry but were less sensitive to water content change when the soil was relatively wet.

One purpose of the frequent (i.e., hourly or more frequent) soil moisture monitoring using the TDR system was to understand the short-term behavior of the soil moisture. However, there was strong noise in the hourly data or even in the daily average data as shown in Figure F.10 and Figure F.11. The strong noise in the data prevented data use for the short-term flow processes. The noise in the data led to very large errors in the calculated 2-m soil water storage and hence limited their use for water balance analysis.

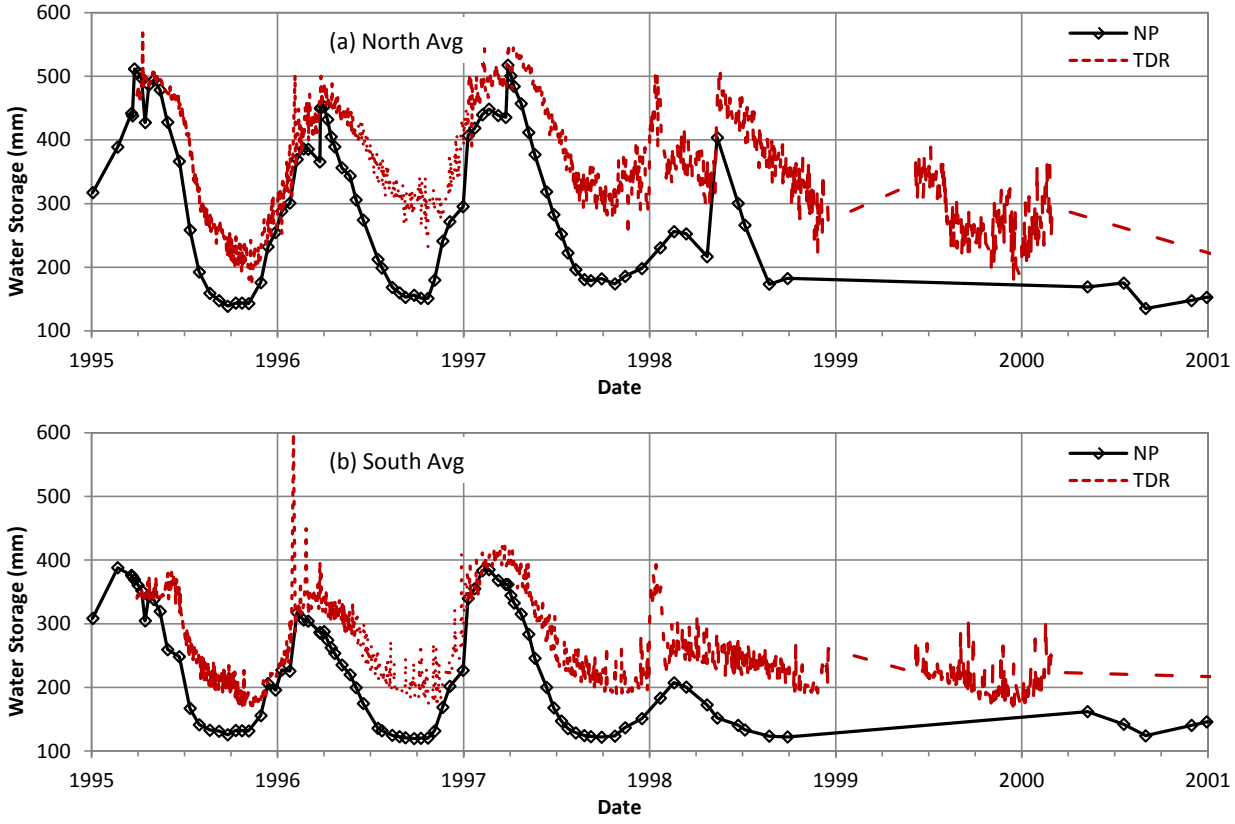

Figure F.10. Spatially averaged water storage from 1995 to 2000 of (top) six monitoring stations in the north section (S01 to S06) and (bottom) six monitoring stations in the south section (S07 to S12). The north section was irrigated to three times the average precipitation from FY95 to FY97. The TDR system was the Soil Moisture MP-917 with the customized 1.85-m-long probes. The TDR data plotted are the daily average values.

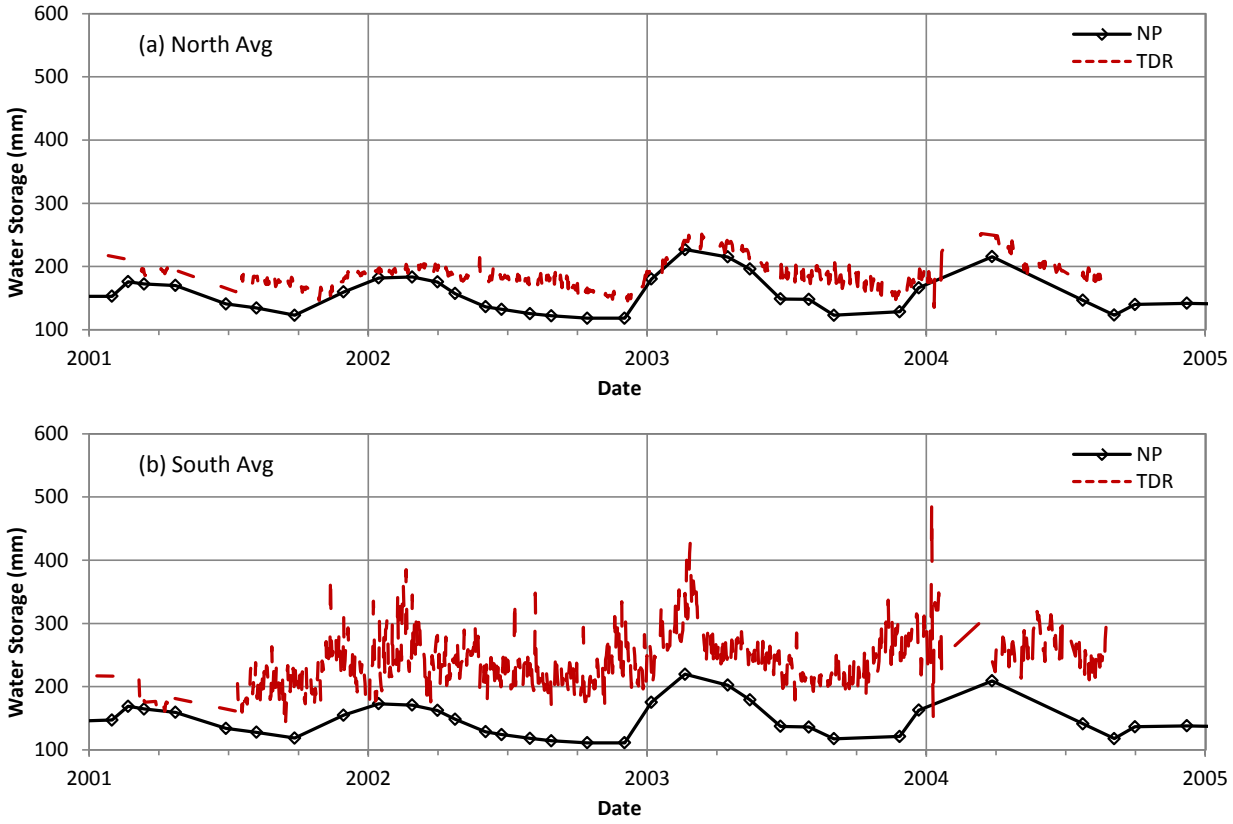

Figure F.11. Spatially averaged water storage from 2001 to 2004 of (top) six monitoring stations in the north section (S01 to S06) and (bottom) six monitoring stations in the south section (S07 to S12). The north section was irrigated to three times the average precipitation from FY95 to FY97. The TDR system was the soil moisture MP-917 with type H and K probes installed in FY01. The TDR data plotted are the daily average values.

Table F.4. Performance of the MP-917 TDR monitoring systems.

		Long TDR Probes		Short TDR Probes	
Performance Type	**Indicator**	**Evaluation Result**	**Performance Grade**	**Evaluation Result**	**Performance Grade**
System Performance	Duration of service (yr)	6	B	6	B
	Data completeness	74%	B	57%	C
	Fraction of valid data	80%	B	94%	A
Sensor Performance	Data instability† (m^3m^{-3})	0.023	B	0.014	B
	Data uncertainty‡ (mm)	-23.9	B	N/A	N/A
Data Representativeness††	Standard deviation (mm)	±49.4	B	±77.9	C

†Deviation of the observations from the 5-day moving average.
††2-m water storage.
‡2-m soil water storage change before and after the simulated 1000-year storms in March of 1996 and 1997.

F.4.3 Instruments for Drainage Measurements

The instruments for measuring drainage in each drainage vault included a dosing counter, a pressure transducer, and a tipping bucket. The vaults and the siphon system were also necessary for drainage measuring using a dosing counter or a pressure transducer. The whole system shared a data logger

powered by a battery and a solar panel. Although the instruments are treated as one measuring system, performance of different types of measuring instruments is described separately as applicable.

System Performance

The drainage monitoring system was in service from 1995 to 2013, with a service duration of 19 years. During the monitoring period, the drainage data were logged generally hourly or more frequently. There were some data gaps, the causes of which were not documented but may have included the lack of system maintenance, system malfunction, or discontinuity of monitoring. The data completeness was 90% or more in 12 of the 19 years (Figure F.12). The data completeness was 89% on average (excluding FY08 and FY09). However, data loss generally had a small impact on the calculation of total drainage because the data were recorded as cumulative values, meaning that the total values could still be correct even with some data loss.

The invalid data consisted of either error codes or negative values. Four of the pressure transducers stopped functioning in the summer of 2012 when they were repaired. The pressure transducer for 5E became noisy in FY04 and produced invalid (negative) values occasionally in this year and the years that followed. In FY95, the dosing counter stopped functioning for 10 days soon after the drainage system started operating. In winter of FY13, the battery voltage was too low (<10 V) for the data logger to correctly record the data. During the whole monitoring period, the fraction of valid data was 99.6% for the dosing counters, 93.4% for the pressure transducers, and 97.2% for the tipping buckets, indicating excellent performance.

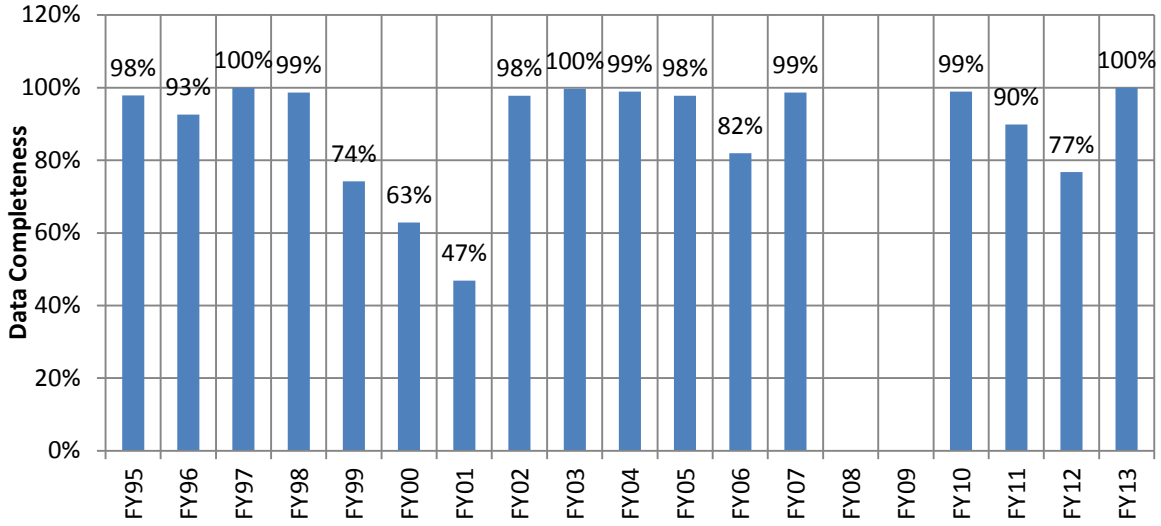

Figure F.12. Drainage data completeness for drainage monitoring system in each fiscal year during the monitoring period.

Sensor Performance

The data instability of dosing volume, response of pressure transducers, and volume of tipping buckets were evaluated based on the differences between two separate calibrations. The dosing volumes of the vaults and pressure transducers were calibrated in 1994 and again in 2000. On average, the difference in dosing volume between the two calibrations ranged from -14.1% to 18.2%, with an average difference of -1.8%.

The responses of the pressure transducers were evaluated based on the soil water pressure per millivolt change in voltage. The responses were between 29.9 and 32.3 cm with an average of 31.3 cm in 1995, and

were between 31.8 and 34.4 cm with an average of 32.8 cm in 2012. The difference between 2012 and 1995 varied from 1.8% to 10.9%, with an average of 4.9%.

The volume of the tipping buckets was calibrated in 1994 and 2012. From 1994 to 2012, the volume change varied between -12% and 47%, with an average of 17%. These values translate to errors of corresponding magnitude in drainage rate by the tipping buckets.

The measurement uncertainty was assessed based on the sensor resolution and the range of measurement. The dosing counters were used to record the counts of siphons. The minimum amount of drainage that can be detected is about 0.6 m^3 using a dosing counter, $10^{-3}m^3$ using a pressure transducer, and about $10^{-5}m^3$ using a tipping bucket.

Data Representativeness

From FY99 to FY12, the difference from the average drainage rate of plots with the same design and under the same hydrological condition was between 0.4 and 12.8 mm yr^{-1} with an average of 5.1 mm yr^{-1} for measurements using dosing counters, between 0.3 and 12.9 mm yr^{-1} with an average of 5.3 mm yr^{-1} using pressure transducers, and between zero and 2.5×10^{-3} mm yr^{-1} with an average of 2.5×10^{-4} mm yr^{-1} using tipping buckets. Generally, the drainage rates had relatively large variability, indicating that replicates are a must in monitoring drainage using these methods.

The performance of the system for measuring drainage is summarized in Table F.5. The low to intermediate performance of data representativeness indicates that replicates for measuring drainage are of critical importance. The applicability of the three methods for measuring drainage rate was limited by the range of measurement for each instrument. The measured annual drainage rates from the three types of instruments are summarized in Table F.6 through Table F.11.

The tipping buckets could measure drainage as small as about 11 ml (3.4×10^{-5} mm for the main plots), which is several orders of magnitude better than those of the dosing counter or pressure transducer. However, the tipping buckets could not respond fast enough when the instant drainage rate was larger than approximately 0.4 L min^{-1}.

The dosing counters had a resolution of 0.6 m^3 (1.8 mm for the main plots). The counters occasionally (approximately once a year or less) missed recording a dose or recorded a fake dose when there was no actual siphoning going on. The causes for these incorrect responses are unknown but added more instability to the measurements. The pressure transducers had a resolution of about 1 L (3.1×10^{-3} mm for the main plots). The measurements of both the dosing counters and the pressure transducers were affected by water loss via evaporation or seepage from a vault. It appears that the drainage rates measured by the dosing counters or pressure transducer were of good quality for the side slope plots (Table F.6 and Table F.7) but were not appropriate for other plots, as indicated by a majority of negative values. The zero or negative drainage rates might be produced because of water loss caused by evaporation or seepage or low resolution.

Hence, data from the tipping buckets are appropriate for determining the drainage rates from the silt loam barrier plots and the transitional plots (Table F.8 through Table F.11) but might underestimate the high drainage rates such as those from the side slopes (Table F.6 and Table F.7). The dosing counters and pressure transducers may only be used to determine the drainage rates from the side slopes. The measurement range of a tipping bucket may be improved by using one with a larger tipping and shorter tipping time.

Table F.5. Performance of monitoring system for measuring drainage.

Performance Type	Indicator	Dosing Counters		Pressure Transducers		Tipping Buckets	
		Evaluation Result	Grade	Evaluation Result	Grade	Evaluation Result	Grade
System	Duration of	19	A	19	A	19	A

Performance	service (yr)						
	Data completeness	89%	A	89%	A	89%	A
	Fraction of valid data	99.6%	A	93.4%	A	97.2%	A
Sensor Performance	Data instability	-1.8%††	A	4.9%§	A	17%‡	B
	Data uncertainty	±0.6 m^3	C	±10^{-3} m^3	B	±10^{-5} m^3	A
Data Represen-tativeness	Difference from average (mm yr^{-1})	5.1	C	5.3	C	2.5×10^{-4}	A

NA: negligible and not evaluated.
† Some malfunctioning sensors were replaced during the period.
†† Dosing volume change between 1994 and 2000.
§ Change in pressure per millivolt change in voltage between 1995 and 2012.
‡ Tipping bucket volume change between 1994 and 2012.

Table F.6. Annual drainage rate (mm yr^{-1}) from the gravel side slope. (The green-yellow-red color scale indicates drainage rates from high to low.)

	South (1W)			**North (4W)**		
	Dosing Counter	**Pressure Transducer**	**Tipping Bucket**	**Dosing Counter**	**Pressure Transducer**	**Tipping Bucket**
FY95	19.5	21.1	6.2	31.0	40.7	28.2
FY96	76.4	72.1	30.0	94.8	139.2	101.2
FY97	156.3	155.5	113.4	167.7	208.8	48.7
FY98	28.4	27.0	17.6	43.8	41.9	14.0
FY99	10.7	8.0	1.9	20.1	19.4	0.0
FY00	16.0	17.0	0.0	29.2	28.4	14.6
FY01	7.1	7.8	0.0	18.2	18.9	0.0
FY02	8.9	10.6	3.9	23.7	23.1	21.1
FY03	0.0	-0.9	24.4	45.6	45.4	12.9
FY04	0.0	0.5	9.8	36.5	36.7	3.2
FY05	0.0	0.5	0.1	0.0	0.6	0.7
FY06	0.0	0.1	10.8	20.1	18.1	16.7
FY07	1.8	1.9	0.1	7.3	4.6	4.4
FY10	0.0	1.8	0.0	1.8	3.6	1.7
FY11	0.0	0.0	0.0	9.1	11.8	8.7
FY12	0.0	0.0	0.0	0.0	-0.2	0.0
Average	20.3	20.2	13.6	34.3	40.1	17.3

†The dosing counter for 4W might not function well in FY97 and earlier.

Table F.7. Annual drainage rate (mm yr^{-1}) from the basalt side slope. (The green-yellow-red color scale indicates drainage rates from high to low.)

	South (1E)			**North (4E)**		
	Dosing Counter	**Pressure Transducer**	**Tipping Bucket**	**Dosing Counter**	**Pressure Transducer**	**Tipping Bucket**

FY95	1.8	3.0	1.1	3.6†	16.5	0.0
FY96	42.9	51.8	7.2	43.0†	143.0	34.7
FY97	132.1	130.3	75.2	267.0	259.5	85.1
FY98	16.1	16.5	12.8	30.5	31.2	25.9
FY99	5.4	6.7	4.1	7.2	6.9	5.9
FY00	10.7	8.9	9.0	14.3	10.2	11.5
FY01	5.4	4.6	0.6	7.2	6.6	0.8
FY02	7.1	7.3	7.7	9.0	9.7	8.1
FY03	30.4	31.0	28.9	35.8	36.2	26.1
FY04	41.1	31.4	30.6	50.2	35.7	29.5
FY05	1.8	2.7	2.9	3.6	3.8	3.5
FY06	0.0	-0.1	0.1	28.7	28.9	16.8
FY07	5.4	-0.9	0.1	17.9	13.6	2.9
FY10	10.7	9.9	9.9	12.5	13.2	12.3
FY11	14.3	0.0	12.3	17.9	17.4	8.6
FY12	7.1	0.0	4.4	12.5	9.4	7.5
Average	20.8	18.9	12.9	35.1	40.1	17.4

†According to BNW-56196 (e.g., page 38), the dosing counter at 4E was malfunctioning for a significant period of FY96. It is possible that this dosing counter was not functioning normally in FY95.

Table F.8. Annual drainage rate (mm yr^{-1}) from the silt loam plots at the west half of the PHB. (Negative values are shown in pink and positive values in green.)

	South (3W)			North (6W)		
	Dosing Counter	**Pressure Transducer**	**Tipping Bucket**	**Dosing Counter**	**Pressure Transducer**	**Tipping Bucket**
FY95	0	-1.52E-01	0	0	-2.13E-01	0
FY96	0	-2.25E-01	3.10E-05	0	-2.98E-01	1.70E-04
FY97	0	-3.86E-01	5.27E-04	0	-3.72E-01	5.11E-04
FY98	0	-7.64E-01	3.72E-04	0	-5.60E-01	3.75E-04
FY99	0	-2.53E-01	0	0	-3.04E-01	0
FY00	0	-2.19E-01	3.41E-04	0	-2.72E-01	3.75E-04
FY01	0	9.17E-03	0	0	-6.72E-01	0
FY02	0	-2.18E-01	0	0	-2.54E-01	3.41E-02
FY03	0	-2.88E-01	0	0	-2.25E-01	3.41E-05
FY04	0	-3.09E-01	0	0	-2.24E-01	3.41E-05
FY05	0	-3.38E-01	2.48E-04	0	-1.71E-01	8.18E-04
FY06	0	-1.40E-01	0	0	-2.18E-01	0
FY07	0	-1.72E-01	0	0	-2.70E-01	5.80E-03
FY10	0	2.42E-01	0	0	-2.77E-01	0
FY11	0	4.26E-02	0	0	-1.81E-01	0
FY12	0	2.03E-01	0	0	5.15E-02	0
Average	0	-1.85E-01	9.50E-05	0	-2.79E-01	2.64E-03

Table F.9. Annual drainage rate (mm yr^{-1}) from the silt loam plots at the east half of the PHB. (Negative values are shown in pink and positive values in green.)

	South (3E)			North (6E)		
	Dosing Counter	**Pressure Transducer**	**Tipping Bucket**	**Dosing Counter**	**Pressure Transducer**	**Tipping Bucket**
FY95	0	-2.95E-01	1.93E-02	0	-1.65E-01	0

FY96	0	-2.24E-01	1.01E-01	0	-2.48E-01	8.50E-04
FY97	0	-6.08E-01	5.14E-04	0	-1.41E-01	1.73E-01
FY98	0	-6.38E-01	5.14E-04	0	-5.31E-01	6.22E-03
FY99	0	-5.56E-01	0	0	-3.04E-01	0
FY00	0	-2.69E-01	1.71E-04	0	-2.98E-01	3.40E-05
FY01	0	-6.55E-02	0	0	-3.57E-01	0
FY02	0	-3.06E-01	0	0	-2.91E-01	3.40E-05
FY03	0	-2.18E-01	3.43E-05	0	-2.15E-01	3.40E-05
FY04	0	-2.11E-01	3.43E-05	0	-2.27E-01	3.40E-05
FY05	0	-1.90E-01	3.43E-05	0	-1.18E-01	0
FY06	0	-1.69E-01	0	0	-1.62E-01	3.40E-05
FY07	0	-3.97E-01	0	0	-3.21E-01	1.36E-04
FY10	0	-1.41E-01	0	0	-1.02E-01	0
FY11	0	-1.68E-01	0	0	-1.10E-01	0
FY12	0	-1.50E-01	0	0	-3.08E-02	0
Average	0	-2.88E-01	7.61E-03	0	-2.26E-01	1.12E-02

Table F.10. Annual drainage rate (mm yr^{-1}) from the transitional plots at the west half of the PHB. (Negative values are shown in pink and positive values in green.)

	South (2W)			North (5W)		
	Dosing Counter	**Pressure Transducer**	**Tipping Bucket**	**Dosing Counter**	**Pressure Transducer**	**Tipping Bucket**
FY95	0	7.36E-01	4.24E-02	6.34E+00	6.73E+00	5.05E+00
FY96	0	-6.87E-01	0	0	4.19E+00	2.98E+00
FY97	0	-6.93E-01	2.79E-04	6.34E+00	6.25E+00	4.05E-01
FY98	0	-8.17E-01	1.53E-03	0	-8.93E-01	1.64E-02
FY99	0	-7.58E-01	1.40E-04	0	4.69E+00	0
FY00	1.28E+01	-8.05E-01	1.95E-03	0	-1.69E+00	7.87E-03
FY01	0	4.18E+00	0	0	-1.42E-01	0
FY02	0	-1.87E-01	2.79E-04	0	1.53E-01	1.09E-04
FY03	0	-5.93E-01	2.79E-04	0	-3.72E-01	0
FY04	0	-5.56E-01	2.79E-04	0	-3.80E-01	0
FY05	0	-4.96E-01	4.19E-04	0	-2.12E-01	0
FY06	0	-4.70E-01	1.40E-04	0	-3.37E-01	0
FY07	0	-1.59E+00	1.40E-04	0	-5.22E-01	0
FY10	0	-4.63E-01	0	0	-1.89E+00	0
FY11	0	-1.40E-10	0	0	4.61E-11	0
FY12	0	4.65E-11	0	0	-9.22E-11	7.65E-04
Average	7.99E-01	-2.00E-01	2.99E-03	7.92E-01	9.74E-01	5.29E-01

Table F.11. Annual drainage rate (mm yr^{-1}) from the transitional plots at the east half of the PHB. (Negative values are shown in pink and positive values in green.)

	South (2E)			North (5E)		
	Dosing Counter	**Pressure Transducer**	**Tipping Bucket**	**Dosing Counter**	**Pressure Transducer**	**Tipping Bucket**
FY95	0	-6.54E-01	0	0	1.02E+00	4.46E-01
FY96	0	-8.31E-01	1.29E-03	0	3.93E+00	4.84E+00
FY97	0	6.35E-02	8.71E-01	6.30E+00	-3.15E-02	7.56E+00
FY98	0	-8.46E-01	1.61E-03	6.30E+00	-3.73E+00	6.75E-03
FY99	0	-7.73E-01	2.15E-04	0	-2.62E+00	0
FY00	6.23E+00	-7.40E-01	8.61E-03	0	-9.91E-01	4.09E-04
FY01	0	1.68E+00	0	0	6.60E+00	0
FY02	0	-1.13E+00	0	0	5.12E+00	9.20E-04
FY03	0	-6.87E-01	0	0	-7.99E-01	4.09E-04
FY04	0	-1.28E-01	0	0	-7.91E-01	3.07E-04
FY05	0	-3.48E-01	1.08E-04	0	-1.96E+00	0
FY06	0	-7.86E-01	0	0	-7.18E-01	0
FY07	0	-8.69E-01	0	0	6.00E-01	1.02E-04
FY10	0	-7.42E-01	0	0	-1.02E+00	0
FY11	0	-1.05E+00	0	0	-1.77E+00	1.02E-04
FY12	0	1.01E+00	0	0	3.15E-01	0
Average	3.89E-01	-4.27E-01	5.52E-02	7.88E-01	1.96E-01	8.03E-01

F.4.4 Heat Dissipation Units

System Performance

The data collection system of the HDUs was more complex than the systems associated with other instruments for a couple of reasons: the HDUs needed to be heated during each measurement and required an excitation module for a constant electric current during measurement. Because of the relatively high power needed, the HDU system was divided into four sub-systems, each with its own battery and solar panel. From FY09 to FY13, only one of the four HDU sub-systems was maintained in operation. The HDU system was in service for 19 years (from FY95 to FY13), with gaps in FY04 through FY06, FY08, and most of FY09. Because of complexity of the HDU system, the HDU system needed considerable setup time in FY95 and maintenance in FY96 and hence had relatively low data completeness of 66% for FY95 and 74% for FY96 (Figure F.13). The system functioned very well in FY97 and FY98, with 100% data completeness. The lack of maintenance in FY99 (because of the discontinuity of funding) reduced the data completeness to 56% for FY99 and only 35% for FY00. After additional maintenance, the data completeness increased to 75% in FY01 and remained at 92% for FY02 and FY03. After a gap of several years, the data completeness remained at 87% or higher from FY09 to FY13. Overall, the data completeness was 81% on average.

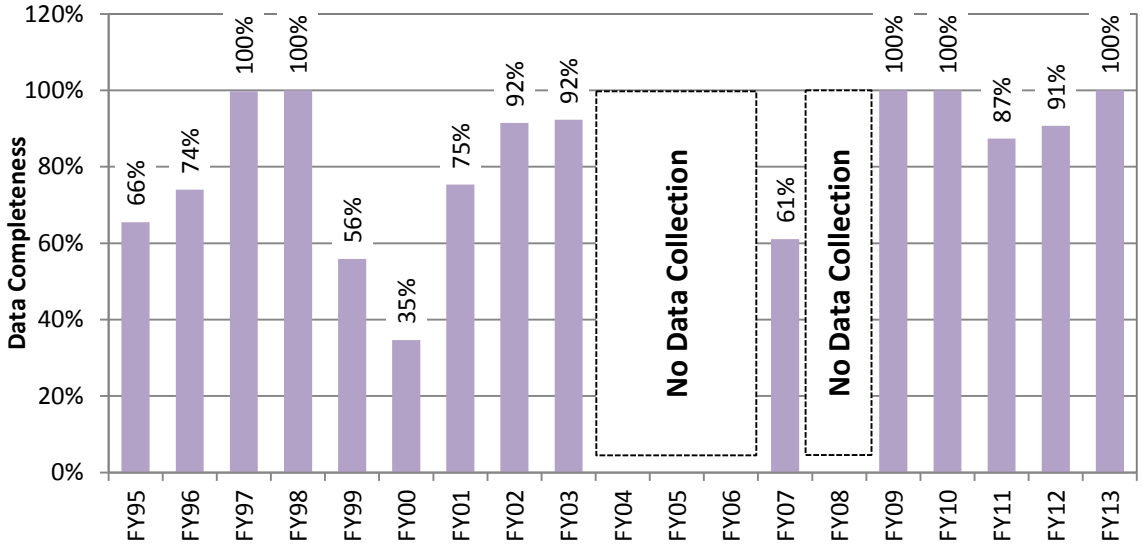

Figure F.13. HDU data compleneteess in each fiscal year.

The fractions of the valid HDU data are shown in Figure F.14. Because 16 of the HDUs functioned poorly during the entire monitoring period, possibly because of a data logger problem, the fraction of valid HDU data was never more than 82%. It was only 56% in FY99 and 45% in FY00 because of battery failure.

After the failed batteries were replaced, the HDU monitoring system was relatively stable (with the fractions of the valid data between 60% and 67%) from FY01 to FY03, but a significant portion of HDUs performed poorly because several more HDUs became nonfunctional for unknown reasons. After a data gap from FY04 to FY06, the system performed poorly again in FY07, with only 40% valid data. On average from FY95 to FY07 (excluding FY04 to FY06) the fraction of valid HDU data was 72%. The main reasons for the nonfunctional HDUs were battery failure and data logger malfunction.

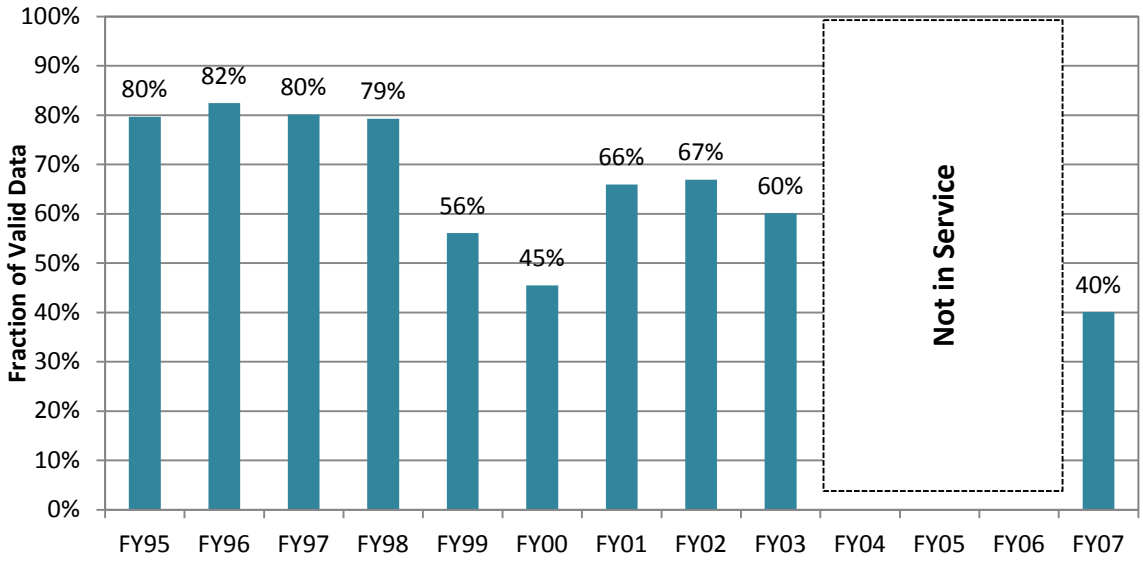

Figure F.14. The fractions of the valid data from the heat dissipation units.

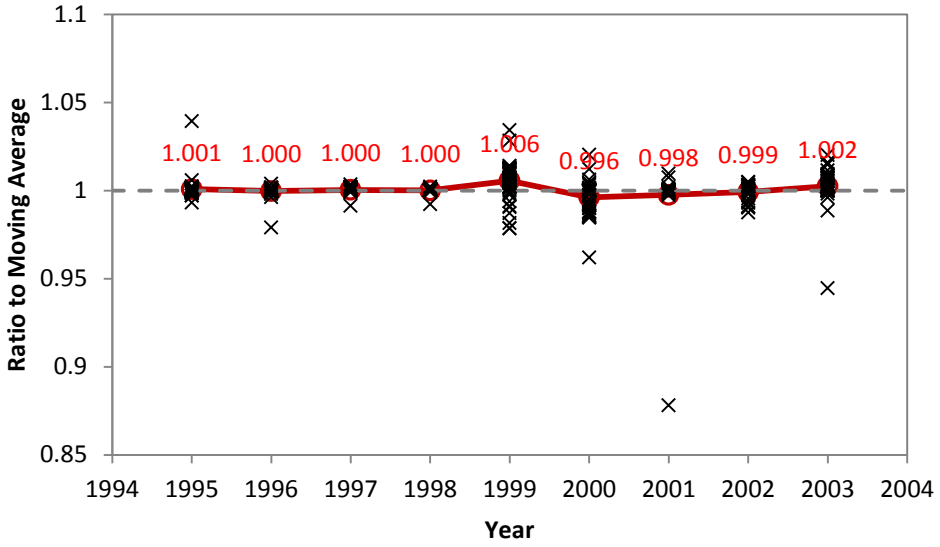

Figure F.15. Ratio of HDU-measured daily average soil-water pressure to the 5-day moving average. The symbols in the plot mark annual averages. The numbers are the mean values for 56 HDUs.

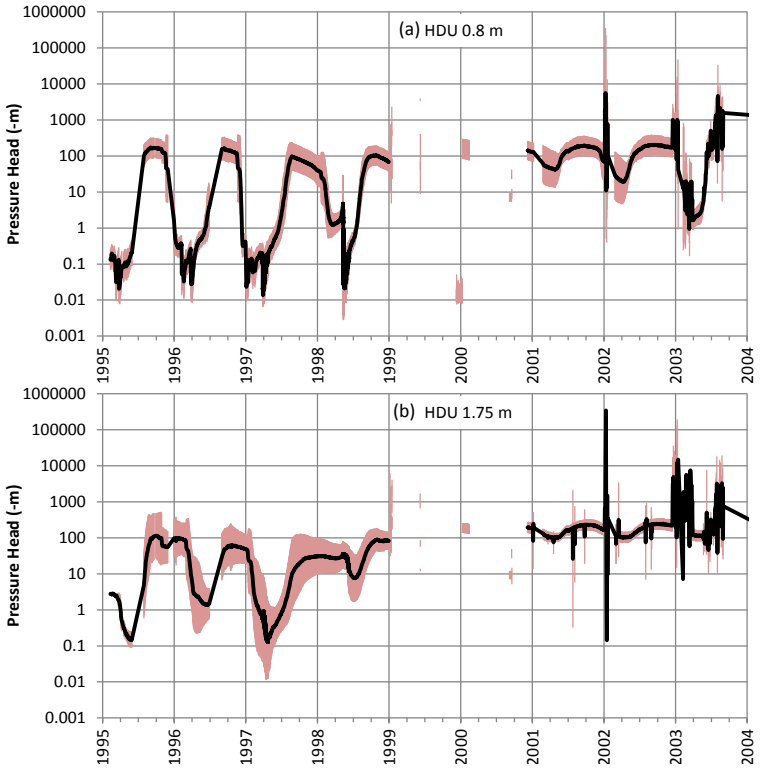

Figure F.16. Variability of soil water pressure head among the six HDUs in the north section of the barrier at 0.8-m and at 1.75-m depths from FY95 to FY98. The shaded area indicates the range of one standard deviation.

Sensor Performance

The noise in the HDU-measured soil water pressure was evaluated by the ratio of the daily average to the 10-day moving average. Here, the geometric average was used because soil water pressure tends to be log-normally distributed. Excluding the 16 non-functional HDUs, the ratio of the 56 functional HDUs and the mean values are shown in Figure F.15. A ratio of unity indicates zero noise. The results show that the noise in the HDU data was no more than about 5% (with one exception, 9%, in 2001). The uncertainty of HDUs was not evaluated due to the lack of more reliable measurements.

Data Representativeness

Figure F.16 demonstrates, as an example, the variation of soil water pressure among the six HDUs at 0.8-m depth and six at 1.75-m depth in the north section of the barrier from FY95 to FY98. The variation was expressed as one standard deviation as shown by the shaded area in Figure F.16. The measured pressure at 0.8-m depth from FY95 to FY98 varied by, on average, a factor of 2.1 relative to the geometric mean, while that for the 1.75-m HDUs varied by factor of 2.9.

The performance of the HDU system is summarized in Table F.12. The system and sensor performance of the HDU system was from intermediate to good, but the data representativeness was poor. Overall, the HDU system was graded as *B* for intermediate performance. A main reason for many problems with the HDU system was the relatively high power consumption by HDUs. Hence, insufficient power supply affected system performance.

Table F.12. Performance of the HDU system.

Performance Type	Indicator	Evaluation Result	Performance Grade
System Performance	Duration of service (yr)	19	A
	Data completeness	89%	B
	Fraction of valid data	72%	B
Sensor Performance	Data instability†	<5%	A
	Data uncertainty	NA	NA
Data Representativeness	Range of variation	A factor‡ of 2 to 3	C
†Noise in data; ‡Relative to the geometric mean			

Discussion: HDU-measured water pressure

Figure F.17 demonstrates the NP-measured water content and HDU-measured soil water pressure at the 0.45-m depth at water balance station S01. Excluding the invalid data, the HDU data from FY95 to FY07 could correctly indicate the hydrological process and soil water pressure within the silt loam barrier. When the soil wetness was very low, usually later in the summer seasons, soil water pressure could change significantly (by an order of magnitude or more) while the soil water content change may be beyond detection. Hence, the HDU data can provide valuable information that other data cannot indicate. The valid monitoring data of NP and HDUs from 1995 to 2003 for four depths at 12 monitoring stations were paired up to determine the field water retention of the silt loam, with and without gravel, of the ETC barrier as reported in Appendix E and Zhang (2015).

The HDU systems have been used to monitor the soil water pressure below interim surfaces in Hanford's T Tank Farm since 2006 and in the TY Tank Farm since 2010. Part of the data was used to evaluate the performance the barrier at the T Tank Farm (Zhang et al. 2012). These systems are still in normal operation at present (verified in September 2015). HDUs were also used in a test of soil desiccation in the laboratory (Oostrom et al. 2012) and in the field (Truex et al. 2012; Truex et al. 2014), and reasonable results were obtained.

The intermediate performance of the HDU system at the PHB was primarily due to the problems with the data logger or batteries, which can be easily corrected in future monitoring.

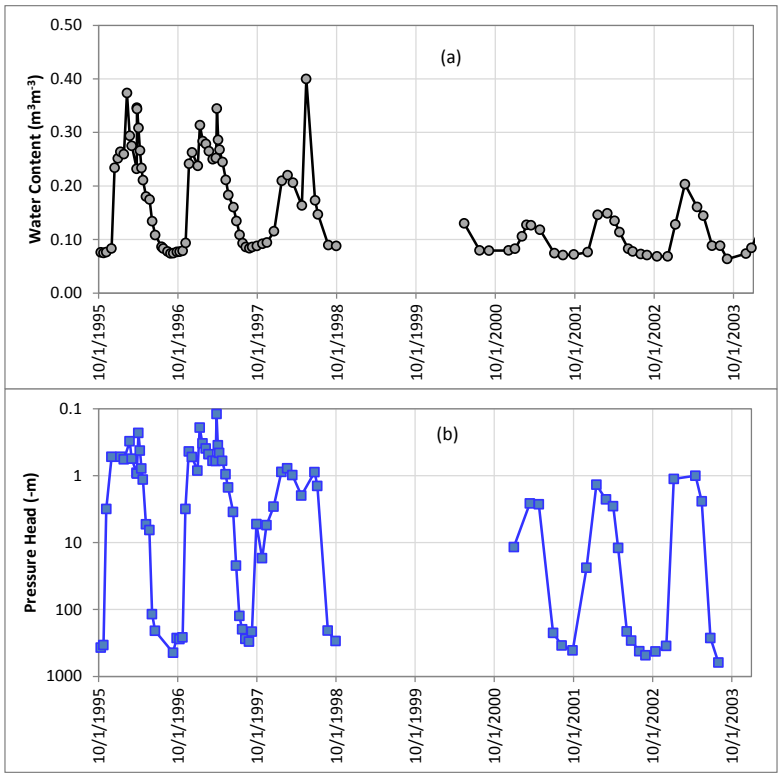

Figure F.17. An example of the field-measured (a) soil water content and (b) soil water pressure at 0.45-m depth at water balance station S01.

F.4.5 Fiberglass Blocks

System Performance

The FGBs (MC-314 Soil Moisture Cells) were in service for 13 years (from FY95 to FY07). During this period, only 1 of the 18 FGBs did not function at all. There were no FGB data collected in FY05 and during a significant portion of FY06. FGB data collection was terminated after FY07.

The data completeness was 75% or better from FY95 to FY04 (Figure F.18). Overall (excluding FY05), the data completeness was 83%. The data from the functional FGBs were rarely beyond the reasonable range and the fraction of valid data was 100%.

Sensor Performance

Most of the functional FGBs showed some instability, as indicated by sudden stair-type drops or jumps illustrated in Figure F.19. These drops or jumps happened occasionally (once every several months or years) during some periods (e.g., from 1995 to 2001) and but more frequently during others (e.g., from 2001 to 2004). A jump or drop often happened to a subset of the sensors instead of individual sensors, indicating a possible electric resistance change of the peripherals, e.g., data logger or battery. There were also outliers that were very different from the trend lines (Figure F.19). These drops or jumps were unexpected because the soil water condition in the sand beneath the AC was expected to be stable and hence a sudden drop of soil water pressure (which would indicate a sudden drier condition) was very unlikely. A possible cause is the instability of some electronic components or poor contact between metals. The instability of the FGB system varied by a factor of about 3 relative to the geometric mean, namely, ranging between h/3 and 3h. For example, if a measurement was -300 m, the range of instability

was between -100 and -900 m. The uncertainty of FGBs was not evaluated due to the lack of more reliable *h* measurements.

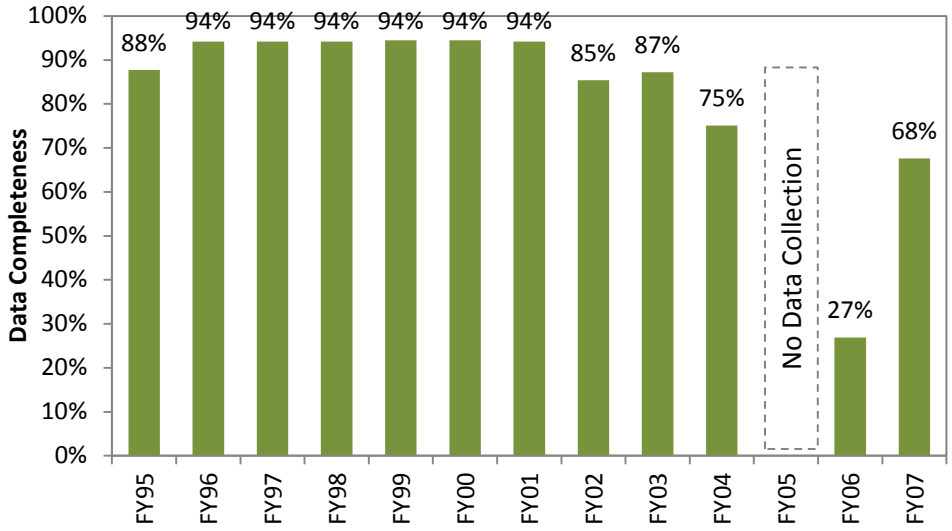

Figure F.18. Completeness of data measured by the fiberglass blocks.

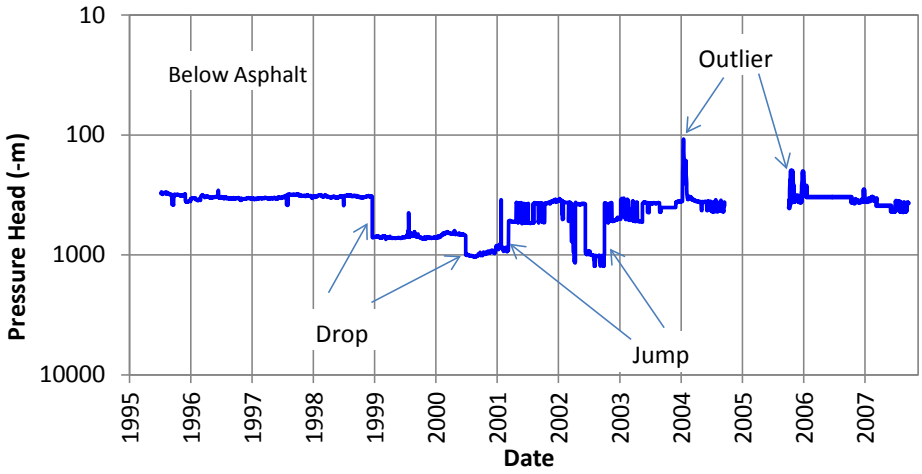

Figure F.19. Geometric mean of the absolute values of the soil water pressure for the six FGBs in the sand beneath the asphalt layer.

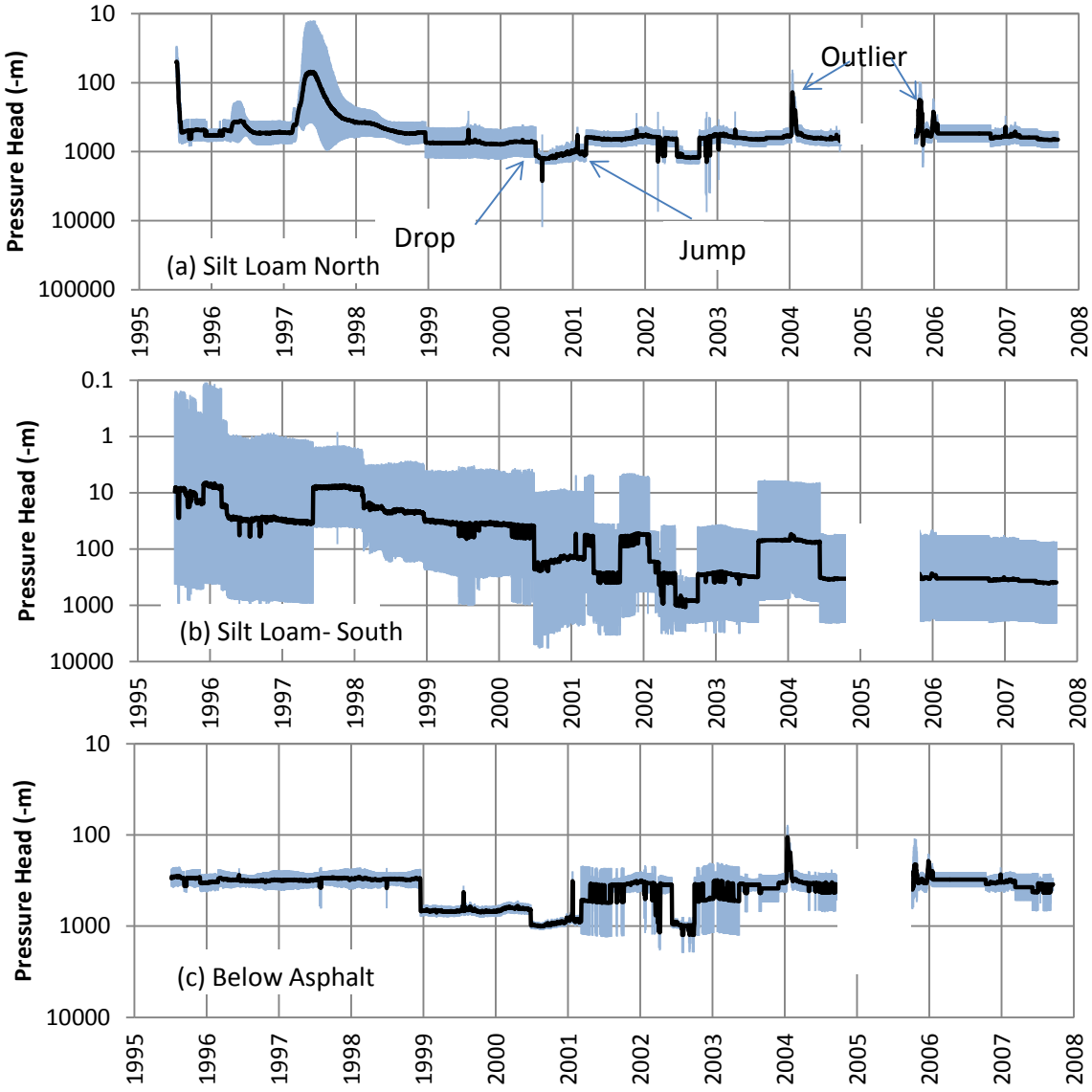

Figure F.20. Variability of the absolute value of soil-water pressure head among the fiberglass blocks from FY95 to FY07. The shaded area indicates the range of one standard deviation.

Data Representativeness

The representativeness of FGBs was evaluated based on the variation of the measurements at the same depth and under the same treatment. There were three groups of FGBs: those near the bottom of the silt loam layer in the north section of the ETC barrier (silt-loam north), those near the bottom of the silt loam layer in the south section of the ETC barrier (silt-loam south), and those beneath the AC barrier. Figure F.20 demonstrates the variability of soil water pressure among the three groups of FGBs from FY95 to FY07. On average, the FGB-measured soil water pressure from FY95 to FY07 varied by a factor of 1.5 for those in silt-loam north, 9.3 in silt-loam south, and 1.3 beneath the AC. Overall, the measurements varied by a factor of 4.0 relative to the geometric mean.

The performance of the FGBs is summarized in Table F.13. The six indicators were graded between *C* and *A*. The large data instability and poor data representativeness were the main concern of the use of FGBs. Hence, the overall system performance was graded as *C* for poor performance. According to

Scanlon et al. (2002), the main sources of error with electrical resistance sensors such as a FGB include the air entry value of the matrix material, soil salinity effects, hysteresis, poor contact, dynamic response of the sensor, and instrument deterioration with time. Thus, they are generally used for crude assessment of soil water status for plant growth, e.g., for the control of an irrigation system.

Table F.13. Performance of the FGB system.

Performance Type	Indicator	Evaluation Result	Performance Grade
System Performance	Duration of service (yr)	13	A
	Data completeness	83%	B
	Fraction of valid data	94%	A
Sensor Performance	Data instability†	a factor of 3	C
	Data uncertainty	NA	NA
Data Representativeness	Range of variation	A factor of 4.0	C
†The range of variation of measurements from FY95 to FY07.			

F.4.6 Pan Lysimeter

System Performance

Percolation through the asphalt concrete was measured by a pan lysimeter equipped with a pump to extract the water and a tipping bucket to measure the volume of water. The system started operation on July 9, 1995, and was in normal function until September 18, 2007. The duration of service was about 13 years. In FY12, when trying to reactivate the system, it was found that the 1.65-mm-diameter stainless steel tubes for venting and pumping were plugged. Pumping of water could not function normally. Because the venting tube was so thin (1.5 mm ID) and very long (tens of feet), attempts to repair it were unsuccessful.

The data completeness was at least 90% from FY95 to FY03 and decreased to 80% in FY04 (Figure F.21). There were no data at all in FY05 and a small fraction of data in FY06. Excluding FY05, the data completeness was 80% on average.

Sensor Performance

All the data were valid and the noise in the data was negligible. The tipping buckets could measure drainage as small as about 11 ml, which is equivalent to resolution in percolation rate of 2.6×10^{-4} mm. Although there were some data gaps, the cumulative drainage data are not thought to be affected.

Data Representativeness

Data representativeness could not be quantified because there was only one pan lysimeter beneath the asphalt layer. A grade of *C* was assigned because of the lack of repetition.

The performance of the pan lysimeter is summarized in Table F.14. The system and sensor performance of the pan lysimeter system was from intermediate to good, but the data representativeness was poor. The overall system performance was graded as *B* for intermediate performance.

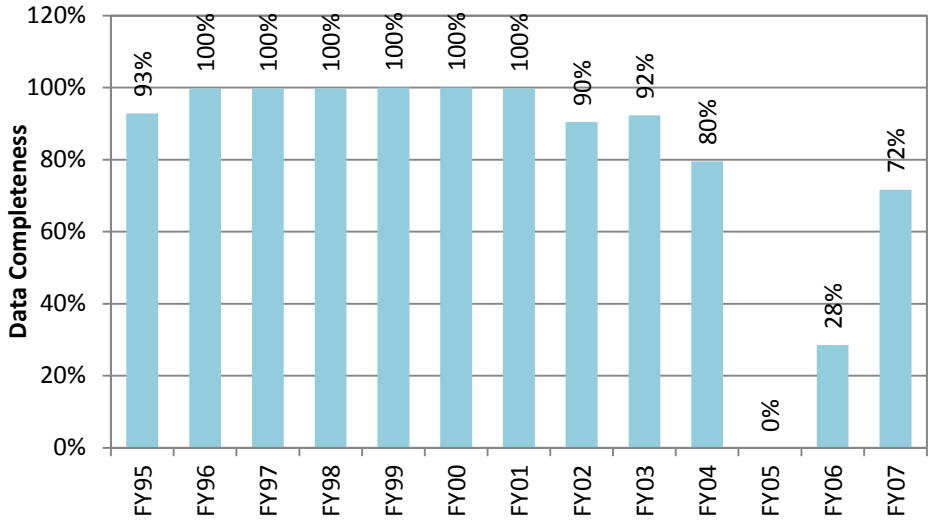

Figure F.21. Completeness of percolation data.

Table F.14. Performance of the pan lysimeter systems.

Performance Type	Indicator	Evaluation Result	Performance Grade
System Performance	Duration of service (yr)	13	B
	Data completeness	80%	B
	Fraction of valid data	100%	A
Sensor Performance	Data instability	Negligible	A
	Data uncertainty (mm)	2.6×10^{-4}	A
Data Representativeness[†]	Standard deviation	Could not be evaluated[†]	C
[†]Could not be evaluated because there was only one pan lysimeter beneath the asphalt layer.			

F.4.7 Rain Gauges

System Performance

The sprinkler system operated from February 1995 to September 1997 and was terminated in May 1998, when the enhanced precipitation test (aka the treatability test) was completed. The duration of service was about 3 years. The data were 100% complete because all operation was manual, and all data were valid.

Sensor Performance

The data instability was negligible. The measurements were taken manually with six rain gauges with a resolution of 0.25 mm.

Data Representativeness

The data representativeness was evaluated by the uniformity of water application because of non-uniform application of water to the ground surface because of factors related to the sprinklers, e.g., the non-uniform distribution of pressure among the sprinklers. Based on the measurements at stations S1 through S6, the average amount of water applied to the barrier surface per fiscal year was between 210 and 247 mm from FY95 to FY98 (Figure F.22). The coefficients of variation of water application ranged from 2.9% in FY95 to 9.7% in FY97, with an average of 6.7%. Station S4, near the middle, received 5.8%

more water than average, while the stations away from the middle (i.e., S1 and S6) received slightly less (2.5% and 4.3%) water from irrigation (Figure **F.23**).

The performance of the rain gauges is summarized in Table F.15. The system and sensor performance of the system was good, but the data representativeness was intermediate because of the slight non-uniformity of water distribution by sprinkler system. The overall performance was graded as *A* for good performance.

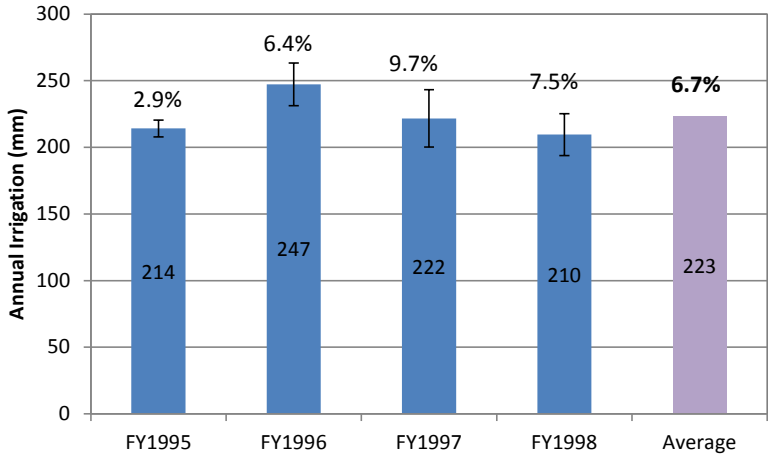

Figure F.22. The average amount of irrigation of each fiscal year. The numbers above each bar indicate the coefficients of variation over the six monitoring stations.

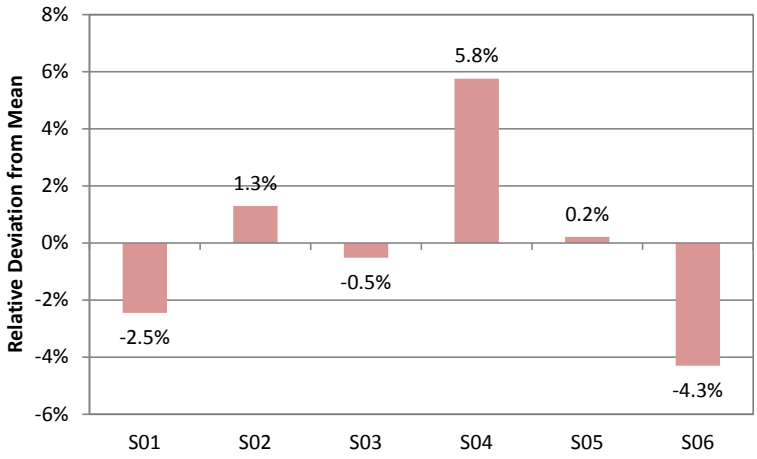

Figure F.23. Relative deviation of irrigation at each station from the average.

Table F.15. Performance of the rain gauges.

Performance Type	Indicator	Evaluation Result	Performance Grade
System Performance	Duration of service (yr)	3	NA†
	Data completeness	100%	A
	Fraction of valid data	100%	A
Sensor Performance	Data instability	Negligible	A
	Data uncertainty	0.25 mm	A
Data Representativeness††	CV	6.7%	B

†The duration of service was not graded because measurement was terminated as planned.
††The uniformity of water application.

F.4.8 Load cells

System Performance

Irrigated and meteoric water was measured by 14 load cells (aka mini-lysimeters) installed at the 14 monitoring stations. The data were logged hourly or more frequently from FY95 to FY98 and hourly thereafter until FY03, when the system was terminated. The system started operation on December 15, 1994, and was terminated in September 2003 due to poor performance. The duration of service was 9 years.

The data completeness (Figure F.24) was 63% and 84% for FY95 and FY96, respectively, because of planned or unintended interruption. There was almost no (<0.3%) data loss in FY97 and FY98. However, the data completeness was no more than 48% in FY99 and after, indicating poor system performance. The average data completeness was 60% over the 9 years of service.

The fraction of valid data ranged from 67% to 100%, with an average of 92% (Figure F.25). For the load cells, the error codes were the primary invalid data.

Sensor Representativeness

Data uncertainty was examined by checking the deviation of the measurements logged at the same time and by comparing the average monthly values from the south unirrigated section with the measurements from the nearby HMS (Figure F.26). Compared with the measurements at the HMS, the measurements at the barrier underestimated the monthly precipitation by an average of 7.0 mm. Negative values were obtained in one or more months from June to August every year. A possible cause was evaporation of water retained in the marbles, especially in the hot summer seasons. However, the measurement at the PHB in January 1997 was significantly higher than at the HMS. The cause is not clear but it could have been due to the heavy snow at that time. It is possible that some snowmelt on frozen ground entered into the load cells.

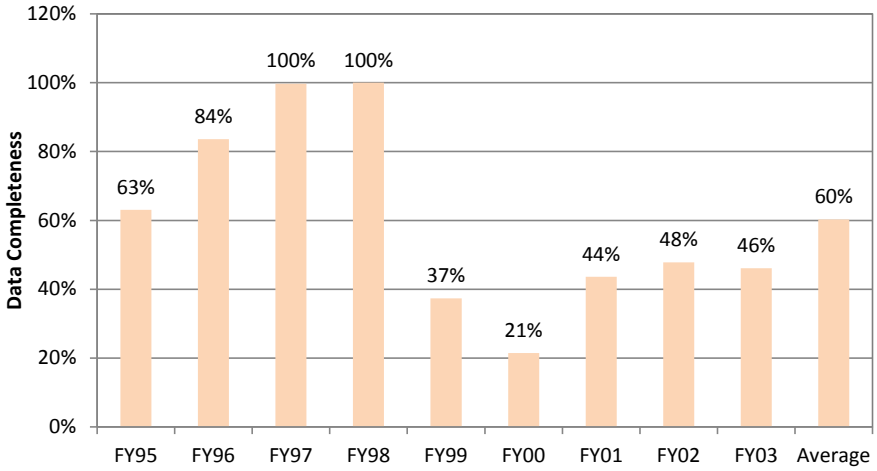

Figure F.24. Data completeness of the load cells for measuring precipitation.

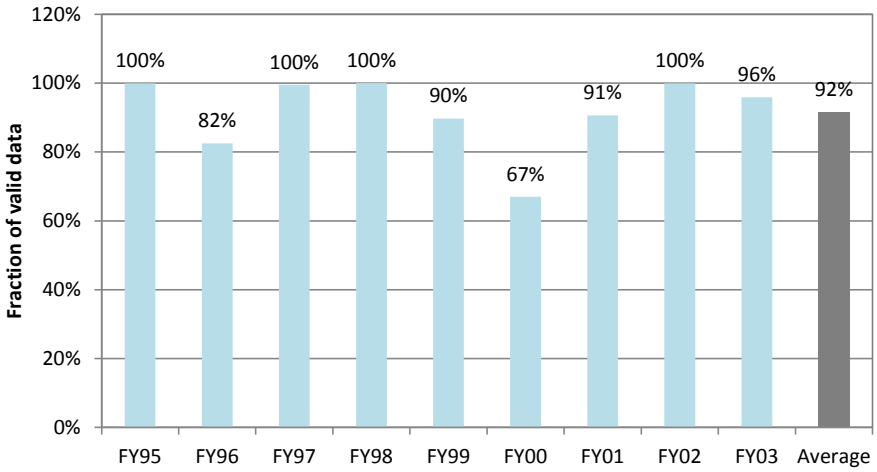

Figure F.25. Fraction of valid data of the load cells for measuring precipitation.

Data Representativeness

Measurement representativeness of load cells was evaluated based on the variation of monthly precipitation measured by the 14 load cells. Generally, the load cell measurements at the barrier had larger variation when the precipitation was relative high (e.g., in the winters of FY95 and FY97) (Figure F.26). On average, the standard deviation of monthly precipitation during the 3-year enhanced precipitation test was 7.9 mm, which is very considerable.

The performance of the load cells is summarized in Table F.16. Problems might exist in the peripherals and the load cells. The overall system performance was graded as *C* for poor performance.

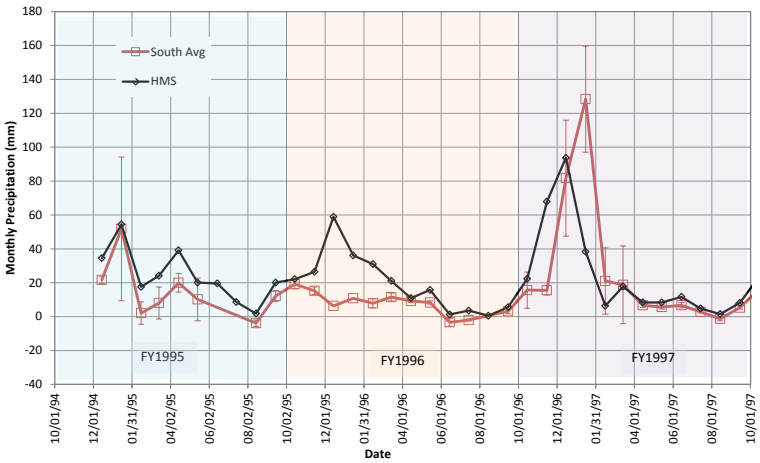

Figure F.26. The measured average monthly precipitation in the south section of the Prototype Hanford Barrier and at the Hanford Meteorological Station. The vertical bars indicate one standard deviation.

Table F.16. Performance of the load cells system.

Performance Type	Indicator	Evaluation Result	Performance Grade
System Performance	Duration of service (yr)	9	B
	Data completeness	60%	C
	Fraction of valid data	92%	A
Sensor Performance	Data instability	Negligible	A
	Data uncertainty †	-7.0 mm	C
Data Representativeness†	Standard deviation	±7.9 mm	C
†Monthly precipitation.			

F.4.9 Summary and Discussion

Based on the above evaluation, the tier-level and overall performance of the monitoring systems at the PHB is summarized in Table F.17**Error! Reference source not found.**. The systems demonstrating good performance (grade *A*) were those for the NP, tipping buckets, and the rain gauges. The systems demonstrating intermediate performance (grade *B*) were those for MP-917 TDR with long probes, the HDUs, and the pan lysimeter. The systems demonstrating poor performance (grade *C*) were those for MP-917 TDR with short probes, the FGBs, and load cells. To best evaluate the performance of the PHB or other future barriers, it is recommended that the data from the *A*-grade monitoring systems be used if possible. Data from the *B*-grade monitoring systems may be used with caution and after proper data screening or as confirmative information. Data from the *C*-grade monitoring systems is not recommended for barrier performance evaluation.

Table F.17. Summary of the performance of the monitoring systems.

Monitoring Systems	System Performance	Sensor Performance	Data Represent-ativeness	Overall System Performance
NP	A	A	A	A
MP-917 TDR (long probes)	B	B	B	B
MP-917 TDR (short probes)	B	B	C	C
Dosing counters	A	B	C	B
Pressure transducers	A	A	C	B
Tipping buckets	A	A	A	A
Rain gauges	A	A	B	A
HDUs	A	A	C	B
FGBs	A	C	C	C
Pan lysimeter	A	A	C	B
Load cells	B	B	C	C

Among the three evaluation tiers (i.e., system performance, sensor performance, and data representativeness), data representativeness for most systems had the lowest grade, *C*. Despite being constructed with consistent procedures, an engineered surface barrier tends to be heterogeneous. The soil surface conditions such as relief and coverage by vegetation and cryptogam varies spatially. The root conditions (e.g., density, capability to absorb soil water) distribute non-uniformly in space. Additionally, the sensing volume differs considerably (e.g., by orders of magnitude) among sensors. Therefore, a robust monitoring system should contain sufficient replicates so that the results can represent the field condition. Without replicates, the representativeness of a measurement cannot be evaluated. For example, very low percolation rate through the AC was measured by only one pan lysimeter. It is very risky to make a decision just by the measurements without duplicates. Furthermore, it is not uncommon for a monitoring system to fail for unexpected reasons, and sometimes the failure cannot be repaired. Replicated measurements will dramatically reduce the chance of complete data loss. Last but not the least, the sensors need to be installed in locations that can represent field conditions. For example, soil water conditions may differ because of the spatial variation of root distribution. Hence, sensors should be installed both within and between the rows of vegetation.

Manual operation with commonly used, maintainable instruments generally can provide reliable long-term (i.e., for decades) but often discrete data (e.g., the neutron probe method). An automated data logging system (e.g., the TDR, HDU, FGB, instruments for drainage monitoring) could provide temporally continuous data but usually needs more maintenance than manually operated methods. Depending on the level of maintenance, the automated systems may use less labor (e.g., instruments for drainage monitoring) or more labor (e.g., TDR) than the manually operated instrument.

It is recognized that the sensor technology (e.g., the TDR technology) has advanced tremendously since the inception of PHB. This advancement needs to be considered in designing the monitoring systems for future barriers. The results of this investigation are useful for the selection and installation/layout of sensors, the design of the monitoring systems, and data collection methods for subsurface hydrological monitoring.

References

Albright, WH, CH Benson, GW Gee, AC Roesler, T Abichou, P Apiwantragoon, BF Lyles, and SA Rock. 2004. "Field Water Balance of Landfill Final Covers," *Journal of Environmental Quality*, 33(6):2317-2332.

Allen, RG, TA Howell, WO Pruitt, IA Walter, and ME Jensen. 1991. *Lysimeters for Evapotranspiration and Environmental Measurements: Proceedings of the International Symposium on Lysimetry*. Am. Soc. of Civ. Eng., New York.

ASTM D2216-10. 2010. *Standard Test Methods for Laboratory Determination of Water (Moisture) Content of Soil and Rock by Mass*, ASTM, West Conshohocken, PA.

Augenstein, M, D Rettenmaier, M Praschak, and H Hötzl. 2010. "Long Term Investigation of Soil Moisture Performance for Structural Monitoring of Landfill Surface Sealing Systems Via Neutron Probe Measuring and Lysimeter Fields," *First European Conference on Loisture Measurement*, Oct. 5-7, 2010, Weimar, Germany.

Bittelli, M. 2011. "Measuring Soil Water Content: A Review," *Hort. Technology*, 21(3):293-300.

Blonquist Jr., JM, SB Jones, and DA Robinson. 2005. "A Time Domain Transmission Sensor with Tdr Performance Characteristics," *Journal of Hydrology*, 314(1-4):235-245. doi:10.1016/j.jhydrol.2005.04.005.

Buckingham, E. 1907. *Studies on the Movement of Soil Moisture*, Soils Bull. 38, U.S. Dep. Agric. Bur.

Campbell, GS and RY Anderson. 1998. "Evaluation of Simple Transmission Line Oscillators for Soil Moisture Measurement," *Computers and Electronics in Agriculture*, 20:31-44.

Chow, L, Z Xing, HW Rees, F Meng, J Monteith, and L Stevens. 2009. "Field Performance of Nine Soil Water Content Sensors on a Sandy Loam Soil in New Brunswick, Maritime Region, Canada," *Sensors*, 9(11):9398-9413. doi:10.3390/s91109398.

Cichota, R, ALB Hurtado, and Q De Jong van Lier. 2008. "Performance of a Multi-Level Tdr System Exposed to Tropical Field Conditions – A Time-Space Comparison with Tensiometry," *Journal of Hydrology*, 352(1-2):181-190. doi:10.1016/j.jhydrol.2008.01.008.

Davis, TW, X Ling, C Kuo, and Y Liang. 2012. "Analysis of Power Characteristics for Sap Flow, Soil Moisture, and Soil Water Potential Sensors in Wireless Sensor Networking Systems," *IEEE Sensors Journal*, 12(6):1933-1945.

Dobriyal, P, A Qureshi, R Badola, and SA Hussain. 2012. "A Review of the Methods Available for Estimating Soil Moisture and Its Implications for Water Resource Management," *Journal of Hydrology*, 458-459:110-117. doi:10.1016/j.jhydrol.2012.06.021.

DOE-RL. 1994. *Constructability Report for the 200-BP-1 Prototype Surface Barrier*, DOE/RL- 94-76, U.S. Department of Energy Richland Operations Office, Richland, Washington.

DOE-RL. 1999. *200-BP-1 Prototype Barrier Treatability Test Report*, DOE/RL-99-11 Rev. 0, U.S. Department of Energy Richland Operations Office, Richland, Washington.

Durner, W and D Or. 2005. "Soil Water Potential Measurement." In *Encyclopedia of Hydrological Sciences*, ed. MG Anderson. John Wiley & Sons, Ltd.

Evett, SR. 2008. "Neutron Moisture Meters." In *Field Estimation of Soil Water Content*, ed. IAEA, pp. 39-54. International Atomic Energy Agency, Vienna, Austria.

Evett, SR, RC Schwartz, JA Tolk, and TA Howell. 2009. "Soil Profile Water Content Determination: Spatiotemporal Variability of Electromagnetic and Neutron Probe Sensors in Access Tubes," *Vadose Zone Journal*, 8(4):926-941. doi:10.2136/vzj2008.0146.

Evett, SR, JA Tolk, and TA Howell. 2005. "Time Domain Reflectometry Laboratory Calibration in Travel Time, Bulk Electrical Conductivity, and Effective Frequency," *Vadose Zone Journal*, 4(4):1020. doi:10.2136/vzj2005.0046.

Gardner, W and D Kirkham. 1952. "Determination of Soil Moisture by Neutron Scattering," *Soil Sci.*, 73:391-402. doi:10.1097/00010694-195205000-00007.

Gee, GW, AL Ward, and MJ Fayer. 1997. "Surface Barrier Research at the Hanford Site," *Land Contamination & Reclamation*, 5(3):233-238.

Hillel, D. 1980. *Fundamentals of Soil Physics*. Academic Press, New York.

Hook, WR, NJ Livingston, ZJ Sun, and PB Hook. 1992. "Remote Diode Shorting Improves Measurement of Soil Water by Time Domain Reflectometry," *Soil Sci. Soc. Am. J.*, 56:1384-1391.

IAEA. 2008. *Field Estimation of Soil Water Content*, Training Course 30, International Atomic Energy Agency, Vienna, Austria.

Imhoff, PT, DR Reinhart, M Englund, R Guerin, N Gawande, B Han, S Jonnalagadda, TG Townsend, and R Yazdani. 2007. "Review of State of the Art Methods for Measuring Water in Landfills," *Waste Management*, 27(6):729-745. doi:10.1016/j.wasman.2006.03.024.

Kamai, T, A Tuli, GJ Kluitenberg, and JW Hopmans. 2008. "Soil Water Flux Density Measurements near 1cm/D Using an Improved Heat Pulse Probe Design," *Water Resources Research*, 44:W00D14. doi:10.1029/2008WR007036.

KEH. 1993. *Prototype Surface Barrier at 200-BP-1 Operable Unit*, W-263-C2 Rev. 0, Kaiser Engineers Hanford Company, Richland, Washington.

Khire, MV and MM Haydar. 2005. "Leachate Recirculation Using Geocomposite Drainage Layer in Engineered Msw Landfills," *GeoFrontier's 05*, Austin, TX. American Society of Civil Engineers, Austin, TX.

Levitt, DG, MJ Hartmann, KC Kisiel, CW Criswell, PD Farley, and C Christensen. 2005. "Comparison of the Water Balance of an Asphalt Cover and an Evapotranspiration Cover at Technical Area 49 at the Los Alamos National Laboratory," *Vadose Zone Journal*, 4(3):789-797. doi:10.2136/vzj2004.0171.

Ochsner, TE, MH Cosh, RH Cuenca, WA Dorigo, CS Draper, Y Hagimoto, YH Kerr, EG Njoku, EE Small, and M Zreda. 2013. "State of the Art in Large-Scale Soil Moisture Monitoring," *Soil Science Society of America Journal*, 77(6):1-32. doi:10.2136/sssaj2013.03.0093.

Olmanson, OK and TE Ochsner. 2006. "Comparing Ambient Temperature Effects on Heat Pulse and Time Domain Reflectometry Soil Water Content Measurements," *Vadose Zone Journal*, 5(2):751-756. doi:10.2136/vzj2005.0114.

Oostrom, M, TW Wietsma, CE Strickland, VL Freedman, and MJ Truex. 2012. "Sensor and Numerical Simulator Evaluation for Porous Medium Desiccation and Rewetting at the Intermediate Laboratory Scale," *Vadose Zone Journal*, 11(1):0. doi:10.2136/vzj2011.0089.

Or, D and JM Wraith. 2001. "Soil Water Content and Water Potential Relationships." In *Soil Physics Companion,* ed. AW Warrick, pp. 49-84. CRC Press, Boca Raton.

Paige, GB and TO Keefer. 2008. "Comparison of Field Performance of Multiple Soil Moisture Sensors in a Semi-Arid Rangeland1," *JAWRA Journal of the American Water Resources Association*, 44(1):121-135. doi:10.1111/j.1752-1688.2007.00142.x.

Pepin, S, NJ Livingston, and WR Hook. 1995. "Temperature-Dependent Measurement Errors in Time Domain Reflectometry Determinations of Soil Water," *Soil Sci. Soc. Am. J.*, 59:38-43.

Robinson, DA, CS Campbell, JW Hopmans, BK Hornbuckle, SB Jones, R Knight, F Ogden, J Selker, and O Wendroth. 2008. "Soil Moisture Measurement for Ecological and Hydrological Watershed-Scale Observatories: A Review," *Vadose Zone Journal*, 7(1):358-389. doi:10.2136/vzj2007.0143.

Robinson, DA, SB Jones, JM Wraith, and SP Friedman. 2003. "A Review of Advances in Dielectric and Electrical Conductivity Measurement in Soils Using Time Domain Reflectometry," *Vadose Zone Journal*, 2(4):444-475.

Romano, N and A Santini. 2002. "Field." In *Methods of Soil Analysis Part 4 Physical Methods,* eds. JH Dane and CT Topp, pp. 721-738. Soil Science Society of America, Inc., Madison, Wisconsin USA.

Scanlon, BR, BJ Andraski, and J Bilskie. 2002. "Miscellaneous Methods for Measuring Matric or Water Potential." In *Methods of Soil Analysis Part 4 Physical Methods,* eds. JH Dane and CT Topp, pp. 643-670. Soil Science Society of America, Inc., Madison, Wisconsin USA.

Staub, MJ, JP Gourc, JP Laurent, C Kintzuger, L Oxarango, H Benbelkacem, R Bayard, and C Morra. 2010. "Long-Term Moisture Measurements in Large-Scale Bioreactor Cells Using Tdr and Neutron Probes," *J Hazard Mater*, 180(1-3):165-172. doi:10.1016/j.jhazmat.2010.04.009.

Topp, CT and PA Ferre. 2002. "Methods for Measuriment of Soil Water Content - Thermogravimetric Using Convective Oven-Drying." In *Methods of Soil Analysis Part 4 Physical Methods,* eds. JH Dane and CT Topp, pp. 422-424. Soil Science Society of America, Inc., Madison, Wisconsin USA.

Topp, GC, JL Davis, and AP Annan. 1980. "Electromagnetic Determination of Soil Water Content: Measurements in Coaxial Transmission Lines," *Water Resources Research*, 16:574-582. doi:10.1029/WR016i003p00574.

Truex, MJ, M Oostrom, CE Strickland, GB Chronister, MW Benecke, and CD Johnson. 2012. "Field-Scale Assessment of Desiccation Implementation for Deep Vadose Zone Contaminants," *Vadose Zone Journal*, 11(4):0. doi:10.2136/vzj2011.0144.

Truex, MJ, CE Strickland, CD Johnson, TC Johnson, RE Clayton, and GB Chronister. 2014. *Deep Vadose Zone Treatability Test for the Hanford Central Plateau: Interim Post-Desiccation Monitoring Results, Fiscal Year 2014*, PNNL-23731, Pacific Northwest National Laboratory, Richland, Washington.

Vaz, CMP, S Jones, M Meding, and M Tuller. 2013. "Evaluation of Standard Calibration Functions for Eight Electromagnetic Soil Moisture Sensors," *Vadose Zone Journal*, 12(2):1-16. doi:10.2136/vzj2012.0160.

Ward, AL and GW Gee. 1997. "Performance Evaluation of a Field-Scale Surface Barrier," *Journal of Environmental Quality*, 26(3):694-705.

Ward, AL, SO Link, KE Draper, and RE Clayton. 2011. *200-BP-1 Prototype Hanford Barrier -- 15 Years of Performance Monitoring*, PNNL-18845 Revision 1, Pacific Northwest National Laboratory, Richland, Washington. Available at http://www.osti.gov/energycitations/servlets/purl/1027194/. (Accessed on Aug. 21, 2015).

Wing, NR and GW Gee. 1994. "Quest for the Perfect Cap," *Civil Engineering*, 64(10):38-41.

Yoder, RE, DL Johnson, JB Wilkerson, and DC Yoder. 1997. "Soil Water Sensor Performance," *Applied Engineering in Agriculture*, 14(2):121-133.

Young, GD, BA Adams, and GC Topp. 2000. " A Portable Data Collection System for Simultaneous Cone Penetrometer Force and Volumetric Soil Water Content Measurements," *Can. J. Soil Sci.*, 80:23-31.

Zhang, ZF. 2015. "Field Soil Water Retention of the Prototype Hanford Barrier and Its Variability with Space and Time," *Vadose Zone Journal*, 14(8):1-10. doi:10.2136/vzj2015.01.0011.

Zhang, ZF, CE Strickland, JG Field, DL Parker, and RE Clayton. 2012. "Evaluating the Performance of a Surface Barrier for Reducing Soil-Water Flow," *Vadose Zone Journal*, 11(3) doi:10.2136/vzj2011.0117.

Appendix G

Nineteen-Year Hydrological Characteristics of the Prototype Hanford Barrier: The Silt Loam Storage Layer

Z. Fred Zhang

Pacific Northwest National Laboratory
Richland, Washington

Content

List of Figures

List of Tables

Abstract

A surface barrier (or cover) is a commonly used technology for subsurface remediation. A key function of the barrier is to reduce or eliminate the movement of meteoric precipitation into the underlying waste zone, where it could mobilize and transport contaminants. Surface barriers are expected to perform for centuries to millennia, yet there are very few examples of performance for periods longer than a decade. The Prototype Hanford Barrier was constructed in 1994 over an existing waste site to demonstrate its constructability and long-term performance for a design period of 1000 years. This barrier is a field-scale evapotranspiration (ET) layer atop a capillary break and is termed as the ETC barrier. The basic concept of an ETC barrier is to store all precipitation in the ET layer, where it can be released later via soil evaporation and plant transpiration such that drainage is always less than the design criterion of 0.5 mm/yr. In this design, the ET layer consists of 2-m-thick silt loam. The 19-year monitoring results show that the store-and-release mechanism for the ETC barrier worked efficiently as the silt loam layer was recharged in the winter season (November to March) and the stored water was released to the atmosphere in the summer season (April to October). The capillary break functioned normally in improving the storage capacity and minimizing drainage. The maximum drainage observed through the ET barrier at any of the monitoring stations was only 0.18 mm yr^{-1} under an enhanced precipitation condition, which is less than the design criterion. A very small amount (38.1 mm in total) of runoff was observed during the 19-year monitoring period. The observed storage capacity of the storage layer was considerably (39%) larger than the estimated value based on the method of equilibrium of water pressure. After a controlled fire in 2008, the newly grown vegetation (primarily shallow-rooted grasses) could still release the stored water and summer precipitation to the atmosphere via ET. These findings suggest that the winter-season precipitation should be used to determine the barrier thickness, which is much less than if the annual precipitation is used, as is the case in the PHB design. The findings are useful for predicting water storage and ET under different precipitation conditions and for the design of future barriers.

G.1 Introduction

A surface barrier (or cover) is a commonly used technology for subsurface remediation. A key function of the barrier is to reduce or eliminate the movement of meteoric precipitation into the underlying waste zone, where it could mobilize and transport contaminants. Conventional surface barriers tend to rely on a layer of material that resists downward water movement. This resistive layer is typically made of compacted clay, geomembranes, geosynthetic clay liners, or a combination of these materials. Conventional barriers are prone to problems such as increasing permeability with time (Benson et al. 2007; Henken-Mellies and Schweizer 2011), preferential flow path development within the barrier (Albright et al. 2004), and cracking because of desiccation (Albrecht and Benson 2001).

Evapotranspiration (ET) barriers are an alternative to conventional surface barriers. Rather than using a resistive layer, ET barriers rely on two natural processes to control water movement into the underlying waste zone: (1) water is stored in the soil, which acts as a natural reservoir for precipitation, and (2) water is released from soil to the atmosphere via natural evaporation from the soil surface and transpiration from the plant community. The integration of these two processes is referred to as the store-and-release mechanism. The ET barrier is a self-renewing biological system and is expected to last much longer than a conventional barrier. ET barriers have also been referred to in the literature as store-and-release covers, water balance covers, and vegetative covers. ET barriers may only be effective in arid, semi-arid, and sub-humid climates where the potential evapotranspiration (PET) exceeds precipitation. The PET at the Hanford Site is about 5 to 10 times the annual precipitation (Gee et al. 1989; Wallace 1977), making the climate at Hanford suitable for ET barriers. According to EPA (2011), ET barriers are increasingly being considered for use at waste disposal sites. The Alternative Cover Assessment Project in 1998 provided a general understanding of the hydrologic behavior of conventional and alternative landfill final covers (Albright et al. 2004; Albright et al. 2002).

The storage capacity of a barrier is the maximum amount of water it can hold without producing drainage. Storage capacity can be enhanced by including a capillary break (CB) beneath the storage layer (Khire et al. 2000; Mancarella et al. 2012; Scanlon et al. 2005). A CB is formed when a fine-textured layer overlays a coarse-textured layer. The interface between the layers acts as barrier to the downward flow of water under unsaturated conditions and effectively increases the storage capacity of the fine-textured soil (Albright et al. 2010). A CB starts taking effect when the wetting front reaches the bottom of the storage layer. Once the water pressure at the CB is higher than the water entry pressure of the coarser layer, water starts flowing across the CB. An ET barrier with a CB is referred to as an evapotranspiration-capillary (ETC) barrier hereafter.

Fayer and Gee (2006) presented the water balance of ETC covers at the Field Lysimeter Test Facility (FLTF) at the Hanford Site near Richland, WA, for periods of up to 17 years. They found that, when irrigated to mimic three times (3X) the average precipitation conditions, the vegetated Hanford Barrier with 1.5-m-thick silt loam underlain by a CB could nearly eliminate drainage (i.e., <0.1 mm yr^{-1}).

Based on systematic investigations at the FLTF and elsewhere, the Prototype Hanford Barrier (PHB) was constructed in 1994 over an existing waste site to demonstrate its constructability and long-term performance (Wing and Gee 1994). The PHB design was a field-scale ETC barrier with a surface slope of 2% and a design life of 1000 years. The barrier was tested from 1994 to 1997 under extreme precipitation conditions not seen in the historical record. Plants on the north section of the barrier were burned with a controlled fire in September 2008 to test the impact of plant loss.

From barrier construction in 1994 until 2013, the monitored components at the PHB included hydrological conditions [i.e., soil water content (θ), drainage (D), and runoff (R)], ecological conditions (i.e., plant species and coverage and animal activities), and the stability of the barrier and side slopes. The nearly two decades' worth of monitoring data over a field-scale surface barrier provide a unique dataset to

evaluate barrier performance and to guide future barrier design. The objective of this appendix is to summarize the temporal variation of the soil water contents and water balance to understand the store-and-release processes within the barrier. The influence of a CB on enhancing water storage in the barrier is discussed. The impacts of the sloped barrier surface and the controlled fire on the barrier's hydrological performance are analyzed. Relationships among water storage (W), ET, and precipitation (P) are established by empirical expressions so that W and ET may be predicted based on precipitation for the site. The appropriate thickness of the storage layer is discussed. It is expected that the 19-year hydrological performance evaluation of the PHB will provide valuable information for future barrier designs at the Hanford Site and elsewhere.

G.2 Climate and the Standardized Precipitation Index at Hanford

The Hanford Site has a steppe (semi-arid) climate with typical dry, hot summers and cool, wet winters (Hoitink et al. 2005). Under the Hanford climate, the most likely season for recharge is between November and March (termed the winter season), when ET is low (Gee et al. 1992; Gee et al. 2005). In addition to winter rains, snowmelt can be an important contributor to recharge. Vegetation consists of shrub-steppe plant communities composed of annual grasses and perennial grasses and shrubs (Rickard and Vaughan 1988). This desert vegetation, a mixture of shallow and deep-rooted plants, generally uses soil water very efficiently from roughly April to October (termed the summer season). To be consistent with the precipitation pattern, a water year (WY) is defined as the 12-month period from November of the previous year to October of the current year. Namely, a WY consists of a 5-month winter season and a 7-month summer season. A specific WY is denoted by "WYyy," in which "yy" is the last two digits of a year. For example, WY1999 is denoted by WY99.

The average recharge rate to the subsurface beneath undisturbed natural vegetation is usually no more than 5.0 mm yr^{-1} (Fayer and Keller 2007). However, without vegetation, the recharge can be as high as 50 to 100 mm yr^{-1}, depending on the texture of the surface soil. A coarser surface soil tends to produce higher recharge.

According to the long-term (67-year from WY48 to WY14) climate record, the WY meteoric precipitation at the Hanford Site had an average, P^{avg}, of 171.3 mm and varied from 101.4 mm ($0.59P^{avg}$) to 293.6 mm ($1.71P^{avg}$). On average, 58.7% (100.6 mm, P_w^{avg}) of the precipitation falls in the winter season and 41.3% (70.7 mm, P_s^{avg}) in the summer season. During the barrier test period from WY95 to WY13, the average precipitation was 185.1 mm yr^{-1}, slightly higher than the long-term average.

Precipitation tends to obey a gamma distribution (Thom 1966). The cumulative probability of an observed precipitation event is described as

$$G(P) = \int_0^P \frac{\xi^{\alpha-1}\exp(-\xi/\beta)}{\beta^{\alpha}\Gamma(\alpha)}d\xi \qquad \text{(G.1)}$$

$$\text{where } \Gamma(\alpha) = \int_0^{\infty} \xi^{\alpha-1}\exp(-\xi)d\xi \qquad for\ P > 0$$

where $\alpha > 0$ is a shape parameter, $\beta > 0$ is a scale parameter, $P > 0$ is the precipitation amount, ξ is the dummy variable of integration, and $\Gamma(\alpha)$ is the gamma function. Based on precipitation measured at Hanford from WY48 to WY14, the precipitation data for the WYs, winter seasons, and summer seasons were used to fit α and β according to Eq. (G.1). Table G.1 shows the precipitation statistics and fitted α and β parameters. Figure **G.1** shows the cumulative probability of precipitation in the WY, winter season, and summer season. Although the model can describe the observed precipitation data well, the estimated precipitation in very low probability (e.g., 0.1%) is subject to extrapolation error.

Table G.1. Precipitation statistics and the fitted parameters α and β for WY48 to WY14.

	Water Year	Winter Season	Summer Season
Min (mm)	101.4	29.7	14.2
Max (mm)	293.6	224.0	157.5
Average (mm)	171.3	100.6	70.7
Median (mm)	167.1	96.1	66.9
α	13.739	7.485	6.149
β	12.465	13.438	11.494

Because the PHB has a design life of 1000 years, the maximum precipitation expected once in 1000 years was quantified by the 99.9% percentile. Based on Eq. (G.1), the estimated precipitation with 0.1% probability at Hanford is 350.0 mm for a WY, 253.0 mm for the winter season, and 191.9 mm for the summer season.

To adequately evaluate the barrier's hydrological performance relative to the precipitation level, the precipitation was categorized with the standardized precipitation index (SPI) developed by McKee et al. (1993). The SPI is a probability index defined as the standard normal random variable (with mean $\mu = 0$ and standard deviation $\sigma = 1$) obtained from the cumulative probability [Eq. (G.1)]. The nature of the SPI allows an anomalously dry or wet event to be quantified at a particular time scale. According to the SPI values, McKee et al. (1995) categorized the precipitation of a given period into seven classes: extreme wet, severe wet, moderate wet, near normal, moderate dry, severe dry, and extreme dry (Table G.2). The calculated SPIs during the barrier test period from WY95 to WY13 for the WYs, winter seasons, and summer seasons are shown in Figure G.2. Regarding the WY precipitation of the 19 test years, 2 years (WY95 and WY97) were extreme wet, 4 moderate wet, 12 near normal, and 1 (WY05) severe dry. This means that the barrier experienced the most precipitation stress in WY95 and WY97, even under the unirrigated section of the barrier.

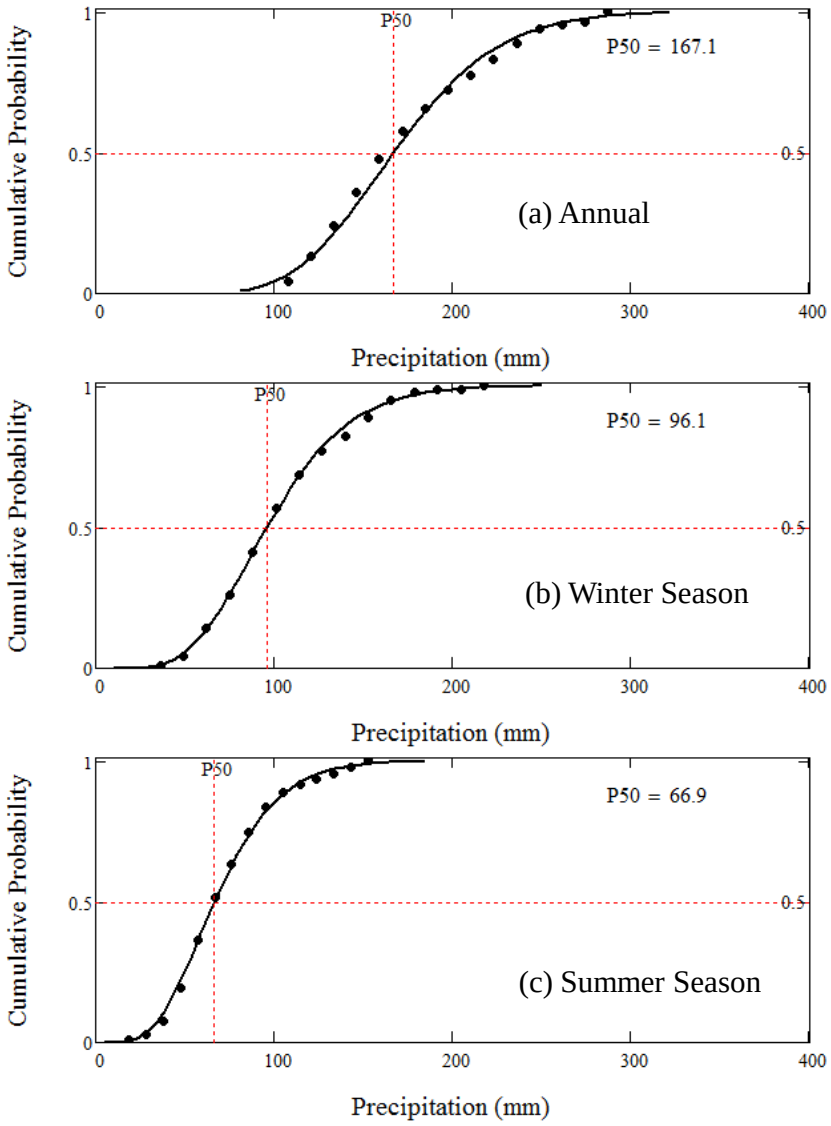

Figure G.1. Cumulative probability of precipitation. The symbols denote data and the curves the best fits. P50 is the median precipitation.

Table G.2. SPI classification following McKee et al. (1995).

SPI Values	Class Name	Class Symbol	Probability of Event (%)
SPI > 2.0	Extreme wet	EW	2.3
1.5 < SPI ≤ 2.0	Severe wet	SW	4.4
1.0 < SPI ≤ 1.5	Moderate wet	MW	9.2
-1.0 < SPI ≤ 1.0	Near normal	NN	68.3
-1.5 < SPI ≤ -1.0	Moderate dry	MD	9.2
-2.0 < SPI ≤ -1.5	Severe dry	SD	4.4
SPI ≤ -2.0	Extreme dry	ED	2.3

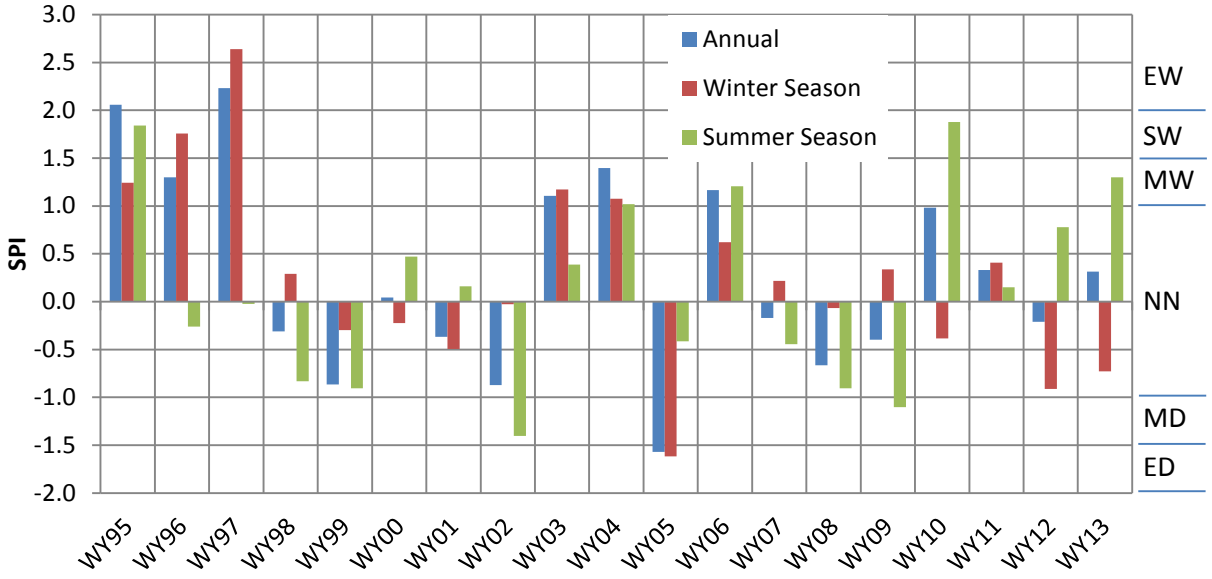

Figure G.2. Standardized precipitation index and precipitation categories during the barrier test period. The definition of precipitation category symbols is given in Table G.2.

G.3 Methods and Materials

G.3.1 Prototype Hanford Barrier Design and Tests

The PHB, with an area of 2.5 ha (6.2 acres), was constructed between late 1993 and 1994 in the 200 East Area of the Hanford Site in southeastern Washington State, and was deployed over the 216-B-57 Crib in the 200-BP-1 Operable Unit (46°34'01.23"N, 119°32'28.43"W). The PHB description and design can be found in other sources (e.g., DOE-RL 1994, 1999; Gee et al. 1997; KEH 1993; Ward and Gee 1997; Wing and Gee 1994). Briefly, the PHB consists of four main components (Figure G.3): (1) a silt loam ET layer with an underlying CB and an intrusion prevention layer, termed the ETC barrier, in the middle; (2) a gentle pit-run gravel side slope in the west (10:1) and in the west portions of the north and south side slopes (5:1 to 3:1); (3) a 2:1 steep basalt riprap side slope in the east and in the east portion of the north and south side slopes; and (4) an asphalt concrete (AC) pad with a polymer-modified fluid applied asphalt coating and a compacted soil layer at the bottom. The ETC barrier is the centerpiece of the PHB and sits directly above the waste zone. It is designed to store precipitation and release the stored water into the atmosphere and to deter intrusion by plants, animals, or humans from the barrier surface. The two side slopes protect the ETC barrier from damage or intrusion from the sides. The AC is the redundant barrier to the overlying ETC barrier to divert drainage and to hinder intrusion.

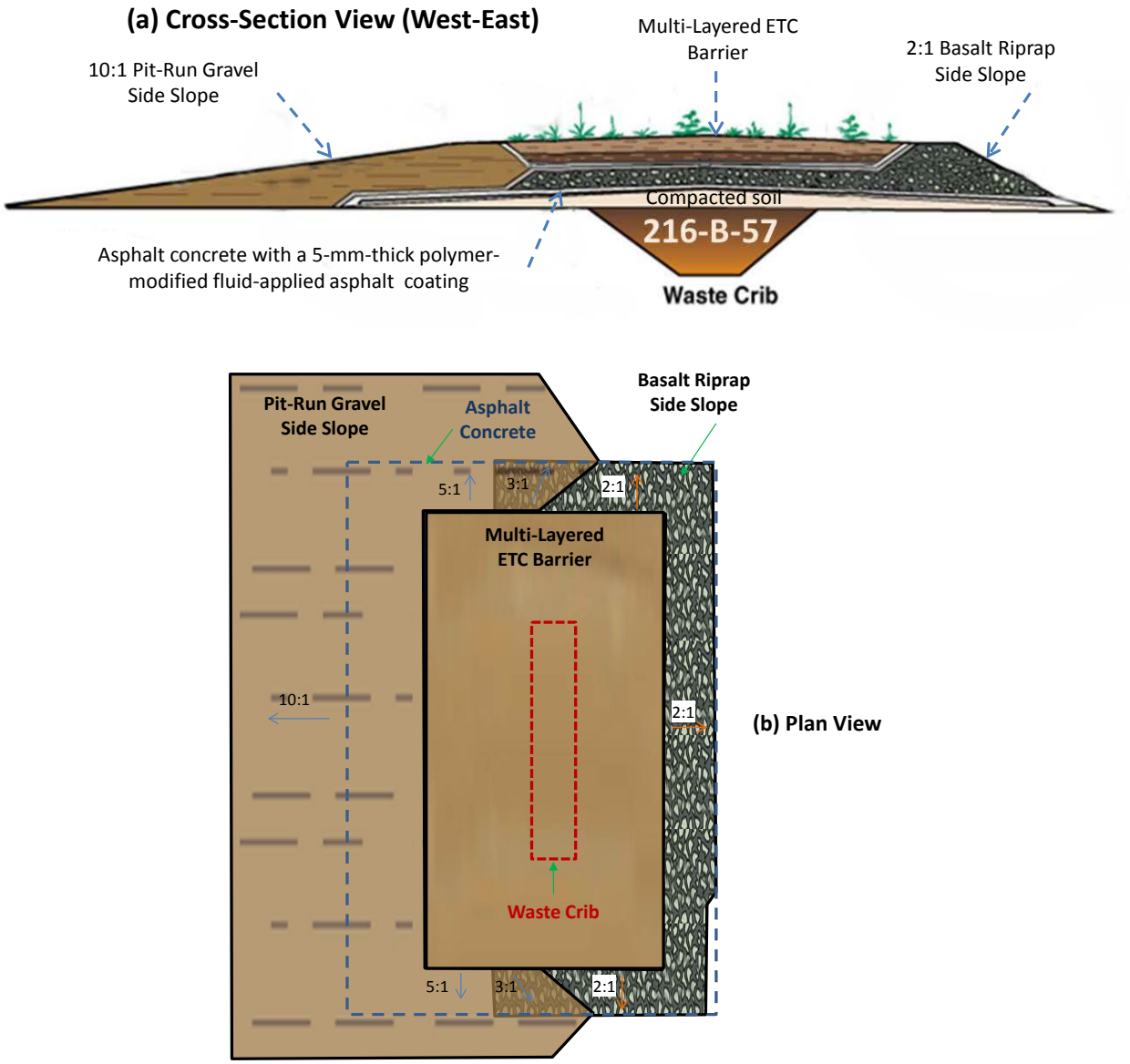

Figure G.3. Schematic of the Prototype Hanford Barrier: (a) cross-section view (west-east) and (b) plan view (approximate scale).

The ETC barrier is a sequence of multiple layers overlying the AC. The 2-m-thick silt-loam layer acts as the storage layer from which ET processes recycle some or all of the stored water back to the atmosphere. The silt loam also provides a medium for the growth of vegetation, which is necessary for transpiration to take place. In addition, the top 1 m of silt loam was amended with 15% w/w pea gravel to minimize wind and water erosion. The dry bulk density of the admix of the ETC barrier after construction was 1380±0.121 kg m^{-3} (Gee et al. 1995). Coarser materials (sand overlying gravel) placed directly below the silt-loam layer create a CB that inhibits the downward percolation of water from the silt loam into the coarser material. The 1.5-m-thick layer of basalt riprap (about 0.25 m in size) helps deter root penetration, animal burrowing, and inadvertent intrusion by humans through the barrier profile. The drainage layer above the AC helps to promote lateral flow of any water that passes through the ETC barrier.

The silt loam (aka Warden silt loam) used for the barrier was from the McGee Ranch about 10 miles west of the site. The average particle size distribution of 16 soil samples was 60.6% sand, 31.1% silt, and 8.3% clay. Zhang (2015) analyzed the field water retention of the silt loam layer at four depths and 12 water balance stations using *in situ* measurements of water content and pressure from 1995 to 2003. The average non-hysteretic field retention parameters with one standard deviation (σ) are saturated water content θ_s = 0.344±0.056 m^3m^{-3}, residual water content θ_r = 0.068±0.012 m^3m^{-3}, van Genuchten α = 5.46×/÷2.33, and van Genuchten n = 1.51±0.13 (Zhang 2015). The spatial variability of the retention properties appeared to be greater than the effects of added 15% w/w pea gravel on the properties. Grouping the data by primary hydrological processes or time showed that neither hysteresis nor time had a discernable effect on the water retention of the silt loam layer. The saturated hydraulic conductivity measured with 16 soil cores at the time of barrier construction had an average of 1.42×10^{-6} m s^{-1}. An average field K_s of 4.31×10^{-6} m s^{-1} was obtained in 2008 using the Guelph permeameter and the two-head data processing method (Ward et al. 2009, Table 3.19).

The barrier was constructed with a 2% slope to the west and east of the barrier crown (the north-to-south centerline). The purpose of the slope is to allow any excessive water on the barrier surface to run off, resulting in less water infiltrating into the center of the barrier and the underlying waste zone.

For testing purposes, the surface barrier was divided into north and south sections separated by a 10-m-wide buffer zone. An enhanced precipitation test (aka treatability test) was used to test the barrier under extreme climate conditions for a period of 3 water years (WY95 to WY97, within a time frame of 4 calendar years). In late March of each year from 1995 to 1997, a 1000-year return, 24-hour rainstorm was simulated on the north section. Although the simulated rainstorm was targeted to deliver 68 mm over a 24-hour period based on the analysis of precipitation from 1947 to 1969 (Stone et al. 1983), in practice, 69.4, 69.5, and 69.7 mm (69.5 mm on average) of water was applied over 8-hour periods (8.7 mm hr^1 or 2.41×10^{-6} m s^{-1}, on average) on March 25 of 1995, March 26 of 1996, and March 27 of 1997, respectively. In May 1998, 209.6 mm of water was added to the entire north section for instrument calibration. The total meteoric precipitation and irrigation received by the north section was 493.3, 493.1, 499.7, and 363.0 mm (SPI = 4.83, 4.83, 4.90, and 3.27) for WY95 through WY98, respectively. The SPI values correspond to precipitation probabilities of 0.67, 0.67, and 0.47 times in 1 million years for WY95, WY96, and WY97, respectively.

From WY99 to WY13, both the north and south sections were exposed to natural precipitation conditions. In September 2008, the vegetation in the north section was burned to test the impact of a natural fire on the barrier performance.

G.3.2 Water Content, Water Pressure, and Drainage Monitoring

Soil water content and pressure of the silt loam barrier were monitored at 12 water balance stations. Six of the stations were located in the north section and spaced 5 m apart. The other six stations were in the south section and also spaced 5 m apart. Barrier water content was monitored at a vertical interval of 0.15 m using a neutron probe (NP) (Hydroprobe Model 503, CPN International, Inc., Martinez, CA) deployed in a vertical (4.8-cm inner diameter) aluminum access tube extending 1.9 m below the barrier surface. The NP was calibrated on April 5, 1995, in the vertical access tube:

$$\theta = a_0 + a_1 N + a_2 N^2 \tag{G.2}$$

where N is the 16-second neutron count, a_0 = -0.01649, $a_1 = 1.449 \times 10^{-5}$, and $a_2 = 3.234 \times 10^{-10}$. On April 20, 2003, the NP received a new neutron counter. Cross-calibration with another NP before and after the installation of the new counter showed that the new counter recorded only 96% of the data recorded using the old counter. Hence, the count values using the new counter were scaled by a factor of 1.041 for vertical logging so that Eq. (G.2) could be used to calculate water content. Radioactive decay was corrected for all measurements before data analysis.

Arrays of heat dissipation units (HDUs) (Model 229L, Campbell Scientific Inc., Logan, Utah) were installed in September 1994 to monitor soil water pressure (h) at depths of 0.075, 0.225, 0.45, 0.80, 1.25, and 1.75 m below ground surface. Before each measurement, the HDU was heated for a fixed period with a needle-type heater inside the HDU. The rate of heat dissipation was controlled by the water content of the HDU's porous matrix because water conducts heat much faster than air. The temperature increase caused a voltage change in the thermocouple in the HDU, and the voltage was measured. The heat dissipation was determined as the difference between two voltages (ΔV), one measured after 1 second of heating and the other measured after a 30 seconds of heating. The relationships between the HDU-measured temperature and output voltage indicated that the variation among the HDUs was very small. Selected HDUs were calibrated in Tempe cells in the laboratory and the general calibration curve (Figure G.1) was used to convert the voltage change to soil-water pressure:

$$h = \begin{cases} a\exp(b\Delta V) & if \quad \Delta V \geq 1000 \\ \\ c(1000-\Delta V)^2 + d(1000-\Delta V) - 1 & if \quad \Delta V < 1000 \end{cases} \tag{G.3}$$

where a = -1.514 × 10^{-3}, b = 6.556 × 10^{-3}, c = -1.338 × 10^{-5}, d = 7.331 × 10^{-3}, , h is soil-water pressure in meters and is negative under unsaturated conditions, and ΔV is voltage change in millivolts. It is noted that the upper limit of water pressure measured by an HDU generally is considered to be approximately -1 m (CSI 2009; Flint et al. 2002; Reece 1996). However, the HDUs used at the PHB were first generation sensors and seemed to lack clear, distinct air entry pressures because of the existence of large pores.

To quantify the total amount of water in the barrier, water storage (W) within the 2-m-thick silt loam layer was calculated based on neutron logging of soil water content at 12 depths between 0.15 and 1.80 m. The measurements at the 0.15-m depth were extrapolated to ground surface and those at 1.80-m depth were extrapolated to the 2-m depth. To calculate the storage change for the winter season (ΔW_w) and the summer season (ΔW_s), the water storages on November 1 and April 1 of each year were estimated by interpolating the two nearest neutron loggings.

The PHB was designed to limit the drainage rate to no more than 1.6×10^{-11} m s^{-1} (0.5 mm yr^{-1}) (Gee et al. 1997; Ward and Gee 1997; Wing and Gee 1994). Under this drainage rate, the drainage water would move only about 5 m in 1000 years, assuming the water content is 0.1 m^3m^{-3}. To confirm the performance, drainage through the silt loam was measured using four 322-m^2 (23-m-long and 14-m-wide) plots, two in the north section and two in the south section. Drainage from each plot was piped to a drainage vault. Once the water level in a vault reached a certain height, it would trigger a siphon system to empty the vault. Each vault was equipped with a tipping bucket, a pressure transducer to measure water level, and a dosing counter to record the counts of siphons. However, because the near-zero drainage through the silt loam barrier was below the detection limits of the pressure transducer and dosing siphon, only the results from the tipping buckets are presented. The tipping buckets had a volume of about 11.0 mL per tip, which is equivalent to 3.4×10^{-5} mm of drainage.

Assuming water flow in the barrier is vertical only, ET can be estimated based on the mass balance equation:

$$ET = P - R - D - \Delta W \tag{G.4}$$

where P is the total precipitation including irrigation water, R is run-off, D is drainage, and ΔW is the change in soil water storage. Using Eq. (G.4), ET was estimated for the north and south sections and for the winter (ET_w) and summer (ET_s) seasons for the years with sufficient data. Monthly ET (ET_m) was calculated for the summer months from WY95 to WY97. There were not enough observations to calculate

the monthly ET for years from WY98 to WY13. The measured precipitation from the Hanford Meteorological Station, which is about 3 miles west of the PHB, was used to calculate ET.

To calculate the storage change (ΔW) for the winter season (ΔW_w) and the summer season (ΔW_s), the water storages on November 1 and April 1 of each year were estimated by interpolating the measured water content of the two nearest neutron loggings. Interpolation of ΔW was conducted for the first day of the month when monthly ET was calculated.

Additionally, the monthly ET for the summer months from WY95 to WY97 was decomposed into the contributions from precipitation (ET_m^p) and soil (ET_m^s). The subscript "m" denotes the monthly value. When calculating ET_m^p and ET_m^s, it was assumed all the monthly precipitation (P_m) was released to the atmosphere via ET in the same month and ET_m^s is the difference between the ET_m and P_m, i.e., $ET_m^p = P_m$, $ET_m^s = ET_m - P_m$. Sometimes negative ET_m^s was produced, suggesting that only part of the P_m contributed ET_m and the rest entered the barrier.

G.4 Results

This section first presents the hydrological processes in the ETC barrier. Then the water balance in the ETC barrier is delineated for the winter seasons, summer seasons, and the water years. Next, presented in sequence are the functionality of the CB, storage capacity of the barrier, water diversion by sloped barrier surface, and the hydrological impacts of controlled fire. Finally, the proper barrier thickness at Hanford is discussed.

G.4.1 Hydrology in the ETC Barrier

From WY95 to WY97, an enhanced precipitation test was carried out in the north section of PHB. In WY98, there was no irrigation in the winter season but there was 209.6 mm of irrigation in the north section in the summer season. The north section of the PHB was under natural precipitation in WY99 and after, while the south section was always under natural precipitation.

The Recharge Process

The total winter season precipitation (meteoric precipitation plus irrigation) on the north section was 252.2, 339.9, 344.2, and 106.9 mm (with an estimated probability of 1.04, 0.009, 0.007, and 3.9 times per 1000 years) for WY95, WY96, WY97, and WY98, respectively. The lower-than-planned P_w for WY95 was due to a delay of the sprinkler system start time.

Because of the low PET in the winter season (Wallace 1977), the barrier had a net gain of water during the winter season of each WY, as shown by the water content (Figure G.4 and Figure G.5) and water pressure (Figure G.6). During each winter season, the infiltration water gradually migrated from shallow to deep soil as more precipitation entered the soil. From WY95 to WY97, the seasonally wetted zone was deeper in the irrigated north section than in the south. For example, water content increased to 0.25 m^3m^{-3} to the depths ranging between 1.65 and 1.80 m in the irrigated north section (Figure G.4a) and to the depths ranging between about 0.8 and 1.2 m in the south section (Figure G.5a). The HDU-measured soil water pressure showed similar responses (Figure G.6).

From WY99 to WY13, the entire barrier was exposed to only natural precipitation. The vegetation in the north section was burned by a controlled fire in September 2008. During this period, the winter season precipitation ranged from 49.3 mm (SPI = -1.62, severe dry) to 144.5 mm (SPI = 1.17, moderate wet), with an average of 96.2 mm. Of the 15 years, the P_w was moderate wet for 2 years, near normal for 12 years, and severe dry for 1 year. Water content is shown in Figure G.4b and Figure G.4c for the north section and in Figure G.5b and Figure G.5c for the south section. The maximum water content was always <0.25 m^3m^{-3} and was less than 0.20 m^3m^{-3} for most years. Water content of 0.1 m^3m^{-3} was generally seen no deeper than 0.8 m and the soil below the 0.8-m depth was < 0.10 m^3m^{-3} in all 15 years.

The soil water pressure also indicates that the barrier was rarely wetter than -1 m and the soil below the 1-m depth was almost always (except in the fall of 2000) drier than -10 m (Figure G.6). These results suggest that in the near-normal precipitation years, the infiltration water was stored primarily in the top 0.8 m of the barrier profile, indicating very little chance to produce drainage.

The Release Process

In the summer season, with a high PET and low precipitation, the barrier had a net loss of soil water via ET as shown in Figure G.4 for the north section and Figure G.5 for the south section. The stored water was released into the atmosphere when ET exceeded precipitation. The soil water in shallow soil (roughly from 0 to 0.4 m deep) was released the quickest because both evaporation and transpiration took effect. The soil water in the intermediate depth (roughly from 0.4 to 1.2 m) was removed almost uniformly; the soil water at large depth (roughly below 1.2 m) was discharged the slowest (when there was plant-available water stored at large depth, e.g., from WY95 to WY98, Figure G.4 and Figure G.5), possibly because there were relatively fewer roots in the deep soil. Observation of plant root density in 1995 and 1996 showed that root length density increased with depth down to about 1.1 to 1.5 m and then decreased with depth (Gee et al. 1995; Gee et al. 1996). The release pattern of soil water to atmosphere is in agreement of the distribution of plant roots.

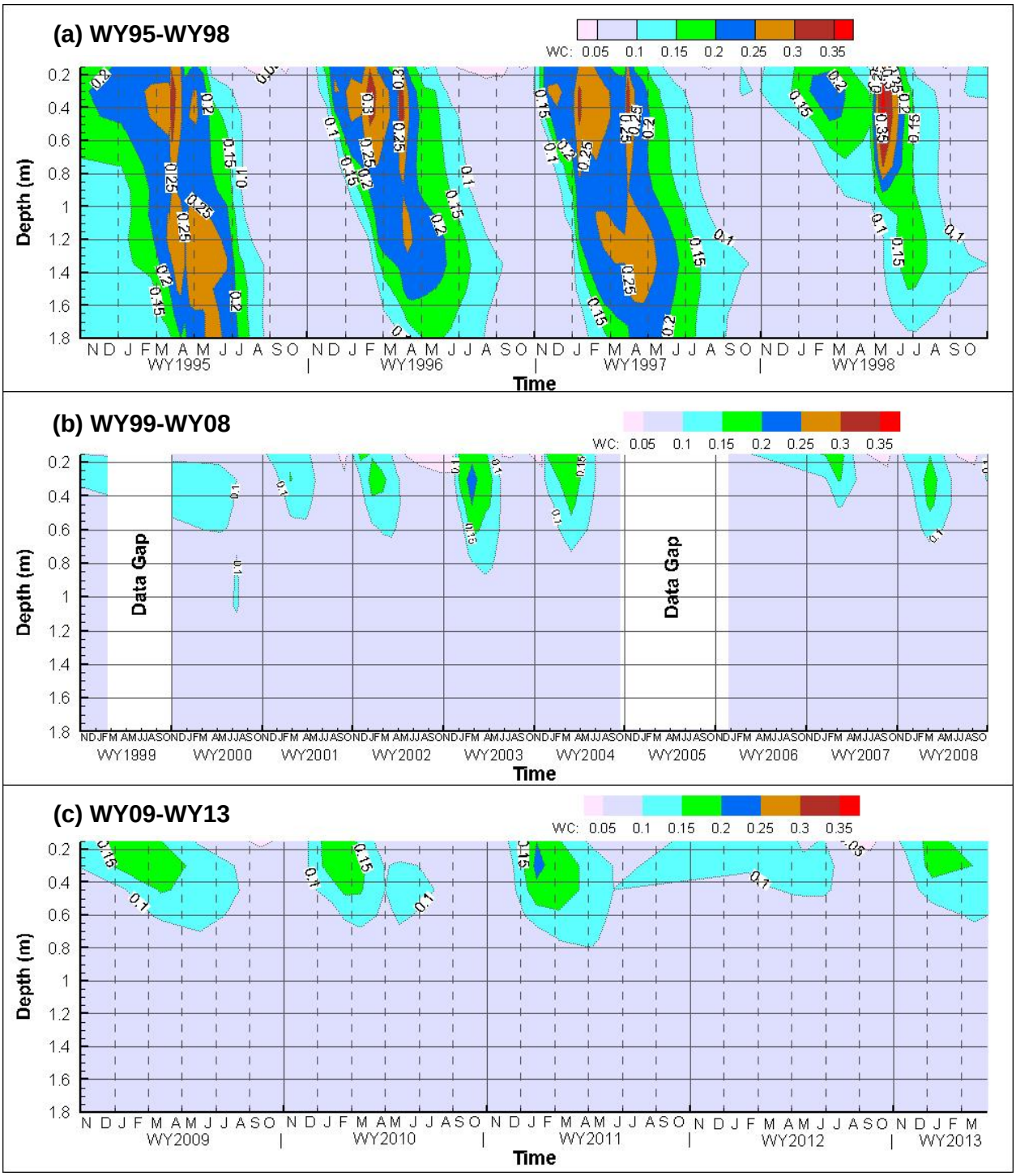

Figure G.4. Average soil water content of 6 monitoring stations for the north section during the periods from (a) WY95 to WY98 with enhanced precipitation in the north section, (b) WY99 to WY08 under the natural condition, and (c) WY09 to WY13 after a controlled fire burned the vegetation in the north section.

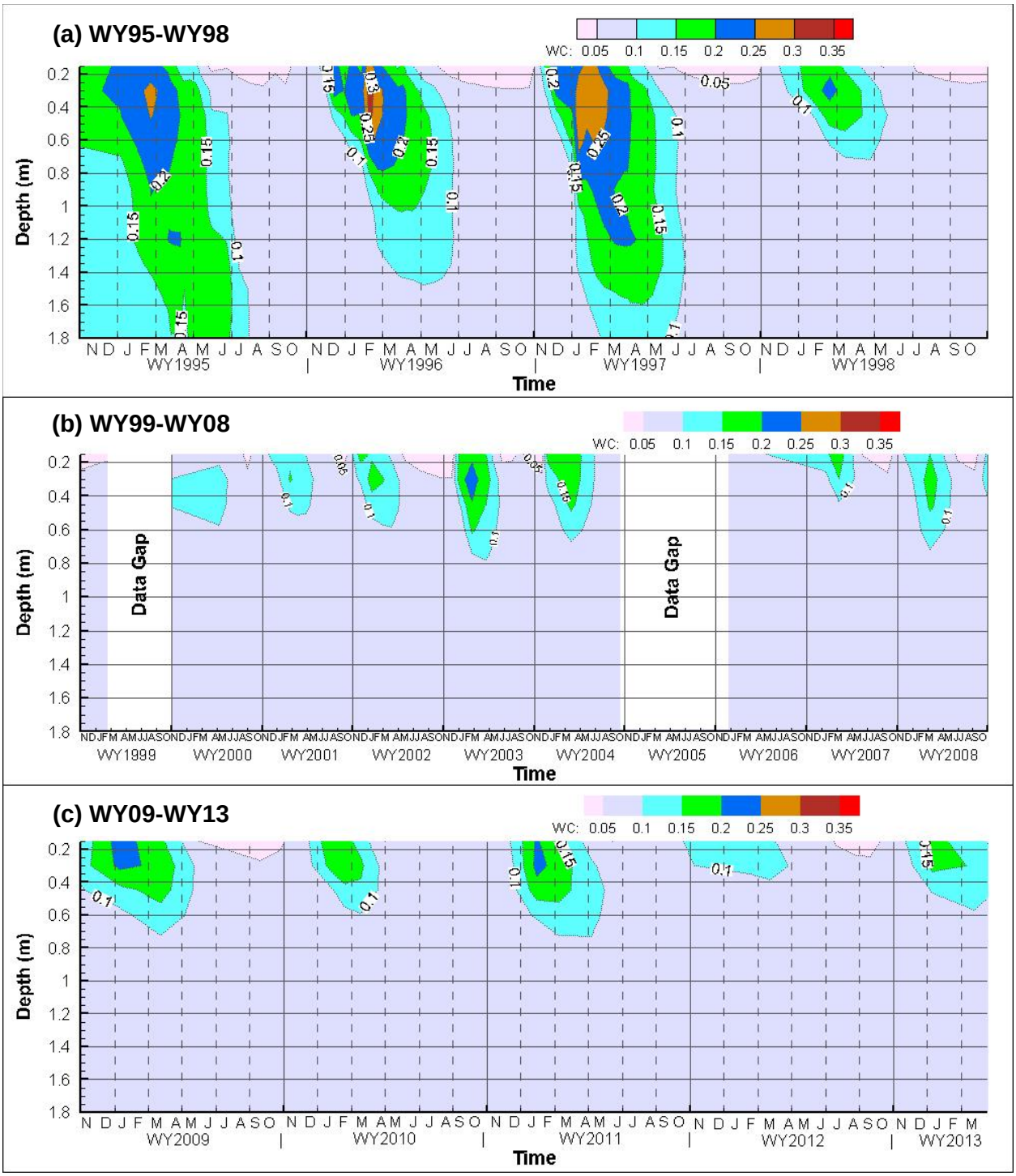

Figure G.5. Average soil water content of 6 monitoring stations for the south section during the periods from (a) WY95 to WY98 with enhanced precipitation in the north section, (b) WY99 to WY08 under the natural condition, and (c) WY09 to WY13 under the natural condition.

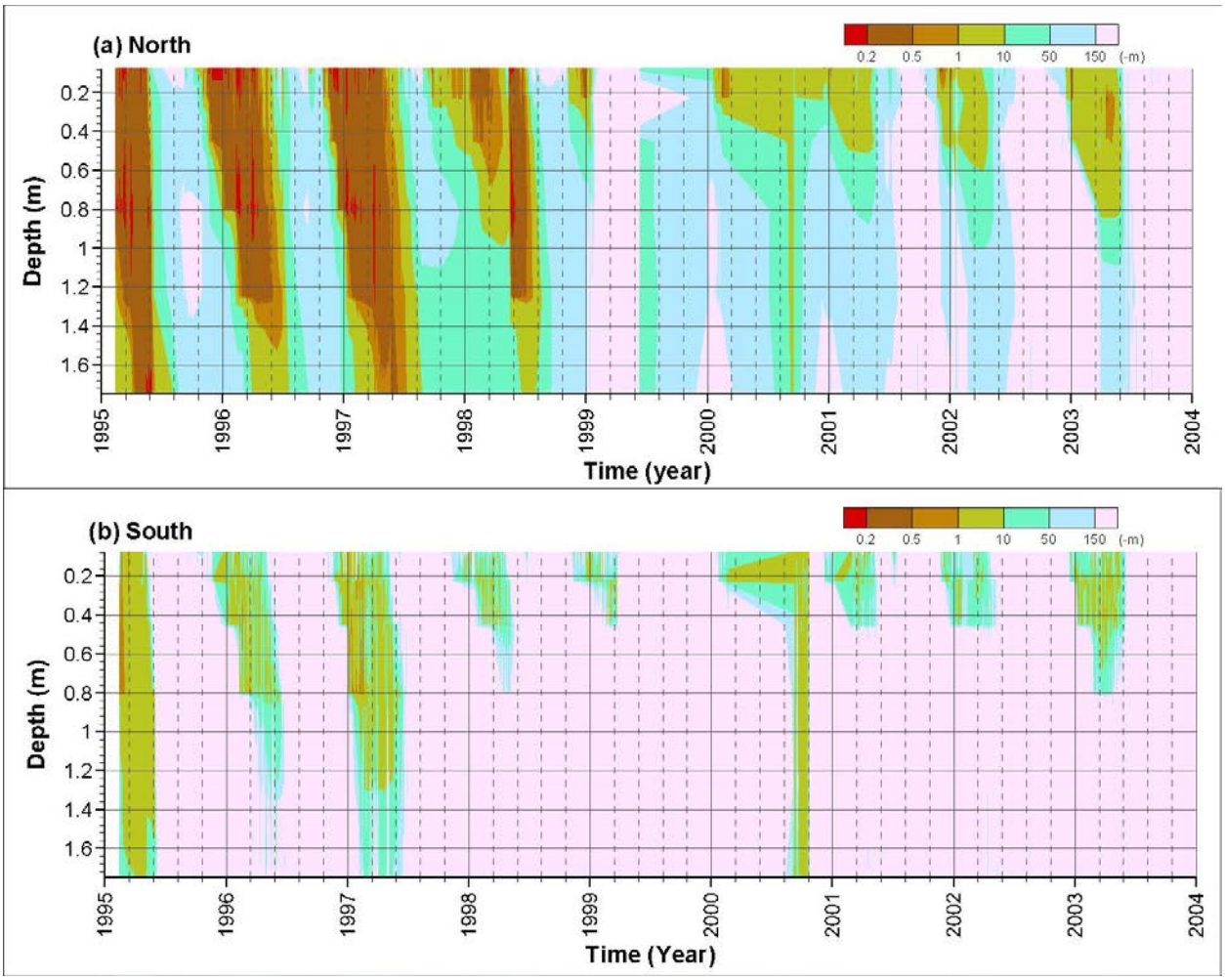

Figure G.6. Geo-averaged soil water pressure of 6 monitoring stations for (a) the north section and (b) the south section during the period from WY95 to WY03. The majority of the HDU monitoring system stopped functioning after 2004.

G.4.2 Water Balance

The water balance components (i.e., precipitation, water storage, runoff, drainage, and ET) are summarized in Table G.3, Table **G.4**, and Table **G.5** for the north section of the PHB during each winter season, summer season, and water year, respectively, and in Table **G.6**, Table **G.7**, and Table **G.8** for the south section. The classes for the corresponding precipitation periods are also listed to provide the relative precipitation level. Each of the other components is described in detail below, except precipitation, which is discussed in Section F.2.

Table G.3. Water balance components (mm) in the north section of the PHB during the winter seasons (November to March).

WY Name	P	P Class	ΔW	R	D	ET
WY95	252.2	EW	210.8	1.8	0.00E+00	39.6
WY96	339.9	EW	308.9	0	2.70E-04	31.0
WY97	344.2	EW	337.9	36.3	1.35E-04	-30.0
WY98	106.9	NN	58.9	0	4.25E-04	48.0
WY99	85.9	NN	#N/A	0	0.00E+00	#N/A
WY00	88.4	NN	#N/A	0	2.07E-04	#N/A
WY01	79.5	NN	27.4	0	0.00E+00	52.1
WY02	95.3	NN	32.8	0	1.70E-05	62.5
WY03	144.5	MW	100.3	0	3.40E-05	44.2
WY04	140.0	MW	86.7	0	3.40E-05	53.3
WY05	49.3	SD	#N/A	0	4.10E-04	#N/A
WY06	120.1	NN	#N/A	0	1.70E-05	#N/A
WY07	104.1	NN	#N/A	0	0.00E+00	#N/A
WY08	93.7	NN	44.9	0	0.00E+00	48.8
WY09	108.7	NN	37.5	0.016	0.00E+00	71.2
WY10	83.1	NN	38.9	0	0.00E+00	44.2
WY11	111.5	NN	47.2	0	9.69E-05	64.3
WY12	67.1	NN	4.2	0	0.00E+00	62.9
WY13	72.4	NN	33.0	0	0.00E+00	39.4
Average	**130.9**	**-**	**45.1**	**2.0**	**8.66E-05**	**45.1**

Table G.4. Water balance components (mm) in the north section of the PHB during the summer seasons (April to October).

WY Name	P	P Class	ΔW	R	D	ET
WY95	241.1	EW	-364.1	0	0.00E+00	605.3
WY96	153.2	EW	-281.1	0	2.40E-04	434.2
WY97	155.5	EW	-331.0	0	9.02E-02	486.5
WY98	256.0	EW	-55.4	0	0.00E+00	311.4
WY99	45.0	NN	#N/A	0	0.00E+00	#N/A
WY00	80.8	NN	#N/A	0	0.00E+00	#N/A
WY01	71.4	NN	-28.2	0	1.70E-05	99.6
WY02	35.3	MD	-57.7	0	0.00E+00	93.0
WY03	78.2	NN	-91.8	0	0.00E+00	170.0
WY04	99.1	MW	-72.5	0	0.00E+00	171.5
WY05	56.1	NN	#N/A	0	0.00E+00	#N/A
WY06	105.9	MW	#N/A	0	0.00E+00	#N/A
WY07	55.4	NN	-40.9	0	2.97E-03	96.3
WY08	45.0	NN	-32.0	0	0.00E+00	77.0
WY09	40.9	MD	-48.6	0	0.00E+00	89.5
WY10	132.8	SW	-31.1	0	0.00E+00	164.0
WY11	71.1	NN	-37.1	0	5.78E-03	108.2
WY12	90.7	NN	-18.4	0	0.00E+00	109.1
WY13	109.5	MW	-25.6	0	0.00E+00	135.1
Average	**101.2**	**-**	**-101.0**	**0**	**5.22E-03**	**210.0**

Table G.5. Water balance components (mm) in the north section of the PHB during the water years.

WY Name	P	P Class	ΔW	R	D	ET
WY95	493.3	EW	-153.4	1.8	0.00E+00	644.9
WY96	493.1	EW	27.9	0	5.10E-04	465.2
WY97	499.7	EW	6.9	36.3	9.03E-02	456.5
WY98	363.0	EW	3.5	0	4.25E-04	359.4
WY99	130.8	NN	#N/A	0	0.00E+00	#N/A
WY00	169.2	NN	#N/A	0	2.07E-04	#N/A
WY01	150.9	NN	-0.8	0	1.70E-05	151.6
WY02	130.6	NN	-24.9	0	1.70E-05	155.5
WY03	222.8	MW	8.6	0	3.40E-05	214.2
WY04	239.0	MW	14.2	0	3.40E-05	224.8
WY05	105.4	SD	#N/A	0	4.10E-04	#N/A
WY06	226.1	MW	#N/A	0	1.70E-05	#N/A
WY07	159.5	NN	#N/A	0	2.97E-03	#N/A
WY08	138.7	NN	12.9	0	0.00E+00	125.8
WY09	149.6	NN	-11.1	0.016	0.00E+00	160.7
WY10	215.9	NN	7.8	0	0.00E+00	208.1
WY11	182.6	NN	10.2	0	5.88E-03	172.4
WY12	157.7	NN	-14.2	0	0.00E+00	171.9
WY13	181.9	NN	7.4	0	0.00E+00	174.5
Average	**232.1**	**-**	**-7.5**	**2.0**	**5.31E-03**	**263.2**

Table G.6. Water balance components (mm) in the south section of the PHB during the winter seasons (November through March).

WY Name	P	P Class	ΔW	R	D	ET
WY95	147.8	MW	77.6	0	0.00E+00	70.2
WY96	173.5	SW	155.1	0	1.55E-05	18.4
WY97	224.0	EW	228.4	0	1.80E-04	-4.4
WY98	106.9	NN	59.9	0	4.10E-04	47.0
WY99	85.9	NN	#N/A	0	0.00E+00	#N/A
WY00	88.4	NN	#N/A	0	2.55E-04	#N/A
WY01	79.5	NN	27.2	0	0.00E+00	52.3
WY02	95.3	NN	23.5	0	0.00E+00	71.8
WY03	144.5	MW	96.3	0	1.70E-05	48.3
WY04	140.0	MW	87.0	0	1.70E-05	53.0
WY05	49.3	SD	#N/A	0	1.42E-04	#N/A
WY06	120.1	NN	#N/A	0	0.00E+00	#N/A
WY07	104.1	NN	#N/A	0	0.00E+00	#N/A
WY08	93.7	NN	51.4	0	0.00E+00	42.3
WY09	108.7	NN	35.9	0	0.00E+00	72.8
WY10	83.1	NN	40.2	0	0.00E+00	42.9
WY11	111.5	NN	45.2	0	6.47E-05	66.3
WY12	67.1	NN	0.8	0	0.00E+00	66.2
WY13	72.4	NN	35.4	0	0.00E+00	37.0
Average	**110.3**	**-**	**68.9**	**0**	**5.80E-05**	**48.9**

Table G.7. Water balance components (mm) in the south section of the PHB during the summer seasons (April through October).

WY Name	P	P Class	ΔW	R	D	ET
WY95	131.3	SW	-231.2	0	0.00E+00	362.6
WY96	59.9	NN	-158.7	0	0.00E+00	218.6
WY97	66.3	NN	-228.4	0	0.00E+00	294.7
WY98	46.5	NN	-63.8	0	0.00E+00	110.3
WY99	45.0	NN	#N/A	0	0.00E+00	#N/A
WY00	80.8	NN	#N/A	0	0.00E+00	#N/A
WY01	71.4	NN	-23.1	0	0.00E+00	94.5
WY02	35.3	MD	-51.5	0	0.00E+00	86.8
WY03	78.2	NN	-87.4	0	0.00E+00	165.6
WY04	99.1	MW	-69.8	0	0.00E+00	168.9
WY05	56.1	NN	#N/A	0	0.00E+00	#N/A
WY06	105.9	MW	#N/A	0	0.00E+00	#N/A
WY07	55.4	NN	-40.5	0	0.00E+00	95.9
WY08	45.0	NN	-25.2	0	0.00E+00	70.2
WY09	40.9	MD	-70.3	0	0.00E+00	111.2
WY10	132.8	SW	-22.6	0	0.00E+00	155.4
WY11	71.1	NN	-37.3	0	0.00E+00	108.4
WY12	90.7	NN	-17.6	0	0.00E+00	108.3
WY13	109.5	MW	-28.2	0	0.00E+00	137.7
Average	**74.8**	**-**	**-77.0**	**0.0**	**0.00E+00**	**152.6**

Table G.8. Water balance components (mm) in the south section of the PHB during the water years.

WY Name	P	P Class	ΔW	R	D	ET
WY95	279.1	EW	-153.6	0	0.00E+00	432.8
WY96	233.4	MW	-3.6	0	1.55E-05	237.0
WY97	290.3	EW	0.0	0	1.80E-04	290.4
WY98	153.4	NN	-3.8	0	4.10E-04	157.3
WY99	130.8	NN	#N/A	0	0.00E+00	#N/A
WY00	169.2	NN	#N/A	0	2.55E-04	#N/A
WY01	150.9	NN	4.0	0	0.00E+00	146.9
WY02	130.6	NN	-28.1	0	0.00E+00	158.6
WY03	222.8	MW	8.9	0	1.70E-05	213.9
WY04	239.0	MW	17.2	0	1.70E-05	221.8
WY05	105.4	SD	#N/A	0	1.42E-04	#N/A
WY06	226.1	MW	#N/A	0	0.00E+00	#N/A
WY07	159.5	NN	#N/A	0	0.00E+00	#N/A
WY08	138.7	NN	26.2	0	0.00E+00	112.5
WY09	149.6	NN	-34.4	0	0.00E+00	184.0
WY10	215.9	NN	17.6	0	0.00E+00	198.3
WY11	182.6	NN	8.0	0	6.47E-05	174.7
WY12	157.7	NN	-16.8	0	0.00E+00	174.5
WY13	181.9	NN	7.2	0	0.00E+00	174.7
Average	**185.1**	**-**	**-10.8**	**0**	**5.80E-05**	**205.5**

G.4.2.1 Water Storage

Figure **G.7** shows the average water storage at the 2-m-thick storage layer of the ETC barrier for the north and south sections. The curves show clear seasonal variation of *W* because of the store-and-release processes of precipitation. From WY95 to WY98 (Figure **G.7**a), the storage was higher in the north section than in the south section because additional water was applied to the north. From WY99 to WY08

(Figure **G.7**b), there was no discernible difference in W between the north and south as expected because they were under the same precipitation and vegetation conditions. From WY09 to WY12 (Figure **G.7**c), there was a slight difference between the two sections after the September 2008 controlled fire.

The highest water storage, W^{high}, generally occurred near the end of the winter season during each year and the lows, W^{low}, near the end of the summer season, as summarized in (Table G.9). For the irrigated section in the period from WY95 to WY97, average W^{low} was 153.7 mm (Table G.9), which is equivalent to an average water content of 0.077 m^3m^{-3}, just slightly above the estimated residual water content of 0.067 m^3m^{-3} as reported in Zhang (2015). For the non-irrigated stations in both the north and south sections, the average W^{low} for the same period was 127.5 mm, which is equivalent to an average water content of 0.064 m^3m^{-3}, slightly less than the estimated residual water content 0.067 m^3m^{-3}. During the 19-year monitoring period, the maximum water storage occurred in late March of 1997 on the irrigated north section (517.5±85.8 mm).

From WY99 to WY12, the average W^{high} with $\pm 1\sigma$ was 194.2±20.2 mm for the north section and 189.4±23.5 mm for the south section, meaning that only a very small fraction of the storage capacity was used, even at the wettest time of a year.

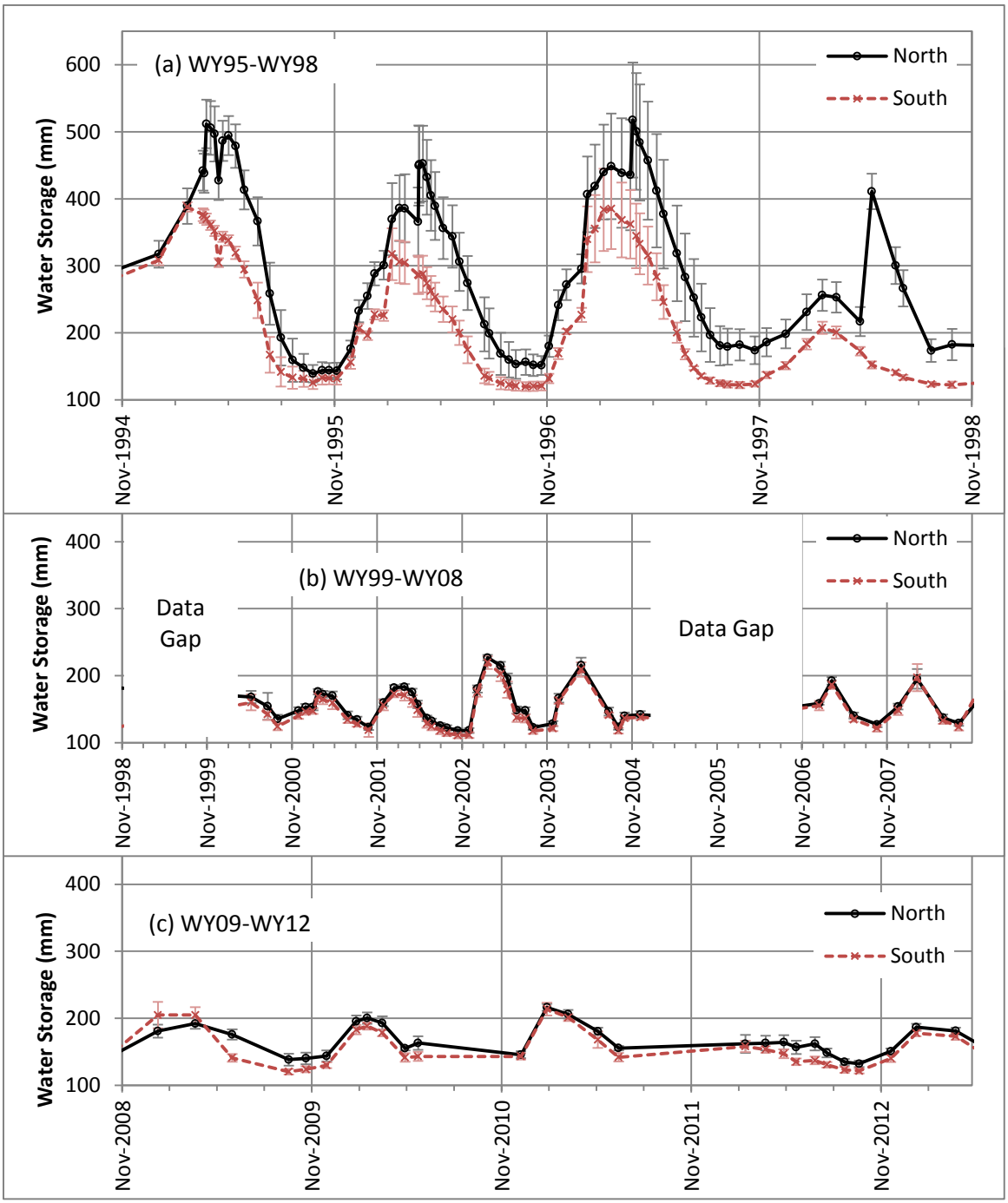

Figure G.7. Average water storage of 6 monitoring stations in the 2-m-thick silt loam storage layer of the ETC barrier (a) during the period (WY95 to WY98) with enhanced precipitation in the north section, (b) during the period (WY99 to WY08) when the entire barrier was under the same treatment of natural conditions, and (c) during the post-fire period (WY90 and after). The vertical lines across each point indicate one standard deviation.

Table G.9. The mean with one standard deviation of the water-year high and low storages (mm).

WY	North		South	
	High	Low	High	Low
WY95	513.3±36.9	138.9±12.9	387.9±7.0	125.5±9.3
WY96	454.7±59.3	149.7±15.1	317.9±37.8	119.4±6.7
WY97	517.5±85.8	172.6±22.3	386.4±60.9	122.0±4.8
WY98	410.8±26.5	170.9±16.5	207.4±9.2	121.9±4.3
WY00	171.5±14.1	135.4±6.2	160.0±11.9	124.1±5.4
WY01	176.1±4.2	122.8±4.0	168.8±7.3	116.1±5.0
WY02	183.4±4.3	118.1±3.9	173.7±6.4	111.1±4.4
WY03	226.9±4.3	122.9±3.6	219.6±9.6	117.5±4.3
WY04	215.7±11.2	123.1±3.6	209.3±10.7	117.7±4.3
WY07	192.4±5.6	127.1±3.8	186.3±6.2	121.5±5.0
WY08	195.2±14.6	128.9±3.7	197.2±20.3	123.4±5.2
WY09	192.0±7.9	138.3±8.9	208.3±16.5	120.4±4.1
WY10	200.3±8.4	145.5±5.1	188.4±5.3	138.4±5.8
WY11	216.3±5.2	155.4±3.2	213.7±9.4	141.8±6.4
WY12	166.2±11.9	132.0±4.8	158.2±8.3	121.4±3.6
WY95-WY97 (Enhanced P in north)	495.2±66.9	153.7±21.7	364.0±51.5	122.3±7.2
WY00-WY12	194.2±20.6	131.8±11.7	189.4±23.5	123.0±10.0
WY95-WY12	-	-	212.3±61.2†	127.5±11.8†
† Includes non-irrigated stations from north section for WY00-WY12				

Water Storage Changes in the Winter and Summer Seasons

An ET barrier functions by storing the precipitation in the winter season in the storage layer and then releasing the stored water into atmosphere in the summer season via ET. To examine the release of stored water, Figure **G.8** shows the water storage changes for the winter and summer seasons. The maximum values of ΔW_w and ΔW_s occurred in WY97 for both the north and south sections. The maximum storage change during the winter season was 338 mm for the north and 228 mm for the south. The maximum change during the summer season was -331 and -228 mm for the north and south sections, respectively. From WY98 to WY13, the water storage changes were in a much smaller range between -92 and 100 mm. On average, 89.1 mm of precipitation was stored in the winter season and 85.4 mm was released in the summer season in the north section; 68.2 mm was stored and 68.0 mm was released in the south section.

Figure **G.9** compares the water storage changes in the winter and summer seasons. All the points fall very close to the 1:1 line, meaning that nearly all the stored water in the winter season was released from the soil the following summer by the store-and-release mechanism.

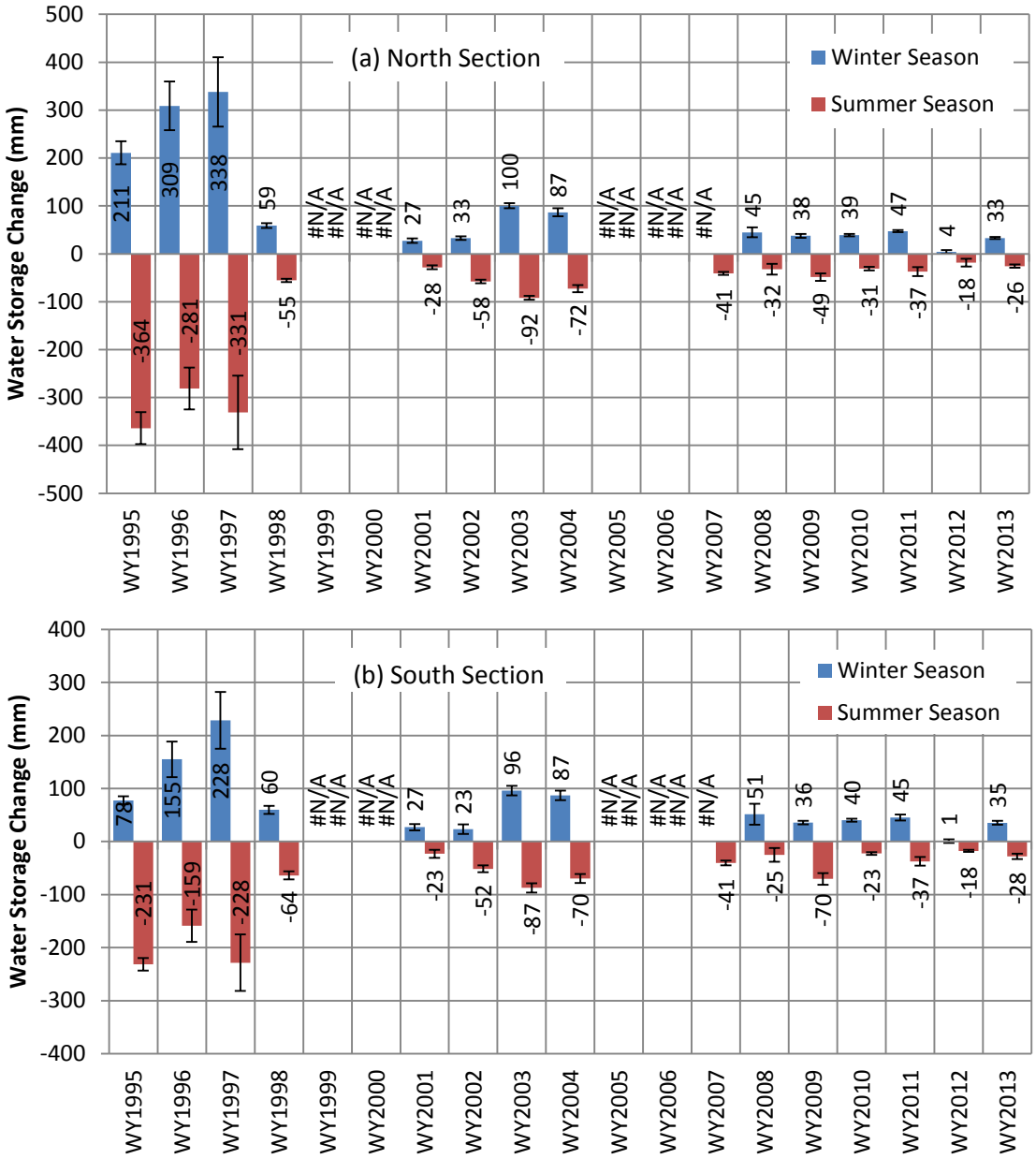

Figure G.8. Soil water storage change (average over 6 monitoring stations) during the winter season (November to March) and the summer season (April to October) for (a) the north section of the barrier and (b) the south section of the barrier. The standard deviation was calculated among the six monitoring stations of each section and is shown as a capped vertical line at each bar. #N/A means no data or insufficient data to calculate storage change.

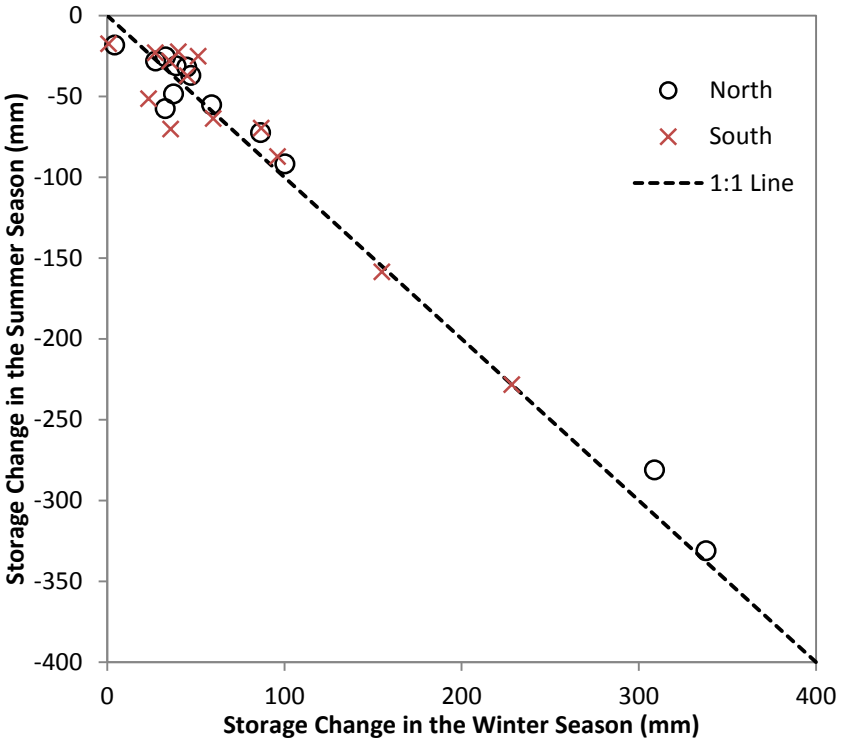

Figure G.9. A comparison of the water storage changes in the winter and summer seasons. (Data for WY95 were excluded because the very high initial water content at the beginning of the WY as a result of water introduced during barrier construction in 1994.)

G.4.2.2 Drainage Rate

A key quantitative performance measure of the enhanced precipitation test from WY95 to WY97 was to determine the amount of drainage through the ETC barrier. The maximum drainage rate of 0.18 mm yr^{-1} was observed in WY97 in the northeast part of the barrier (Figure **G.10**, 6E). The average drainage rate from WY95 to WY12 through the ETC barrier was 0.005 mm yr^{-1}. After the enhanced precipitation test, the maximum drainage rate measured was 5.8×10^{-3} mm yr^{-1} and occurred in the northwest part of the barrier in WY07; all other measurements were either zero or at the magnitude of 10^{-5} to 10^{-4} mm yr^{-1}.These drainage rates were much less than the design drainage criterion of 0.5 mm yr^{-1}.

Studies at the FLTF have demonstrated that a vegetated, 1.5-m-thick silt loam overlying sand and gravel layers prevented drainage from an annual precipitation of greater than 480 mm (Fayer and Gee 2006). Albright et al. (2004) reported the water balance of the monolithic or capillary barriers at 11 sites, 8 of which had an arid, semiarid, or sub-humid climate, for a test period up to 5 years. They found that the drainage rates from the capillary barriers (with storage layer thickness ranging between 0.6 and 2.5 m) in the arid, semiarid, and sub-humid sites were less than 1.5 mm yr^{-1} (0.4% of precipitation). Apiwantragoon et al. (2015) evaluated the water balance of monolithic and capillary barriers at 22 sites across the U.S. They found that, at semiarid and arid sites having low annual precipitation (<250 mm yr^{-1}), the drainage rates from capillary barriers of variable depths typically are less than 5 mm yr^{-1} and are frequently less than 1 mm yr^{-1}. Hence, the drainage rates measured at the PHB are in agreement with those observed by others under similar conditions.

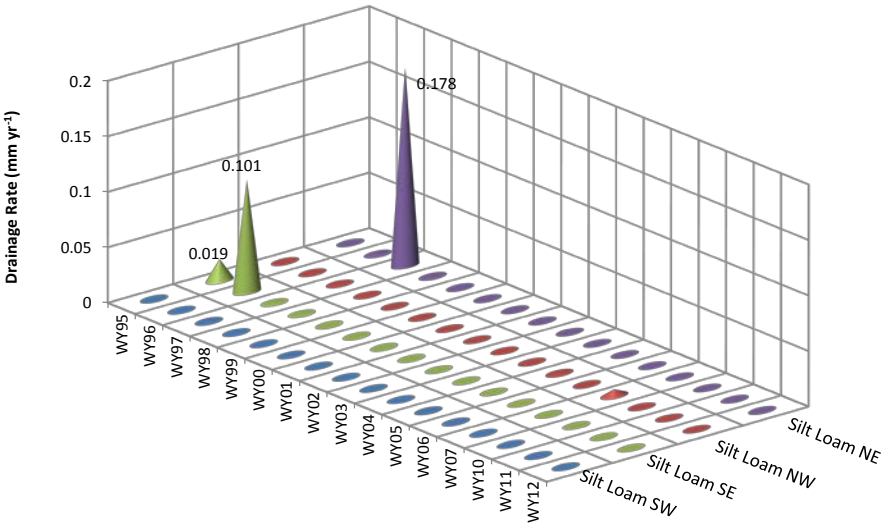

Figure G.10. Drainage rate through the silt loam barrier plots (SE: southwest; SE: southeast; NW: northwest; NE: northeast).

G.4.2.3 Runoff

Runoff occurs when rainfall intensity is higher than the soil's infiltration capacity. In this report, runoff refers to the water flowed out of the side boundary of the ETC barrier because of surface flow. Runoff may occur during a high-intensity rainstorm or when the soil hydraulic conductivity is considerably reduced by processes such as freezing conditions or the soil has become hydrophobic, e.g., from a wildfire. In March 1995, after the simulated 1000-year, 24-hour rainstorm to the newly vegetated surface, 1.79 mm of runoff was measured (Gee et al. 1995). The relatively low runoff was attributed to the relatively high K_s of the storage layer. Runoff of 36.3 mm was observed in the winter of 1997 and was attributed to the record precipitation of 93.7 mm in December 1996 and snowmelt on frozen ground (Ward et al. 1997). In January 2009, 4 months after the controlled fire, 0.016 mm of runoff was observed. No runoff was observed during the rest of the monitoring period, including during the simulated 1000-year rainstorms in 1996 and 1997, during the severe rainstorm in May 2004 (that generated runoff near the east riprap side slope of the PHB), and after the controlled burn in 2008. Hence, the total runoff observed was 38.1 mm with an average of 2.0 mm yr^{-1} during the 19-year monitoring period.

The primary reasons for the lack of runoff were the sufficiently high soil hydraulic conductivity and the increased coverage of vegetation on the ground surface. The 15% by weight pea gravel in the top 1 m of the barrier protects the barrier surface from erosion and against the formation of runoff channels such as rills or gullies (Gilmore and Walters 1993).The anti-erosion capability of gravel appears to the primary reason for the sustainability of natural bergmounds formed from the ice-rafted debris about 13,000 years ago (Bjornstad 2014; Chamness 1993; Fecht and Tallman 1978).

The above results indicate that snowmelt events on frozen ground pose a higher risk than the 1000-year return, 24-hour rainstorms for generating runoff. This is because the ice in frozen soil blocks a fraction of the soil pores and the hydraulic conductivity of a frozen soil is decreased. The magnitude of the decrease depends on the ice content. A snowmelt event on frozen ground happens once approximately in a decade or longer. For example, the previous snowmelt-caused ponding occurred in March 1985 and caused ponding of water at ground surface (Gee 1987).

G.4.2.4 Evapotranspiration

The ET processes in the winter and summer seasons differ dramatically because of variations in weather and the biological process of vegetation. Hence, ET is discussed separately here for the two seasons.

Winter ET

The estimated winter ET (ET_w) averaged 47.0 mm with a σ of 23.1 mm and showed no obvious trend (Figure G.11a) from WY95 to WY13. The lack of correlation between ET_w and P_w suggests that ET_w was nearly independent of P_w. Because of the low temperature and near-dormant vegetation in the winter season, transpiration is nearly zero in the winter season. Nevertheless, there can be some water loss to the atmosphere through evaporation and occasional sublimation. Wallace (1977,Table 2) estimated a 38.7-mm PET for the winter season at Hanford using the Thornthwaite-Mather method (Thornthwaite and Mather 1955). The winter PET is about 38% of the average winter precipitation at Hanford, suggesting ET_w is primarily controlled by the winter PET, and an average of 62% of P_w is stored in the barrier. Because temperature, radiation, and wind, the main factors that determine PET, vary less than precipitation across years, ET_w had a relatively small variation across years and was nearly constant. As presented above, the runoff and drainage from the ETC barrier is negligibly small relative to *P* and ET (Table G.3 through Table **G.8**). Thus, the relationship between ΔW_w and P_w is approximated by

$$\Delta W_w = P_w - ET_{w0} \tag{G.5}$$

where ET_{w0} = 47.0 mm is the *ET* during the winter season by fitting Eq. (G.5) to data and is very similar to the winter PET. This means that, on average, about 47.0 mm of P_w was released to the atmosphere during the winter season while the remaining precipitation contributed to an increase of water storage.

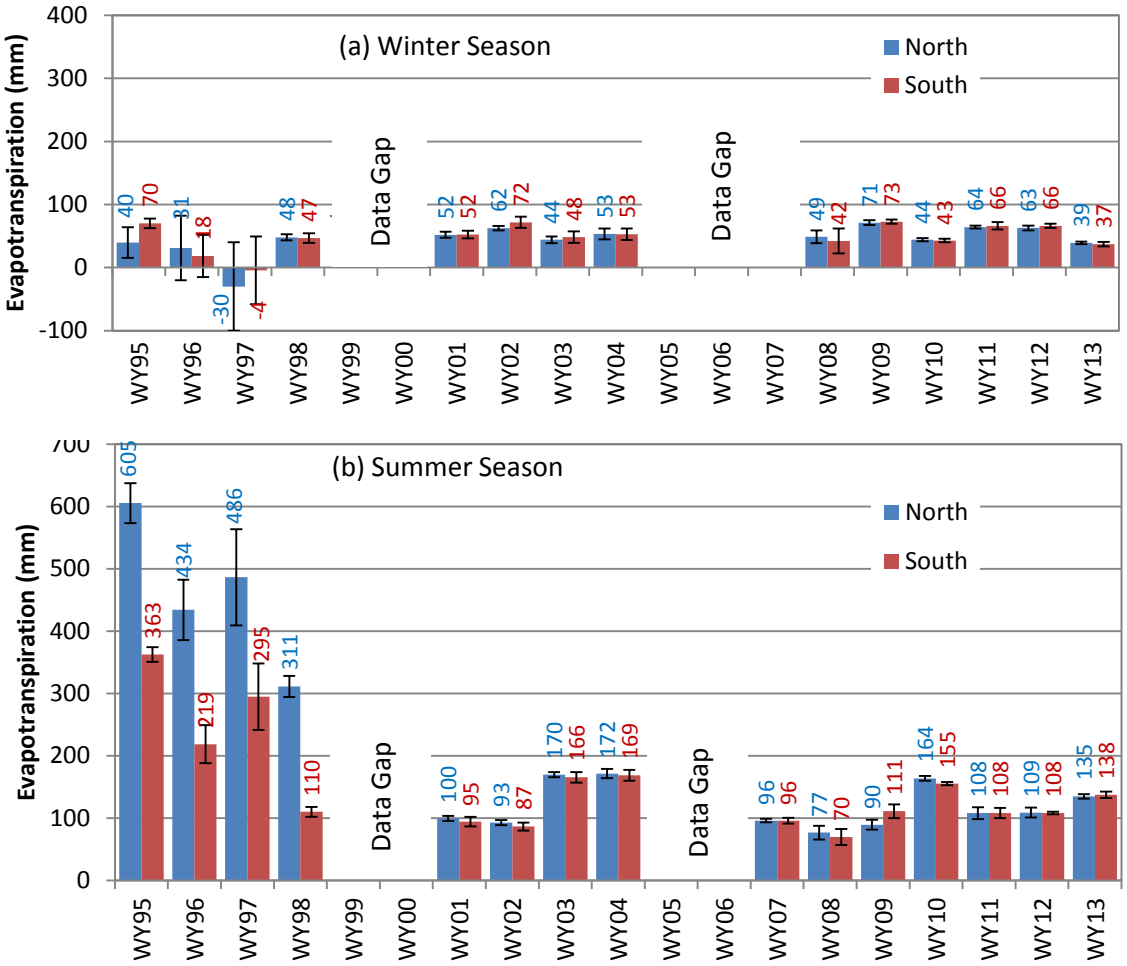

Figure G.11. Average evapotranspiration of 6 monitoring stations in (a) the winter season and (b) the summer season. The numbers indicate the actual ET at corresponding WY. The standard deviation was calculated among the six monitoring stations of each section and is shown as a capped vertical line at each bar.

Summer ET

In contrast to ET_w, the ET_s shows a clear temporal variation, with much higher values from WY95 to WY97 for both the north and south sections than in other years (Figure G.11b). The primary reason is that the meteoric precipitation in these years was much higher than usual and was categorized as extreme wet, moderate wet, and extreme wet for WY95, WY96, and WY97, respectively. Additionally, supplemental water was applied to the north section.

Based on Eqs. (G.4) and (G.5), the relationship between ET_s and P_a ($P_a = P_w + P_s$) is therefore

$$ET_s = P_a - ET_{w0} \tag{G.6}$$

According to Eq. (G.6), about 47.0 mm of precipitation is released into the atmosphere in the winter season and the rest is released in the summer season. To demonstrate the use of Eq. (G.6), the predicted ET_s for both the north and south sections is shown in Figure **G.12** as a function of WY precipitation. Generally, Eq. (G.6) yielded good predictions of ET_s (with a predicted σ of 21.6 mm), with minor

overestimation when P_a was relatively low (e.g., P_a < 250 mm) and slight underestimation when P_a was high (e.g., P_a > 250 mm).

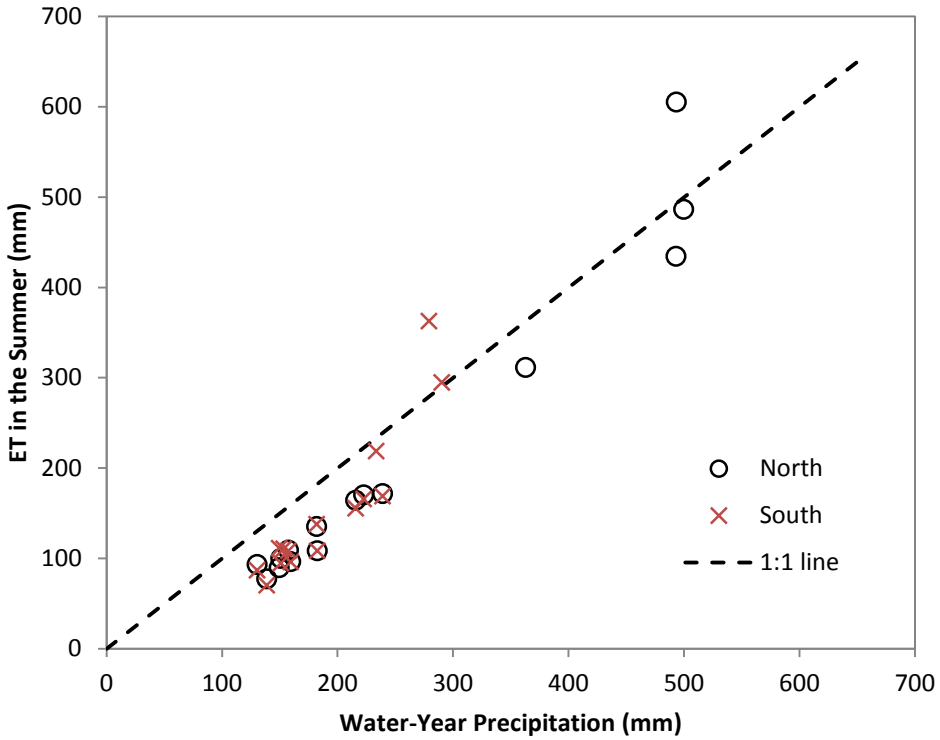

Figure G.12. Observed and predicted summer ET in the north and south sections of the barrier.

To further examine the release process of the stored water via ET, Figure G.13 demonstrates the monthly *ET* fraction from the soil from WY95 to WY97. In WY95, ET_m^s first increased with time, reached the maximum in July, and then decreased in both the north and south sections. However, in WY96 and WY97, ET_m^s was nearly stable from April to June and then decreased with time. The different response in WY95 was probably because the vegetation, which was planted in November 1994, was much smaller and hence the seedlings probably had limited need for soil water in the early summer of 1995. As the plants grew bigger, the low ET_m^s in April and May led to high available soil water and hence a very high ET_m^s in July 1995. The decrease of ET_m^s started in June or July, when the ET process was constrained by the supply of soil water. For all cases, ET_m^s approached nearly zero in September every year, meaning there was not much soil water available for the vegetation. In October, some negative ET_m^s values meant that the barrier soil had a net gain of water from precipitation in some years.

These results indicate that ET could release most of the available water from roughly April to June at a rate controlled by the weather and plant conditions from WY95 to WY97. Plants can release nearly all the remaining available water from July to September, but at a lower rate possibly controlled by soil conditions. The results indicate that ET processes were strong enough to release to the atmosphere nearly all the stored water in the 2-m-thick barrier even before the end of the summer season.

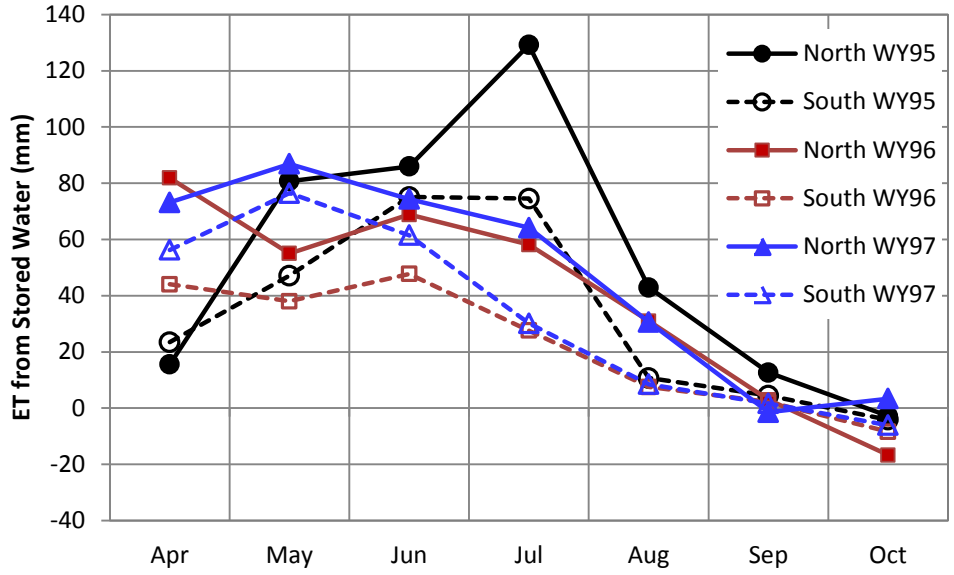

Figure G.13. Monthly contribution of soil water (averaged over 6 monitoring stations) to ET during the summer seasons from WY95 to WY97.

G.4.3 Functionality of the Capillary Break

The functionality of the ETC barrier of the PHB was not directly monitored. However, the functionality can be inferred by the measured soil water content and pressure approximately 0.15 m above the texture interface—the CB. Theoretically, water flow in the finer layer does not enter the coarser layer until the water pressure at the interface exceeds the water-entry pressure of the coarser material (Albright et al. 2010; Stormont and Morris 1998).

At the PHB, when the silt loam is underlain by 0.15-m-thick coarse sand and 0.3-m-thick gravel, a strong CB is formed. Because the hydraulic properties of the coarse sand are not available, a water entry, h_{we}, of -0.15 m is assumed. This h_{we} corresponds to a water content of 0.297 m^3m^{-3}, using the average non-hysteretic hydraulic parameters (θ_s = 0.344 m^3m^{-3}, θ_r = 0.068 m^3m^{-3}, α = 5.46 m^{-1}, and n = 1.51) (Zhang 2015).

Vertical neutron logging at six stations in March when the barrier was wettest during WY95, WY96, and WY97 (Figure G.14) indicated that the water content at 0.20 m above the CB was generally below 0.25 m^3m^{-3}, except at the west end in 1997. Horizontal neutron logging at 0.15 m above the CB (see Appendix H) also showed that water content was no more than 0.25 m^3m^{-3}. The high water content at the west end in 1997 (Figure **G.14**c) was not observed by the horizontal neutron logging, suggesting this high water content might happen locally. The measured h at 0.25 m above the CB generally was less than -0.5 m, except h = -0.23 m at station S1 in March 1997. All of these results indicate that, although soil water increased near the bottom of the storage layer, the soil wetness near the bottom of the storage layer was still much lower than the near-saturation value needed to initiate water movement through the CB. Consequently, very little drainage occurred in spite of the enhanced precipitation. Based on the water content measurements (Figure **G.4**a) and drainage rates (Figure **G.10**), it appears that only minimal water flow across the CB occurred for the 3 years with enhanced precipitation.

The above results indicate that, in the winter seasons of the enhanced precipitation period, the infiltration water indeed reached the CB. However, both the observed soil water content and water pressure were lower than the entry values, suggesting mass flow of water did not enter the coarser layer, meaning the CB functioned normally. This is in agreement with the very low drainage observed (≤0.18 mm yr^{-1}).

It is recognized that the heterogeneity exists in the ETC barrier due to multiple causes, such as non-uniformity at construction, root ingress, animal burrowing, and soil genesis. Additionally, the barrier surface has a 2% slope. The vegetation and micro-relief of barrier surface may cause non-uniform distribution of precipitation at ground surface. Hence, soil wetness near the CB varies laterally across the ETC barrier. The small amount of drainage might be caused by water breaking through the CB at some location that had higher water content than the entry value. This does not imply a failure of the CB but rather indicates an exceptionally wet local condition.

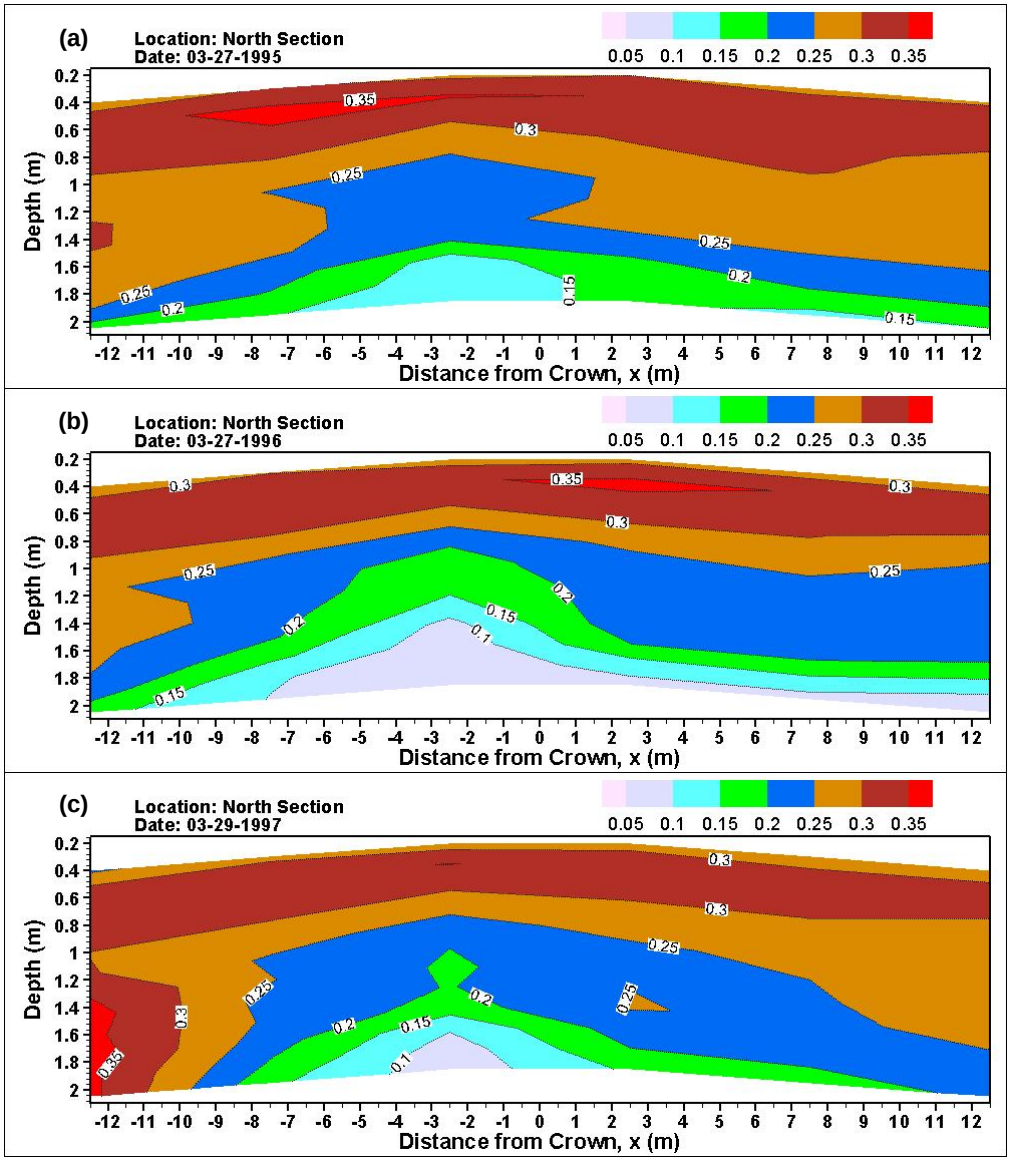

Figure G.14. Average water of 6 monitoring stations contents for a west-east cross-section of the north section in late March when the barrier was the wettest in WY95, WY96, and WY97. The irrigation treatment was in effect in all 3 years.

G.4.4 Available Storage of the ETC Barrier

For a given ETC barrier, the upper limit of water storage (W^{max}) is the maximum amount of water the barrier can store without water breaking through the CB. It is also called the storage of the barrier. The lower limit, W^{min}, is the storage of water that the ET process cannot remove. The available storage, W^{a}, is

the difference of the two, i.e., $W^a = W^{max} - W^{min}$. W^{max} and W^{min} were not directly measured at the PHB but approximated by the observed W^{high} and W^{low} values.

During the 3-year enhanced precipitation test, the observed maximum storage was 518±86 mm (Table G.3). The observed very low (≤0.18 mm yr^{-1}) drainage in this period suggested that the W^{high} values at the barrier probably was close to W^{max}. However, this does not mean that all of the additional infiltration water will become drainage. The very small drainage could happen at a certain location as preferential flow while there is no drainage of the barrier elsewhere. If so, when more precipitation infiltrates the barrier, most of the infiltration water will still be stored in the barrier but some may drain at the already-draining locations and possibly at new locations as preferential flow. A lysimeter test of a 1.5-m-thick Warden silt loam barrier showed that drainage did not occur as mass flow under 3X long-term precipitation (i.e., 480 mm yr^{-1}) in the lysimeters with vegetation (Fayer and Gee 2006; Gee et al. 1993). The test at the FLTF showed that the 1.5-m-thick barrier can store at least about 500 mm of water.

The observed W^{max} of 518±85 mm is consistent with the findings at the FLTF but is considerably (39%) larger than the estimated value of 373 mm (assuming a water entry of -0.15 m), based on the equilibrium of water pressure (e.g.,Khire et al. 2000). The soil freezing and low temperature in the winter season might contribute to the substantial difference. For example, the normal monthly air temperature at Hanford is -0.2°C for December and -0.5°C for January; on average, each year there are 23 days with the daily air temperature and 106 days with the minimum air temperature below freezing point (Hoitink et al. 2005). The soil freezing process is analogous to a drying process by pulling water to the freezing front, with ice accumulation in a zone above the freezing front (Miller 1980). Additionally, the low air temperature creates an upward temperature gradient that can cause upward movement of water (Fayer 2000; Scanlon et al. 2003). Because frozen water (i.e., ice or snow) is immobile in the soil and ice formation in the soil reduces soil permeability, it is more difficulty for fluid water to migrate downward in frozen soils. The transient process may be another reason for the much higher observed W^{max}. Field observation shows that, when the barrier was wettest, the upper part of the profile was generally wetter than the lower part (Figure G.4).

W^{min} corresponds to the soil water that is held so tightly within the smallest soil pores that evaporation and transpiration cannot remove it, making those pores unavailable for the storage of infiltration water. According to Zhang (2015), the Warden silt loam has an average plant unavailable water content (θ_u) of 0.058 m^3m^{-3}, which translates to 116 mm of storage for a 2-m-thick storage layer. It is noted that θ_u is also dependent on the type of vegetation type and climate. For the steppe vegetation on the PHB at the semi-arid Hanford climate, θ_u of the silt loam is actually less than θ_r (0.068 m^3m^{-3}). Hence, an extended water retention function (e.g, Webb 2000; Zhang 2011) should be used for more accurate simulation of water flow in a barrier.

Hence, the available capacity of the PHB is approximately 402 (= 518 – 116) mm. In other words, drainage from the 2-m-thick silt loam layer will not occur if the winter precipitation is less than 449 (= 402 + 47) mm, Eq. (G.6).

G.4.5 Water Diversion by the Sloped Barrier Surface

The ground surface of the ETC barrier was designed with a 2% slope away from the crown to promote runoff, since the waste zone is directly beneath the barrier crown, so that water will not pond near the crown area, especially during rainstorms. The lateral water movement away from the crown is considered water diversion. The water content distribution in the west-east cross-section of the irrigated north section from WY95 to WY97 (Figure G.14) shows that in late March, when the irrigated section was the wettest, there was a relatively low water content zone in the lower portion of the barrier profile near the crown in each of the 3 years. In contrast, water content near the edges was higher, likely due to water diversion. To confirm that the observed water diversion was not caused by measurement errors, the HDU-measured h 0.25 m above the CB on March 29 of the 3 years was analyzed (Figure G.15). The soil near the crown

showed more negative *h* values, indicating a relatively drier condition. Additionally, the horizontal NP logging at 0.15 m above the CB also confirmed the existence of the drier zone below the crown. During the same period, this diversion process was not as obvious in the ambient south section as it was in the north section. These results indicate that the water-diversion process due to the 2% slope enhanced the barrier's ability to protect the area near the crown against heavy rainstorms.

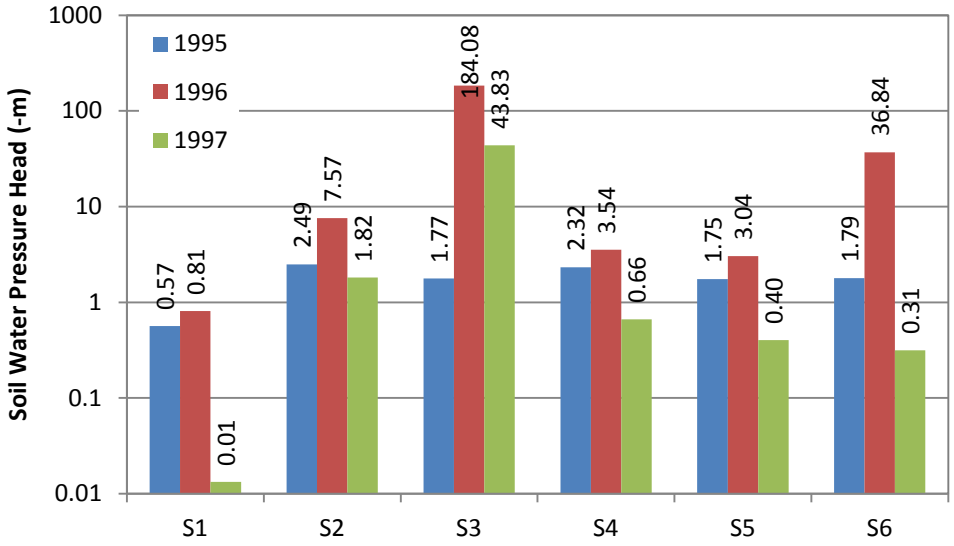

Figure G.15. Soil water pressure 0.25 m above the capillary break on March 29 of 1995 through 1997. (S1 through S6 stand for six water balance monitoring stations. S1 is the west-most station and the barrier crown is between S3 and S4.)

G.4.6 Hydrological Impacts of Controlled Fire

The impact of the controlled fire in September 2008 on soil water processes within the ETC barrier was delineated by comparing the water content distribution of the north (Figure **G.4**c) and south (Figure G.5c) sections. The results indicate that the ET rate in early summer was slightly less in the burned north section than in the unburned south section. However, the ET in the burned section appeared high enough to release the stored water to the atmosphere, albeit over a slightly longer period. For both the burned and unburned sections, there was no detectible drainage and zero runoff except in 2009 (0.016 mm). This suggests that the barrier can still perform well after a wildfire eliminates the vegetation. In a separate test of a 1.5-m-thick Warden silt loam barrier at the Hanford FLTF, for the treatment without vegetation, the average drainage rate was no more than 0.2 mm yr^{-1} from 1987 to 2004 under ambient precipitation and was no more than 16.4 mm yr^{-1} from 1987 to 2002 under the enhanced (2X before 1990 and 3X thereafter) precipitation condition (Fayer and Gee 2006).

It is noted that annual precipitation during the monitoring period after the fire (WY09 to WY13) was near normal. If extremely wet years follow a fire, performance may be different. A comparable scenario was the 1000-year return, 24-hour rainstorm in March 1995 when the vegetation planted in November 1994 was still very small and the barrier surface was nearly bare. During this simulated rainstorm, 1.79 mm of runoff and 72 kg ha^{-1} of soil erosion was observed.

G.4.7 Implication on Barrier Thickness

The findings at the PHB have an important implication for the determination of appropriate thickness (*L*) of the storage layer. Before the construction of PHB, the required storage capacity of the ETC barrier was estimated based on annual precipitation. Field data demonstrate that the precipitation in the summer

season (April to October) does not contribute to the storage at the PHB. During the winter season (November to March), all but an average of 47 mm of the precipitation infiltrates into the barrier. Hence, it is more proper to determine the required storage capacity based on winter precipitation rather than annual values. Based on the analysis of winter precipitation [Eq. (G.1)], the estimated P_w with 99.9% percentile (probability of 0.1%, approximately once in 1000 years) is 253 mm.

The observed storage capacity had a standard deviation of 86 mm. To be conservative, the following analysis uses the average value 518 mm and ET_w of 20 mm (less than half of the ET_{w0}). Assuming that the storage capacity is uniform over the whole thickness of the storage layer, the test at the PHB suggests that a 1-m-thick barrier has 201 mm of available storage. The relationship between P_w, the percentile of P_w, and the required barrier thickness is shown in Figure G.16. The 1000-year return P_w of 253 mm would need a 1.2-m-thick barrier. The 100-year return P_w of 205 mm would need a 0.9-m-thick barrier. The estimated median P_w of 96 mm can be stored in a 0.4-m-thick barrier. Hence, for an ETC barrier that can store the 1000-year return P_w, the lower portion of the barrier will be at very low water content for most of the years.

Note that the total winter precipitation (including irrigation) for WY96 and WY97 was very high, such that this magnitude of precipitation has a very low probability of occurring (0.001 times) during the design life of 1000 years. Studies at FLTF have demonstrated that a vegetated, 1.5-m-thick silt loam layer overlying sand and gravel layers has a storage capacity of over 500 mm (Gee et al. 1993). This suggests that the storage layer of the future surface barrier at the Hanford can be less than 2 m. It is important to note that the above calculation of barrier thickness is a rough approximation that does not consider the flow process in the silt loam layer. Further, the plant and animal population and the erodability of the barrier would be different when the barrier thickness changes.

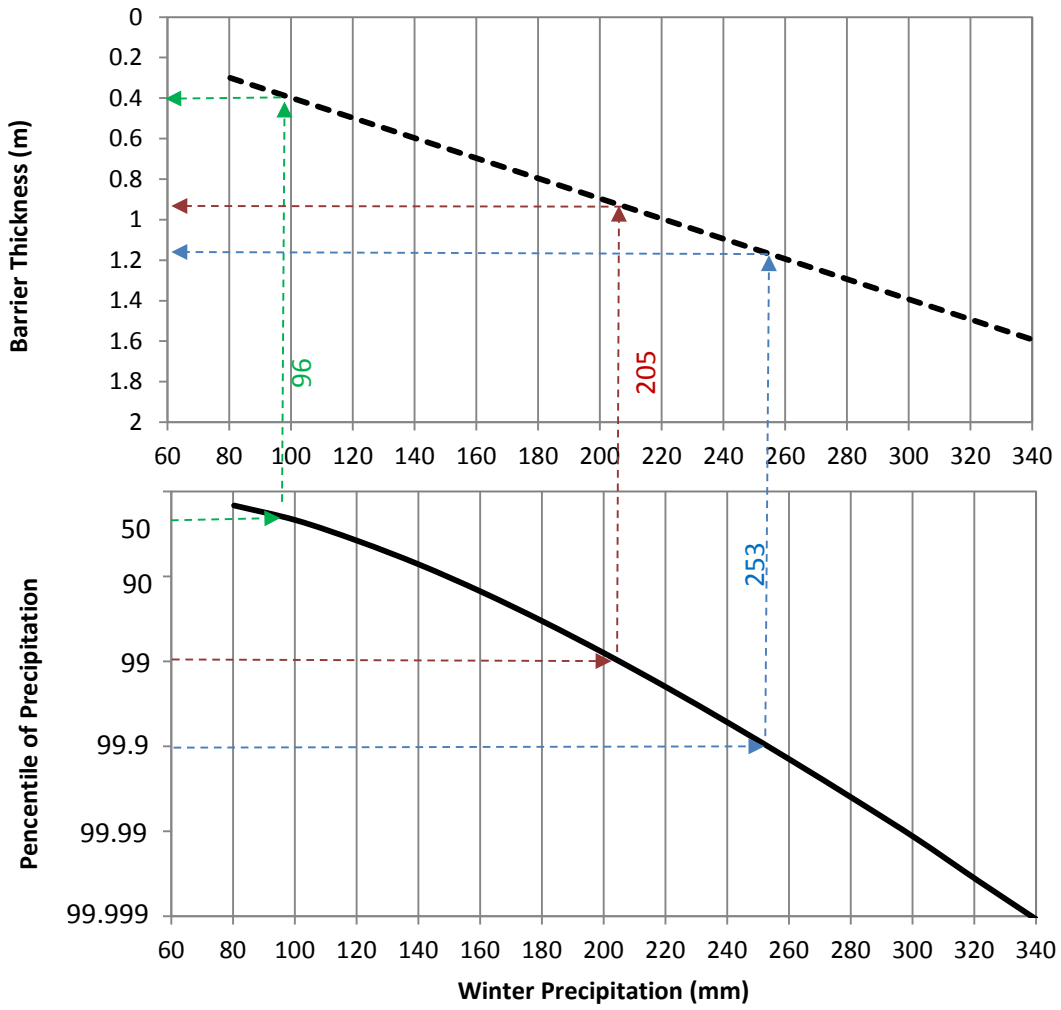

Figure G.16. Relationship between P_w, the percentile of P_w, and the required barrier thickness.

G.5 Summary

The Prototype Hanford Barrier was constructed in 1994 and its 2-m-thick storage layer was built up with the local Warden silt loam. The following summarizes the main findings based on the 19-year (from WY95 to WY13) monitoring data on barrier hydrology.

- *Store-and-release mechanism*. The store-and-release mechanism for the ETC surface barrier worked efficiently. The silt loam layer was recharged in the winter season (from November to March) from top to bottom. Nearly all the stored water and precipitation in the summer season (from April to October) was released into the atmosphere via ET.

- *Water balance*. The maximum drainage observed was only 0.18 mm yr^{-1}, less than the design criterion of 0.5 mm yr^{-1}. A very small amount (2.0 mm yr^{-1} on average) of runoff was observed. The ET in the winter season was at a nearly constant rate of approximately 47 mm, which is comparable to the PET of the season. The ET in the summer season is approximately the sum of the stored water in the previous winter and the precipitation in the summer.

- *Capillary break*. The CB functioned normally. During the test of enhanced precipitation, infiltration water reached the CB but the wetness was lower than the entry value. The drainage observed was also near zero.
- *Storage capacity*. The observed maximum storage of the storage layer was 517.5±85.8 mm, which is considerably (39%) larger than the estimated value of 373 mm based on the method of equilibrium of water pressure.
- *Water diversion*. Water diversion due to the 2% slope of the barrier surface was observed in the irrigated north section but not in the non-irrigated south section from WY95 to WY97.
- *Hydrological impacts of controlled fire*. The newly grown vegetation (primarily shallow-rooted grasses) after the controlled fire could still release the stored water and summer precipitation to the atmosphere via ET.
- *Proper barrier thickness*. It is more appropriate to estimate the thickness of the storage layer based on the 1000-year return winter-season precipitation rather than annual precipitation. The estimated thickness of the storage layer appeared to be less than 2 m for the Prototype Hanford Barrier.

The results indicate that the ETC barrier of the PHB was working very efficiently and nearly eliminated all precipitation from migrating through the underlying waste zone. The results are useful for surface barrier design with optimum thickness.

References

Albrecht, BA and CH Benson. 2001. "Effect of Desiccation on Compacted Natural Clays," *Journal of Geotechnical and Geoenvironmental Engineering*, 127(1):67-75. doi:10.1061/(asce)1090-0241.

Albright, WH, CH Benson, GW Gee, AC Roesler, T Abichou, P Apiwantragoon, BF Lyles, and SA Rock. 2004. "Field Water Balance of Landfill Final Covers," *Journal of Environmental Quality*, 33(6):2317-2332.

Albright, WH, CH Benson, and WJ Waugh. 2010. *Water Balance Covers for Waste Containment Principles and Practices*. ASCE Press, Reston, Virginia.

Albright, WH, GW Gee, GV Wilson, and MJ Fayer. 2002. *Alternative Cover Assessment Project Phase I Report*, 41183, Desert Research Institute, Las Vegas, NV.

Apiwantragoon, P, CH Benson, and WH Albright. 2015. "Field Hydrology of Water Balance Covers for Waste Containment," *Journal of Geotechnical and Geoenvironmental Engineering*, 141(2):04014101. doi:10.1061/(asce)gt.1943-5606.0001195.

Benson, CH, A Sawangsuriya, B Trzebiatowski, and WH Albright. 2007. "Postconstruction Changes in the Hydraulic Properties of Water Balance Cover Soils," *Journal of Geotechnical and Geoenvironmental Engineering*, 133(4):349-359. doi:10.1061/(asce)1090-0241(2007)133:4(349).

Bjornstad, BN. 2014. "Ice-Rafted Erratics and Bergmounds from Pleistocene Outburst Floods, Rattlesnake Mountain, Washington, USA," *Quaternary Science Journal*, 63(1):44-59. doi:10.3285/eg.63.1.03.

Chamness, MA. 1993. *An Investigation of Bergmounds as Analogs to Erosion Control Factors on Protective Barriers,* PNL-8841, Pacific Northwest Laboratory, Richland, Washington. Available at http://www.iaea.org/inis/collection/NCLCollectionStore/_Public/25/059/25059205.pdf.

CSI. 2009. *229 Heat Dissipation Matric Water Potential Sensor,* Campbell Scientisic, Inc., Logan, Utah.

DOE-RL. 1994. *Constructability Report for the 200-BP-1 Prototype Surface Barrier,* DOE/RL- 94-76, U.S. Department of Energy Richland Operations Office, Richland, Washington.

DOE-RL. 1999. *200-BP-1 Prototype Barrier Treatability Test Report,* DOE/RL-99-11 Rev. 0, U.S. Department of Energy Richland Operations Office, Richland, Washington.

EPA. 2011. *Fact Sheet on Evapotranspiration Cover Systems for Waste Containment,* EPA 542-F-11-001, www.clu-in.org/download/remed/epa542f03015.pdf.

Fayer, MJ. 2000. *UNSAT-H Version 3.0: Unsaturated Soil Water and Heat Flow Model: Theory, User Manual, and Examples,* PNNL-13249, Pacific Northwest National Laboratory, Richland, Washington. Available at http://www.pnl.gov/main/publications/external/technical_reports/PNNL-13249.pdf. (Accessed on Aug. 28, 2015).

Fayer, MJ and GW Gee. 2006. "Multiple-Year Water Balance of Soil Covers in a Semiarid Setting," *Journal of Environmental Quality*, 35(1):366-377.

Fayer, MJ and JM Keller. 2007. *Recharge Data Package for Hanford Single-Shell Tank Waste Management Areas,* PNNL-16688, Pacific Northwest National Labratory, Richland, Washington. Available at http://www.osti.gov/energycitations/servlets/purl/917585-FNQXEV/.

Fecht, KR and AM Tallman. 1978. *Bergmounds Along the Western Margin of the Channeled Scablands, South-Central Washington* RHO-BWI-SA-11, Rockwell International, Richland, Washington. Available at http://www.osti.gov/scitech/servlets/purl/6431635.

Flint, AL, GS Campbell, KM Ellett, and C Calissendorff. 2002. "Calibration and Temperature Correction of Heat Dissipation Matric Potential Sensors," *Soil Sci. Soc. Am. J.*, 66:1439-1445.

Gee, GW. 1987. *Recharge at the Hanford Site: Status Report,* PNL-6403, Pacific Northwest laboratory, Richland, Washington.

Gee, GW, MD Campbell, GS Campbell, and JH Campbell. 1992. "Rapid Measurement of Low Soil Water Potentials Using a Water Activity Meter," *Soil Sci. Soc. Am. J.*, 56:1068-1070.

Gee, GW, D Felmy, JC Ritter, RR Kirkham, SO Link, JL Downs, and MJ Fayer. 1993. *Field Lysimeter Test Facility: Status Report IV,* PNL-8911, Pacific Northwest Laboratory, Richland, WA.

Gee, GW, JM Keller, and AL Ward. 2005. "Measurement and Prediction of Deep Drainage from Bare Sediments at a Semiarid Site," *Vadose Zone Journal*, 4:32-40.

Gee, GW, ML Rockhold, and JL Downs. 1989. *Status of FY 1988 Soil-Water Balance Studies on the Hanford Site,* PNL-6750, Pacific Northwest National Laboratory, Richland, Washington.

Gee, GW, AL Ward, and MJ Fayer. 1997. "Surface Barrier Research at the Hanford Site," *Land Contamination & Reclamation*, 5(3):233-238.

Gee, GW, AL Ward, BG Gilmore, MW Ligotke, and SO Link. 1995. *Hanford Prototype-Barrier Status Report: FY 1995*, PNL-10872, Pacific Northwest National Laboratory, Richland, Washington. Available at http://www.osti.gov/energycitations/servlets/purl/177965-nd9isN/webviewable/.

Gee, GW, AL Ward, BG Gilmore, SO Link, GW Dennis, and TK O`Neil. 1996. *Hanford Prototype-Barrier Status Report FY 1996*, PNNL-11367, Pacific Northwest National Laboratory, Richland, Washington. Available at http://www.osti.gov/energycitations/servlets/purl/444009-twIbfZ/webviewable/.

Gilmore, BG and WH Walters. 1993. *Water Erosion Field Tests for Hanford Protective Barriers: FY 1992 Status Report*, PNL-8949 UC-603, Pacific Northwest Laboratory, Richland, Washington.

Henken-Mellies, WU and A Schweizer. 2011. "Long-Term Performance of Landfill Covers - Results of Lysimeter Test Fields in Bavaria (Germany)," *Waste Manag Res*, 29(1):59-68. doi:10.1177/0734242X10385748.

Hoitink, DJ, KW Burk, JV Ramsdell (Jr.), and WJ Shaw. 2005. *Hanford Site Climatological Summary 2004 with Historical Data*, PNNL-15160, Pacific Northwest National Laboratory, Richland, Washington.

KEH. 1993. *Prototype Surface Barrier at 200-BP-1 Operable Unit*, W-263-C2 Rev. 0, Kaiser Engineers Hanford Company, Richland, Washington.

Khire, MV, CH Benson, and PJ Bosscher. 2000. "Capillary Barriers: Design Variables and Water Balance," *Journal of Geotechnical and Geoenvironmental Engineering*, 126(8):695-708. doi:10.1061/(asce)1090-0241.

Mancarella, D, A Doglioni, and V Simeone. 2012. "On Capillary Barrier Effects and Debris Slide Triggering in Unsaturated Layered Covers," *Engineering Geology*, 147:14-27. doi:10.1016/j.enggeo.2012.07.003.

McKee, TB, NJ Doesken, and J Kleist. 1993. "The Relationship of Drought Frequency and Duration of Time Scales," *Eighth Conference on Applied Climatology, American Meteorological Society,* 179-186 pp. Jan. 17-23, 1993, Anaheim, California.

McKee, TB, NJ Doesken, and J Kleist. 1995. "Drought Monitoring with Multiple Time Scales," *9th Conference on Applied Climatology,* Am. Meteorol. Soc., Dallas, Texas.

Miller, RD. 1980. "Freezing Phenomena in Soils." In *Applications of Soil Physics*, ed. D Hillel, pp. 254-299. Academic Press, New York.

Reece, CF. 1996. "Evaluation of Line Heat Dissipation Sensor for Measuring Soil Matic Potential," *Soil Sci. Soc. Am. J.*, 60:1022-1028.

Rickard, WH and BE Vaughan. 1988. "Plant Community Characteristics and Responses." In *Shrub-Steppe: Balance and Change in a Semi-Arid Terrestrial Ecosystem, Developments in Agricultural and Managed-Forest Ecology*, eds. WH Rickard, BE Vaughan, and LE Rogers, Vol 20, pp. 109-179. Elsevier, Amsterdam.

Scanlon, BR, K Keese, RC Reedy, J Simunek, and BJ Andraski. 2003. "Variations in Flow and Transport in Thick Desert Vadose Zones in Response to Paleoclimatic Forcing (0-90 Kyr): Field Measurements, Modeling, and Uncertainties," *Water Resources Research*, 39(7) doi:10.1029/2002wr001604.

Scanlon, BR, RC Reedy, KE Keese, and SF Dwyer. 2005. "Evaluation of Evapotranspirative Covers for Waste Containment in Arid and Semiarid Regions in the Southwestern USA," *Vadose Zone Journal*, 4(1):55-71.

Stone, WA, JM Thorp, OP Gifford, and DJ Hoitink. 1983. *Climatological Summary for the Hanford Area*, PNL-4622, Pacific Northwest Laboratory, Richland, Washington.

Stormont, JC and CE Morris. 1998. "Method to Estimate Water Storage Capacity of Capillary Barriers," *Journal of Geotechnical and Geoenvironmental Engineering*, 124(4):297-302.

Thom, HCS. 1966. *Some Methods of Climatological Analysis*, WMO Technical note 81, Secretariat of the WMO, Geneva, Switzerland.

Thornthwaite, CW and JR Mather. 1955. "The Water Balance," *Publications in Climatology, Drexel Institute of Climatology, Centerton, NJ*, 8(1):1-104.

Wallace, RW. 1977. *A Comparision of Evapotranspiration Estimates Using ERDA Hanford Climatological Data*, PNL-2698, Battelle Pacific Northwest Laboratories, Richland, Washington.

Ward, AL and GW Gee. 1997. "Performance Evaluation of a Field-Scale Surface Barrier," *Journal of Environmental Quality*, 26(3):694-705.

Ward, AL, GW Gee, and SO Link. 1997. *Hanford Prototype-Barrier Status Report: FY 1997*, PNNL--11789, Pacific Northwest National Laboratory, Richland, Washington. Available at http://www.osti.gov/energycitations/servlets/purl/569021-3NLXw0/webviewable/.

Ward, AL, N Hasan, SO Link, and KE Draper. 2009. *The Effects of Fire on the Function of the 200-BP-1 Engineered Surface Barrier*, PNNL-18934, Pacific Northwest National Laboratory, Richland, Washington.

Webb, SW. 2000. "A Simple Extension of Two-Phase Characteristic Curves to Include the Dry Region," *Water Resources Research*, 36(6):1425-1430.

Wing, NR and GW Gee. 1994. "Quest for the Perfect Cap," *Civil Engineering*, 64(10):38-41.

Zhang, ZF. 2011. "Soil Water Retention and Relative Permeability for Conditions from Oven-Dry to Full Saturation," *Vadose Zone Journal*, 10(4):1-10. doi:10.2136/vzj2011.0019.

Zhang, ZF. 2015. "Field Soil Water Retention of the Prototype Hanford Barrier and Its Variability with Space and Time," *Vadose Zone Journal*, 14(8):1-10. doi:10.2136/vzj2015.01.0011.

Appendix H

Nineteen-Year Hydrological Characteristics of a Surface Barrier: The Side Slopes and Asphalt Concrete Barrier

Z. Fred Zhang

Pacific Northwest National Laboratory
Richland, Washington

Content

List of Figures

List of Tables

Abstract

A surface infiltration and waste isolation barrier is usually protected by side slopes to prevent wind and water erosion and damage by other natural or human activities. A low-permeability bottom layer is often used to intercept the drainage from the overlying layers. The hydrological characteristics may affect the mechanical strength of the side slopes and low-permeability layer and hence are critical to ensuring the normal function of the barrier. The Prototype Hanford Barrier (PHB), constructed between late 1993 and 1994 at the Hanford Site, WA, was protected by a gravel side slope on the west side and a riprap side slope on the east side. At the bottom of the multi-layered PHB was an asphalt concrete (AC) barrier coated with fluid-applied asphalt. The soil water content in the gravel side slope, drainage through the side slopes and the barrier side boundaries, and effects of the AC were monitored from 1994 to 2013. Results show that the drainage through the side slopes had a clear seasonal pattern, with the highest drainage rate generally in January or February and the lowest rate usually in the summer or early fall. The drainage rate was nearly zero if annual precipitation was less than about 100 mm yr^{-1}. When precipitation was larger than about 100 mm yr^{-1}, approximately half of the additional precipitation ended up as drainage. No obvious difference was observed between the two types of side slopes in either the seasonal pattern of drainage or the drainage rate through the side slopes. Lateral flow along the barrier boundaries was significant only under the enhanced (3 times average) precipitation treatment and was minimal under natural precipitation. The stable or decreasing water content, stable water pressure, and very low percolation rate indicate negligible water percolation through the AC.

H.1 Introduction

Surface barriers are used to reduce or prevent infiltration water from entering the underlying waste zone and to isolate the waste from plant, animal, and human intrusion. Evapotranspiration (ET) barriers use two natural processes—the storage process to store precipitation (P) in the soil (i.e., the soil water reservoir) and the ET process to empty the soil water reservoir—to control infiltration into the underlying waste zone. The performance of an ET barrier can be enhanced by including a capillary break (CB) beneath the soil layer. For convenience, an ET barrier with a CB is referred to as an ETC barrier and the soil layer of such a barrier as the storage layer hereafter. The side boundaries of the storage layer are usually protected by side slopes to prevent wind and water erosion and damage by other natural or human activities. A low-permeability bottom layer is often used to intercept drainage from the overlying layers and redirect it laterally to beyond the edge of the low-permeability layer. The hydrological characteristics of the side slopes and low-permeability layer may affect the mechanical strength of the side slopes and hence are critical to the normal function of the barrier.

Side slopes are often constructed of coarse-textured materials that have low water-holding capacity and very high permeability so as to prevent water in the side slopes from entering the area protected by the barrier and maintain the mechanical strength of the side slopes. In this design, most of the precipitation that infiltrates the side slopes can quickly migrate to a large depth and has little chance of moving laterally. Fast drainage will also ensure that a side slope remains unsaturated, which keeps effective stress high and ensures good mechanical strength. Generally, a high fraction of precipitation on the side slopes ends up as deep drainage. The fate of this drainage is a concern because it could move into the soil under the barrier if not properly managed.

At the bottom of a surface barrier, a nearly impermeable layer is often constructed to prevent any drainage from penetrating into the underlying waste zone and to inhibit any noxious gas in the waste zone from migrating to the atmosphere. Conventional barrier layers are constructed of compacted clay, geomembranes, geosynthetic clay liners, or combinations of these materials. The conventional compacted barrier may suffer problems such as increasing permeability with time (Benson et al. 2007; Henken-Mellies and Schweizer 2011), preferential flow path development within the barrier (Albright et al. 2004), and cracking because of desiccation (Albrecht and Benson 2001). An alternative to the clay liners is an asphalt-based layer because asphalt has the properties of water repellency, impermeability, and longevity (Freeman and Romine 1994). Hot-mix asphalt concrete (AC) was found to have low permeability and improved mechanically stable compositions (Terrel 1991; Tuffour and Ishai 1990). However, the AC may crack if it is not well formulated or constructed. For example, a 2- to 20-cm-thick asphalt cover was constructed in 1961 over a contaminated site at Technical Area 49 at Los Alamos National Laboratory (Levitt et al. 2005). A few years later, this barrier cracked and collapsed in some areas. To reduce the cracking and hydraulic conductivity of AC, polymer may be added to the AC to increase its strength and resist cracking. Fluid-applied asphalt (FAA) coating also can be applied to AC to reduce its permeability (Freeman and Romine 1994; Wing and Gee 1994).

There are very few long-term field data on the hydrological performance of side slopes and an AC. The Prototype Hanford Barrier (PHB), constructed in 1994 at the Hanford Site, WA, consists of a 40-m by 80-m ETC barrier, whose side boundaries are protected by a gravel slope on the west and a riprap slope on the east. At the bottom of the surface barrier is an FAA-coated AC, which intercepts the drainage through the barrier or the side slopes. To understand the hydrological processes and verify the performance of the side slopes and the AC, water content in the gravel side slope and below the asphalt concrete layer, drainage through the side slopes, drainage through the barrier side boundaries, and percolation through the AC were monitored from 1994 to 2013. This paper summarizes the hydrological characteristics of the side boundaries of the ETC barrier, the side slopes, and the AC and evaluates their performance. The

hydrological characteristics of the storage layer of the ETC are reported in Appendix G. The results reported here are useful for the design of side slopes and AC for future barriers.

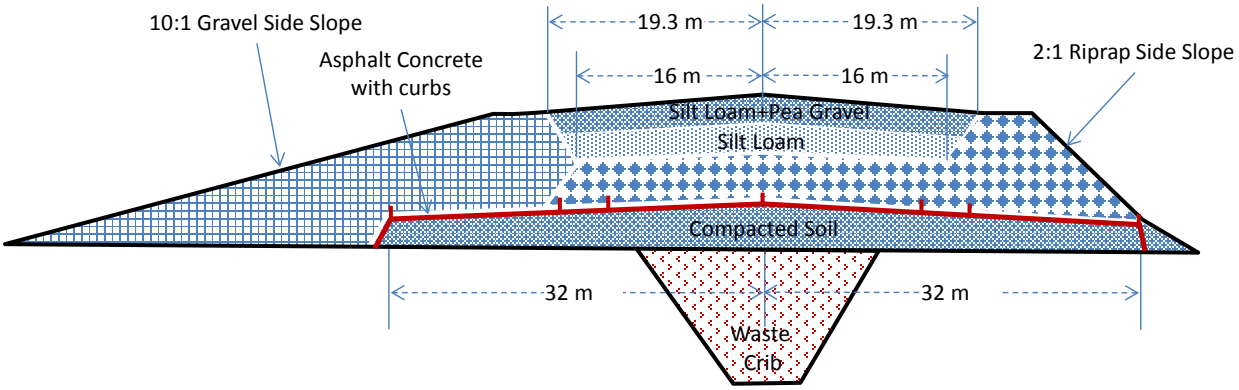

Figure H.1. Schematic of west-to-east cross-section showing the main components of the PHB. (Approximate scale; 2X vertical exaggeration)

H.2 Methods and Materials

H.2.1 Design of the Prototype Hanford Barrier and Field Tests

The description and design of the PHB was reported in other sources such as Wing and Gee (1994), Gee et al. (1997), and Ward and Gee (1997). The PHB, with an area of 2.5 ha, consists of an ETC barrier, a west 10:1 (horizontal:vertical) pit-run gravel (aka clean-fill dike) side slope, and an east 2:1 basalt riprap side slope (Figure H.1). The thickness of the side slopes varies from 5 m near the boundaries of the ETC barrier to zero at the slope toes. The angularity of the riprap provides many interlocking surfaces between adjacent rocks, allowing the creation of a relatively steep yet stable side slope. The coarse materials for the side slopes provide such a condition that infiltration water drains freely. The west side slope of the PHB contains a small amount of fine (e.g., sand and silt) particles. The east side slope is made of the basalt riprap with a size range of from 0.2 to 0.3 m diameter that had a near-zero water holding capacity.

The ETC barrier was constructed with a 2% slope to the west and east from the crown (north-to-south center line) of the barrier. The west and the east boundaries of the storage layer have an approximate 30° angle such that the cross section of the ETC barrier looks like an inverted trapezoid, approximately. The distance from the west edge to the east edge of the ETC barrier is 40 m at the top and 32 m at the bottom. A filter that transitions from sand to gravel was applied between the silt loam and the side slopes to prevent the fine soil from entering the side slopes.

During the monitoring period from 1994 to 2013, there was no vegetation on the riprap side slope but sparse vegetation on the gravel side slope. Below the 5-m-thick ETC barrier is a 0.15-m-thick 64 × 105 m^2 AC with a 5-mm-thick polymer-modified FAA coating (DOE-RL 1994). The distance from the west edge to the east edge of the AC is 64 m, which is 22 m longer than the ETC barrier so that the AC extended below the side slopes.

For testing purposes, the ETC barrier and the AC were divided into a north section and a south section separated by a 10-m-wide buffer zone. From November 1994 to October 1997, the north section received an enhanced amount of precipitation (natural precipitation plus supplemental irrigation) to simulate extreme climate conditions [about 3 times (3X) the long-term precipitation], while the south section received only natural precipitation. To synchronize with the natural storage and release processes in the

barrier, the irrigation was conducted on a water-year (WY) basis. A water year starts in November of the previous year and ends in October of current year. In May 1998, water was added to the north section for instrument testing. The total meteoric precipitation and irrigation was 493.3, 493.1, 499.7, and 363.0 mm for WY95 through WY98, respectively. After that, both the north and south sections were exposed to natural precipitation only. In September 2008, the vegetation in the north section was burned to test the impact of a natural fire on the barrier performance.

Characterization of the precipitation at the test site based on the standardized precipitation index (McKee et al. 1993, 1995) is reported in Appendix A. Regarding the WY precipitation of the 19 test years, 2 years (WY95 and WY97) were extreme wet, 4 moderate wet, 12 near normal, and 1 (WY05) severe dry. This means that the barrier had the most precipitation stress in WY95 and WY97, even under the unirrigated section of the barrier.

H.2.2 Monitoring of Water Content and Water Pressure

Water contents were monitored vertically in the gravel side slope, laterally at the base of the barrier's silt loam storage layer, and laterally at three depths beneath the AC. Details of the lateral measurements are presented in Sections 2.3 and 2.4. Details of the vertical measurements are given below.

Water content, θ (m^3m^{-3}) of the soil 0.05 m above the bottom of the silt loam storage layer was monitored with eight horizontally oriented neutron probe (NP) access tubes to examine the impacts of side boundaries and the CB at the bottom on water movement. Water content beneath the AC was monitored with six horizontally oriented NP access tubes installed at the depths of 1, 2, and 3 m below the AC. The layout of the access tubes is shown in Figure H.2. To monitor the water contents under different treatment, four of the NP access tubes in the storage layer (i.e., AA1, AA2, AA5, and AA6) were installed in the north section and four (i.e., AA3, AA4, AA7, and AA8) in the south section. All the NP access tubes below the AC (BA1 through BA6 in Figure H.2) were placed at the north section, where there was a higher chance of percolation through the AC. Water content was monitored at a horizontal interval of 1.0 m using an NP (Hydroprobe Model 503, CPN International, Inc., Martinez, CA) in 76-mm ID aluminum tubes. A sleeve was used around the NP to keep it in the center of the access tubes during each horizontal logging. Water contents in the gravel side slope were monitored at two locations, i.e., S13 and S14 in Figure H.2, at a vertical interval of 0.15 m using an NP deployed in a vertical (48-mm inner diameter) aluminum access tube extending 1.9 m below the barrier surface.

The soil used to construct the storage layer was Warden silt loam, and the soil below the AC was local sand. The retention properties of the silt loam are reported in Appendix E. Three separate calibrations were conducted for NP H33115140 in April 1995 for different combinations of soil and NP access tube:

48-mm tube in gravel side slope $$\theta = a_0 + a_1 N + a_2 N^2 \quad \text{(H.1)}$$

76-mm tube in silt loam $$\theta = \exp(b_0 + b_1 N) \quad \text{(H.2)}$$

76-mm tube in sand $$\theta = c_0 + c_1 N \quad \text{(H.3)}$$

where N is the 16-sec. neutron count, a_0 = -0.0165, $a_1 = 1.449 \times 10^{-5}$, $a_2 = 3.234 \times 10^{-10}$, b_0 = -2.9328, $b_1 = 8.869 \times 10^{-5}$, c_0 = -0.02822, and $c_1 = 1.83 \times 10^{-5}$. On April 20, 2003, the neutron probe received a new neutron counter and a new sleeve. Hence, after this date, the N values needed to be scaled by a factor of 1.041 for vertical loggings and 0.988 for horizontal loggings. Radioactive decay was corrected for all the measurements before data analysis.

Soil water pressure, h (m), at the northeast section of the barrier below the AC was monitored with six fiberglass blocks (FGBs, MC-314 Soil Moisture Cells). The FGBs were calibrated in the laboratory and a single calibration was used for the FGBs to convert the measured electrical resistance, R (k Ohm), into soil-water pressure:

$$h = -3.1696R^{1.4317} \tag{H.4}$$

The NP monitoring was conducted from WY95 to WY13, with some data gaps in WY99, WY05, and WY06. The FGB monitoring was discontinued in FY07 because of a system malfunction.

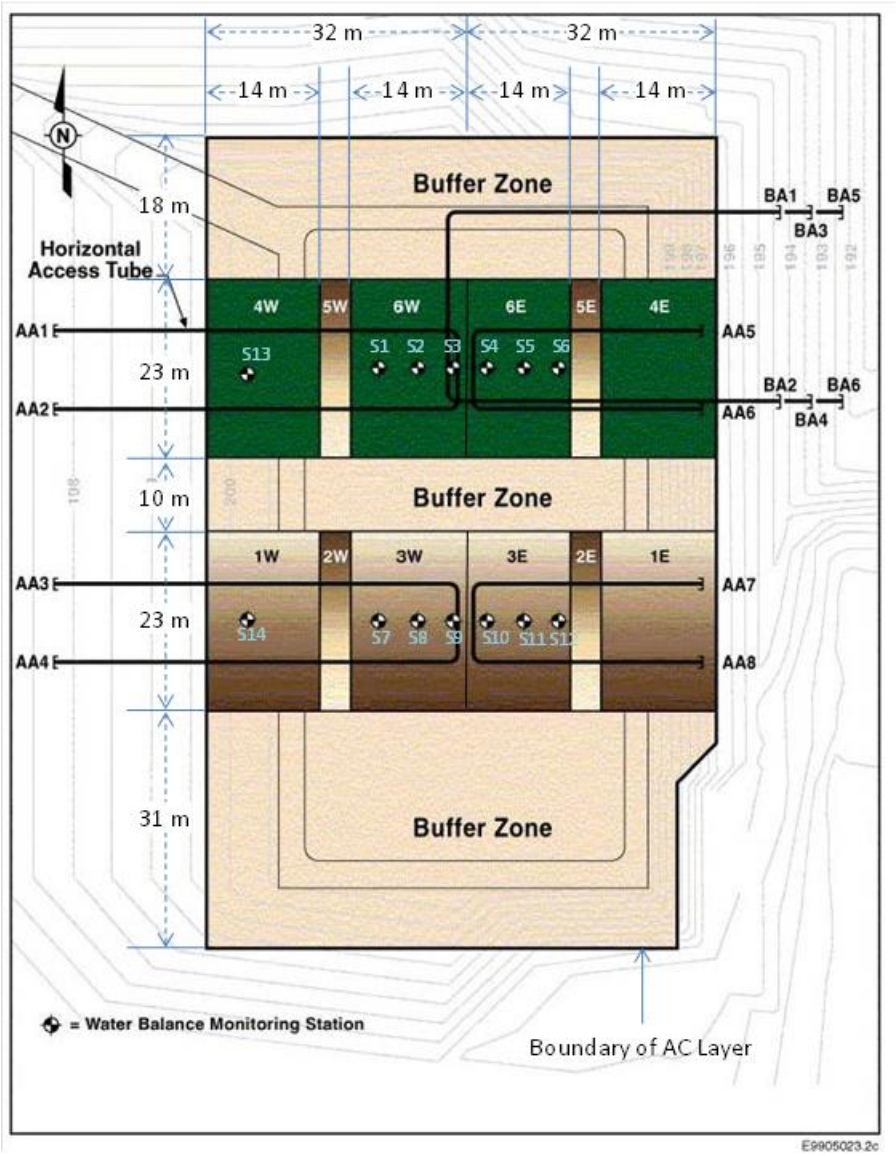

Figure H.2. The horizontal neutron probe access tubes shown by the U-shaped lines. Tubes AA1 through AA8 are located 0.05 m above the silt-sand interface. Tubes BA1 and BA2 are 1 m below, BA3 and BA4 are 2 m below, and BA5 and BA6 are 3 m below the asphalt concrete layer with fluid applied asphalt coating. Symbols 1W through 6W and 1E through 6E denote that 12 zones for drainage monitoring. (Approximate scale.)

H.2.3 Monitoring Drainage off the Asphalt Concrete

The low-permeability FAA-coated AC was built with a 2% slope, parallel to the barrier surface, to the east and west of the barrier crown. The entire surface of the AC barrier was covered with a 0.3-m-thick layer of gravel to facilitate lateral water movement toward the lower slope positions of each collection zone. A series of curbs divided a portion of the AC surface into 12 water collection zones, denoted by 1W through 6W and 1E through 6E in Figure H.2. Most of the area of plots 1W and 4W was below the gravel side slope, while most of the area of plots 1E and 4E below the riprap side slope. These four plots are referred to as the side slope plots. For the side slope plots, of the 14-m width, about 1 m was below the silt loam boundary and 4 m was below the unvegetated road, which was constructed by placed gravels over the leveled portion of the side slopes. The effects of the silt loam boundary and road on drainage added complexity in interpreting the drainage data from the side slope plots. Plots 2W and 5W were primarily below the west boundary of the ETC barrier and 2E and 5E below the east boundary. These four plots are referred to as the barrier boundary or transitional plots. Approximately 1 m of the 4-m width was below the ETC barrier boundary plots. The remaining four plots were below the ETC barrier and drainage from them is reported in Appendix G. The water intercepted by the AC in the plots was conveyed through a network of PVC pipes to collection vaults for measurement. The water intercepted in other area of the AC was transferred to a disposal pond north of the collection vaults. An exception was that the east half of the north buffer zone (i.e., the NE corner) of the AC was un-curbed at the east edge. For this un-curbed AC surface area, the intercepted water flowed off the surface at the east edge of the AC.

Each of the 12 drainage plots was plumbed to a separate concrete vault containing a drainage monitoring system. Each vault contained an Orenco dosing siphon system[1] (Orenco Systems, Inc., Sutherlin, OR) that discharged the collected water (i.e., the dosing volume) once the maximum water level was reached. The average dosing volume was 0.591 m^3, which was equivalent to 1.8 mm of drainage through the side slope plots and 6.3 mm of drainage through the smaller barrier boundary plots. The drainage rate from each plot was also measured with a tipping bucket and a pressure transducer. Drainage water flowed into each vault via a tipping bucket, which allowed monitoring of low flows, e.g., through the ETC barrier (Appendix F) or the ETC barrier boundaries. The tipping buckets might not have responded fast enough to high flow rates through the side slopes and hence the results from tipping buckets are not discussed below. A submerged Druck pressure transducer (Instrumart, South Burlington, VT) monitored the intermediate-to-high flow rates by recording hydrostatic pressure at intervals ranging from 10 minutes to 1 hour. The drainage rate (D) reported in this paper was based on the pressure transducer measurements after and converting volume changes to drainage rates.

Each vault was equipped with a lid to prevent precipitation from entering. The lid was covered with a thick tarp to prevent the water in the vault from freezing in the winter or evaporating in the summer. This monitoring was conducted from WY95 to WY13, with some data gaps in WY99, WY05, and WY06.

H.2.4 Monitoring Percolation through the Asphalt Concrete

Percolation through the AC was expected to be very small. To confirm that hypothesis, a pan lysimeter (6.5-m wide, 0.3-m deep) was installed beneath plot 4E on the riprap side slope (Figure H.2). This location was chosen to maximize the potential for drainage (it was irrigated to supplement precipitation and achieve 3X annual average precipitation from WY95 to WY97). The pan lysimeter was shaped like an inverted pyramid and filled with a 0.1-m-thick layer of drainage gravel and 0.2-m-thick layer of top course gravel with a geotextile in between (DOE-RL 1994). The perimeter of the lysimeter was sealed to the underside of the AC. Paired 1.65-mm-diameter stainless steel tubes were used for venting and siphoning water from the bottom of the lysimeter (Myers and Duranceau 1994). The siphon tube was

[1] http://www.orencostore.com/img/nsu-si-si-2.pdf, accessed on March 11, 2015.

connected to a monitoring system, which consisted of a pump and tipping-bucket rain gauge controlled by a datalogger. This monitoring was discontinued in 2007 because of a system malfunction.

H.3 Results

The seasonal variation of soil water in the gravel side slope is discussed first (note that the water content of the riprap slope was not monitored because the riprap was assumed to have very little water holding capacity when the monitoring system was designed.) Next, the impacts of the west and east boundaries of the ETC barrier on the distribution of water contents are presented. Then the drainage through the barrier boundaries and the side slopes is delineated, and finally, the percolation through the AC barrier is analyzed.

H.3.1 Seasonal Variation of Soil Water in the Gravel Side Slope

Figure H.3 shows the water content contours on the gravel side slope from 1995 to 2013. In agreement with seasonal variation of the precipitation, the gravel side slope was wetter during the winter seasons than the summer seasons. Because of the low water holding capacity of the pit-run gravel, the maximum water content generally was no more than 0.15 m^3m^{-3}, indicating additional water migrated downward as drainage. During the summer seasons, it appears that there was still plenty of water available for plants in the soil profile, evidenced by the blue color in Figure H.3. This suggests that the water stored in the intermediate and large depths could not be completely released into the atmosphere by the ET process because of very sparse vegetation.

The water storage in the top two meters of the gravel side slope from 1995 to 2013 varied between about 118 mm and 239 mm (Figure H.4). Although the north section was irrigated to an average precipitation of 495.4 mm (approximately 3X the average precipitation) from WY95 to WY97, there was little difference in water storage between the irrigated and the non-irrigated sections during winter seasons, meaning the maximum storage of the gravel was reached. The water storage of the irrigated north section in the summer of 1996 and 1997 was slightly higher than it was in the non-irrigated section, implying limited capability of the ET process to consume the stored water.

As a comparison, the 2-m water storage in the ETC barrier varied between about 111 mm and 518 mm, as reported in Appendix G. Although the high values for the gravel side slope were much lower than those for the ETC barrier, the low values for the former were nearly the same as those for the latter. These results indicate that soil type has a strong impact on its storage capacity and great care needs to be taken when selecting the construction material for the ETC barrier.

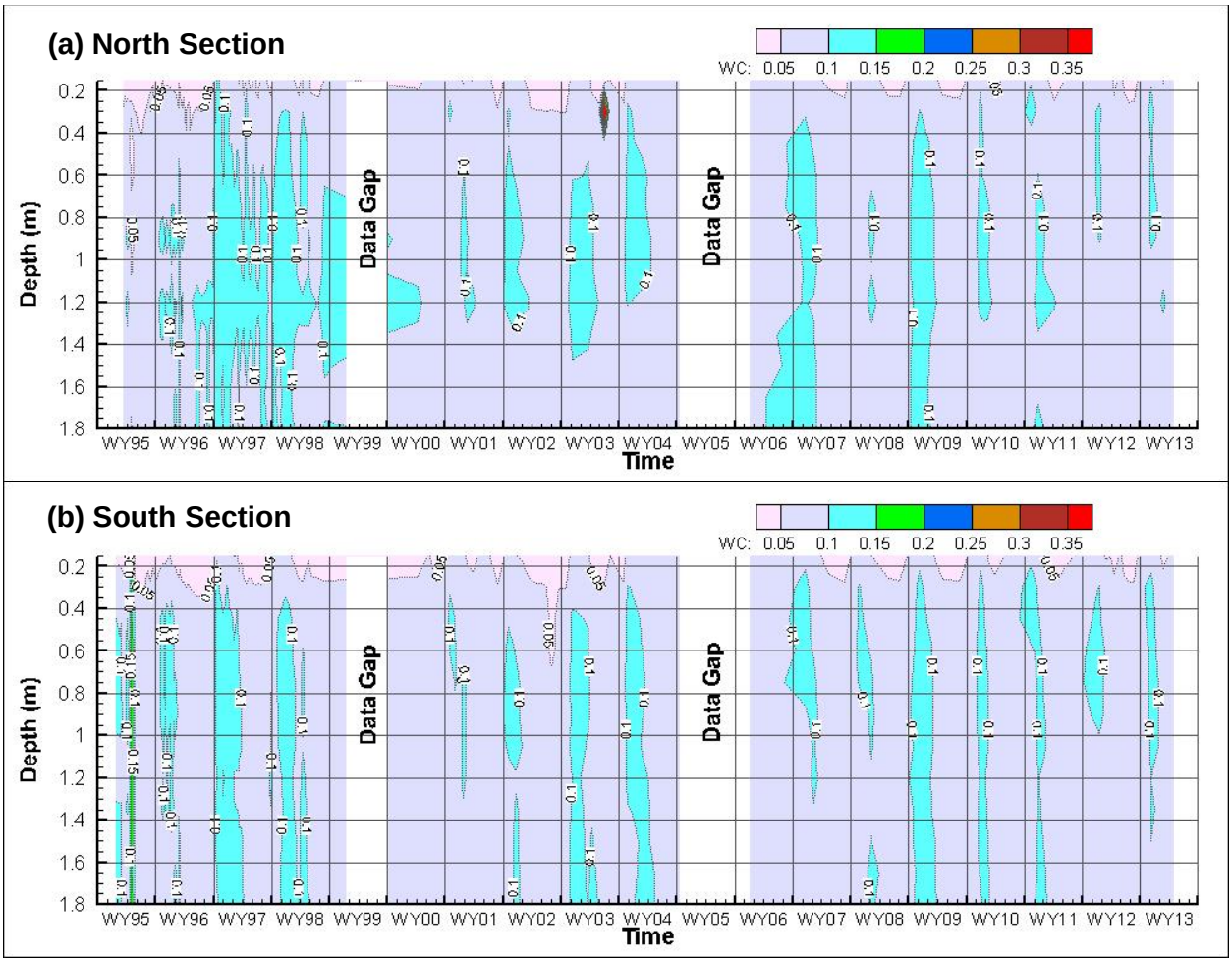

Figure H.3. Water content distribution in two vertical access tubes in the gravel side slope from 1995 to 2014.

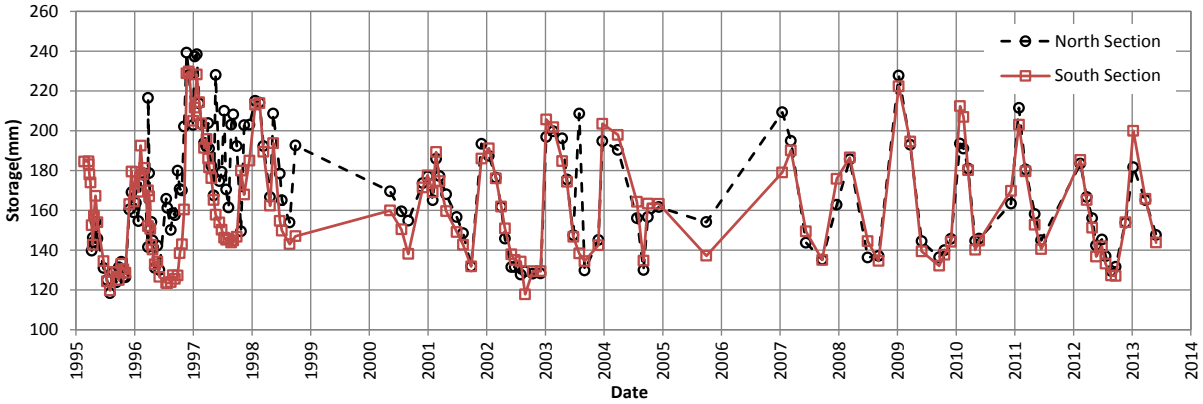

Figure H.4. Variation of water storage in the top 2 m of the gravel side slope.

H.3.2 Drainage through Side Slopes

The monthly drainage rates for the two types of side slopes from 1995 to 2012 varied seasonally (Figure H.5). The highest drainage rates generally occurred around January or February of each year and the lowest rates usually in the summer or early fall. The drainage rates in the summer were very low and the minimum monthly rates were no more than 3 mm per month regardless of the use of irrigation. This means that most of the summer precipitation on the side slopes probably was released into the atmosphere via ET. This pattern is in agreement with the seasonal variation of P and ET.

Figure H.6 compares the rates or WY drainage through the side slopes. Because the drainage measuring system was not ready until March 1995, the drainage for WY95 was a cumulative value from March to October. During the monitoring period, the maximum D was 283.0 mm yr^{-1} for the riprap side slope and 231.1 mm yr^{-1} for the gravel side slope when they were under enhanced precipitation. The maximum D under natural precipitation was 143.1 mm yr^{-1} for the riprap side slope and 171.4 mm yr^{-1} for the gravel side slope. All maximums occurred in WY97, which had the highest (290 mm, 1.7X the average) precipitation during the monitoring period. The average P_a over the three-year enhanced precipitation condition was 495.3 mm yr^{-1} and average drainage rates was 130.7 mm yr^{-1} (i.e., $0.26P_a$) at the gravel side slope and 139.9 mm yr^{-1} (i.e., $0.28P_a$) at the riprap side slope. During the same period, the average P_a under ambient condition was 367.6 mm yr^{-1} and average drainage rates was 83.5 mm yr^{-1} (i.e., $0.31P_a$) at the gravel side slope and 61.7 mm yr^{-1} (i.e., $0.23P_a$) at the riprap side slope.

From WY98 to WY12, natural precipitation (from 0.81X to 1.32X average precipitation, with an average of 172.6 mm yr^{-1} for the south section and 188.7 mm yr^{-1} for the north) was near normal and hence the drainage rate was relatively low, with an average of 12.4 mm yr^{-1} (i.e., $0.067P_a$) for the gravel side slope and 13.1 mm yr^{-1} (i.e., $0.072P_a$) for the riprap slope. The results indicate that the precipitation played a critical role to the drainage rate through the side slopes.

The monitoring results demonstrate that there was no obvious difference in either the seasonal pattern of drainage (Figure H.5) or the drainage rates (Figure H.6) between the two types of side slopes. Intuitively, one may think the drainage rate through the riprap side slope would be larger than that through the gravel side slope because the former did not contain any fine particles and no vegetation grew on it. In fact, a small but not negligible amount of precipitation can be held by the riprap, e.g., as a thin water film. Internal evaporation could occur within the riprap side slope through two different mechanisms that might be insignificant for the gravel side slope. 1) The very large pore space among the riprap blocks could allow the convection of air flow in the large (about 1s to 10s cm) pores and remove the water vapor from the slope. 2) Because of the lack of fine particles, the riprap slope tended to have a higher summer temperature and hence higher evaporation than the gravel side slope.

Figure H.7 shows the relationship between WY drainage rate and annual precipitation. For both types of side slopes, when P_a was less than about 140 mm yr^{-1}, the drainage approached zero, indicating nearly all the annual precipitation was first stored in the side slope soil and then released into the atmosphere via ET for the gravel side slope and via evaporation for the riprap side slope. When P was larger than about 140 mm yr^{-1}, roughly 46% (43% for the gravel slope and 49% for the riprap slope) of the additional annual precipitation ended up as drainage.

In other words, when $P_a \leq 140$ mm $yr^{-}1$, all the precipitation ends up as ET; when $P_a > 140$ mm $yr^{-}1$, about 54% of the additional precipitation becomes as ET, i.e., $ET \approx 140+0.54(P_a - 140)$. For example, for an average year with 172 mm yr^{-1} precipitation, the estimated drainage is 14.7 mm yr^{-1} (8.6% of P_a) and ET is 157.3 mm yr^{-1} (91.4% of P_a). These results indicate that ET can release most of the precipitation back to the atmosphere despite the low storage capacity of the side slopes.

The above analysis did not consider the impacts of the silt loam boundary and the road on drainage through the side slopes. Because about 10% of the side slope plots was below the silt loam boundary and 30% below the gravel covered road, the drainage rates measured could be different from the case if 100% of the plots would be under the side slopes. The impact of the gravel road might be small because the

gravel had relative large permeability and would allow the infiltration of precipitation. However, the silt loam boundary might lead to an underestimation of drainage rate.

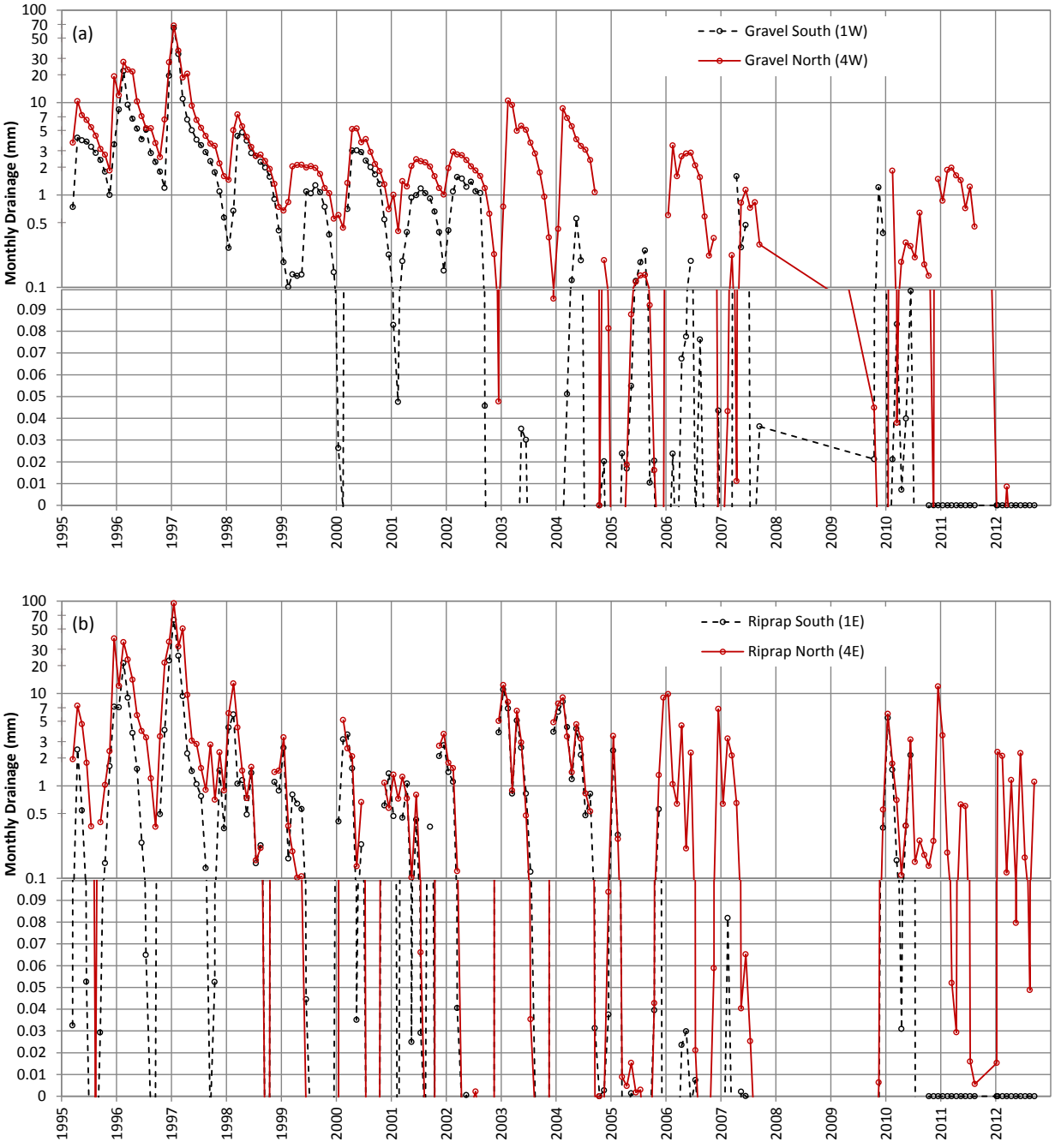

Figure H.5. Monthly drainage through the (a) gravel side slope and (b) riprap side slope. To clearly show the low values, each plot contains two portions, the upper is in log-scale for values > 0.1 mm and the lower in normal scale for values < 0.1 mm. The north section was irrigated from WY95 to WY97 so that the total precipitation was approximately 3X the average.

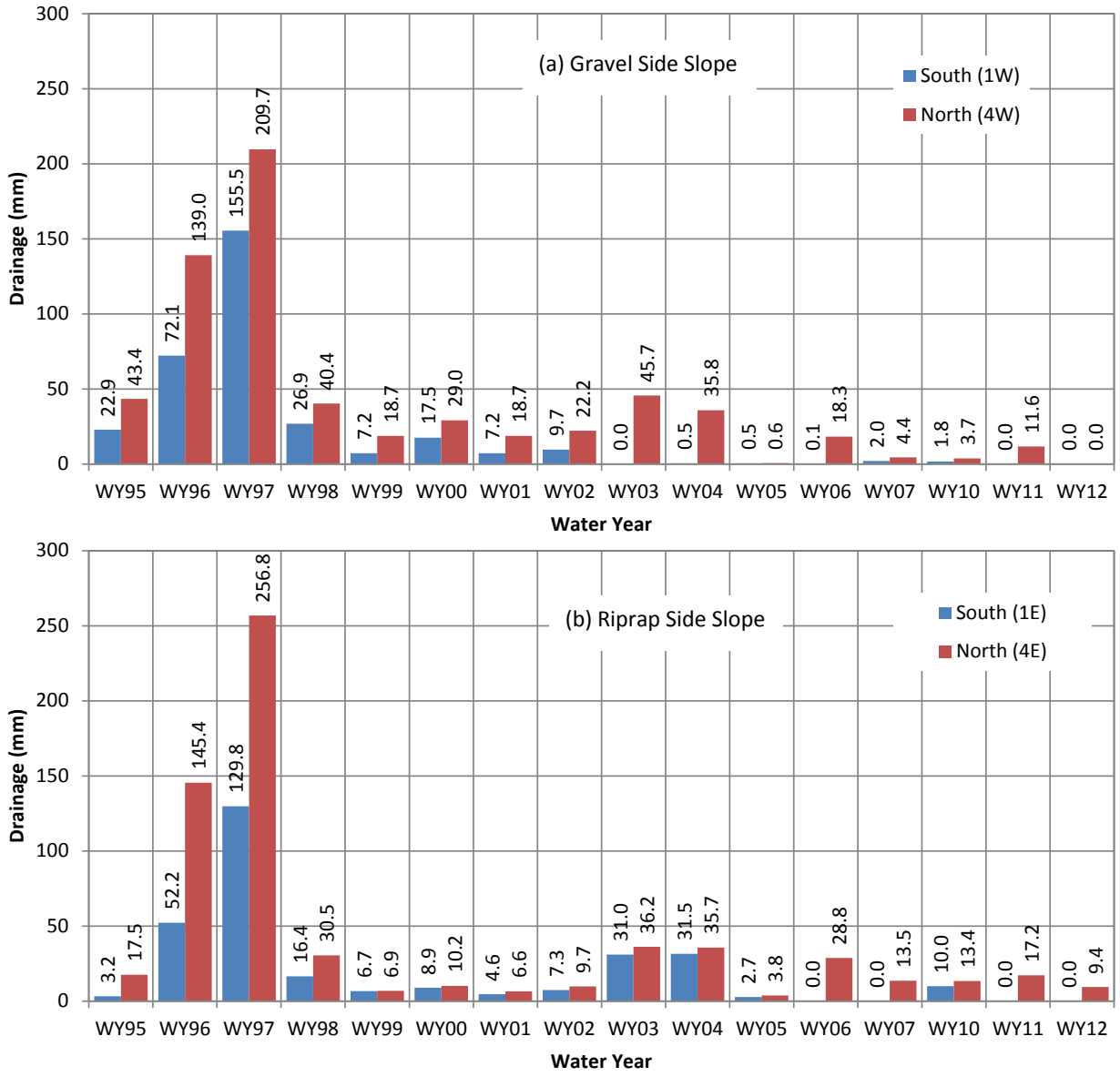

Figure H.6. Annual drainage through the (a) gravel side slope and (b) the riprap side slope. The north section was irrigated from WY95 to WY98. The drainage for WY95 was from March to October.

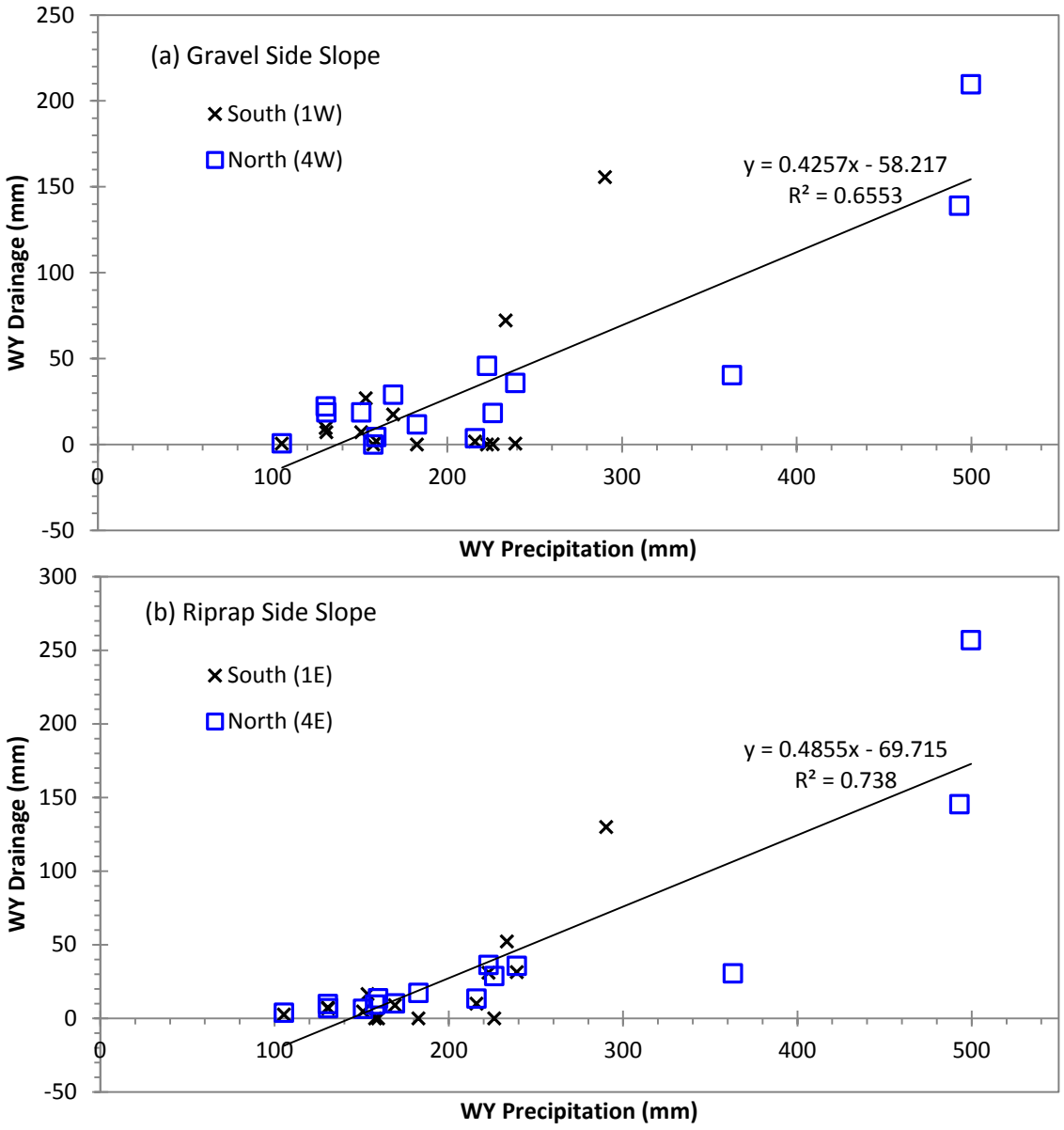

Figure H.7. The relation between drainage and precipitation for (a) the gravel side slope and (b) the riprap side slope. The lines indicate linear regressions. The observations from WY95 were excluded because the measuring system was not completely ready.

H.3.3 Flow at the Transition Zones

The silt loam-sand interface as the side boundaries of the storage layer forms a CB so that the capillary water in the silt loam could not enter the coarser materials unless the silt loam was nearly saturated. Because the storage layer had a shape similar to an inverted isosceles trapezoid, the silt loam near the boundaries was thinner than that inside the layer. As a result, the silt loam above the slanted CB had less storage capacity.

Different from that inside the ETC barrier, where flow tends to be one-dimensional vertically, the flow in the silt loam near the boundary is expected to be and likely migrate both vertically and laterally because of the slanted interface between silt loam and sand. Theoretically, after the infiltrating water reaches the slanted side CB, the water is expected to move downward along the slanted boundary. After arriving at the bottom of the silt loam layer, the infiltration water tends to move laterally into the silt loam because of the CB at the bottom. When sufficient water is at the bottom to overcome the capillary break, some water will enter into the underlying coarser layers and end up as drainage.

Figure H.8 shows θ measurements as time-space planes along two lateral monitoring lines, one for the north section and the other for the south section. From WY95 to WY97, there was a seasonal variation of water content at the bottom of the silt loam of the irrigated north section (Figure H.8a), indicating the infiltration water reached the bottom of the silt loam layer in the winter seasons. The increase in θ during the winter seasons was much more pronounced near boundaries than in the middle of the storage layer. For instance, along the line of AA1-AA5 on March 29, 1997, the maximum θ was 0.238 m^3m^{-3} near the west boundary, 0.201m^3m^{-3} near the east boundary, and 0.069 m^3m^{-3} in the middle, meaning infiltration water accumulated near the slanted side boundaries of the barrier. Figure H.8a also signifies that the infiltration water moved laterally toward the inside of the storage layer by as much as about 10 m in the irrigated north section in WY95 and WY97. However, the θ was still much less than the near saturation condition (θ_s = 0.378 m^3m^{-3}), indicating no drainage occurred across the capillary break at the bottom of the silt loam layer. In the non-irrigated south section, the infiltration water reached the bottom of the storage layer near the side boundaries only in the spring of 1997, when the winter precipitation was 2.2X the average precipitation. From 1998 to 2013, P was moderate wet for only 1 year and near normal or less in other years. Thus, the water content at the bottom of the silt loam layer stayed at low θ (<0.075 m^3m^{-3}) almost all the time (Figure H.8a, b), suggesting the infiltration water never reached the bottom of the silt loam layer, even at the side boundaries, for these years. The above results show that the moisture accumulation along the silt loam boundaries was evident only under the enhanced (3X average) precipitation conditions. No moisture accumulation was observed under natural precipitation conditions.

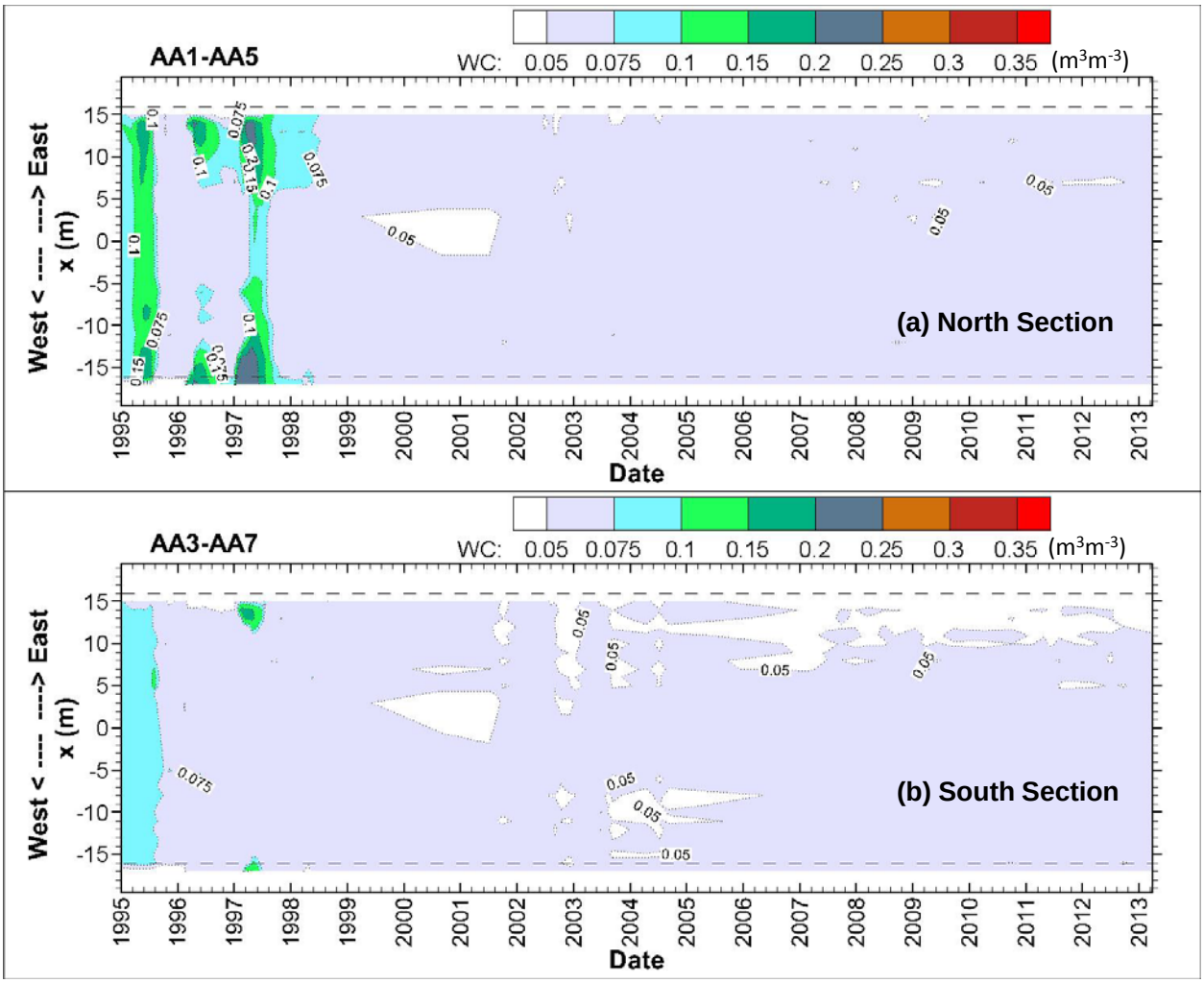

Figure H.8. Soil water content near the bottom of the silt loam in the time-space plane along the horizontal lines (a) in the north section and (b) in the south section. The edges of the silt loam layer at the ground surface were at x = -19.3 m and x = 19.3 m and those at the bottom of the silt loam layer at x = -16 m and x = 16 m (marked by the horizontal dashed lines).

The annual drainage rates through the boundaries are given in Table H.1. The greater-than-0.5 mm yr^{-1} (the design criterion) drainage rates occurred in five instances during the 19-year monitoring period. Four instances occurred in the irrigated section and the other case (i.e., 0.9 mm yr^{-1}) occurred in the ambient east boundary in WY97 with a 2.2X winter precipitation. The maximum drainage rate was 7.5 mm yr^{-1} and occurred in the irrigated northeast boundary in WY97. The maximum drainage rate through the side boundaries was much larger than the maximum drainage rate through the silt loam of 0.18 mm yr^{-1} (Appendix G) but much less than the rate through the side slopes of 283.0 mm yr^{-1} reported above. From WY98 to WY13, the drainage rate through the side boundary was no more than 0.002 mm yr^{-1} when the winter precipitation was no more than 1.4X of the long-term average.

The above results indicate there is an edge effect on the flow in the ETC barrier and the strength of this effect is dependent on the water storage near the barrier edge. Hence, it is necessary that the horizontal extent of the ETC barrier is larger than that of the underlying waste zone. For the worst-case scenario during the 3X enhanced irrigation test, the distance of lateral was about 10 m. Fayer (1987) conducted a series of numerical simulation and found that a 10-m overhand was sufficient to mitigate the edge effect

of a barrier over a loam sand. They also pointed that a finer soil beneath the barrier would have stronger edge effect.

Table H.1. Drainage through the west and east boundaries of the silt loam layer (transition zones, mm yr^{-1})

	West Boundary		East Boundary	
	South (2W)	North (5W)	South (2E)	North (5E)
WY1995	4.2E-2	5.5	0	4.5E-1
WY1996	0	2.7	1.3E-3	4.9
WY1997	2.8E-4	2.8E-1	0.9	7.5
WY1998	1.5E-3	1.4E-3	1.6E-3	1.2E-3
WY1999	1.4E-4	0	2.2E-4	0
WY2000	2.0E-3	7.9E-3	8.6E-3	4.1E-4
WY2001	0	0	0	8.2E-4
WY2002	2.8E-4	1.1E-4	0	1.0E-4
WY2003	2.8E-4	0	0	4.1E-4
WY2004	2.8E-4	0	0	3.1E-4
WY2005	4.2E-4	0	1.1E-4	0
WY2006	1.4E-4	0	0	0
WY2007	1.4E-4	0	0	1.0E-4
WY2010	0	0	0	0
WY2011	0	0	0	1.0E-4
WY2012	0	7.7E-4	0	0

H.3.4 Effects of Asphalt Concrete

Figure H.9 shows the water content distribution for the region beneath the AC (the lower portion below the dashed line, x = 0 to 32 m) and the region beyond the AC edge (upper portion above the dashed line, x > 32 m). In the sand beyond the AC edge, drainage was expected to flow freely down to the deep sand. Hence, water content in the sand near the edge was expected to be higher than that beneath the AC, as evidenced in the upper portion of each plot in Figure H.9. A clear edging effect of the AC on flow is shown by the higher θ near the edge, with one exception (a low θ zone in Figure H.9b). This effect appears to be stronger for the uncurbed AC (Figure H.9a, c and e) than the curbed AC (Figure H.9b, d, and f) because the intercepted drainage at the uncurbed portion would flow off the edge into the sand. The low θ zone in Figure H.9b might be due to local anomaly, e.g., cobbles near the point of neutron logging. The edging effect caused some of the drainage water to move laterally into the sand below the AC by as much as 2 to 3 m at the depth of 1 m (Figure H.9a and b) and by 4 to 5 m at the depths of 2 or 3 m (Figure H.9c through f).

The water content of the sand beneath the AC, except the portion near the edge, was either stable or decreasing slightly over the 19-year monitoring period (Figure H.9). To quantitatively examine the variation of water content beneath the AC, the average θ of 26 observations below the AC barrier (excluding the outer 6 m, i.e., x = 0 to 26 m), is illustrated in Figure H.10. From 1995 to about 2000 there

was a trend of decreasing θ, but the changes were generally very small (< 0.005 m^3m^{-3}) because the initial θ at the time of construction was relatively low (about 0.10 m^3m^{-3}). The trend of decreasing water content suggests the soil was losing water likely because of downward movement of antecedent soil water due to gravity. If there was any water input from above during this period, it was smaller than the water loss from this zone. From 2000 to 2013, the water content stayed relatively stable, meaning the soil water was nearly immobile. Note that the neuron counter and probe sleeve for the NP used were replaced by new parts in April 2003, and this might have caused a slight (< 0.005 m^3m^{-3}) increase in observation starting in early 2003.

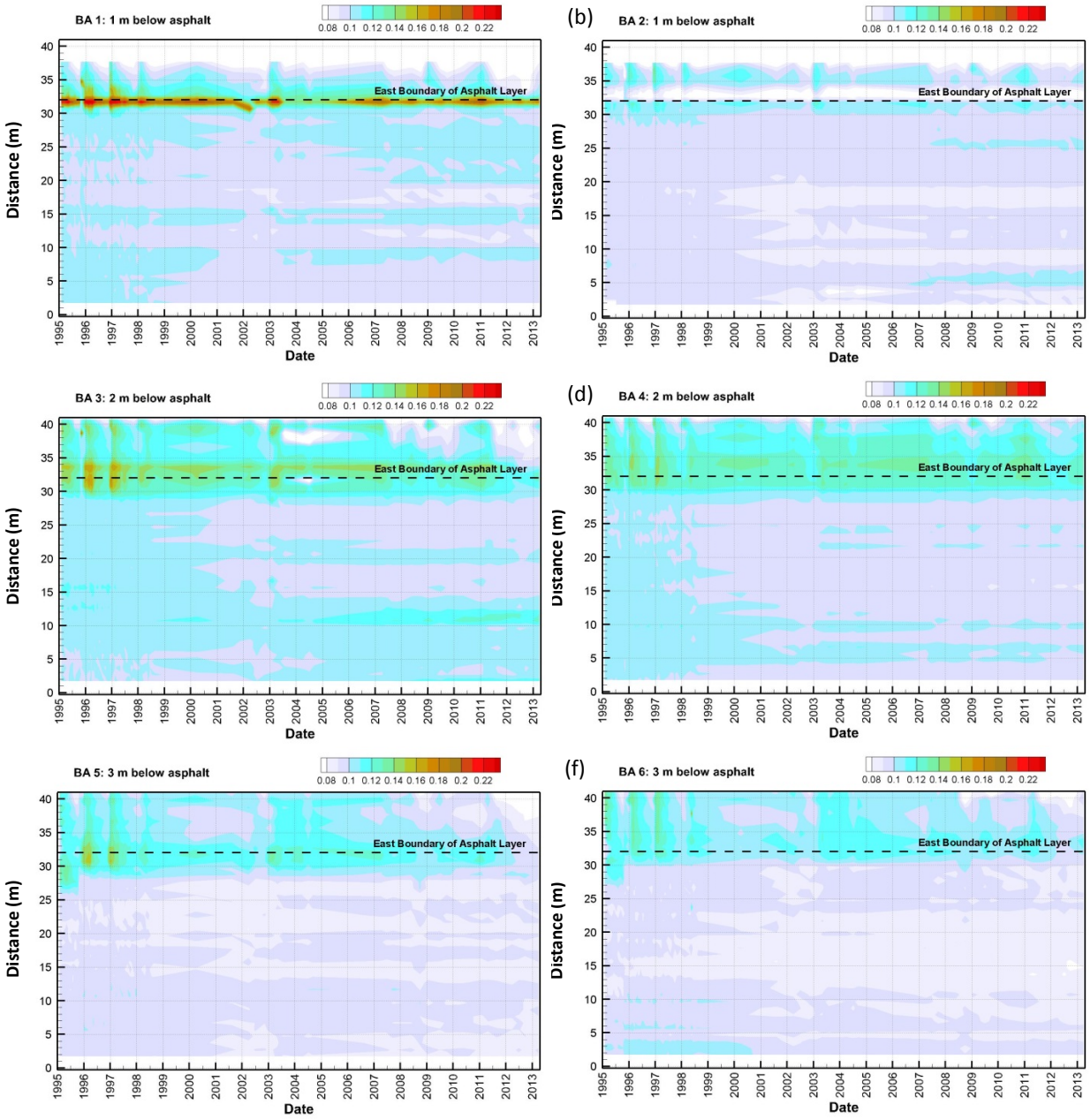

Figure H.9. Water contents at depths of 1 m, 2 m, and 3 m below the asphalt layer in the time-space plane. The vertical axis is the distance from the center line of the silt loam barrier. BA2, BA4, and

BA6 were below the area of curbed AC, while BA1, BA3, and BA5 below the area of uncurbed AC.

The soil water pressure below the AC barrier measured at the northeast section with six FGBs was almost always less than -300 m. Despite the large uncertainty of FGB-measured *h* of about a factor of 3, the measured *h* was comparable to the commonly used permanent wilting point of -150 m (Or and Wraith 2001; Romano and Santini 2002).The cumulative percolation through the AC barrier measured with the pan lysimeter was only 0.14 mm (average 0.012 mm yr^{-1}) over a period of about 12 years. The percolation through the AC barrier is considered very low compared with the design criterion of 0.5 mm yr^{-1}.

In summary, the stable or decreasing water content, stable soil water pressure, and very low percolation rate all demonstrate negligible water percolation through the AC barrier over the 19-yr monitoring period. However, pan lysimeter data suggest that the FAA-coated AC barrier should not be impermeable.

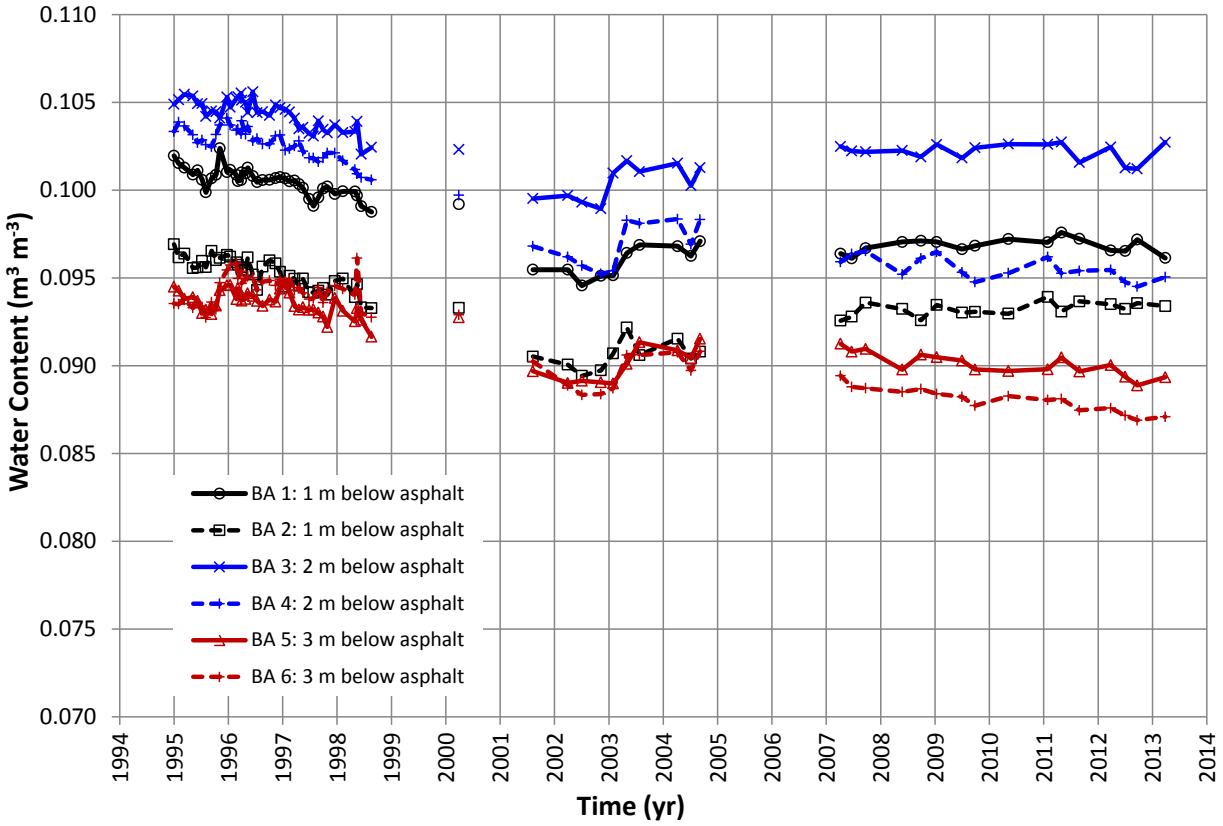

Figure H.10. The average water content from x = 0 to 26 m. (x is the distance from the center line of the barrier. The edge of the AC barrier is at x = 32 m.)

H.4 Summary

Based on the monitoring results from 1994 to 2013 at the Prototype Hanford Barrier, the hydrological characteristics at the side slopes and the asphalt concrete layer are summarized below.

The variation of water content of the gravel side slope had a seasonal pattern. During the cold, wet winter season, the maximum water content generally was no more than 0.15 m^3m^{-3} because of the low water holding capacity of the gravel sand. During the hot, dry summer season, it appeared that the stored water in the intermediate and large depths could not be completely released to the atmosphere by the ET process. The drainage rate through the two types of side slopes also varied seasonally, with the highest drainage rate generally in January or February and lowest rate usually in the summer or early fall. The WY drainage was nearly zero when the annual *P* was less than about 140 mm yr^{-1}, meaning nearly all the P was released from the side slopes into the atmosphere via ET. When P was larger than 140 mm yr^{-1}, approximately half of the additional precipitation ended up as drainage. The results indicate that ET is an important mechanism to release most of the precipitation back to the atmosphere. No obvious difference was observed between the two types of side slopes in either the seasonal pattern of drainage or the rate of drainage through the side slopes.

Different from the flow inside the barrier, which was generally one-dimensional vertically, the flow in the silt loam near the side boundaries migrated both vertically and laterally. After arriving at the bottom of the silt loam layer, the infiltration water tended to move laterally into the silt loam because of the CB at the bottom. When sufficient water was at the bottom, some water entered into the underlying coarser layers and ended up as drainage. The measured maximum drainage rate through the side boundaries was much higher than the rate through the silt loam layer but much less than the rate through the side slopes. The lateral flow along the silt loam boundaries was significant only under the enhanced (3X average) precipitation conditions and was minimal under natural precipitation conditions.

The water content beneath the AC, except the portion near the edge, was either stable or decreasing over the 19-year monitoring period. The soil water pressure below the AC was almost always less than -300 m, which was comparable to the permanent wilting point, meaning the soil water was tightly bound on soil particles. The cumulative percolation through the AC was only 0.14 mm (average 0.012 mm yr^{-1}) over a period of about 12 years. The stable or decreasing water content, stable water pressure, and very low percolation rate all indicate that negligible water percolated through the AC.

References

Albrecht, BA and CH Benson. 2001. "Effect of Desiccation on Compacted Natural Clays," *Journal of Geotechnical and Geoenvironmental Engineering*, 127(1):67-75. doi:10.1061/(asce)1090-0241.

Albright, WH, CH Benson, GW Gee, AC Roesler, T Abichou, P Apiwantragoon, BF Lyles, and SA Rock. 2004. "Field Water Balance of Landfill Final Covers," *Journal of Environmental Quality*, 33(6):2317-2332.

Benson, CH, A Sawangsuriya, B Trzebiatowski, and WH Albright. 2007. "Postconstruction Changes in the Hydraulic Properties of Water Balance Cover Soils," *Journal of Geotechnical and Geoenvironmental Engineering*, 133(4):349-359. doi:10.1061/(asce)1090-0241(2007)133:4(349).

DOE-RL. 1994. *Constructability Report for the 200-BP-1 Prototype Surface Barrier*, DOE/RL- 94-76, U.S. Department of Energy Richland Operations Office, Richland, Washington.

Fayer, MJ. 1987. *Model Assessment of Protective Barrier Designs: Part II*, PNL-6297, Pacific Northwest Laboratory, Richland, WA.

Freeman, HD and RA Romine. 1994. Hanford Permanent Isolation Barrier Program: Asphalt Technology Development. In GW Gee and NR Wing *Proceedings of Thirty-Third Hanford Symposium on Health and*

the Environment-- In-Situ Remediation: Scientific Basis for Current and Future Technologies, Battelle Press, Richland, Washington.

Gee, GW, AL Ward, and MJ Fayer. 1997. "Surface Barrier Research at the Hanford Site," *Land Contamination & Reclamation,* 5(3):233-238.

Henken-Mellies, WU and A Schweizer. 2011. "Long-Term Performance of Landfill Covers - Results of Lysimeter Test Fields in Bavaria (Germany)," *Waste Manag Res*, 29(1):59-68. doi:10.1177/0734242X10385748.

Levitt, DG, MJ Hartmann, KC Kisiel, CW Criswell, PD Farley, and C Christensen. 2005. "Comparison of the Water Balance of an Asphalt Cover and an Evapotranspiration Cover at Technical Area 49 at the Los Alamos National Laboratory," *Vadose Zone Journal*, 4(3):789-797. doi:10.2136/vzj2004.0171.

McKee, TB, NJ Doesken, and J Kleist. 1993. "The Relationship of Drought Frequency and Duration of Time Scales," *Eighth Conference on Applied Climatology, American Meteorological Society,* 179-186 pp. Jan. 17-23, 1993, Anaheim, California.

McKee, TB, NJ Doesken, and J Kleist. 1995. "Drought Monitoring with Multiple Time Scales," *9th Conference on Applied Climatology,* Am. Meteorol. Soc., Dallas, Texas.

Myers, DR and DA Duranceau. 1994. *Prototype Hanford Surface Barrier: Design Basis Document,* BHI-00007 Rev.0, Bechtel Hanford, Inc., Richland, Washington.

Or, D and JM Wraith. 2001. "Soil Water Content and Water Potential Relationships." In *Soil Physics Companion,* ed. AW Warrick, pp. 49-84. CRC Press, Boca Raton.

Romano, N and A Santini. 2002. "Field." In *Methods of Soil Analysis Part 4 Physical Methods,* eds. JH Dane and CT Topp, pp. 721-738. Soil Science Society of America, Inc., Madison, Wisconsin USA.

Terrel, RL. 1991. "Polymer-Modified Hot-Mix Asphalt for Environmental Liners," *Hot Mix Asphalt Technology,* (Spring):14-17.

Tuffour, YA and I Ishai. 1990. "The Difision Model and Asphalt Age-Hardening," *Association of Asphalt Paving Technologist*, 59:73-92.

Ward, AL and GW Gee. 1997. "Performance Evaluation of a Field-Scale Surface Barrier," *Journal of Environmental Quality*, 26(3):694-705.

Wing, NR and GW Gee. 1994. "Quest for the Perfect Cap," *Civil Engineering*, 64(10):38-41.

Appendix I

Structural Stability of the Prototype Hanford Barrier

Z. Fred Zhang

Pacific Northwest National Laboratory
Richland, Washington

Content

List of Figures

List of Tables

Abstract

Stability and integrity are critical to the normal function of surface barriers for waste isolation and infiltration control. Wind and water erosion, compression and settlement of the barrier, and displacement in the side slope were monitored for a prototype barrier at the Hanford Site near Richland, WA, USA. During a 3-year monitoring of wind erosion, wind speeds at heights of 0.25 and 0.5 m had decreasing trends, while wind friction velocity had an increasing trend with time as the vegetation grew. No water erosion was observed except for a small amount during the first 1000-year return 24-hour rainstorm in 1995. Over the 19-year period of monitoring (1994 to 2012), the elevation change of the asphalt layer (underlying the evapotranspiration layer) varied between -0.03 and 0.02 m. On average the elevation of the barrier surface decreased by 0.002 m with creep gauges moving an average of 0.024 m downslope to the east, 0.021 m to the north, and -0.006 m lower in elevation. These results indicate that the barrier surface and side slopes were very stable and nearly free from wind and water erosion.

I.1 Introduction

A surface infiltration and waste isolation barrier (cover) is one of the remediation technologies for the underground radioactive waste at the U.S. Department of Energy's Hanford Site near Richland, WA (DOE-RL 2013). Its primary function is to isolate waste from animal, vegetation, and human intrusion and to reduce or eliminate infiltration of precipitation into the waste zone. Maintaining integrity and stability is critical for the normal function of the surface barrier. To achieve this, barrier design must address factors that may lead to barrier failure.

Structural failure of a surface barrier can happen in different ways, such as the differential settlement of the barrier or barrier foundation (Benson et al. 1999; Jessberger and Stone 1991; Lagatta 1992; Levitt et al. 2005) or sliding of the side slope, which may be caused by excessive pore water pressure (Blight 2008; Koerner and Soong 2000; Merry et al. 2005). Elevating water pressure will reduce the barrier's effective stress and shear strength. The existence of slopes may increase the chance of sliding at the interfaces between components such as liner, drainage layer, filter layer, or protection layer (Reddy and Munwarbasha 2014).

Barrier cover designs, such as those recommended by the U.S. Environmental Protection Agency, have a short design life of 30 years (EPA 1991). Many wastes (e.g., nuclear waste) must be isolated for much longer periods, from centuries to millennia. Consequently, additional factors that may lead to barrier failure need to be addressed. For example, many synthetic construction materials that might be effective for decades cannot be relied on to perform satisfactorily for longer time periods. The barrier needs to be protected from wind and water erosion or deposition of dune sand and intrusion by plants, animals, and humans (Bowerman and Redente 1998; Waugh et al. 2007).

Although numerous landfill covers are in service around the world, there is little information about the design and long-term testing of surface barriers. At the Hanford Site, surface barriers are needed for in-place disposal and for disposal sites, mixed-waste disposal trenches, and some other facilities (DOE-RL 2013). The Prototype Hanford Barrier (PHB) was designed for this purpose and was constructed in 1994 as a demonstration (Wing and Gee 1994). The PHB consists of a 40- by 80-m evapotranspiration (ET) barrier underlain by a capillary (C) break. This combination is referred to as an ETC barrier. The side boundaries of the ETC barrier are protected by a gentle gravel slope in the west and a steep riprap slope in the east. The barrier was designed to be maintenance-free; resist plant, animal, and human intrusion; minimize erosion-related problems; and isolate wastes for at least 1000 years (DOE-RL 1999). Barrier stability was tracked by monitoring the degree of vertical deformation of the silt-loam surface and subgrade, change of the steep riprap side slope, and wind and water erosion from 1994 through 2013. The following summarizes the monitoring results over that period. These results are useful for the evaluation and design of stable long-term barriers.

I.2 Barrier design and test

The description and design of the PHB can be found in other sources such as Wing and Gee (1994), Gee et al. (1997), and Ward and Gee (1997). Briefly, the PHB consists of an ETC barrier, a west 10:1 gentle pit-run gravel (aka clean-fill dike) side slope, and an east 2:1 steep basalt riprap side slope. It was constructed in 1994 over a 2.5 ha area overlying an existing waste site, resulting in a surface feature that is elevated relative to the previous ground surface. The dry bulk density of the admix of the ETC barrier after construction was 1380 ± 0.121 kg m^{-3} (Gee et al. 1995). The function of the side slopes was to keep the ETC barrier stable and protect it from damage by natural processes or human activities. During the monitoring period (1994 to 2013), there was no vegetation in the riprap side slope but there was sparse vegetation in the gravel side slope. The ETC barrier was about 5 m thick and below it was a 0.15-m-thick, 64×105 m^2 asphalt concrete (AC) barrier with a 5-mm thick polymer-modified FAA coating (DOE-RL 1994).

The barrier is intended to perform for at least 1000 years without maintenance, making stability crucial to its success. Issues that could affect barrier stability or longevity were addressed in the design.

- Material degradation. The synthetic materials used for conventional barrier are not expected to last for the life of the barrier. Natural construction materials (e.g., fine soil, sand, gravel, cobble, basalt, asphalt) were selected for barrier construction. Most of these materials are known to have existed for thousands of years.
- Wind and water erosion. To reduce soil erosion, the PHB uses both a pea-gravel admix and vegetation to reduce water and wind erosion. The gravel admix was blended with the soil during construction and vegetation was planted after construction. The surface layer (top 1 m of soil) was amended by adding about 15 wt% (dry weight) pea gravel. The gravel was added to act as an agent to reduce erosion during periods following construction, wildfires, droughts, or other periods of susceptibility to eolian stresses. The decision to use 15 wt% pea gravel was based in part on the results of wind tunnel tests (Ligotke 1993; Ligotke and Klopfer 1990), and was also a compromise with the needs of water storage in the surface layer.
- Intrusion. The side slopes guard the barrier against plant, animal, and human intrusion from the sides and the 1.5-m-thick basalt riprap layer below the storage layer guards the barrier against the intrusion from the barrier surface.
- Settlement. A compacted soil foundation was constructed to prevent settlement of the barrier foundation, which could lead to cracking of or other types of damage to the barrier. The 0.15-m-thick asphalt concrete layer at the bottom of the barrier was built with a 2% slope away from the crown (north-to-south centerline) so that any drainage water through the barrier or side slope will flow away freely and no standing water will form at the covered area. In this way, both the barrier and the side slopes can maintain their shear strength and structural stability.
- Slope stability. The angularity of the riprap provides many interlocking surfaces between adjacent rocks, allowing a relatively steep yet stable side slope.

For testing purposes, the surface barrier was divided into north and south sections separated by a 10-m-wide buffer zone. To be consistent with the precipitation pattern, a water year (WY) is defined as the 12-month period from November of the previous year to October of the current year. From WY95 to WY97, the north section received natural precipitation plus enough irrigation to simulate an extreme climate condition (about 3 times the long-term average precipitation), while the south section received only natural precipitation. In March of each year, about 70 mm of water was applied over an 8-hour period to simulate a 1000-year return 24-hour rainstorm. In May 1998, 209.6 mm of water was added to the entire north section for an instrument test. From WY99 to WY13, both the north and south sections were exposed to natural precipitation conditions. In September 2008, the vegetation in the north section was burned to test the impact of a natural fire on the barrier performance.

I.3 Monitoring of Structural Stability

To verify performance, PHB stability was evaluated by measuring the water and wind erosion from the barrier surface, settlement of the barrier below the AC, elevation change of the barrier surface, and displacement in the riprap side slope. Figure I.1 is the plan view schematic showing the monitoring stations for wind erosion, settlement and elevation markers, the creep gauges (CGs), and the water erosion flume. The methodology of the measurements is presented below.

I.3.1 Wind and Water Erosion

PHB stability was evaluated by measuring the water and wind erosion from the barrier surface, settlement of the subgrade below the AC, elevation change of the barrier surface, and displacement in the riprap side slope.

Two wind monitors were installed on top of the barrier and a third was installed on the gravel side slope (Figure I.1). Wind speed sensors were installed at elevations of 0.25, 0.50, 1.0, and 2.0 m above the surface. Monitoring was carried out from 1994 through 1997. To quantify the shear stress exerted on the barrier surface, the time-averaged (monthly) wind velocity distribution was described by the semi-empirical relationship of a log wind profile (Oke 1987):

$$u_z = \frac{u_*}{k} \ln\left(\frac{z}{z_0}\right) \quad (1)$$

where u_z is wind velocity (m s^{-1}) at height z, u_* is friction or shear velocity (m s^{-1}), $k \approx 0.41$ is the von Karman's constant, and z_0 is the surface roughness (m). The surface roughness accounts for the effect of objects on a surface on wind. Typically, the roughness length is between 1/10 and 1/30 of the height of the objects (e.g., vegetation) on the ground.

Three sand saltation stations were installed at the southeast quadrant of the barrier surface (Figure I.1). The measurement was terminated because of a lack of saltation source as a result of the rapid growth rate of vegetation and the high soil moisture content at the barrier surface. Water erosion were monitored by measuring runoff and sediment yield from a 6 × 15 m flume installed on the soil surface (Figure I.1). The flume was constructed of timber with an opening at the downslope end. A collector system was designed to receive the water-sediment runoff and to convey the runoff to the monitoring system.

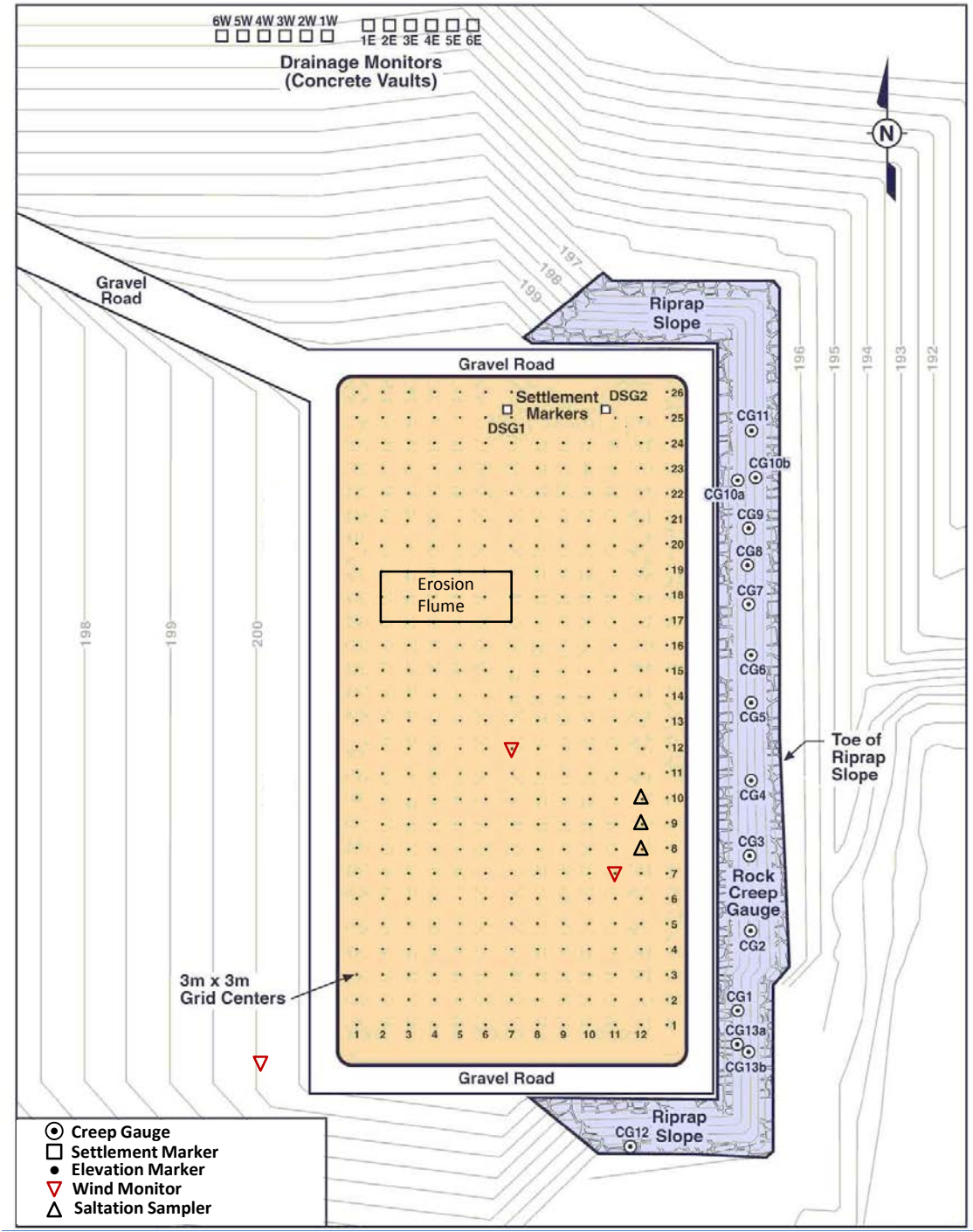

Figure I.1. Plan view schematic showing the 338 settlement markers, 2 elevation markers, 3 wind monitors, 3 saltation samplers, 15 creep gauges, and the erosion flume.

I.3.2 Elevation and Location Survey

Subsidence or setting of the AC barrier was quantified by measuring the change in the elevation of settlement markers, DSG1 and DSG2 (Figure I.1), attached to the AC barrier. These two settlement markers, 14 m apart, were installed at the north end of the barrier during construction of the barrier. Each marker consisted of a 4.2-m-long galvanized steel rod (0.025-m diameter) welded to a 0.6-m square plate, which was set on the surface of the asphalt concrete. The markers were protected by cast iron monument cases whose tops were set 0.025±0.01 m above the ground surface (Myers and Duranceau 1994). The lower 1.95-m portion of each rod that extended downward from the gravel filter to the plate was encased in a 0.1-m-diameter galvanized steel pipe to prevent binding between the rod and the riprap material. Changes in rod elevations were measured using the EDM or RTK system.

Elevation changes of a barrier surface indicate the inflation or deflation of the barrier as well as subsidence. Elevation surveys were taken at 338 (13 × 26) locations marked by wood stakes, 3 m apart (Figure I.1).

Because of the steepness of the riprap side slope (2:1), this slope was considered to have the potential for movement. A total of 15 CGs were installed at 13 locations (Figure I.1) in the riprap slope during or after barrier construction to monitor slope displacement. Each CG consisted of a 3-m-long steel rebar encased in a mortar-filled, 0.3-m-long × 0.076-m-diameter PVC tube. The 0.013-m-diameter head of a large nail embedded in the mortar was used as the benchmark for monitoring CG movement. A CG was installed at the mid-slope on the riprap slope at 11 of the 13 locations. Two CGs were installed at the upper (CG10a and CG13a) and lower (CG10b and CG13b) at positions 10 and 13, respectively.

From the start of monitoring in 1994 through 2003, measurements of elevation and horizontal locations were made by an electronic distance measurement (EDM) system. From 2004 to 2013, a real-time-kinematic global positioning system (Trimble Navigation Ltd., Sunnyvale, CA) was used because of a malfunction in the EDM system. The data for 1998 are questionable because they deviate considerably from other years, and hence these data were not included in the analysis. In total, 18 surveys were conducted for the elevation stakes, 19 for settlement markers, and 19 for the CGs. The survey in May 2004 was conducted for the first time at the PHB using the RTK system. The apparent departure from the relatively small changes in the previous years was considered invalid (Ward et al. 2005). A partial EDM elevation survey was also conducted in 2004 and was used to correct the RTK survey in 2004.

I.4 Results

The observed results of erosion, elevation changes of the AC barrier and barrier surface, and displacement of the riprap side slope, are presented and discussed below.

I.4.1 Wind and Water Erosion

Wind Erosion

Wind stress was monitored from September 1994 to September 1997. The average wind speed was 3.1 m s^{-1} at the 2-m height above the silt loam surface and 2.6 m s^{-1} at the gravel side slope (Table I.1). The peak gust during the monitoring period was 21.4 m s^{-1}, and occurred on December 12, 1995. Figure I.2 shows the monthly average wind speed at four heights for the three monitoring stations. The wind generally was stronger in late spring and summer than in the fall and winter. During the 3-year monitoring period, the wind speeds at the 2-m and 1-m heights showed slightly increasing trends with time, while those at the 0.25-m and 0.5-m heights had decreasing trends. The decreasing trend was attributed to vegetation growth on the surface.

Table I.1. Time-averaged or extreme values (from 09/1994 to 09/1997) of the measurements at three wind stress monitoring stations.

Variable Names	Station 1 (South of PHB)	Station 2 (SE of PHB)	Average of Stations 1 and 2	Station 3 (SW to PHB, off barrier surface)
Air Temperature (C°)	13.3	13.1	13.2	13.3
Wind Direction (degree)	225	213	219.2	224
Wind Speed at 0.25 m (m s^{-1})	1.5	1.2	1.3	0.8
Wind Speed at 0.5 m (m s^{-1})	1.8	1.6	1.7	1.4
Wind Speed at 1 m (m s^{-1})	2.6	2.4	2.5	2.1
Wind Speed at 2 m (m s^{-1})	3.2	3.0	3.1	2.6
Max. Wind Speed at 2 m (m s^{-1})	22.0	20.8	21.4	17.6
Date of the Max. Wind Speed	12/12/1995	12/12/1995	12/12/1995	12/12/1995
Direction of Max. Wind (Degree)	210	204	207.4	209

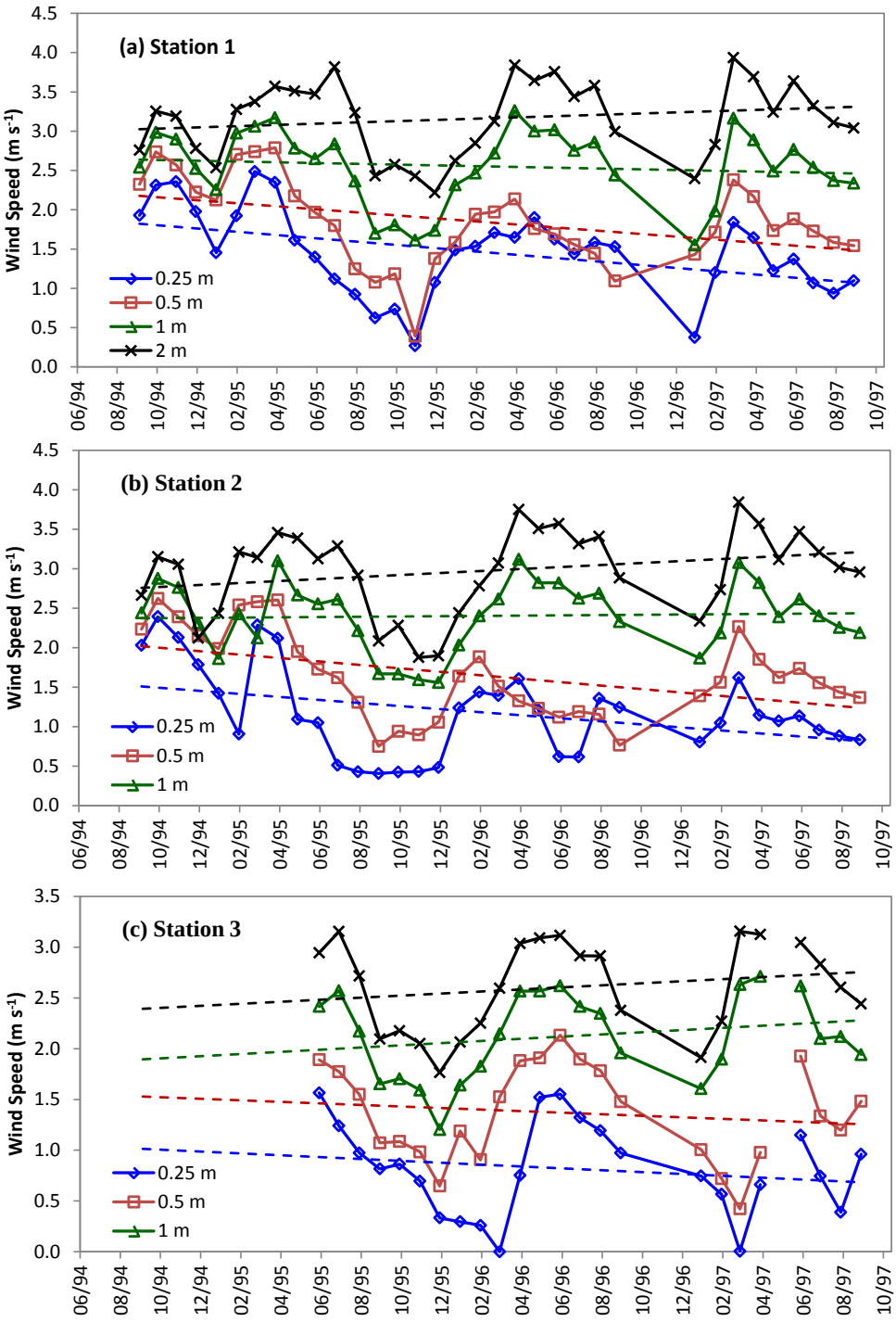

Figure I.2. Monthly average wind speed at three monitoring stations and four heights.

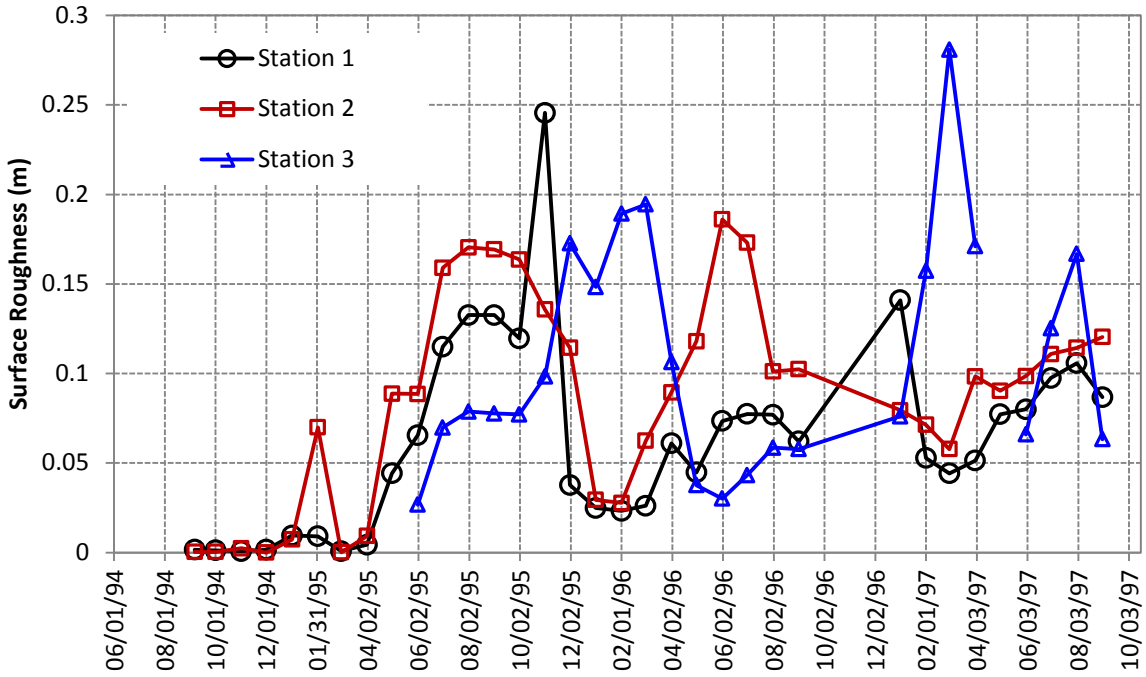

Figure I.3. Barrier surface roughness based on monthly average wind profiles.

As air moves over most surfaces, vegetation is an obstruction to the flow of air above the ground surface. The effectiveness of vegetation in protecting ground surface against wind erosion is quantified by surface roughness, which is the height at which wind velocity reduces zero. Higher surface roughness means better protection again wind erosion. Surface roughness generally increases with the height and/or coverage of vegetation. Based on the monthly average wind speed profile and Eq. (1), the barrier surface roughness for each month was estimated and is shown as points in Figure I.3. From the revegetation on the barrier in November 1994 to about April 1995, the surface roughness was near zero (Figure I.3). After May 1995 when the vegetation grew up, the surface roughness varied seasonally, with higher values generally in the summer season. This is most likely due to more leaves and/or flowers of sagebrush and higher coverage of annuals and limited bi-annuals. Hence the vegetation had a greater ability to reduce wind in the summer. This implies that, for a given year, the barrier was more resistant to wind erosion in the summer season than in the winter season. Across different years, the low values of z_0 at stations 1 and 2 on the barrier surface (roughly in early spring) increased from near zero in 1995 to about 0.05 m in 1997. This increase suggests that the barrier was likely well protected from wind erosion year round in 1997.

Comparing Figure I.2 and Figure I.3 shows that the stronger wind in late spring and summer coincided with higher surface roughness. As a result, the strong wind in the spring/summer probably was overcome by higher roughness of the barrier surface. The results indicate that the vegetation increased the height of zero wind velocity above the barrier surface and suggest reduced possibility of wind erosion.

Water Erosion

Water erosion only happens when there is runoff and soil erodibility is low. In general, runoff occurs when rainfall intensity is higher than the hydraulic conductivity of the soil. This may occur during a high-intensity rainstorm or when the soil hydraulic conductivity is considerably reduced by freezing conditions. Soil erodibility is dependent on soil physical properties, vegetation cover, or other cover (e.g.,

gravel). In March 1995, after the simulated 1000-year 24-hour rainstorm (69.4 mm of water over an 8-hour period) to the newly vegetated surface, 1.79 mm of runoff was measured (Gee et al. 1995). Initial sediment concentrations collected during the test were approximately 7 g L^{-1}. This amount fell to approximately 1 g L^{-1} at the end of the water application. The results showed a decreasing pattern of erosion, indicating less soil was eroded possibly because more pea gravel was exposed. The estimated soil erosion was 72 kg ha^{-1} in total. No soil erosion was observed during the rest of the monitoring period, including during the 1000-year storms in 1996 and 1997, the snowmelt event in the January 1997, and after the burn in 2008.

The primary reasons for the lack of runoff and erosion were the sufficiently high soil hydraulic conductivity and the increased coverage of vegetation on the ground surface. The 15% by weight pea gravel in the top 1 m of the barrier protects the barrier surface from erosion because of its weight and hence against the formation of runoff channels such as rills or gullies (Gilmore and Walters 1993).The anti-erosion capability of gravel appears to the primary reason for the sustainability of natural bergmounds formed from the ice-rafted debris about 13,000 years ago (Bjornstad 2014; Chamness 1993; Fecht and Tallman 1978).

The above results indicate that the vegetation and the pea gravel added to the soil protected the surface of the ETC barrier from wind or water erosion. It is expected that, in the future, if combined natural hazards occur (e.g., a heavy storm after a wild fire), the pea gravel can still protect the barrier surface against erosion.

I.4.2 Barrier Settlement and Compression

From 1994 to 2012, the average elevations with $\pm 1\sigma$ of the two settlement markers were 201.956±0.007 m and 201.685±0.012 m, respectively, without clear trends over time (Figure I.4a). For both markers, the elevation variations were between -0.03 and 0.02 m (Figure I.4b), indicating near-zero settlement. Because the small variations were probably measurement noise, the results suggest a very stable AC barrier, subgrade, and waste zone.

The contour maps of the barrier surface for the 18 surveys from 1994 to 2012 are shown in Figure I.5. The results reflect the 2% slope from the crown. During the 18-year monitoring period, the shape of the barrier surface stayed nearly the same.

The time course of the spatially averaged elevation change is shown in Figure I.6. From 1994 to 2012, the average elevation change with 1σ was 0.003±0.018 m, which was negligibly small. There was no noticeable difference between the north and the south sections. The north section was irrigated to three times the long-term average precipitation from WY95 to WY97 and the vegetation on it was burned by a controlled fire in 2008, while the south section was exposed under the natural conditions all the time.

The above results indicate that both the base and barrier had an appropriate density, so neither settlement nor compression happened during the reported monitoring period of 18 years.

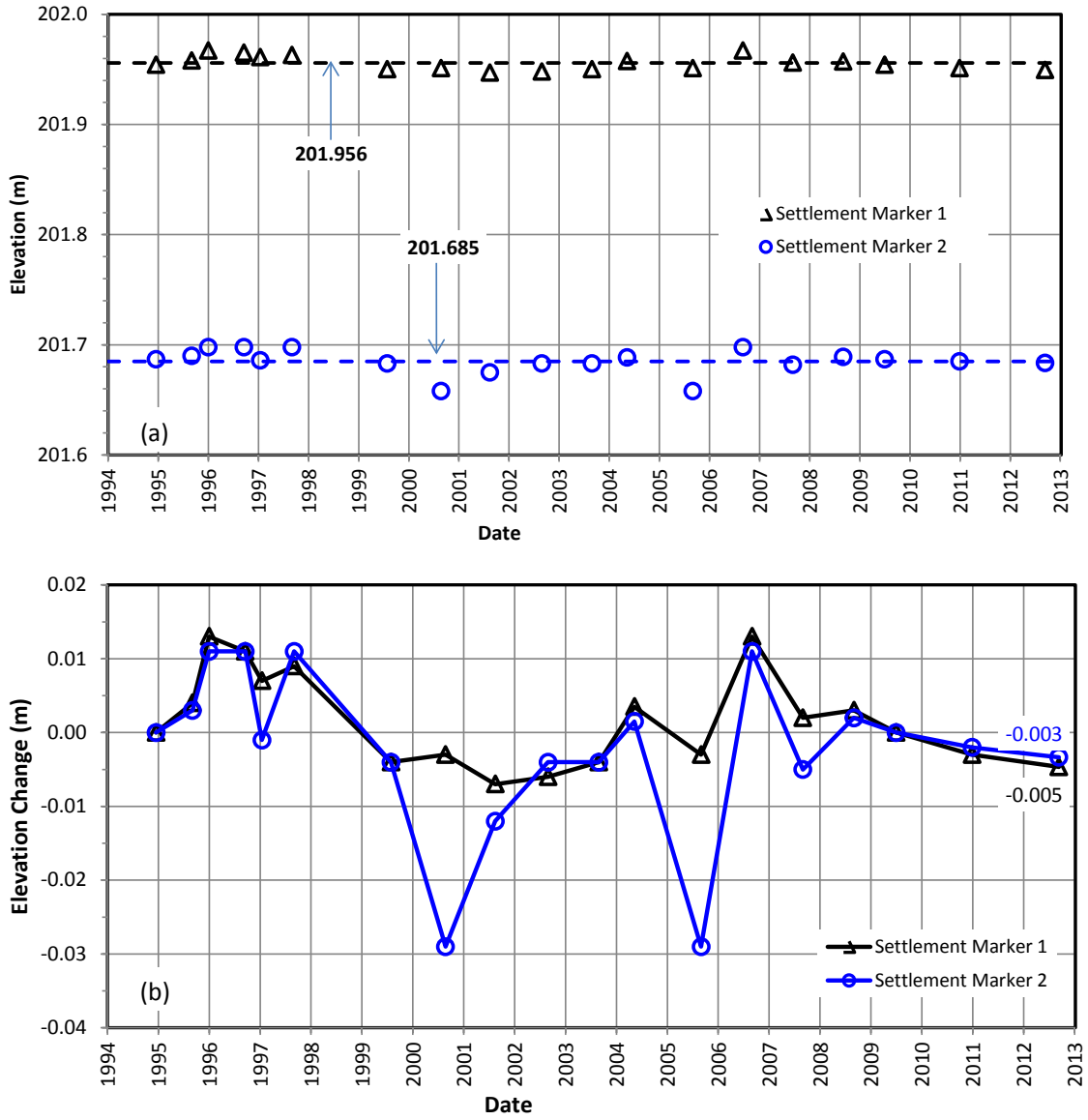

Figure I.4. Variation of (a) the elevation of settlement markers and (b) elevation change relative to the initial values. The dashed lines indicate the average values.

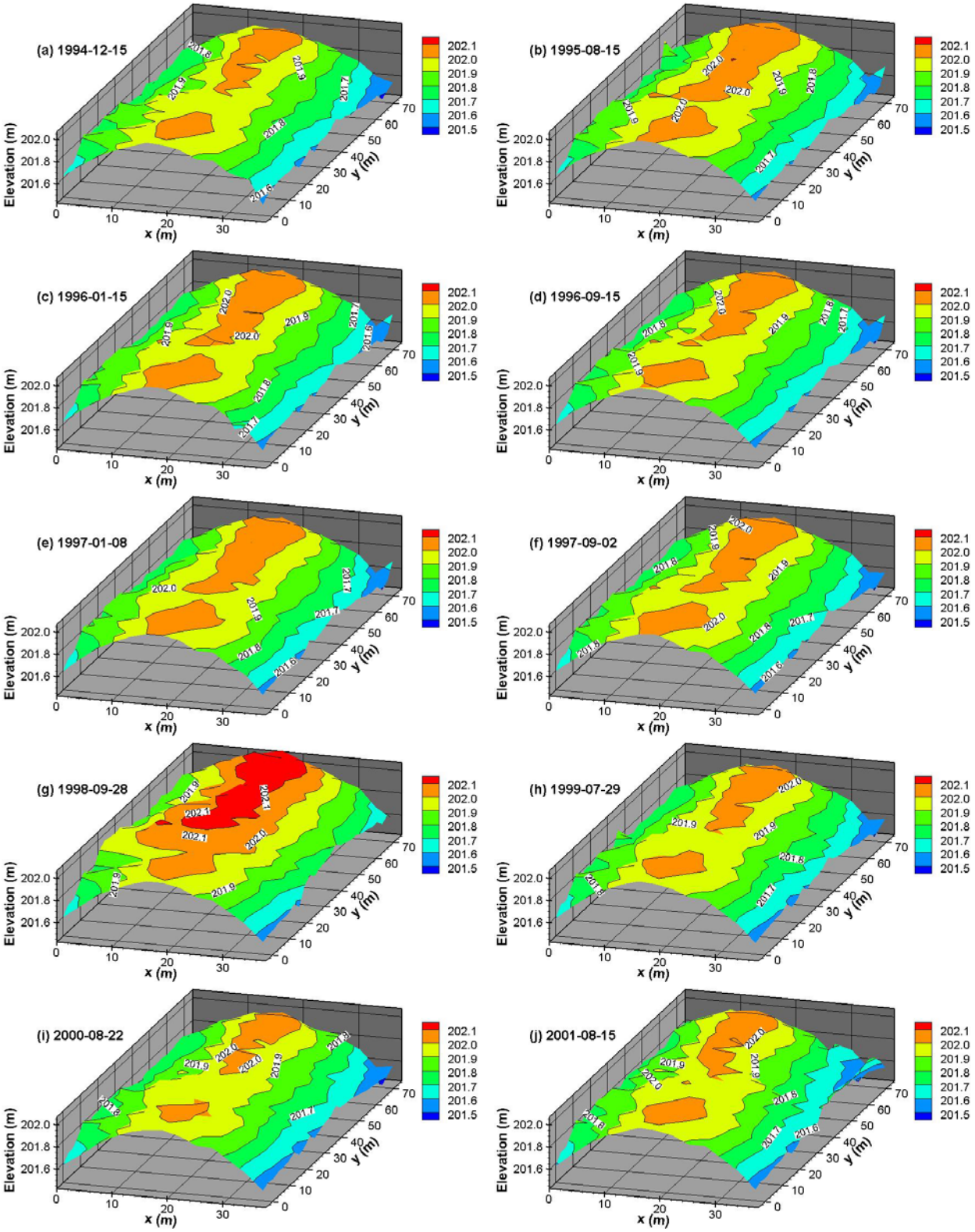

Figure I.5. Contour of the surface elevation of the Prototype Hanford Barrier.

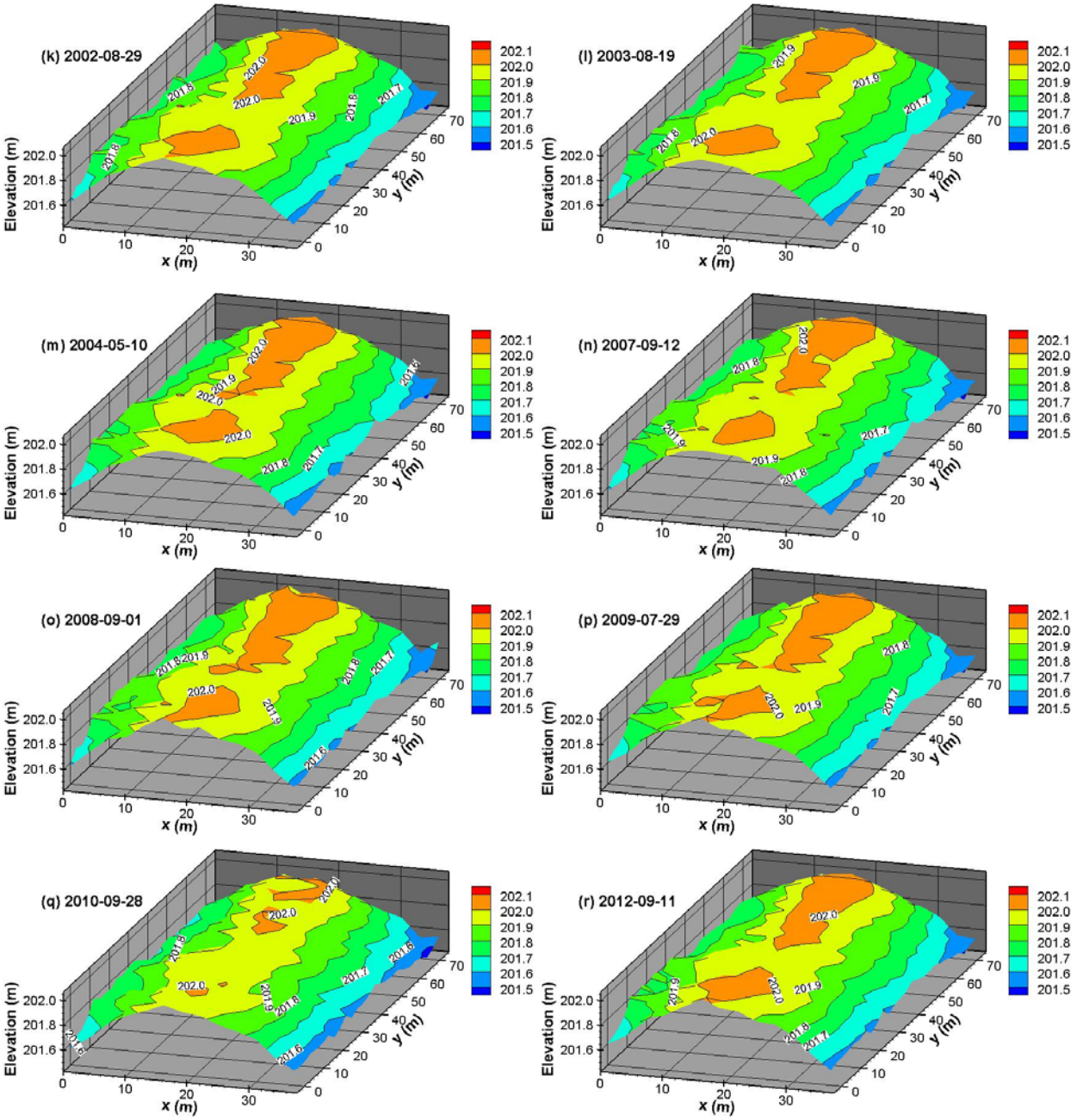

Figure I.5. Contour of the surface elevation of the Prototype Hanford Barrier. (Cont.)

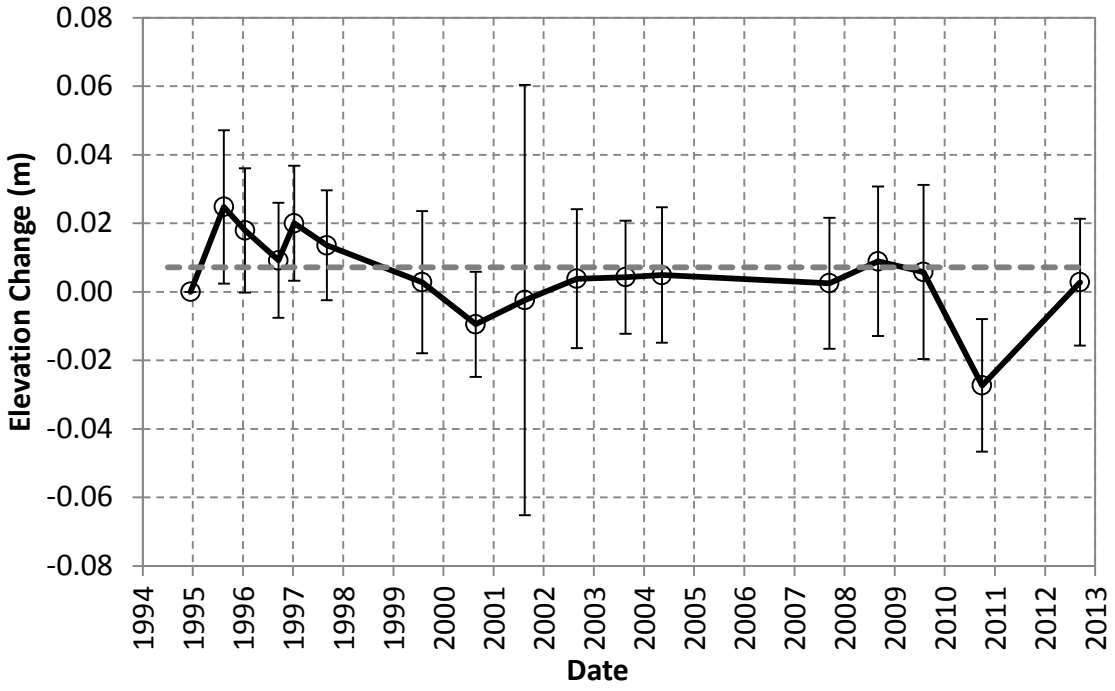

Figure I.6. Average surface elevation change of 338 observations. The vertical lines indicate one standard deviation.

Table I.2. Statistics of creep gauge positions in 2012 relative to their initial positions.

	dx	dy	dz
Mean (m)	0.023	0.020	-0.007
Standard Deviation (m)	0.032	0.012	0.006
Max (m)	0.083	0.033	0.003
Min (m)	-0.032	-0.008	-0.018

I.4.3 Riprap Side Slope Displacement

The riprap side slope displacement was determined by the changes in position, i.e., easting (dx) northing (dy), and vertical coordinates (dz), with time of 15 CGs, as shown in Figure I.7. The positive change in dx means the lateral movement of the riprap side slope outward. Any inward movement of the riprap side slope was very unlikely and thus the small negative changes in dx were possibly caused by measurement error.

Figure I.7a shows that the changes in dx ranged between -0.032 m and 0.115 m, with an average of 0.012 m, indicating a negligible outward movement of the riprap side slope. The changes in dy were between -0.251 to 0.062 m, with a near-zero average of 0.006 m (Figure I.7b). The dz values were the changes in the vertical direction and were between -0.096 and 0.029 m, with an average of -0.005 m (Figure I.7c).

The positions of the CGs in the final survey in 2012 (2011 for CG12 and 2010 for CG10a) relative to their corresponding initial positions in 1994 are shown in Figure I.8. The mean, standard deviation, maximum, and minimum of the last survey are summarized in Table I.2. Of the 15 CGs, 12 had positive changes up to 0.083 m to the downslope east, 13 had positive changes up to 0.033 m to the north, and 13

had negative changes down to -0.018 m (shown as the empty circles) in the vertical direction. On average over the 15 CGs, the changes with 1σ are dx = 0.023±0.032 m, dy = 0.020±0.012 m, and dz = -0.007±0.006 m. The average changes are comparable to the standard deviation, indicating that the riprap side slope was very stable during the monitoring period.

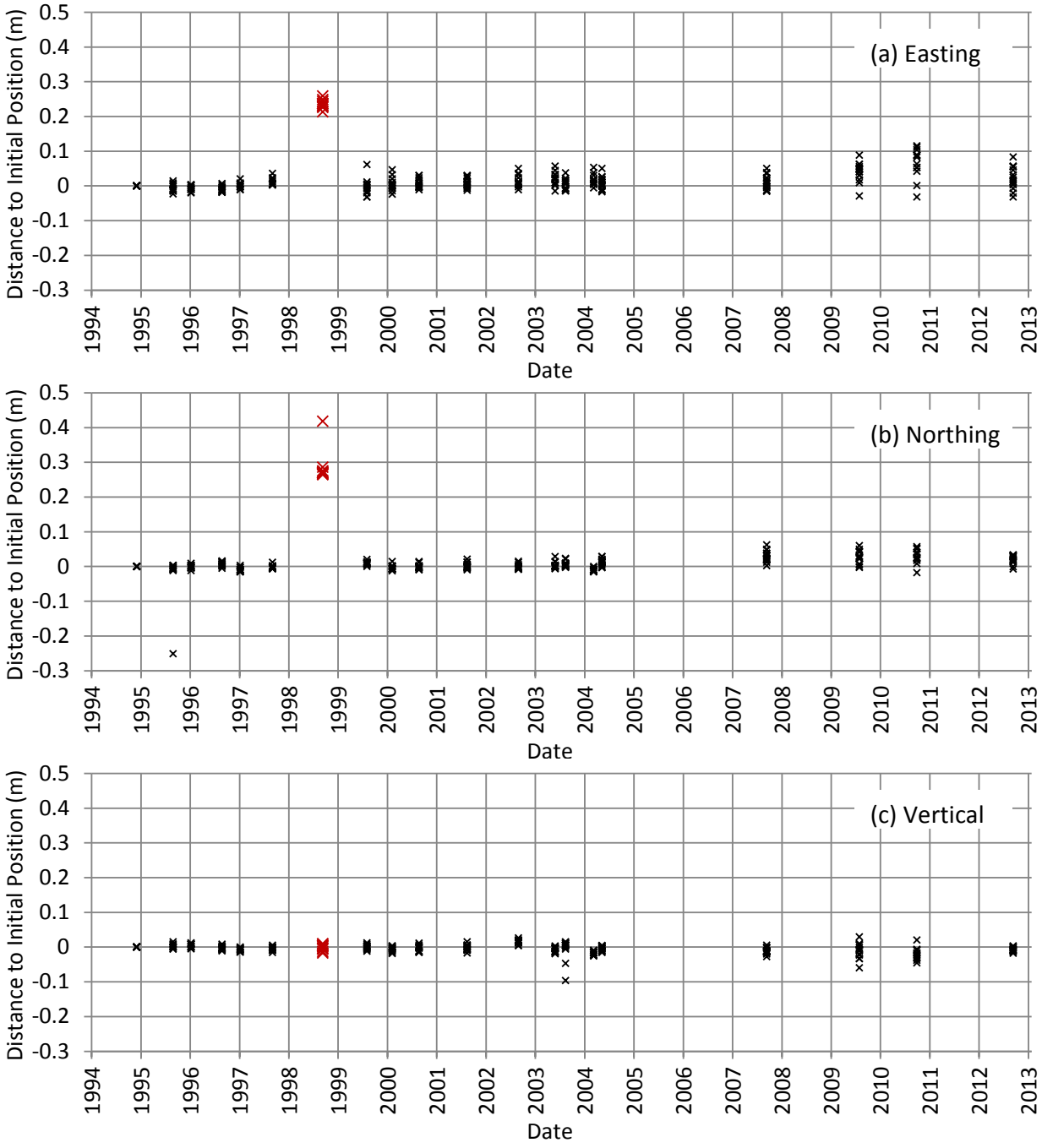

Figure I.7. Time course of the positions, represented by the easting, northing, and vertical coordinates, of 15 creep gauges relative to their initial values.

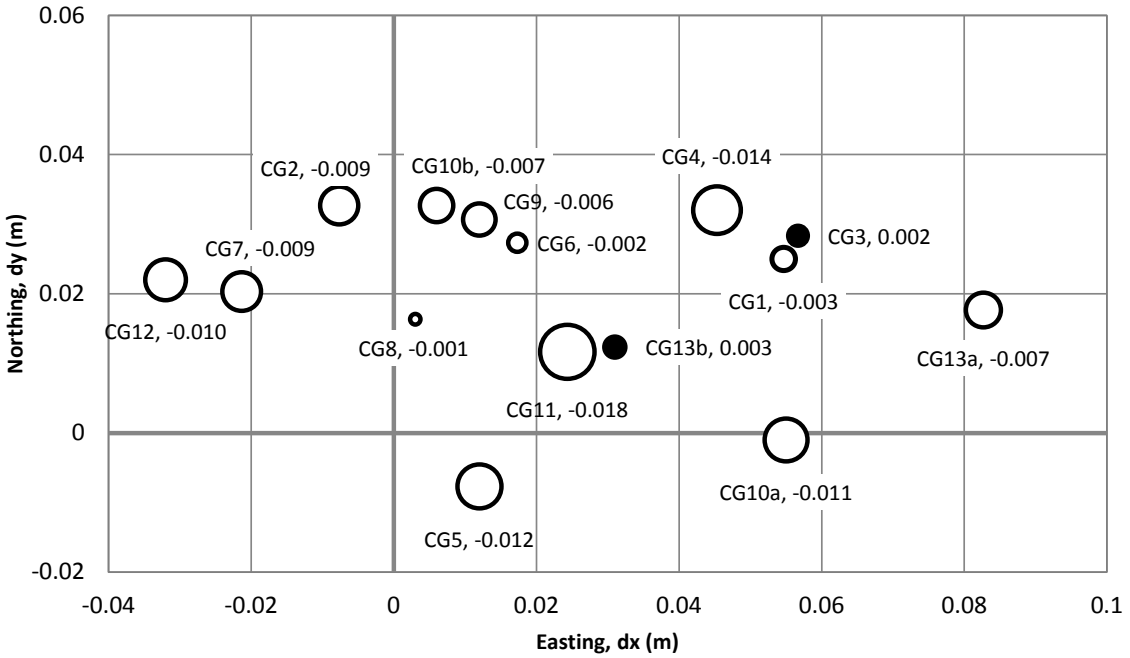

Figure I.8. Positions of the creep gauges in 2012 (2011 for CG12 and 2010 for CG10a) relative to their corresponding initial positions. A filled bubble indicates an increase in CG elevation while an empty bubble indicates a decrease. The area of the bubble indicates the change in elevation as shown by the number nearby. Positive dx value indicates lateral movement of the side slope outward.

I.4.4 Barrier Maintenance

After the completion of the PHB construction and revegetation in 1994, there was very little maintenance at the PHB, other than instrumentation, except the filling of an animal hole that was about 0.6 m deep with a 0.3 m diameter. In May 2004, after severe thunderstorms, runoff water from the elevated BY-BX Tank Farm surface (southeast to the PHB) flowed down-gradient to the region between the Tank Farm and the PHB, eroding a channel about 1.1 m deep at the base of the east side of barrier side slope (Figure I.9). The channel extended into the sandy structural fill layer below the riprap side slope. A repair was made in fiscal year 2005.

The occurrence of the flood indicates that the topology around the barrier, the resultant run-on/runoff, as well as the surrounding surface hydrology can play an important role to the integrity of the barrier and hence protecting the toe of the riprap side slope needs to be considered in the design. The current side slopes have constant gradients (10:1 in the west and 2:1 in the east), while natural analog indicate that a more stable slope usually has a convex shape in the upper portion and a concave shape near the toe (Schor and Gray 2007). The low elevation areas around the barrier will have high probability to be future runoff channels and hence proper protection (e.g., with gravels and vegetation) is needed for soil erosion.

Figure I.9. North-facing photograph taken on June 16, 2004. The orange lines indicate the path and direction of the runoff water in May 2004 after severe thunderstorms.

I.5 Summary

Wind and water erosion, settlement of the barrier subgrade below the asphalt layer, barrier compression, and displacement in the riprap side slope were monitored for the PHB. Wind erosion was monitored from 1995 to 1997. During these 3 years, wind speeds at the 0.25-m and 0.5-m heights had decreasing trends, while the wind friction velocity had increasing treads with time because of the growth of vegetation on the barrier. The stronger wind in late spring and summer coincided approximately with higher surface roughness when the vegetation had leaves. As a result, the seasonal variation of wind appeared to have little erosive impact on the barrier surface. A small amount of soil erosion was observed during the first simulated 1000-year return 24-hour rainstorm. No soil erosion was observed during the rest of the monitoring period, including during the 1000-year rainstorms in 1996 and 1997 and after the burn in 2008.

The elevation of the asphalt layer varied between -0.03 and 0.02 m, indicating near-zero settlement and a very stable asphalt surface and subgrade. From 1994 to 2012, the spatially averaged elevation of barrier surface decreased by only 0.002 m, meaning negligible soil loss or gain because of soil or wind erosion or barrier compression. During the 18-year monitoring period, the CGs moved an average of 0.024 m outward to the east, 0.021 m to the north, and 0.006 m lower in elevation. These small changes demonstrate that the riprap side slope was very stable during the monitoring period.

Overall, the results for the 18-year monitoring period show that the PHB is robust with high structural stability. Although the period of monitoring is short relative to the design life of 1000 years, all indications are that the PHB will perform as expected if future conditions are similar to those that occurred during monitoring period. These conditions included irrigation to simulate precipitation rates of up to 3X greater than the long-term average, 1000-year rainstorm events, and wildfires. However, protection of the side slopes needs to be considered in the design of surface barriers.

References

Benson, CH, DE Daniel, and GP Boutwell. 1999. "Field Performance of Compacted Clay Liners," *Journal of Geotechnical and Geoenvironmental Engineering*, 125:390-403.

Bjornstad, BN. 2014. "Ice-Rafted Erratics and Bergmounds from Pleistocene Outburst Floods, Rattlesnake Mountain, Washington, USA," *Quaternary Science Journal*, 63(1):44-59. doi:10.3285/eg.63.1.03.

Blight, G. 2008. "Slope Failures in Municipal Solid Waste Dumps and Landfills: A Review," *Waste Management & Research*, 26:448-463.

Bowerman, G and EF Redente. 1998. "Biointrusion of Protective Barriers as Hazardous Waste Sites," *Journal of Environmental Quality*, 27:625-632.

Chamness, MA. 1993. *An Investigation of Bergmounds as Analogs to Erosion Control Factors on Protective Barriers*, PNL-8841, Pacific Northwest Laboratory, Richland, Washington. Available at http://www.iaea.org/inis/collection/NCLCollectionStore/_Public/25/059/25059205.pdf.

DOE-RL. 1994. *Constructability Report for the 200-BP-1 Prototype Surface Barrier*, DOE/RL- 94-76, U.S. Department of Energy Richland Operations Office, Richland, Washington.

DOE-RL. 1999. *200-BP-1 Prototype Barrier Treatability Test Report*, DOE/RL-99-11 Rev. 0, U.S. Department of Energy Richland Operations Office, Richland, Washington.

DOE-RL. 2013. *Hanford Site Cleanup Completion Framework*, DOE/RL-2009-10, Rev. 1, U.S. Department of Energy Richland Operations Office, Richland, Washington. Available at http://www.hanford.gov/files.cfm/Comp_Framework_Jan_%201-23-13-lfm.pdf.

EPA. 1991. *Design and Construction of RCRA/CERCLA Final Covers* EPA/625/4-91/025, Office of Research and Development, US EPA, Washington, DC.

Fecht, KR and AM Tallman. 1978. *Bergmounds Along the Western Margin of the Channeled Scablands, South-Central Washington* RHO-BWI-SA-11, Rockwell International, Richland, Washington. Available at http://www.osti.gov/scitech/servlets/purl/6431635.

Gee, GW, AL Ward, and MJ Fayer. 1997. "Surface Barrier Research at the Hanford Site," *Land Contamination & Reclamation*, 5(3):233-238.

Gee, GW, AL Ward, BG Gilmore, MW Ligotke, and SO Link. 1995. *Hanford Prototype-Barrier Status Report: FY 1995*, PNL-10872, Pacific Northwest National Laboratory, Richland, Washington. Available at http://www.osti.gov/energycitations/servlets/purl/177965-nd9isN/webviewable/.

Gilmore, BG and WH Walters. 1993. *Water Erosion Field Tests for Hanford Protective Barriers: FY 1992 Status Report*, PNL-8949 UC-603, Pacific Northwest Laboratory, Richland, Washington.

Jessberger, HL and K Stone. 1991. "Subsidence Effects on Clay Barrier," *Geotech*, 41:185-194.

Koerner, R and T Soong. 2000. "Stability Assessment of Ten Large Landfill Failures," *Advances in transportation and geoenvironmental systems using geosynthetics (GeoDenver 2000)*, 1-38 pp. Geotechnical Special Publication (GPS 103),

Lagatta, MD. 1992. "Hydraulic Conductivity Tests on Geosynthetic Clay Liners Subjected to Differential Settlement," MS Thesis, University of Texas, Austin, Texas.

Levitt, DG, MJ Hartmann, KC Kisiel, CW Criswell, PD Farley, and C Christensen. 2005. "Comparison of the Water Balance of an Asphalt Cover and an Evapotranspiration Cover at Technical Area 49 at the Los Alamos National Laboratory," *Vadose Zone Journal*, 4(3):789-797. doi:10.2136/vzj2004.0171.

Ligotke, MW. 1993. *Soil Erosion Rates Caused by Wind and Saltating Sand Stresses in a Wind Tunnel*, PNL-8478, Pacific Northwest Laboratory, Richland, Washington. Available at http://www.osti.gov/energycitations/servlets/purl/6377761/.

Ligotke, MW and DC Klopfer. 1990. *Soil Erosion Rates from Mixed Soil and Gravel Surfaces in a Wind Tunnel*, PNL-7435, Pacific Northwest Laboratory, Richland, Washington.

Merry, SM, E Kavazanjian, and WU Fritz. 2005. "Reconnaisance of the July 10 2000 Payatas Landfill Failure," *ASCE Journal of Performance of Constructed Facilities*, 19:100-107.

Myers, DR and DA Duranceau. 1994. *Prototype Hanford Surface Barrier: Design Basis Document*, BHI-00007 Rev.0, Bechtel Hanford, Inc., Richland, Washington.

Oke, TR. 1987. *Boundary Layer Climates*. Second ed., Methuen, London.

Reddy, K and B Munwarbasha. 2014. Slope Stability of Waste Dumps and Landfills: State-of-the-Art and Future Challenges. In *Proceedings of Indian Geotechnical Conference IGC-2014*, Andhra Pradesh, India.

Schor, HJ and DH Gray. 2007. *Landforming: An Environmental Approach to Hillside Development, Mine Reclamation and Watershed Restoration*. John Wiley & Sons, Inc., Hoboken, New Jersey.

Ward, AL and GW Gee. 1997. "Performance Evaluation of a Field-Scale Surface Barrier," *Journal of Environmental Quality*, 26(3):694-705.

Ward, AL, JK Linville, JM Keller, and GH Seedahmed. 2005. *200-BP-1 Prototype Hanford Barrier Annual Monitoring Report for Fiscal Year 2004*, PNNL-14960, Pacific Northwest National Laboratory, Richland, Washington. Available at http://www.osti.gov/energycitations/servlets/purl/15020831-RBQnP9/.

Waugh, WJ, G Smith, B Danforth, GW Gee, V Kothari, and T Pauling. 2007. "Performance Evaluation of the Engineered Cover at the Lakeview, Oregon, Uranium Mill Tailings Site," *Proceedings of Waste Management 2007*, Tucson, AZ.

Wing, NR and GW Gee. 1994. "Quest for the Perfect Cap," *Civil Engineering*, 64(10):38-41.

Appendix J

Plant Community Dynamics after Revegetation, Irrigation, and Fire at the Prototype Hanford Barrier

Steven O. Link

Content

List of Figures

List of Tables

Abstract

Vegetation was planted on the Prototype Hanford Barrier in November 1994. Observations were taken on vegetation almost every year from 1995 to 2011, including species composition and cover. Species composition was also determined on the north and west side-slopes of the barrier. Soil seed banks were characterized before and after a fire on the surface. In addition, data collected on unburned and recently burned sites were compared. This allowed the composition of species, cover, and seed banks on the native soils of two McGee Ranch analog sites to be compared with that of the barrier before and after the fire. Forty-nine species were observed between 1995 and 2011, with the highest number of species occurring two years after construction (35 species) and 2 years after the fire (34 species). The minimum number of species was 11 in 2008 before the fire. *Artemisia tridentata* (big sagebrush) was the dominant plant until after the fire, when *Machaeranthera canescens* (hoary tansyaster) became dominant on the burned section. The two plant communities on the barrier surface were more similar to each other than to burned and unburned plant communities at the McGee Ranch analog site. *Artemisia tridentata* density on the unburned section of the surface was 0.77 plants per m^{-2}, which was significantly higher than at the McGee Ranch unburned site (0.437 plants per m^{-2}). *Artemisia tridentata* did naturally reestablish from the seed bank on the burned section after the fire. *Bromus tectorum* (cheatgrass) increased on the burned section.

J.1 Introduction

Engineered surface barriers are an integral component of the U.S. Department of Energy (DOE) waste management strategy, serving as an alternative to the removal, treatment, and disposal of near-surface contaminants at a variety of waste sites (DOE-RL 1993). Several locations at the Hanford Site may have significant amounts of contaminants deep in the vadose zone that may be remediated using surface barriers (DOE-RL 2013). Evapotranspiration covers and multilayered designs with a vegetated evapotranspirative surface layer have been effective in arid and semiarid climates in most cases, but have failed in others because of inadequate storage capacity and vegetation (Albright et al. 2004; Anderson 1993; Hauser et al. 2001).

Concerns associated with vegetation include possible gradual and catastrophic changes sufficient to compromise cover function (Anderson and Forman 2002). Gradual changes such as those associated with plant community dynamics and succession may increase the risk of failure on covers. There is uncertainty about the relationship between initial vegetation and persistent climax species (Albright et al. 2004). Fire can cause catastrophic changes in plant community composition and structure, particularly increases in *Bromus tectorum* cover (Whisenant 1990). Increases in *B. tectorum* cover are generally concurrent with decreased perennial plant cover, reducing evapotranspirative potential at least in the short-term (Anderson and Forman 2002). Few if any studies examine plant community dynamics on engineered barriers over periods sufficient to address concerns about catastrophic and gradual risks for vegetation. Increasing stakeholder acceptance of barrier technology requires demonstration of barrier longevity and the assurance of adequate performance over the design life.

The purpose of this research is to investigate risks of failure associated with plant community dynamics on an engineered barrier receiving three times average precipitation for 3 years, in the long-term (17 years), and after a fire. In August 1994, the Prototype Hanford Barrier (PHB), a multilayered capillary barrier with an evapotranspiration surface layer, was constructed over the 216 B-57 radioactive liquid-waste disposal crib in Hanford's 200 East Area. The barrier was designed with a storage capacity of 600 mm to limit recharge to <0.5 mm/yr (1.6×10^{-9} cm/s), minimize erosion, and isolate wastes for at least 1000 years (Ward and Gee 1997; Wing and Gee 1994). In the semi-arid shrub-steppe, well-designed barriers are likely to be stabilized and eliminate recharge to underlying wastes for thousands of years if native perennial plants dominate the surface (Link et al. 1994a). If such a barrier were to become dominated by shallow-rooted annuals such as *Bromus tectorum*, drainage (Anderson and Ratzlaff 1996; Seyfried et al. 2005) and failure could occur. The prediction of drainage is based on the observation that a silt-loam soil at Hanford dominated by *B. tectorum* with high levels of litter retained water below the rooting zone after a wet year (Cline et al. 1977).

Vegetation on the PHB was monitored almost every year from 1994 to 2011. Ecological responses monitored included species composition and cover. Species composition was also determined on the north and west side slopes of the barrier. Soil seed banks were characterized before and after a fire on the surface. In addition, comparisons were made using data collected on unburned and recently burned analog sites (Waugh et al. 1994). This allowed the composition of species, cover, and seed banks on the native soils of two McGee Ranch analog sites to be compared with that of the PHB before and after the fire. This appendix summarizes the data collected over 17 years on vegetation dynamics as affected by increased precipitation and fire on the PHB.

J.2 Methodology

J.2.1 Study Sites

The study was conducted at the DOE Hanford Site in south central Washington state. The PHB is located (46°34'01.23"N, 119°32'28.43"W) on the 200 Area Plateau at an elevation of 194 m a.s.l. The old burn analog site at McGee Ranch is at about 46°35'05.64"N, 119°43'51.71"W and at an elevation of 245 m a.s.l. The unburned McGee Ranch analog site is at about 46°34'40.24"N, 119°44'33.02"W and at an elevation of 247 m a.s.l. Characteristics of McGee Ranch are described in Link et al. (1994b). The climate is semiarid with hot dry summers and cool wet winters (Stone et al. 1983). Average yearly precipitation at the nearby Hanford Meteorological Station is about 167 mm. Snowfall ranges from trace amounts to 137 cm, but averages 35 cm.

J.2.2 Barrier Characteristics and Treatments

The surface area of the entire PHB is 2 ha. The surface is elevated with one relatively steep (2:1 horizontal to vertical) protective side slope that is covered with basalt riprap. The other side slope is shallow (10:1) and consists of local pit run gravel backfill. The barrier is constructed of 2 m of fine soils over coarser material. The soil used in the upper layers of the PHB is a Warden silt loam (Gee 1987; Hajek 1966).

The north section of the PHB was irrigated during a treatability test from 1994 to 1998, while the south section was not irrigated. This test included irrigation at a rate of about 480 mm/yr, including a simulated 1000-yr return storm each March when about 70 mm of water was applied over an 8-hour period to gain insight into barrier performance under elevated precipitation conditions. No further manipulations occurred until September 2008, when the north section of the barrier was burned (Ward et al. 2008; Ward et al. 2009a; Ward et al. 2009b). The surface was gridded into three-hundred 9-m^2 quadrats with 144 quadrats in the south area and 156 quadrats in the north area for ecological surveys.

J.2.3 Revegetation

The PHB surface and surrounding disturbed areas were planted in the fall of 1994. Planting was done separately for the perennial shrubs and perennial grasses. Perennial shrubs were established by collecting seeds, growing seedlings, and planting them on the surface of the barrier. Seeds of *A. tridentata* and *E. nauseosa* (gray rabbitbrush) were collected from local populations growing on the silt loam soil used for the upper layer of the barrier. Seeds were collected on December 23, 1993. The entire inflorescence of *A. tridentata* and the fruits of *E. nauseosa* were harvested and stored in plastic bags in the field. The material was transported to a laboratory, removed from the plastic bags, and placed on tabletops to dry. Material was stored in the dark and at room temperature until shipped to a nursery. The seeds were cleaned by April 12 and sown on May 4, 1994. Seedlings were grown in 164-cm^3 tubes until they were approximately 20 cm tall. Planting was initiated on November 7, 1994, and completed the next day. A total of 2700 holes were drilled at a density of 1-hole m^{-2} on the PHB surface. Two seedlings were placed in each hole. A total of 1350 *E. nauseosa* and 4050 *A. tridentata* seedlings were planted. All shrubs of each species were counted in all quadrats in 1995 and 1997. These data were used to compute percent survival in 1997 as (#live in 1997) *100/(#planted in 1995).

Perennial grasses were established by hydroseeding the surface and surrounding slopes. The hydroseeding mix included seeds, fertilizer, mulch, and a tacking agent. The native perennial grass seed mixture included *Poa secunda* (Sandberg's bluegrass; 34 kg ha^{-1}), *Elymus lanceolatus* (5.6 kg ha^{-1}), *Achnatherum*

hymenoides (22 kg ha^{-1}), *Poa ampla* (Sherman big bluegrass; 11 kg ha^{-1}), *Hesperostipa comata* (5.6 kg ha^{-1}), *Elymus wawawaiensis* (14 kg ha^{-1}), and *Elymus elymoides* (3.4 kg ha^{-1}). Seeds of *E. elymoides* were collected in June 1994 from grasses in the silt loam soils within 20 km of the barrier. The other perennial grasses originated from sources in the semi-arid West. The fertilizer was applied as 67 kg ha^{-1} of total nitrogen, 67 kg ha^{-1} of available phosphoric acid (P_2O_5), and 67 kg ha^{-1} of soluble potash (K_2O) in solution. The mulch was applied as 2240 kg ha^{-1} of Eco-Fibre 100% virgin wood fiber. Degradable glue was added to the mulch as a tackifier at 67 kg ha^{-1}. Hydroseeding occurred on November 10, 1994, with the above material in a slurry form. The material was mixed with water using power augers in a large tank on a truck and then dispersed under pressure from large hoses onto the surface.

In 1995, grasses were sampled about 6 months after seeding in each of the three-hundred 9-m^2 quadrats. Grasses were assessed by counting shoots within a 0.1 m^2 quadrat (Daubenmire 1959) located in the southwest corner of each 9-m^2 quadrat. Invasive species were counted in each quadrat.

In 1997, data were collected to test the hypothesis that irrigation reduces the percentage of *Artemisia tridentata* shrubs with mature seed heads compared with the non-irrigated treatment. Data to test the hypothesis were obtained by estimating the percentage of *A. tridentata* shrubs with mature seed heads that were present in both treatments. Sampling was done by selecting the 3rd row and the 6th through 15th rows south of the north border in the irrigated treatment area and the 3rd row and 6th through 15th rows north of the south border in the non-irrigated treatment area. In each row, the number of individual shrubs with mature floral heads present and absent was recorded.

In 2007, observations were made on shrub recruitment on the barrier surface. A few naturally seeded *A. tridentata* shrubs were cut and their age was determined by counting growth rings. Observations were made on *A. tridentata* flowering.

J.2.4 Vegetative Composition

The vegetative composition reflects the condition of the transpirative and stabilization potential of the surface. Plant species composition was determined in every observation year on the surface by several inspections. Species composition was also determined on the barrier side slopes and at the McGee Ranch analog sites. Identifications were made using Hitchcock and Cronquist (1973), USDA NRCS (2010), and Sackschewsky and Downs (2001). Soil cryptogams reflect the condition of the surface with respect to evaporation and stabilization potential of the surface. Soil cryptogams were identified (Link et al. 2000) on both the north and south sections of the barrier surface.

J.2.5 Cover

Cover is the fraction of the ground surface covered by certain types of vegetation, litter, cryptogams, rocks, and soil. High cover by plants or litter is expected to have less evaporation and greater transpiration, and to be more resistant to wind and water erosion. Cover estimates (Daubenmire 1959; DOE-RL 1999) of grasses, shrubs, herbaceous forbs, litter, and bare soil/soil cryptogams were made on each 9-m^2 quadrat on the surface and on the side slopes. Soil cryptogam cover was determined separately from bare soil starting in 2007. Cover of pea gravel was determined starting in 2009.

Cover was determined at the two McGee Ranch analog sites in 2009 by sampling areas of the same size and shape as the barrier surface. At each analog site, 21 quadrats were established, as was done on the barrier surface. The study areas at each site were marked as rectangles like the barrier surface. These analog sites were 40 m by 80 m.

Cover was estimated for grasses, shrubs, and herbaceous forbs as groups from 1996 to 2007. Cover in each quadrat was determined for each species by visual inspection in every quadrat after 2007. Cover was assigned values for percentage ranges as 0%, 0% to 5%, 5% to 25%, 25% to 50%, 50% to 75%, 75% to 95%, and 95% to 100%, and percent cover was assigned the value of the mid-point of each cover range after Rebele and Lehmann (2002).

A more accurate estimate of the cover of pea gravel was made in 2010 on the burned and unburned sections of the PHB surface using a modified Daubenmire technique. This technique uses a 0.5 m^2 rectangular plot frame gridded into fifty 1- dm^2 quadrats. Of the 50 quadrats in the frame, only those that were soil and gravel only were used for the estimate. Quadrats were also included if plant material was over the surface but not on the surface, allowing for a clear view of the soil and gravel surface. These were counted. The 1-dm^2 quadrats were then visually divided into nine parts and the number of 0.11 dm^2 parts that were only covered by gravel were then estimated and counted. The gravel "parts" were then summed and divided by nine for the number of 1-dm^2 quadrats completely covered with gravel. This number was then divided by the number of soil and gravel only quadrats in the frame and multiplied by 100 to estimate the percent of pea gravel cover. Six plots were used to compute average pea gravel cover in the burned and unburned sections of the barrier surface. These were located near the east and west sides and in the center. Two transects of each of three plots were arrayed on each section of the surface.

Cover on the side slopes was assessed using the modified Daubenmire technique. This approach allows for less than 1% cover resolution. Observations were taken in 1997 (Ward et al. 1997) using five line transects that were placed equidistant on the west-facing surface and oriented up and down the slope. On each line transect, the cover was sampled at 10-m intervals from the toe to the top of the slope. In 2007 and 2009, 15 plots were located on the west side slope, five in each of three transects from the top of the slope to the bottom. On the north side, nine plots were located, with three in each of three transects from the top to the bottom of the slope. All plots were grouped to compare cover types (n = 24). In 2010 and 2011, 12 plots were located on both the west and north side slopes, four in each of three transects from the top of the slope to the bottom. Estimates were made for each species and each cover class as was done on the surface.

J.2.6 Shrub Density

All shrubs were counted in each quadrat on the barrier surface after the fire and on the unburned section of the barrier, and at both McGee Ranch analog sites. In each plot, the number of shrubs in three age classes (new seedlings, midsize young, and old large) was counted. At each analog site, 21 plots were established to characterize each site. The study areas at each site were marked as rectangles as was done for the barrier surface. These analog sites were 40 m by 80 m. At the old burn McGee Ranch analog site, plots were the same size as quadrats on the barrier (3 m by 3 m). At the unburned McGee Ranch analog site, plots were larger (6 m by 6 m) to efficiently capture variation in *A. tridentata* populations.

J.2.7 Seed Bank Assessment

Seedling emergence tests (Roberts 1981) were used to quantify the impact of fire on the seed content of the barrier soils and for comparison with the McGee Ranch sites. Soil samples were collected from the various sites just before the fire (September 17 and 18, 2008) and just after the fire (September 30, 2008). Samples were physically paired on the surface for the before and after comparison. Samples were collected along the west, north, and east edges and randomly chosen under the canopy and between canopy pairs throughout the center of the burned area. Samples were collected at the old burn McGee Ranch analog site between December 9 and 11, 2008, and at the undisturbed mature plant community at the unburned McGee Ranch analog site on November 18 and December 1, 2008. The McGee Ranch old-

burn site burned in 1996 (Easterly and Salstrom 2003). The depth of the sample, which was about 3 cm deep, captured the majority of seeds in these soils (Boudell et al. 2002). Samples were placed in paper bags and stored dry at room temperature until they were placed in a greenhouse in flats.

Soil samples were spread in trays in the climate-controlled Washington State University Tri-Cities Native Plant Greenhouse. The greenhouse conditions were ambient light, temperatures above 20°C, and daily watering. Generally, the samples were spread in a layer 1 cm thick on top of potting soil in a flat (0.142 m^2). Barrier samples were placed in the greenhouse in flats between February 23 and March 5, 2009. McGee Ranch samples were placed in the greenhouse in flats between August 6 and 11, 2009. Observations were taken for approximately 1 year for each set.

Germinated seedlings were identified and counted. The seed banks of the barrier before (n = 36) and after the fire (n = 36), the old burn community at McGee Ranch (n = 36), and the unburned mature community at McGee Ranch (n = 36) were compared.

J.2.8 Data Analysis

Species composition of sites was compared using the Jaccard similarity index (Jaccard 1901):

$$J = M_{11}/(M_{01} + M_{10} + M_{11})$$

where M_{11} is the number of species in common between two (A, B) sites, M_{01} is the number of species absent in A and present in B, and M_{10} is the number of species present in A and absent in B.

Prior to statistical analysis, percent survival data were transformed (normalized) using the arcsine transform with radian units (Steele and Torrie 1960) as follows:

$$\arcsin\sqrt{\frac{\%Live}{100}}$$

Density data were also normalized by using the square root transformation (Steele and Torrie 1960).

The percentage of shrubs with mature seed heads (P) was computed as:

$$P = 100\ (N/T)$$

where N is the number of shrubs in each row with mature seed heads and T is the total number of shrubs in the row. Each row is considered an experimental unit where P is the observation. A total of five replicate experimental units were observed in each treatment. Student's t-test was used to test the hypothesis.

Means are presented using untransformed data with error bars based on untransformed data for interpretation. Multiple range comparisons were done using the Tukey-Kramer HSD test. Error terms are 1 standard error of the mean (1 SEM). Significance was tested at the $\alpha = 0.05$ level. Analyses were done using JMP version 5.0 software (SAS Institute 2002).

J.3 Results

In this section, results are presented describing plant establishment from 1995 to 1997 and species composition and cover on the barrier surface from 1995 to 2011. Species composition on the side slopes is presented in association with post-fire succession. Comparisons are made with two analog sites in 2009 as well as seed banks for all sites.

J.3.1 Plant Establishment, Survivorship, and Reproduction

In 1995 and 1997, a census of live and dead shrubs was conducted in all 300 quadrats. The mean survivorship of the shrubs in 1997 based on the number of planted shrubs in 1995 was compared with respect to the treatment. *E. nauseosa* survivorship was significantly ($p < 0.00001$) greater in the irrigated treatment (72.5 ± 3.07%) than in the ambient precipitation treatment (38.0 ± 3.23%). In contrast, survivorship of *A. tridentata* was significantly ($p < 0.00001$) greater in the ambient precipitation treatment (97.6 ± 0.87%) than in the irrigated treatment (90.8 ± 0.84%).

In 1995, grass density about 6 months after planting was highly variable, ranging from 140 to 1975 shoots per m^{-2} across the entire surface. The number of native and invasive alien forbs ranged from 0 to 15 per 9-m^2 quadrat. There was no effect of irrigation ($p > 0.05$) on average forb numbers per 9-m^2 quadrat (ambient precipitation: 3.62 ± 0.22; irrigated: 4.15 ± 0.22). Invasive alien species were not common in the spring, but *S. kali* became the dominant species by July.

In 1997, the percentage of *A. tridentata* with mature seed heads in the irrigated treatment (62.3 ± 3.7) was significantly ($p = 0.009$) lower than in the non-irrigated treatment (80.6 ± 3.8). This result is another indication (Gee et al. 1996) that *A. tridentata* is less viable on this surface with three times normal precipitation than with non-irrigated precipitation.

Observations were also made of seedling establishment of *A. tridentata* and *E. nauseosa* in 1997. In late spring, numerous seedlings of both species occurred in both treatment areas. By late summer, most of the seedlings had perished. Even so, a significant number of *A. tridentata* seedlings were at least 1 year old and were up to 5 cm tall.

In 2007, *A. tridentata* flowers were observed on many shrubs in the north and in south sections of the barrier. Most *A. tridentata* shrubs had only a few flowering stems while other individuals had many flowering stems. *Artemisia tridentata* had reproduced with a number of cohorts. Seedlings that were about 6 cm tall were 2 years old, seedlings about 14 cm tall were 4 years old, and shrubs about 27 cm tall were 8 years old,

In 2010, 83% of the surveyed *A. tridentata* shrubs in the unburned section of the barrier were in flower. None of the *A. tridentata* shrubs in the burned section had flowered.

In 2011, 97% of the surveyed *A. tridentata* shrubs in the unburned section of the barrier were in flower. Seven percent of the *A. tridentata* shrubs in the burned section had flowered.

J.3.2 Botanical Composition on the Barrier

Forty-nine species were observed between 1995 and 2011 (Table J.1) on the surface. There were 14 families present, of which Asteraceae, Brassicaceae, and Poaceae accounted for 71% of the 49 species. The 49 species included 3 shrubs, 33 forbs and 13 grass species. Of these, 36% were non-native species and 44% were perennial species. Over all observation years, nine species occurred in only 7% of the years

while seven species occurred in 100% of the years (Table J.1). Of the highest frequency species, five were grasses and two were members of Asteraceae. Five of these species had been planted. Species that were becoming established included *Centaurea diffusa* and *Chrysothamnus viscidiflorus* (Table J.1). Annual and biennial species that can be classified as ruderal, based on presence after the initial construction (1995, 1996, 1997) and fire (2009, 2010, 2011) disturbances are *Conyza canadensis, Descurainia pinnata, Chenopodium leptophyllum, Erodium cicutarium,* and *Verbena bracteata. Melilotus officinalis* can also be considered ruderal, as it was present from 1995 to 2001 and then after the fire. Comparing species composition in 1997 (35 species) and 2010 (34 species), the years with the greatest number of species, indicates 23 were common to both years. Fourteen species found after the initial disturbance, but absent after the fire are *Ambrosia acanthicarpa, Cardaria draba, Chorispora tenella, Draba verna, Convolvulus arvensis, Lupinus pusillus, Agropyron cristatum, Elymus lanceolatus, Hesperostipa comata, Sphaeralcea munroana, Thinopyrum intermedium, Triticum aestivum, Phacelia linearis* and *Epilobium brachycarpum.* Only *E. brachycarpum* has wind-dispersed seed. Eight species that were found after the fire, but not after the initial disturbance include *C. diffusa, Chaenactis douglasii, Erigeron filifolius, Erigeron piperianus, Lagophylla ramosissima, Pseudognaphalium canescens, Stephanomeria paniculata,* and *Chenopodium album.* Seven of these species have wind-dispersed seed. Of the 34 species found on the surface in 2010, 47% have wind-dispersed seed. These data indicate that the original plantings largely maintained themselves on the surface and that species are likely to establish and maintain themselves on the surface after disturbances. These data also provide information to support possible vegetation management plans for long-term maintenance of barrier function. The initial plantings and subsequent natural vegetation dynamics have maintained barrier function.

Table J.1. Plant species observed on the barrier surface between 1995 and 2011. Species type are "n" = native, "a" = alien, "af" = annual forb, "ag" = annual grass, "bf" = biennial forb, "pf" = perennial forb, "pg" = perennial grass, "s" = shrub, "r" = seeded or planted species, and "w" = wind dispersed seed. Permanence is the percent of years a species is present on the surface.

Family *Species*	**Type**	**1995**	**1996**	**1997**	**1999**	**2000**	**2001**	**2002**	**2003**	**2004**	**2007**	**2008**	**2009**	**2010**	**2011**	**Permanence**
Asteraceae																
Achillea millefolium common yarrow	n,pf	1		1	1	1	1				1		1	1	1	64
Ambrosia acanthicarpa flatspine bur ragweed	n,af	1		1		1										21
Artemisia tridentata big sagebrush	n,s,r	1	1	1	1	1	1	1	1	1	1	1	1	1	1	100
Centaurea diffusa diffuse knapweed	a,bf										1	1	1	1	1	36
Chaenactis douglasii Douglas' dustymaiden	n,bf													1	1	14
Chrysothamnus viscidiflorus yellow rabbitbrush	n,s			1							1	1	1	1	1	43
Conyza canadensis Canadian horseweed	n,af			1										1		14
Ericameria nauseosa rubber rabbitbrush	n,s,r	1	1	1	1	1	1	1	1	1	1	1	1	1	1	100
Erigeron filifolius	n,pf													1		7

Family *Species*	**Type**	**1995**	**1996**	**1997**	**1999**	**2000**	**2001**	**2002**	**2003**	**2004**	**2007**	**2008**	**2009**	**2010**	**2011**	**Permanence**
threadleaf fleabane																
Erigeron piperianus Piper's fleabane	n,pf													1		7
Erigeron pumilus shaggy fleabane	n,pf							1	1					1	1	29
Lactuca serriola prickly lettuce	a,af	1	1	1	1	1			1	1			1	1		64
Lagophylla ramosissima branched lagophylla	n,af													1		7
Machaeranthera canescens hoary tansyaster	n,bf		1	1	1	1	1		1	1	1	1	1	1	1	86
Pseudognaphalium canescens Wright's cudweed	n,af													1		7
Stephanomeria paniculata tufted wirelettuce	n,af												1	1		14
Tragopogon dubius yellow salsify	a,af		1	1	1	1	1			1			1	1		57
Boraginaceae																
Amsinckia lycopsoides tarweed fiddleneck	n,af	1	1	1	1	1	1	1	1	1			1	1	1	86
Brassicaceae																
Cardaria draba whitetop	a,pf		1	1	1	1										29
Chorispora tenella crossflower	a,af	1		1												14
Descurainia pinnata western tansymustard	n,af	1	1	1									1	1		36
Draba verna spring draba	a,af	1	1	1	1	1	1	1								50
Sisymbrium altissimum tall tumbleweed mustard	a,af	1	1	1		1			1				1	1	1	57
Caryophyllaceae																
Holosteum umbellatum jagged chickweed	a,af				1	1	1	1	1						1	43
Chenopodiaceae																
Chenopodium album lambsquarters	a,af													1		7
Chenopodium leptophyllum narrowleaf goosefoot	n,af	1	1	1									1	1		35
Salsola kali prickly Russian thistle	a,af	1	1	1	1	1	1		1	1		1	1	1		79
Convolvulaceae																
Convolvulus arvensis	a,pf		1	1												14

Family *Species*	**Type**	**1995**	**1996**	**1997**	**1999**	**2000**	**2001**	**2002**	**2003**	**2004**	**2007**	**2008**	**2009**	**2010**	**2011**	**Permanence**
field bindweed																
Fabaceae																
Astragalus caricinus buckwheat milkvetch	n,pf			1	1	1	1				1		1	1		50
Lupinus pusillus rusty lupine	n,af			1												7
Melilotus officinalis sweetclover	a,af		1	1	1	1	1						1	1		50
Geraniaceae																
Erodium cicutarium redstem storks bill	a,af	1	1	1	1	1	1	1	1	1			1	1		79
Hydrophyllaceae																
Phacelia linearis threadleaf phacelia	n,af	1														7
Laminaceae																
Agastache occidentalis western giant hyssop	n,pf				1											7
Malvaceae																
Sphaeralcea munroana Munro's globemallow	n,pf		1	1	1	1	1		1	1						50
Onagraceae																
Epilobium brachycarpum tall annual willowherb	n,af		1	1	1	1	1									36
Poaceae																
Achnatherum hymenoides Indian ricegrass	n,pg,r	1	1	1			1							1		36
Agropyron cristatum crested wheatgrass	a,pg		1	1	1											21
Bromus tectorum cheatgrass	a,ag	1	1	1	1	1	1	1	1	1	1	1	1	1	1	100
Elymus elymoides squirreltail	n,pg,r	1				1								1		21
Elymus lanceolatus thickspike wheatgrass	n,pg,r	1	1	1												21
Elymus wawawaiensis Snake River wheatgrass	n,pg,r	1	1	1	1	1	1	1	1	1	1	1	1	1	1	100
Hesperostipa comata needle and thread	n,pg,r	1		1												14
Poa ampla *big bluegrass*	n,pg,r	1	1	1	1	1	1	1	1	1	1	1	1	1	1	100
Poa bulbosa bulbous bluegrass	a,pg	1	1	1	1	1	1	1	1	1	1	1	1	1	1	100
Poa secunda Sandberg's bluegrass	n,pg,r	1	1	1	1	1	1	1	1	1	1	1	1	1	1	100

Family *Species*	**Type**	**1995**	**1996**	**1997**	**1999**	**2000**	**2001**	**2002**	**2003**	**2004**	**2007**	**2008**	**2009**	**2010**	**2011**	**Permanence**
Thinopyrum intermedium intermediate wheatgrass	a,pg		1	1		1	1	1	1							43
Triticum aestivum common wheat	a,ag	1														7
Vulpia microstachys small fescue	n,ag						1	1		1			1	1	1	43
Verbenaceae																
Verbena bracteata bigbract verbena	n,af		1	1									1	1		29

Plant species on the burned and unburned sections of the barrier were identified in 2009 (Table J.2). There were more ruderal annuals and biennial species on the burned section (13) of the surface than on the unburned section (6) in 2009. *Stephanomeria paniculata* appeared for the first time in 2009 and remained in 2010 (Table J.3). This annual forb has windblown seed and likely arrived in the wind. *Descurainia pinnata, C. leptophyllum, M. officinalis,* and *V. bracteata* reappeared in 2009 and remained in 2010. All were present after the initial construction disturbance. None of these annual forbs have windblown seed. The large number of species appearing after the fire is a normal response to disturbance and is not likely to affect barrier performance based on the conditions of the test.

Plant species on the burned and unburned sections of the barrier were identified again in 2010 (Table J.3). There were substantially more ruderal annuals and biennial species on the burned section (20) of the surface than on the unburned section (8) in 2010. There were *Chaenactis douglasii, E. filifolius, E. piperianus, L. ramosissima, P. canescens,* and *C. album* that were not present on the surface until 2010. Four of these species were found in the burned area, and only *C. douglasii* remained in 2011 (Table J.4). Seeds of four of the five species are windblown, suggesting that they arrived from some distance, as they have not been observed on the side slopes of the barrier. Many of the species observed after the fire had not been observed for several years (Table J.1). Some of these species may have resided in the seed bank waiting for a fire to create conditions conducive to germination and establishment. The number of species found on the unburned section of the surface in 2010 was 18, which is substantially greater than the low value of 11 observed in 2007 and 2008 before the fire. It was observed that species from the burned section of the surface were appearing in the unburned section of the surface. It is likely that the increase in species richness is partially due to the high species richness in the burned section of the surface. It also has been observed that *A. tridentata* shrubs have been gradually dying in the unburned section of the surface, opening sites where new species can establish. The substantially large number of species appearing 2 years after the fire is a normal response to disturbance and is unlikely to affect barrier performance based on the conditions of the test.

Substantial changes in species composition and richness occurred in 2011 (Fig. J.3, Table J.4). Species richness decreased to 45% of that in 2010(Table J.3). This decrease was greater and more rapid than the change from 1997 to 1999, after the effects of the initial construction disturbance. If *M. canescens* had retained high cover after 2011 (see Table J.8), species richness may have continued to decrease, possibly returning to the low values achieved just before the fire. If so, then *M. canescens* may be considered a highly competitive early invasive species. It is classified as an annual, biennial, and perennial (USDA NRCS 2011). Although the lifespan of *M. canescens* is not well studied, it is considered a ruderal species

(Lesica and Cooper 1999). The reduction in species after the fire is a normal response to disturbance and is unlikely to affect barrier performance under the conditions of the test.

Table J.2. Plant species observed in 2009 on the burned and unburned sections of the barrier

Family ***Species***	**Perennial**	**Annual/ Biennial**	**Native**	**Alien**	**Burned**	**Unburned**
Asteraceae						
Achillea millefolium	1		1		1	
Artemisia tridentata	1		1		1	1
Centaurea diffusa		1		1	1	1
Chrysothamnus viscidiflorus	1		1		1	1
Ericameria nauseosa	1		1		1	1
Lactuca serriola		1		1	1	
Machaeranthera canescens		1	1		1	1
Stephanomeria paniculata		1	1		1	
Tragopogon dubius		1		1	1	
Boraginaceae						
Amsinckia lycopsoides		1	1		1	1
Brassicaceae						
Descurainia pinnata		1	1		1	
Sisymbrium altissimum		1		1	1	
Chenopodiaceae						
Chenopodium leptophyllum		1	1		1	
Salsola kali		1		1	1	1
Fabaceae						
Astragalus caricinus	1		1		1	
Melilotus officinalis	1			1	1	
Geraniaceae						
Erodium cicutarium		1		1	1	
Poaceae						
Bromus tectorum		1		1	1	1
Elymus wawawaiensis	1		1		1	1
Poa ampla	1		1		1	1
Poa bulbosa	1			1	1	1
Poa secunda	1		1		1	
Vulpia microstachys		1	1		1	1
Verbenaceae						
Verbena bracteata		1	1		1	
Total number of species	10	14	15	9	24	12
Burned	10	13	15	9		
Unburned	6	6	8	4		

Table J.3. Plant species observed in 2010 on the burned and unburned sections of the barrier

Family ***Species***	**Perennial**	**Annual/ Biennial**	**Native**	**Alien**	**Burned**	**Unburned**
Asteraceae						
Achillea millefolium	1		1		1	1
Artemisia tridentata	1		1		1	1
Centaurea diffusa		1		1	1	1
Chaenactis douglasii		1	1		1	
Chrysothamnus viscidiflorus	1		1		1	1
Conyza canadensis		1	1		1	
Ericameria nauseosa	1		1		1	1
Erigeron filifolius	1		1			1
Erigeron piperianus	1		1		1	
Erigeron pumilus	1		1		1	1
Lagophylla ramosissima		1	1		1	
Lactuca serriola		1		1	1	
Machaeranthera canescens		1	1		1	1
Pseudognaphalium canescens		1	1		1	
Stephanomeria paniculata		1	1		1	
Tragopogon dubius		1		1	1	1
Boraginaceae						
Amsinckia lycopsoides		1	1		1	1
Brassicaceae						
Descurainia pinnata		1	1		1	1
Sisymbrium altissimum		1		1	1	
Chenopodiaceae						
Chenopodium album		1		1	1	
Chenopodium leptophyllum		1	1		1	
Salsola kali		1		1	1	1
Fabaceae						
Astragalus caricinus	1		1		1	
Melilotus officinalis		1		1	1	
Geraniaceae						
Erodium cicutarium		1		1	1	
Poaceae						
Achnatherum hymenoides	1		1		1	
Bromus tectorum		1		1	1	1
Elymus elymoides	1		1		1	
Elymus wawawaiensis	1		1		1	1
Poa ampla	1		1		1	1
Poa bulbosa	1			1	1	1
Poa secunda	1		1		1	1
Vulpia microstachys		1	1		1	1
Verbenaceae						

Family ***Species***	**Perennial**	**Annual/ Biennial**	**Native**	**Alien**	**Burned**	**Unburned**
Verbena bracteata		1	1		1	
Total number of species	14	20	24	10	33	18
Burned	13	20	23	10		
Unburned	10	8	13	5		

Table J.4. Plant species observed in 2011 on the burned and unburned sections of the barrier

Family ***Species***	**Perennial**	**Annual/ Biennial**	**Native**	**Alien**	**Burned**	**Unburned**
Asteraceae						
Achillea millefolium	1		1		1	1
Artemisia tridentata	1		1		1	1
Centaurea diffusa		1		1	1	1
Chaenactis douglasii	1		1		1	
Chrysothamnus viscidiflorus	1		1		1	
Ericameria nauseosa	1		1		1	1
Erigeron pumilus	1		1		1	
Machaeranthera canescens		1	1		1	1
Boraginaceae						
Amsinckia lycopsoides		1	1		1	
Brassicaceae						
Sisymbrium altissimum		1		1	1	
Poaceae						
Bromus tectorum		1		1	1	1
Elymus wawawaiensis	1		1		1	1
Poa ampla	1		1		1	1
Poa bulbosa	1			1		1
Poa secunda	1		1		1	1
Vulpia microstachys		1	1		1	1
Total number of species	10	6	12	4	15	11
Burned	9	6	12	3		
Unburned	7	4	8	3		

Species composition on the side slopes (Table J.5) adjacent to the barrier surface was compared with species composition on the barrier surface in 2007 and 2010 (Table J.1). Jaccard's similarity index is nearly the same in 2007 and 2010 and less than 0.5, indicating that the fire did not affect similarity in the adjacent community. The new species on the barrier surface after the fire did not move to the side slope. Only 33% of the species on the side slope in 2007 have windblown seed, which is nearly the same as the 27% of species that are windblown in 2010. Most of the species with windblown seed are members of the Asteraceae family, which has the most species in the area (Sackschewsky and Downs 2001). Species observed on the north and west side slopes in 2010 and 2011 while collecting cover data are found in Table J.9 and Table J.10.

Table J.5. Species composition on the barrier side slopes in 2007 and 2010

Family Species	Seed dispersal mechanism	2007	2010
Asteraceae			
A. millefolium	none	1	1
A. acanthicarpa	animal		1
A. tridentata	none	1	1
C. diffusa	wind	1	1
C. douglasii	wind	1	
C. viscidiflorus	wind	1	1
E. nauseosa	wind	1	1
M. canescens	wind	1	1
T. dubius	wind	1	
Boraginaceae			
A. lycopsoides	animal	1	1
Brassicaceae			
S. altissimum	none	1	1
Caryophyllaceae			
H. umbellatum	none	1	1
Chenopodiaceae			
S. kali	wind	1	1
Fabaceae			
A. caricinus	none	1	1
A. succumbens	none	1	
M. officinalis	none	1	1
Geraniaceae			
E. cicutarium	animal	1	1
Graminae			
A. cristatum	none	1	
B. tectorum	animal	1	1
E. lanceolatus	none		1
E. wawawaiensis	none	1	1
H. comata	none		1
P. bulbosa	none		1
P. secunda	none	1	1
V. microstachys	none	1	1
Onagraceae			
E. brachycarpum	wind		1
Number of Species Present		21	22
Jaccard similarity coefficient (Eq. 1) where B is the barrier surface		0.455	0.436

Species richness (Fig. J.1) rose to 35 two years after the initial construction disturbance, dropping to 11 in 2008 before the fire, rising again to 34 two years after the fire, and then falling to 17 species in 2011. The number of perennials was similar to the number of annuals and biennials through the entire period until 2007, when there were only 3 annuals and biennials compared with 9 perennials. Two years after the fire there were 20 annuals and biennials and 14 perennials. The number of annuals and biennials dropped to 7 and the number of perennials dropped to 10 three years after the fire.

J.3.3 Cover on the Barrier

Cover was evaluated using the mean, median, and mode. The median is the value for which half of the observations are below and half are above. The mode is the most common observation. Daubenmire classes are ordinal and technically should not be analyzed using arithmetic means. The median and modes are useful for such data and are reported here. Computed means based on midpoint values of each class is a common approach (Rebele and Lehmann 2002) and is used here to allow comparison with other published values. The mean, median, and mode cover classes for each cover type in the north and the south sections of the barrier are presented in Table J.6. The ranges are the cover classes as defined by Daubenmire (1959).

Table J.6. Median, mode, and mean percent cover classes. The north section was irrigated from 1995 to 1998 and was burned in 2008. The south section was not treated.

Cover Class	Treatment	Water Year	Median	Mode	Mean
Grass	North Section	1996	25–50	5–25	25–50
		1997	50–75	50–75	50–75
		1999	75–95	75–95	50–75
		2000	75–95	75–95	50–75
		2001	75–95	75–95	25–50
		2002	5–25	5–25	5–25
		2003	5–25	5–25	5–25
		2004	5–25	5–25	25–50
		2007	0–5	0–5	5–25
		2009	0–5	0–5	0–5
		2010	5–25	5–25	5–25
		2011	5–25	0–5	5–25
	South Section	1996	5–25	5–25	5–25
		1997	25–50	25–50	25–50
		1999	25–50	25–50	25–50
		2000	5–25	5–25	25–50
		2001	5–25	5–25	5–25
		2002	0–5	0–5	0–5
		2003	5–25	0–5	5–25
		2004	0–5	0–5	5–25
		2007	0–5	0–5	0–5
		2009	0–5	0–5	0–5
		2010	0–5	5–25	0–5

Cover Class	Treatment	Water Year	Median	Mode	Mean
		2011	0–5	0–5	0–5
Shrub	North Section	1996	0–5	0–5	0–5
		1997	25–50	25–50	25–50
		1999	25–50	25–50	25–50
		2000	50–75	50–75	25–50
		2001	25–50	25–50	25–50
		2002	25–50	25–50	25–50
		2003	25–50	25–50	25–50
		2004	25–50	25–50	25–50
		2007	25–50	25–50	25–50
		2009	0–5	0–5	0–5
		2010	5–25	5–25	0–5
		2011	0–5	0–5	0–5
	South Section	1996	0–5	0–5	0–5
		1997	25–50	25–50	25–50
		1999	25–50	25–50	25–50
		2000	25–50	25–50	25–50
		2001	25–50	25–50	25–50
		2002	5–25	5–25	5–25
		2003	25–50	25–50	25–50
		2004	25–50	25–50	25–50
		2007	25–50	25–50	25–50
		2009	25–50	25–50	25–50
		2010	5–25	5–25	25–50
		2011	25–50	25–50	25–50

Cover Class	Treatment	Water Year	Median	Mode	Mean
Litter	North Section	1996	5–25	5–25	5–25
		1997	50–75	50–75	50–75
		1999	75–95	95–100	75–95
		2000	75–95	75–95	50–75
		2001	25–50	25–50	50–75
		2002	50–75	25–50	50–75
		2003	25–50	25–50	25–50
		2004	50–75	50–75	50–75
		2007	5–25	5–25	25–50
		2009	0–5	5–25	5–25
		2010	0–5	0–5	5–25
		2011	0–5	0–5	5–25
	South Section	1996	5–25	5–25	5–25
		1997	25–50	25 –50	25 –50
		1999	50–75	50–75	50–75
		2000	25–50	25–50	25–50
		2001	25–50	5–25	25–50
		2002	25–50	25–50	25–50
		2003	5–25	5–25	5–25
		2004	25–50	25–50	25–50
		2007	5–25	5–25	25–50
		2009	25–50	25–50	25–50
		2010	25–50	5–25	25–50
		2011	25–50	5–25	25–50
Bare Ground	North Section	1996	5–25	5–25	5–25
		1997	5–25	25–50	5–25
		1999	5–25	0–5	5–25
		2000	5–25	5–25	5–25
		2001	5–25	5–25	5–25
		2002	25–50	25–50	25–50
		2003	50–75	50–75	25–50
		2004	25–50	50–75	25–50
		2007	50–75	50–75	50–75
		2009	75–95	75–95	75–95
		2010	50–75	50–75	50–75
		2011	50–75	50–75	50–75
	South Section	1996	5–25	5–25	25–50
		1997	25–50	25–50	25–50
		1999	5–25	5–25	25–50
		2000	25–50	50–75	25–50
		2001	25–50	25–50	25–50

Cover Class	Treatment	Water Year	Median	Mode	Mean
		2002	25–50	25–50	25–50
		2003	50–75	75–95	50–75
		2004	50–75	50–75	50–75
		2007	50–75	50–75	50–75
		2009	50–75	50–75	50–75
		2010	25–50	50–75	25–50
		2011	25–50	25–50	25–50

Class	Percent Cover	Midpoint
1	0 to 5	2.5
2	5 to 25	15
3	25 to 50	37.5
4	50 to 75	62.5
5	75 to 95	85
6	95 to 100	97.5

Percent cover of grasses (Fig. J.1) on the barrier surface was significantly higher in the north section of the surface than in the south section in all years except 2003. Note that error bars are smaller than the size of the symbol in nearly all cases (Fig. J.1). Grass cover generally has decreased on both sections of the barrier since 1997, reaching minimal values in 2009. Grass cover increased after the fire on the burned section by up to 10% by 2011 (Fig. J.1).

Shrub cover (Fig. J.1) was similar on both sections of the surface until the fire, when shrub cover was reduced to near zero on the burned section of the surface. Shrub cover naturally increased in 2010 and then decreased in 2011 to 3.3% in the burned area. Shrub cover decreased slowly between 2004 and 2011 on the unburned section of the surface.

Litter cover (Fig. J.1) reached maximal values in 1999 and was significantly greater in the north section of the surface than in the south section until 2007. After the fire, litter cover was sharply reduced in the burned section of the surface compared with the unburned section.

Forb cover (Fig. J.1) was significantly greater than zero in 1996, the second year after planting. Forb cover remained very low and was the same on both sections of the surface until just before the fire in 2008. Forb cover increased strongly after the fire to 43.8% in 2010 and then dropped to 28.2% in 2011. Forb cover remained very low on the unburned section of the surface during the study period.

Soil cryptogam cover in 2009 was significantly ($p < 0.0001$) greater in the unburned section (28.3 ± 1.63%) than in the burned section (0%). Similarly, soil cryptogam cover in 2010 was significantly ($p < 0.0001$) greater in the unburned section (23.5 ± 1.29%) than in the burned section (0%). By 2011, soil cryptogam cover was recognizable in the burned area with soil cryptogam cover significantly (<0.0001) greater in the unburned section (22.9 ± 1.39%) than in the burned section (0.1 ± 0.04 %).

Bare surface cover (soil plus soil cryptogams) has generally increased since the initial planting (Fig. J.1). Before the fire bare surface cover was greater in the south section of the surface than in the north section except in 2002 and 2007, when they were the same. Bare surface cover decreased in the south section of the surface between 2007 and 2011, while it increased on the north section right after the fire to a maximal level. Bare ground cover decreased from 2009 to 2010, remaining the same as 2010 in 2011 in

the unburned area. Bare ground cover decreased from 2009 to 2011 in the burned area (Table J.6). While bare surface cover increased right after the fire, the risk posed to barrier performance is low because naturally occurring forb plant cover was sufficiently high right after the fire.

Pea gravel cover was significantly lower in the unburned section (12.1 ± 0.44 %) of the surface than on the burned section (15%) in 2009. Pea gravel cover was significantly ($p < 0.0001$) lower in the unburned section (10.9 ± 0.53 %) of the surface than on the burned section (15%) in 2010. Similarly, in 2011, pea gravel cover was significantly ($p < 0.0001$) lower in the unburned section (10.5 ± 0.5 %) than in the burned section (16.4 ± 0.46 %).

In 2010, cover of rocks (mostly pea gravel) was estimated to be 15% in the burned area and 10.9% in the unburned area using the coarse cover classes noted below Table J.6. Using the finer gridded cover frame allowed for a more accurate estimate of pea gravel cover. These observations were taken only in areas where there was little other cover and were used to provide an estimate that is relevant to the development of a surface pavement. The more accurate estimate of percent pea gravel cover (mean ± 1 SEM) on the burned and unburned sections of the surface indicates that cover (9.73 ± 0.78%) on the burned section of the surface was significantly ($p = 0.0024$) greater than that (6.33 ± 0.31%) on the unburned section of the surface.

Cover maps for 1996 are provided in Gee et al. (1996); for 1997 in Ward et al. (1997); and for 2007 in Ward et al. (2009a). Cover maps of the major surface classes after the fire are in Figure J.2 to Figure J.6 for 2009, 2010, and 2011. Litter cover (Fig. J.2) is very low in the burned area over the 3 years, with high levels in the unburned area near the edges. This is associated with higher shrub cover near the edges that also hold tumbleweed skeletons blown in by the wind. Forb cover (Fig. J.3) is high and variable in the burned area with maximal cover in 2010. There is very little forb cover in the unburned area. Grass cover (Fig. J.4) increased across the 3 years, with increases associated with the *E. wawawaiensis* patch in the northeast corner of the burned area. *Elymus wawawaiensis* and *B. tectorum* are both increasing in the burned area (Tables J.3 and J.4). Shrub cover (Fig. J.5) is variable in the unburned area, with lower cover appearing in the southeast corner of the surface in 2011. Shrub cover is highest at the edges of the surface. Bare areas (Fig. J.6) are roughly the inverse of litter and vegetation patterns with decreases in the burned area over time.

Plant cover was sufficient from the beginning of the trial to minimize the risk of infiltration and erosion. Through 2011, the fire had not substantially increased these risks because naturally occurring forbs dominated the surface after the fire. Shrub cover became more variable across the untreated section of the surface and may eventually increase risks. Variation in shrub cover may indicate potential increases in soil water if they become far apart and there is little deep-rooted vegetation between shrubs. Large shrubs along edges can indicate that more water is in the soil profile with increased potential for drainage.

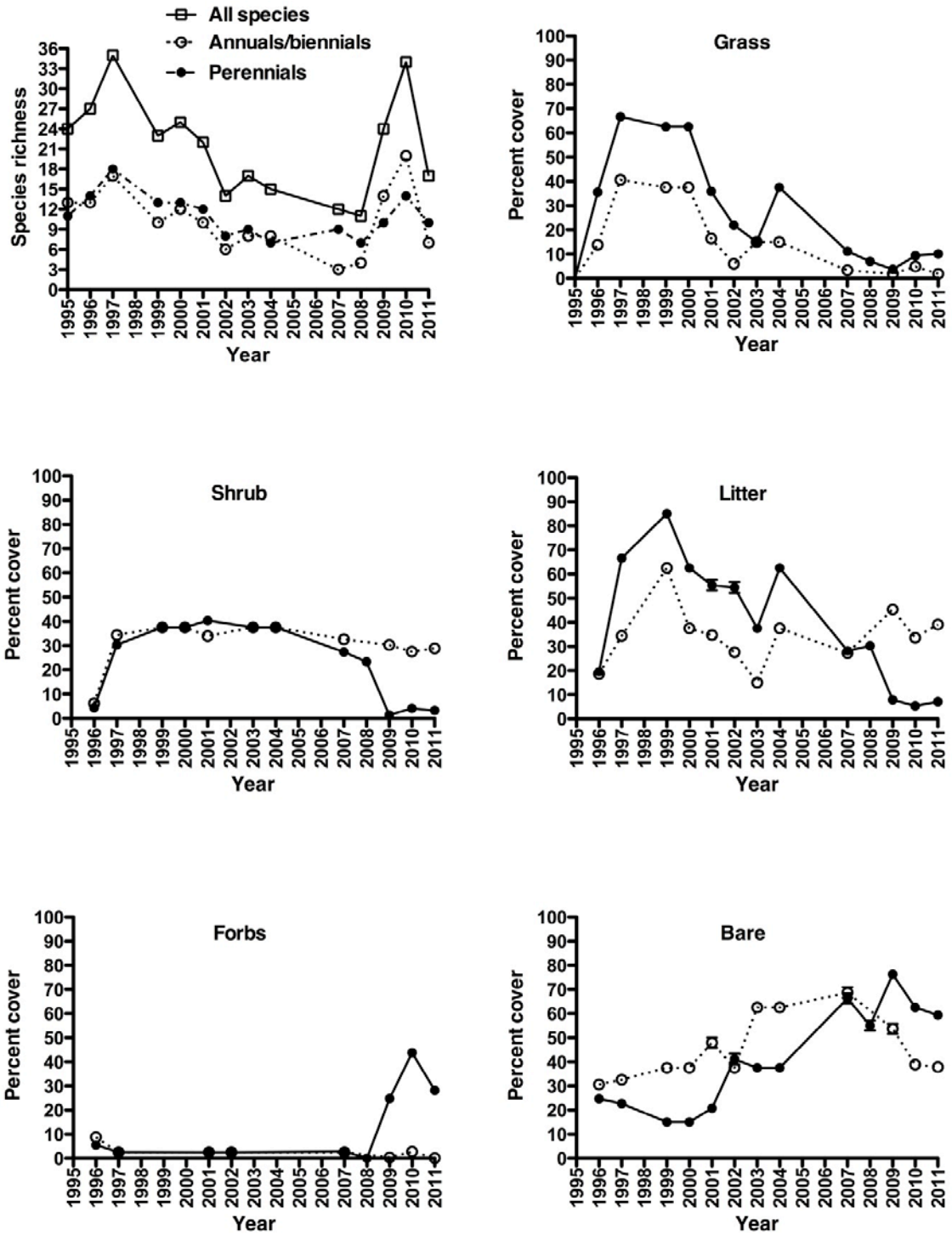

Figure J.1. Species richness and cover (o - south section, • - north section) dynamics on the Prototype Hanford Barrier. The north section was irrigated from 1994 to 1998 and burned in September 2008.

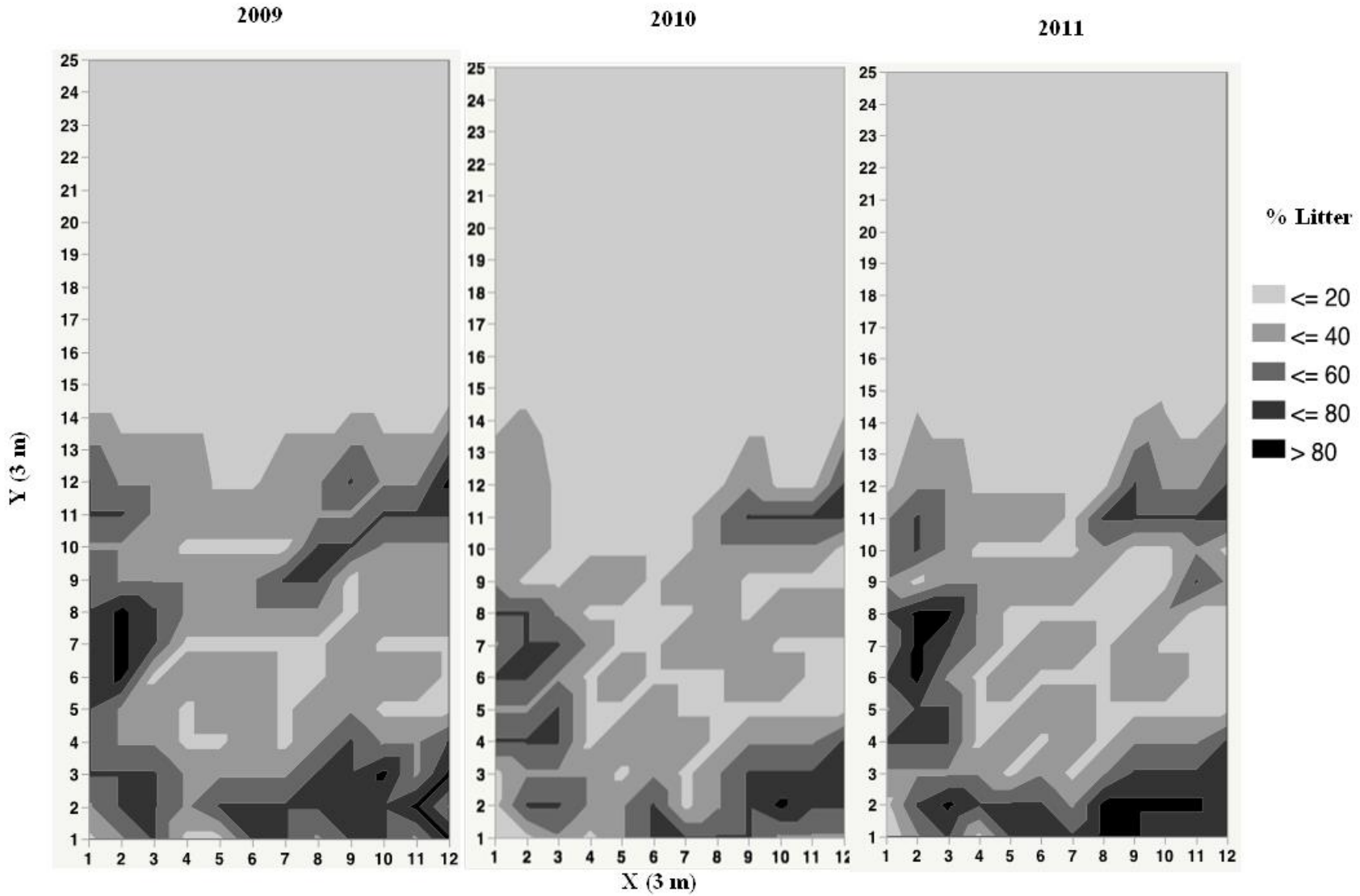

Figure J.2. Litter percent cover in 2009, 2010, and 2011.

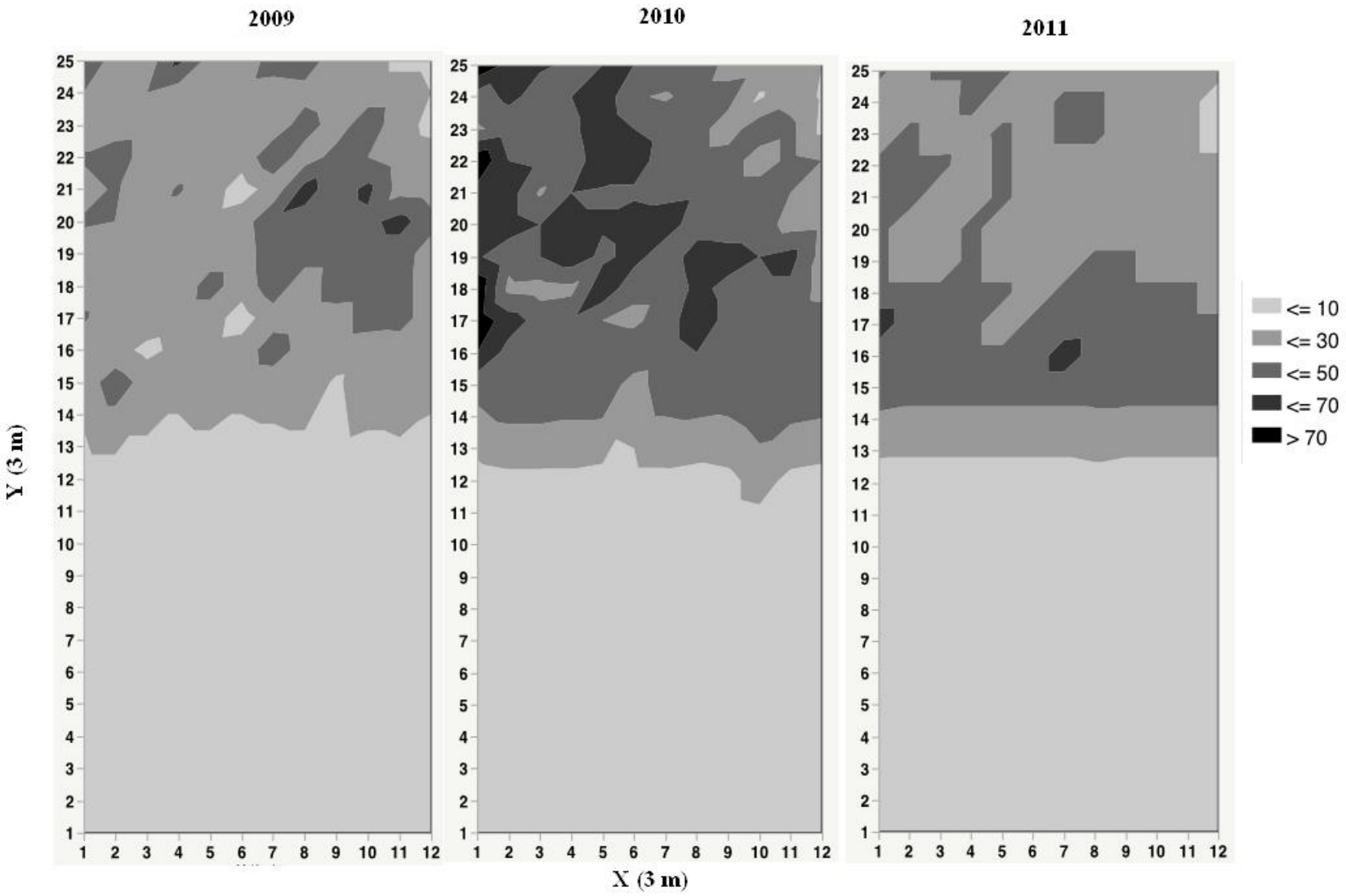

Figure J.3. Forb percent cover in 2009, 2010, and 2011.

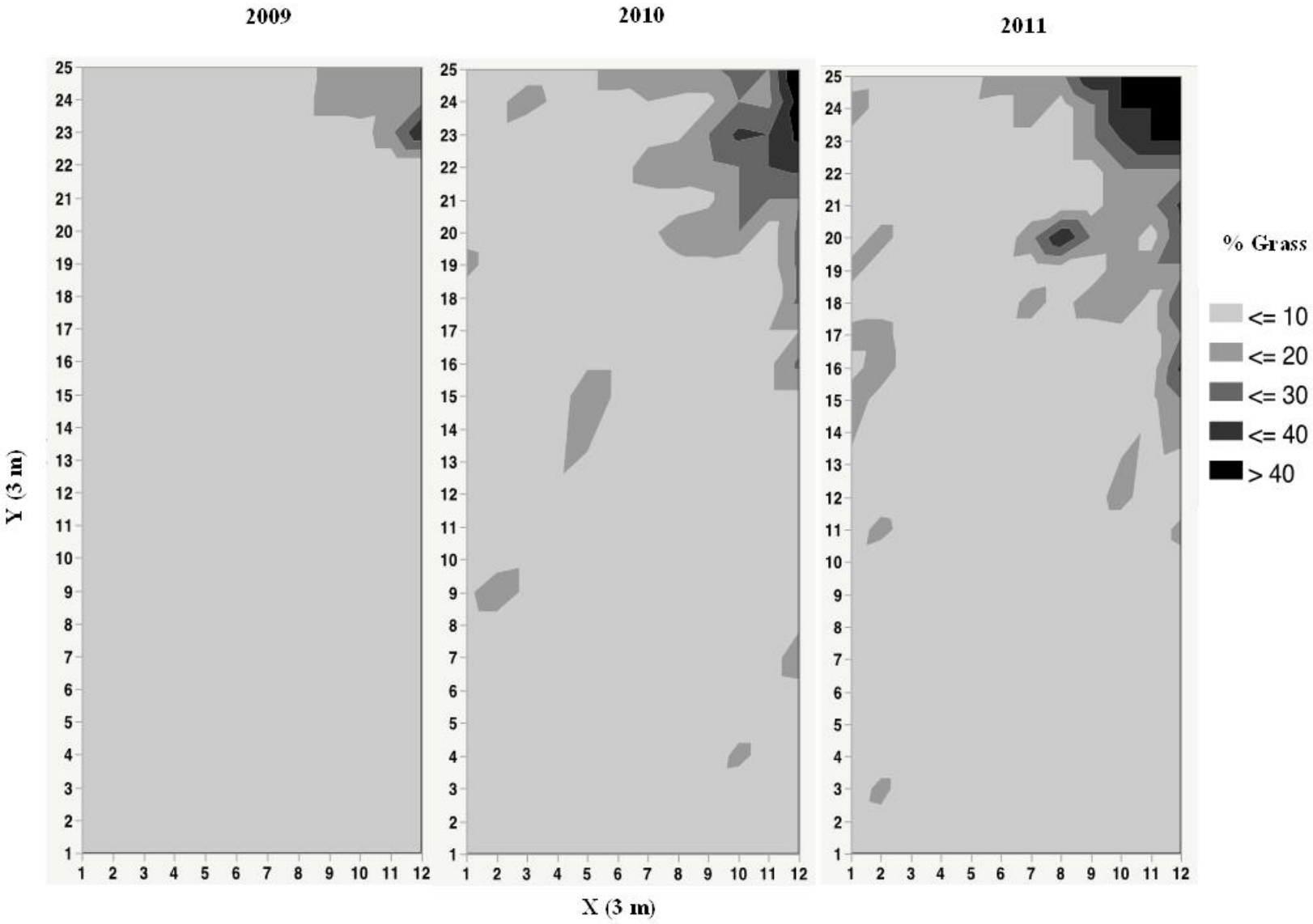

Figure J.4. Grass percent cover in 2009, 2010, and 2011.

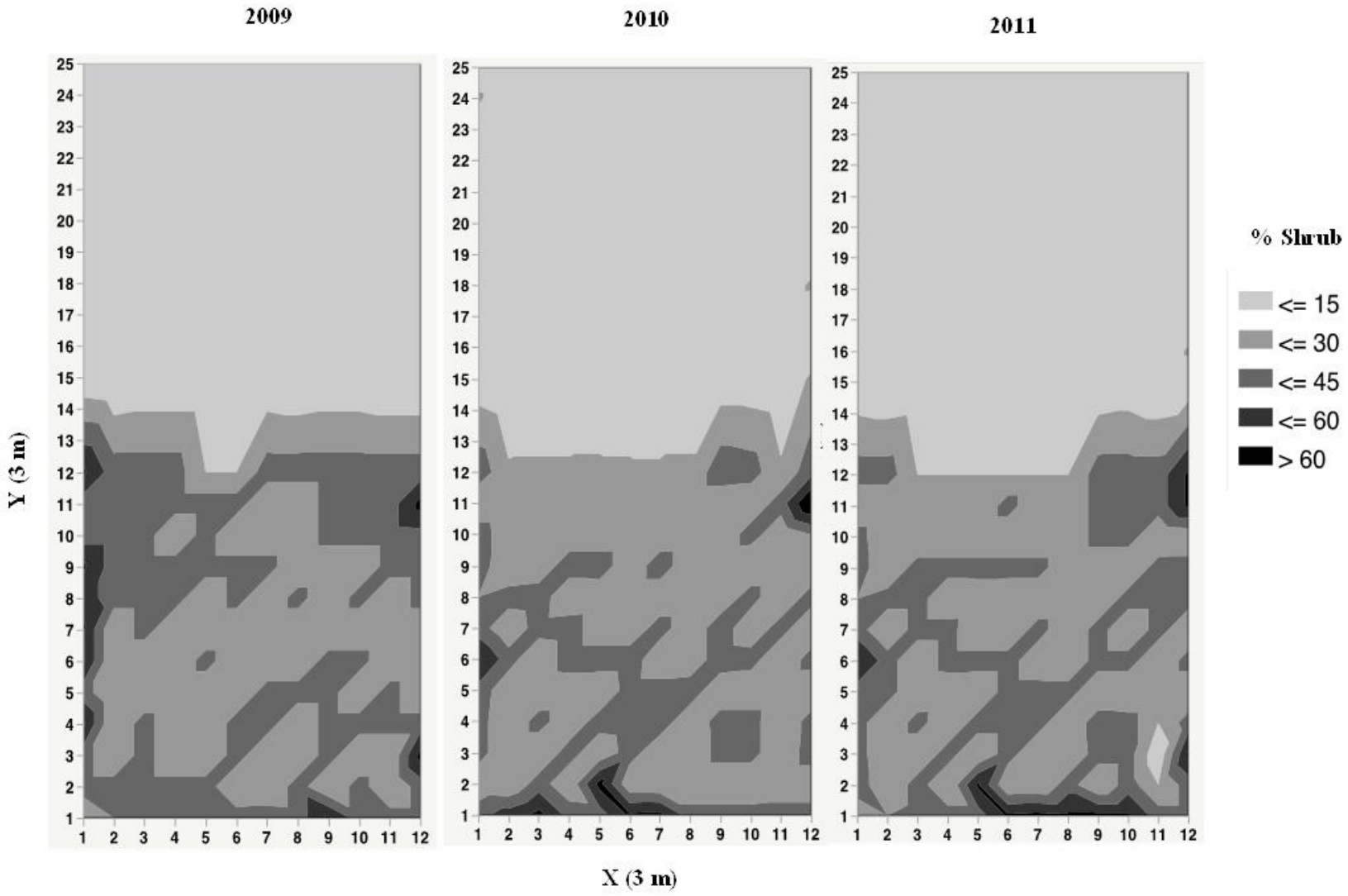

Figure J.5. Shrub percent cover in 2009, 2010, and 2011.

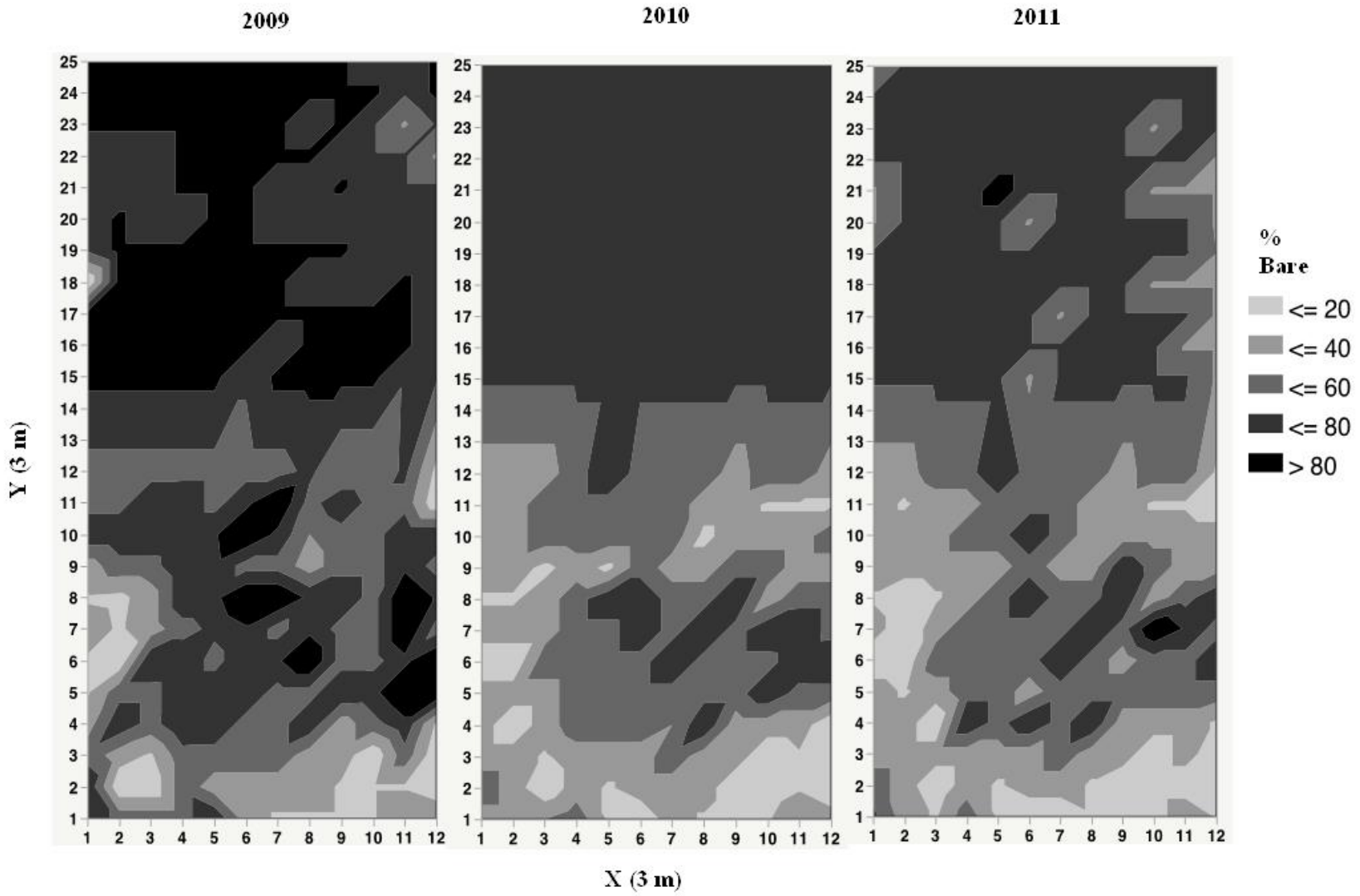

Figure J.6. Bare (soil + soil cryptogam) percent cover in 2009, 2010, and 2011.

J.3.4 Species Cover after the Fire

Sagebrush dominates the unburned section of the Prototype Hanford Barrier (Fig. J.7).

Figure J.7. Prototype Hanford Barrier cover dominated by *Artemisia tridentata* in 2010, 16 years after establishment on the unburned section of the surface.

After the prescribed fire on the north section of the barrier, the deep-rooted *A. tridentata* shrub was no longer dominant. *Machaeranthera canescens*, a biennial forb with roots growing to a depth of 1.55 m (Klepper et al. 1985), dominated in 2010 (Fig. J.8) and 2011 (Fig. J.9).

Figure J.8. Vegetation cover on the north section in 2010 dominated by biennial forb, *Machaeranthera canescens*.

Figure J.9. Vegetation cover on the north section in 2011 dominated by biennial forb, *Machaeranthera canescens*.

Cover of each species was determined on both sections of the barrier surface in 2009 (see Table J.12), 2010 (Table J.7), and 2011 (Table J.8). Thirty-one species were observed in 2010. Cover of seven species was very low and not significantly different from zero (Table J.7). Of 31 species, 19 had significantly greater cover on the burned section of the surface compared with the unburned section. *Artemisia tridentata* cover was significantly greater than zero 2 years after the fire on the burned section of the surface. *Machaeranthera canescens* cover was highly significant at 27.9% on the burned section of the surface and much greater than on the unburned section of the surface. Only cover of *A. tridentata* and *P. bulbosa* was significantly greater on the unburned section than on the burned section of the surface.

Table J.7. Mean percent cover (± 1 SEM) of plant species and other categories observed in 2010 on the burned and unburned sections of the barrier. Statistically significant differences between burned and unburned sections are set at $p <= 0.05$.

Species/categories	**Barrier burn**	**Barrier unburned**	**p**
A. millifolium	0.12 ± 0.05	0.02 ± 0.02	0.0320
A. hymenoides	0.02 ± 0.02	0	0.3182
A. lycopsoides	0.99 ± 0.10	0.03 ± 0.02	<0.0001
A. tridentata	1.52 ± 0.10	25.7 ± 1.11	<0.0001
A. caricinus	0.03 ± 0.02	0	0.1569
B. tectorum	3.61 ± 0.32	2.15 ± 0.12	<0.0001
C. diffusa	0.09 ± 0.04	0	0.0241

Species/categories	Barrier burn	Barrier unburned	p
C. douglasii	0.03 ± 0.02	0	0.1569
C. album	0.10 ± 0.04	0	0.0132
C. leptophyllum	0.35 ± 0.07	0	<0.0001
C. viscidiflorus	0.05 ± 0.03	0.10 ± 0.10	0.6311
C. canadensis	0.36 ± 0.07	0	<0.0001
D. pinnata	1.27 ± 0.11	0.02 ± 0.02	<0.0001
E. wawawaiensis	3.78 ± 0.58	0.54 ± 0.13	<0.0001
E. nauseosa	2.69 ± 0.23	1.79 ± 0.19	0.0008
E. piperianus	0.02 ± 0.02	0	0.3182
E. pumilus	0.03 ± 0.02	0	0.1569
E. cicutarium	0.47 ± 0.08	0	<0.0001
L. ramosissima	0.05 ± 0.03	0.02 ± 0.02	0.3158
M. canescens	27.9 ± 0.98	1.35 ± 0.14	<0.0001
M. officinalis	3.00 ± 0.77	0	<0.0001
P. ampla	0.40 ± 0.12	0.03 ± 0.02	0.0038
P. bulbosa	0.47 ± 0.08	1.20 ± 0.14	<0.0001
P. secunda	0.73 ± 0.10	0.99 ± 0.10	0.0631
P. canescens	0.04 ± 0.02	0	0.1569
S. kali	6.30 ± 0.48	1.41 ± 0.10	<0.0001
S. altissimum	2.10 ± 0.12	0	<0.0001
S. paniculata	0.31 ± 0.07	0	<0.0001
T. dubius	0.09 ± 0.04	0	0.0241
V. bracteata	0.23 ± 0.06	0	0.0002
V. microstachys	0	0.02 ± 0.02	0.3182

Cover was determined on both sections of the barrier surface in 2011 (Table J.8). Only 13 species were observed. Cover of five species was very low and not significantly different from zero. Six of 13 species had significantly greater cover on the burned section of the surface compared with the unburned section. *Artemisia tridentata* cover was significantly greater than zero 3 years after the fire on the burned section of the surface. *Bromus tectorum* cover was significantly greater on the burned section of the surface than on the unburned section. *Ericameria nauseosa* cover was significantly greater on the burned section than on the unburned section of the surface. *Machaeranthera canescens* cover was highly significant at 28% on the burned section of the surface and much greater than on the unburned section of the surface.

These results indicate that vegetation can naturally recover from fire under the conditions of the test. Dominance by *M. canescens* after the fire, in part, takes over the role of *A. tridentata* with respect to minimizing infiltration risk.

Table J.8. Mean percent cover (± 1 SEM) of plant species and other categories observed in 2011 on the burned and unburned sections of the barrier. Statistically significant differences between burned and unburned sections are set at $p <= 0.05$.

Species/categories	Barrier burn	Barrier unburned	*p*
A. millifolium	0.1 ± 0.04	0	0.0132

Species/categories	Barrier burn	Barrier unburned	*p*
A. tridentata	1.27 ± 0.1	28.5 ± 1.2	<0.0001
B. tectorum	4.43 ± 0.43	1.28 ± 0.2	<0.0001
C. viscidiflorus	0.02 ± 0.02	0	0.3182
E. wawawaiensis	5.21 ± 0.82	0.17 ± 0.05	<0.0001
E. nauseosa	1.98 ± 0.25	0.36 ± 0.15	<0.0001
E. pumilus	0.02 ± 0.02	0	0.3182
M. canescens	28 ± 1.04	0.16 ± 0.05	<0.0001
P. ampla	0.12 ± 0.04	0	0.0073
P. bulbosa	0.02 ± 0.02	0.05 ± 0.03	0.3156
P. secunda	0.26 ± 0.06	0.28 ± 0.07	0.8499
S. altissimum	0.03 ± 0.02	0	0.1569
V. microstachys	0.03 ± 0.02	0.1 ± 0.1	0.5169

J.3.5 Cover on the Barrier Side Slopes

The side slopes and the surface were hydroseeded in late 1994 at the same time. The same perennial grass seed mix that was applied to the surface was applied to the side slope. The primary difference between the side slope and the surface is soil texture. The side slope is gravel and the upper surface is a silt-pea gravel admixture as previously described.

After construction, vegetative cover was greatest at the toe of the side slope, decreasing toward the top of the slope (Figure J.10). Annual or biennial species had the largest cover, nearly 30% at the toe, but less than 10% elsewhere. Perennial grass cover was less than 10% at all locations, with the greatest cover occurring at 10, 20, and 30 m from the toe. Litter cover was substantial (near 70%), only at the toe, and less than 10% elsewhere. Bare ground cover was near 15% at the toe, gradually rising to more than 90% at the top. Combined vegetation and litter cover was the greatest at the toe, gradually decreasing toward the top. The combination cover was nearly 30% at 10 and 20 m from the toe (Ward et al. 1997).

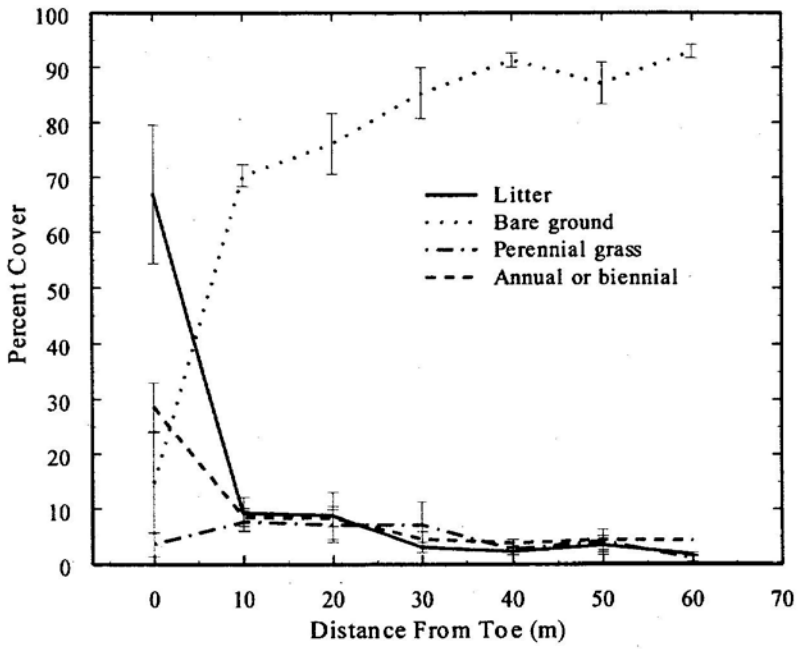

Figure J.10. Percent cover of litter, bare ground, and perennial grasses plus annual or biennial plant species on the west-facing side slope. Error bars are 1 SEM based on five replicates. Figure taken from Ward et al. (1997).

The greater cover of vegetation at the toe may be due to location, relative to the surrounding seed sources. The annual or biennial species found near the toe were primarily *B. tectorum* and *S. kali* that were also found near the toe, but outside the assessment area. The toe also may be more conducive to plant establishment because of greater litter cover. This litter contains seeds and will aid in establishment by protecting germinating seeds from desiccation (drying out). Very little litter cover was found further up the slope. More vegetative cover was also observed in the areas on the gravel slope where silt had been inadvertently distributed during construction. These areas have only a very thin layer of silt that is enough to support vegetative establishment. This assertion has not been tested (Ward et al. 1997).

In 2007, cover on the north and west side slopes was relatively uniform, thus data were combined (Figure J.11). Rock cover was much greater than cover of other classes while cover of shrubs and grasses were similar (Ward et al. 2007).

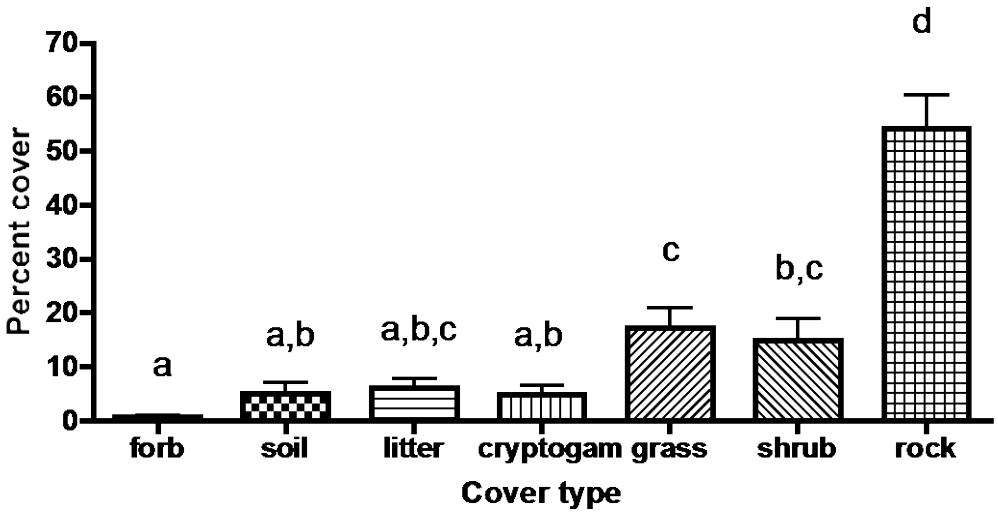

Figure J.11. Mean cover on the north and west side slopes of the barrier in 2007. Error bars are 1 SEM. Different letters indicate significant differences. After Figure 3.10 of Ward et al. (2009a).

In 2009, cover on the north and west side slopes was relatively uniform, thus data were combined (Figure J.12). Rock cover was much greater than cover of other classes while cover of shrubs and grasses were similar, but lower than in 2007.

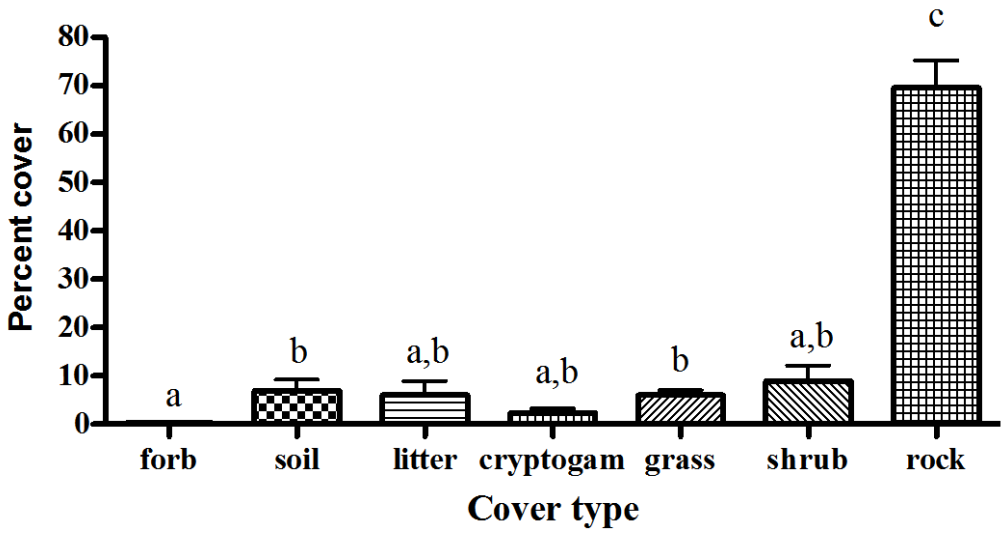

Figure J.12. Mean cover on the north and west side slopes of the barrier in 2009. Error bars are 1 SEM. Different letters indicate significant differences.

In 2010 cover on the side slopes (Table J.9) was the same on north- and west-facing slopes for most categories. *Bromus tectorum* and *P. secunda* cover was significantly greater on the north slope than on the west slope. Gravel cover was significantly less on the north slope than on the west slope.

Table J.9. Mean percent cover (± 1 SEM) of plant species and other categories observed in 2010 on the north and west side slopes of the barrier. Statistically significant differences between the north and west side slopes are noted by $p <= 0.05$.

Species/categories	North	West	*p*
Ambrosia acanthicarpa	0	0.02 ± 0.02	0.3282
Bromus tectorum	13.6 ± 3.05	5.22 ± 1.71	0.0124
Centaurea diffusa	0	0.5 ± 0.5	0.3282
Chrysothamnus viscidiflorus	0	0.02 ± 0.02	0.3282
Elymus wawawaiensis	3.17 ± 1.55	3.58 ± 2.71	0.8174
Epilobium brachycarpum	0.02 ± 0.02	0	0.3282
Ericameria nauseosa	16.8 ± 6.77	9.47 ± 4.59	0.2391
Holosteum umbellatum	0.03 ± 0.02	0	0.1522
Machaeranthera canescens	0	0.17 ± 0.17	0.3282
Poa bulbosa	0	0.05 ± 0.04	0.1591
Poa secunda	1.83 ± 1.14	0.1 ± 0.07	0.0379
Salsola kali	0.05 ± 0.03	0.25 ± 0.14	0.2625
Gravel	39.1 ± 9.92	71.6 ± 8.80	0.0228
Litter	18.3 ± 5.29	9.75 ± 4.41	0.1288
Soil	8.73 ± 6.17	1.7 ± 0.97	0.1694
Soil cryptogams	3.92 ± 1.10	5.55 ± 2.94	0.7561

In 2011, cover on the side slopes (Table J.10) was the same on north- and west-facing slopes for most categories. *Bromus tectorum* cover was significantly greater on the north slope than on the west slope. Gravel cover was significantly less on the north slope than on the west slope. Litter was significantly greater on the north slope than on the west slope.

There were differences in species composition in the sample plots between 2010 and 2011. This was found for low cover species and it is likely that species composition differences are by chance with location of plots. There has been no effort to sample the same physical location across the years.

The relatively low vegetative and high gravel cover on the side slopes likely reduces the risk of fire being carried across the side slopes, reducing fire risk for the barrier surface. This was noted while shrubs were ignited on the side slope during the fire test in 2008. Fire did not carry across the side slope. Vegetation on the side slopes provides seed for naturally populating the barrier surface.

Table J.10. Mean percent cover (± 1 SEM) of plant species and other categories observed in 2011 on the north and west side slopes of the barrier. Statistically significant differences between the north and west side slopes are noted by $p <= 0.05$.

Species/categories	North	West	p
Artemisia tridentata	0	2.67 ± 2.67	0.3282
Bromus tectorum	14.1 ± 3.45	4.50 ± 1.30	0.0164
Elymus wawawaiensis	1.67 ± 0.84	0.83 ± 0.41	0.3803
Ericameria nauseosa	16 ± 5.56	7.83 ± 5.58	0.3159

Species/categories	North	West	p
Holosteum umbellatum	0.02 ± 0.02	0.005 ± 0.003	0.4359
Poa secunda	2.83 ± 2.65	0.08 ± 0.08	0.3116
Salsola kali	0.002 ± 0.002	0.04 ± 0.04	0.3479
Vulpia microstachys	0.002 ± 0.002	0	0.3282
Gravel	41.6 ± 9.60	70.9 ± 9.09	0.0375
Litter	17 ± 4.55	4.25 ± 1.58	0.0147
Soil	6.06 ± 3.65	6.71 ± 6.16	0.9287
Soil cryptogams	6.39 ± 3.76	4.79 ± 3.66	0.7633

J.3.6 Analog Community Comparisons with the Barrier Surface

Species richness of the two McGee Ranch analog sites was essentially the same as at the unburned section of the barrier (Table J.11). Species richness of the burned section of the barrier was much greater than at the other three sites. The percent of perennials observed in the flora decreased from 69% at the unburned McGee Ranch site (Fig. J.13) and 56% at the burned (fire in 1996) McGee Ranch site (Fig. J.14) to 47% at the unburned barrier surface and only 38% at the burned barrier surface.

Figure J.13. Unburned mature plant community at McGee Ranch.

Figure J.14. Old burned plant community at McGee Ranch. The fire occurred in 1996.

Jaccard similarity values indicate that the old burn McGee Ranch site is more similar to the unburned McGee Ranch site than to either the unburned or burned sections of the barrier surface. The unburned barrier section is more similar to the McGee Ranch old burn site than is the burned section of the barrier. Finally, the two sections of the barrier are much more similar to each other than any other comparison (Table J.11).

Table J.11. Plant species observed in 2009 on the burned and unburned sections of the barrier and at the two McGee Ranch analog sites.

Family *Species*	**Barrier burned**	**Barrier unburned**	**McGee old burn**	**McGee unburned**
Asteraceae				
A. millifolium	1			
A. tridentata	1	1	1	1
Balsamorhiza careyana			1	
C. diffusa	1	1	1	
C. viscidiflorus	1	1		
C. atribarba				1
E. nauseosa	1	1	1	
E. filifolius				1
E. piperianus				1
E. poliospermus				1
H. cusickii			1	1

Family *Species*	**Barrier burned**	**Barrier unburned**	**McGee old burn**	**McGee unburned**
L. serriola	1			
M. canescens	1	1	1	1
S. paniculata	1			
T. dubius	1		1	
Boraginaceae				
A. lycopsoides	1	1		
Brassicaceae				
D. pinnata	1		1	1
S. altissimum	1	1	1	
Chenopodiaceae				
C. leptophyllum	1			
G. spinosa				1
S. kali	1	1	1	1
Fabaceae				
A. caricinus	1			
M. officinalis	1			
Geraniaceae				
E. cicutarium	1	1		
Malvaceae				
S. munroana			1	1
Poaceae				
A. hymenoides			1	1
B. tectorum	1	1	1	1
E. elymoides			1	1
E. wawawaiensis	1	1		
P. ampla	1	1		
P. bulbosa	1	1		
P. secunda	1	1	1	1
V. microstachys	1	1		1
Polemoniaceae				
P. longifolia			1	
Verbenaceae				
V. bracteata	1			
Number of Species Present	**24**	**15**	**16**	**16**
Number of Annuals/biennials	**15**	**8**	**7**	**5**
Number of Perennials	**9**	**7**	**9**	**11**
Jaccard similarity coefficient	**0.184**	**0.208**	**0.478**	**B**
	0.278	**0.348**	**B**	

Family *Species*	**Barrier burned**	**Barrier unburned**	**McGee old burn**	**McGee unburned**
	0.652	**B**		

Cover of eight species at all four sites was very low and not significantly different from zero (Table J.12). Cover of *A. tridentata* was 37% greater on the unburned section of the barrier than at the unburned McGee Ranch site. *Bromus tectorum* cover was significantly greater at the McGee Ranch old burn site than at the other three sites, which were all statistically the same. Cover of *H. cusickii* was about 10% at the McGee Ranch old burn site and over 4% at the unburned McGee Ranch site. None occurred at the barrier. Cover of *M. canescens* was the greatest at the McGee Ranch old burn site and significantly greater than at the three other sites. *Poa secunda* cover was substantially greater at the two McGee Ranch sites than at the two barrier sites. *Salsola kali* cover was significantly greater at the barrier burn site than at the other three sites. *Sisymbrium altissimum* cover was the same at both burned sites and both sites had significantly greater cover than the two unburned sites. Grass cover was substantially greater at the two McGee Ranch sites than at the two barrier sites. Forb cover was substantially greater at the two burned sites than at the unburned sites. The McGee Ranch unburned site had significantly more forb cover than the unburned portion of the barrier. Soil cryptogams had the greatest cover at the unburned McGee Ranch site, less at the unburned barrier site, less at the McGee Ranch old burn, and none at the barrier burn site. All sites were significantly different from one another. Litter cover was the greatest at the McGee Ranch old burn and barrier unburned sites, which were not significantly different. Litter cover was mid-range at the McGee Ranch unburned site and significantly greater than at the barrier burn site, which had the lowest cover. Rock cover was significantly greater at the burned barrier site than at the unburned barrier site and both were significantly greater than at the two McGee Ranch sites. Bare ground was the greatest at the burned barrier site and significantly greater than at the other three sites, which had similar bare cover.

These results indicate that efforts to mimic natural processes that may allow similarity to be achieved between a manipulated site and its natural analog did not occur. The soils for the barrier surface were taken from McGee Ranch. Initial revegetation efforts were not able to acquire or propagate a majority of native species found at the unburned McGee Ranch site, which likely resulted in little similarity between the unburned McGee Ranch site and the barrier surface 17 years after planting. The planting of a higher density of *A. tridentata* than occurs naturally caused barrier plant community dynamics to become dominated by *A. tridentata*, excluding the establishment of a more diverse plant community such as occurs at the McGee Ranch unburned site. The characteristics of the McGee Ranch old burn site may be realized on the barrier burned surface after several more years. This is of concern given that cover of *B. tectorum* is 39.4% at the McGee Ranch old burn site. Prediction of plant community dynamics is difficult.

Table J.12. Mean cover (± 1 SEM) of plant species and other categories observed in 2009 on the burned and unburned sections of the barrier and at two McGee Ranch analog sites. Comparisons with differing letters are significantly different.

Species/categories	**Barrier burned**	**Barrier unburned**	**McGee old burn**	**McGee unburned**
A. millifolium	0.02 ± 0.02 a	0 a	0 a	0 a
A. hymenoides	0 a	0 a	1.19 ± 0.72 b	0.71 ± 0.25 ab
A. lycopsoides	0.09 ± 0.04 a	0.02 ± 0.02 a	0 a	0 a
A. tridentata	0.35 ± 0.12 a	30 ± 1.12 b	0.36 ± 0.2 a	21.9 ± 2.53 c
B. tectorum	1.53 ± 0.1 a	1.06 ± 0.1 a	39.4 ± 5.71 b	4.88 ± 1.1 a
C. diffusa	0.05 ± 0.03 a	0 a	0 a	0 a

Species/categories	Barrier burned	Barrier unburned	McGee old burn	McGee unburned
C. leptophyllum	0.16 ± 0.05 a	0 ab	0 ab	0 ab
C. viscidiflorus	0.02 ± 0.02 a	0.1 ± 0.1 a	0 a	0 a
C. atribarba	0 a	0 a	0 a	0.24 ± 0.16 a
D. pinnata	0.07 ± 0.03 a	0 a	0.24 ± 0.16 a	0.83 ± 0.26 b
E. elymoides	0 a	0 a	0.36 ± 0.2 a	1.55 ± 0.27 b
E. wawawaiensis	1.84 ± 0.39 a	0.3 ± 0.07 b	0	0
E. nauseosa	1.09 ± 0.1 a	0.19 ± 0.11 b	0.12 ± 0.12 b	0 b
E. filifolius	0 a	0 a	0 a	0.36 ± 0.2 a
E. cicutarium	0.02 ± 0.02 a	0.02 ± 0.02 a	0 a	0 a
G. spinosa	0 a	0 a	0 a	0.12 ± 0.12 a
H. cusickii	0 a	0 a	10.8 ± 2.83 b	4.64 ± 1.32 b
M. canescens	1.11 ± 0.14 a	0.05 ± 0.03 b	3.1 ± 1.12 c	0.6 ± 0.24 ab
M. officinalis	1.56 ± 0.37 a	0 b	0 b	0 b
P. ampla	0.03 ± 0.02 a	0.19 ± 0.06 b	0	0
P. bulbosa	0 b	0.12 ± 0.04 a	0 ab	0 ab
P. secunda	0.07 ± 0.03 a	0.16 ± 0.05 a	18 ± 2.66 b	15.4 ± 1.88 b
S. kali	19.5 ± 0.86 a	0 b	2.02 ± 0.7 b	0.12 ± 0.12 b
S. altissimum	2.1 ± 0.23 a	0.31 ± 0.07 b	2.86 ± 1.14 a	0 b
S. munroana	0 a	0 a	0.12 ± 0.12 a	1.31 ± 0.28 b
T. dubius	0.03 ± 0.02 a	0 a	0.6 ± 0.24 b	0 a
V. microstachys	0.03 ± 0.02 a	0.03 ± 0.02 a	0 a	0.6 ± 0.24 b
Grass	3.51 ± 0.42 a	1.86 ± 0.18 b	58.9 ± 4.88 c	23.1 ± 1.82 d
Shrubs	1.46 ± 0.16 a	30.3 ± 1.13 b	0.48 ± 0.22 a	22 ± 2.57 c
Forbs	24.7 ± 0.97 a	0.4 ± 0.1 b	19.8 ± 2.19 a	8.1 ± 1.4 c
Soil cryptogams	0 a	28.3 ± 1.63 b	6.79 ± 1.98 c	42.6 ± 3.57 d
Litter	7.95 ± 0.52 a	45.3 ± 1.7 b	53.1 ± 4.72 b	28 ± 2.19 c
Soil	76.6 ± 1.09 a	25.5 ± 1.22 b	40.5 ± 4.59 c	19.3 ± 1.98 b
Rock	15 ± 0 a	12.1 ± 0.44 b	2.26 ± 0.16 c	2.5 ± 0 c
Bare ground	76.6 ± 1.09 a	53.8 ± 2.06 b	47.3 ± 5.22 b	61.9 ± 3.47 b

Soil cryptogam composition (Table J.13) varied widely at the four study sites. There were no soil cryptogams observed on the burned surface of the barrier. There was only one soil lichen found at the McGee Ranch old burn site. The unburned section of the barrier surface had 7 species and the unburned McGee Ranch site had 12 species. Soil cryptogams stabilize soil surfaces, reducing the risk of erosion. The diversity of soil cryptogams on the unburned portion of the barrier had not yet achieved that of the McGee unburned area by 2011.

Table J.13. Lichens and mosses occurring on soils of the barrier surface and at the burned and unburned McGee Ranch analog communities.

Lichens	Barrier Unburned	McGee Old Burn	McGee Unburned
Acarospora schleicheri (Ach.) A. Massal.		*	
Caloplaca tominii Savicz	*		*
Candelaria concolor (Dickson) Stein	*		
Candelariella terrigena Rasanen	*		*
Cladonia pyxidata (L.) Hoffm.			*
Lecanora muralis (Schreb.) Rabenh.			*
Physconia enteroxantha (Nyl.) Poelt			*
Physconia isidiigera (Zahlbr.) Essl.	*		*
Psora globifera (Ach.) Mass.			*
Psora luridella (Tuck.) Fink	*		*
Trapeliopsis steppica McCune & Camacho			*
Mosses			
Bryum argenteum Hedw.			*
Bryum cf *caespiticium* Hedw. (sterile)	*		*
Syntrichia ruralis var. *papillosissima* (Copp.) Loeske.	*		*

Shrub density varied among the four study sites (Table J.14). *Artemisia tridentata* density was very low and was the same after the barrier burn and at the McGee old burn site. Density was significantly greater at the unburned area on the barrier than at the McGee Ranch unburned analog site. *Ericameria nauseosa* established in significant, but still low, numbers after the fire on the barrier surface. This shrub and the other shrubs were present only in low numbers (Table J.14).

Table J.14. Mean shrub density (plants m^{-2}) ± 1 SEM.

	Site			
Species	Barrier burn	Barrier unburned	McGee old burn	McGee unburned
Artemisia tridentata	0.0146 ± 0.00539 a	0.77 ± 0.0121 b	0.0147 ± 0.00308 a	0.437 ± 0.0331 c
Ericameria nauseosa	0.113 ± 0.0127 a	0.00386 ± 0.00202 b	0.00125 ± 0.00051 b	0
Chrysothamnus viscidiflorus	0	0.0107 ± 0.00609	0	0
Grayia spinosa	0	0	0	0.00126 ± 0.00126

Shrub density varied by size and age class among the four sites (Table J.15). At the McGee unburned site about 79% of the shrubs were old while 96% were old on the barrier unburned site. This indicates that the shrubs, while reproducing, were not reproducing at the rate found at the mature plant community. The shrubs in the unburned section of the barrier likely will die faster than they are recruited until the density of large shrubs is closer to that in the mature community. When density has been sufficiently reduced, it is likely that the *A. tridentata* population will achieve a more natural size and age distribution. The population distribution at the McGee Ranch old burn site has 32% of individuals that are large and/or old.

This distribution may be partly a consequence of an incomplete burn leaving a few old plants. Shrubs were not cut to age them, but were assumed to be old. After the burn on the barrier surface a significant number of shrubs germinated from the seed bank and/or from seed that arrived at the site. *A. tridentata* was observed in the seed bank, so it is likely that those found on the burned barrier surface are from the seed bank. *Artemisia tridentata* seed is not wind-borne. In contrast, while 88% of the new shrubs on the burned barrier surface were *E. nauseosa*, none were found in the seed bank. If they were in the seed bank, they may not have had the appropriate conditions to germinate. It is possible that these new recruits arrived from nearby plants that released wind-borne seed after the fire. While there were few *E. nauseosa* plants in the adjacent unburned barrier surface, there were numerous shrubs on the adjacent side slopes that could be the source of the new recruits on the burned surface.

Table J.15. Mean size/age density (plants m^{-2}) ± 1 SEM of *A. tridentata* at the four study sites.

	Site			
Size/age class	Barrier burn	Barrier unburned	McGee old burn	McGee unburned
Large/old	0	0.743 ± 0.0104	0.00469 ± 0.00139	0.344 ± 0.0304
Mid-size	0	0.027 ± 0.00712	0.00781 ± 0.00164	0.0688 ± 0.0125
Small/young	0.0146 ± 0.00539	0	0.00218 ± 0.00148	0.0238 ± 0.00615

J.3.7 Seed Banks

The seed bank of *A. tridentata* was very large at the McGee Ranch old burn site and significantly larger than that of the two barrier observations before and after the fire (Table J.16). The fire had no effect on the *A. tridentata* seed bank. The most interesting observation is emergence of *A. tridentata* from the seed bank after the fire, which suggests that this dominant shrub will return after fire. This observation is in contrast to the general belief that *A. tridentata* does not recover after fire. There was no re-sprouting after the fire.

The seed bank of *A. hymenoides* was significantly greater than zero at the McGee Ranch unburned site and was the same as that for the McGee Ranch old burn site (Table J.16). The seed bank of *B. tectorum* was very large at the McGee Ranch old burn site and significantly larger than that observed on the two barrier surfaces before and after the fire. The fire had no effect on the *B. tectorum* seed bank, although variation was high before the burn. The *D. pinnata* seed bank was very large at the unburned McGee Ranch site and significantly greater than at the McGee Ranch old burn site, which was significantly greater than the seed bank before the burn. There was a significant *E. elymoides* seed bank at the McGee Ranch unburned site, which was significantly greater than zero. The *E. wawawaiensis* seed bank was highly variable before and after the fire, and thus was not significantly greater than zero. The *M. canescens* seed bank was highly variable before the burn and at the McGee Ranch old burn site and thus was not significantly different from zero. No seeds emerged from the other two conditions. The *P. bulbosa* seed (propagule) bank was significantly different from zero only before the burn on the barrier. The *S. kali* seed bank was the greatest at the McGee Ranch old burn site, which was significantly greater than at the McGee Ranch unburned site. There was no seed bank on the barrier surface. The *S. altissimum* seed bank was the greatest at the McGee Ranch old burn site, which was significantly greater than at the McGee Ranch unburned site. The seed bank on the barrier surface was not significantly different from zero. The *V. bracteata* seed bank was significantly greater than zero after the burn, but was not significantly different from that before the burn. The *V. microstachys* seed bank at the McGee Ranch unburned site was the largest of all species and significantly greater than the McGee Ranch burned site. The species was not present in the barrier seed bank.

When emerged seedlings of all species were combined in each experimental unit for the high (n = 17) and low (n = 19) fuel load areas on the barrier surface there was no significant (p = 0.86) effect of fire

intensity on seedling density. There were 48.2 ± 12.7 seedlings m^{-2} in the high fuel load area and 57.9 ± 24.3 seedlings m^{-2} in the low fuel load area. When high and low fuel samples were combined, there was no significant (p = 0.76) effect of the fire on seedling density. There were 51.7 ± 10.8 seedlings m^{-2} (n = 36) before the fire and 50.6 ± 13.9 seedlings m^{-2} (n = 36) after the fire.

There was no difference in the number of species emerging from the seed bank before and after the fire on the barrier (Table J.16). The number of species in the seed bank of the four sets of observations ranged from 8 to 11. The percent of the flora that is perennial was similar for the four sets of observations and ranged from 33% to 40%.

The Jaccard similarity index is the greatest for the two McGee Ranch sites. The index is very low when comparing the two barrier burn assessments with the unburned McGee Ranch site or the old burn McGee Ranch site. The two burn conditions on the barrier had mid-range similarity (Table J.16).

The seed bank comparisons reflect the results for the vegetation comparisons for the barrier and the McGee Ranch sites. The barrier is not similar to the two McGee Ranch sites, which are more similar to each other. There was no effect other than a reduction in the seed bank of *P. bulbosa* after the fire on the barrier. This indicates that a fire on a barrier surface will not affect the potential vegetative recovery arising from the seed bank under the conditions of the test.

Table J.16. Presence and mean seedling density (plants m^{-2}) ± 1 SEM of species emerging from the seed bank before and after the fire on the barrier surface and at the two McGee Ranch analog sites. Comparisons with differing letters are significantly different

Species	Barrier After Burn (n = 36)	Barrier Before Burn (n = 36)	McGee Old Burn (n = 36)	McGee Unburned (n = 36)
A. hymenoides	0*b*	0*b*	3.89 ± 1.92*a,b*	6.67 ± 2.11*a*
A. tridentata	5.56 ± 3.25*b*	1.67 ± 0.934*b*	175 ± 83.8*a*	21.1 ± 7.68*a,b*
B. tectorum	1.11 ± 0.774*c*	24.4 ± 9.05*b,c*	139 ± 38.5*a*	56.7 ± 17.4*b*
D. pinnata	0*a*	2.22 ± 1.33*a*	59.4 ± 19.9*b*	201 ± 35.1*c*
E. elymoides	0*a*	0*a*	4.44 ± 2.41*a,b*	9.44 ± 3.42*b*
E. wawawaiensis	13.9 ± 13.3*a*	4.44 ± 3.91*a*		
E. cicutarium	1.67 ± 1.23*a*	0*a*	0*a*	0*a*
H. umbellatum	3.89 ± 3.36*a*	0.56 ± 0.56*a*	0.56 ± 0.56*a*	18.9 ± 6.32*b*
L. serriola	0*a*	2.78 ± 1.81*a*	0*a*	0*a*
M. canescens	0*a*	2.78 ± 1.81*a*	26.1 ± 25.0*a*	0*a*
P. bulbosa	1.11 ± 0.774*a*	3.89 ± 1.56*b*	0*a*	0*a*
S. kali	0	0	80 ± 35*a*	12.8 ± 5.53*b*
S. altissimum	3.33 ± 2.03*b,c*	0*c*	41.7 ± 9.41*a*	12.2 ± 3.50*b*
S. munroana	0*a*	0*a*	0.56 ± 0.56*a*	2.22 ± 1.33*a*
V. bracteata	10 ± 3.69*a*	3.89 ± 1.34*a,b*	0*b*	0*b*
V. microstachys	0	0	8.89 ± 3.86*a*	473 ± 111*b*
Number of Annuals/biennials	5	6	7	6
Number of Perennials	3	3	4	4
Number of Species	8	9	11	10

Species	Barrier After Burn (*n* = 36)	Barrier Before Burn (*n* = 36)	McGee Old Burn (*n* = 36)	McGee Unburned (*n* = 36)
Jaccard similarity coefficient	0.286	0.267	0.909	B
	0.267	0.333	B	
	0.545	B		

Seedling density was very high under *A. tridentata* canopies in the old burn area (Table J.17). There were few *A. tridentata* plants in the area, but they likely produce large amounts of seed given that there is little competition for water. Competition by the dominant *B. tectorum* likely restricts rapid establishment of *A. tridentata.* At the unburned site, *A. tridentata* was much more common across sample sites, but seedling numbers were low. It is likely that low amounts of seed are produced for each individual plant given that they are common at the site and likely compete with each other for water. *Bromus tectorum* was very common under *S. kali* canopies at the old burn site and was significantly denser than in other conditions other than under *A. tridentata.* There was little effect of condition on *B. tectorum* seedling density at the unburned site. There was little effect of condition at either analog site for *D. pinnata*. The seed bank for *P. secunda* was similar across conditions at both analog sites. The only significant effect was much greater density under bunchgrass canopies that in the bare swales at the unburned site. *Salsola kali* seedling density was significantly greater under its canopy than in any of the other conditions at both sites. *Sisymbrium altissimum* was evenly distributed among the conditions at both sites.

These results provide an assessment of how existing analog communities potentially can reproduce. Even though the barrier plant communities currently are not like the analog communities, it is possible that they will become more similar in time. A potential risk should be recognized with respect to *S. kali* as a nurse plant for *B. tectorum. Salsola kali* appears to protect or encourage germination of *B. tectorum* in large numbers compared with other conditions at the burned analog site. Given that *S. kali* accumulates along the edges of the barrier, getting caught in *A. tridentata* canopies, it is possible the *B. tectorum* will more easily establish along the edges.

Table J.17. Mean seedling density (± 1 SEM) from the seed bank at six conditions at the two McGee Ranch analog sites (b = old burn, u = unburned).

Species	trt	Under *S. kali*	Under *A. tridentata*	Bunchgrass	Hummock	Cryptogamic swale	Bare swale
A. tridentata	b	0a	1040 ± 339b	0a	0a	0a	10 ± 6.83a
	u	10 ± 6.83a	56.7 ± 38.8a	0a	6.67 ± 4.22a	6.67 ± 6.67a	46.7 ± 16.9a
B. tectorum	b	463 ± 138a	193 ± 104ab	93.3 ± 25.6b	63.3 ± 40.5b	13.3 ± 8.43b	6.67 ± 4.22b
	u	40 ± 25.8ab	76.7 ± 61.4ab	147 ± 68.1a	50 ± 30.4ab	26.7 ± 12.3ab	0b
D. pinnata	b	50 ± 26.2ab	3.33 ± 3.33b	20 ± 12.6ab	217 ± 96.8a	26.7 ± 12.3ab	40 ± 11.5ab
	u	117 ± 28a	113 ± 38.5a	360 ± 138a	270 ± 74.1a	227 ± 76.9a	120 ± 93.2a
P. secunda	b	26.7 ± 19.8a	10 ± 4.47a	10 ± 10a	3.33 ± 3.33a	3.33 ± 3.33a	0 ± 0a
	u	357 ± 104ab	420 ± 151ab	967 ± 383a	773 ± 455ab	287 ± 127ab	36.7 ± 15.8b
S. kali	b	387 ± 164a	13.3 ± 13.3b	26.7 ± 16.1b	33.3 ± 29.5b	16.7 ± 16.7b	3.33 ± 3.33b
	u	66.7 ± 22.9a	0b	3.33 ± 3.33b	6.67 ± 6.67b	0b	0b
S. altissimum	b	100 ± 44.1a	20 ± 10.3ab	13.3 ± 6.67b	40 ± 11.5ab	46.7 ± 18.4ab	30 ± 13.4ab
	u	36.7 ± 14.1a	6.67 ± 4.22a	3.33 ± 3.33a	6.67 ± 4.22a	6.67 ± 4.22a	13.3 ± 9.89a

J.4 Discussion

The PHB has been effective in preventing drainage since its inception, under the stress of three times normal precipitation, and after a fire sharply reduced vegetative cover through 2009 (Ward et al. 2010). Concerns remain and are associated with the risk of gross changes to the vegetative cover. A plant community dominated by, or with significant patches of the barrier surface dominated by, shallow-rooted *B. tectorum* (cheatgrass) may increase the risk of failure. The risk of failure associated with even patchy dominance by *B. tectorum* is based on increased soil water storage recorded in October 1974 below its rooting depth on similar soils (Cline et al. 1977). Concerns have been raised (Albright et al. 2004; Hauser et al. 2001; Seyfried et al. 2005) about failure because of the uncertainty associated with the direction of plant community succession. Here we discuss detailed observations on plant community dynamics at the PHB and associated analog sites located nearby at McGee Ranch on the same soils used to construct the barrier surface. The relationship between initial vegetation and persistent climax species, which is one of the concerns discussed by Albright et al. (2004), is discussed, along with the long-term dynamics of species composition and cover on the barrier as affected by initial enhanced precipitation and a later fire. These responses are compared with those documented recently at the McGee Ranch analog site that had experienced a fire in 1996. The likelihood that *B. tectorum* will gain dominance on the barrier surface in patches is assessed and possible strategies to minimize these risks are provided.

J.4.1 Plant Establishment and Survivorship

The initial vegetation on the barrier surface was a combination of planted shrub seedlings, seeded grasses, and species that arrived by uncontrolled seed transport. The much greater survivorship of *A. tridentata* compared with *E. nauseosa* reflects the differential competitive characteristics of these two species. *Ericameria nauseosa* is an early seral species (Wagner et al. 1978). Its survival rate of only 38% in comparison with 97.6% survival of *A. tridentata* after three seasons demonstrates its rapid rate of decline when under significant competitive stress. As an early seral species, it increased cover early on the north section of the surface after the burn and significantly more so than *A. tridentata* in 2010. In 2011, cover of both species decreased and was no longer significantly different. In contrast, *A. tridentata* rapidly became the dominant species on the surface after planting and likely is the reason that seeded bunchgrass cover declined even when grasses had high initial cover on the north section of the surface in the first 3 years after planting. *Artemisia tridentata* is recognized as a late-to-mid seral species in the shrub-steppe (Daubenmire 1970).

The only seeded grass to establish in significant numbers was *E. wawawaiensis,* and only on the north section of the surface. The two seeded *Poa* species (*Poa ampla* has been grouped with *Poa secunda*, but the two grasses as seeded are substantially different in size and for this analysis seen functionally as separate species) are present on both the north and south sections of the surface, but in very small numbers.

Many species arrived at the surface in 1995 as a result of uncontrolled seed transport. This effect was significant because *S. kali* dominated the surface in the first summer after planting and then quickly became a minor component of the surface (Gee et al. 1996). This species is an early invader on disturbed soils and becomes only a minor component after the perennial species become established (Allen and Allen 1988).

While the other species that arrived in the first summer do not have classically defined wind-transported seed, this analysis assumed that seed was transported by vehicles and potentially dust devils that may have lifted seeds with the soil and deposited them. While it is possible that some species were incorporated onto the surface with the transported soil, this is felt be a minor contribution because the

soils for the surface were sub-soils (at least 1 m below the surface) and are not likely to contain many seeds. Most seeds in the soil bank in the shrub-steppe are within 2 cm of the surface (Kemp 1989).

The relationship between initial vegetation and persistent climax species at the barrier surface was driven by the large number of *A. tridentata* seedlings planted on the surface. This species rapidly became dominant and was the persistent climax species at least through the first 16 years of the barrier. A reduction in percent cover to 28.5 ± 1.2% on the unburned south section of the surface in 2011 to levels similar to the unburned McGee Ranch analog site (21.9 ± 2.53%) observed in 2009. The reductions may be associated with losses due to insect galls and poor seed production. Significant damage associated with gall formation and low recruitment from local seed (data not presented) with the planted *A. tridentata* on the barrier was observed. With continued reductions in *A. tridentata* cover, it is possible that the community will become similar to that at the McGee unburned site, which is classified as an *A. tridentata/P. secunda* association (Daubenmire 1970), although it would take a long time given the small populations of *P. secunda* on the surface. It is also possible that after the burn the community will become an *A. tridentata/B. tectorum* association given that cover of *B. tectorum* increased after the fire from near zero (Ward et al. 2009) to 4.43 %. It is possible that *B. tectorum* can increase its cover and become a significant component of the climax community. The *B. tectorum* cover at the unburned McGee Ranch community was 4.88 %, but was 39.4% at the McGee Ranch burned site. While there is no detailed knowledge of *B. tectorum* cover at the McGee Ranch burned site before the fire, it has been recognized that fires tend to increase *B. tectorum* cover, especially if an ecosystem already has significant *B. tectorum* cover and a patchy or discontinuous perennial component (Whisenant 1990). The long-term persistent climax species can be *B. tectorum* that is associated with decadent stands of *A. tridentata* in the shrub-steppe (Daubenmire 1970; Howard 1999). This climax association occurs at the Hanford Site, especially in areas that have been heavily disturbed. Continued monitoring is needed at the barrier to determine if *B. tectorum* cover continues to increase.

J.4.2 Long-term Dynamics of Species Composition and Cover on the Barrier

Plant species composition and richness was highly variable on the barrier surface over the entire observation period. The high species richness observed after the two disturbances and the gradual decline after the first disturbance are common responses by plant communities to disturbance (Anderson 2007). Much of the variation can be associated with the initial construction disturbance and the consequences of the fire. A comparison of the two disturbances revealed that the initial disturbance had many species that did not have wind-driven seed, while after the fire many of the species had wind-driven seed. It is possible that the initial species composition was influenced by the construction activity, with seeds arriving with vehicles and humans working on the surface. The prevalence of species with wind-driven seed after the fire may be a realization of an accumulation of species stored in the seed bank, or the seeds may have arrived naturally after the fire and then been able to establish. It is likely that some of the species with wind-blown seed arrived from the adjacent side slope community, but there were eight species (all Asteraceae) with wind-blown seed on the barrier surface after the fire that did not exist on the side slopes, suggesting that these seed arrived from plants some distance from the barrier. This observation is similar to that by Robinson and Handel (1993), who did not find a relationship between wind-driven seeded species on a landfill cap and distance to nearby source plants. It has been observed that seed can travel up to 20 km for many species and considerably further by animal/human transport (Cain et al. 2000).

Another difference between the two disturbances was that there were almost as many annuals/biennial species as perennial species from 1995 through 2004, but the former became fewer in 2007 and 2008. This is in contrast to the reversal after the fire, where annuals/biennials became more numerous than the perennials. The high species richness and preponderance of annual/biennials after the fire is a classic

response to fire disturbance (Bond and Wilgen 1996). Early species such as annuals and biennials commonly dominate for the first 2 years after fire and then decrease as perennials begin to competitively exclude the early ruderals (Bond and Wilgen 1996).

This analysis of vegetation dynamics and cover is for a longer period than found elsewhere in arid regions. A similar study, but with only a 3-year observation period in New Mexico (Dwyer et al. 2000), noted the strong effect of initial establishment success on subsequent vegetation characteristics. The study found that seeding in a wet year resulted in substantially more perennial grass establishment than seeding in a dry year. This effect resulted in associated high cover of weedy species on the dry plots. These effects remained during the 3 years of the study. The effect of initial conditions on differential plant establishment remained even when the plots were irrigated. In this study, initial irrigation treatment resulted in increased grass and litter cover compared with the unirrigated section of the barrier, but the effect of initial conditions on plant community characteristics was very reduced 13 years after planting. Both conditions studied were dominated by perennials in contrast with the dominance of weedy species on the initially dry section of the (Dwyer et al. 2000) plots. It is possible that the dry plots of Dwyer et al. (2000) have remained weedy. In Berlin, Germany, Rebele and Lehmann (2002) examined 5 years of plant community dynamics from bare soil on a naturally vegetated landfill cover and found species richness did not change, even with changing species composition and cover. Annuals were never prominent, with perennial cover increasing linearly over time to about 80%. This response is similar to the one found at the PHB after revegetation, but was unlike the PHB response after fire with annual/biennials dominant.

The significant increase in cover of *M. canescens* in 2010 (27.9%) after the fire was likely caused by wind-blown seed from some distance, as there were none in the seed bank after the fire and only 1% cover of *M. canescens* in 2009 to provide seed for 2010. *Machaeranthera canescens* is an early-to-mid or late successional stage species after fire (Koniak 1985), as are the other annuals/biennials, but it had assumed the position of dominance compared with all other species on the burned section of the surface with cover at 28% in 2011.

Litter on the surface before the fire was largely that of *A. tridentata* leaves and did have an inhibitory effect on bunchgrass germination (Schlatterer and Tisdale 1969).

J.4.3 Seed Bank

The most interesting observation was the emergence of *A. tridentata* from the seed bank after the fire, which suggests that this dominant shrub will return after a fire. This observation is in contrast to the general belief that *A. tridentata* does not recover after a fire (Tirmenstein 1999). There was no resprouting after the fire. There were no significant differences among the barrier plots before and after the fire and the unburned McGee Ranch site. Both *S. kali* and *S. altissimum* were significantly greater on the old burn McGee Ranch site than at the unburned McGee Ranch site, while there were no seedlings observed from any of the barrier samples. Both species were found growing on the barrier surface after the fire, suggesting that either viable seed was in the seed bank, and they did not germinate from the samples in the greenhouse, or the seed arrived on the surface after the fire from surrounding seed sources. Both species are recognized as responding favorably to fire. *Verbena bracteata* seedlings were found in the seed bank of samples before and after the fire. None were found at the two McGee Ranch sites. There is little correlation between current vegetation and the species composition of seed banks (Henderson et al. 1988).

Given that the fire had little effect on the seed bank on the barrier, it can be concluded that fires pose little risk to the potential plant communities that can arise from the naturally occurring seed bank. A potential risk should be recognized with respect to *S. kali* as a nurse plant for *B. tectorum. Salsola kali* appears to

protect or encourage germination of *B. tectorum* in large numbers compared with other conditions at the burned analog site. Given that *S. kali* accumulates along the edges of the barrier, getting caught in *A. tridentata* canopies, it is possible the *B. tectorum* will more easily establish along the edges.

J.4.4 Likelihood of *Bromus tectorum* Invasion

Bromus tectorum more than doubled its cover on the burned section of the barrier from 2009 to 2010, but only to 3.61%. Cover continued to increase in 2011 to 4.34%. The likelihood that its cover will continue to increase to a co-dominant level, or that it will become dominant in patches on the surface, may put the functionality of the barrier at risk. The risk of drainage or failure because of *B. tectorum* cover has been addressed on lysimeters at Hanford by Fayer and Gee (2006), who concluded, under the conditions of the test, that there is no risk of failure if *B. tectorum* cover should become significant on the surface. This finding differs from the result of Cline et al. (1977) who found significantly increased soil moisture stored below the 0.5-m depth in a *B. tectorum* field in October after a year of 31 cm (or about double normal) precipitation. This finding was at a silt loam soil site within 10 km of the barrier and lysimeters. A possible contributing factor is the retention of water associated with a deep layer of litter in the *B. tectorum* dominated old-field. Litter has been noted to significantly reduce soil evaporation in arid sites (Villegas et al. 2010). In addition, Link et al. (1990) observed increased soil moisture storage below 1.25 m in a *Pseudoroegneria spicata* community that had been an *A. tridentata* dominated community before it was killed by a fire. The risk that *B. tectorum* will become prominent on the surface after the fire depends on how successfully it competes with other species on the surface. It has been recognized that after fire and loss of perennials, *B. tectorum* can increase its cover by outcompeting perennial seedlings (Chambers et al. 2007). Whether *B. tectorum* will form a patch where it is dominant remains to be seen. If such a patch were to occur near the edges of the barrier surface, where additional water has allowed plants to become much larger, the likelihood of failure may be higher because of increased *B. tectorum* seed availability. The more seed available, the more likely it will be that *B. tectorum* can move across the barrier.

J.4.5 Management Implications

Management implications based on the results of this research are associated with efforts to initiate revegetation on future landfill caps, the need to institute continued vegetation monitoring, and the need to institute vegetation management on future landfill caps. The effort to revegetate the PHB was not sufficient to achieve similarity with the McGee Ranch unburned analog site. Only 2 shrub species and 7 bunchgrass species were used to initiate the plant community on the PHB, while 17 native species were observed at the two McGee Ranch sites. Future revegetation efforts should attempt to match an analog site to confer a higher likelihood of long-term functionality to landfill caps. Efforts to recreate an existing analog plant community on constructed barrier surfaces will require vegetation management efforts to modify community structure for a few years after initial plantings to achieve higher similarity and to maintain this condition by keeping *B. tectorum* under control. The unburned McGee Ranch community had only 4.88% cover of *B. tectorum*, much higher bunchgrass cover, higher forb cover, lower shrub cover, and higher soil cryptogam cover. This combination likely has maintained *B. tectorum* at low levels, which likely would not compromise barrier functionality.

Yearly vegetation monitoring should be instituted to ensure that small problems such as *B. tectorum* invasion or significant losses of controlling species such as *A. tridentata,* as appears to be occurring on the PHB because of insect infestations (see Appendix L), can be corrected inexpensively. Regular vegetation monitoring becomes part of regular vegetation management on landfill caps. Yearly monitoring and management is likely the less expensive approach to maintaining functionality and stakeholder confidence for the use landfill caps at Hanford.

J.4.6 Implications on Barrier Performance

Implications on barrier performance are simple based on the conditions of the test. During the monitoring period, the PHB performed as intended, even with 4 years of additional irrigation and with vegetation changes after a fire. Vegetation changes that may pose a risk to barrier performance are associated with loss of deep-rooted perennials and increases in the shallow-rooted *Bromus tectorum*. Further testing of the ability of barriers to prevent drainage if portions were to be dominated by *B. tectorum* or when dominant along barrier edges is warranted given the differences noted between artificial lysimeter conditions and those from undisturbed field observations.

J.5 Conclusions

The Prototype Hanford Barrier was able to return all precipitation to the atmosphere, preventing drainage when subjected to three times normal precipitation and nearly all after a fire. The revegetation actions were successful, but resulted in a near monoculture of *A. tridentata*. The species richness (number of species) on the surface increased after the initial construction disturbance, then dropped to low levels after 12 years. Species richness then increased after the fire disturbance and subsequently dropped. Shrub cover was significantly reduced after the fire, but forb and grass cover increased. The barrier plant community has not achieved similarity with its analog site at McGee Ranch. The burned and unburned barrier communities were more similar to each other than to either of the McGee Ranch analog sites, which in turn were more similar to each other. The large element of species with wind-blown seed appearing after the fire implies that general seed rain will be the source of future species on landfill covers. It is possible to increase the number of wind-blown seed species and their cover near construction sites to increase the likelihood that they will spontaneously revegetate such areas. The seed bank on the barrier was not affected by the fire. The unanticipated high cover of *M. canescens* after the fire suggests that this species may be able to resist *B. tectorum* invasions and possibly may be a useful species for general fire restoration efforts. Finally, further testing of the ability of barriers to prevent drainage if portions were to be dominated by *B. tectorum* or when dominant along barrier edges is warranted given the differences noted between artificial lysimeter conditions and those from undisturbed field observations.

Acknowledgement

Research was funded by the U.S. Department of Energy under Contract DE-AC06-76RLO 1830 with the Pacific Northwest National Laboratory. We thank Glendon Gee for conceiving the Hanford Prototype Barrier and early support. We thank Kevin Leary for initiating, helping with, and funding the fire portion of the study. We thank Bill Mast, Jere Boudell, Traci Degerman, Jennifer Lewinsohn, Sally Simmons, Karen Barton, Andrew Pomiak, Dale Loth, Jenifer Linville, and Janice Maya for technical assistance.

References

Albright, WH, CH Benson, GW Gee, AC Roesler, T Abichou, P Apiwantragoon, BF Lyles, and SA Rock. 2004. "Field Water Balance of Landfill Final Covers," *Journal of Environmental Quality*, 33(6):2317-2332.

Allen, EB and MF Allen. 1988. "Facilitation of Succession by the Nonmycotrophic Colonizer *Salsola Kali* (Chenopodiaceae) on a Harsh Site: Effects of Mycorrhizal Fungi.," *American Journal of Botany*, 75:257-266.

Anderson, CE and TD Ratzlaff. 1996. "Protective Cap/Biobarrier Experiment II: A Comparison of Water Use by Annual and Perennial Species on Simulated Waste Burial Plots at the Idaho National Engineering Laboratory." In *Environmental Science and Research Foundation Annual Technical Report, Calendar Year 1995*, eds. TD Reynolds and RC Morris, pp. 45-48. Environmental Science and Research Foundation, Idaho Fall, Idaho.

Anderson, JE. 1993. "Managing Soil Moisture on Waste Burial Sites in Arid Regions. ," *Journal of Environmental Quality*, 22:62-69.

Anderson, JE and AD Forman. 2002. *The Protective Cap/Biobarrier Experiment a Study of Alternative Evapotranspiration Caps for the Idaho National Engineering and Environmental Laboratory*, Stoller-ESER-46 Stoller Corporation, Idaha Falls, Idaho.

Anderson, KJ. 2007. "Temporal Patterns in Rates of Community Change During Succession," *The American Naturalist*, 169:780-793.

Bond, WJ and BWV Wilgen. 1996. *Fire and Plants*. Chapman and Hall, London.

Boudell, JA, SO Link, and JR Johansen. 2002. "Effect of Soil Microtopography on Seed Bank Distribution in the Shrub-Steppe," *Western North American Naturalist*, 62:14-24.

Cain, ML, BG Milligan, and AE Strand. 2000. "Long-Distance Seed Dispersal in Plant Populations," *American Journal of Botany*, 87:1217-1227.

Chambers, JC, BA Roundy, RR Blank, SE Meyer, and A Whittaker. 2007. "Hat Makes Great Basin Sagebrush Ecosystems Invasible by *Bromus tectorum*?," *Ecological Monographs*, 77:117-145.

Cline, JF, DW Uresk, and WH Rickard. 1977. "Comparison of Soil Water Used by a Sagebrush-Bunchgrass and a Cheatgrass Community," *Journal of Range Management*, 30:199-201.

Daubenmire, R. 1959. "A Canopy-Coverage Method of Vegetational Analysis," *Northwest Science*, 33:43-64.

Daubenmire, R. 1970. *Steppe Vegetation of Washington*. Washington Agricultural Experiment Station Technical Bulletin Number 62, Pullman, Washington.

DOE-RL. 1993. *Treatability Test Plan for the 200-BP-1 Prototype Surface Barrier*, DOE/RL-93-27, U.S. Department of Energy Richland Operations Office, Richland, Washington.

DOE-RL. 1999. *200-BP-1 Prototype Barrier Treatability Test Report*, DOE/RL-99-11 Rev. 0, U.S. Department of Energy Richland Operations Office, Richland, Washington.

DOE-RL. 2013. *Hanford Site Cleanup Completion Framework*, DOE/RL-2009-10, Rev. 1, U.S. Department of Energy Richland Operations Office, Richland, Washington.

Dwyer, SF, GL Wolters, and G Newman. 2000. *FY 97-99 Vegetation Analysis of ALCD Soil Amended Landfill Cover Plots*, SAND2000-2900, Sandia National Laboratories, Albuquerque, New Mexico.

Easterly, R and D Salstrom. 2003. *Current Vegetation Map of McGee-Riverland Unit, Hanford Reach National Monument*. Accessed on Feb. 20, 2015, at http://Nerp.Pnnl.Gov/Docs/Ecology/Biodiversity/Easterly2003.Pdf (last updated 2003).

Fayer, MJ and GW Gee. 2006. "Multiple-Year Water Balance of Soil Covers in a Semiarid Setting," *J. Environ. Qual.*, 35:366–377.

Gee, GW. 1987. *Recharge at the Hanford Site:Status Report*, Pacific Northwest Laboratory, PNL-6403, Richland, Washington.

Gee, GW, AL Ward, BG Gilmore, SO Link, GW Dennis, and TK O`Neil. 1996. *Hanford Prototype-Barrier Status Report FY 1996*, PNNL-11367, Pacific Northwest National Laboratory, Richland, Washington.

Hajek, BF. 1966. *Soil Survey, Hanford Project in Benton County, Washington*, Pacific Northwest Laboratory, BNWL-243, Richland, Washington.

Hauser, VL, BL Weand, and MD Gill. 2001. "Natural Covers for Landfills and Buried Waste. Journal of Environmental Engineering," *Journal of Environmental Engineering*, 127:768-775.

Henderson, CB, KE Petersen, and RA Redak. 1988. "Spatial and Temporal Patterns in the Seed Bank and Vegetation of a Desert Grassland Community," *Journal of Ecology*, 76:717-728.

Hitchcock, CL and A Cronquist. 1973. *Flora of the Pacific Northwest*. University of Washington Press, Seattle, Washisngton.

Howard, JL. 1999. *Artemisia tridentata subsp. Wyomingensis. In: Fire Effects Information System.* Accessed on Feb. 2/28/2015, at http://www.feis-crs.org/beta/ (last updated Jan. 8, 2015).

Jaccard, P. 1901. "Étude Comparative De La Distribution Florale Dans Une Portion Des Alpes Et Des Jura," *Bulletin de la Société Vaudoise des Sciences Naturelles*, 37:547-579.

Kemp, PR. 1989. "Seed Banks and Vegetation Processes in Deserts." In *Ecology of Soil Seed Banks.*, eds. MA Leck, VT Parker and LR Simpson. Academic Press, Inc., San Diego, California.

Klepper, EL, KA Gano, and LL Cadwell. 1985. *Rooting Depth and Distributions of Deep-Rooted Plants in the 200 Area Control Zone of the Hanford Site*, PNL-5247, Pacific Northwest Laboratory, Richland, Washington.

Koniak, S. 1985. "Succession in Pinyon-Juniper Woodlands Following Wildfire in the Great Basin," *Great Basin Naturalist*, 45:556-566.

Lesica, P and SV Cooper. 1999. "Succession and Disturbance in Sandhills Vegetation: Constructing Models for Managing Biological Diversity," *Conservation Biology*, (13):293-302.

Link, SO, GW Gee, ME Thiede, and PA Beedlow. 1990. "Response of a Shrub-Steppe Ecosystem to Fire: Soil Water and Vegetational Change," *Arid Soils Research and Rehabilitation*, 4:163-172.

Link, SO, BD Ryan, JL Downs, LL Cadwell, J Soll, MA Hawke, and J Ponzetti. 2000. "Lichens and Mosses on Shrub-Steppe Soils in Southeastern Washington," *Northwest Science*, 74:50-56.

Link, SO, WJ Waugh, and JL Downs. 1994a. " The Role of Plants on Isolation Barriers Systems." In *Insitu Remediation: Scientific Basis for Current and Future Technologies, Proceedings of the 33rd*

Hanford Symposium on Health and Environment, eds. GW Gee and NR Wing, pp. 561-592. Battelle Press, Columbus.

Link, SO, WJ Waugh, JL Downs, ME Thiede, JC Chatters, and GW Gee. 1994b. "Effects of Coppice Dune Topography and Vegetation on Soil Water Dynamics in a Cold-Desert Ecosystem," *Journal of Arid Environments*, 27:265-278.

Rebele, F and C Lehmann. 2002. "Restoration of a Landfill Site in Berlin, Germany by Spontaneous and Directed Succession," *Restoration Ecology*, 10:340-347.

Roberts, HA. 1981. *Seed Banks in the Soil - Advances in Applied Biology*. 6, Academic Press, Cambridge.

Robinson, GR and SN Handel. 1993. "Forest Restoration on a Closed Landfill: Rapid Addition of New Species by Bird Dispersal," *Conservation Biology*, 7:271-278.

Sackschewsky, MR and JL Downs. 2001. *Vascular Plants of the Hanford Site*, PNL-13688, Pacific Northwest National Laboratory, Richland, WA.

SAS Institute. 2002. *JMP Statistics and Graphics Guide, Version 5*. SAS Institute Inc, Cary.

Schlatterer, EF and EW Tisdale. 1969. "Effects of Litter of *Artemisia*, *Chrysothamnus*, and *Tortula* on Germination and Growth of Three Perennial Grasses," *Ecology*, 50:869-873.

Seyfried, MS, S Schwinning, MA Walvoord, WT Pockman, BD Newman, RB Jackson, and FM Phillip. 2005. "Ecohydrological Control of Deep Drainage in Arid and Semiarid Regions," *Ecology*, 86:277-287.

Steele, RBD and JH Torrie. 1960. *Principals and Procedures of Statistics*. McGraw-Hill, New York.

Stone, WA, JM Thorp, OP Gifford, and DJ Hoitink. 1983. *Climatological Summary for the Hanford Area.*, Pacific Northwest Laboratory, PNL-4622, Richland, Washington.

Tirmenstein, D. 1999. "*Artemisia Tridentata* spp. *tridentata*." In *Fire Effects Information System*, ed. U.S. Department of Agriculture Forest Service. Rocky Mountain Research Station, Fire Sciences Laboratory (http://www.fs.fed.us/database/feis).

USDA NRCS. 2010. "*The Plants Database*." National Plant Data Center (http://plants.usda.gov), Baton Rouge, LA 70874-4490 USA.

USDA NRCS. 2011. "*The Plants Database*." National Plant Data Center (http://plants.usda.gov), Baton Rouge, LA 70874-4490 USA.

Villegas, JC, DD Breshears, CB Zou, and DJ Law. 2010. "Ecohydrological Controls of Soil Evaporation in Deciduous Drylands: How the Hierarchical Effects of Litter, Patch and Vegetation Mosaic Cover Interact with Phenology and Season," *Journal of Arid Environments*, 74:595-602.

Wagner, WL, WC Martin, and EF Aldon. 1978. "Natural Succession on Strip-Mined Lands in Northwestern New Mexico," *Reclamation Review*, 1:67-73.

Ward, AL, GT Berlin, JW Cammann, KD Leary, and SO Link. 2008. *Test Plan to Assess Fire Effects on the Function of an Engineered Surface Barrier,* PNNL-17859, Pacific Northwest National Laboratory, Richland, Washington.

Ward, AL and GW Gee. 1997. "Performance and Water Balance Evaluation of a Field-Scale Surface Barrier," *J. Environ. Qual,* 2:694-705.

Ward, AL, GW Gee, and SO Link. 1997. *Hanford Prototype-Barrier Status Report: FY 1997,* PNNL--11789, Pacific Northwest National Laboratory, Richland, Washington.

Ward, AL, N Hasan, SO Link, and KE Draper. 2009a. *The Effects of Fire on the Function of the 200-BP-1 Engineered Surface Barrier,* PNNL-18934, Pacific Northwest National Laboratory, Richland, Washington.

Ward, AL, KD Leary, SO Link, GT Berlin, JW Cammann, ML Mandis, and LC Buelow. 2009b. "Short and Long-Term Fire Impacts on Hanford Barrier Performance," *Waste Management Symposium 09,* Phoenix, Arizona.

Ward, AL, SO Link, CE Strickland, KE Draper, and RE Clayton. 2007. *200-BP-1 Prototype Hanford Barrier Annual Monitoring Report for Fiscal Years 2005 through 2007,* PNNL-17176, Pacific Northwest National Laboratory, Richland, Washington.

Ward, AL, SO Link, CD Wittreich, KD Leary, GT Berlin, and GW Gee. 2010. "Quest for the Perfect Cap: The Prototype Hanford Barrier 15 Years Later," *36th Annual radioactive waste management symposium,* 939-956 pp.Phoenix, Arizona.

Waugh, WJ, KL Petersen, SO Link, BN Bjornstad, and GW Gee. 1994. "Natural Analogs of the Long-Term Performance of Engineered Covers," *In-Situ Remediation: Scientific Basis for Current and Future Technologies. Parts 1-2. Thirty Third Hanford Symposium on Health and the Environment. November 7-11, 1994,* 379- 410 pp.Pasco WA Battelle Press, Columbus, Ohio.

Whisenant, SG. 1990. *Changing Fire Frequencies on Idaho's Snake River Plains: Ecological and Management Implication*. Proceeding-Symposium on Cheatgrass Invasion, Shrub Die-Off, and Other Aspects of Shrub Biology and Management, USDA Forest Service Intermountain Research Station General Technical Report: INT-276:4-10.

Wing, NR and GW Gee. 1994. "Quest for the Perfect Cap," *Civil Engineering,* Oct:38-41.

Appendix K

Plant Structure and Function at the Prototype Hanford Barrier

Steven O. Link

Content

List of Figures

List of Tables

Abstract

Observations were taken on plant structure and function at the Prototype Hanford Barrier (PHB) from 1995 to 2011. Information on plant physiology and structure is useful for parameterizing soil moisture models needed to predict possible outcomes on the PHB. Plants are also useful as a tool to estimate soil water potential. In 2009, mean leaf area index (LAI) on the unburned section of the barrier (1.13 ± 0.087) was significantly greater than on the burned section of the barrier (0.254 ± 0.02). A surface with a high LAI can transpire more water than a surface with a low LAI. Pre-dawn xylem pressure potential values can be used as an estimate of soil water potential. Values measured on *Machaeranthera canescens* were highly variable across the surface, ranging from an average of -18.8 to -76.3 bars, indicating highly variable soil moisture patterns across the surface. Transpiration rates of *Artemisia tridentata* ranged from 0.75 mmol $m^{-2}s^{-1}$ in February to 19.7 mmol $m^{-2}s^{-1}$ in late July of 2009. Roots grew to the bottom of the assessment tube viewing position (about 175 cm) in the first year after planting in the irrigated section and by the second year in the ambient precipitation section. These roots are primarily those of *A. tridentata.* This indicates that deep-rooted *A. tridentata* shrubs will rapidly access nearly the entire soil profile for barriers after construction.

K.1 Introduction

Engineered surface barriers are an integral component of the U.S. Department of Energy (DOE) waste management strategy, serving as an alternative to the removal, treatment, and disposal of near-surface contaminants at a variety of waste sites (DOE-RL 1993). Several locations at the Hanford Site may have significant amounts of contaminants deep in the vadose zone that may be remediated using surface barriers (DOE-RL 2013). Evapotranspiration (ET) covers and multilayered designs with a vegetated evapotranspirative surface layer have been effective in arid and semiarid climates in most cases, but have failed in others because of inadequate storage capacity and vegetation (Albright et al. 2004; Anderson 1993; Hauser et al. 2001).

Concerns associated with vegetation include possible gradual and catastrophic changes sufficient to compromise cover function (Anderson and Forman 2002). Gradual changes such as those associated with plant community dynamics and succession may increase the risk of failure on ET covers. Gall forming insects can cause the death of *Artemisia tridentata* or sagebrush (Haws et al. 1990). Loss of this deep-rooted shrub from the barrier surface will reduce transpiration potential. Catastrophic changes associated with fire can lead to increasing *Bromus tectorum* (cheatgrass) cover (Whisenant 1990) and reductions in transpiration potential at least in the short-term (Anderson and Forman 2002). Assessments of plant function related to ET have been reviewed, examined on other surfaces and covers, and modeled (Cui and Zornberg 2008; Donovan et al. 2001; Haws et al. 1990; Piet et al. 2003; Ritchie and Hinckley 1975; Scanlon et al. 2005; Ward et al. 2005a). Modeling of ET can be used to assess barrier performance over the long-term as a function of plant community dynamics (Ward et al. 2005a). Such assessments can increase stakeholder acceptance of barrier technology.

Plant xylem pressure potential data can be used as an estimate of soil moisture pressure potential and can be gathered anywhere on the surface, unlike soil water potential sensors. Plant xylem water potential has been thought to be at equilibrium with soil water potential just before dawn and in equilibrium in the wettest portion of the soil where roots exist, usually where the roots are deepest (Ritchie and Hinckley 1975). The xylem water potential of some species, such as *A. tridentata*, can be a few bars dryer than the soil water potential of well-watered soil (Donovan et al. 2001). Although soil water potential and pre-dawn xylem pressure potential may not be exactly the same, the xylem pressure can be used to examine variability across the surface. Another characteristic of plants associated with water status is the ability to produce flowers. This study examined flowering status with respect to the irrigation treatment and location on the barrier surface.

The purpose of this research was to provide basic information on plant structure and function. This information can be used to parameterize models for the prediction of ET and to provide information on the spatial variability of xylem potential. Plant information was gathered on the PHB after three times average precipitation for 4 years, in the long-term, and after a fire. Plant structure information included plant height, canopy dimensions and canopy leaf area, leaf area index (LAI), rooting depth, and root length density. Information on plant function included xylem water potential, transpiration, and net photosynthesis. Information on soil/root respiration was also gathered to assess biological activity after the fire. Observations were taken on the PHB surface and at the McGee Ranch analog site.

K.2 Methodology

K.2.1 Study Site

The study was conducted at the DOE Hanford Site in south central Washington state. The PHB is located (46°34’01.23”N, 119°32’28.43”W) on the 200 Area Plateau at an elevation of 194 m a.s.l. The old burn

analog site at McGee Ranch is at about 46°35'05.64"N, 119°43'51.71"W and at an elevation of 245 m a.s.l. The unburned McGee Ranch analog site is at about 46°34'40.24"N, 119°44'33.02"W and at an elevation of 247 m a.s.l. Characteristics of McGee Ranch are described in Link et al. (1994a) and Link et al. (1994b).The climate is semiarid with hot dry summers and cool wet winters (Stone et al. 1983). Average yearly precipitation at the nearby Hanford Meteorological Station is about 167 mm. Snowfall ranges from trace amounts to 137 cm, but averages 35 cm.

K.2.2 Barrier Characteristics and Treatments

The surface area of the entire barrier is 2.5 hectares. The surface is elevated with one relatively steep (2:1 horizontal to vertical) protective side slope that is covered with basalt riprap. The other side slope is shallow (10:1) and consists of local pit run gravel backfill. The PHB is constructed with 2 m of fine soils over coarser material. The soil used in the upper layers of the PHB is a Warden silt loam (Gee 1987; Hajek 1966).

The north section was irrigated during treatability testing from 1994 to 1998 while the south section was not irrigated. This test included irrigation at a rate of 480 mm/yr, including a simulated 1000-yr return storm each March in which about 70 mm of water was applied over an 8-hour period to gain insight into barrier performance under elevated precipitation conditions. No further manipulations occurred until September 2008, when the north section of the barrier was burned (Ward et al. 2008; Ward et al. 2009a; Ward et al. 2009b). The surface was gridded into three-hundred 9-m^2 quadrats, with 144 quadrats in the unirrigated area and 156 quadrats in the irrigated area for ecological surveys.

K.2.3 Plant Canopy Dimensions, Leaf Area, and Leaf Area Index

Plant height of *A. tridentata* and *Ericameria nauseosa* (gray rabbitbrush) was measured with a meter stick in the irrigated and non-irrigated portions of the barrier in 1995, 1996, and 1997. Observations were made on the height of *Salsola kali* (Russian thistle) and *Elymus lanceolatus* (thickspike wheatgrass) in each treatment. Observations were taken on at least nine individuals of *S. kali, A. tridentata,* and *E. nauseosa* in each of the treatments on July 26, 1995, on *E. lanceolatus* in each treatment on May 23, 1996, and again on *S. kali, A. tridentata, and E. lanceolatus* in each treatment on August 1, 1996. Height of *A. tridentata* and *E. nauseosa* was measured in each treatment in 2003, 2004, and between June 14 and August 18, 2007. In 2008, plant height was measured on all sagebrush plants in 84 of the 9-m^2 quadrats in the unburned section of the surface.

Differences between treatments for height data in 1995, 1996, and 1997 were assessed by comparing regression relationships in time using a linear test approach (Neter and Wasserman 1974).

Observations were taken on April 15, May 15, and June 15, 1997 to describe canopy characteristics, leaf area, and LAI dynamics. Canopy characteristics were measured to estimate leaf area, as described in Link et al. (1990). Canopy characteristics of the same individual shrubs were measured on the three dates. Shrubs were randomly chosen (20 from the non-irrigated treatment and 20 from the irrigated treatment), then labeled with metal tags numbered 1 through 40.

The leaf area of *A. tridentata* was measured by double sampling, using a model relating leaf area to canopy measures. This model was developed by measuring the height, the greatest projected canopy diameter, and the diameter perpendicular to the greatest diameter, then relating these measures to harvested leaf area. These measurements were taken on five shrubs in April and seven shrubs in May and June in both treatment areas. Plants were chosen to encompass all possible shrub sizes found in both treatments. The shrubs were measured and then harvested to determine leaf area.

Harvested shrubs were placed in plastic bags and taken to a laboratory for measurement of mass and leaf area. Because the shrubs were large, each one was broken into similar pieces for sampling. The entire shrub was weighed and about 10% taken to measure leaf area. The mass of the sample piece was recorded. Leaves were then stripped from stems and single-sided green leaf area was determined with a LI-COR 3100 Leaf Area Meter (LI-COR, Inc., Lincoln, NE). The leaf area of the entire shrub was determined as:

$$LA_{shrub} = Mass_{shrub} \times LA_{sample} / Mass_{sample} \quad \text{(K.1)}$$

where LA_{shrub} is the total leaf area of the shrub (cm^2), LA_{sample} is the leaf area of the weighed sample, $Mass_{shrub}$ is the mass of the entire shrub (g), and $Mass_{sample}$ is the mass of the sample (g).

The model for leaf area is:

$$Y = b_0 + b_1 d + b_2 h + b_3 w + b_4 pw + b_5 trt + b_6 h^2 + b_7 w^2 + b_8 hwpw + b_9 wtrt \quad \text{(K.2)}$$

where

Y = leaf area (cm^2)
d = day of the year (1 to 365)
h = plant height (cm)
w = greatest projected canopy diameter (cm)
pw = diameter 90° to w (cm)
trt = treatment code (1 = irrigated, 0 = non-irrigated).

The coefficients of the polynomial defined in Eq. (K.1) are:

b_0 = -1959	b_5 = 1100
b_1 = -11.96	b_6 = -0.822
b_2 = 56.52	b_7 = -3.827
b_3 = 225.3	b_8 = 0.0579
b_4 = -51.65	b_9 = -50.88

This model (Eq. (K.1)) was used to compute the leaf area of the 40 tagged shrubs.

Canopy leaf area measurements were expressed as LAI (m^2 green leaf area / m^2 ground area). For this purpose, the mean predicted canopy leaf area was multiplied by the number of *A. tridentata* individuals in each treatment (non-irrigated = 1977, irrigated = 1686), divided by 10,000 to convert square centimeters to square meters, and then divided by 1296 m^2 (the area in each section of the surface without the middle row).

In 2003, 2004, and 2007, canopy measurements were taken on the PHB. In 2007, the measurements were taken between June 14 and August 18. Variables measured were shrub height and canopy dimensions. Canopy dimensions of about 25 shrubs each in the north (irrigated in 1995, 1996, and 1997) and south (non-irrigated) sections of the barrier surface were measured consistent with the methods used in DOE-RL (1999). The height of the highest stem, the greatest canopy diameter (*A*), and the diameter at the center of the plant perpendicular to the greatest diameter (*B*) were measured. The canopy area was determined as the product of *A* and *B*. The measured shrubs (*A. tridentata* and *E. nauseosa*) were chosen randomly.

In 2008, pre-burn *A. tridentata* height was measured on all live plants in 84 of the 9-m^2 quadrats from the

south side of the burn area to the north section. In 2009, the greatest shrub height, greatest canopy diameter, and the diameter at the center of the plant perpendicular to the greatest diameter were measured on 24 shrubs in the unburned section and on 10 shrubs in the burned section of the barrier. In 2010 and 2011, greatest height, greatest canopy diameter, and the diameter at the center of the plant perpendicular to the greatest diameter were measured on 30 individuals of *A. tridentata*, *E. nauseosa*, *Machaeranthera canescens* (hoary aster), and *Elymus wawawaiensis* (Snake River wheatgrass) on the burned section of the barrier and on 30 individuals of *A. tridentata* on the unburned section of the barrier. In 2011, 11 *E. nauseosa* individuals were measured on the unburned section of the barrier. The location on the surface (edges and center) was noted for *A. tridentata* as well as flowering status. In 2010, measurements on *E. wawawaiensis* were taken on old and young individuals as well as evidence of herbivory. The ellipsoidal volume of each canopy was computed. In 2011, measurements on *E. wawawaiensis* were taken without regard to age or herbivory. Location on the surface was noted.

In 2011, flowering status was recorded as occurring or not and the relative amount of flowers was noted as either few flower heads or abundant flower production.

The LAI provides a measure of physiologically active vegetation and is used in agricultural applications to provide models with a measure of leaf area. The measure is useful also to help provide a measure of leaf area for arid land plant-physiology models. For the applications at the barrier and analog sites, the response is a combination of green leaf area and other shading, but not inactive material such as dry grass leaves. It is useful to compare plant community types for potential active leaf area. It may provide a response close to a true value in *A. tridentata* where leaves are evergreen.

The LAI was measured in 2008 and 2009 using an AccuPAR LP80 Ceptometer (Decagon Devices, Pullman, WA). The LAI was measured on each study plot used to determine cover at the burned and unburned barrier areas and at the two McGee Ranch analog sites. Observations were taken in the center of each plot. Pre-burn LAI observations were made in the center of each quadrat in seven east/west rows. There were 12 quadrats in each row for a total of 83 observations. Quadrat 1 is on the west edge, and 13 is on the east edge of the surface with $n = 7$ in each quadrat set. One quadrat value was lost. Observations were also taken in 21 plots in each of the two analog sites. The LAI values were transformed using the square root because data were Poisson distributed (many very small values and few large values). Comparisons are made using transformed data while untransformed values are presented for easy interpretation.

K.2.4 Xylem Water Status

Predawn xylem pressure potential data were gathered on August 1,1996, with a pressure chamber (Soilmoisture Equipment Co., Santa Barbara, CA), after Scholander et al. (1965). Data were gathered on *A. tridentata* and *E. nauseosa* in both irrigated and ambient precipitation treatments. Xylem pressure potential data were obtained by placing cut stems (about 10 cm in length) in the pressure chamber and slowly pressurizing with nitrogen gas until the tip of the stem first showed evidence of a color change due to expressed water. A wet paper towel was placed in the chamber to maintain a humid atmosphere around the stem and leaf material during pressurization. Treatment effects on xylem pressure potential were compared using Student's t-test (Steele and Torrie 1960) within species.

Measurements of water potential of plant leaves, or more exactly, the plant xylem pressure potential, are useful for comparing plant activity and soil water status. Xylem pressure potential was measured on plants with a Model 1005 Pressure Chamber Instrument (PMS Instrument Company, Albany, OR) in the burned and unburned sections of the barrier. In 2009, measurements were taken just before dawn to assess maximal xylem pressure potential. Observations were made on *A. tridentata*, *S. kali*, and *M. officinalis* in

the west, central, and east sides of the surface. In addition, measurements were taken on *A. tridentata* in the unburned condition in late afternoon to determine the lowest possible values. Data were collected on September 5. In 2010, observations were taken on *A. tridentata* and *M. canescens* in the west, central, and east sides of the surface. Data were collected on August 27.

K.2.5 Plant Gas Exchange

Plant gas exchange data were collected in 1995 and 1996. Transpiration and net photosynthetic data are presented in this section. Such data are a useful indicator of the ability of shrubs to remove water from the surface. Comparisons are made for the effect of the irrigation treatment on gas exchange rates for *A. tridentata.* Previous gas exchange data collected for *E. nauseosa* indicate similar rates as for *A. tridentata* (Gee et al. 1996). Because of the similarity and the decreasing importance of *E. nauseosa* on the surface, only data for *A. tridentata* are presented in this appendix. These data are graphically presented with earlier data, as in Gee et al. (1996), to interpret long-term trends in plant gas exchange.

Gas exchange data were gathered with a LI-COR 6200 gas exchange system. Such data are collected by placing a chamber over plant stem tips and allowing water vapor and CO_2 to change over a few minutes. In 1997, a 10-cm length of stem was placed in the chamber for plants in the non-irrigated treatment and a shorter piece (less than 5 cm long) was used in the irrigated treatment. The varying amounts of exposed leaf area were used to maintain similar vapor pressures for the two treatment samples in the chamber. After observations were made, the stem was cut and a single-sided leaf area was measured, using a LI-COR 3100 Leaf Area Meter. All gas exchange observations were taken at midday and in full sun.

K.2.6 Post-Burn Biological Activity and Soil Carbon Dioxide Flux

Soil respiration after fire generally decreases with reductions in biological activity and organic carbon. Biological activity was assessed nearly 1 year after the fire by comparing activity on the unburned and burned sections of the barrier surface. Respiration rates were compared under very dry surface soil conditions and after a rain that wetted the top 33 mm of the soil profile. Measurements of soil CO_2 were made *in situ* with a Vaisala CARBOCAP® Hand-Held Model GMP343 CO_2 probe and a Model G70 CARBOCAP® hand-held CO_2 meter. Measurements were taken in a static diffusion chamber made of glass (Figure K.1). Before each measurement, the edges were sealed with a small berm of dry soil placed along the bottom edge. The chamber then was covered with a black cloth that allowed essentially no photosynthetically active radiation to enter the chamber. This was measured with an AccuPAR LP80 Ceptometer. Observations were taken for 15 minutes. Steady-state respiration rates were achieved within a few minutes before data were recorded. Six replicates were taken for each condition. The depth to the bottom of the wetting front was measured with a meter stick for wetted soil tests.

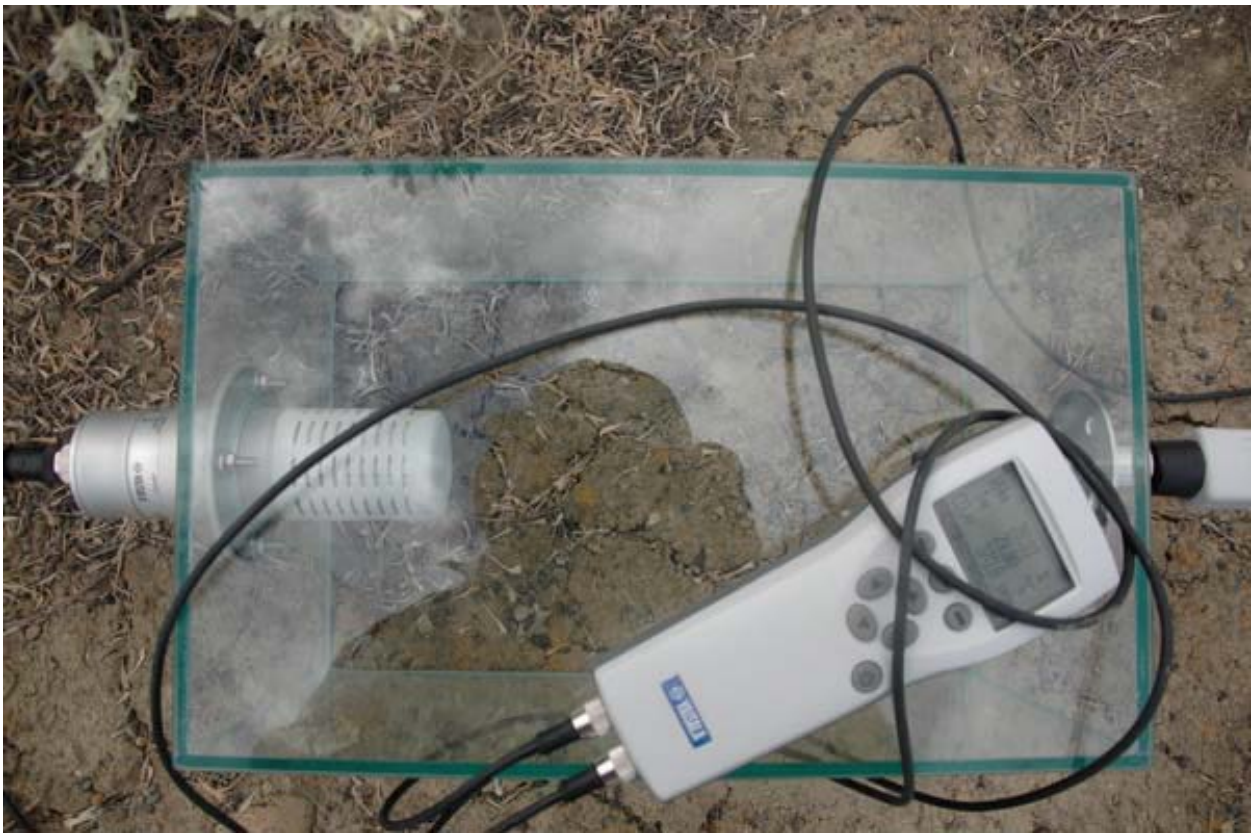

Figure K.1. Static Diffusion Chamber with Sensors and Readout Device

K.2.7 Roots

Root observations were taken using a Circon Agricultural Camera in clear mini-rhizotron tubes inclined at a 45° angle. Six mini-rhizotrons were placed in the irrigated and non-irrigated sections of the surface. Observations were taken from July 13 to July 21 in 1995, in June 1996, and on September 18, 1997. In 1997, only three tubes were examined in each treatment. The videos of each root tube were examined to compute root length density. The method was to count each root that intersected with the tube surface and each intersecting branching root from a root already in contact with the tube. In 1995 and 1996, all roots observed were considered alive. In 1997, live and dead roots were counted separately. Live roots are white to brown and turgid, with some roots having root hairs. Dead roots are dark in color and contracted within root channels in the soil. Differentiating live from dead roots is subjective. Root counts were taken in an area the width of the viewing area (1.55 cm) and 10 cm long. Count data were then divided by the observation area to yield a root length density value (Upchurch and Ritchie 1983).

K.2.8 Data Analysis

Student's t-test was used for single comparisons (Steele and Torrie 1960). Multiple range comparisons were done using the Tukey-Kramer HSD test. Linear regression was used to define relationships and test treatments effects (Neter and Wasserman 1974). Error terms are 1 standard error of the mean (1 SEM). Significance was tested at the $\alpha = 0.05$ level. Data analyses used JMP version 2.0.2 software (Sall et al. 1991) and JMP version 5.0 software (SAS Institute 2002). Mean data are presented with one standard error.

K.3 Results

K.3.1 Plant Canopy Dimensions, Leaf Area, and Leaf Area Index

Ericameria nauseosa grew significantly taller from 1995 through 1997 and were taller in the irrigated treatment than in the non-irrigated treatment (Figure K.2). Plants in the irrigated treatment increased from 37.8 to 54.1 cm and those in the non-irrigated treatment increased from 31.4 to 42.9 cm from 1995 to 1997 (Figure K.2). Linear regressions were significantly different for the two treatments ($F' = 7.43 > F[0.95;2,61] = 3.15$); see the linear test approach in Neter and Wasserman (1974). Although no height differences appeared between the treatments in any year, when all data were combined, plants in the irrigated treatment were significantly taller than those in the non-irrigated treatment (Figure K.2).

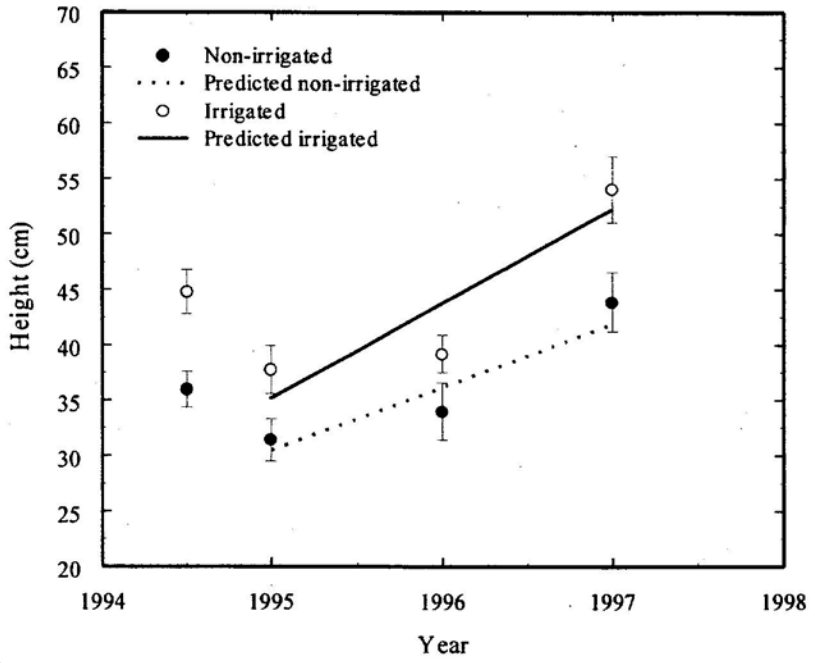

Figure K.2. Height of *E. nauseosa* from 1995 to 1997 in Irrigated and Non-irrigated Treatments. The two means displayed outside the fitted data sets are the combined means over time for each treatment. These two means are significantly different. Error bars are 1 SEM (After Figure 5.8 of Ward et al. 1997).

Artemisia tridentata grew significantly taller over the 3 years, but was not affected by irrigation (Figure K.3). Plants in the irrigated treatment increased from 45 to 59.3 cm, and those in the non-irrigated treatment increased from 37.1 to 64.7 cm from 1995 to 1997 (Figure K.3). Linear regressions were not significantly different for the two treatments ($F' = 3.03 < F'[0.95;2,101] = 3.10$; see Neter and Wasserman 1974). Thus, the data were combined to produce the linear regression line in Figure K.4. No differences between the treatments were observed in any year or when all data were combined.

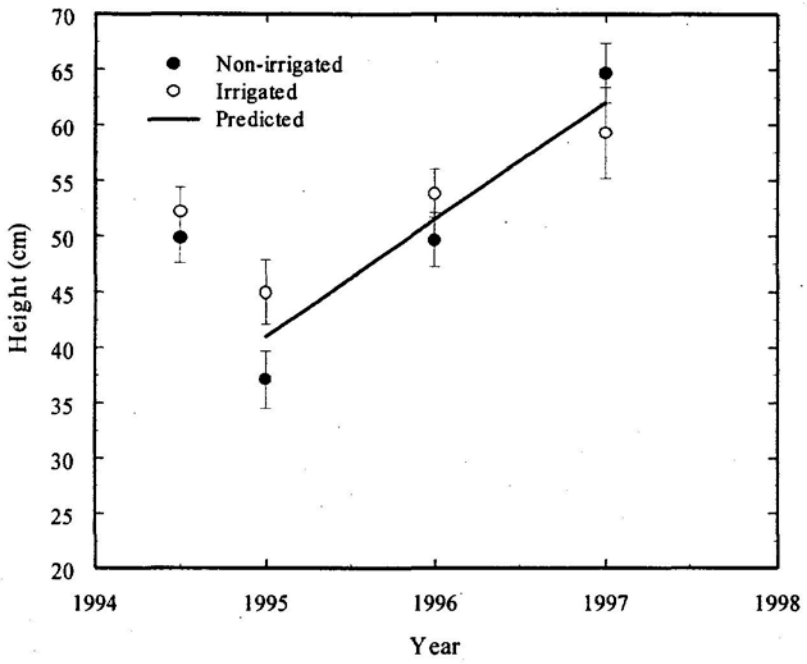

Figure K.3. Height of *A. tridentata* from 1995 to 1997 in Irrigated and Non-irrigated Treatments. The two means displayed outside the fitted data set are the combined means over time for each treatment. These two means are significantly different. Error bars are 1 SEM. (After Figure 5.9 of Ward et al. 1997).

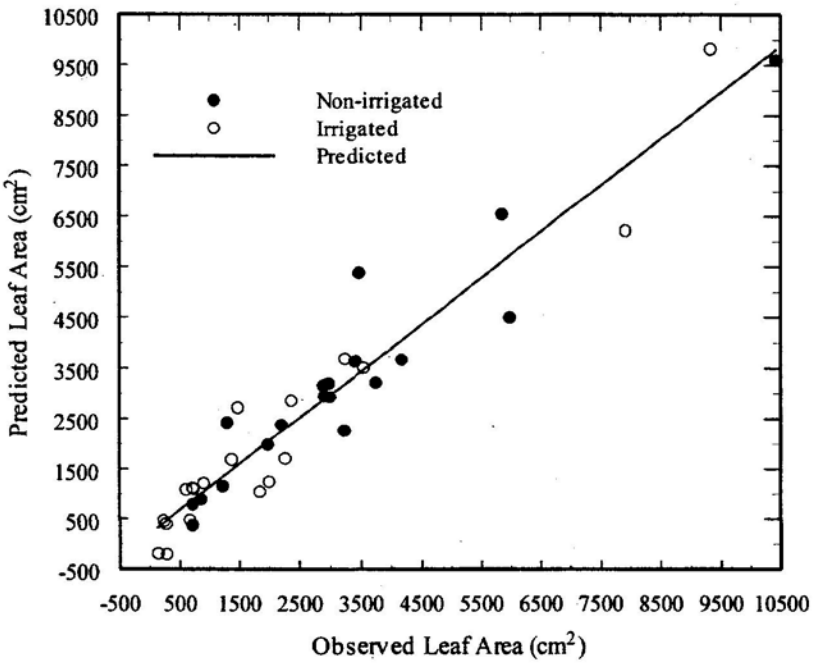

Figure K.4. Predicted Leaf Area Using Equation 5.2 Correlated with Observed Leaf Area for *A. tridentata* (After Figure 5.10 of Ward et al. 1997).

In 1997, the canopy characteristics, leaf area, and LAI were investigated for *A. tridentata*. This investigation supported efforts to understand the hydrology of the surface with respect to the two treatments. To compute ET rates, it is necessary to compute plant transpiration rates. The transpiration

rates for *A. tridentata* were estimated because it is the dominant shrub on the surface; it also will likely account for a large portion of plant transpiration from the surface. Computing transpiration rates for the entire shrub requires a measure of its entire leaf area. Canopy morphological measures were used to estimate canopy leaf area and LAI. Knowing the canopy leaf area and transpiration rates permits an estimate of canopy transpiration rates, as discussed in Section K.3.3.

The 38 plants divided between the treatments were used to create the model described in Eq. (K.2). The regression resulted in a significant [$F = (35.5; p < 0.00001; 8) = 0.92$] relation between observed and predicted values of leaf area (Figure K.4). The correlation between predicted and observed data resulted in a slope of 0.92 ± 0.045 (1 SEM) that is not significantly different from one; an intercept of 214 ± 163 is not significantly different from zero. Therefore, the use of Eq. (K.2) to predict leaf area of *A. tridentata* is justified.

Leaf area of *A. tridentata* was analyzed, based on the day when plants were harvested, to create the model that also was within a few days of the time when the 40 individual shrubs in the two treatments were measured morphologically. The results of model predictions are presented in Figure K.5 for both treatments over time in 1997. Of the 40 individual shrubs, four were smaller than the smallest individual used to create the model, which predicted negative values for these four; thus they were eliminated from further analysis. In the non-irrigated treatment, mean predicted canopy leaf area ranged from 301.5 to 483.1 cm^2 from mid-April to mid-June. However, values ranged only from 1524 to 2329 cm^2 in the irrigated treatment (Figure K.5). Linear regressions were significantly different for the two treatments [$F = 12.63 > F(0.95;2,106) = 3.10$]. The only significant difference between mean predicted canopy leaf area in the non-irrigated and irrigated treatments occurred in April 3.

LAI increased over time and was larger in the non-irrigated treatment than in the irrigated treatment (Table K.1). Values ranged from 0.198 to 0.303 in the irrigated treatment and from 0.460 to 0.737 in the non-irrigated treatment. These estimated LAI values are comparable to those observed for *A. tridentata* on the Fitzner-Eberhardt Arid Lands Ecology Reserve (Link et al. 1990). Leaf area index values in Link et al. (1990) averaged 0.25 in a mature ecosystem dominated by *A. tridentata*. The values computed in the non-irrigated treatment were three times larger in June than those observed in Link et al. (1990). It is likely that over time the *A. tridentata* element of the plant community will come into a steady state condition, if there are no fires, with an LAI closer to 0.25. The density of individuals on the PHB surface is probably greater than in comparable natural communities. Such a comparison has not been made.

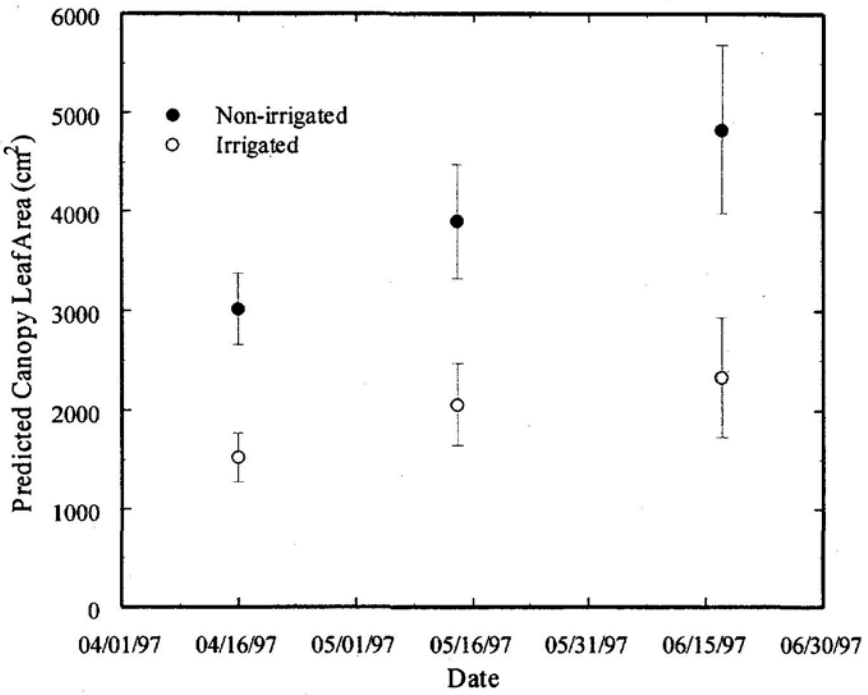

Figure K.5. Predicted Mean Canopy Leaf Area of *A. tridentata* for the Irrigated and Non-irrigated Treatments over 3 Months in 1997. Error bars are 1 SEM. (After Figure 5.11 of Ward et al. 1997).

Table K.1. Estimated Leaf Area Index of *A. tridentata* in Each Treatment in 1997 (After Table 5.11 of Ward et al. 1997).

Treatment	Date	Leaf Area Index
Irrigated	April 16	0.198
	May 14	0.268
	June 17	0.303
Non-Irrigated	April 16	0.460
	May 14	0.595
	June 17	0.737

The mean height and canopy area of individual sagebrush increased slightly from 2003 to 2004 in the north and south sections of the barrier (Table K.2). The mean height and canopy area of rabbitbrush shrubs in the north section increased slightly, while the height and area of rabbitbrush in the non-irrigated treatment has remained relatively the same between 2003 and 2004. Summarized shrub measurement results are shown in Table K.1.

Table K.2. Shrub Measurement Summary Data of 2003 and 2004 on the Prototype Hanford Barrier (After Table 4.1 of Ward et al. 2005b)

Dimension	North Section		South Section	
	Mean[(a)]	Range[(a)]	Mean[(a)]	Range[(a)]
Sagebrush				
Area (cm^2)	4,449 (3,294)	370-15,456 (690-6,975)	4,808 (3,224)	504-8,200 (481-8,187)
Height (cm)	69 (65)	30-118 (40-80)	66 (61)	40-92 (20-82)

Rabbitbrush[(b)]				
Area (cm^2)	3,600 (2,851)	680-9,188 (325-2,950)	821 (850)	782-860 (240-1,250)
Height (cm)	54 (66)	38-68 (42-64)	35 (31)	30-39 (21-50)

(a) 2003 measurements are shown in parentheses.
(b) Note for north section rabbitbrush, $n = 5$; for south section rabbitbrush, $n = 2$.

The mean height and canopy area of sagebrush was the same in 2004 and 2007 in the north and south sections of the barrier (Table K.3). Sagebrush height and canopy area were not significantly different in the south (Table K.3) and north (Table K.3) sections of the barrier in 2007. The mean height of rabbitbrush in the north section was the same in 2004 and 2007. The canopy area was not significantly different (Table K.3) in 2007 than in 2004 in the north section of the barrier. In the south section of the barrier, the height and canopy area of rabbitbrush were apparently larger in 2007 than in 2004. This may be an artifact given that only two shrubs were measured in 2004. There was no significant difference (Table K.3) in rabbitbrush height and canopy area between the north and south sections of the barrier in 2007 (Table K.3). Seedlings in 2007 that were about 6 cm tall were 2 years old, seedlings about 14 cm tall were 4 years old, and shrubs about 27 cm tall were 8 years old.

Table K.3**.** Shrub Measurement Summary Data of 2004 and 2007 on the Prototype Hanford Barrier (After Table 4.1 of Ward et al. 2007).

Dimension	North Section		South Section	
	Mean[(a)]	Range[(a)]	Mean[(a)]	Range[(a)]
Sagebrush				
Area (cm^2)	4,449 (4,449)	72-19,050 (370-15,456)	5,283 (4,808)	504-13,000 (504-8,200)
Height (cm)	69 (69)	18-129 (30-118)	65 (66)	28-86 (40-92)
Rabbitbrush[(b)]				
Area (cm^2)	7,520 (3,600)	680-9,188 (325-2,950)	5,584 (821)	1,769-9,379 (782-860)
Height (cm)	56 (54)	23-76 (38-68)	57 (35)	48-69 (30-39)

(a) 2004 measurements are shown in parentheses.
(b) Note for north section rabbitbrush, $n = 5$; for south section rabbitbrush, $n = 2$ in 2004 and $n = 5$ in 2007.

In 2008, the height of sagebrush was consistently larger in all quadrats except those in the 25th row near the north section of the barrier (Figure K.6). Sagebrush on the north edge of the burned area was much shorter than in the interior of the burned area. This is because there is significantly more recruitment along the north edge of the burned area where there is less competition.

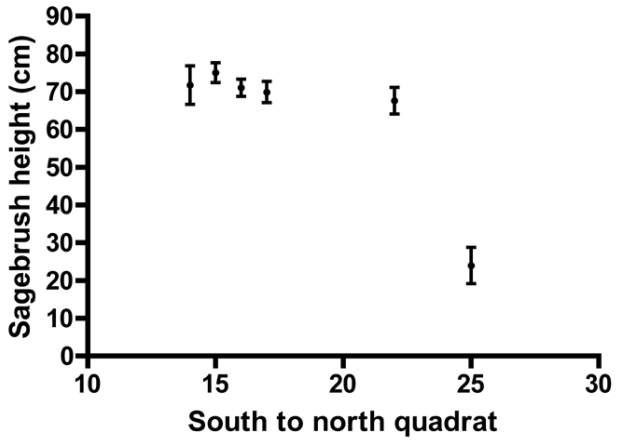

Figure K.6. Mean Height of Sagebrush Plants in Quadrats from the South Side of the Burned Area to the North Side in 2008. (After Figure 3.3 of Ward et al. 2009a)

In 2009, the mean height of *A. tridentata* in the unburned section was 64.5 ± 3.34 cm and 6.95 ± 1.18 cm in the burned section for new seedlings. The canopy volume of *A. tridentata* in the unburned section was 150.8 ± 19.7 dm^3 and only 0.165 ± 0.483 dm^3 in burned section for new seedlings.

In 2010, *A. tridentata* was significantly taller near the edge of the barrier than in the center of the barrier (Table K.4). Plants were about two times taller in both sections of the barrier. Young *E. wawawaiensis* plants that likely germinated after the fire were significantly shorter, but were 82% as tall as older plants. Eighty-three percent of the surveyed *A. tridentata* shrubs in the unburned section of the barrier were in flower. None of the *A. tridentata* shrubs in the burned section had flowered.

Table K.4**.** Mean canopy dimensions ± (1 SEM, *n*) in 2010 of plants in the burned and unburned sections of the barrier where "*n*" is the number of samples.

Species	Burned		Unburned	
	Height (cm), *n*	Volume (dm^3)	Height (cm)	Volume (dm^3)
Artemisia tridentata	*p* = 0.0063	*p* = 0.0908	*p* = 0.0005	*p* = 0.0001
Plot edge	23.6 ± 2.09, 15	6.96 ± 1.31	112.7 ± 7.69, 3	1100 ± 345.9
Plot center	12.1 ± 2.71, 9	2.79 ± 1.81	66.4 ± 3.82, 27	157.5 ± 22.9
Machaeranthera canescens	47.2 ± 4.04, 30	71.8 ± 14.9		
Ericameria nauseosa	27.9 ± 1.71, 30	15.6 ± 3.04		
Elymus wawawaiensis	P = 0.0001	P = 0.0082		
Old	66.3 ± 1.45, 19	64.9 ± 7.56		
Young	54.6 ± 1.42, 11	34.8 ± 4.50		

In 2011, sampling density at the edges was insufficient to test for effects at the species level (Table K.5). Combining all data to compare the effect of the edge on plant height and volume was adequate to detect effects. Plant height was significantly (*p* = 0.0005) higher at the edge than in the center of the surface. *Elymus wawawaiensis* was taller in 2011 than in 2010. Ninety-seven percent of the surveyed *A. tridentata* shrubs in the unburned section of the barrier were in flower. Seven percent of the *A. tridentata* shrubs in the burned section had flowered.

Table K.5**.** Mean canopy dimensions ± (1 SEM, *n*) in 2011 of plants in the burned and unburned sections of the barrier where "*n*" is the number of samples.

Species	Burned		Unburned	
	Height (cm), *n*	Volume (dm^3)	Height (cm), *n*	Volume (dm^3)
Artemisia tridentata				
Plot edge	34.7 ± 7.84, 3	10.6 ± 4.52	124 ± 31.3, 3	788 ± 375
Plot center	15.4 ± 1.00, 27	1.57 ± 0.45	85.0 ± 7.82, 27	246 ± 27.6
Machaeranthera canescens				
Plot edge	59 ± 1, 2	63.2 ± 5.14		
Plot center	43.7 ± 2.12, 28	14.1 ± 3.17		
Ericameria nauseosa				
Plot edge	40.5 ± 0.5, 2	25.0 ± 15.5	82.3 ± 3.93, 3	497 ± 191
Plot center	31.1 ± 1.88, 28	13.4 ± 1.98	34.6 ± 7.82, 8	49.4 ± 34.5
Elymus wawawaiensis				
Plot edge	86.3 ± 2.65, 6	79.8 ± 22.7		
Plot center	81.3 ± 3.06, 24	35.7 ± 6.25		

In 2008, LAI values ranged from 0 in apparently very low to non-existent canopy conditions to 4.75 in the dense cover conditions in the first quadrat along the west edge of the surface. Quadrats along the two edges were combined ($n = 28$) and compared with quadrats in the center of the test area ($n = 55$). Mean LAI (1.34 ± 0.17) along the edges was significantly ($p < 0.0001$) greater than in the center (0.47 ± 0.043). The pattern of LAI across the surface (Figure K.7) demonstrates the effect of location on canopy structure.

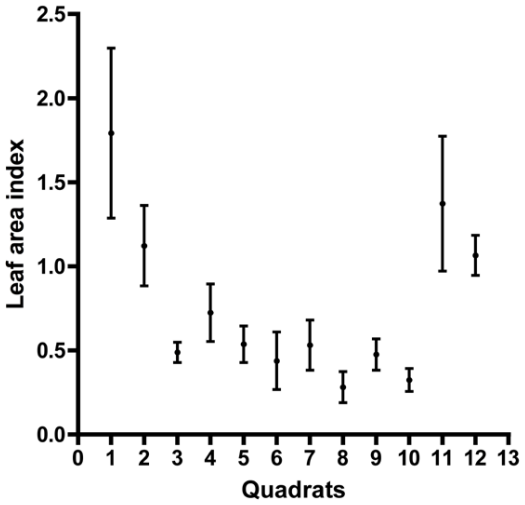

Figure K.7. Pre-Burn LAI Across the Barrier Surface. (After Figure 3.11 of Ward et al. 2009a)

In 2009, post-burn measurements of LAI show that the mean LAI on the unburned section of the barrier (1.13 ± 0.087) was not significantly different from the mean LAI in the McGee Ranch unburned plant community (0.692 ± 0.129). The mean LAI in the burned section of the barrier (0.254 ± 0.02) was not significantly different from the mean LAI in the McGee Ranch old burn plant community (0.103 ± 0.0.031). Values in the two burned areas were significantly lower than those in the two unburned areas.

K.3.2 Xylem Water Status

In 1996, xylem pressure potential values were significantly lower in the ambient precipitation treatment than in the irrigated treatment (Table K.6). Both species had almost identical mean values within treatments, with more variation in the ambient precipitation treatment than in the irrigated treatment. Values ranged from -7 to -12 bars in the irrigated treatment and -27 to -55 bars in the ambient precipitation treatment.

Table K.6**.** Mean Pre-Dawn Xylem Pressure Potential with One Standard Error (SE, n = 5 to 6) in 1996. Note that 1 MPa =10 bars and *C. nauseosus* = *E. nauseosa.* (After Table 5.6 of Gee et al. 1996)

Species	Treatment	Mean Xylem Pressure Potential (bar)	SE
A. tridentata	irrigated	-9.2	0.086
	ambient	-38.7	0.418
E. nauseosa	irrigated	-9.2	0.066
	ambient	-38.8	0.305

In 2009, xylem pressure potential was measured on plants in the burned and unburned conditions. Measurements were made just before dawn to assess maximal xylem pressure potential. *Artemisia tridentata*, *S. kali*, and *M. officinalis* were measured on the west, central, and east sides of the surface. In addition, *A. tridentata* was measured in the unburned condition in late afternoon to determine the lowest possible values. There was no significant (p = 0.570) effect of species on xylem pressure potential for early morning readings in the burned condition. These values were then combined to test the effect of location on xylem pressure potential in the burned condition. Location had a significant (p = 0.0045) effect on xylem pressure potential. Plants on the west third of the surface had significantly greater xylem pressure (-17.5 ± 0.89 bars, n = 12) than those on the middle and east thirds of the surface (-26.3 ± 2.49 bars, n = 13). This observation suggests that similar variation in the soil water potential may exist on the burned section of the barrier.

Early morning and late afternoon observations were compared on *A. tridentata* in the unburned condition. There was no significant (p = 0.523) effect of observation time on xylem pressure potential. The mean value for all combined observations was -74.3 ± 3.19 bars (n = 11). Having early morning pressure potential values as low as those in late afternoon means that *A. tridentata* has essentially extracted all water available to it from the soil profile at this time of year. The species is nearly inactive under these conditions. Values ranged from -51 to -87.5 bars.

In 2010, xylem pressure potential was measured on plants in the burned and unburned conditions. *Artemisia tridentata* xylem pressure potential was not significantly (p = 0.2963) different among samples collected near ports 1, 3, and 6 on the unburned section of the barrier. The mean values are -50.0, -44.7, and -46.3 for ports 1, 3, and 6, respectively. *Machaeranthera canescens* plants ranged from short to tall throughout the burned section of the barrier. The effect of height on xylem pressure potential was compared (n = 5). Short plants were less than 20 cm tall while taller plants were at least 50 cm tall. There was no significant (p = 0.7135) effect of height on xylem pressure potential. The mean value of all 10 plants used in this test was -40 ± 6 bars. *Machaeranthera canescens* xylem pressure potential was

measured on three plants near each of the six neutron probe ports in the burned section of the barrier (Table K.7). There was significant variability among plants at the six ports.

Table K.7. Mean (± 1 SEM) *Machaeranthera canescens* xylem Pressure Potential (bars) near the Six Neutron Probe Ports on the Burned Section of the Barrier. Means with the same letter are not significantly different. Observations were taken on August 27, 2010.

Port	Mean ± 1 SEM	Tukey's HSD test
1	-58.7 ± 2.03	a,b
2	-56 ± 4	a,b
3	-76.3 ± 4.84	b
4	-47.3 ± 3.93	a
5	-69 ± 6.08	b
6	-69 ± 4.58	b

Further observations were made at points on the surface and along the edge of the surface on the burned section of the barrier (Table K.8). These data along with those of Table K.7 indicate significant spatial variation in pre-dawn xylem pressure potential across the surface. The highest values were along the east and west edges, which also have larger plants. This indicates that more water is stored in the soil along the edges. An unusually wet location at quad (9, 16) is similar to edge locations (Table K.3). The three individual plant values in this quad were -14, -14, and -32 bars. The range of observations was from -10 to -86 bars. Some of this variation may be attributed to more soil water near the edges and less in the drier center of the surface. Other possible sources include variation in rooting depth. If the soils are wettest deep in the profile, then only plants with deep roots will reach this depth and have the highest xylem pressure potential values. There is only one observation of rooting depth for *M. canescens* at the Hanford Site and roots were found down to 155 cm deep (Link et al. 1994a). It is possible that *M. canescens* has deeper roots. It would be necessary to determine rooting depth of many individuals or a community of this species to obtain better rooting depth estimates. It is also possible that roots do reach the 2-m depth of the surface and that there is considerable variation in soil water storage patterns on the surface.

Table K.8. Mean (± 1 SEM) *Machaeranthera canescens* xylem pressure potential (bars) near the Six Locations on the Burned Section of the Barrier. Means with the same letter are not significantly different. Observations were taken on August 27, 2010.

Location	Mean ± 1 SEM	Tukey's HSD test
Quad (3,16)	-56 ± 1.53	b
Quad (6, 16)	-55.3 ± 3.48	b
Quad (9, 16)	-20 ± 6	a
Eastern edge	-21.3 ± 0.88	a
Western edge	-18.8 ± 2.13	a
Northeast corner	-34 ± 7.57	a

K.3.3 Gas Exchange

Transpiration and net photosynthetic data based on leaf area are presented here for 1995, 1996, and 1997. Stomatal conductance values used to compute transpiration are presented for 1995 and 1996 in Gee et al. (1996). In the non-irrigated treatment, transpiration rate had the low value near 0.75 mmol $m^{-2}s^{-1}$ in February 1995 and the high value of 19.7 mmol $m^{-2}s^{-1}$ in late July 1996. In the irrigated treatment, values were at a maximum of 14.2 mmol $m^{-2}s^{-1}$ in June 1997 (Figure K.8). The only difference between treatments on any of the 5 observations was in July 1996, when the transpiration rate in the non-irrigated treatment was significantly greater than in the irrigated treatment (p = 0.033).

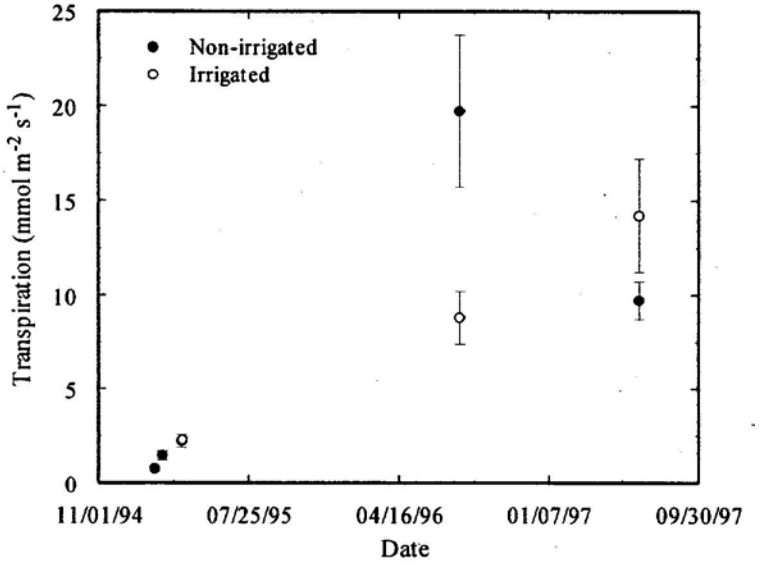

Figure K.8. Transpiration Rates for *A. tridentata* Collected in 1995, 1996, and 1997 in the Irrigated and Non-irrigated Treatments. Data in 1997 were collected on June 18. Error bars are 1 SEM. (After Figure 5.12 of Ward et al. 1997)

Combining these transpiration data with leaf area data for the surface provides an estimate of the water loss rate from the surface through *A. tridentata*. This estimate assumes that transpiration rates of the entire shrub are similar to that of the stem tips used to collect the transpiration data. Estimates were computed by converting transpiration rates for June 18, 1997 (14.2 mmol $m^{-2}s^{-1}$ for irrigated, 9.7 mmol $m^{-2}s^{-1}$ for non-irrigated) to the equivalent that would leave the surface for the entire leaf area (393 m^2 for irrigated, 955 m^2 for non-irrigated) on the surface in 1 hour (20,090 mol h^{-1} for irrigated, 33,352 mo1 h^{-1} for non-irrigated). This figure was then converted to the equivalent depth of water on the surface (0.46 mm h^{-1} for non-irrigated, 0.28 mm h^{-1} for irrigated). These rates are only estimates of the true rate, one that is difficult to measure. The rates presented here are based on stem tips and are likely to be higher than rates for the entire canopy. This possibility has been demonstrated for *Bromus tectorum* canopies by Link et al. (1995). The rates observed in this study are probably near maximum values for the day as they were collected just prior to midday. Rates will be lower at other times during the day. A better estimate would be achieved by the use of whole plant gas exchange data collected over an entire day.

The transpiration values obtained here should not be used to estimate the components of ET. They are not representative of all the vegetation on the surface nor are they representative of the time scale used in ET estimates for the surface. These values can be considered maximal for estimation purposes.

Net photosynthetic rates were near 3 μmol $m^{-2}s^{-1}$ in February 1995 and 19.7 μmol $m^{-2}s^{-1}$ in July 1996 in the non-irrigated treatment. In the irrigated treatment, values were at a maximum of 17.9 μmol $m^{-2}s^{-1}$ in June 1997 (Figure K.9). No differences were found in treatments on any of the 5 observations ($p > 0.05$).

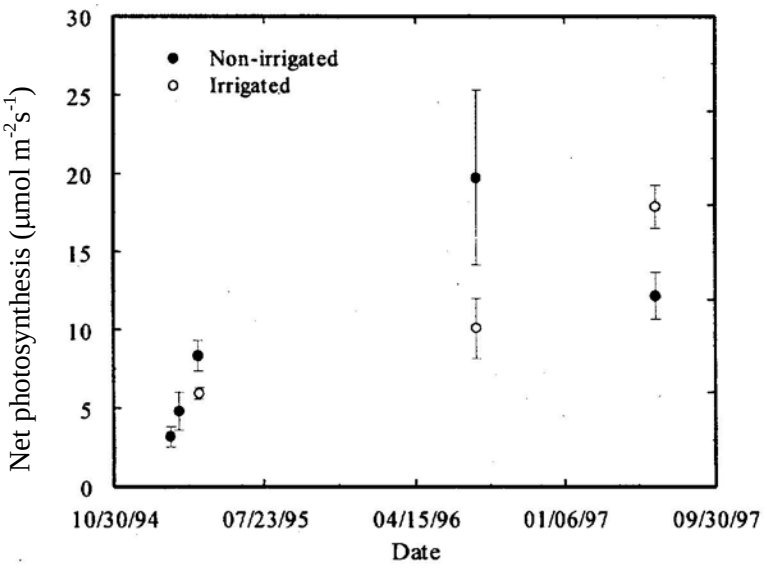

Figure K.9. Net Photosynthesis in *A. tridentata* Collected in 1995, 1996, and 1997 in the Irrigated and Non-irrigated Treatments. Data in 1997 were collected on June 18. Error bars are 1 SEM. (After Figure 5.13 of Ward et al. 1997. Note that the original label for the vertical axis was in error.)

K.3.4 Biological Activity and Soil Carbon Dioxide Flux

In 2009, soil respiration rates in the burned and unburned conditions were compared when surface soils were dry and when surface soils had been wetted by rain to an average depth of 33.8 ± 1.1 mm (Table K.9). When the upper soil profile was dry, soil respiration rates were significantly ($p = 0.0205$) greater in the burned treatment than in the unburned treatment. When the upper soil profile had been wetted, there was no significant ($p = 0.339$) difference between the treatments. Given that observations were taken from the same location in wet and dry conditions, dry rates were subtracted from wet rates and compared between the treatments. These differences were not significantly ($p = 0.194$) different; thus, observations in the treatments were combined to compare wet and dry rates. Soil respiration rates (μmol CO_2 m^{-2} s^{-1}) were significantly ($p < 0.0001$, $n = 12$) greater in the wet surface soils (0.834 ± 0.0725) than in the dry surface soils (0.104 ± 0.0137).

Table K.9. Mean Soil Respiration Rates ± 1 SEM (μmol CO_2 m^{-2} s^{-1}) Measured in 2009 (After Table 3.11 of Ward et al. 2009a).

Condition	Treatments	
	Unburned	Burned
Dry	0.074±0.013 a	0.134±0.018 b
Wet	0.907±0.124 c	0.76±0.074 c
Different letters within conditions indicate significant differences between		

treatments (n = 6)

The higher respiration under dry conditions in the burned area compared with the unburned area is likely a result of the wetter soil profile. The wetter soil profile, as evidenced by plants with higher water potential values, yields more active plants that have higher root-respiration rates. It is likely that soil respiration is primarily root respiration given that the soil surface was very dry, limiting surface microbial activity. When the surface soils were wetted, it is likely that a significant component of the respiration was microbial. Given that soil organic matter increased or decreased depending on the assessment method after the fire, it is possible that there was enough organic carbon in the burned soil to support respiration rates as high as in the unburned soil. While there was no attempt to account for the root activity or biomass in the wetted soil zone, it is likely that these roots were more active when wetted by the rain. Roots were observed in the upper few centimeters of the soil in the burned area, suggesting that they had not yet decomposed after the fire or that they were, in part, new roots from active vegetation.

K.3.5 Root Study

Root length data are presented with respect to treatment, year, and depth in Figure K.10. Root length density exhibits little pattern with depth other than a decrease near the bottom in 1997.

Mean root length density over depths and holes was significantly greater in the irrigated treatment than in the non-irrigated treatment in 1996 and 1997 (Figure K.11).

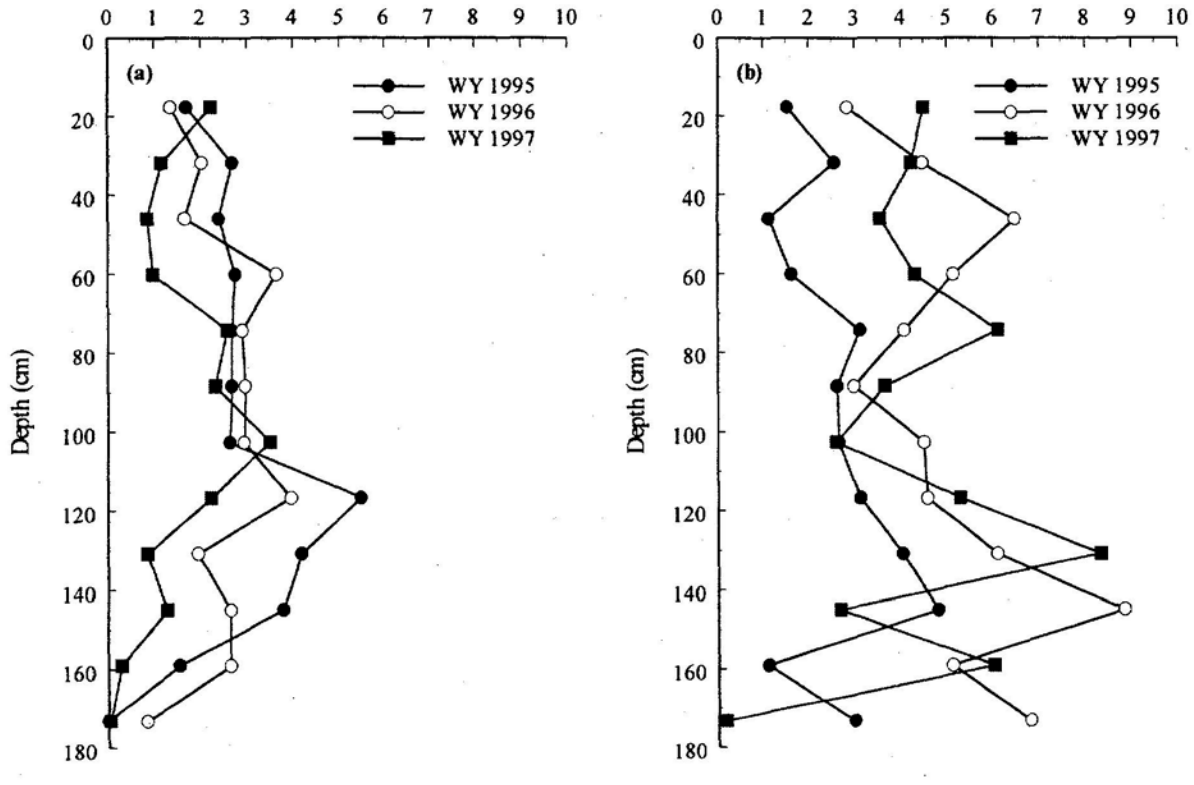

Figure K.10. Mean Root Length Density as a Function of Depth in 1995, 1996, and 1997: (a) the non-irrigated treatment and (b) the irrigated treatment (after Figure 5.14 of Ward et al. 1997).

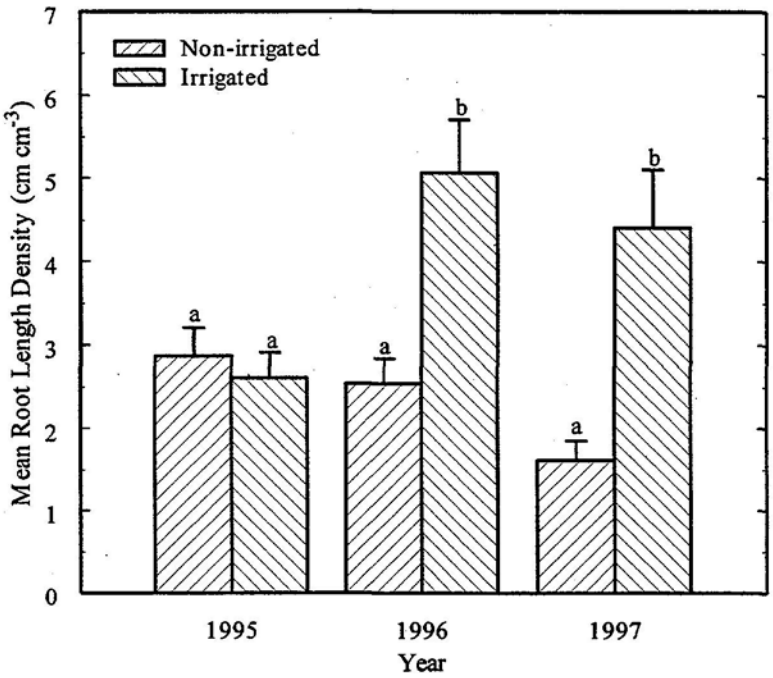

Figure K.11. Mean Root Length Density over Depths and Holes in 1995, 1996, and 1997 for the Non-irrigated and Irrigated Treatments. Error bars are 1 SEM. Means with differing letters within years are significantly different (After Figure 5.15 of Ward et al. 1997).

During 1995 and 1996, no attempt was made to distinguish live from dead roots. By 1997, dead roots became obvious, and both live and dead root length density were quantified. This data is expressed as the ratio of dead to live root length density with depth (Figure K.12). The mean ratio of dead to live root length density over depths and holes was significantly different with a ratio of 0.25 ± 0.08 in the irrigated treatment and 1.14 ± 0.24 in the non-irrigated treatment.

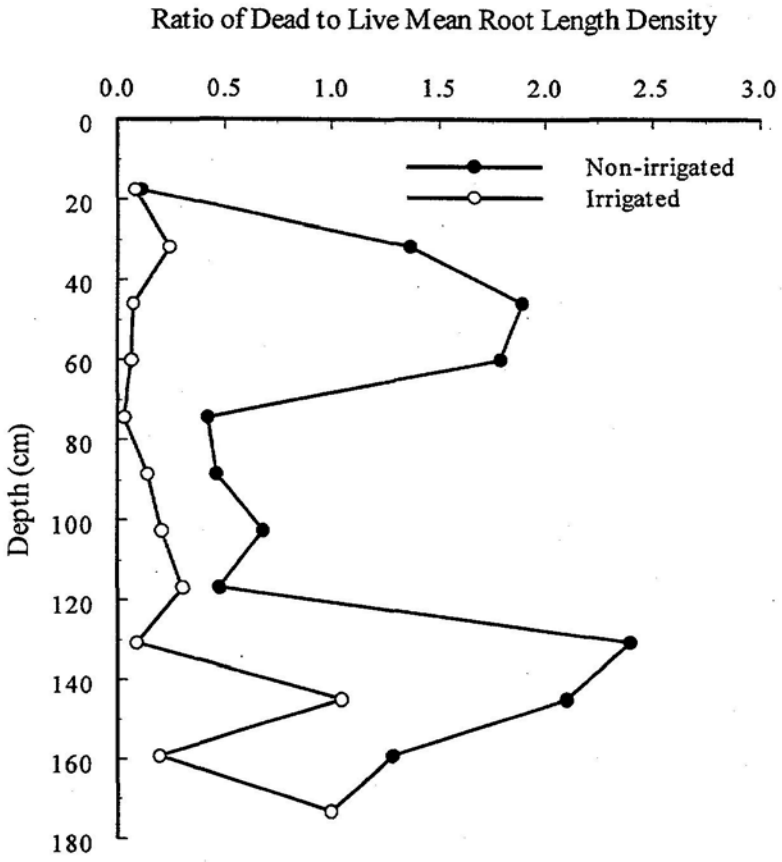

Figure K.12. Mean Ratio of Dead to Live Root Length Density in 1997 for the Non-irrigated and Irrigated Treatments (After Figure 5.16 of Ward et al. 1997).

K.4 Discussion

The purpose of this research was to provide basic information on plant structure and function that can be used to parameterize models for the ET prediction and to gain insight into soil moisture patterns associated with plant size and of pre-dawn xylem water potential. Plant height, canopy dimensions and canopy leaf area, LAI, rooting depth, and root length density are discussed. Plant physiological characteristics of xylem water potential, transpiration, and net photosynthesis are assessed. Soil/root respiration data were also gathered to assess biological activity after the fire.

K.4.1 Plant Canopy Dimensions, Leaf Area, and Leaf Area Index

The dominant plant on the surface was *A. tridentata.* This species was dominant on all portions of the surface until the fire. After the fire, *A. tridentata* became a minor element of the burned area. Most of the plant structural measurements were performed on *A. tridentata.* Average *A. tridentata* height increased to a little over 60 cm by 1997 and remained between about 65 cm and 70 cm average after that, except in the unburned section in 2011, where average height was 85 cm in the center of the section. Height varied across the surface, rising to 124 cm along the edges. Taller plants near the edges indicate there has been more water available along the edges. Some of this extra water may have infiltrated into the cap soils

from the adjacent graveled road. The STOMP model used canopy height as a parameter (Ward et al. 2005a). Efforts to model ET for barriers at Hanford can focus on *A. tridentata*, but should also be able to incorporate plant community dynamics based on the changes after the fire and other potential planting mixes as appropriate for differing locations and soils at Hanford.

The LAI determined for *A. tridentata* is used in a number of models to predict ET (Bohnhoff et al. 2009; Roesler et al. 2002; Ward et al. 2005a). The LAI determined in this study provides values from April to June 1997 as a function of the irrigation treatments and in 2008 and 2009 as a function of location on the barrier surface and the fire. These values can be used for ET models for the PHB or other similar barriers at Hanford. The LAI of the PHB was not significantly different from that of the natural analog McGee Ranch sites; thus, physiological performance based on LAI has been achieved.

K.4.2 Plant Xylem Water Status

Observations of plant xylem water status indicated that there was considerable variation across the surface. The edges were wetter than interior portions of the surface before dawn. There also was considerable variation in the interior portions of the surface after the burn. Variation was noted on plants growing next to probe ports. An examination of soil moisture values at the ports to see if there is a relationship with the pre-dawn plant xylem water values would be useful and may allow the use of plants as soil moisture sensors across the surface. One location [quad (9,16)] on the surface had values as high as that of edge plants. The use of plants as soil moisture sensors may not be perfect (Donovan et al. 2001), but they will allow for a dense assessment of soil water status across surfaces.

Soil moisture models such as UNSAT-H (Fayer 2000), as noted in Roesler et al. (2002) for landfill covers, make assumptions about the wilting point of plants as transpiration parameters. These assumptions are related to minimum soil moisture contents at the driest point in the season and deep in the root zone (Gee et al. 1999), as noted in Roesler et al. (2002). The lowest values noted are -61.3 bar as the wilting point suction. This study compared pre-dawn and late afternoon values on *A. tridentata* and found no difference. The mean value for all combined observations was -74.3 ± 3.19 bars (n = 11). Having early morning pressure potential values as low as those in late afternoon means that *A. tridentata* has essentially extracted all water available to it from the soil profile at this time of year. The species is nearly inactive under these conditions. Values ranged from -51 to -87.5 bars. It is possible for values to be much lower, as the lowest value observed was -87.5 bars. These arid land plants do not technically have a wilting point. They have a quiescent point. *Artemisia tridentata* does not wilt, but will drop spring leaves, leaving smaller green leaves on the shrub through the season. Soil moisture models can be re-parameterized using such information. The differences between soil moisture status and pre-dawn xylem pressure status could be characterized to determine any offsets (Donovan et al. 2001). Another assumption noted by Roesler et al. (2002) is the topsoil layer was excluded from wilting point determinations because the soil is dried to lower water content by ET. This assumption does not take into account the phenomenon of hydraulic lift (Caldwell et al. 1998), where moisture is moved by roots from the deepest wettest soil root zone at night to the drier upper layers and leaked into the rhizosphere. This water is rapidly removed by transpiration during the day.

K.4.3 Gas Exchange

The gas exchange data collected in 1995 through 1997 provided an upper estimate of *A. tridentata* transpiration and net photosynthesis at midday and in full sun. These values can be useful for models by providing an assessment of activity through a growing season and as affected by three times the normal precipitation. It should be noted that gas exchange rates in 1996 were lower in the irrigated treatment than in the ambient precipitation treatment and indicate high water stress on *A. tridentata.*

K.4.4 Biological Activity and Soil Carbon Dioxide Flux

The assessment of soil carbon dioxide flux in the year after the fire revealed that rates were higher in the burned section than in the unburned section when surface soils were dry. This may be because the soils in the burned section were wetter and thus there was more root respiration than in the drier unburned section. Upon wetting there were no longer differences between the two sections. This indicates that the soil microbiological potential as affected by the fire was not significant in the season after the fire and is not a concern for barrier performance.

K.4.5 Root Study

Roots grew to the bottom of the assessment tube viewing position (about 175 cm) in the first year after planting in the irrigated section and by the second year in the ambient precipitation section. These roots were primarily those of *A. tridentata*. This indicates that deep-rooted *A. tridentata* shrubs rapidly accessed nearly the entire soil profile for barriers after construction.

Root data gathered in the first 3 years after construction provided rooting depth and root length density information needed by soil moisture models as discussed in Roesler et al. (2002), Piet et al. (2003), Ward et al. (2005), and Bohnhoff et al. (2009).

K.4.6 Management Implications

Implications for management based on plant structure and function are twofold. The first implication is that soil moisture patterns on barrier surfaces are significant and may be mapped using plants as soil moisture sensors. Deep-rooted plants to be used on barriers offer soil moisture assessments for the deepest and wettest root zone. While using pre-dawn measures of plant xylem water potential may not be perfect, it does allow for assessment of spatial patterns. An effort to relate pre-dawn measures of plant xylem water potential to values obtained with soil moisture probes or by destructive sampling would offer the ability to assess spatial variation in soil moisture on barriers. The ability to finely assess such patterns would improve stakeholder confidence in barriers.

The second implication is that while the plant structure and function information gathered will be helpful for soil moisture models, the information is not sufficient to parameterize or drive such models without making a number of assumptions. Insufficient information has been gathered for root structure and function. The root observation tubes remain in place and can be reassessed. A new root camera was obtained for this purpose by one of the stakeholders (The Confederated Tribes of the Umatilla Indian Reservation) and its use is justified to determine root characteristics after nearly 20 years. Efforts to define LAI, plant water status, and transpiration in much more detail are justified to allow soil moisture models to predict soil moisture dynamics on barriers. There has been no effort to incorporate the existing plant function and structure data into soil moisture models for the PHB. Improving the predictive abilities of such models, especially for differing plant types, would improve stakeholder confidence in barriers.

K.4.7 Implications for Barrier Performance

Implications for barrier performance are related to observed variations in pre-dawn measures of plant xylem water potential. The significant variations in pre-dawn measures of plant xylem water potential across the surface indicate that barrier performance may not have been assessed adequately with the current distribution of soil moisture probes on the surface. The edges and points in the interior of the surface are significantly wetter than other areas on the surface. It may be possible that weak points on the

surface exist but are not well recognized. This can be assessed by measuring pre-dawn plant xylem water potential in an intensive mapping effort across the surface.

K.5 Conclusion

Plant structure and function was assessed on the Prototype Hanford Barrier as a function of revegetation, irrigation, and fire. The dominant plant has been the deep-rooted *A. tridentata* shrub, although it was nearly eliminated by the fire at the north section. The dominant plant after the fire was the 1.55 m deep-rooted forb, *M. canescens* (Link et al. 1994b) on the burned section of the surface. The *A. tridentata* had nearly reached full height 3 years after planting. It can be concluded that revegetating was functionally rapid and that the deep-rooted shrub, *A. tridentata*, served to dominate such surfaces. Leaf area index values were highest along the barrier edges where there was more available water. Plant xylem water potential was variable across the surface, indicating that soil moisture was also variable across the surface. Plant gas exchange information gathered for 3 years after initiation of the plantings provided useful information for soil moisture models as do plant height, LAI, plant xylem water potential, rooting depth, and root length density information.

Acknowledgement

Research was funded by the U.S. Department of Energy under Contract DE-AC06-76RLO 1830 with the Pacific Northwest National Laboratory. We thank Glendon Gee for conceiving the Prototype Hanford Barrier and early support. We thank Kevin Leary for initiating, helping with, and funding the fire portion of the study. We thank Bill Mast, Jere Boudell, Traci Degerman, Jennifer Lewinsohn, Sally Simmons, Karen Barton, Andrew Pomiak, Dale Loth, Jenifer Linville, and Janice Maya for technical assistance.

References

Albright, WH, CH Benson, GW Gee, AC Roesler, T Abichou, P Apiwantragoon, BF Lyles, and SA Rock. 2004. "Field Water Balance of Landfill Final Covers," *Journal of Environmental Quality*, 33(6):2317-2332.

Anderson, JE. 1993. "Managing Soil Moisture on Waste Burial Sites in Arid Regions. ," *Journal of Environmental Quality*, 22:62-69.

Anderson, JE and AD Forman. 2002. *The Protective Cap/Biobarrier Experiment a Study of Alternative Evapotranspiration Caps for the Idaho National Engineering and Environmental Laboratory*, Stoller-ESER-46 Stoller Corporation, Idaha Falls, Idaho. Available at http://www.gsseser.com/PDF/PCBESummaryweb.pdf.

Bohnhoff, GL, AS Ogorzalek, CH Benson, CD Shackelford, and P Apiwantragoon. 2009. "Field Data and Water-Balance Predictions for a Monolithic Cover in a Semiarid Climate," *Journal of Geotechnical and Geoenvironmental Engineering*, 135:333-348.

Caldwell, MM, TE Dawson, and JH Richards. 1998. "Hydraulic Lift: Consequences of Water Efflux from the Roots of Plants," *Oecologia*, 113:151-161.

Cui, Y-J and JG Zornberg. 2008. "Water Balance and Evapotranspiration Monitoring in Geotechnical and Geoenvironmental Engineering," *Geotech. Geol. Eng.*, 26(6):783-798.

DOE-RL. 1993. *Treatability Test Plan for the 200-BP-1 Prototype Surface Barrier*, DOE/RL-93-27, U.S. Department of Energy Richland Operations Office, Richland, Washington. Available at http://www.osti.gov/energycitations/servlets/purl/10185012-iIHFSc/.

DOE-RL. 1999. *200-BP-1 Prototype Barrier Treatability Test Report*, DOE/RL-99-11 Rev. 0, U.S. Department of Energy Richland Operations Office, Richland, Washington.

DOE-RL. 2013. *Hanford Site Cleanup Completion Framework*, DOE/RL-2009-10, Rev. 1, U.S. Department of Energy Richland Operations Office, Richland, Washington. Available at http://www.hanford.gov/files.cfm/Comp_Framework_Jan_%201-23-13-lfm.pdf.

Donovan, LA, MJ Linton, and JH Richards. 2001. "Predawn Plant Water Potential Does Not Necessarily Equilibrate with Soil Water Potential under Well-Watered Conditions," *Oecologia*, 129:328-335. doi:10.1007/s004420100738.

Fayer, MJ. 2000. *UNSAT-H Version 3.0: Unsaturated Soil Water and Heat Flow Model: Theory, User Manual, and Examples*, PNNL-13249, Pacific Northwest National Laboratory, Richland, Washington. Available at http://www.pnl.gov/main/publications/external/technical_reports/PNNL-13249.pdf. (Accessed on Aug. 28, 2015).

Gee, GW. 1987. *Recharge at the Hanford Site: Status Report*, Pacific Northwest Laboratory, PNL-6403, Richland, Washington.

Gee, GW, AL Ward, BG Gilmore, SO Link, GW Dennis, and TK O`Neil. 1996. *Hanford Prototype-Barrier Status Report FY 1996*, PNNL-11367, Pacific Northwest National Laboratory, Richland, Washington. Available at http://www.osti.gov/energycitations/servlets/purl/444009-twIbfZ/webviewable/.

Gee, GW, AL Ward, and P Meyer. 1999. "Discussion of "Method to Estimate Water Storage Capacity of Capillary Barriers," by J. Stormont and C. Morris," *J. of Geotechnical and Geoenvironmental Engineering*, 125(10):918-920.

Hajek, BF. 1966. *Soil Survey, Hanford Project in Benton County, Washington*, Pacific Northwest Laboratory, BNWL-243, Richland, Washington.

Hauser, VL, BL Weand, and MD Gill. 2001. "Natural Covers for Landfills and Buried Waste. Journal of Environmental Engineering," *Journal of Environmental Engineering*, 127:768-775.

Haws, BA, GE Bohart, CR Nelson, and DL Nelson. 1990. Insects and Shrub Die-Off in Western States: 1986-89 Survey Results. In ED Mcarthur, EM Romney, SD Smith, and PT Tueller *Proceedings of Symposium on cheatgrass invasion, shrub die-off, and other aspects of shrub biology and management*, U.S. Department of Agriculture, Forest Service, Intermountain Research Station, Ogden, UT.

Link, SO, H Bolton (Jr.), ME Thiede, and WH Rickard. 1995. "Responses of Downy Brome to Nitrogen and Water," *J. Range Management*, 48:292-297.

Link, SO, GW Gee, ME Thiede, and PA Beedlow. 1990. "Response of a Shrub-Steppe Ecosystem to Fire: Soil Water and Vegetational Change," *Arid Soils Research and Rehabilitation*, 4:163-172.

Link, SO, WJ Waugh, and JL Downs. 1994a. The Role of Plants on Isolation Barriers Systems. In GW Gee and NR Wing *Proceedings of The 33rd Hanford Symposium on Health and Environment - In Situ Remediation: Scientific Basis for Current and Future Technologies* Battelle Press, Columbus, OH.

Link, SO, WJ Waugh, JL Downs, ME Thiede, JC Chatters, and GW Gee. 1994b. "Effects of Coppice Dune Topography and Vegetation on Soil Water Dynamics in a Cold-Desert Ecosystem," *Journal of Arid Environments*, 27:265-278.

Neter, J and W Wasserman. 1974. *Applied Linear Statistical Models: Regression, Analysis of Variance, and Experimental Designs*. Richard D. Irwin, Inc., Homewood, Ill.

Piet, SJ, JJ Jacobson, P Martian, R Martineau, and R Soto. 2003. "Modeling and Simulation of Long-Term Performance of near-Surface Barriers," *WM'03 Conference*, Tucson, AZ.

Ritchie, GA and TM Hinckley. 1975. "The Pressure Chamber as an Instrument for Ecological Research," *Adv Ecol Res*, 9:165-254.

Roesler, AC, CH Benson, and WH Albright. 2002. *Field Hydrology and Model Predictions for Final Covers in the Alternative Assessment Program - 2002*, Geo Engineering Report No. 02-08, University of Wisconsin-Madison, Madision, WI.

Sall, J, K Ng, and M Hecht. 1991. *Statistical Visualization Forthe Macintosh (JMP).* SAS Institution, Inc., Cary, NC.

SAS Institute. 2002. *JMP Statistics and Graphics Guide, Version 5*. SAS Institute Inc, Cary.

Scanlon, BR, RC Reedy, KE Keese, and SF Dwyer. 2005. "Evaluation of Evapotranspirative Covers for Waste Containment in Arid and Semiarid Regions in the Southwestern USA," *Vadose Zone Journal*, 4(1):55-71.

Scholander, TF, HT Hammel, ED Bradstreet, and EA Hemmingsen. 1965. "Sap Pressure in Vascular Plants," *Science*, 148:339-346.

Steele, RBD and JH Torrie. 1960. *Principals and Procedures of Statistics*. McGraw-Hill, New York.

Stone, WA, JM Thorp, OP Gifford, and DJ Hoitink. 1983. *Climatological Summary for the Hanford Area.*, Pacific Northwest Laboratory, PNL-4622, Richland, Washington.

Upchurch, DR and JT Ritchie. 1983. "Root Observations Using a Video Recording System in Minirhizotrons. Agron. J. 75:1009-15," *Agron. J.*, 75:109-1015.

Ward, AL, GT Berlin, JW Cammann, KD Leary, and SO Link. 2008. *Test Plan to Assess Fire Effects on the Function of an Engineered Surface Barrier*, PNNL-17859, Pacific Northwest National Laboratory, Richland, Washington.

Ward, AL, EJ Freeman, MD White, and ZF Zhang. 2005a. *STOMP: Subsurface Transport over Multiple Phases Version 1.0 Addendum: Sparse Vegetation Evapotranspiration Model for the Water-Air-Energy Operational Mode*, PNNL-15465, Pacific Northwest National Laboratory, Richland, Washington.

Ward, AL, GW Gee, and SO Link. 1997. *Hanford Prototype-Barrier Status Report: FY 1997*, PNNL--11789, Pacific Northwest National Laboratory, Richland, Washington. Available at http://www.osti.gov/energycitations/servlets/purl/569021-3NLXw0/webviewable/.

Ward, AL, N Hasan, SO Link, and KE Draper. 2009a. *The Effects of Fire on the Function of the 200-BP-1 Engineered Surface Barrier*, PNNL-18934, Pacific Northwest National Laboratory, Richland, Washington.

Ward, AL, KD Leary, SO Link, GT Berlin, JW Cammann, ML Mandis, and LC Buelow. 2009b. "Short and Long-Term Fire Impacts on Hanford Barrier Performance," *Waste Management Symposium 09*, Phoenix, Arizona.

Ward, AL, SO Link, CE Strickland, KE Draper, and RE Clayton. 2007. *200-BP-1 Prototype Hanford Barrier Annual Monitoring Report for Fiscal Years 2005 through 2007*, PNNL-17176, Pacific Northwest National Laboratory, Richland, Washington. Available at http://www.osti.gov/energycitations/servlets/purl/927493-58wmF0/.

Ward, AL, JK Linville, JM Keller, and GH Seedahmed. 2005b. *200-BP-1 Prototype Hanford Barrier Annual Monitoring Report for Fiscal Year 2004*, PNNL-14960, Pacific Northwest National Laboratory, Richland, Washington. Available at http://www.osti.gov/energycitations/servlets/purl/15020831-RBQnP9/.

Whisenant, SG. 1990. *Changing Fire Frequencies on Idaho's Snake River Plains: Ecological and Management Implication*. Proceeding-Symposium on Cheatgrass Invasion, Shrub Die-Off, and Other Aspects of Shrub Biology and Management, USDA Forest Service Intermountain Research Station General Technical Report: INT-276:4-10.

Appendix L

Animal Activities at the Prototype Hanford Barrier

Steven O. Link

Content

List of Figures

Abstract

Animal activity on the Prototype Hanford Barrier was monitored for several years. Potential risks for barrier function include the formation of large holes, mounding, and damage to plants. The number and size of holes on the surface were not significant factors for barrier function. The largest hole was 9 cm in diameter and 30 cm deep. There was one mound observed that was 9 cm tall. Rabbits were noted on the surface by the presence of feces. These feces were positively correlated with percent cover of *Elymus wawawaiensis*. Insect galls were found on *Artemisia tridentata* making the plants appear to be under stress. There was little risk to barrier function in association with these animal observations. Insect gall presence on *A. tridentata* may eventually weaken the shrubs with heavy infestation that can lead to their death.

L.1 Introduction

Engineered surface barriers are an integral component of the U.S. Department of Energy (DOE) waste management strategy, serving as an alternative to the removal, treatment, and disposal of near-surface contaminants at a variety of waste sites (DOE-RL 1993). Several locations at the Hanford Site may have significant amounts of contaminants deep in the vadose zone that may be remediated using surface barriers (DOE-RL 2013). Evapotranspiration covers and multilayered designs with a vegetated evapotranspirative surface layer have been effective in arid and semiarid climates in most cases, but have failed in others because of inadequate storage capacity and vegetation (Albright et al. 2004; Anderson 1993; Hauser et al. 2001). There also has been concern that animal bioturbation may affect soil water storage or lead to preferential flow to the bottom of the evapotranspiration layer (Landeen 1994a). Landeen (1994a), in a lysimeter study on animal burrows concluded that animal burrows had no effect on soil moisture storage. While this study was done on a relatively small lysimeter, it has remained a concern on the much larger barrier surface.

At the Hanford Site, prominent species of small mammals include Great Basin pocket mice (*Perognathus parvus*), deer mice (*Peromyscus maniculatus*), northern pocket gophers (*Thomomys talpoides*), western harvest mice (*Reithrodontomys megalotus*), and Northern grasshopper mice (*Onychomys lucogaster*). Additionally, other organisms, such as darkling beetles, spiders, lizards, coyotes, and badgers are responsible for reworking the surface soils. These organisms' use of an area can be greatly influenced by the wildfires.

In addition, animals can affect the plants on the surface. Gall forming insects have been recognized to reduce growth and reproduction in *Artemisia tridentata* (Takahashi and Huntly 2010). Rabbits (*Sylvilagus nuttallii*) can use the bunchgrasses.

The purpose of this research was to investigate risks of failure associated with animal bioturbation and negative effects on plants on an engineered barrier after three times the average precipitation for 3 years, in the long-term (17 years), and after a fire.

The Prototype Hanford Barrier (PHB) was monitored almost continuously for 17 years (1994 to 2011). This paper summarizes the data collected over the monitoring period on animal presence, their bioturbation, and insect infestations as affected by increased precipitation and fire on the barrier.

L.2 Methodology

L.2.1 Study Site

The study was conducted at the DOE Hanford Site in south central Washington state. The PHB is located (46°34'01.23"N, 119°32'28.43"W) on the 200 Area Plateau at an elevation of 194 m a.s.l. The climate is semiarid with hot dry summers and cool wet winters (Stone et al. 1983). Average yearly precipitation at the nearby Hanford Meteorological Station is about 167 mm. Snowfall ranges from trace amounts to 137 cm, but averages 35 cm.

L.2.2 Barrier Characteristics and Treatments

The surface area of the entire barrier is 2.5 hectares. The surface is elevated with one relatively steep (2:1 horizontal to vertical) protective side slope that is covered with basalt riprap. The other side slope is gentle (10:1) and consists of local pit run gravel backfill. The barrier is constructed with 2 m of fine soils

over coarser materials. The soil used in the upper layers of the prototype barrier is a Warden silt loam (Gee 1987; Hajek 1966).

The north section was irrigated during treatability test from 1994 to 1998 while the south section was not irrigated. This test included irrigation at a rate of about 480 mm/yr, including a simulated 1000-yr return storm each March when about 70 mm of water was applied over an 8-hour period to gain insight into barrier performance under elevated precipitation conditions. No further manipulations occurred until September 2008, when the north section of the barrier was burned (Ward et al. 2008; Ward et al. 2009a; Ward et al. 2009b). The surface was gridded into three-hundred 9-m^2 quadrats, with 144 quadrats in the south section and 156 quadrats in the north section for ecological surveys. A quadrat may also be referred to as a plot.

L.2.3 Animal Observations

During the monitoring period, animal observations were taken in 1995 through 1997 and 2007 through 2011. Animal evidence on the surface was casually noted in 1995 and measured in 1996. In 1996 and 1997, evidence of animal presence (feces, burrows) was noted by inspection in all 300 quadrats on the surface. Observations in 1996 were made between May 24 and June 7. In 1997, observations were made on April 25; the depths of selected holes were measured on September 12. Hole sizes were not classed into small and large holes for measurements before 2007.

In 2007, the barrier surface was examined for evidence of use and intrusion (burrowing) by insects and small mammals on August 18. This was done by carefully inspecting 20 of 300 sample squares on the surface. Indications of animal use included direct observation and presence of droppings, tracks, nests, burrows, or holes. The greatest width, the width at 90° to the greatest width, and the depth of 11 holes and burrows were measured. Hole depth and volume were analyzed. The side slopes were examined for animal evidence.

In 2008, pre-burn surveys were conducted across the entire surface to document evidence of use and intrusion (burrowing) by insects and small mammals. Small mammal traps were used to positively identify vertebrates on the surface. Evidence of animal use was observed on the surface and included direct observation (traps) as well as the presence of droppings, tracks, nests, burrows, holes, and resting spots. A small mammal trapping event and reconnaissance of indirect evidence of animal activity was performed in September 2008, just before the controlled burn of the north section of the surface barrier area on September 28.

After the burn, two small mammal arrays, containing nine traps each, of Sherman live traps were placed on the surface; one array was located in the burned section and the other in the unburned section. Each array consisted of three trap lines, each with three traps spaced 10 m apart (30 m × 30 m area). The traps were placed in the field on September 15, 2008, and left for 1 day before baiting and opening to allow small mammals to acclimate to the new objects. Both small mammal arrays were opened the evening of September 16, 2008, and then checked and re-baited with a mixture of peanut butter and oatmeal each morning until the survey was completed. Species, age, and sex were determined for all small mammals captured, and each animal was given a mark to identify the occurrence of recaptured specimens. The relative abundance of small mammals was estimated for two areas by dividing the total number of traps and number of nights by the total number of new captures and then multiplied by 100. Animal activity such as scat, tracks, and burrows were noted in each area while field crews were mobilizing and demobilizing and performing daily trap checks.

In 2009, the barrier surface was examined for evidence of use and intrusion (burrowing) by insects and small mammals on September 13. This was done by carefully inspecting 288 of 300 sample squares on the surface. The row between the burned and unburned portions of the surface was not assessed. Indications of animal use included direct observation and presence of droppings, tracks, nests, burrows, or holes, and gall formation on *A. tridentata*. Hole size was classed as large (>~2 cm diameter) or small. Holes in each class were counted in each plot. The degree of gall formation and amount of feces were classed into high and low groups. A high degree of gall formation was noted when any shrub had numerous (>~50) galls. A high amount of rabbit feces was noted when feces were concentrated in patches, while a plot with few feces that were widely distributed was classed as low. The Van der Waerden non-parametric test (van Der Waerden 1952) was used when data were not normally distributed to compare responses in the burned and unburned treatments. The relationship between rabbit (*Sylvilagus nuttallii*) feces and cover of *Elymus wawawaiensis* was determined by relating the percent of plots in each of 25 rows that had feces with mean percent cover of *E. wawawaiensis* in each row. Each of the 25 rows had 12 plots. The relationship was determined using linear regression.

In 2010 and 2011, the barrier surface was examined for evidence of use and intrusion (burrowing) by insects and small mammals between June 3 and July 13, 2010 and in early August 2011. This was done by inspecting 300 sample squares on the surface. In 2010, all holes were recognized whether new or old and occurring under litter. In 2011, as in earlier years, only well-formed new holes were counted and no effort was made to count holes under litter. Holes that were counted were about 1 cm in diameter or larger. Animal activity on the side slopes was noted by inspection. Indications of animal use included direct observation and presence of droppings, tracks, nests, burrows, or holes, and gall formation on *A. tridentata*. The greatest width, the width at 90° to the greatest width, and the depth of burrows were measured.

L.2.4 Data Analysis

The dimensions of animal holes were described by the greatest width (d_1), the width at 90° to the greatest width (d_2), and the maximum depth (d_3). The hole size is the average of the two widths. The holes smaller than 2 cm were defined as large and the rest as small. It was assumed that the cross section of the holes were constant vertically and the hole volume (in cubic centimeters) was estimated by the elliptical area times the maximum depth of the hole:

$$\text{Volume} = \pi\, d_1 d_2 d_3/4 \qquad \text{(L.1)}$$

Means were computed. Error terms are one standard error of the mean. Significance was tested at the $\alpha = 0.05$ level. Analyses were done using JMP version 5.0 software (SAS Institute 2002).

L.3 Results

In 1995, birds were observed frequently on the surface consuming seeds. There were no mammals or the evidence of mammals on the surface. Some of the most interesting insect observations were made while examining roots. A colony of what appeared to be termites at a depth of about 80 cm along one of the root tubes was observed (see Appendix K).

In 1996, evidence of animals on the surface was documented in early June. Evidence consisted of the presence of rabbit and bird feces and holes in the ground. There was evidence in 20% of the quadrats in the non-irrigated section of the barrier and in 8% of the quadrats in the irrigated section. A total of nine large holes (0.0033 m^{-2}) were observed on the surface.

In 1997, animal use of the surface was documented in April and September. Rabbit feces were present in 93% of the quadrats in the non-irrigated section of the barrier and in 69% of the quadrats in the irrigated section. Ten holes were observed on the surface.

In 2007, animal use of the surface was evident and widespread. Rabbit use, indicated by the presence of droppings, was most evident in the northeast corner of the north section of the barrier where grass cover is highest (Figure L.1). Numerous small (<2 cm diameter) holes were observed on the barrier surface. Larger holes were observed in 14 of 20 plots with a total of about 31 holes in the 20 plots (0.172 m^{-2}). Based on the sample, 70% of the observation plots had animal burrows. These holes (Figures L.2 and L.4), dug by insects and small mammals, were distributed throughout the surface with little obvious pattern associated with disturbance, concrete, instruments, or other items on the surface. Eleven holes were measured and were 2 to 9 cm wide and up to 30 cm deep. Average hole diameter was 3.9 ± 0.8 cm, area was 13.8 ± 5.5 cm^2, depth was 12 ± 2.6 cm, and volume was 164 ± 75 cm^3. A few mounds were observed on the north edge of the barrier surface. No darkling beetles or other burrowing insects were noted on the surface except ants on the north edge of the barrier surface.

Animal activity on the gravel slopes was restricted to the lower elevations where fine soils were common. In these areas, there were numerous holes from small mammals or insects. These holes were not measured or counted. There were large ant colonies in the fine soils. There was little if any recognizable animal activity in the gravels on the west and north slopes.

Figure L.1. Rabbit droppings in association with high grass cover in the northeast corner of the barrier surface.

In 2008, a pre-burn survey was conducted across the entire surface to document evidence of use and intrusion (burrowing) by insects and small mammals. Evidence of animal use was observed on the surface and included direct observation (traps) as well as the presence of droppings, tracks, nests, burrows, holes, and resting spots. The most common mammal found on the surface by trapping was deer mice (*Peromyscus* sp.).

Another survey was conducted several days after the burn. Two species were captured during a total of 50 trap nights. The predominant species in both areas was the deer mouse (*P. maniculatus*). One great basin pocket mouse (*P. parvus*) was trapped in the unburned region. The relative abundance of small mammals was higher in the burned area trapping grid; estimated at 21 new captures per 100 trap nights, as opposed to 4 new captures per 100 trap nights measured in the unburned trapping grid. Adults and juveniles were captured, indicating that the small mammals were residents to the area, as opposed to dispersed migrants from other areas. No reproductively active specimens were encountered. In addition, a number of side-blotched lizards (*Uta stansburiana*) were observed during the trapping event.

Figure L.2. Small Animal Hole on the Barrier Surface. Note recent digging activity in the upper left hand corner.

Indirect indices of animal activity, such as evidence of use by rabbits, coyotes, lizards, and invertebrates (in addition to small mammals), were common in both areas. A number of small, relatively shallow (less than 10 cm deep) excavations were noted throughout both trapping areas. Most were assumed to have been made by resident lizards, but there was evidence that some excavations were also made by darkling beetles and small mammals. Two areas in the unburned trapping grid contained evidence of underground small mammal burrow systems likely constructed by resident pocket mice.

In 2009, the barrier surface was again examined for evidence of use and intrusion (burrowing) by insects and small mammals on September 13, almost 1 year after the fire. Animal holes were significantly ($p < 0.0001$) more prevalent on the unburned section (0.041 ± 0.0074 holes m^{-2}) than on the burned section (0.0054 ± 0.002 holes m^{-2}). Of 61 holes found in all the plots, 31 were large and 30 were small. Of 21 holes dug by rodents, 20 were large. Of 38 holes dug by insects, 9 (23.7%) were large. There were no significant ($p > 0.05$) linear relationships between location (X, Y) and hole density. Rabbit use, indicated by the percent of plots with feces in each of 25 rows, was positively correlated (Fig. L.3) with mean percent cover of *E. wawawaiensis*:

$$\%\text{plots with feces} = 27.8 \pm 3.9 + (4.8 \pm 1.8) * \text{mean \% cover}; \; p = 0.0151 \qquad \text{(L.2)}$$

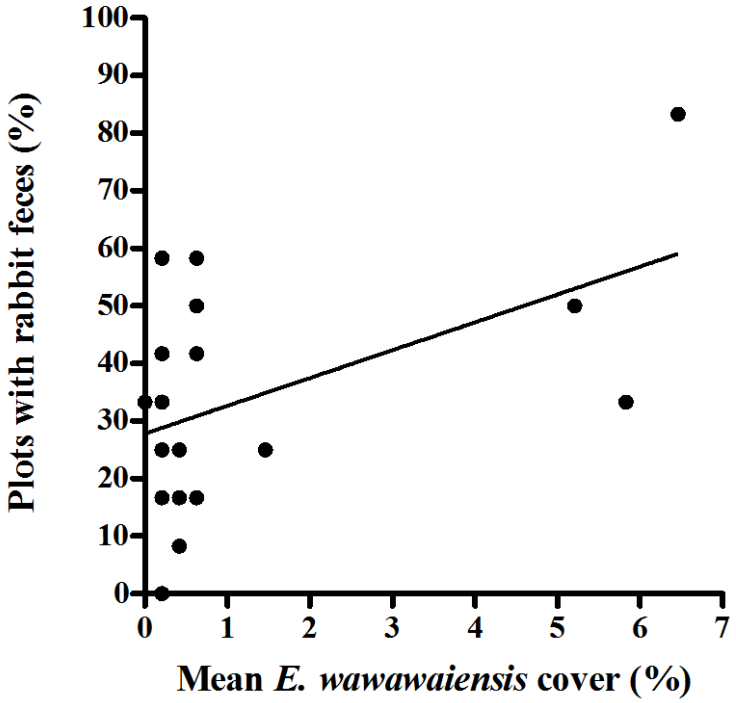

Figure L.3. Relationship (Eq. L.2) between Mean *E. wawawaiensis* Percent Cover and Percent of Plots with Rabbit Feces.

Most *E. wawawaiensis* plants had experienced herbivory. Coyote feces were noted in two locations on the surface.

Galls, most likely attributed to flies or wasps, were found infesting a number of *A. tridentata* plants. Some of the *A. tridentata* were heavily infested, damaging the shrub. Of 144 plots in the unburned section of the barrier, 100 (69%) had infested shrubs and 19% had heavily infested shrubs. Heavy infestation is a condition where nearly all leafy stems have numerous galls. This infestation will likely reduce the population density of *A. tridentata* in future years. Only one plot in the burned section of the surface had galls on an *A. tridentata* seedling.

Figure L.4. Typical Animal Hole on the Surface of the Barrier.

In 2010, the intensive examination found 101 holes (0.078 holes m^{-2}) in the burned and 208 holes (0.16 holes m^{-2}) in the unburned portions of the surface. Some holes were observed within larger holes. Old holes were counted even though some had partially caved in. In 2011, 8 well-formed newer holes were observed in the burned portion and 23 holes without litter were observed in the unburned portion of the barrier. The larger number of holes in the unburned portion of the surface may be because some are older than the holes in the burned portion. The fire appeared to change soil stability, as noted in by the soil inflation and deflation patterns (Appendix M). Loose soils can cover animal holes and may be a cause for the reduced numbers. In addition, the unburned portion has been stable, has more litter providing cover, and has more biomass that may improve habitat for burrowing mice, large insects, and spiders increasing their numbers and thus holes.

In 2011, the majority of holes were 1 to 6 cm wide and up to 18 cm long. A single hole had an area of 1014 cm^2 and was about 4 cm deep. This hole was not used to compute means. Average largest ellipsoidal diameter was 3.15 ± 0.19 cm, area was 7.12 ± 0.78 cm^2, below-ground length was 7.08 ± 0.75 cm, and volume was 53.9 ± 8.39 cm^3 (n = 30). Most holes were at roughly 45° angle to the surface. Thus, the average vertical depth was about 3.5 cm. The deepest vertical hole was 6 cm. Figure L.5 shows a typical animal hole. A larger hole with nearby smaller holes also had a mound with a height of about 9 cm (Figure L.6).

Rabbit use, indicated by the presence of droppings, was most evident in the northeast corner of the burned portion of the barrier where grass cover is highest. In 2011, the unburned portion of the surface had rabbit pellets in 1 plot while there were 11 plots with rabbit pellets on the burned portion of the surface. Coyote feces were noted in three plots (10,6; 6,16; 6,18) on the surface.

Galls were noted on *A. tridentata* for several years. In 2011, galls were recognized in a plot if observed on any shrub in the plot. On the unburned section of the surface, galls were found in 105 of 144 plots, or 73% of the plots. While this study did not specifically try to relate gall infestation pressure with shrub condition, heavily infested shrubs appeared to be under stress and more likely to die.

Figure L.5. Small Animal Hole on the Burned Section of the Barrier Surface.

Figure L.6. Large Animal Hole with Five Nearby Holes on the Burned Section of the Barrier Surface.

L.4 Summary and Discussion

Animal presence on the surface was widespread by the third year after construction and remained widespread until the fire in 2008. The fire reduced the number of animal holes and the reduction remained through 2011. In 1996, nine holes were observed. By 2010, there were 309 holes observed. A total of 309 holes greater than 1 cm in diameter and with an average diameter of 3.15 cm yields a total area of about 2,408 cm^2 on the surface, which is only 0.0089 % of the barrier surface area. The holes are shallow and make up a very small portion of the surface. They do not appear to have created a risk for the function of the barrier (Landeen 1994a). There were only a few small mounds on the surface and thus the creation of mounds and variability associated with mounding was not significant for the function of the barrier. There was never any evidence of large holes associated with badgers or coyotes.

In 2008, a Great Basin pocket mouse was trapped on the unburned section of the surface. These mice will create burrow systems. Two burrow systems were observed on the unburned section of the surface. Based on several species of pocket mice, Kennedy et al. (1985) found that 50% of the burrow system is distributed within the top 0.5 m below ground surface and 90% is distributed within the top meter. Pocket mice typically construct burrows less than 2.5 cm in diameter, and other small mammal burrows common to the site are typically wider; for example, deer mouse burrows are up to 10 cm in diameter (Laundré 1989). These systems are not likely to create a risk for barrier function as Landeen (1994a) observed no increase in soil water storage with pocket gophers.

Use of *E. wawawaiensis* by rabbits was significant. Herbivory was significant and potentially can lead to a reduction in *E. wawawaiensis*, especially if seed production is reduced. There were seeds of *E. wawawaiensis* in the seed bank (Appendix J), but it is not known if their number would be greater without herbivory. Insect galls on *A. tridentata* were significant and damaged shrubs with heavy infestation. Insects have been recognized to reduce growth and reproduction in *A. tridentata* (Takahashi and Huntly 2010). This infestation likely will continue to reduce *A. tridentata* populations. Reduction of the *A. tridentata* population opens the opportunity for *B. tectorum* to establish.

After 17 years and under the conditions of the test, it can be concluded that burrowing animals will not have an effect on barrier function. The most significant animal risk is associated with insect damage to *A. tridentata.* Loss of *A. tridentata* can eventually increase the risk that *B. tectorum* will become more prominent and may reduce the ability of the barrier to control infiltration.

Although one of the objectives of the PHB being maintenance free was not met due to the presence of a few larger burrowing animal holes. However, studies (Cadwell et al. 1989; Landeen 1990, 1991, 1994b) indicate that most animal burrows do not extend below 1 m depth since most favorable environmental conditions (e.g., food, water, shelter, and temperature) are found within the top 1 m below ground surface with the exception of the Western harvester ant (Gano and States 1982). An Animal Intrusion Lysimeter Facility was constructed in FY88 to evaluate the impacts of burrowing animals on engineered surface barrier performance. The results of the studies are (Cadwell et al. 1989; Landeen 1990, 1991, 1994b):

- Although deep percolation can occur, most water is later removed by a variety of processes (e.g., drying via ventilation effects from open burrows and transpiration from invader species like mustards). Abandoned badger burrows are often quickly backfilled with soil and organic debris.
- The presence of small mammal burrows does not have a considerable impact on deep percolation through the barrier.
- The soil brought to the surface by burrowing animals can be more susceptible to erosion. However, the erosion can be mitigated by the addition of gravel admix into the upper portion of the soil or the installation of a bio-barrier.

Acknowledgements

Research was funded by the U.S. Department of Energy under Contract DE-AC06-76RLO 1830 with the Pacific Northwest National Laboratory. We thank Glendon Gee for conceiving the Hanford Prototype Barrier and early support. We thank Kevin Leary for initiating, helping with, and funding the fire portion of the study. Brett Tiller of Environmental Assessment Services made animal observations in 2008.

Reference

Albright, WH, CH Benson, GW Gee, AC Roesler, T Abichou, P Apiwantragoon, BF Lyles, and SA Rock. 2004. "Field Water Balance of Landfill Final Covers," *Journal of Environmental Quality*, 33(6):2317-2332.

Anderson, JE. 1993. "Managing Soil Moisture on Waste Burial Sites in Arid Regions. ," *Journal of Environmental Quality*, 22:62-69.

Cadwell, LL, LE Eberhardt, and MA Simmons. 1989. *Animal Intrusion Studies for Protective Barriers: Status Report for FY 1988,* PNL-6869, Pacific Northwest Laboratory, Richland, WA.

DOE-RL. 1993. *Treatability Test Plan for the 200-BP-1 Prototype Surface Barrier,* DOE/RL-93-27, U.S. Department of Energy Richland Operations Office, Richland, Washington.

DOE-RL. 2013. *Hanford Site Cleanup Completion Framework,* DOE/RL-2009-10, Rev. 1, U.S. Department of Energy Richland Operations Office, Richland, Washington.

Gano, KA and JB States. 1982. *Habitat Requirements and Burrowing Depths of Rodents in Relation to Shallow Waste Burial Sites,* PNL-4140, Pacific Northwest Laboratory, Richland, Washington.

Gee, GW. 1987. *Recharge at the Hanford Site: Status Report*, Pacific Northwest Laboratory, PNL-6403, Richland, Washington.

Hajek, BF. 1966. *Soil Survey, Hanford Project in Benton County, Washington*, Pacific Northwest Laboratory, BNWL-243, Richland, Washington.

Hauser, VL, BL Weand, and MD Gill. 2001. "Natural Covers for Landfills and Buried Waste. Journal of Environmental Engineering," *Journal of Environmental Engineering*, 127:768-775.

Kennedy, WE, LL Cadwell, and DH Mckenzie. 1985. "Biotic Transport of Radionuclides from a Low-Level Radioactive Site," *Health Phys*, 49:11-24.

Landeen, DS. 1990. *Animal Intrusion Status Report for Fiscal Year 1989,* WHC-EP-0299, Westinghouse Hanford Company, Richland, Washington.

Landeen, DS. 1991. *Animal Intrusion Status Report for Fiscal Year 1990,* WHC-EP-0398, Westinghouse Hanford Company, Richland, Washington.

Landeen, DS. 1994a. The Influence of Small-Mammal Burrowing Activity on Water Storage at the Hanford Site. In GW Gee and NR Wing *Proceedings of Thirty-Third Hanford Symposium on Health and the Environment,* Battelle Press, Columbus, Ohio.

Landeen, DS. 1994b. *The Influence of Small Mammal Burrowing Activity on Water Storage at the Hanford Site,* WHC-EP-0730, Westinghouse Hanford Company, Richland, Washington.

Laundré, JW. 1989. "Horizontal and Vertical Diameter of Burrows of Five Small Mammal Species in Southeastern Idaho," *Great Basin Nat,* 49:646-649.

SAS Institute. 2002. *JMP Statistics and Graphics Guide, Version 5*. SAS Institute Inc, Cary.

Stone, WA, JM Thorp, OP Gifford, and DJ Hoitink. 1983. *Climatological Summary for the Hanford Area.*, Pacific Northwest Laboratory, PNL-4622, Richland, Washington.

Takahashi, M and N Huntly. 2010. "Herbivorous Insects Reduce Growth and Reproduction of Big Sagebrush (Artemisia tridentata)," *Arthropod-Plant Interactions*, 4:257-266.

van Der Waerden, BL. 1952. "Order Tests for the Two-Sample Problem and Their Power," *Indagationes Mathematicae*, 14:453-458.

Ward, AL, GT Berlin, JW Cammann, KD Leary, and SO Link. 2008. *Test Plan to Assess Fire Effects on the Function of an Engineered Surface Barrier,* PNNL-17859, Pacific Northwest National Laboratory, Richland, Washington.

Ward, AL, N Hasan, SO Link, and KE Draper. 2009a. *The Effects of Fire on the Function of the 200-BP-1 Engineered Surface Barrier,* PNNL-18934, Pacific Northwest National Laboratory, Richland, Washington.

Ward, AL, KD Leary, SO Link, GT Berlin, JW Cammann, ML Mandis, and LC Buelow. 2009b. "Short and Long-Term Fire Impacts on Hanford Barrier Performance," *Waste Management Symposium 09,* Phoenix, Arizona.

Appendix M

Controlled Fire at the Prototype Hanford Barrier

Steven O. Link

Content

List of Figures

Abstract

A controlled fire was conducted in 2008 to determine if the stress of a fire was sufficient to affect aspects of the Prototype Hanford Barrier function. The fire was ignited on September 26. The maximum flame heights exceeded 9 m, and maximum temperatures ranged from 250°C at 1.5 cm below the surface to over 700°C at 1 m above the surface. Fuel load and fire intensity were highly variable across the surface. The total fuel load on the low-fuel plots was around 10.54 tonnes compared to 12.8 tonnes/ha on the high-fuel plots. Based on the measurements with erosion pins before and nearly a year after the fire, the average change in measurement with one standard deviation was 1.3±7.1 cm. The large uncertainty in the measurements suggests the measurements with erosion pins were inclusive on inflation and deflation.

M.1 Introduction

Engineered surface barriers are an integral component of the U.S. Department of Energy (DOE) waste management strategy, serving as an alternative to the removal, treatment, and disposal of near-surface contaminants at a variety of waste sites (DOE-RL 1993). Several locations at the Hanford Site may have significant amounts of contaminants deep in the vadose zone that may be remediated using surface barriers (DOE-RL 2013). The primary function of engineered barriers is to control infiltration of meteoric water through the surface. This function is typically accomplished through a water storage and release mechanism in which water is stored in fine-textured soils during the rainy season and recycled to the atmosphere by evapotranspiration (Ward et al. 2009a). Over the functional life of an engineered barrier, the barrier will be subjected to extreme events such as wildfires. The effect of a simulated wildfire on the Prototype Hanford Barrier (PHB) was described in Ward et al. (2009a). Here, elements of the fire study are described, including fuel loading, fire characteristics, and soil inflation and deflation.

M.2 Methodology

M.2.1 Study Site

The study was conducted at the DOE Hanford Site in south central Washington state. The PHB is located (46°34’01.23”N, 119°32’28.43”W) on the 200 Area Plateau at an elevation of 194 m a.s.l. The climate is semiarid with hot dry summers and cool wet winters (Stone et al. 1983). Average yearly precipitation at the nearby Hanford Meteorological Station is about 167 mm. Snowfall ranges from trace amounts to 137 cm, but averages 35 cm.

M.2.2 Barrier Characteristics and Treatments

The surface area of the entire PHB is 2.5 hectares. The surface is elevated with one relatively steep (2:1 horizontal to vertical) protective side slope that is covered with basalt riprap. The other side slope is gentle (10:1) and consists of local pit run gravel backfill. The barrier is constructed with 2 m of fine soils over coarser material. The soil used in the upper layers of the PHB is a Warden silt loam (Gee 1987; Hajek 1966).

During construction in 1994, the top 1 m of silt loam was amended by adding 15% by weight of pea gravel. The gravel was added to minimize wind and water erosion of the silt loam soil immediately after construction, when the surface was bare, and during periods of drought, wildfire, or any other period of increased eolian or aqueous stresses.

The north section was irrigated during treatability test from 1994 to 1998 while the south section was not irrigated. This test included irrigation to a total precipitation of about 480 mm yr^{-1}, including a simulated 1000-yr return storm each March when about 70 mm of water was applied over an 8-hour period to gain insight into barrier performance under elevated precipitation conditions. No further manipulations occurred until September 2008, when the north section of the barrier was burned (Ward et al. 2008; Ward et al. 2009a; Ward et al. 2009b). The surface was gridded into three-hundred 9-m^2 quadrats, with 144 quadrats in the unirrigated area and 156 quadrats in the irrigated area for ecological surveys. Revegetation and plant community dynamics are described in Appendix J.

M.2.3 Monitoring the Fire

Responses to the fire potentially vary according to the intensity of the fire, and the site was configured and instrumented to permit monitoring. The simulated fire was limited to the north section of the barrier, which was divided into nine 12-m x 12-m plots (Figure M.1). Nine flame-height poles fitted with thermocouples (Figure M.2) were installed at the center of each plot for visual observation of flame height and to quantify fire intensity during the fire. Flame height was used to estimate radiation intensity of flames, which is directly related the rate of spread of a fire (Johnson and Miyanash 2001). Two theoretical definitions of flame height are (1) the height where flames reach the maximum temperature and (2) the vertical distance from the flame base or ground to the time-averaged yellow flame tip (Johnson and Miyanash 2001). During the fire, the scorch height was measured by recording the elevation of the scorch marks on flame-height rods mounted within each plot. Flame height poles were constructed of galvanized pipe and painted alternating colors to permit easy determination of scorch height. The poles were painted in 10-cm sections from 57 cm to a height of 297 cm above ground. Each unit was self-supporting, allowing installation without the need to core into the barrier surface.

The degree of fire intensity was scored on a scale of 1 to 5, with little or no effect (bright white) assigned a value of 1 and the darkest carbonized areas assigned a value of 5. White painted strips were examined every 40 cm for seven assessments on each pole. Values were averaged on each pole, and the pole average was used to create a fire intensity map. To verify flame heights inferred from ocular observation and to track soil temperatures, Type-K thermocouples (ThermoWorks, Lindon, UT) were installed on the flame height rods at 1.5 cm (0.6 in.) below the soil surface and at 0 cm (Figure M.3a). In addition, thermocouples were installed at five additional heights above the surface (Figure M.3b): 1 cm (0.4 in.), 10 cm (4 in.), 30 cm (12 in.), 100 cm (39.4 in.), and 200 cm (78.7 in.). A thermocouple wire can be seen mounted at a right angle to the pole at a height of 2 m (Figure M.3b). Each of the 63 thermocouples was attached to a HOBO data-logger (Onset, Bourne, MA) to record temperatures. Temperatures were measured once per second starting 3 hours before the fire until about 9 hours after the fire. The resulting data were used to map the relative intensity of the fire across the burned surface.

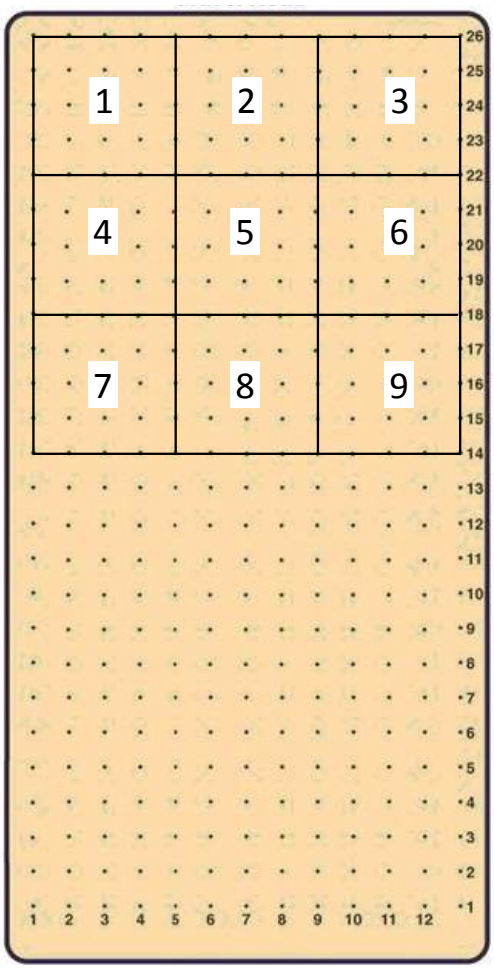

Figure M.1. Schematic plan view of the barrier's surface showing the 3 × 3 m grid and the nine (1 through 9) 12 × 12 m plots to be used for comparing effects of fuel loads on fire intensity.

Figure M.2**.** Photograph of fire pole used to measure flame characteristics and to secure thermocouples (After Figure 2.7 of Ward et al. 2009a).

(a) (b)

Figure M.3**.** Thermocouples for measuring soil and air temperature installed on flame height scaffold: (a) thermocouples were installed 1.5 cm deep, at the surface (0 cm), 1 cm, 10 cm, and 30 cm, and (b), aboveground thermocouples were installed at 100 cm and 200 cm (After Figure 2.8 of Ward et al. 2009a).

M.2.4 Fuel-Load Characterization and Modification

Fuel-load plays an important role in the extent of combustion of vegetation and the long-term changes in soil organic matter as well as total and available fractions of nutrients and trace elements (De Marco et

al. 2005). Thus, pre-burn site characterization included assessing the available fuel load. As shown in Figure M.4, significant differences in plant density and fuel load were observed on the surface.

Figure M.4. Photographs of the PHB surface: (a) sparse vegetation on the surface suggesting need for increased fuel load to emulate realistic conditions. Some *Salsola kali* (tumbleweed) was already lodged among sagebrush plants, and (b) the riprap side slope of the barrier shows an accumulation of tumbleweed. Dead sagebrush and tumbleweed were imported to the barrier surface to increase the fuel load. (After Figure 2.9 of Ward et al. 2009a).

Shrub biomass that could serve as fuel was determined by measuring the canopy characteristics, including height, greatest width, and greatest diameter at right angles to the greatest width on the shrubs. Measurements were taken on 18 individual shrubs off the barrier surface that spanned the range of shrub sizes on the barrier surface. These shrubs were then harvested, weighed, dried, and weighed again to the fuel moisture content. Canopy characteristics were then measured on 81 individual *A. tridentata* shrubs on the barrier surface to estimate shrub fuel density. The biomass of other fuel components on the surface was also estimated. Some areas of the barrier surface were quite sparse in vegetative cover and required an increase in biomass to reach representative fire intensities and severities (e.g., Figure M.4a). Other fuel components included *Salsola kali* (tumbleweed). Tumbleweed was already lodged among the *A. tridentata* shrubs on the surface, and more were brought in to confirm a complete burn of the surface. Although some tumbleweed was found near the barrier, it was still necessary to import tumbleweed from other areas. A truck was used to collect and transport tumbleweed across the Hanford Site to the barrier (Figure M.5).

Over 2 tonnes of clean tumbleweeds were brought to the barrier from around the 200 East Area. Tumbleweeds were dumped onto the gravel road to the north of the barrier and distributed from there. Subsamples of the imported fuel were weighed and dried to determine the moisture content. The dry tumbleweeds were spread across the surface of the barrier by hand (Figure M.6) to achieve the randomly assigned fuel loads. Two fuel loads of approximately 10.5 and 12.8 tonnes/ha were assigned to the nine 12 × 12 m plots.

Figure M.5**.** Unloading of tumbleweed brought to the barrier to increase fuel load. Over 2 tonnes of tumbleweed was added to the surface. (After Figure 2.10 of Ward et al. 2009a)

Figure M.6**.** Redistribution of imported tumbleweed across the barrier to achieve different fuel loads for the controlled burn. Captain Jerry Keeling of the Hanford Fire Patrol is shown redistributing tumbleweed with a rake. (After Figure 2.11 of Ward et al. 2009a).

M.2.5 Surface-Layer Inflation/Deflation

Soil inflation and deflation are likely to occur after a fire with the loss of plant cover. The pattern of inflation and deflation was mapped using 66 erosion pins on the burned section of the barrier. Measurements were taken before and after the fire. These data should reveal the ability of the surface to resist erosive stresses after fire and provide insight into changes in surface composition relative to the bulk composition of the top 1 m of admix. The height above the soil surface at the 66 steel stakes was measured with a meter stick. The 66 measurement stakes were distributed around the edges and throughout the central region of the surface (Figure M.7). A metal washer was placed on the west side of each stake and used as a measuring base. The measuring technique was used before the fire on September 22, 2008, and repeated on August 13, 2009 and August 21, 2010, nearly 11 months after the fire. Measurements were taken by viewing the interception of the top of the metal stake with the millimeter-ruled meter stick. This was done in the same manner before and after the fire to minimize bias and parallax.

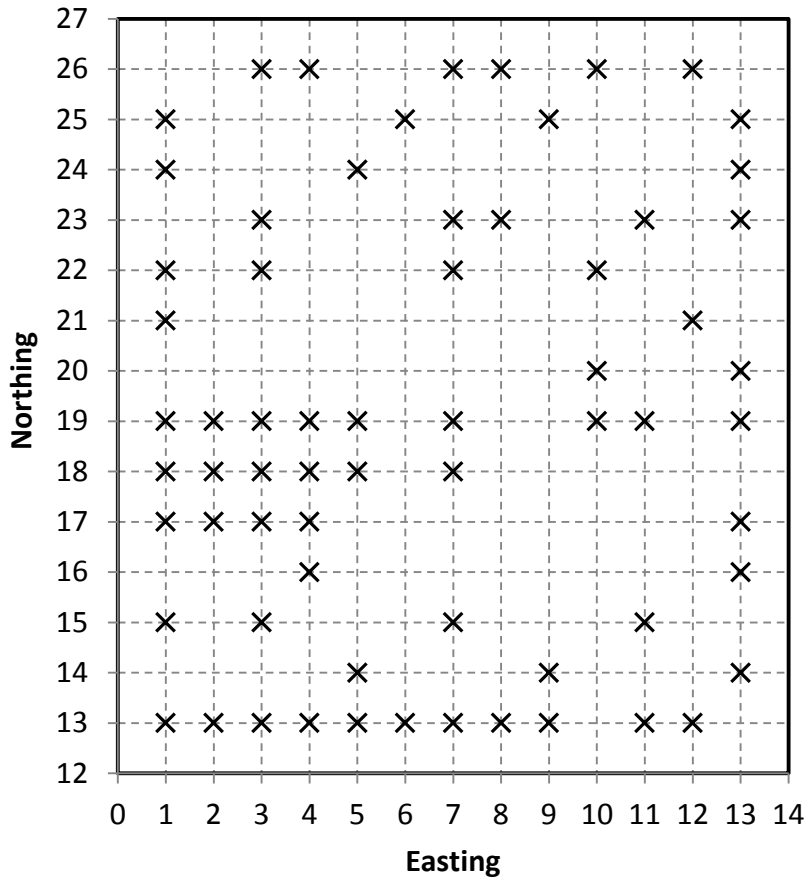

Figure M.7**.** Locations of the 66 erosion pins. The distance between coordinate values is 3 meters.

M.3 Results and Discussion

M.3.1 Fuel cover and biomass

The ground cover was used to estimate the amount of fuel (see Appendix J). Percent cover was estimated for shrubs, *S. kali*, grasses, forbs, and litter. These cover estimates were summed and in some cases exceeded 100%. The spatial distribution of percent cover (Figure M.7) was quite variable. The existing fuel before the adding *S. kali* to the surface was determined visually.

Biomass was estimated across the surface by assessing *A. tridentata* and *S. kali* litter. The canopy structure of *A. tridentata* was measured and related to the harvested biomass. Measurements were taken on 18 plants covering the range of sizes on the barrier surface. Data recorded included maximum height (z), maximum diameter in the longitudinal direction (x), and maximum diameter in the transverse direction (y). These individuals were then harvested and weighed. The relationship used to predict biomass is:

$$Y = \alpha + \beta e^{(\gamma x + \delta y + \varepsilon z)}$$

where α, β, γ, δ, and ε are nonlinear regression parameters. The estimated parameters resulted in a highly significant predictive relationship ($r^2 = 0.95$, $p < 0.001$). The parameter values are $\alpha = -182 \pm 144$, $\beta = 129 \pm 101$, $\gamma = 0.0124 \pm 0.00603$, $\delta = 0.00762 \pm 0.00457$, and $\varepsilon = 0.00369 \pm 0.00263$. Eighty-one *A. tridentata* shrubs were measured for canopy characteristics across the burn area, resulting in an average predicted wet biomass of 1.15 ± 0.05 lb (522 ± 55 g). Shrubs were counted in 84 quadrats, resulting in an average of 13.2 ± 0.65 shrubs in each quadrat. Thus, there were about 1894 shrubs on the surface with a total estimated wet biomass of 988 kg (2178 lb). The mean water content was 22.4 ± 0.87% by weight; thus, the oven-dried biomass was 767 kg (1691 lb). There was about 383.7 kg (846 lb) of oven-dried shrub mass in each of the high- and low-fuel treatments on the surface. The area of the burn area is 0.32 acres (0.129 ha), so the mean shrub fuel load was around 5.92 tonnes/ha (2.64 tonnes/Ac).

Biomass of *S. kali* was determined by estimating the amount present and the amount added to the surface. The amount added to the surface was similar to amounts already present in the low-fuel treatments, but was distributed fully across the surface while that already present was clumped. The average wet mass added to the low-fuel treatment was 3.67 kg (8.1 lb) in each quadrat. The mean water content was 4.21 ± 0.327%, resulting in an oven-dried biomass added of 3.52 kg (7.76 lb). About 253.6 kg (559 lb) of dried mass was added to low-fuel treatment. The added fuel load was about 3.92 tonnes/ha (1.75 tonnes/Ac). The average wet mass added to the high fuel section was 5.51 kg (12.15 lb) in each quadrat. Thus, the dried biomass added was 5.29 kg (11.7 lb). There was about 380.7 kg (839 lb) of oven-dried mass added to the high fuel section. The added fuel was about 5.9 tonnes/ha (2.63 tonnes/Ac).

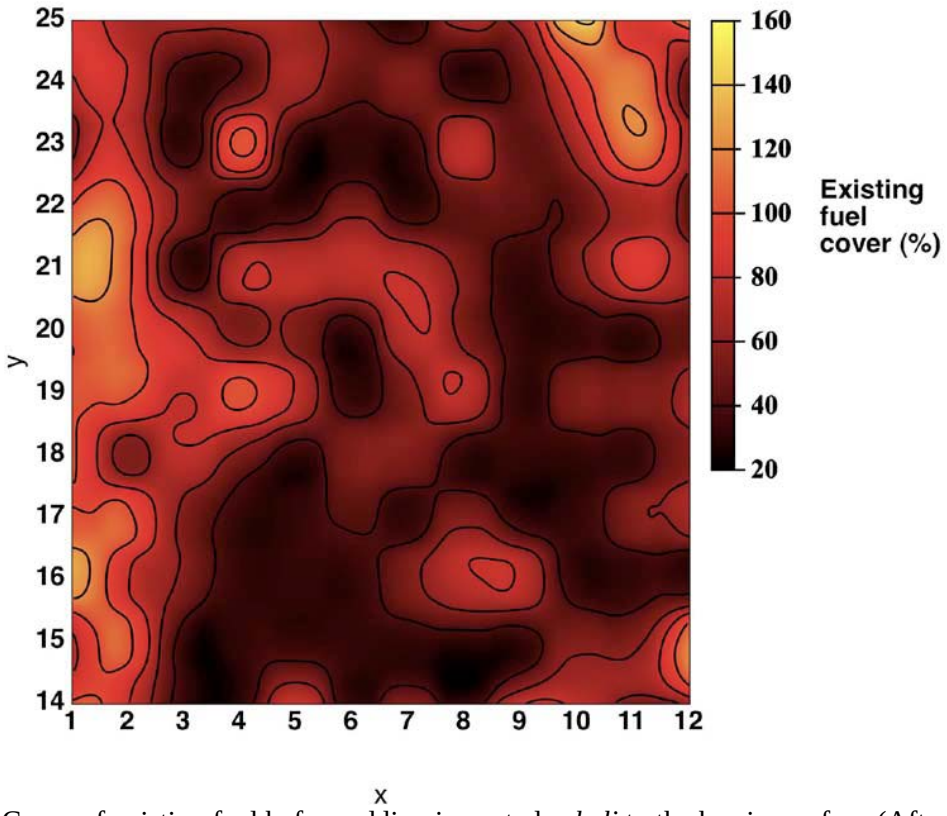

Figure M.8**.** Cover of existing fuel before adding imported *s. kali* to the barrier surface (After Figure 3.5 of Ward et al. 2009a).

The biomass already present in the low-fuel treatment was estimated by relating the mass of added fuel that provides generally high cover of about 90% to existing cover in each quadrat. The cover was visually estimated in each quadrat. The resulting estimate was 0.63 ± 0.08 kg (1.39 ± 0.176 lb) in each quadrat. There was about 45.4 kg (100 lb) existing in the low fuel section of the surface. The existing fuel load was about 0.695 tonnes/ha (0.31 tonnes/Ac).

The existing biomass on the high-fuel treatment was estimated at 1.31 ± 0.14 kg (2.88 ± 0.31 lb) in each quadrat. There was about 94.3 kg (207.89 lb) existing in the high-fuel treatment. The existing fuel load was about 1.457 tonnes/ha (0.65 tonnes/Ac). The total fuel load on the low-fuel plots was around 10.54 tonnes/ha (4.7 tonnes/Ac) compared to 12.8 tonnes/ha (5.71 tonnes/Ac) on the high-fuel plots. The fuel load contributed by bunchgrasses and other plants was minor and was not used for the total-fuel-load estimate.

The fuel depth is the shrub height, which ranged from about an average of 70 cm to about 25 cm on the north edge of the burn area (see Figure K.6 in Appendix K). Most of the burn area had average heights near 70 cm (2.3 feet).

The fuel load and plant composition are similar to that of shrub fuel type SH2 (142), with heights on average less than 3 ft tall (Appendix K) in the “Moderate Load Dry Climate” used in standard fire behavior fuel models (Scott and Burgan 2005). The SH2 (142) fuel type is a moderate load dry climate shrub (Scott and Burgan 2005). The shrub fuel type may be rated higher as SH3 (143) because of deeper fuel loading than SH2. The SH3 (143) fuel type is a moderate load humid climate shrub (Scott and Burgan 2005). Average canopy heights determined in Appendix K do not represent the relevant fuel loading depth that is more closely aligned with the tallest shrubs. Shrub height was not classed into taller

and shorter groups. The shrubs and tumbleweed had a water content of less than 30%, which classifies them as fully cured fuels (Scott and Burgan 2005). The upper fuel load in this study was 12.8 tonnes/ha, which is midrange compared with a high value of about 22.3 tonnes/ha in other big sagebrush ecosystems (Wright and Pritchard 2006). Similar fuel cover and biomass can be expected on future barriers at Hanford that are planted densely with *A. tridentata.*

M.3.2 Simulated Fire

Weather conditions on the day of the burn were sunny with a mean temperature of 24°C (75°F) and a slight wind from the south. A liquid foam line was applied before the fire was initiated to separate the area to be burned (north section) from the south section.

As discussed in Ward et al. (2009a), the fire was ignited at 3:15 PM by three ground fire crewmembers. The fire on top of the barrier was fast moving with flames reaching as high as 9 m (30 ft). Flame heights exceeded the 6-m (20-ft) flame-height rods but were estimated using video records with nearby infrastructure being used as a scale. Not all of the vegetation near the edges of the barrier was initially consumed. The fire ground crew revisited unburned areas and ignited unburned or partially burned plants with drip torches. The lower burn efficiency around the edges of the barrier may be related to the size and moisture content of the biomass. Plants around the edges of the barrier were typically bigger, perhaps because of a larger amount of available moisture that accumulates at the capillary break near the edge. Figures L.8 and L.9 show different stages of the fire.

Flame lengths were up to 30 feet, which classifies the fire as extreme (Scott and Burgan 2005). With such a long flame length, the shrub fuel type grades into a SH5 class characterized by heavy shrub load, with a fuel depth of 4 to 6 feet (Scott and Burgan 2005). The higher flame lengths observed in the fire may have resulted from the extra placement of tumbleweed fuel amongst the shrub canopies. It is likely that future barriers at Hanford that are planted densely with *A. tridentata* will have similar fire characteristics, especially if they trap *S. kali* amongst their canopies.

M.3.3 Fire Intensity

Figure M.10 shows the relative fire or scorch intensity for the burned area. The relative fire or scorch intensity was the greatest on the north to northwest and west sides while the lowest values were found along the northeast corner and southeast corners. This pattern is similar to the fuel load and air temperature patterns. After the burn, the surface was examined to identify any mosaic patterns that might indicate variable fire severity.

Fire intensity was verified by soil and air temperature measurements. The time-course of temperature before, during, and after the fire was recorded and examples of these data are shown in Figure M.11. These two temperature time-courses were taken from one tower at the hottest part of the barrier surface. Temperatures ranged from 250°C (482°F) at 1.5 cm (0.6 in.) below the surface to over 700°C (1292°F) at 1 m (3.3 ft) above the surface (Figure M.12). Air temperature rose much higher than the soil temperature. This can be expected because of the large amount of fuel on the surface and the flame heights. In addition, the thermal conductivity of soil is strongly dependent on moisture, with dry soils being very poor thermal conductors. With little soil organic matter, the only other possible source of fuel in the subsurface would have been live roots, and as a result, there would have been little transmission of heat in the subsurface.

After the peak temperature was attained, the air temperature also decreased much more rapidly than the soil temperature. The effect of the fire on soil temperature persisted for about 2 hours (Figure M.11).

Figure M.9. A View of the fire from southwestern edge of the plot about 4 minutes after ignition. the photograph was taken from atop of the Hanford Fire Department bush rig. (After Figure 3.16 of Ward et al. 2009a).

Figure M.10. Painted fire pole in foreground showing a thermocouple mounted perpendicular to the pole at a height of 2 m (After Figure 3.17 of Ward et al. 2009a).

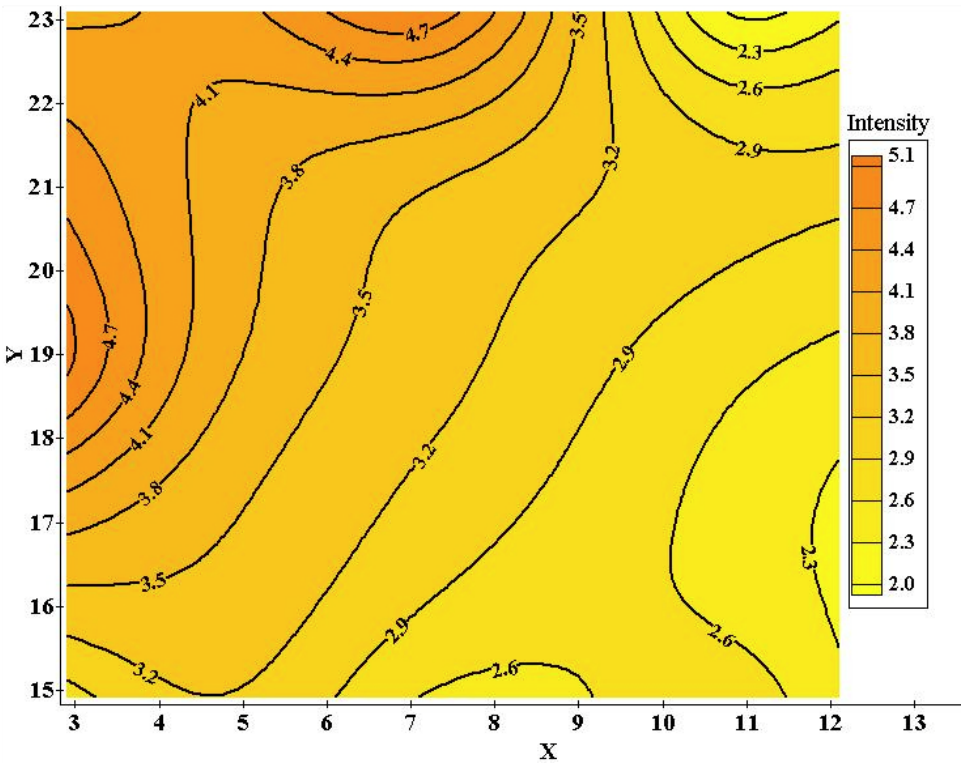

Figure M.11. Fire or scorch intensity mapped across the burned area at the end of the fire. The X and Y edges denote positions on the surface. The distance between coordinate values is 3 meters. (After Figure 3.18 of Ward et al. 2009a).

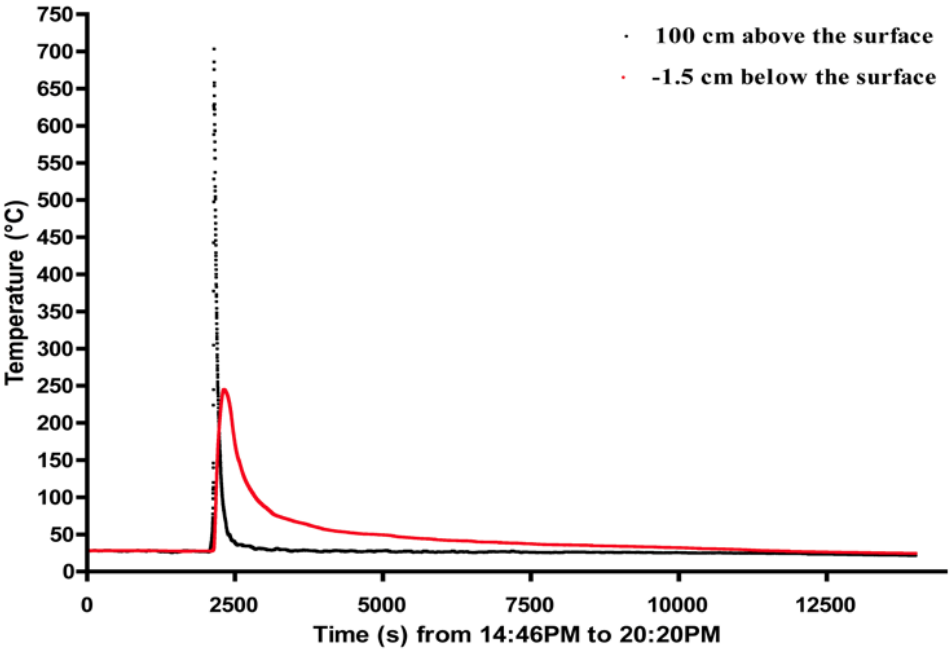

Figure M.12. Temperature in the air and soil before, during, and after the fire (After Figure 3.19 of Ward et al. 2009a).

These differences can again be attributed to differences in thermal conductivity between the soil and air

and differences in the effects of wind circulation on the redistribution of heat. The mean maximum temperatures were the lowest below the surface, rising to a maximum at 10 cm above the surface. Temperatures then decreased with increasing height (Figure M.12). The total duration of elevated temperature above that just before the fire was lower as the thermocouple became higher above the ground surface (Figure M.13). Below ground, there is an apparent reduction of integrated temperature compared with that at the ground surface, but the effect is not statistically significant. The temperature was integrated over a 2.61-hour period until temperatures fell to those observed before the fire. Soil and air temperatures measured at the fire poles were used to generate contour plots of the spatial distribution of temperature above and below the surface. Figure M.14 shows a plot of maximum temperatures recorded across the burned area. Both air temperature (Figure M.14a) and soil temperature (Figure M.14b) maps show that the highest temperatures were recorded in the plots with the higher fuel load, e.g., between x = 3 and 7 in Figure M.14. These results are consistent with those inferred from the scorch intensity measures on the fire poles. Scorch intensities were greatest on the north to northwest and west sides while the lowest values were found along the northeast corner and southeast corners. The gravel road surrounding the barrier acted as a natural firebreak and prevented the fire from spreading to the side slopes. The fire lasted approximately 7 minutes, by which time all of the imported fuel and most of the natural biomass had been consumed.

Following completion of the fire on the surface of the barrier, attempts were made to ignite the north portion of the gravel side slope. The toe of the gravel side slope did not burn very well, perhaps due to the high-moisture conditions of the plant biomass and the low plant density that resulted in large open areas between plants. The fire consumed only the plants that were lit by the drip torch, but did not transfer between plants. Winds were also very mild and were not a major factor in transporting the fire from plant colony to colony. Note that no imported fuel was added to the side slope.

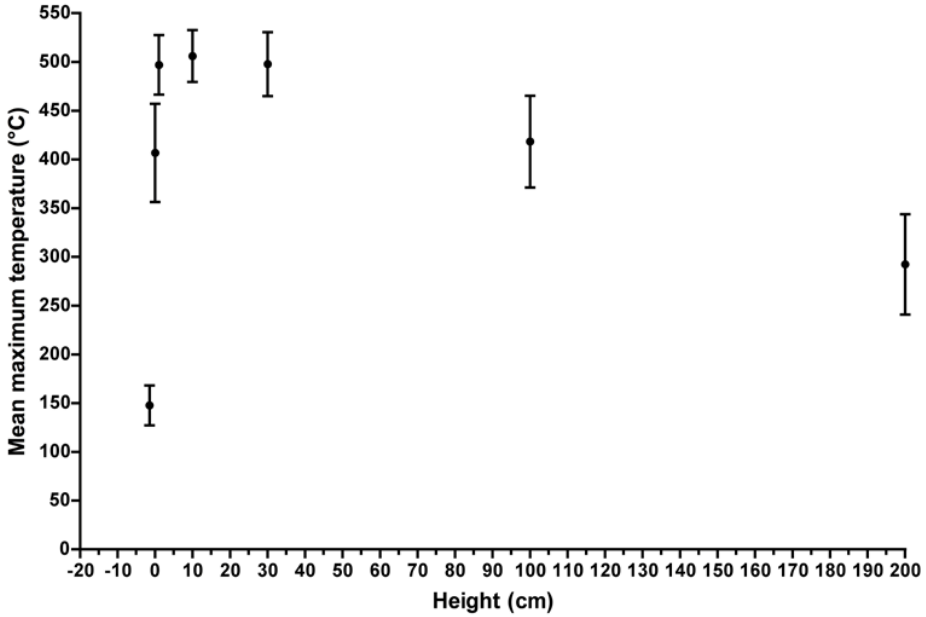

Figure M.13**.** Relationship between the average of maximum temperatures over the burned area and height from about 1.5 cm below ground to 200 cm above the ground. Error bars are 1 standard error of the mean. (After Figure 3.20 of Ward et al. 2009a).

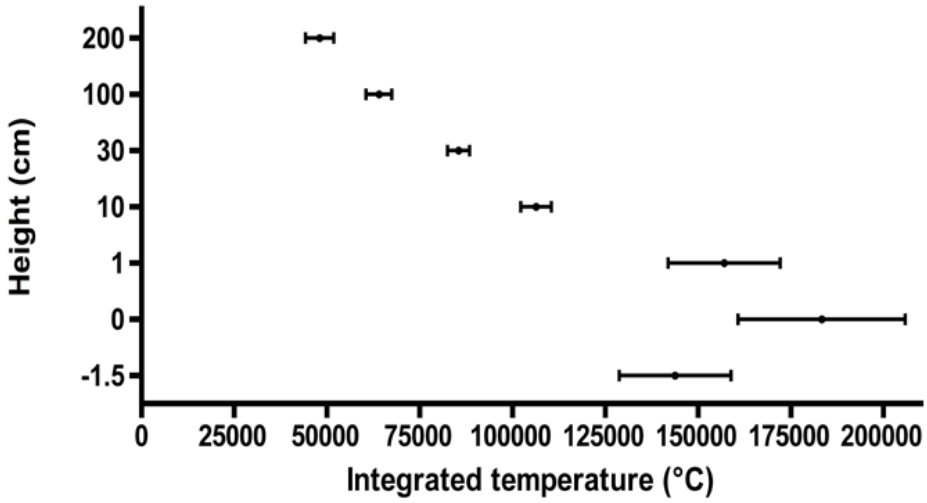

Figure M.14. Integrated temperature (°C sec). Bars are 1 standard error of the mean (After Figure 3.21 of Ward et al. 2009a).

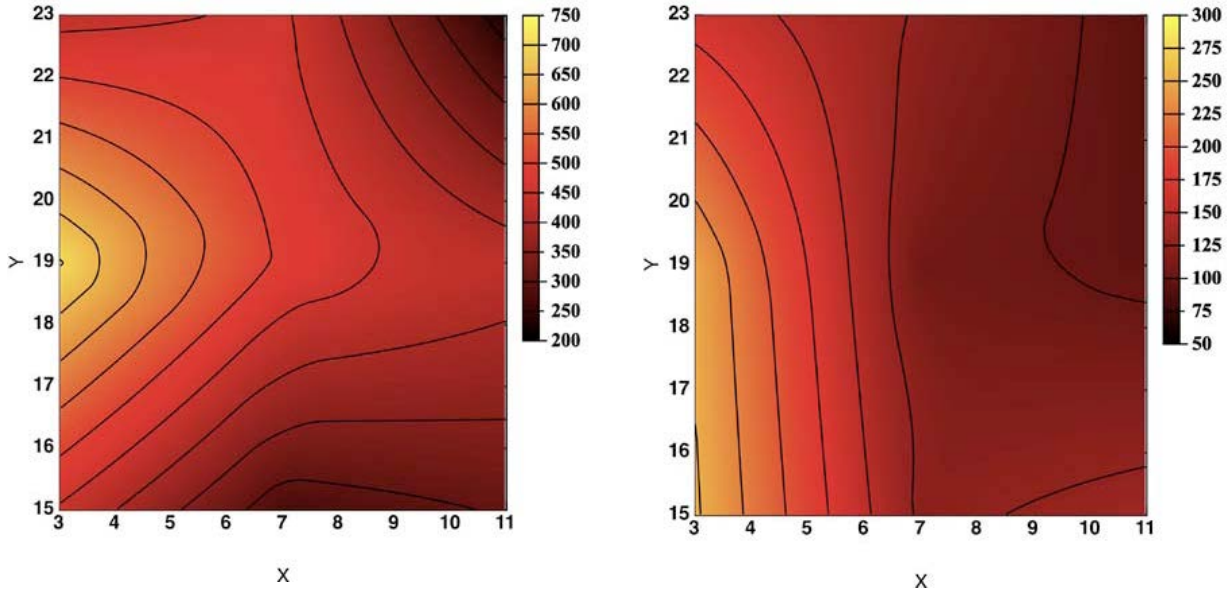

(a) (b)

Figure M.15. Peak temperatures observed on the burned section of the barrier: (a) air temperature measured 100 cm above the surface and (b) soil temperature measured 1.5 cm below the surface on the burn area. Unit is degrees Celsius (After Figure 3.22 of Ward et al. 2009a).

The greatest fire temperature observed was a little more the 700°C. This is lower than maximal modeled wildfire temperature (about 1200°C) in the Simi Fire in Southern California (Dennison et al. 2006). The lower temperature in the barrier fire likely is associated with lower fuel loads than in Southern California.

M.3.4 Surface Inflation/Deflation

Although gravel contents do not indicate any short-term inflationary pressures (Ward et al. 2009b), there

is circumstantial evidence that some soil may have been transported across the surface since the fire. Evidence of soil migration was observed after a snowfall on December 16, 2008. Soil dust was evident on the snow surface owing to its contrast with the bright snow found in footprints that were shielded from the deposition (Figure M.15) but the source of the dust uncertainty. The average change in measurement with one standard deviation was 1.3±7.1 cm in 2009 and 0.6±7.5 cm in 2010. The large uncertainty in the measurements suggests the measurements with erosion pins were inconclusive on inflation and deflation (Figure M.16). Based on the surveys of ground surface elevation using a real-time-kinematic global positioning system at the 338 locations on September 1, 2008 and July 29, 2009, the average change in elevation with one standard deviation was -0.3±2.2 cm in 2009 and -3.6±1.7 cm in 2010, which are inconsistent with the observation using the erosion pins, indicating no detectable change in ground surface elevation.

Figure M.16**.** Soil deposition patterns on a snow-covered surface on December 16, 2008 (After Figure 3.28 of Ward et al. 2009a).

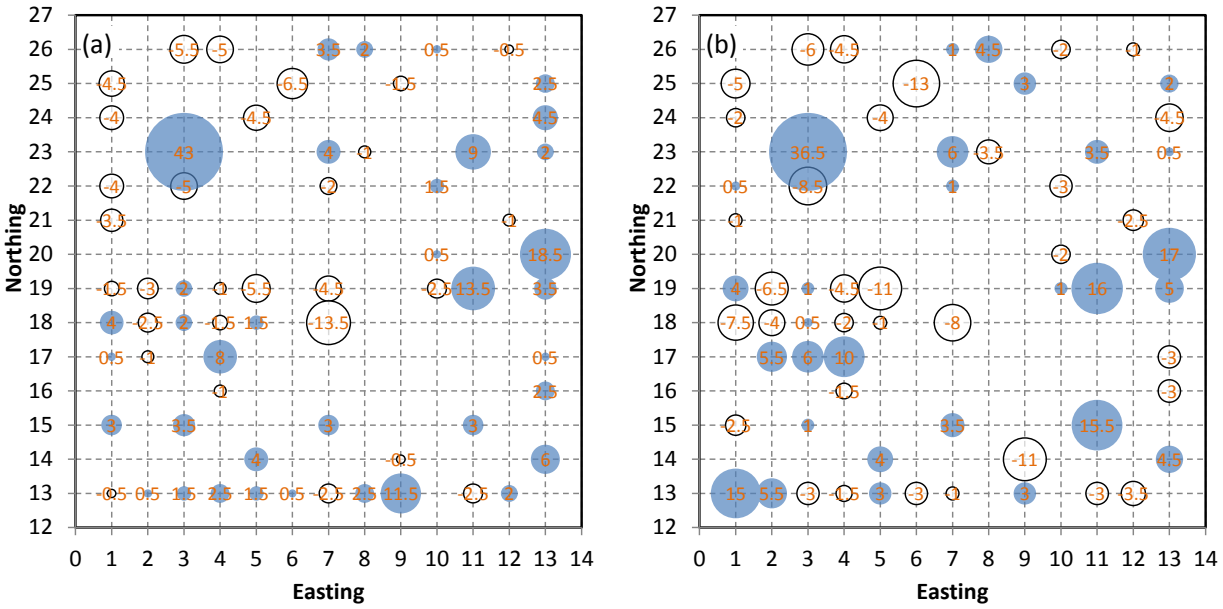

Figure M.17. Soil Inflation and Deflation Patterns on the Burned Area Relative to the 2008 Pre-Burn Condition in (a) 2009 and (b) 2010. The x and y edges denote positions on the surface. The distance between coordinate values is 3 meters.

These changes may be due to localized redistribution of soil from the burned area (Figure M.16). During the period of monitoring for the treatability test, very little erosion was observed. The only measurable loss of soil by wind occurred during the first 3 months when the surface was bare, with estimates ranging from 7.4 to 744 mg/m^2 (DOE-RL 1999). After the fire there were losses of up to 0.8% of the depth of surface soils (1.6 cm out of 200 cm). Areas with lower temperatures and fuels had gains of up to 1% of the depth of the surface soils. Surface inflation and deflation may be coarsely associated with fire temperatures. Fires are associated with increased wind erosion (Vermeire et al. 2005), and Ravi et al. (2006) did observe that fire-induced water repellency enhances erodibility. It is possible that soil losses were associated with higher fire temperatures compared to areas with lower soil losses or gains. This has not been assessed. It is not likely that significant amounts of soil will be lost from the surface after fires. It is also possible, but not measured at the barrier, that soils will deposit on the surface when vegetation cover is high given that the drier portions of the Columbia Basin are subject to wind erosion of soils (Feng et al. 2011).

M.3.5 Management Implications

Management implications are that the effects of a wildfire are not likely to compromise the function of the barrier under the conditions of the test. Monitoring ended in 2011. How the plant community recovered after the fire and the implications for future functionality should be assessed.

M.3.6 Implications on Barrier Performance

Implications for barrier performance are similar to management implications and are associated with understanding barrier condition and function beyond 2011. If soil erosion and deposition has continued, more surface variability may now be evident. This potentially can create weak spots on the surface.

M.4 Conclusions

The fire was similar to other shrub-steppe fires. The fuel load was about midrange compared with other shrub-steppe ecosystems. The fire exhibited great flame lengths, classifying the fire as extreme. The effect of the fire on the surface was noted by patterns of deposition (up to 1.0%) and erosion (up to 0.8%). The erosion and deposition patterns are not likely to cause a loss in functionality of the barrier under the conditions of the test.

Acknowledgement

Research was funded by the U.S. Department of Energy under Contract DE-AC06-76RLO 1830 with the Pacific Northwest National Laboratory. We thank Glendon Gee for conceiving the Hanford Prototype Barrier and early support. We thank Kevin Leary for initiating, helping with, and funding the fire portion of the study. We thank Anderson Ward, Karen Barton, Andrew Pomiak, Dale Loth, Jenifer Linville, and Janice Maya for technical assistance.

References

De Marco, A, AE Gentile, C Arena, and AV Virzo De Santo. 2005. "Organic Matter, Nutrient Content and Biological Activity in Burned and Unburned Soils of a Mediterranean Maquis Area of Southern Italy," *International Journal of Wildland Fire*, 14:365-377.

Dennison, PE, K Charoensiri, DA Roberts, SH Peterson, and RO Green. 2006. "Wildfire Temperature and Land Cover Modeling Using Hyperspectral Data," *Remote Sensing of Environment*, 100:212-222.

DOE-RL. 1993. *Treatability Test Plan for the 200-BP-1 Prototype Surface Barrier*, DOE/RL-93-27, U.S. Department of Energy Richland Operations Office, Richland, Washington. Available at http://www.osti.gov/energycitations/servlets/purl/10185012-iIHFSc/.

DOE-RL. 1999. *200-BP-1 Prototype Barrier Treatability Test Report*, DOE/RL-99-11 Rev. 0, U.S. Department of Energy Richland Operations Office, Richland, Washington.

DOE-RL. 2013. *Hanford Site Cleanup Completion Framework*, DOE/RL-2009-10, Rev. 1, U.S. Department of Energy Richland Operations Office, Richland, Washington. Available at http://www.hanford.gov/files.cfm/Comp_Framework_Jan_%201-23-13-lfm.pdf.

Feng, G, B Sharratt, and L Wendling. 2011. "Fine Particle Emission Potential from Loam Soils in a Semiarid Region," *Soil Sci. Soc. Am. J.*, 75:2262-2270.

Gee, GW. 1987. *Recharge at the Hanford Site: Status Report*, Pacific Northwest Laboratory, PNL-6403, Richland, Washington.

Hajek, BF. 1966. *Soil Survey, Hanford Project in Benton County, Washington*, Pacific Northwest Laboratory, BNWL-243, Richland, Washington.

Johnson, EA and K Miyanash. 2001. *Forest Fires: Behavior and Ecological Effects*. Academic Press, San Diego.

Ravi, S, P D'odorico, B Herbert, T Zobeck, and TM Over. 2006. "Enhancement of Wind Erosion by Fire-Induced Water Repellency," *Water Resources Research*, 42:1-9.

Scott, JH and RE Burgan. 2005. *Standard Fire Behavior Fuel Models: A Comprehensive Set for Use with Rothermel's Surface Fire Spread Model*, USDA Forest Service RMRS-GTR-153.

Stone, WA, JM Thorp, OP Gifford, and DJ Hoitink. 1983. *Climatological Summary for the Hanford Area.*, Pacific Northwest Laboratory, PNL-4622, Richland, Washington.

Vermeire, LT, DB Wester, RB Mitchell, and SD Fuhlendorf. 2005. "Fire and Grazing Effects on Wind Erosion, Soil Water Content, and Soil Temperature," *J. Environ. Qual.*, 34:1559-1565.

Ward, AL, GT Berlin, JW Cammann, KD Leary, and SO Link. 2008. *Test Plan to Assess Fire Effects on the Function of an Engineered Surface Barrier*, PNNL-17859, Pacific Northwest National Laboratory, Richland, Washington.

Ward, AL, N Hasan, SO Link, and KE Draper. 2009a. *The Effects of Fire on the Function of the 200-BP-1 Engineered Surface Barrier*, PNNL-18934, Pacific Northwest National Laboratory, Richland, Washington.

Ward, AL, KD Leary, SO Link, GT Berlin, JW Cammann, ML Mandis, and LC Buelow. 2009b. "Short and Long-Term Fire Impacts on Hanford Barrier Performance," *Waste Management Symposium 09*, Phoenix, Arizona.

Wright, CS and SJ Pritchard. 2006. Biomass Consumption During Prescribed Fires in Big Sagebrush Ecosystems. In PL Andrews and BW Butler *Proceedings of Fuels Management—How to Measure Success*, U.S. Department of Agriculture, Forest Service, Rocky Mountain Research Station, Fort Collins, Colorado.

Appendix N

Fire Impacts on the Performance of the Prototype Hanford Barrier[1]

A. L. Ward
Pacific Northwest National Laboratories
P.O. Box 999 MSIN K9-33, Richland, WA 99354
K. D. Leary
U.S. Department of Energy, Richland Operations Office
825 Jadwin Avenue, Richland, WA 99352
S. O. Link
Washington State University Extension Service
G. T. Berlin and J.W. Camman
CH2M Hill Plateau Remediation Company
P.O. Box 1600, Richland, WA 99352
M.L. Mandis
Washington State Dept. of Ecology 3100 Pobb Blvd, Richland, WA
L.C. Buelow
U.S. Environmental Protection Agency, 309 Bradley Street, Suite 115, Richland, WA 99352

[1]This is a reformatted version of a published article: Ward, AL, SO Link, KD Leary, and GT Berlin. 2010. "Fire Impacts on an Engineered Barrier's Performance: The Hanford Barrier One Year after a Controlled Burn," *WM 2010 conference*, March 7-11, 2010, Phoenix, Arizona.

Content

List of Figures

List of Tables

Abstract

A critical unknown for long-term engineered barrier performance is the effect of wild fire during a post-institutional control environment where routine maintenance may be limited or non-existent. In September 2008, a controlled burn was conducted on one half of a vegetated, multilayered capillary barrier emplaced over a Hanford waste site. The effects on barrier performance have been monitored and documented over the past year. Soil physical, chemical, and hydrologic properties; plant floristics and density; and animal-use were characterized before and after the fire with the unburned half of the barrier serving as a control. Temperatures during the controlled burn ranged from 250 °C 1.5 cm below the surface to over 700 °C, 1 m above the surface. Significant decreases in hydraulic conductivity and surface-soil wettability were observed immediately after the fire. Post-fire concentrations of major soil nutrients, pH, and electrical conductivity remain elevated. Dense stands of sagebrush were destroyed from the fire allowing many more species to emerge, thereby increasing species diversity. Seed sources contributing to this species diversification were from either the existing seedbank and/or wind-blown sources. There were significant differences in the rate of accumulation and loss of soil moisture on the burned and unburned sections. On the burned section, water storage was higher during the fall; it increased more slowly with the onset of winter precipitation (owing to higher evaporation); and it decreased more slowly in the spring (owing to lower evapotranspiration). There were significant differences in storage between the burned and unburned sections by end of October 2009 although barrier effectiveness has not been compromised.

N.1 Introduction

Enhanced capacitive covers combine natural or modified soil materials with evapotranspirative surface layers to control infiltrating surface water. They are now accepted as an alternative to the removal, treatment, and disposal of near-surface contaminants in arid and semiarid regions where potential evapotranspiration (PET) significantly exceeds precipitation. Over their functional life, barriers will be subjected to extreme events including erosive stresses and abnormal precipitation events. On bare surfaces, such as those which may result from wildfire, these events could adversely impact barrier performance. Thus, understanding how an engineered barrier responds to, and ultimately recovers from, such disturbances is important for predicting long-term performance and obtaining public and regulatory acceptance of barrier technology.

Perhaps the biggest unknown is the effect of wild fire on the evapotranspirative soil layer and ultimately the function on these engineered ecosystems. Research in rangeland and forest ecosystems show that the effects of fire can be quite complex. These range from the reduction, or even elimination, of above-ground biomass, to changes in soil physical and chemical properties, and alteration to microbial mediated processes (Doerr and Cerdà 2005; Feis-Fire Effects Information Service). Wildfire can directly or indirectly alter soil aggregate stability, water repellency, surface runoff response, mineralogy, pH, and nutrient availability as well as fundamental ecological processes such as biomass productivity, vegetation re-sprouting, plant species recruitment, microbial composition, and animal habitat. The damage sustained by plants has been shown to be proportional to the intensity and duration of the fire and the long-term effect is a change in the floristic composition of plant communities. A more immediate effect is the destruction of surface litter and vegetation, leading to a reduction in the protection offered to the soil from raindrop impact and increased runoff (Neary et al. 1999; Powers et al. 1998). Runoff is also enhanced by fire-induced water repellency in the near surface owing to the coating of soil aggregates with hydrophobic organic compounds (Debano 1981). Increased runoff is often accompanied by loss of soil from the evapotranspirative soil layer, a reduction in available soil nutrients, and a decrease in water holding capacity.

Owing to the strong coupling between soil properties and ecological processes, fire-induced alterations are sitespecific and cannot be easily extrapolated to other ecosystems. However, in engineered ecosystems where nutrients may be already limiting, soil and nutrient loss could inhibit processes necessary for successful barrier performance and recovery from fire. The main objectives of this study were to document fire effects on: (i) soil hydrophysical and geochemical properties, and (ii) ecological processes controlling barrier performance and function as a recovering ecosystem. It is hypothesized that the interplay between fire-induced changes in hydrophysical and geochemical properties and post-fire plant dynamics can affect nutrient availability and soil water balance. To this end, a controlled burn was conducted on one half of the surface of the prototype Hanford barrier in September 2008. The effects of the fire were monitored over the last year and this paper provides a summary of the results to date.

N.2 Materials and Methods

N.2.1 Physical Setting

The prototype barrier is in 200 East central plateau of the Hanford Site, which is located in semiarid south central Washington State. The long-term average (LTA) annual precipitation from 1946 to the present is 6.85 in (174 mm) with almost half occurring in the winter (November through February). Temperature

ranges from as low as 10 °F (- 12 °C) in the winter to as high as 115 °F (46 °C) in the summer. Actual evapotranspiration (AET) ranges from 4.4 in. (11.1 cm) to 6.3 in. (159 mm) whereas potential evapotranspiration (PET) ranges from 29.5 in. (750 mm) to 54.7 in. (1390 mm). The thick vadose zone on the central plateau (> 300 ft [100 m]) is comprised mostly of coarse glaciofluvial sediments ranging from loamy sand to sandy loam. The relatively deep vadose zone and the difference between AET and PET make this site ideal for use of engineered barriers for waste isolation.

The prototype barrier consists of a 2-m thick silt-loam layer overlying other, coarser materials including sand, gravel, and basalt riprap with each layer serving a distinct purpose (Ward et al. 1997). The top 1 m of silt loam contains 15% by weight of pea gravel to minimize wind erosion. The entire silt-loam layer is a medium for plant growth and therefore forms the evapotranspiration layer. The design water storage capacity is 600 mm, which is more than three times the LTA precipitation for the site. Additional layers below the silt-loam serve several functions including the establishment of a capillary break and a biointrusion layer (Ward et al. 1997; Ward et al. 2007).

N.2.2 Site Vegetation

Prior to construction of the barrier, the native vegetation at the site was a mix of *Artemisia tridentata* (sagebrush), *Ericameria nauseosa* (gray rabbitbrush), and *Poa secunda* (Sandberg's bluegrass). The silt loam used to construct the barrier was mined at the nearby McGee Ranch where the vegetation is mostly shrubs (22%), with *A. tridentata* being dominant, and grass (23%) with *Poa secunda* accounting for 15.4%. Following construction of the barrier, the surface was vegetated with a mixture of shrubs (*A. tridentata* and *E. nauseosa*) and grasses including *Agropyron dasystacyum* (thickspike wheatgrass), *Hesperostipa comata* (needle and thread grass), *Elymus elymoides* (squirreltail), *Elymus wawawaiensis* (Snake River wheatgrass), and *Poa secunda* (Sandberg's bluegrass). Knowledge of the composition of the plant community is an important aspect of this study as fire can affect the floristic composition and the rate of re-establishment of vegetation that will, in part, be controlled by the existing seedbank.

N.2.3 Performance Monitoring

The barrier is instrumented for monitoring components of the water balance including precipitation, runoff, water storage, and percolation out of the root zone. Water storage is monitored using a neutron hydroprobe and vertically installed shorting-diode time domain reflectometry (TDR) probes. Matric potential and soil temperature are measured by heat dissipation units (HDUs). Percolation is monitored using a system of 12 concrete vaults located to the north and down-gradient from the asphalt layer where water is collected by gravity flow and the hydrograph recorded automatically using tipping buckets and pressure transducers (Doerr and Cerdà 2005; Feis-Fire Effects Information Service). Monitoring of deep percolation is facilitated by a 6.5 m × 6.5 m pan lysimeter installed under the northeast section of the asphalt layer (Doerr and Cerdà 2005; Feis-Fire Effects Information Service). Horizontal access tubes facilitate monitoring of water content at the capillary break (1.95 m deep) and beneath the asphalt pad by neutron hydroprobe. Barrier and sideslope stability is monitored using elevation measurements whereas erosion is monitored using erosion pins and any sediment collected from the runoff plot.

N.2.4 Simulated Fire

The simulated fire was limited to the north half of the barrier, which was divided into nine 12 × 12 m plots. Two fuel loads were used in the study, 4.7 and 5.71 tons/acre (10.5 and 12.8 tonnes/ha). The heavier fuel load was on the west and the lighter fuel load on the east side of the barrier surface. A flame height rod was installed in the center of each plot for visual observation of the flame height during the fire and for monitoring temperature. For temperature measurements, type K thermocouples connected to a HOBO® datalogger, were installed 1.5 cm below the soil surface, at the surface (0 cm) and elevations of 1, 10, 30, 100, and 200 cm. Measurements started 3 hrs prior to the fire and continued for some 9 hrs after the fire. Water balance monitoring during and after the fire made use of instruments. Near surface sensors,

instrument boxes, and solar panels were covered with fiberglass insulation, aluminum fire blankets for protection (Ward et al. 2008).

N.2.5 Characterization of Soil Properties

Soil physical and chemical properties were measured before the fire and at one week, 6 months, and 1 year after the fire. The field-saturated hydraulic conductivity, K_{fs}, was measured at nine different locations on each 12 m × 12 m plot using a Guelph permeameter (Reynolds and Elrick 1985). On an engineered barrier, water movement typically occurs as unsaturated flow, which is controlled by the unsaturated hydraulic conductivity, $K(\psi)$ rather than saturated conditions. To gain insight into any possible effects of the fire infiltration, field measurements of $K(\psi)$ were also measured on each 12 m × 12 m plots using a Guelph tension infiltrometer (Reynolds 1993). Within each 12 m × 12 m plot, four measurements were made, one on each 3 m × 3 m quadrant, to provide representative values before and after the burn. Both methods allowed estimation of the α parameter, which is the inverse of the air entry pressure, *Pe*, and can be expected to change with changes in soil structure. Changes in the surface layer composition may be expected as the barrier ages under both deflationary and inflationary influences of soil loss or gain. Such changes could be enhanced in post-fire environment and were therefore investigated by measuring the particle-size distribution of samples collected from 0 cm to 2 cm and 2 cm to 10 on a 3 m × 3 m grid. Soil samples were separated into four grain-size fractions, namely, gravel, sand, silt, and clay, and sub classes (very coarse, coarse, medium, fine, and very fine). The pattern of inflation and deflation was mapped by comparing 1-yr post-burn measurements on 66 erosion pins with pre-burn measurements on the north half of the barrier. An important phenomenon affecting infiltration or water movement in soils after fire is the hydrophobization of originally wettable aggregates by coatings with organic substances of plant origins (Wallis and Horne 1992). To quantify the importance of this phenomenon at the barrier, soil water repellency was measured *in situ* and on pre- and post-burn soil samples using the water-drop penetration time (WDPT) test (Dekker and Ritsema 1994). Following the initial measurement, three additional measurements were made with the final set being made almost 1 yr after the fire. The effect of fire on soil moisture profiles and water storage was determined from neutron probe measurements of soil water content. Water-content profiles were measured at approximate 1-month intervals following the fire to document changes in storage. Measurements were taken at 0.15-m intervals in the 2-m-thick fine-soil layer. In addition to hydrophysical properties, geochemical properties were also determined on pre- and post-burn soil samples collected on a similar schedule. Soil samples were analyzed for macronutrients (N,P,K) and micronutrients (Ca, Mg, Na) by Northwest Agricultural Consultants (NWAg) of Kennewick, Washington using procedures described by Gavlak et al. (2003). In addition to soil nutrients, samples were also analyzed to quantify pH, electrical conductivity, soil organic matter, cation exchange capacity, and specific surface area. Selected samples were also analyzed by X-ray diffraction (XRD) methods to determine the effects of fire on mineralogy.

N.2.6 Characterization of Ecological Properties

Plant species composition, including the occurrence of soil cryptograms, was determined for the functional portion of the barrier as well as the north and west sideslopes. The occurrence and density of the dominant shrubs, *A. tridentata* and *E. nauseosa*, were determined by counting the number of shrubs in three age classes (new seedlings, midsized-young, and large-old). In addition, shrub height, greatest canopy diameter, and the diameter at the center of the plant perpendicular to the greatest diameter were measured on 25 shrubs each from the north and south sections of the barrier. Ground cover of grass, shrubs, forbs, litter, soil, and soil cryptogams was also determined for the barrier and side-slopes by visual inspection for each species according to Daubenmire (1959). The LAI was measured on each study plot used to determine cover at the burned and unburned barrier areas and at the two McGee Ranch analog sites. Leaf area index (LAI) was measured with an AccuPAR LP80 Ceptometer at the center of each plot. The LAI values were transformed using the square root because data were Poisson distributed. Pre-dawn xylem pressure potential was measured with a Model 1005 pressure chamber instrument (PMS

Instruments) on *A. tridentata*, *S. kali*, and *M. officinalis* on the burned and unburned sections of the barrier. To better understand the effects of fire on post-fire vegetation regeneration, soil seed banks were assessed for the pre- and post-burn conditions using seedling emergence tests. Soil samples were collected from the top 3 cm and stored dry at room temperature until the emergence tests, which were conducted in the climate-controlled greenhouse at Washington State University. Germinated seedlings were identified and counted and the resulting data analyzed separately for each of the most common species. All of these measurements were repeated at two analog sites at the McGee Ranch (the source of silt loam used in the construction of the barrier), one which has not burned in decades and the other which burned about 8 years ago, thereby providing context to the communities on the barrier. After the fire, general assessments of shrub survival, re-sprouting, and recruitment were made at the barrier. In addition, cover was determined at the two McGee Ranch analog sites (old burn and unburned) to provide a comparison for the barrier

N.3 Results and Discussion

N.3.1 Simulated Fire

The fire was ignited at 3:15 PM on September 26, 2008 using drip torches. The fire on top of the barrier was fast moving with flames reaching as high as 9 m (30 ft). The fire lasted approximately 7 minutes by which time all of the imported fuel and most of the natural biomass had been consumed. Flame heights exceeded the 6-m (20-ft) flame-height rods but were estimated using video records with nearby infrastructure being used as a scale (Figure **N**.**1**). The time-course of temperature before, during, and after the fire was recorded with HOBO® data loggers. These two temperature time-courses were taken from one tower at the hottest part of the barrier surface. Temperatures ranged from 250 °C (482 °F) at 1.5 cm (0.6 in.) below the surface to over 700 °C (1292 °F) at 1 m (3.3 ft) above the surface. Air temperature increased much higher than the soil temperature, which can be expected. The soil thermal conductivity is strongly dependent on moisture with dry soils being very poor thermal conductors. This coupled with the absence of significant subsurface fuel would have limited the depth of penetration of elevated temperatures. The effect of the fire on soil temperature persisted for about 2 hours. Fire intensity was verified by soil and air temperature measurements. The relative scorch intensity was greatest on the north to northwest and west sides of the barrier while the lowest values were found along the northeast corner and southeast corners. This pattern is similar to the fuel load and air temperature patterns. After the burn, the surface was examined to identify any mosaic patterns that might be indicative of variable fire severity. Some of the vegetation, particularly near the edges of the barrier was not initially consumed but were later ignited by the fire crew. The lower burn efficiency around the edges may be related to the size and moisture content of the biomass. Plants around the edges of the barrier were typically bigger, perhaps because of a larger amount of available moisture that accumulates near the edge.

Figure N.1. Painted fire pole in foreground showing thermocouple mounted perpendicular to the pole at a height of 2 m.

N.3.2 Fire Effects on Soil Properties

N.3.2.1 Hydraulic Properties

The one-head and two-head K_{fs} measurements made with the Guelph permeameter before the fire were remarkably similar given the variability typically found in K_{fs} measurements. Nonetheless, these data provide a good reference point for quantifying the effects of fire. A comparison of pre- and post-burn (1 wk, and 1 yr) measurements of K_{fs} measured shows a significant decrease from pre-burn values (Figure N.2). However, after 1 year, K_{fs} had returned to pre-burn values at three out of eight measurement locations. Plots 1, 3, and 7 showed essentially the same K_{fs} values as before the fire, whereas reduced K_{fs} values persisted on Plots 2, 4, 5, 6, and 8. Estimates of the K_{fs} derived from the tension infiltrometer showed a mean of 1.33×10^{-3} cm/s (3.77 ft/day) with a standard error of 0.009. This value is roughly one order of magnitude larger than the K_{fs} measured in the laboratory on repacked silt-loam samples prior to barrier construction. A reduction in K_{fs} is indicative of a reduction in the volume fraction of large pores or the overall porosity. Such a change is consistent with the loss of soil structure that typically results from wildfire. During the first week, the post-fire estimates of α also decreased from pre-fire conditions. The mean pre-burn α was 0.085 cm^{-1} (0.216 in.-1), which is equivalent to a P_e of about 12 cm (4.7 in.). This value is somewhat small for a silt loam but is consistent with a gravel amended field soil with some structure. The inverse, α^{-1}, is a measure of the air entry pressure, P_e, and a decrease in α is therefore equivalent to an increase in P_e. This can be expected with a decrease in mean pore size or an increase in fines content. The only reasonable explanation for such an increase could be pore plugging due to an increase in ash in the near-surface layers. Estimates of α derived from tension infiltrometer measurements 1 yr after the fire also show that only three out of eight plots had returned to pre-burn values (Plots 1, 3, and 7), whereas five showed essentially the same α as before the fire. Both K_{fs} and α are strongly influenced by pore-size distribution and therefore soil structure. It is clear that for the Warden silt loam used at the barrier, 1 yr is too soon to see a regeneration of the structure that may have been destroyed by

the fire. This can be expected as the regeneration of structure will depend on the ground cover and organic matter derived from plant biomass which is still mostly absent. The specific surface area, which controls sorption and the hyper-dry region of the moisture retention function, was also measured. The mean value for the surface soil, sieved to pass a 2-mm (0.08-in.) sieve, was 9.92 m^2/g. This value compares well with independent measurements that range from 8 to 11 m^2/g and remained unchanged after the fire.

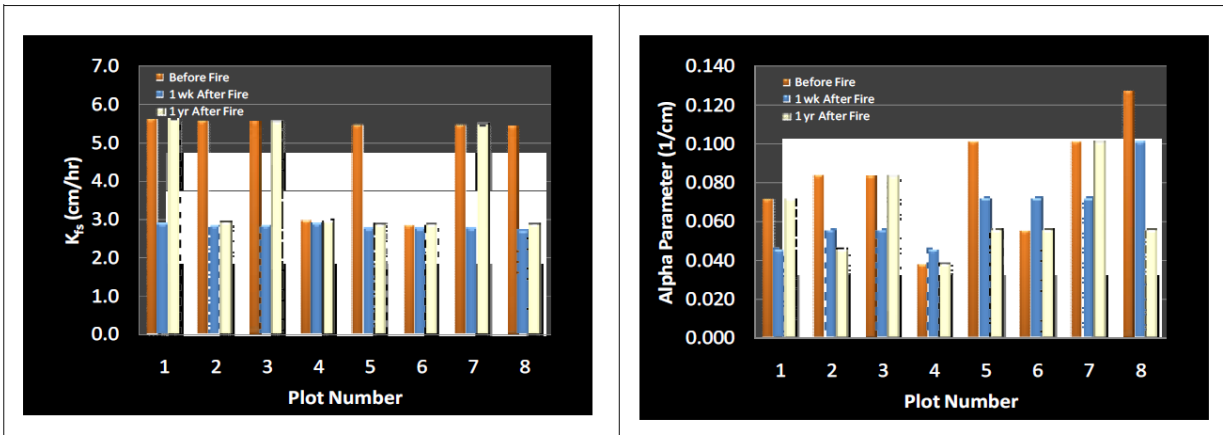

Figure N.2. comparison of *in-situ* pre-burn and post-burn field hydraulic properties, (a) saturated hydraulic conductivity, K_{fs}, and (b) α parameter, the inverse of air entry pressure, P_e.

N.3.2.2 Surface Layer Composition and Inflation/Deflation

Measurements with erosion pins also show evidence of inflation and deflation. The greatest loss of soil was 13.5 mm, and the greatest accumulation of soil was 18.5 mm. The greatest deflationary losses of soil occurred on the northwest through the center of the burned area. The greatest inflationary accumulation of soil occurred in the east side of the surface[2]. These changes may be due to localized redistribution of soil from the burned area. In spite of these short-term changes, particle size analyses showed a significant increase in the near-surface gravel content over the last 15 years, which is indicative of deflation in the surface. During the 3-yr of treatability test conducted from 1994-1997, very little erosion was observed. Thus, the increase in gravel in the near surface could be due partly to freeze-thaw processes. The difference between the two sections of the barrier was attributed to deflation due to the simulated 1,000-yr return precipitation events on the north. Long-term freeze-thaw cycles, when coupled with the development of root biomass, could have an impact on the soil bulk density in the near surface. The mean pre-burn dry bulk density on the north section was 1.46 ± 0.054 g/cm3 whereas the mean post-burn density was 1.442 ± 0.07 g/cm3, not a significant difference. Some observed changes were largest near sagebrush stumps, suggesting a relationship between with the location of large ash accumulations on the surface. Nonetheless, the short-term decrease in dry bulk density is not statistically significant.

N.3.2.3 Soil Hydrophobicity

Pre-burn *in-situ* and laboratory water repellency measurements resulted in water-drop penetration times all less than 5 seconds, an indication of fully wettable soils. Immediately after the burn and for 2 months after, field and laboratory measurements showed a significant decrease in wettability. In general, water repellant conditions in unburned areas were found in the leaf litter and at the surface immediately beneath shrubs, before the fire. After the fire, water repellant areas were typically found parallel to the surface but at deeper depths. Water drops penetrated immediately into wettable soils, which were typically bare soil

[2] Further data analysis showed the result on barrier inflation/deflation based on erosion pins is inconclusive. Please refer to appendix M, section M.3.4.

areas (no evidence of plants) and ash-free zones, i.e., free of organic matter before the fire (Figure N.3). However, water-drop penetration tests near shrubs suggested the presence of water-repellant soils with repellency ranging from slightly water repellant to strongly water repellant. Results indicated some general relationships between soil temperature resulting from wild fire and water repellency: 1) essentially no change in water repellency when soil temperatures were less than 200 °C, 2) strong water repellency when soil temperatures were between 200 and 250°C, and (3) absence of water repellency when soil temperatures between 250 and 400°C were recorded. These ranges are consistent with those reported by Debano (2000). Measurements taken over time showed that the intense snowfall in the winter of 2008 resulted in a loss of water repellency by early January 2009, and repellency remained relatively low throughout the winter. Measurements made 1 year later when the soil surface was quite dry still showed evidence of reduced wettability. Only 16% of samples show showed signs of decreased wettability after 1 yr. Under these conditions water repellency appears to be reversible; disappearing when the soil is wet and returning after the soil dries out. For fires occurring in the late summer, elevated water repellency may persist for at least 1 yr under Hanford conditions. Published reports suggest that the time to dissipate can range from less than 1 yr (Huffman et al. 2001) to over 6 yr (Dyrness 1976). These observations are of significance to the runoff response of the barrier.

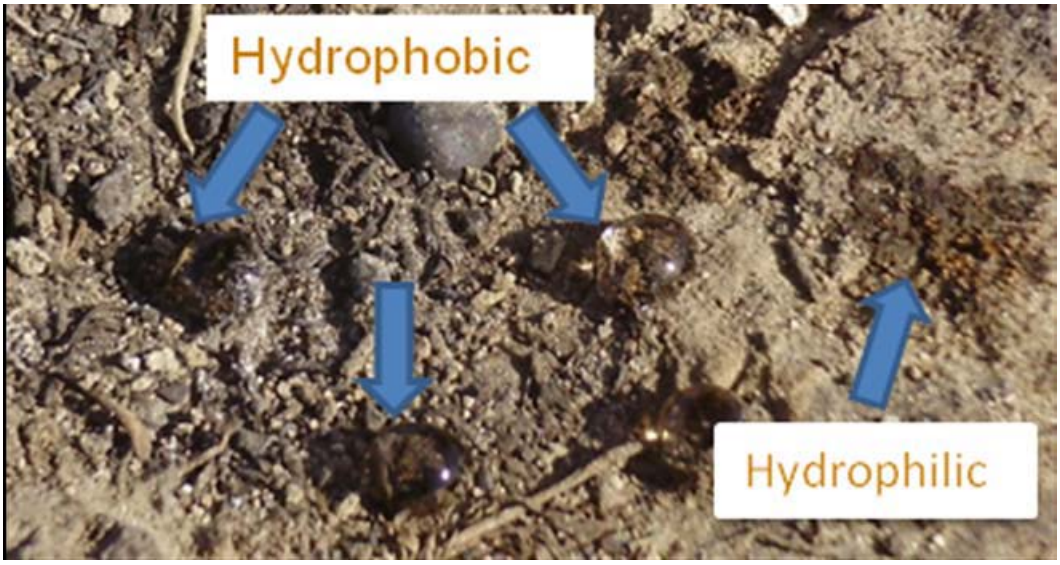

Figure N.3**.** Photograph of burned surface during water drop penetration test.

N.3.2.4 Fire Effects on Soil Water Storage

Water balance is the most comprehensive approach for assessing the field-scale hydrologic performance of an engineered barrier. Thus, observing differences in the water- balance components between the burned and unburned sections should provide insight into the effects of the fire. Robichaud and Miller (2000) suggested that under fire-induced water- repellent conditions, runoff rates should quickly peak and then begin declining as the hydrophobic substances of the soil are broken down, thus increasing infiltration over time. Before the fire, runoff had been recorded at the barrier on only two occasions, once when the surface was bare, and once after a rapid snowmelt event on frozen surface soil. In the winter of 1997, Chinook winds on frozen surface soils resulted in 36.3 mm of surface runoff with no sediment loss. In January 2009, following the fire, a total of 1.6 L of runoff was recorded. This is equivalent to 0.016 mm, quite small compared to previous events but the first observed in over 15 years. It can be attributed directly to the effects of the fire. A comparison of the soil water profiles measured on the burned (north) and unburned (south) sections over the last year also show significant differences that can be directly attributed to the fire. These differences are best interpreted in terms of soil water storage, W (Figure N.4). In September 2008, just before the fire, the soil water storage was mostly depleted, and the north and

south sides showed no differences in water-content distributions. By January 2009, after a relatively wet winter, a difference in the water-content profiles could be seen between the north and south sections with the south section being considerably wetter in the top 0.7 m and with the north section showing slightly wetter conditions at depth (0.8 to 1.6 m). With both sides receiving the same amount of precipitation, the difference in water-content distribution is due to changes induced by the fire, although the discrepancy is somewhat counter intuitive. The lower near-surface water content can be attributed to increased evaporation from the bare surface whereas the developing moisture front at depth is due to redistribution of water that moved beyond the evaporative depth. The wetting front developing at depth is more obvious in the Mar profile. After the start of spring, the depletion in moisture content (owing to plant uptake) increased, and there was a sharp reduction of moisture in the 0 to 0.8 m depth on the south side, whereas the water content at depth continued to increase. The rapid decrease in the top 0.8 m is likely due to uptake by evergreen *A. tridentata* and sparse shallow rooted active bunchgrasses. By June, the profiles had reversed with the burned north section being considerably wetter than the south unburned section with the leading edge of the wetting front persisting at depth. By July, the difference between the burned and unburned sections was much smaller, although the burned section was still wetter.

Perhaps the most striking observation is that despite the removal of plants from the north section, the soil water content was depleted to an amount almost identical to the unburned section. Owing to the relatively low ground cover on the recovering burnt section and the relatively small plants, it is unlikely that this much water was removed by transpiration. Thus, evaporation may have been the dominant mechanism. If due entirely to evaporation, the evaporative depth appears to extend much deeper than the top few centimeters that is typically assumed in uncoupled models for predicting water-balance processes. An alternative explanation is higher than expected transpiration on the burned area. While there was relatively little leaf area in the burned area compared with the unburned area, it is possible that root zones were larger and that transpiration rates are relatively high given the strong vapor potential gradient. This would result in a much higher draw-down than on a truly bare soil.

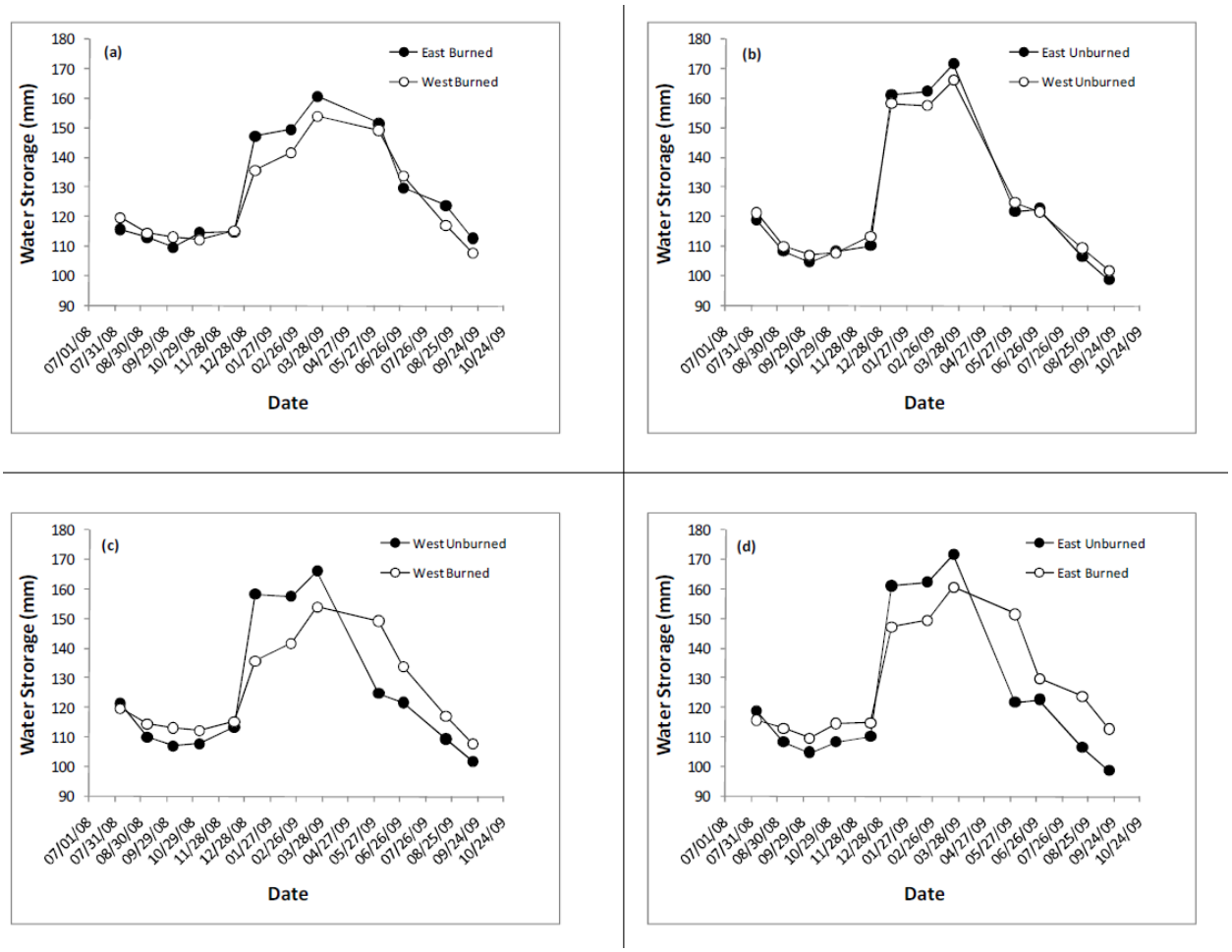

Figure N.4. Post-fire average water storage at the barrier, (a) north plots, (b) south plots, (c) northwest and southwest plots, and (d) northeast and southeast plots.

N.3.2.5 Fire Effects on Soil Nutrients

To assess the effects of fire on the soil chemical system, a number of geochemical properties were measured pre- and post-burn. The results are summarized in Table **N.1**. Soil pH is known to control the availability of most nutrients, and this is important in nutrient-limiting environments, like engineered ecosystems, where fertilizer is typically not applied. Within the first week of the fire, mean pH increased significantly but subsequently decreased over time. One year after the fire, pH has declined from the immediate post-burn value but remained significantly different from pre-burn conditions. Increases in pH can be attributed to ash accretion (Ahlgren and Ahlgren 1960; Smith 1970). The release of minerals as oxides or carbonates is usually an alkaline reaction (Debano 2000; Youngberg 1953). An increase in pH typically increases the cycling of various elements critical for plant growth. Although pH does not directly control N availability, it does affect soil microbial activity which can affect N availability. Acidic conditions (low pH) limits microbial activity and slows down N mineralization and nitrification whereas high pH can increases N loss by volatilization. The availability of P is strongly influenced by soil pH, reaching a maximum between pH values of 5.5 and 7.5. Basic soil conditions (pH > 7.5) result in an excess of Ca in the soil solution, which can also precipitate with phosphorus, rendering it unavailable.

The pre-burn organic matter (OM) content measured by the Walkley-Black method was 0.916% and increased to 1.256% and 1.374% after one week and one year, respectively. After one year, OM appears to have increased by about 50% from pre-burn conditions. The OM content is often used as an indication

of soil productivity and can be used to estimate the N release. The amount of available N released to the plant is about 28 to 56 kg of actual N per hectare per year for each percent of OM and depends on a number of factors including soil water content, temperature, and length of growing season. The pre-burn OM is equivalent to 26 to 51 kg of nitrogen per hectare per year compared to 35 to 70 kg of N per hectare per year after one week and 38 to 77 kg of N per hectare per year after 1 year. These results are somewhat counter intuitive as heating the soil to temperatures between 220 and 460 oC is known to destroy organic matter to depths of up to 80 mm. There is no physical explanation of the apparent increase in OM by the Walkley-Black method. However, OM determined by loss on ignition showed an 8% decrease over the same period. Decrease in OM can alter the CEC, however, as shown in Table **N**.**1**, CEC did not show any statistically significant changes between pre- and post-burn conditions.

Electrical conductivity measured on 1:1 extracts, EC1:1, showed a significant increase from 0.189 mmho/cm to 0.493 mmho/cm within the first week but had decreased to 0.261 mmho/cm one year later. Electrical conductivity of the soil is a measure of the amount of soluble salts present and hence the salinity. The tendency of fire to volatilize nutrients, increase soil concentrations of mineral elements, and reduce available moisture is consistent with the observed increase in EC1:1. In fact, soil elemental analyses indicate that concentrations of major nutrients increased following the fire. While this could potentially result in a short-term increase in nutrient availability, it also results in an increase in salinity, which could have detrimental effects on establishment of vegetation. EC1:1 alone, however, is insufficient to assess the effects of salinity on plant growth because the salt concentration at the root surface can be much greater than in the bulk soil. The saturated paste value, ECe, is a better measure and can be estimated from EC1:1 as ECe = 2.2 EC1:1. The estimated ECe before the fire was 0.416 dS/m. The estimated ECe one week after the fire was 1.085 dS/m, compared to 0.574 dS/m one year after the fire. Soils with ECe values in the range 0 to 2 dS/m are considered non-saline and are not expected to have any effect on plant growth.

The responses of individual nutrients to fire are different. Furthermore, each nutrient has an inherent temperature threshold where volatilization occurs (Debano 2000; Raison 1979). These thresholds can be divided into three general nutrient categories: sensitive, moderately sensitive, and relatively insensitive. Nitrogen (Hosking 1938) and S (Tiedemann 1987) are considered sensitive because they have thresholds as low as 200 to 375°C, respectively. Potassium (K) and P are moderately sensitive, having threshold temperatures of 774 °C (Raison 1979). Magnesium (Mg), Ca, and Mn are relatively insensitive, with high threshold temperatures of 1,107 °C, 1,484 °C, and 1,962 °C, respectively. Because the threshold temperatures of N, P, and K are lower than the flaming temperatures of woody fuels (100 °C) and, except for P, lower than glowing combustion temperatures (650 °C), these nutrients are readily volatilized from soil organic matter during combustion. Thus, significant changes in the soil concentration of N, P, and K can be expected.

On a plot-by-plot basis, the responses of N to the fire varied with different fuel load and soil temperature. Post-burn NH4-N concentration increased from 4.050 mg/kg to 15.511 mg/kg, a 282% increase after one week but subsequently decreased to 10.47 mg/kg after one year. Concentrations of NH4-N can increase, decrease, or remain unchanged, depending on fire severity and duration. Increases in NH4-N immediately following the fire appear to be related to the soil temperature reached. Debano (1981) suggested that most of the soil N is volatilized by high-severity fires, particularly on or near the surface with only small amounts being transferred downward through the soil. Conversely, large amounts of NH4-N are typically found in ash and underlying soil after low-severity fires. Heat can intensify physiochemical processes including the decomposition of nitrogen-containing organic matter and the release of ammonia from soil minerals (Arefyeva and Kolesnikov 1964). Ammonia loss peaks at 250 to 300oC as a result of volatilization, which explains why NH4-N increased while organic N decreased (Raison 1979). Nonetheless, increases in the soil NH4 + pool is appears to have been only temporary and has shown a gradual decrease since reaching 10.47 mg/kg one year after the fire. This is consistent with observations

of Wan et al. (2001) who reported a gradual decrease to pre-fire levels after about 1 year. The NO3-N also showed a significant increase following the fire (Table **N**.**1**). The mean concentration of NO3-N after one week increased from 3.6 mg/kg to 5.206 mg/kg and to 16.72 mg/kg after one year, an increase of over 300%. Comparatively small increases (24%) have been reported in the soil NO3−N pool immediately after a fire with a continued increase over time reaching a maximum of approximately three times the pre-fire level within 0.5 to 1 years after fire, followed by a decline (Wan et al. 2001). Studies of prescribed fires show an increase in nitrogen for 2 or 3 months following the fire (Pyke 2002).

The mean pre-burn P concentration was 11.389 meq/100 g compared to a post-burn value of 26.03 meq/100 g at one week and 32.5 meq/100 g at one year after the fire. This represents a 124% increase in P after one week and a 185% increase after one year. Phosphorus is known to respond differently to elevated temperatures than N. As much as 60% of the total P is typically lost by non-particulate transfer when organic matter is totally combusted (Raison 1979). As a result, relatively large amounts of highly available P can be found in the ash and on the soil surface immediately following fire. However, this P can be quickly immobilized in insoluble compounds especially if soil is rich in Ca. While there have been numerous reports on the effects of fire on the availability of N and P, comparatively few studies discuss other nutrients like K, Ca, Na, and Mg. Table **N**.**1** shows that K increased by 58.6% immediately after the fire but subsequently declined to 326.6 meq/100 or 36% above pre-burn levels. Soil concentration of Mg increased by 91% after one week but had returned to pre-burn levels after 1 year. In contrast, Ca and Na remained statistically unchanged. These results are therefore consistent with published reports, which suggest that all of these cations may increase after fire (Christensen 1976; Raison 1979). Increases in soluble K in the litter and A horizon, or topsoil, have been reported when temperatures remain below 200°C whereas Ca, Fe, and Mn have been reported to decrease (Ohr and Bragg 1985). However, they also found that if the plot burned in consecutive years, then K, Cu, Fe, and Zn availability increased.

Table N.1. Effect of fire on soil nutrient status.

Variable	Sampling	Mean	Variance	t_{stat}	P(T≤t) Two-Tail	t_{crit} Two-Tail
pH	Pre-burn	8.036	0.046	-12.52	1.74E-14	2.03
	1 week	8.978	0.147	-1.25E+01	1.74E-14	2.03
	1 year	7.572	0.021	1.29E+01	6.94E-15	2.03
Organic Matter (%)	Pre-burn	0.916	0.053			
	1 week	1.256	0.105	-5.449	4.11E-06	2.03
	1 year	1.374	0.221	-5.622	2.43E-06	2.03
CEC (meq/100 g)	Pre-burn	10.323	0.0023	-0.3979	0.7025	2.36
	1 week	10.4	0.291	-0.3979	0.7025	2.36
	1 year	9.761	0.387	1.692	1.29E-01	2.31
Electrical Conductivity	Pre-burn	0.189	0.001			
(mmho/cm)	1 week	0.493	0.012	-1.59E+01	1.37E-17	2.03
	1 year	0.261	0.005	-6.18E+00	4.52E-07	2.03
Ammonium-N (mg/kg)	Pre-burn	4.05	9.693			
	1 week	15.511	20.559	-12.477	1.93E-14	2.03
	1 year	10.472	24.393	-7.358	1.32E-08	2.03
Nitrate-N (mg/kg)	Pre-burn	3.622	3.461			
	1 week	5.206	2.821	-3.464	0.001422	2.03

	1 year	16.719	71.939	-9.355	4.71E-11	2.03
P-Bicarbonate (meq/100 g)	Pre-burn	11.389	17.787			
	1 week	26.028	49.056	-9.844	1.28E-11	2.03
	1 year	32.528	108.542	-11.747	1.07E-13	2.03
K-Bicarbonate (meq/100g)	Pre-burn	239.75	4276.25	-7.589	6.75E-09	2.03
	1 week	26.028	49.056	-9.844	1.28E-11	2.03
	1 year	32.528	108.542	-11.747	1.07E-13	2.03
Calcium	Pre-burn	17.508	0.646			
	1 week	17.692	0.645	-0.935	0.356426	2.03
	1 year	16.253	0.787	7.448	1.02E-08	2.03
Magnesium	Pre-burn	1.409	0.027			
	1 week	2.686	9.328	-2.479	0.018127	2.03
	1 year	1.672	0.037	-6.275	3.36E-07	2.03
Sodium	Pre-burn	0.054	0.001			
	1 week	0.095	0.015	-1.953	0.058824	2.03
	1 year	0.081	0.001	-4.62	5.03E-05	2.03

N.3.2.6 Fire Effects on Ecological Properties

Ground Cover

Figure N.5 shows an aerial photograph of barrier on September 30, 2009, one year after the controlled burn. One year after the fire, as can be expected, bare ground is now higher in the burned section (76.6 ± 1.09 %) compared to the unburned section (53.8 ± 2.06%) of the barrier. The burned (north) section now has the same ground cover of grasses (3.51 ± 0.42 %) as the unburned (south) section (1.86 ± 0.18%). However, shrub cover in the burned section (1.46 ± 0.16%) is much lower than in the unburned section (30.3 ± 1.13%). Plant litter (dead leaves, twigs etc) is also now lower in the burned section (7.95 ± 0.52 %) compared to the unburned section (45.3 ± 1.7 %). Ground cover values at the prototype barrier are in sharp contrast to those observed at the two analogue sites at the McGee Ranch. Grass cover on the barrier is quite low when compared to the McGee Ranch old burn (58.9 ± 4.88 %) and unburned (23.1± 1.82 %) sites. Shrub cover in the McGee Ranch unburned area is lower (22 ± 2.57 %) than that in the unburned area on the barrier (30.3 ± 1.13 %). Forb cover is similar in the two burned areas, 24.7 ± 0.97 % at the barrier and 19.8± 2.19 % at the McGee Ranch old burn, than in the unburned barrier (0.4 ± 0.1 %) and unburned McGee Ranch (8.1± 1.4 %). There was no soil cryptogam on the burned half of the barrier, but low cover percentages were observed at the McGee Ranch burned area (6.79 ± 1.98 %) compared to those at the unburned barrier (28.3 ± 1.63 %) and unburned McGee Ranch (42.6 ± 3.57 %).

Figure N.5**.** South facing aerial view of the barrier on September 30, 2009 showing the burnt north and unburned south section 1 yr after the fire.

Table **N.2** identifies the plant species on the burned and unburned treatments of the barrier and at the two McGee Ranch analog sites. Figure N.6 compares the total number of species on the barrier surface from 1995 through 2009. Species richness on the barrier has dropped from 35 in 1997 to 10 in 2008 just before the fire. Nearly 1 year after the fire, species richness increased to 15 in the unburned half of the surface and increased markedly to 24 species on the burned half of the surface. Species richness at the two analog sites is essentially the same as on the unburned half of the barrier. Annual and biennial species are 32% of

the flora in the long-term undisturbed community at the McGee Ranch, 44% in the McGee Ranch old burn, 53% in the unburned barrier surface, and increasing to 58% on the burned half of the barrier. The dominance of *A. tridentata* on the unburned half of the barrier surface may contribute to continued reductions in species richness on the surface. Similar species richness was found at the unburned McGee Ranch analog site that is also dominated by *A. tridentata*. This is in contrast to the similar richness at the burned McGee Ranch analog site, even though *A. tridentata* has very low cover. Factors other than dominance by *A. tridentata* are determinants of species richness. It is likely that the increase in species richness after fire is a short-lived consequence of fire given that the old burn at McGee Ranch had essentially the same species richness.

Table N.2. Plant species observed in 2009 on the burned and unburned sections of the barrier plus at two McGee Ranch analog sites

Family	Species	Barrier Burn	Barrier Unburned	McGee Old Burn	McGee Unburned
Asteraceae	*Achillea millifolium*	X			
	Artemisia tridentate	X	X	X	X
	Balsamorhiza careyana			X	
	Centaurea diffusa	X	X	X	
	Chrysothamnus viscidiflorus	X	X		
	Crepis atribarba				X
	Ericameria nauseosa	X	X	X	
	Erigeron filifolius				X
	Erigeron piperianus				X
	Erigeron poliospermus				X
	Helianthus cusickii			X	X
	Lactuca serriola	X			
	Machaeranthera canescens	X	X	X	X
	Stephanomeria paniculata	X			
	Tragopogon dubius	X		X	
Boraginaceae	*Amsinckia lycopsoides*	X	X		
Brassicaceae	*Descurainia pinnata*	X		X	X
	Sisymbrium altissimum	X	X	X	
Chenopodiaceae	*Chenopodium leptophyllum*	X			
	Grayia spinosa				X
	Salsola kali	X	X	X	X
Fabaceae	*Astragalus caricinus*	X			
	Melilotus officinalis	X			
Geraniaceae	*Erodium cicutarium*	X	X		
Malvaceae	*Sphaeralcea munroana*			X	X

Table (contd)

Family	Species	Barrier Burn	Barrier Unburned	McGee Old Burn	McGee Unburned
Poaceae	*Achnatherum hymenoides*			X	X
	Bromus tectorum	X	X	X	X
	Elymus elymoides			X	X
	Elymus wawawaiensis	X	X		
	Poa ampla	X	X		
	Poa bulbosa	X	X		
	Poa secunda	X	X	X	X
	Vulpia microstachys	X	X		X
Polemoniaceae	*Phlox longifolia*			X	
Verbenaceae	*Verbena bracteata*	X			
	Total Number of Species Present	24	15	16	16

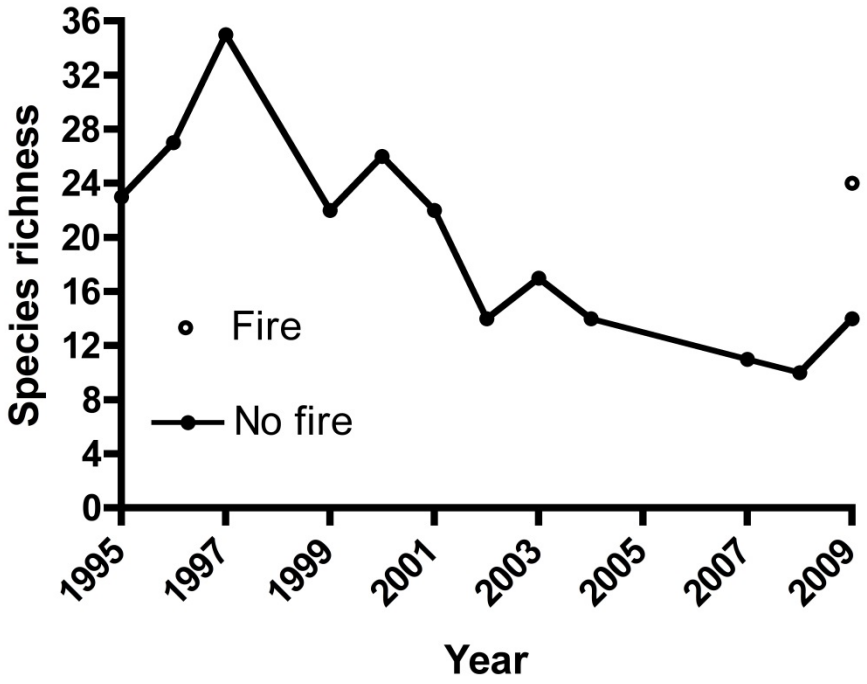

Figure N.6**.** Temporal variation in the number of species on the Prototype Hanford Barrier from inception through September 2009, 1 year after the fire.

Shrub Density

Post-burn shrub density varied among the four study sites. After one year, the density (plants per m2) of *A. tridentata* was very low on the burned section of the barrier (0.0146 ± 0.0054) and essentially equivalent to that at the McGee Ranch old burn site (0.0147 ± 0.0031). The density was significantly higher on the unburned barrier (0.77 ± 0.0121) than at the McGee Ranch unburned analog site (0.437 ± 0.0331). *E.*

nauseosa established in significant, but low numbers (0.00386 ± 0.00202) after the fire on the barrier surface. This and other shrubs were present only in low numbers.

Seed Bank Assessment

After the burn on the barrier surface, a significant number of shrubs germinated from the seed bank and/or from seed that arrived at the site. However, there was no difference in the number of species emerging from the seed bank before and after the fire. The most interesting observation is the emergence of *A. tridentata* from the seed bank after the fire, which suggests that this dominant shrub will return after fire. This observation is in contrast to the general belief that *A. tridentata* does not recover after a fire. There was no evidence of re-sprouting after the fire. There is evidence of *A. tridentata* in the seed bank, so it is likely that those found on the burned barrier surface are from the seed bank. *A. tridentata* seed is not wind-borne. In contrast, while 88% of the new shrubs on the burned barrier surface were *E. nauseosa*, none were found in the seed bank. If they were in the seed bank, they may not have had the appropriate conditions to germinate. It is possible that these new recruits arrived from nearby plants that released wind-borne seed after the fire. While there are few *E. nauseosa* plants in the adjacent unburned barrier surface, there are numerous shrubs on the adjacent side slopes that can be the source of the new recruits on the burned surface. There were no significant differences among the barrier plots before and after the fire and the unburned McGee Ranch site. Both *S. kali* and *S. altissimum* were significantly greater on the old burn McGee Ranch site than at the unburned McGee Ranch site while there were no seedlings observed from any of the barrier samples. Both species were found growing on the barrier surface after the fire, suggesting that viable seed is either in the seed bank, and they did not germinate from the samples in the greenhouse, or the seed arrived on the surface after the fire from surrounding seed sources. Both species are recognized as responding favorably to fire. *Verbena bracteata* seedlings were found in the seed bank of samples before and after the fire. None were found on the side slope or at the two McGee Ranch sites. When emerged seedlings of all species were combined in each experimental unit for the high (n = 17) and low (n = 19) fuel load areas on the barrier surface, there was no significant (p = 0.86) effect of fire intensity on seedling density.

Leaf Area Index and Plant Water Status

Post-burn measurements of LAI show that the mean LAI on the unburned half of the barrier (1.13 ± 0.087) was not significantly different from mean LAI in the McGee unburned plant community (0.692 ± 0.129). The mean LAI in the burned half of the barrier (0.254 ± 0.02) was not significantly different from the mean LAI in the McGee old burn plant community (0.103 ± 0.0.031). Values in the two burned areas were significantly lower than those in the two unburned areas. The xylem pressure potential was measured on plants in the burned and unburned conditions. Measurements were made just before dawn to assess maximal xylem pressure potential. There was no significant (p = 0.570) effect of species on xylem pressure potential for early morning readings in the burned condition. These values were then combined to test the effect of location on xylem pressure potential in the burned condition. Location had a significant (p = 0.0045) effect on xylem pressure potential. Plants on the west third of the surface had significantly greater xylem pressure (-17.5 ± 0.89 bars, n = 12) than those on the middle and east thirds of the surface (-26.3 ± 2.49 bars, n = 13). This observation suggests that similar variation in the soil water potential may exist on the burned half of the barrier.

Biological Activity and Soil Carbon Dioxide Flux

Soil respiration rates in the burned and unburned conditions were compared when surface soils were dry and when surface soils had been wetted by rain to an average depth of 33.8 ± 1.1 mm. When the upper soil profile was dry, soil respiration rates (μmol CO2 m^{-2} s^{-1}) were significantly (p = 0.0205) greater in the burned treatment (0.134 ± 0.018) than in the unburned treatment (0.074 ± 0.013). After wetting the upper soil profile, there was no significant (p = 0.3394) difference between the treatments. Given that

observations were taken from the same location in wet and dry conditions, dry rates were subtracted from wet rates and compared between the treatments. These differences were not significantly ($p = 0.1936$) different. Thus, observations in the treatments were combined to compare wet and dry rates. Soil respiration rates were significantly ($p < 0.0001$, $n = 12$) greater in the wet surface soils (0.834 ± 0.0725) than in the dry surface soils (0.104 ± 0.0137). The higher respiration under dry conditions in the burned area compared with the unburned area is likely a result of the wetter soil profile. The wetter soil profile, as evidenced by plants with higher water potential values, yields more active plants that have higher root-respiration rates. It is likely that soil respiration is primarily root respiration given that the soil surface was very dry, limiting surface microbial activity. When the surface soils were wetted, it is likely that a significant component of the respiration was microbial. Given that soil organic matter increased or decreased depending on the assessment method after the fire, it is possible that there was enough organic carbon in the burned soil to support respiration rates as high as in the unburned soil.

N.4 Summary and Conclusions

A critical unknown in long-term engineered surface barrier use for waste site remediation is the post-fire hydrologic function where institutional controls are intact, but there are no resources to implement maintenance activities, such as re-planting of vegetation. A study was recently conducted at the Hanford Site to gain insight into the effects of wildfire on the function of an engineered barrier. The north half of the barrier was amended with imported fuel with the west side getting the largest load and the east side getting the lowest fuel load. The barrier was ignited along the perimeter and the surface was completely burnt in about 7 minutes with flame heights exceeding 9 m (30 ft), and temperatures ranging from 250 °C (482 °F) at 1.5 cm (0.6 in.) below the surface to over 700 °C (1292 °F) at 1 m (3.3 ft) above the surface. The relative fire intensity was consistent with the fuel distribution.

One week after the fire, non-destructive and destructive measurements were made to quantify changes in soil hydrophysical and geochemical properties, including nutrient status. Post-fire analysis of soil properties shows significant decreases in wettability, hydraulic conductivity, air-entry pressure, organic matter, and porosity relative to pre-fire conditions, whereas dry bulk density increased. Decreases in hydraulic conductivity and wettability, one week after the fire, are implicated in a surface runoff event that occurred in January 2009, the first runoff event in 13 years. There was a significant increase in macro-nutrients, pH, and electrical conductivity. Measurements repeated after one year show that hydrophobicity has returned to pre-burn levels with only 16% of the samples still showing signs of decreased wettability. Over the same period, hydraulic conductivity and air-entry pressure returned to preburn levels at one third of the locations but remained identical to values recorded immediately after the fire at the other two thirds. Soil nutrients, pH, and electrical conductivity remain elevated. Species composition on the burned surface changed markedly from prior years relative to the unburned surface and two analogue sites. There was an increase in the proportion of annuals and biennials, which is characteristic of burned surfaces that have become dominated by ruderal species. However, it anticipated that native perennial species will come to dominate the burned area again as *A. tridentata* and *E. nauseosa* have started to re-establish. Observations at the old burn analogue site suggests that *A. tridentata* will produce an abundance of seed as long as competition remains low, and there is access to stored water to support the high seed production. Greenhouse seedling emergence tests conducted to assess the seed bank at the barrier and analogues sites show no difference in the number of species emerging from pre- and post-burn soils. However, there were fewer species emerging from the side-slope seed bank whereas more emerged from two analogue sites. Xylem pressure potentials were considerably higher on the burned half of the barrier in September 2009, suggesting that not all the water in the soil profile may be removed before the fall rains begin. Greater soil respiration rates under dry surface conditions in the burned area compared with the unburned area observations support the supposition that plants experiencing wetter soil

profiles will show more active root respiration. Continued soil respiration observations may be a good surrogate of root activity as the vegetation recovers.

There were significant differences in the rate of accumulation and loss of soil moisture on the burned and unburned sections. On the burned section, water storage was higher during the fall, increased more slowly with the onset of winter precipitation owing to higher evaporation, and decreased more slowly in the spring owing to lower evapotranspiration. The result was significantly higher water storage on the burned section at the end October 2009, which translates into a lower storage capacity prior to the onset of winter precipitation. Nonetheless, barrier effectiveness has not been compromised as the storage capacity is some 600 mm. The results of this study are contributing to a better understanding of barrier performance after major disturbances in a post-institutional control environment. Such an understanding is needed to enhance stakeholder acceptance regarding the long-term efficacy of engineered barriers.

References

Ahlgren, IF and CE Ahlgren. 1960. "Ecological Effects of Forest Fires," *Bot. Rev.*, 26:483-533.

Arefyeva, ZN and BP Kolesnikov. 1964. "Dynamics of Ammonia and Nitrate Nitrogen in Forest Soils of the Transurals at High and Low Temperatures," *Soviet Soil Science*, 3:246-260.

Christensen, NL. 1976. "Short-Term Effects of Mowing and Burning on Soil Nutrients in Big Meadows, Shenandoah National Park," *Journal of Range Management*, 29:208-509.

Daubenmire, R. 1959. "A Canopy-Coverage Method of Vegetational Analysis," *Northwest Science*, 33:43-64.

Debano, LF. 1981. *Water Repellent Soils: A State of the Art*, General Technical Report PSW-46, Pacific Southwest Forest and Range Exp. Sta., U.S. Department of Agriculture Forest Service, Berkeley, California.

Debano, LF. 2000. "Water Repellency in Soils: A Historical Overview," *Journal of Hydrology*, 231/232:4-32.

Dekker, LW and CJ Ritsema. 1994. "How Water Moves in a Water-Repellent Sandy Soil: I. Potential and Actual Water Repellency," *Water Resources Research*, 30:2507-2517.

Doerr, SH and A Cerdà. 2005. "Fire Effects on Soil System Functioning: New Insights and Future Challenges," *International Journal of Wildland Fire*, 14(4):339-342.

Dyrness, CT. 1976. *Effect of Wildfire on Soil Wettability in the High Cascades of Oregon*, USDA Forest Service Res. Pap. PNW-202, USDA Forest Service, Corvallis, OR.

Feis-Fire Effects Information Service. *Fire Effects Information. U.S. Department of Agriculture Forest Service*. Accessed on November, 2009 at http://www.fs.fed.us/database/feis/plants/index.html.

Gavlak, R, D Horneck, RO Miller, and J Kotuby-Amacher. 2003. *Soil, Plant and Water Reference Methods for the Western Region*, WCC 103 publication WREP 125, 2nd edition, Oregon State University, Corvallis, OR.

Hosking, JS. 1938. "The Ignition at Low Temperatures of the Organic Matter in Soils," *Journal of Agricultural Science* 38(3):393-400.

Huffman, EL, LH Macdonald, and JD Stednick. 2001. "Strength and Persistence of Fire-Induced Soil Hydrophobicity under Ponderosa and Lodgepole Pine, Colorado Front Range," *Hydrological Processes*, 15:2877-2892.

Neary, DG, CC Klopatek, LF Debano, and PF Ffolliott. 1999. "Fire Effects on Belowground Sustainability: A Review and Synthesis," *Forest Ecology and Management*, 122:51-71.

Ohr, KM and TB Bragg. 1985. "Effects of Fire on Nutrient and Energy Concentration of Five Prairie Grass Species," *Prairie Nat.*, 17:113-126.

Powers, RF, DH Alban, RE Miller, AE Tiarks, CG Wells, PE Avers, RG Cline, RO Fitzgerald, and NS Loftus. 1998. Sustaining Site Productivity in North American Forests: Problems and Prospects. In SA Gessel, et al. *Proceedings of the 7th North American Forest Soils Conference,* Vancouver, British Columbia.

Pyke, DA. 2002. *Born of Fire-Restoring Sagebrush Steppe,* USGS FS-126-02, Science Center, Corvallis, OR.

Raison, RJ. 1979. "Modifications of the Soil Environment by Vegetation Fires, with Particular Reference to Nitrogen Transformations: A Review," *Plant and Soil* 51:73-108.

Reynolds, WD. 1993. "Unsaturated Hydraulic Conductivity: Field Measurement." In *Soil Sampling and Methods of Analysis*, ed. MR Carter, Canadian Society of Soil Science, pp. 633-644. Lewis Publishers, Boca Raton, Florida.

Reynolds, WD and DE Elrick. 1985. "In Situ Measurement of Field-Saturated Hydraulic Conductivity, Sorptivity and the A-Parameter Using the Guelph Permeameter," *Soil Science*, 140(4):292-302.

Robichaud, PR and SM Miller. 2000. "Spatial Simulations to Describe Duff Consumption of Prescribed Fire," *International Journal of Wildland Fire*, 9:17-143.

Smith, DW. 1970. "Concentrations of Soil Nutrients before and after Fire," *Can. J. Soil Sci.*, 50:17-29.

Tiedemann, AR. 1987. Nutrient Accumulations in Pinyon-Juniper Ecosystems—Managing for Future Site Productivity. In RL Everett *Proceedings of Proceedings—Pinyon-Juniper Conference, compiler. USDA-FS, Intermountain. Gen. Tech. Rep. INT-215,* Inter. For. and Range Res. Sta., Ogden, Utah.

Wallis, MG and DJ Horne. 1992. "Soil Water Repellency," *Advances in Soil Science*, 20:91-146.

Wan, SD, D Hui, and Y Luo. 2001. "Fire Effects on Nitrogen Pools and Dynamics in Terrestrial Ecosystems: A Meta-Analysis," *Ecological Applications*, 11:1349-1365.

Ward, AL, GT Berlin, JW Cammann, KD Leary, and SO Link. 2008. *Test Plan to Assess Fire Effects on the Function of an Engineered Surface Barrier*, PNNL-17859, Pacific Northwest National Laboratory, Richland, Washington.

Ward, AL, GW Gee, and SO Link. 1997. *Hanford Prototype-Barrier Status Report: FY 1997*, PNNL--11789, Pacific Northwest National Laboratory, Richland, Washington. http://www.osti.gov/energycitations/servlets/purl/569021-3NLXw0/webviewable/.

Ward, AL, SO Link, CE Strickland, KE Draper, and RE Clayton. 2007. *200-BP-1 Prototype Hanford Barrier Annual Monitoring Report for Fiscal Years 2005 through 2007*, PNNL-17176, Pacific Northwest National Laboratory, Richland, Washington. http://www.osti.gov/energycitations/servlets/purl/927493-58wmF0/.

Youngberg, CT. 1953. "Slash Burning and Soil Organic Matter Maintenance," *J. Forest.* , 51:202-203.

Appendix O

Aerial Photographs of the Prototype Hanford Barrier

Z. Fred Zhang

Pacific Northwest National Laboratory
Richland, Washington

Contents

List of Figures

Abstract

The conditions of the Prototype Hanford Barrier (PHB) above the ground surface were recorded periodically (roughly annually or once every 2 or 3 years) by aerial photos. This appendix compiles the aerial photos of the PHB during the monitoring period from 1994 to 2015.

This appendix compiles the aerial photos of the Prototype Hanford Barrier (PHB) during the monitoring period from 1994 to 2015.

O.1 Methodology

The conditions of the PHB above the ground surface were recorded periodically (roughly annually or once every 2 or 3 years) by aerial photos on the following dates:

- 08/09/1994
- 08/09/1995
- 09/14/1996
- 09/18/1997
- 06/02/1999
- 09/17/2002
- 01/03/2003
- 09/09/2005
- 09/20/2008
- 09/30/2009
- 08/18/2011
- 09/13/2012

Additionally, aerial photos of the PHB on June 8, 2013, and May 6, 2015, were obtained from Google Earth (Google. Inc.). The altitude and longitude coordinates of the PHB are 46°34'01.50" N and 119°32'28.44" W, respectively. The most recent view available at Google Maps (https://www.google.com/maps) can be seen using the coordinates of (46.567006,-119.541256) m.

O.2 Results

The following photos provide visual data to complement other monitoring data and may be useful for further image analysis. One image was selected for each of the above dates (Figure O.1 through Figure O.14). These images are original except those from 2003 and 2005, which were stitched together from three or four separate images using Photoshop® (Adobe Systems Inc., San Jose, CA).

These images show the topology and the spatial distribution of the vegetation of the PHB and surrounding area.

Figure O.1. The Prototype Hanford Barrier on August 9, 1994 (southwest-facing view). The two side-slope configurations and drainage monitoring system are to the north.

Figure O.2. The Prototype Hanford Barrier on August 9, 1995 (southwest-facing view). The green vegetation seen in the photo is non-native Russian thistle (tumbleweeds), not the planted native sagebrush and rabbitbrush, which were still seedlings and were much smaller than the Russian thistle, and cannot be seen in the image. The Russian thistle might come with the imported silt loam.

Figure O.3. The Prototype Hanford Barrier on September 14, 1996 (southwest-facing view). The Russian thistle (tumbleweeds) had died and been blown off the barrier surface by wind.

Figure O.4. The Prototype Hanford Barrier on September 18, 1997 (southwest-facing view). The planted native species (sagebrush and rabbitbrush) were developing in rows.

Figure O.5. The Prototype Hanford Barrier on June 2, 1999 (southwest-facing view).

Figure O.6. The Prototype Hanford Barrier on September 17, 2002 (southwest-facing view).

Figure O.7. The Prototype Hanford Barrier on January 3, 2003 (southwest-facing view).

Figure O.8. The Prototype Hanford Barrier on September 9, 2005 (south-facing view).

Figure O.9. The Prototype Hanford Barrier on September 20, 2008, 1 week prior to the controlled burn (south-facing view).

Figure O.10. The Prototype Hanford Barrier on September 30, 2009, 1 year after the controlled burn (south-facing view). The north half was still mostly free of vegetation.

Figure O.11. The Prototype Hanford Barrier on August 18, 2011 (south-facing view).

Figure O.12. The Prototype Hanford Barrier on September 13, 2012 (south-facing view).

Figure O.13. The Prototype Hanford Barrier on June 8, 2013 (south-facing view) (Source: Google Earth).

Figure O.14. The Prototype Hanford Barrier on May 6, 2015 (south-facing view) (Source: Google Earth).

Appendix P

Prototype Hanford Barrier: Elements Worked, Lessons Learned and Recommendations

Z. Fred Zhang

Pacific Northwest National Laboratory
Richland, Washington

Content

Abstract

The design and performance of a surface barrier at Hanford is supported by the 19-year field-scale performance data from the Prototype Hanford Barrier (PHB). The success elements, lessons learned during the monitoring of the PHB and the recommendations are helpful for improving barrier design and monitoring, and for future deployment.

The success elements are

- Comprehensive and thorough pre-barrier investigation were carried out
- The pre-PHB tests and PHB demonstration were well documented
- The information about the PHB was well communicated
- PHB deployment, revegetation, three-year treatability test, and the controlled burn test were successful
- The drainage monitoring system was well-designed and function well
- The neutron probe worked very well
- The mechanical stability of PHB was thoroughly addressed

Lessons learned on barrier design/construction are as follows:

- Curbs on the asphalt layer should be aligned with the side slope boundaries.
- The toe of the side slopes needs to be properly protected.

Lessons learned on barrier monitoring are as follows:

- The capacitance probe has a low sensitivity; load cells underestimated precipitation; the runoff system did not have sufficient sensitivity.
  The Fiberglass blocks had a large uncertainty and the time domain reflectometry system could not provide accurate results because of noise.
- The vent tubes for the pan lysimeter were too thin.
- The locations of some sensors could not be identified.
- The automated data logging may not always be better than manual logging.
- The batteries at barrier surface should be replaced regularly.

Recommendations are as follows:

- Optimize and adapt the design of the PHB to the conditions of different sites.
- Evaluate new monitoring capabilities and sensors.
- Demonstrate and test barrier evaluation tools.
- Investigate of affecting extent of a surface barrier and evaluate other flow mechanisms across the capillary break.
- Evaluate the integration of a surface barrier with other remediation technologies.

The design, construction, and operation of the Prototype Hanford Barrier (PHB) for 19 years present a unique opportunity to improve the design and use of barriers as a remediation technology.

Conducting an experiment spanning 19 years is challenging for several reasons. First, personnel change. Whether it is project managers, scientists, technicians, staff at the Depart of Energy (DOE), or regulators, changes in personnel can create the conditions for programmatic and technical knowledge to be lost or compromised. Second, funding levels change. DOE budgets are reviewed annually and prioritized according to high-priority concerns. Monitoring plans start out based on expectations of funding, but they have to be adjusted to each year's fiscal reality. Lastly, equipment and sensors change. The causes include aging, corrosion, clogging, physical adjustment, biotic interference, human action, weather impacts, or some combination thereof.

Although the challenges described above existed throughout the 19 years, a core of the monitoring program for the PHB survived. In this Section, we review the successful elements, identify lessons learned from what did not work, and provide recommendation to guide deployment efforts.

P.1 Successful Elements

P.1.1 Management

Comprehensive and thorough pre-barrier investigation were carried out
Before the construction of PHB, multi-year barrier development program was conducted to develop, test, and evaluate the effectiveness of various barrier designs. A team of engineers and scientists directed the barrier development effort. The barrier program was organized to develop and evaluate the technology for permanent, long-term containment of near-surface radioactive waste.

The pre-PHB tests and PHB demonstration were well documented
As listed in Appendix O, over 150 reports or journal publications were published to document the data, compare expectations, and identify needs. Preparing the report was also important because it encouraged the project to analyze and review the data rather than defer to reduce costs.

The information about the PHB was well communicated
Conference presentations, journal articles, and site tours exposed the data to scientific scrutiny and provided transparency to the public.

P.1.2 Field Barrier Demonstration

PHB deployment was successful
The PHB construction and monitoring system installation were deployed as planned.

The revegetation was successful
Perennial shrubs were established by collecting seeds, growing seedlings, and planting them on the surface of the barrier. Perennial grasses were established by hydroseeding the surface and surrounding slopes. They formed normal vegetation at the barrier surface.

The three-year treatability test was successful
The irrigation system provided a successful test of barrier performance during extreme wet events.

The controlled burn test was successful
It provided a successful test of barrier performance during the complete loss of vegetation.

The drainage monitoring system was well-designed and functioned well
The drainage plots and drainage vaults worked consistently and provided a nearly continuous dataset. The large size of the plots helped to minimize concerns about spatial variability.

The neutron probe worked very well
The neutron probe worked consistently and provided a nearly continuous high-quality dataset. These data were critical to understand the hydrological processes and barrier storage capability.

The mechanical stability of PHB was thoroughly addressed
The 2 settlement markers, 338 elevation markers, and 15 creep gauges were surveyed nearly annually and provided nearly continuous high-quality dataset to address the mechanical stability of PHB.

P.2 Lessons Learned

P.2.1 Barrier Design and Construction

Curbs on the asphalt layer should be aligned with the side slope boundaries
Each of the drainage plots for the side slopes included the 4-m-wide road and about 1 m of the silt loam boundary. Hence, the drainage measured was not solely for the side slopes. The drainage contribution through the roads and silt loam boundary could not be distinguished from that through the side slopes.

The toe of the side slopes needs to be properly protected
In May 2004, after severe thunderstorms, runoff water from the elevated BY-BX Tank Farm surface (southeast of the PHB) flowed down-gradient to the region between the tank farms and the PHB, eroding a channel about 1.1 m deep at the base of the east side of barrier side slope. The channel extended into the sandy structural fill layer of the riprap toe slope.

The surface barrier needs to mimic stable natural landforms
The PHB has a rectangular shape and the slopes have linear and constant gradient. Hills and mounts tend to be curvilinear and the natural stable hillslopes often has a convex shape in the upper portion and a concave shape near the toe. Landform grading concept needs to be considered in the design of surface barriers to mimic stable natural landforms at the surround landscape.

P.2.2 Monitoring

The capacitance probe has a low sensitivity
The Troxler Sentry 200 capacitance probe was used only for one year and then its use was terminated partially because of its low insensitivity to high water content (Gee et al. 1995).

Load cells underestimated precipitation
The load cells generally underestimated the precipitation because of several problems.

1) Although the load cells measured the precipitation continuously, each of them reached a maximum value when the 20-L (equivalent to about 300 mm of precipitation) container for collecting the water was full, unless the water was dumped manually.

2) The system has the output resolution of 0.001 volts, which translates to about 22 g of water or about 0.3 mm of precipitation. Hence, any precipitation event of less than 3 mm could not be detected.
3) Although the system was designed to measure both liquid and solid water (i.e., snow) without being heated, it appeared that the load cells did not function well for measuring snow because the snow above the load cells tended to stick together with the snow in the surrounding area. Hence, the weight of snow could not be measured correctly.
4) When the vegetation was well developed, it might have some impacts on the local distribution of precipitation and hence the measurements of load cells.

The runoff system did not have sufficient sensitivity
The runoff system was designed to be activated if runoff occurred that caused the flow rate to exceed the minimum rate. The system appeared to not function well during the monitoring period, possibly because it was not sensitive enough to handle any very small runoff.

The Fiberglass blocks had a large uncertainty
The fiberglass blocks had large data instability and poor data representativeness.

The MP-917 time domain reflectometry (TDR) system could not provide accurate results because of noise
One purpose of the frequent (i.e., hourly) soil moisture monitoring using the TDR system was to understand the short-term behavior of the soil moisture. However, the noise in the hourly data or even in the daily average data prevented the data use for this purpose. The noise also limited the use of for water balance analysis.

The vent tubes for the pan lysimeter were too thin
In fiscal year 2012, when trying to reactivate the system associated with the pan lysimeter, it was found that the 1.65-mm-diameter stainless steel tubes for venting and pumping were plugged, and hence pumping of water could not be completed. Because the venting tube was so thin and very long (several tens of feet), attempts to repair it were unsuccessful.

The locations of some sensors could not be identified
The specific locations of the following sensors could not be identified:
- Heat dissipation units and temperature sensors installed in the runoff flume
- Fiberglass blocks below the AC layer

The automated data logging may not always be better than manual logging
Automated data collection systems provide high-frequency datasets that can be used to understand processes occurring within or below the barrier system. Additionally, automated systems offer the ability to reduce labor costs and to collect data at all times of the day and in all types of weather. The usually overlooked disadvantages of automated systems are the cost to set up and operate (e.g., power), the labor to monitor regularly, and the labor involved in the receipt, processing, and storage of very large amounts of data. Too often the expectation of reduced labor costs from automation leads to reduced oversight and deferred data processing in order to realize the expected savings in labor costs.

The batteries at barrier surface should be replaced regularly
The batteries may be less efficient after several (e.g., 4 or 5) years of service. To reduce the chance of data loss because of low battery voltage, all the batteries should be replaced after about 5 years.

P.3 Limitation of the Field Demonstration

Not everything relevant to the performance of the barrier has been assessed at the PHB demonstration for all kinds of reasons, e.g., the constraint of technology, time, and cost. The migration contaminant plume below the PHB has not been monitored and hence the reduction of plume movement has not been confirmed. Up to now (2015) the length of the demonstration time is only about 2% of the 1000-year design life of the cover. Large uncertainty exists to extrapolation the results to the future.

P.4 Recommendations for the PHB

The PHB has provided valuable dataset to understand its performance in a period of two decades. Despite of the excellent performance of the PHB, it is recommended that monitoring of PHB performance be continued for several reasons. The two-decade monitoring period accounts only 2% of the 1000-year design life. Extrapolation of the past performance for the future is subject to large uncertainty. Extreme events happen once in decades or a longer period of time. For example, since the inception of the PHB, snowmelt on frozen ground and a 0.3-m-deep badger hole were observed at the barrier surface. In May 2004, after severe thunderstorms, runoff water from the elevated BY-BX Tank Farm surface eroded a channel about 1.1 m deep at the base of the east side of barrier side slope. So far, the vegetation at the north section of the PHB is still dominated by the shallow-rooted grasses 7 years after the controlled burn, while the meteoric precipitation since then has been at the normal level. It is necessary to monitor the recovery of the vegetation and the performance of the PHB if higher precipitation or sever rainstorms happen. One of the most challenging issues for the acceptance of the barrier technology is to convince the stakeholders that the technology is effective and long-lasting. Although it is impractical to substantially extend the length of data record, continued monitoring is achievable and is the best can be done in order to address stakeholders' concerns about the surface barrier technology.

In addition, because of uncertainty in future climate, the hydrology at the PHB can vary substantially within a year and from year to year, requiring continued annual performance monitoring. Although the barrier structure and ecological conditions have been relatively stable over the monitoring period to date, changes in climate may impact the barrier ecology and structure, which could impact hydrologic performance. These changes make it necessary to periodically monitor the hydrology of the barrier, perform ecological surveys, monitor the elevation of the surface barrier, and assess the stability of the riprap side slopes. The monitoring systems with good performance are recommended for the necessary items for continued hydrological monitoring at the accepted frequency.

- It is necessary to monitor the hydrology. This will include
    - Neutron logging to monitor water contents and storage (manual logging, quarterly)
    - Drainage from 12 plots (automated logging, hourly)
    - Runoff (automated logging, hourly)
- It is necessary to monitor the elevation of the surface barrier, stability of the riprap side slope, and ecological survey once every 5 years.
- The above monitoring activities may be carried out if a severe unexpected event (e.g., fire, flooding, severe erosion, slope slide, death of a large portion of vegetation, considerable change in elevation in part or the whole barrier) occurs at the PHB.

Besides the regular monitoring, it is recommended to decommission the unused items and repair the monitoring systems. Currently the drainage monitoring system needs to be retrofitted for several reasons. A couple of the drainage vaults are leaking. Several dosing siphons do not function normally. Repairing the dosing siphons is challenging and costly because the bottom of them is buried in the concrete. The dosing siphons and pressure transducers do not have sufficient resolution for the drainage through the silt loam plots. A system of dual-tipping-bucket in tandem, with a smaller one above a large one, is recommended for drainage measurement.

P.5 Recommendations for Future Barrier Development

Although the monitoring results at the PHB have confirmed that the barrier has performed as or even better than designed, several recommendations are provided to guide and enhance future barrier design and deployment efforts.

P.5.1 Establish Institutional Control

Human activities are unpredictable without proper institutional control in place. Vandalism or stealing of the barrier materials may happen because the silt loam is a fertile soil suit for, e.g., farming and gardening and the riprap can be used for other purposes. Entertaining activities involving the use of large quantity of water at or near a barrier may compromise the barrier's protection capability.

P.5.2 Initiate Barrier Design for Various Sites

The PHB included two side slope designs and both designs provided adequate stability to the barrier. The fate of drainage through the side slopes needs to be addressed in the design. The drainage through the side slopes needs to be properly managed. It is recommended that methods be developed so that design of PHB can be optimized and adapted to the conditions of different sites. Based on the results of the PHB demonstration, it appears that a slightly thinner barrier may be sufficient for the wastes at Hanford. Protection of the toes of the side slopes need to be addressed in the design. Some specific questions need to be addressed in future barrier design include (but are not limited to):

- Which waste site is appropriate for the use of an ET cover?
- Can the thickness of the silt loam layer be reduced and how will this affect the performance?
- Can the thickness of the riprap penetration layer be reduced?
- Is a capillary break needed at all locations and under what conditions the capillary break is needed?
- When are rip-rap side slopes needed and at what locations are they un- necessary?
- How to protect the toe of the side slopes?

P.5.3 Evaluate New Monitoring Technologies

Sensor technology is continually evolving as are other aspects critical to successful monitoring, including components to be monitored, monitoring locations and frequency, and the layout of monitoring sensors. We recommend that new monitoring capabilities and sensors be evaluated relative to the existing suite of sensors. Final selections can be based on factors such as performance, cost, and new capabilities.

Evaluate the remote sensing technology for long-term cost-effective monitoring of vegetation, elevation, and stability monitoring. The technology can be based on near ground (e.g., 50 to 150 feet) aerial over flights or satellite imagery. This technology is expected to be very efficient for monitoring spatially distributed sites.

P.5.4 Assess Future Performance of Barriers

The existing modeling technologies such as UNSAT-H (Fayer 2000) and HELP (Schroeder et al. 1994) are sufficiently robust and qualified to be used for evaluations of simple surface barrier deployments above low-risk vadose zone contamination. For complex deployments above high-risk vadose zone contamination areas that receive remediation treatment (e.g., desiccation), more robust software tools are necessary. The STOMP software (specifically, STOMP-WAE-B and eSTOMP-WAE-B) (Ward et al. 2005; White et al. 2015) provide the simulation capabilities needed to address complex vadose zone problems and uncertainties. It is recommended that test barrier evaluation tools be demonstrated and tested. The worst-case scenarios of a variety of natural stresses (e.g., changes in climate, ecology, geomorphology, barrier properties) need to be investigated.

P.5.5 Investigate Barrier Affecting Depth and Other Flow Mechanisms

During the demonstration of the PHB, the affecting extent of a surface barrier was not examined. When the depth of a contaminant plume is very large, its migration may not be reduced by the deployment of a surface barrier because of there is a time delay before the barrier can take effect. In addition, the portion of the barrier near the edge is not as effective as the inside of the barrier. Some flow mechanisms are important under relatively dry conditions. For example, film flow can occur when capillary flow is negligible; fingering of flow may happen under some conditions; the shape of the fine/coarse interface can cause local lateral flow; and the intrusion of fine particles into the underlying coarser material will affect the capability of barrier storage. It is recommended to investigate the affecting extent of a surface barrier and evaluate other flow mechanisms across the capillary break.

P.5.6 Evaluate the Integration of Remediation Technologies

Depending on the site characteristics and depth of the waste, a surface barrier may not have a measureable impact on contaminant flux for years to decades following deployment because of water already present in the vadose zone. Therefore, we recommend integrating a surface barrier with other remediation technologies such as vadose zone desiccation.

References

Fayer, MJ. 2000. *UNSAT-H Version 3.0: Unsaturated Soil Water and Heat Flow Model: Theory, User Manual, and Examples*, PNNL-13249, Pacific Northwest National Laboratory, Richland, Washington.

Gee, GW, AL Ward, BG Gilmore, MW Ligotke, and SO Link. 1995. *Hanford Prototype-Barrier Status Report: FY 1995*, PNL-10872, Pacific Northwest National Laboratory, Richland, Washington.

Schroeder, PR, TS Dozier, PA Zappi, BM Mcenroe, JW Sjostrom, and RL Peyton. 1994. *The Hydrologic Evaluation of Landfill Performance (HELP) Model: Engineering Documentation for Version 3*, EPA/600/R-94/168b, U.S. Environmental Protection Agency, Risk Reduction Engineering Laboratory, Cincinnati, OH.

Ward, AL, EJ Freeman, MD White, and ZF Zhang. 2005. *STOMP: Subsurface Transport over Multiple Phases Version 1.0 Addendum: Sparse Vegetation Evapotranspiration Model for the Water-Air-Energy Operational Mode,* PNNL-15465.

White, MD, D Appriou, DH Bacon, Y Fang, VL Freedman, ML Rockhold, CM Ruprecht, GD Tartakovsky, SK White, and ZF Zhang. 2015. *STOMP/eSTOMP User Guide PNNL-SA-108766.* Accessed on March 27, 2015 at http://stomp.pnnl.gov/estomp_guide/eSTOMP_guide.stm (last updated March 2015).

Appendix Q

Prototype Hanford Barrier Publications

Pub No.	Citation	Pub Type[(a)]
1	Phillips SJ, MR Adams, TW Gilbert, CC Meinhardt, RM Mitchell, and WJ Waugh. 1985. *Engineered Barrier Test Facility Status Report: 1984*. RHO-WM-SR-3P, Rockwell Hanford Operations, Richland, Washington.	C
2	Phillips SJ, TW Gilbert, and MR Adams. 1985. *Preliminary Engineering Specifications for a Test Demonstration Multilayer Protective Barrier Cover System*. RHO-WM-EV-8 P, Rockwell Hanford Operations, Richland, Washington.	C
3	Fayer MJ, W Conbere, PR Heller, and GW Gee. 1985. *Model Assessment of Protective Barrier Designs*. PNL-5604, Pacific Northwest Laboratory, Richland, Washington.	PNNL
4	Myers DR. 1985. *Disposal Materials Study*. RHO-WP-EV-12P, Rockwell Hanford Operations, Richland, Washington.	C
5	Adams MR and MF Kaplan. 1986. Marker Development for Hanford Waste Site Disposal. In *Waste Management '86, Volume* 1, ed. RG Post, pp. 425–431. University of Arizona, College of Engineering and Mines, Tucson.	PROC
6	Phillips SJ and JN Hartley. 1986. Protective Barrier Systems for Final Disposal of Hanford Waste Sites. *In Waste Management '86, Volume 1,* ed. RG Post, pp. 433–437. University of Arizona, College of Engineering and Mines, Tucson.	PROC
7	Kaplan M F and MR Adams. 1986. Using the Past to Protect the Future: Marking Nuclear Waste Disposal Sites. *Archaeology* 39(5):51–54.	J
8	Adams MR and NR Wing. 1986. *Protective Barrier and Warning Marker System Development Plan*. RHO-RE-OL-35P, Rockwell Hanford Operations, Richland, Washington.	C
9	Fayer MJ. 1987. *Model Assessment of Protective Barrier Designs: Part II*. PNL-6297, Pacific Northwest Laboratory, Richland, Washington.	PNNL
10	Last GV, MA Glennon, MA Young, and GW Gee. 1987. *Protective Barrier Materials Analysis: Fine Soil Site Characterization.* PNL-6314, Pacific Northwest Laboratory, Richland, Washington.	PNNL
11	Gee GW. 1987. Preliminary Analysis of the Performance of the Protective Barrier and Marker System. In *Final Environmental Impact Statement – Disposal of Hanford Defense High-Level Transuranic and Tank Wastes, Appendix M*. DOE/EIS-0113, U.S. Department of Energy Richland, Operations Office, Richland, Washington.	DOE
12	Kirkham RR, GW Gee, and JL Downs. 1987. *Field Lysimeter Test Facility for Protective Barriers: Experimental Plan*. PNL-6351, Pacific Northwest Laboratory, Richland, Washington.	PNNL
13	Waugh WJ and SO Link. 1988. *Barrier Erosion Control Test Plan: Gravel Mulch, Vegetation, and Soil Water Interactions*. WHC-EP-0067, Westinghouse Hanford Company, Richland, Washington.	C
14	Wing NR, MD Campbell, JL Downs, GW Gee, RR Kirkham, and SJ Phillips. 1988. Protective Barrier Development: The Field Lysimeter Test Facility. In *Proceedings of the International Topical Meeting on Nuclear and Hazardous Waste Management Spectrum '88*, pp. 196–198. American Nuclear Society, Inc., La Grange Park, Illinois.	PROC
15	Phillips SJ, MS Ruben, and RR Kirkham. 1988. Engineered Surface Barriers for Waste Disposal Sites: Lysimeter Facility Design and Construction. In *DOE Model Conference Proceedings, Volume 4*, pp. 1227–1238. CONF-881054,	PROC

Pub No.	Citation	Pub Type[(a)]
	Martin Marietta, Oak Ridge, Tennessee.	
16	Ligotke MW. 1988. *Soil Erosion Rates from Mixed Soil and Gravel Surfaces in a Wind Tunnel: A Preliminary Report*. PNL-6677, Pacific Northwest Laboratory, Richland, Washington.	PNNL
17	Waugh WJ and MG Foley. 1988. *Protective Barrier Climate-Change Impacts: Technical Workshop Findings and Recommendations*. PNL-6615, Pacific Northwest Laboratory, Richland, Washington.	PNNL
18	Ligotke MW. 1989. *Surface Stability Test Plan for Protective Barriers*. PNL-6722, Pacific Northwest Laboratory, Richland, Washington.	PNNL
19	Gee GW, RR Kirkham, JL Downs, and MD Campbell. 1989. *The Field Lysimeter Test Facility (FLTF) at the Hanford Site: Installation and Initial Tests*. PNL-6810, Pacific Northwest Laboratory, Richland, Washington.	PNNL
20	Gee GW, MD Campbell, HD Freeman, and JF Cline. 1989. *Assessment of Cover Systems at the Grand Junction, Colorado, Uranium Mill Tailings Pile: 1987 Field Measurements*. PNL-6762, Pacific Northwest Laboratory, Richland, Washington.	PNNL
21	Petersen KL. 1989. The Long-Term Climate Change Assessment Task of the Hanford Site, Washington, Protective Barrier Development Program. In *In-Situ Remediation: Scientific Basis for Current and Future Technologies, Parts 1–2*, eds. GW Gee and NR Wing, pp. 633–648. Battelle Press, Columbus, Ohio.	C
22	Cadwell LL, LE Eberhardt, and MA Simmons. 1989. *Animal Intrusion Studies for Protective Barriers: Status Report for FY 1988*. PNL-6869, Pacific Northwest Laboratory, Richland, Washington.	PNNL
23	Freeman HD, GW Gee, and JF Relyea. 1989. *Field Study Plan for Alternate Barriers*. PNL-6840, Pacific Northwest Laboratory, Richland, Washington.	PNNL
24	Freeman HD and GW Gee. 1989. *Hanford Protective Barriers Program: Asphalt Barrier Studies – FY 1988*. PNL-6874, Pacific Northwest Laboratory, Richland, Washington.	PNNL
25	Waugh WJ. 1989. *Gravel Admix, Vegetation and Soil Water Interactions in Protective Barriers: Experimental Design, Construction and Initial Conditions*. PNL-6616, Pacific Northwest Laboratory, Richland, Washington.	PNNL
26	Freeman HD and GW Gee. 1989. *Hanford Protective Barriers Program: Status of Asphalt Barrier Study – FY 1989*. PNL-7513, Pacific Northwest Laboratory, Richland, Washington.	PNNL
27	Link SO and WJ Waugh. 1989. *Evapotranspiration Studies for Protective Barriers: Experimental Plans*. PNL-6899, Pacific Northwest Laboratory, Richland, Washington.	PNNL
28	Petersen KL. 1990. The Long-Term Climate Change Assessment Task of the Protective Barrier Development Program for Low-Level Waste Site Remediation at the Hanford Site, Washington. In *High Level Radioactive Waste Management, Volume 2*, pp. 1235–1239. American Nuclear Society, La Grange Park, Illinois.	PROC

Pub No.	Citation	Pub Type[(a)]
29	Fayer MJ. 1990. *Test Plan for Hydrologic Modeling of Protective Barriers*. PNL-7152, Pacific Northwest Laboratory, Richland, Washington.	PNNL
30	Wing N R and GW Gee, eds. 1990. *Hanford Site Protective Barrier Development Program: Fiscal Year 1989 Highlights*. WHC-EP-0318, Westinghouse Hanford Company, Richland, Washington.	C
31	Campbell MD, GW Gee, MJ Kanyid, and ML Rockhold. 1990. *Field Lysimeter Test Facility: Second Year (FY 1989) Test Results*. PNL-7209, Pacific Northwest Laboratory, Richland, Washington.	PNNL
32	Landeen DS, LL Cadwell, LE Eberhardt, RE Fitzner, and MA Simmons. 1990. *Animal Intrusion Field Test Plan*. WHC-EP-0253, Westinghouse Hanford Company, Richland, Washington.	C
33	Link SO, ME Thiede, RD Evans, JL Downs, and WJ Waugh. 1990. *Evapotranspiration Studies or Protective Barriers: FY 1988 Status Report*. PNL-6985, Pacific Northwest Laboratory, Richland, Washington.	PNNL
34	Relyea JF, MR Sackschewsky, and WJ Waugh. 1989. *Small-Tube Lysimeter Facility Status Report for Fiscal Year 1989*. WHC-EP-0297, Westinghouse Hanford Company, Richland, Washington.	C
35	Walters WH, KA Hoover, and LL Cadwell. 1990. *Project Test Plan for Runoff and Erosion on Fine-Soil Barrier Surfaces and Rock-Covered Side Slopes*. PNL-6791, Pacific Northwest Laboratory, Richland, Washington.	PNNL
36	Hoover KA, LL Cadwell, and WH Walters. 1990. *Hanford Protective Barriers Program: Water Erosion Studies – FY 1989*. PNL-7214, Pacific Northwest Laboratory, Richland, Washington.	PNNL
37	Landeen DS. 1990. *Animal Intrusion Status Report for Fiscal Year 1989*. WHC-EP-0299, Westinghouse Hanford Company, Richland, Washington.	C
38	Ligotke MW and DC Klopfer. 1990. *Soil Erosion Rates from Mixed Soil and Gravel Surfaces in a Wind Tunnel*. PNL-7435, Pacific Northwest Laboratory, Richland, Washington.	PNNL
39	Waugh WJ, ME Thiede, CJ Kemp, LL Cadwell, and SO Link. 1990. *Field Study of Gravel Admix, Vegetation, and Soil Water Interactions: Protective Barrier Program Status Report – FY 1989*. PNL-7440, Pacific Northwest Laboratory, Richland, Washington.	PNNL
40	Hunter CR, AJ Busacca, and WJ Waugh. 1990. *A Feasibility Study of Modeling Pedogenic Carbonates in Soils and Sediments at the U.S. Department of Energy's Hanford Site*. PNL-7413, Pacific Northwest Laboratory, Richland, Washington.	PNNL
41	Wing NR and GW Gee. 1990. Protective Barrier Development: Overview. In *Proceedings of the Twenty-Eighth Hanford Symposium on Health and the Environment – Environmental Monitoring, Restoration and Assessment: What Have We Learned?*, ed. RH. Gray, pp. 147–151. CONF-891053, Pacific Northwest Laboratory, Richland, Washington.	C
42	Wing NR and GW Gee. 1990. Protective Barrier Development: Overview. In *Proceedings of the International Topical Meeting on Nuclear and Hazardous Waste Management Spectrum '90*, pp. 335–337. American Nuclear Society, Inc., La Grange Park, Illinois.	C

Pub No.	Citation	Pub Type[(a)]
43	Glantz CS, MN Schwartz, KW Burk, RB Kaspar, MW Ligotke, and DJ Perrault. 1990. *Climatological Summary of Wind and Temperature Data for the Hanford Meteorology Monitoring Network*. PNL-7471, Pacific Northwest Laboratory, Richland, Washington.	PNNL
44	Campbell MD and GW Gee. 1990. *Field Lysimeter Test Facility: Protective Barrier Test Results (FY 1990, The Third Year)*. PNL-7558, Pacific Northwest Laboratory, Richland, Washington.	PNNL
45	Sackschewsky MR, JC Chatters, SO Link, and CA Brandt. 1991. *Protective Barrier Program: Test Plan for Plant Community Dynamics*. WHC-EP-0380, Westinghouse Hanford Company, Richland, Washington.	C
46	Nichols WE. 1991. *Comparative Simulations of a Two-Layer Landfill Barrier Using the Help Version 2.0 and UNSAT-H Version 2.0 Computer Codes*. PNL-7583, Pacific Northwest Laboratory, Richland, Washington.	PNNL
47	Landeen DS. 1991. *Animal Intrusion Status Report for Fiscal Year 1990*. WHC-EP-0398, Westinghouse Hanford Company, Richland, Washington.	C
48	Campbell MD, GW Gee, RR Kirkham, SJ Phillips, and NR Wing. 1991. Water Balance Lysimetry at a Nuclear·Waste Site. In *Proceedings of the International Symposium on Lysimetry*, ed. RG Allen, pp. 125–134. American Society of Civil Engineers, New York.	PROC
49	Kirkham RR, ML Rockhold, GW Gee, MJ Fayer, MD Campbell, and LJ Fritschen. 1991. Lysimeters: Data Acquisition and Analysis. In *Proceedings of the International Symposium on Lysimetry*, ed. RG Allen, pp. 362–370. American Society of Civil Engineers, New York.	PROC
50	Phillips SJ, JF Relyea, CJ Kemp, NR Wing, MD Campbell, GW Gee, MJ Graham, RR Kirkham, and MS Rubin. 1991. Development of Hanford Site Lysimeter Facilities. In *Proceedings of the International Symposium on Lysimetry*, ed. RG Allen, pp. 1–27. American Society of Civil Engineers, New York.	PROC
51	Waugh WJ, ME Thiede, LL Cadwell, GW Gee, HD Freeman, MR Sackschewsky, and JF Relyea. 1991. Small Lysimeters for Documenting Arid Site Water Balance. In *Proceedings of the International Symposium on Lysimetry*, ed. RG Allen, pp. 151–159. American Society of Civil Engineers, New York.	PROC
52	Cadwell LL, ed. 1991. *Hanford Site Protective Barrier Development Program: Fiscal Year 1990 Highlights*. PNL-7831, Pacific Northwest Laboratory, Richland, Washington.	PNNL
53	Petersen KL. 1991. *Modern and Pleistocene Climatic Patterns in the West*. WHC-EP-0523, Westinghouse Hanford Company, Richland, Washington.	C
54	Chatters JC and HA Gard. 1991. *Archaeological Mounds as Analogs of Engineered Covers for Waste Disposal Sites: Literature Review and Progress Report*. PNL-7718, Pacific Northwest Laboratory, Richland, Washington.	PNNL
55	Sackschewsky MR, CJ Kemp, LL Cadwell, ME Thiede, and WJ Waugh. 1991. *Status Report for the Small-Tube Lysimeter Facility – Fiscal Year 1990*. WHC-EP-0381, Westinghouse Hanford Company, Richland, Washington.	C
56	Fayer MJ, ML Rockhold, and DJ Holford. 1992. *Model Assessment of Protective Barriers: Part Ill – Status of FY 1990 Work*. PNL-7975, Pacific Northwest Laboratory, Richland, Washington.	PNNL

Pub No.	Citation	Pub Type[(a)]
57	Petersen KL. 1992. A warm and wet little climate optimum and a cold and dry little ice age in the southern Rocky Mountains, U.S.A. *Climatic Change* 26(2–3):243–269. .	J
58	Link SO, JL Downs, ME Thiede, DJ Lettau, TR Twaddell, and RA Black. 1992. *Evapotranspiration Studies for Protective Barriers: FY 1990 Status Report*. PNL-8032, Pacific Northwest Laboratory, Richland, Washington.	PNNL
59	Link SO, ME Thiede, JL Downs, DJ Lettau, and WJ Waugh. 1992. *Evapotranspiration Studies for Protective Barriers: FY 1989 Status Report*. PNL-8033, Pacific Northwest Laboratory, Richland, Washington.	PNNL
60	Fayer MJ, ML Rockhold, and MD Campbell. 1992. Hydrologic Modeling of Protective Barriers: Comparison of Field Data and Simulation Results. *Soil Science Society of America Journal* 56:690–700.	J
61	Wing NR. 1992. *A Peer Review of the Hanford Site Permanent Isolation Surface Barrier Development Program*. WHC-MR-0392, Westinghouse Hanford Company, Richland, Washington.	C
62	Gee GW, MJ Fayer, ML Rockhold, and MD Campbell. 1992. Variations in Recharge at the Hanford Site. *Northwest Science* 66:237–250.	J
63	Gee GW, MD Campbell, GS Campbell, and JH Campbell. 1992. Rapid Measurement of Low Soil Water Potentials Using a Water Activity Meter. *Soil Science Society of America Journal* 56:1068–1070.	J
64	Ligotke MW. 1993. *Soil Erosion Rates Caused by Wind and Saltating Sand Stresses in a Wind Tunnel*. PNL-8478, Pacific Northwest Laboratory, Richland, Washington.	PNNL
65	Fayer MJ. 1993. *Model Assessment of Protective Barriers: Part IV – Status of FY 1992 Work*. PNL-8498, Pacific Northwest Laboratory, Richland, Washington.	PNNL
66	Wing NR and GW Gee. 1993. The Development of Permanent Isolation Surface Barriers: Hanford Site, Richland, Washington, U.S.A. In *Geology and Confinement of Toxic Wastes: Proceedings of the International Symposium Geoconfine 93*, eds. M Arnould, M Barrès, and B Coûme, pp. 357–362. A.A. Balkema, Rotterdam.	PROC
67	Petersen KL, JC Chatters, and WJ Waugh. 1993. *Long-Term Climate Change Assessment Study Plan for the Hanford Site Permanent Isolation Barrier Development Program*. WHC-EP-0569 Rev. 1, Westinghouse Hanford Company, Richland, Washington.	C
68	Wing NR. 1993. The Results of Laboratory Tests to Determine the Physical Properties of Various Barrier Construction Materials. WHC-SD-ER-DP-006, Rev. 0, Westinghouse Hanford Company, Richland, Washington.	C
69	Gee GW, LL Cadwell, HD Freeman, MW Ligotke, SO Link, RA Romine, and WH Walters, Jr. 1993. *Testing and Monitoring Plan for the Permanent Isolation Surface Barrier Prototype*. PNL-8391, Pacific Northwest Laboratory, Richland, Washington.	PNNL
70	Cadwell LL, SO Link, and GW Gee. 1993. *Hanford Site Permanent Isolation Surface Barrier Development Program: Fiscal Year 1992 and 1993 Highlights*. PNL-8741, Pacific Northwest Laboratory, Richland, Washington.	PNNL

Pub No.	Citation	Pub Type[(a)]
71	Link SO, RN Kickert, MJ Fayer, and GW Gee. 1993. *A Comparison of Simulation Models for Predicting Soil Water Dynamics in Bare and Vegetated Lysimeters.* PNL-8675, Pacific Northwest Laboratory, Richland, Washington.	PNNL
72	Sackschewsky MR, CJ Kemp, and LL Cadwell. 1993. *Status Report for the Small-Tube Lysimeter Facility – Fiscal Year 1992*. WHC-EP-0597, Westinghouse Hanford Company, Richland, Washington.	C
73	Petersen KL and JC Chatters. 1993. *Long-Term Climate Change Assessment Task for the Hanford Site Permanent Isolation Barrier Development Program: Status through FY 1992.* WHC-EP-0644, Westinghouse Hanford Company, Richland, Washington.	C
74	Chamness M. 1993. *An Investigation of Bergmounds as Analogs to Erosion Control Factors on Protective Barriers*. PNL-8841, Pacific Northwest Laboratory, Richland, Washington.	PNNL
75	Bjornstad BN and SS Teel. 1993. *Natural Analog Study of Engineered Protective Barriers at the Hanford Site*. PNL-8840, Pacific Northwest Laboratory, Richland, Washington.	PNNL
76	DOE-RL. 1993. *Treatability Test Plan for the 200-BP-1 Prototype Surface Barrier*. DOE/RL-93-27, U.S. Department of Energy Richland Operations Office, Richland, Washington.	DOE
77	Gee GW, D Felmy, JC Ritter, MD Campbell, JL Downs, MJ Fayer, RR Kirkham, and SO Link. 1993. *Field Lysimeter Test Facility Status Report IV: FY 1993*. PNL-8911, Pacific Northwest Laboratory, Richland, Washington.	PNNL
78	Wing NR. 1993. *Permanent Isolation Surface Barrier: Functional Performance*. WHC-EP-0650, Westinghouse Hanford Company, Richland, Washington.	C
79	Gaylord DR, LD Stetler, GD Smith, and RW Mars. 1993. *Summary of 1990 Eolian Characterization Studies, Hanford Site, Washington*. PNL-8862, Pacific Northwest Laboratory, Richland, Washington.	PNNL
80	Gilmore BG and WH Walters. 1993. *Water Erosion Field Tests for Hanford Protective Barriers: FY 1992 Status Report*. PNL-8949, Pacific Northwest Laboratory, Richland, Washington.	PNNL
81	Kirkham RR. 1993. *Comparison of Surface Energy Fluxes with Satellite-Derived Surface Energy Flux Estimates from a Shrub-Steppe*. PNL-9003, Pacific Northwest Laboratory, Richland, Washington.	PNNL
82	U.S. Army Corps of Engineers, Walla Walla and Kansas City Districts. 1993. *Report on Value Engineering Study of Permanent Isolation Surface Barrier and Warning Marker System Development Plan at the Hanford Site.* DOE/RL/12074--8, Revision 0, U.S. Department of Energy Richland Operations Office, Richland, Washington.	DOE
83	Wing NR. 1994. *Permanent Isolation Surface Barrier Development Plan*. WHC-EP-0673, Westinghouse Hanford Company, Richland, Washington.	C
84	Waugh WJ, JC Chatters, GV Last, BN Bjornstad, SO Link, and CR Hunter. 1994. *Barrier Analogs: Long-Term Performance Issues, Preliminary Studies, and Recommendations*. PNL-9004, Pacific Northwest Laboratory, Richland, Washington.	PNNL
85	Link SO, LL Cadwell, CA Brandt, JL Downs, RE Rossi, and GW Gee. 1994. *Biointrusion Test Plan for the Permanent Isolation Surface Barrier*	PNNL

Pub No.	Citation	Pub Type[(a)]
	Prototype. PNL-9411, Pacific Northwest Laboratory, Richland, Washington.	
86	Kirkham RR and GW Gee. 1994. *Experimental Plan and Construction Guidance for Hanford Protective Barrier Test at Hill AFB, Utah*. PNL-9412, Pacific Northwest Laboratory, Richland, Washington.	PNNL
87	Freeman HD and RA Romine. 1994. *Hanford Permanent Isolation Barrier Program: Asphalt Technology Test Plan*. PNL-9336, Pacific Northwest Laboratory, Richland, Washington.	PNNL
88	Link SO, WJ Waugh, JL Downs, ME Thiede, JC Chatters, and GW Gee. 1994. Effects of Coppice Dune Topography and Vegetation on Soil Water Dynamics in a Cold-Desert Ecosystem. *Journal of Arid Environments* 27:265–278.	J
89	Waugh WJ, ME Thiede, DJ Bates, LL Cadwell, GW Gee, and CJ Kemp. 1994. Plant Cover and Water Balance in Gravel Admixtures at an Arid Waste-Burial Site. *Journal of Environmental Quality* 23:676–685.	J
90	Landeen DS. 1994. *The Influence of Small Mammal Burrowing Activity on Water Storage at the Hanford Site*. WHC-EP-0730, Westinghouse Hanford Company, Richland, Washington.	C
91	DOE-RL. 1994. *Constructability Report for the 200-BP-1 Prototype Surface Barrier*. DOE/RL-94-76, Rev. 1, U.S. Department of Energy Richland Operations Office, Richland, Washington.	DOE
92	Myers DR and DA Duranceau, eds. 1994. *Prototype Hanford Surface Barrier: Design Basis Document*. BID-00007, Rev. 00, Bechtel Hanford, Inc., Richland, Washington.	C
93	Wing NR and GW Gee. 1994. Quest for the Perfect Cap. *Civil Engineering* 64(10):38–41.	J
94	Gee GW and NR Wing, eds. 1994. *In-Situ Remediation: Scientific Basis for Current and Future Technologies, Parts 1–2*. Battelle Press, Columbus, Ohio.	PROC
95	Wing NR and GW Gee. 1994. The Development of Surface Barriers at the Hanford Site. In *In-Situ Remediation: Scientific Basis for Current and Future Technologies, Parts 1–2*, eds. GW Gee and NR Wing, pp. 427–440. Battelle Press, Columbus, Ohio.	PROC
96	Waugh WJ, KL Petersen, SO Link, BN Bjornstad, and GW Gee. 1994. Natural Analogs of the Long-Term Performance of Engineered Covers. In *In-Situ Remediation: Scientific Basis for Current and Future Technologies, Parts 1–2*, eds. GW Gee and NR Wing, pp. 379–410. Battelle Press, Columbus, Ohio.	PROC
97	Freeman HD and RA Romine. 1994. Hanford Permanent Isolation Barrier Program: Asphalt Technology Development. In *In-Situ Remediation: Scientific Basis for Current and Future Technologies, Parts 1–2*, eds. GW Gee and NR Wing, pp. 491–506. Battelle Press, Columbus, Ohio.	PROC
98	Gilmore BG and WH Walters. 1994. Summary of Methods to Develop a Representative Equation for Soil Loss from the Hanford Permanent Isolation Barrier. In *In-Situ Remediation: Scientific Basis for Current and Future Technologies, Parts 1–2*, eds. GW Gee and NR Wing, pp. 507–522. Battelle Press, Columbus, Ohio.	PROC

Pub No.	Citation	Pub Type[(a)]
99	Landeen DS. 1994. The Influence of Small-Mammal Burrowing Activity on Water Storage at the Hanford Site. In *In-Situ Remediation: Scientific Basis for Current and Future Technologies, Parts 1–2*, eds. GW Gee and NR Wing, pp. 523–544. Battelle Press, Columbus, Ohio.	PROC
100	Ligotke MW. 1994. Control of Eolian Soil Erosion from Waste-Site Surface Barriers. In *In-Situ Remediation: Scientific Basis for Current and Future Technologies, Parts 1–2*, eds. GW Gee and NR Wing, pp. 545–560. Battelle Press, Columbus, Ohio.	PROC
101	Link SO,WJ Waugh, and JL Downs. ·1994. The Role of Plants in Isolation Barrier · Systems. In *In-Situ Remediation: Scientific Basis for Current and Future Technologies, Parts 1–2*, eds. GW Gee and NR Wing, pp. 561–592. Battelle Press, Columbus, Ohio.	PROC
102	Myers DR and NR Wing. 1994. Hanford Site Protective Isolation Surface Barrier: Taking Research and Development to Engineered Application. In *In-Situ Remediation: Scientific Basis for Current and Future Technologies, Parts 1–2*, eds. GW Gee and NR Wing, pp. 613–624. Battelle Press, Columbus, Ohio.	PROC
103	Petersen KL. 1994. The Long-Term Climate Change Task of the Hanford Permanent Isolation Barrier Development Program. In *In-Situ Remediation: Scientific Basis for Current and Future Technologies, Parts 1–2*, eds. GW Gee and NR Wing, pp. 663–648, Battelle Press, Columbus, Ohio.	PROC
104	Gee GW, HD Freeman, WH Walters, MW Ligotke, MD Campbell, AL Ward, SO Link, SK Smith, BG Gilmore, and RA Romine. 1994. *Hanford Prototype Surface Barrier Status Report: FY 1994*. PNL-10275, Pacific Northwest Laboratory, Richland, Washington.	PNNL
105	Gaylord PR and LD Stetler. 1994. Aeolian-Climate Thresholds and Sand Dunes at the Hanford Site, South-Central Washington, U.S.A. *Journal of Arid Environments* 28:95–116.	J
106	Freeman HD, RA Romine, and AH Zacher. 1994. *Hanford Permanent Isolation Barrier Program: Asphalt Technology Data and Status Report – FY 1994*. PNL-10194, Pacific Northwest Laboratory, Richland, Washington.	PNNL
107	Wing NR, GW Gee, and JW Cammann. 1995. Program Management of a Multi-Year Technology Development Effort. *PM Network* 9(3):47–50.	J
108	Sackschewsky MR, CJ Kemp, SO Link, and WJ Waugh. 1995. Soil Water Balance Changes in Engineered Soil Surfaces. *Journal of Environmental Quality* 24:352–359.	J
109	Rockhold ML, MJ Fayer, CT Kincaid, and GW Gee. 1995. *Estimation of Natural Ground Water Recharge for the Performance Assessment of a Low-Level Waste Disposal Facility at the Hanford Site*. PNL-10508, Pacific Northwest Laboratory, Richland, Washington.	PNNL
110	Link SO, ME Thiede, RD Evans, JL Downs, and GW Gee. 1995. Responses of Big Sagebrush and Spiny Hopsage to Increasing Water Stress. In *Proceedings of the Wildland Shrub and Arid Land Restoration Symposium*, eds. BA Roundy, ED McArthur, JS Haley, and DK Mann, pp. 196–201. U.S. Department of Agriculture-Forest Service, Intermountain Research Station, Ogden, Utah.	PROC
111	Wing NR, FM Corpuz, KL Petersen, and AM Tallman. 1995. *Physical Stability of Long-Term Surface Barriers – Assessment of Potentially Disruptive Natural*	C

Pub No.	Citation	Pub Type[(a)]
	Events. BID-00145, Bechtel Hanford, Inc., Richland, Washington.	
112	Wing NR, KL Petersen, C Whitlock, and RL Burk. 1995. *Long-Term Climate Change Effects Task for the Hanford Site Permanent Isolation Barrier Development Program: Final Report*. BID-00144, Bechtel Hanford, Inc., Richland, Washington.	C
113	Duranceau DA. 1995. *Site Evaluation Report for Candidate Basalt Quarry Sites*. BID-00005, Bechtel Hanford, Inc., Richland, Washington.	C
114	Fayer MJ and CS Simmons. 1995. Modified soil water retention functions for all matric suctions. *Water Resources Research* 31:1233–1238.	J
115	Petersen KL, SO Link, and GW Gee. 1995. *Hanford Site Long-Term Surface Barrier Development Program: Fiscal Year 1994 Highlights*. PNL-10605, Pacific Northwest Laboratory, Richland, Washington.	PNNL
116	Link SO, NR Wing, and GW Gee. 1995. The development of permanent isolation barriers for buried wastes in cold deserts: Hanford, Washington. *Journal of Arid Land Studies* 4:215–224.	J
117	Link SO, LL Cadwell, KL Petersen, MR Sackshewsky, and DS Landeen. 1995. *The Role of Plants and Animals in Isolation Barriers at Hanford, Washington*. PNL-10788, Pacific Northwest Laboratory, Richland, Washington.	PNNL
118	Gee GW, AL Ward, BG Gilmore, MW Ligotke, and SO Link. 1995. *Hanford Prototype Barrier Status Report: FY 1995*. PNL-10872, Pacific Northwest National Laboratory, Richland, Washington.	PNNL
119	Gee GW, AL Ward, BG Gilmore, SO Link, GW Dennis, and TK O'Neil. 1996. *Hanford Prototype Barrier Status Report: FY 1996*. PNNL-11367, Pacific Northwest National Laboratory, Richland, Washington.	PNNL
120	Bechtel Hanford, Inc. 1996. *Focused Feasibility Study of Engineered Barriers for Waste Management Units in the 200 Areas*. DOE/RL-93-33, Rev. 1, U.S. Department of Energy Richland Operations Office, Richland, Washington.	DOE
121	Ward AL and GW Gee. 1997. Performance evaluation of a field-scale surface barrier. *Journal of Environmental Quality* 26:694–705.	J
122	Gee GW, NR Wing, and AL Ward. 1997. Development and Testing of Permanent Isolation Surface Barriers at the Hanford Site. In *Barrier Technologies for Environmental Management – Summary of a Workshop*, pp. D-3–D-22. National Academy Press, Washington, D.C.	B
123	Gee GW and AL Ward. 1997. Still in Quest of the Perfect Cap. In *Landfill Capping in the Semi-Arid West: Problems, Perspectives and Solutions*, eds. TD Reynolds and RC Morris, pp. 145–164. Environmental Science and Research Foundation, Idaho Falls, Idaho.	PROC
124	Fayer JJ and GW Gee. 1997. Hydrologic Model Tests for Landfill Covers Using field data. In *Landfill Capping in the Semi-Arid West: Problems, Perspectives and Solutions*, eds. TD Reynolds and RC Morris, pp. 53–68. Environmental Science and Research Foundation, Idaho Falls, Idaho.	PROC
125	Gee GW, AL Ward, and MJ Fayer. 1997. Surface barrier research at the Hanford Site. *Land Contamination & Reclamation* 5(3):233–238.	J
126	Ward AL, GW Gee, and SO Link. 1997. *Hanford Prototype Barrier Status Report: FY 1997*. PNNL-11789, Pacific Northwest National Laboratory, Richland, Washington.	PNNL

Pub No.	Citation	Pub Type[(a)]
127	Gee GW, AL Ward, and RR Kirkham. 1997. Long-term performance of surface covers estimated with short-term testing. In *Proceedings of the Long-Term Stewardship Workshop*, pp. 67–81. CONF-980652, U.S. Department of Energy, Grand Junction, Colorado.	PROC
128	DOE-RL. 1999. *200-BP-1 Prototype Barrier Treatability Test Report*. DOE/RL-99-11, Rev 0, U.S. Department of Energy Richland Operations Office, Richland, Washington.	DOE
129	Ward AL and GW Gee. 2000. Hanford Site surface barrier technology. In *Vadose Zone: Science and Technology Solutions*, eds. BB Looney and RW Falta, pp. 1415–1423. Battelle Press, Columbus, Ohio.	BC
130	Gee, GW and AL Ward. 2000. Moisture Accumulating under Asphalt Cover at Radioactive Waste-Burial Site: Discussion. *Practice Periodical of Hazardous, Toxic, and Radioactive Waste Management*, 4(1):40-41.	J
131	Miller CW and CD Wittreich. 2001. *Alternative Fine-Grained Soil Borrow Source Study Work Plan*. BHI-01478, Bechtel Hanford, Inc., Richland, Washington.	C
132	Galgoul MJ and C Sump. 2002. *Alternative Fine-Grained Soil Borrow Source Study Final Report*. BHI-01551, Rev. 0, Bechtel Hanford, Inc., Richland, Washington.	C
133	Gee GW, AL Ward, and CD Wittreich. 2002. *The Hanford Site 1000-Year Cap Design Test*. PNNL-14143, Pacific Northwest National Laboratory, Richland, Washington.	PNNL
134	Wittreich CD, JK Linville, GW Gee, and AL Ward. 2003. *200-BP-1 Prototype Hanford Barrier Annual Monitoring Report for Fiscal Year 2002*. CP-14873 Rev. 0, Fluor Hanford, Inc., Richland, Washington.	C
135	Ward AL, JK Linville, JM Keller, and GH Seedahmed. 2005. 2*00-BP-1 Prototype Hanford Barrier Annual Monitoring Report for Fiscal Year 2004*. PNNL-14960, Pacific Northwest National Laboratory, Richland, Washington.	PNNL
136	Ward AL, SO Link, CE Strickland, KE Draper, and RE Clayton. 2007. *200-BP-1 Prototype Hanford Barrier Annual Monitoring Report for Fiscal Years 2005 Through 2007*. PNNL-17176, Pacific Northwest National Laboratory, Richland, Washington.	PNNL
137	Sackschewsky MR, CJ Kemp, and WM Hayward. 1993. *Surface Stabilization and Revegetation Test Plots – Fiscal Year 1993 Status Report*. WHC-EP-0684, Westinghouse Hanford Company, Richland, Washington.	C
138	Skelly WA. 1994. *Material Properties Data and Volume Estimate of Silt Loam Soil at the NRDWL Reserve, McGee Ranch*. WHC-SD-EN-TI-218, Revision 0, Westinghouse Hanford Company, Richland, Washington.	C
139	Buckmaster MA. 1995. *Construction Quality Assurance Report for the Prototype Surface Barrier*. BHI-00432 Rev. 0, Bechtel Hanford, Inc., Richland, Washington.	C
140	Fayer MJ and GW Gee. 2006. Multiple-Year Water Balance of Soil Covers in a Semiarid Setting. *Journal of Environmental Quality* 35:366–377.	J
141	Ward AL. 2007. *Geotechnical, Hydrogeologic, and Vegetation Data Package for 200-UW-1 Waste Site Engineered Surface Barrier Design*. PNNL-17134, Pacific Northwest National Laboratory, Richland, Washington.	PNNL
142	Ward AL, GT Berlin, JW Cammann, KD Leary, and SO Link. 2008. *Test Plan to Assess Fire Effects on the Function of an Engineered Surface Barrier*.	PNNL

Pub No.	Citation	Pub Type[(a)]
	PNNL-17859, Pacific Northwest National Laboratory, Richland, Washington.	
143	Ward AL, SO Link, KE Draper, and RE Clayton. 2009. *200-BP-1 Prototype Hanford Barrier – 15 Years of Performance Monitoring*. PNNL-18845, Pacific Northwest National Laboratory, Richland, Washington.	PNNL
144	Ward AL, N Hasan, SO Link, and KE Draper. 2009. *The Effects of Fire on the Function of the 200-BP-1 Engineered Surface Barrier*. PNNL-18934, Pacific Northwest National Laboratory, Richland, Washington.	PNNL
145	Ward AL, KD Leary, SO Link, GT Berlin, JW Cammann, ML Mandis, and LC Buelow. 2009. Short and Long-term Fire Impacts on Hanford Barrier Performance. In *WM 2009 – Waste Management for the Nuclear Renaissance*, Paper 9449. WM Symposia, Phoenix, Arizona. Available from http://www.wmsym.org/archives/2009/pdfs/9449.pdf (May 2013).	PROC
146	Fayer MJ, AL Ward, and VL Freedman. 2010. *Technical Basis for Evaluating Surface Barriers to Protect Groundwater from Deep Vadose Zone Contamination*. PNNL-18661, Pacific Northwest National Laboratory, Richland, Washington.	PNNL
147	Ward AL, GW Gee, SO Link, CD Wittreich, KD Leary, and GT Berlin. 2010. Quest for the Perfect Cap: The Prototype Hanford Barrier 15 Years Later. In *WM 2010 – Improving the Future by Dealing with the Past*, Paper 10419. WM Symposia, Phoenix, Arizona. Available from http://www.wmsym.org/archives/2010/pdfs/10419.pdf (May 2013).	PROC
148	Ward AL, SO Link, KD Leary, and GT Berlin. 2010. Fire Impacts on an Engineered Barrier's Performance: The Hanford Barrier One Year After a Controlled Burn. In *WM 2010 – Improving the Future by Dealing with the Past*, Paper 10472. WM Symposia, Phoenix, Arizona. Available from http://www.wmsym.org/ archives/2010/pdfs/10472.pdf (May 2013).	PROC
149	Strickland CE, AL Ward, WP Clement, and KE Draper. 2010. Engineered surface barrier monitoring using ground-penetrating radar, time-domain reflectometry, and neutron-scattering techniques. *Vadose Zone Journal* 9:415–423.	J
150	Ward AL, KE Draper, SO Link, and RE Clayton. 2011. *200-BP-1 Prototype Hanford Barrier – 15 Years of Performance Monitoring*. PNNL-18845, Revision 1, Pacific Northwest National Laboratory, Richland, Washington.	PNNL
151	KEH. 1993. *Construction Specification for Prototype Surface Barrier at 200-BP-1 Operable Unit*. W-263-C2, Rev 0, Kaiser Engineers Hanford Company, Richland, Washington.	C
152	PNL. 1995. Letter report to Bechtel Hanford, Inc., from Pacific Northwest Laboratory, "Milestone 0.204, Performance evaluation of the water balance monitoring systems at the prototype surface barrier," June 16, 1995, Richland, Washington.	PNNL
153	Graham MJ. 1999. Letter CCN 073428 to BL Foley (U.S. Department of Energy Richland Operations Office) from MJ Graham (Bechtel Hanford, Inc.), "200-BP-1 Prototype Hanford Barrier Annual Monitoring Report for FY 1999," September 30, 1999, Richland, Washington.	C

Pub No.	Citation	Pub Type[(a)]
154	Graham MJ. 2000. Letter CCN 083132 to BL Foley (U.S. Department of Energy Richland Operations Office) from MJ Graham (Bechtel Hanford, Inc.), "200-BP-1 Prototype Hanford Barrier Annual Monitoring Report for Fiscal Year 2000," October 19, 2000, Richland, Washington.	C
154	Graham MJ. 2002. Letter CCN 100381 to BL Foley (U.S. Department of Energy Richland Operations Office) from MJ Graham (Bechtel Hanford, Inc.), "200-BP-1 Prototype Hanford Barrier Annual Monitoring Report for Fiscal Year 2001,"June 18, 2002, Richland, Washington.	C

(a) J = journal article; DOE = DOE report; PNNL = PNNL report; C = Hanford = Hanford contractor report; PROC = conference proceedings; BC = book chapter.

Appendix R

Monitoring Data

Z. Fred Zhang, Chris E. Strickland, Ray E. Clayton, Jonathan N. Thomle

Pacific Northwest National Laboratory
Richland, Washington

Contents

This appendix describes the data collected at the Prototype Hanford Barrier (PHB) and the data collected at the Field Lysimeter Test Facility (FLTF). The data in digital form are provided separately on CD.

R.1 Data Collected at the PHB

R.1.1 Neutron Probe Data

This dataset contains the raw neutron counts during each field logging from 1994 to 2013. The logging is divided into three categories:

1. vertical neutron logging
2. horizontal neutron logging at the bottom of the silt loam
3. horizontal neutron logging below the asphalt layer

Name of folder: PHB\001_Neutron_logging

Name of data file: QA-Data-Neutron.xlsx

R.1.2 Time-Domain-Reflectometry (TDR) Data

This dataset contains the raw TDR data from 1995 to 2007.

Name of folder: PHB\001_TDR

Names of data files:

QA_data_TDR_FY1995.xlsx
QA_data_TDR_FY1996.xlsx
QA_data_TDR_FY1997.xlsx
QA_data_TDR_FY1998.xlsx
QA_data_TDR_FY1999.xlsx
QA_data_TDR_FY2000.xlsx
QA_data_TDR_FY2001.xlsx
QA_data_TDR_FY2002.xlsx
QA_data_TDR_FY2003.xlsx
QA_data_TDR_FY2004.xlsx
QA_data_TDR_FY2007.xlsx

R.1.3 Drainage Data

This dataset contains the raw thermocouple temperature, tipping bucket cumulative tip counts, pressure transducer voltage, and dosing siphon flush counts from the 12 drainage vaults, which were logged from 1995 to 2013.

Name of folder: \PHB\003_Drainage

Names of data files:

- QA_Data_Drainage_FY1995-1998.xlsx
- QA_Data_Drainage_FY1999-2003.xlsx
- QA_Data_Drainage_FY2004-2009.xlsx
- QA_Data_Drainage_FY2010-2013.xlsx

R.1.4 Heat Dissipation Unit (HDU) and Precipitation Data

This dataset contains the HDU and mini-lysimeter (aka load cells) data from 1995 to 2013.

Name of folder: PHB\004_HDU_Precip

Names of data files:

- QA_HDU_Precip_FY1995_1998.xlsx
- QA_HDU_Precip_FY1999_2002.xlsx
- QA_HDU_Precip_FY2003_2007.xlsx
- QA_HDU Precip FY2008_2013.xlsx

R.1.5 Pan Lysimeter and Fiberglass Block Data

This dataset contains the drainage from the pan lysimeter, fiberglass blocks, several HDUs, and thermocouple sensors.

Name of folder: PHB\005_PanLysimeter_FGB

Names of data files: QA_204 Pan Lysimeter FGB TC.xlsx

R.1.6 Wind Erosion Data

This dataset contains data on the dry density of barrier, surface gravel content, wind speed at different heights for three wind stations, and saltation of sand particles.

Name of folder: PHB\007_WindErosion

Names of data files:

- QA_Saltation.xlsx
- QA_Surface gravel content.xlsx
- QA_Wind_Stations.xlsx

R.1.7 Stability Data

This dataset contains the survey results of barrier stability from 1994 to 2012. The surveys are divided into three categories: (1) barrier elevation, (2) barrier settlement, and (3) locations of creep gauges.

Name of folder: PHB\008_Stability

Name of data file: QA_Data_Stability.xlsx

R.1.8 Soil Properties

This dataset contains the properties of mineralogy, retention, particle size distribution, organic matter and bulk density of the silt loam, and the saturated hydraulic conductivity of the asphalt concrete for barrier construction.

Name of folder: PHB\009 Soil Properties

Name of data file: QA_phb_physical_properties.xlsx

R.1.9 Ecology Data

This dataset contains files for surveys of plant community, plant physiology, and animal activities.

Name of folder: PHB\011_ecology

Names of data files:

Plant Community\Files\2007 notebook.docx
Plant Community\Files\analog seed bank 9-09.xlsx
Plant Community\Files\animalpltcover 96, 97.xlsx
Plant Community\Files\artr can 7-16-10.xlsx
Plant Community\Files\barr dry seed bank 9-09.xlsx
Plant Community\Files\burned half shrub cnt8-15-9.xlsx Plant Community\Files\canopy8-6-11.xlsx
Plant Community\Files\cov 9,10,11.xlsx
Plant Community\Files\cover 8-4-07.xlsx
Plant Community\Files\cover.d 6-3-96.xlsx
Plant Community\Files\covslope 07,09,10.xlsx
Plant Community\Files\grass 4-95.xlsx
Plant Community\Files\live_dead shrub 95,96,97.xlsx
Plant Community\Files\mcgee cov 2009.xlsx
Plant Community\Files\mcgee old burn shrub cnt 8-29-09.xlsx
Plant Community\Files\mcgee spe list.docx
Plant Community\Files\sage seedheads 1-30-97.xlsx
Plant Community\Files\shrub mature count8-29-09.xlsx
Plant Community\Files\slope cov 10, 11 c.xlsx
Plant Community\Files\spe freq 8-15-12a p.xlsx
Plant Community\Files\unburned shrub den 8-29-09.xlsx

Plant Community\Files\w sideslope cover 6-18-97.xlsx Plant Community\Files\weeds 4-95.xlsx
Plant Physiology\Files\artr can 7-16-10.xlsx
Plant Physiology\Files\artr can dim 10-16-09.xlsx
Plant Physiology\Files\Canopy 8-4-07.xlsx
Plant Physiology\Files\canopy8-6-11.xlsx
Plant Physiology\Files\co2 w-d 9-6-09.xlsx
Plant Physiology\Files\elwa can 7-16-10.xlsx
Plant Physiology\Files\erna can 7-16-10.xlsx
Plant Physiology\Files\gasex 6-18-97.sas.xlsx
Plant Physiology\Files\gasex2-8-95.xlsx
Plant Physiology\Files\gasex8-1-96.xlsx
Plant Physiology\Files\ht 95,96,97.xlsx
Plant Physiology\Files\la harv 4-16-97.xlsx
Plant Physiology\Files\la pred 1997.xlsx
Plant Physiology\Files\maca can 7-16-10.xlsx
Plant Physiology\Files\par 9-21-08.xlsx
Plant Physiology\Files\par lai 8-17-09.xlsx
Plant Physiology\Files\Pre-burn Artr Height 9-15-08.xlsx Plant Physiology\Files\root.dat 95,96,97.xlsx
Plant Physiology\Files\xyl 8-27-10.xlsx
Plant Physiology\Files\xyl 9-5-09.xlsx
Plant Physiology\Files\xyl press pot 8-1-96.xlsx
Animal activities\Files\animal g, plt cnts 8-6-11a.xlsx
Animal activities\Files\animal hole 10, 11 6-8-11b.xlsx
Animal activities\Files\animal hole size 6-8-11.xlsx
Animal activities\Files\animal holes b 8-13-9.xlsx
Animal activities\Files\animal holes8-18-07.xlsx
Animal activities\Files\animal presence 6-8-2011.xlsx
Animal activities\Files\animal.d 5-24-96.xlsx
Animal activities\Files\animalpltcover 96, 97.xlsx
Animal activities\Files\p.29 hardcopy 2007 notebook.docx
Animal activities\Files\pellets 3-24-15.xlsx

R.1.10 Controlled Burn – Temperature Data

This dataset contains the raw loggings of the soil or air temperature at 62 locations.

Name of folder: PHB\012 Controlled burn - Temperature

Name of data file: QA_Fire Temperature.xlsx

R.1.11 Controlled Burn – Soil Properties Data

This dataset contains particle size distribution, soil repellency, physical properties, and nutrient concentration before and after the controlled burn.

Name of folder: PHB\013 Controlled burn - Soil Properties

Names of data file:

QA_Geochemical.xlsx
QA_Pre-and-Post_burn_properties.xlsx
QA_PSB_PostBurn_LaserParticleSize.xls

R.1.12 Capacitance Probe Data

This dataset contains the measured frequency data that can be converted into soil water content with a calibration curve.

Name of folder: PHB\016 Capacitance Probe

Name of data file: QA_capacitance.xlsx

R.1.13 Irrigation Data

This dataset contains the irrigation quantity measured with rain gauges.

Name of folder: PHB\ 021_Irrigation

Name of data file: QA_PHB_irrigation.xlsx

R.2 Data Collected at the FLTF

R.2.1 Neutron Probe Data

This dataset contains the neutron logging data from the FLTF from 1987 to 2013.

Name of folder: FLTF\022_Neutron

Name of data file: QA_FLTF_Neutron_data.xlsx

R.2.2 Tensiometer Data

This dataset contains the tensiometer data from the FLTF from 1988 to 2013.

Name of folder: FLTF\023_Tensiometer

Name of data file: QA_FLTF_Tensions.xls

R.2.3 Irrigation Data

This dataset contains the tensiometer data from the FLTF from 2000 to 2013.

Name of folder: FLTF\024_Irrigation

Name of data file: QA_FLTF_Irrigation Data 2000-2013.xls

R.2.4 Vegetation Data

This dataset contains the vegetation data from the FLTF from 2006 to 2012.

Name of folder: FLTF\025_Vegetation

Name of data file: QA_FLTF Vegetation Observations.xls

R.2.5 Drainage Data

This dataset contains the drainage data from the FLTF from 1990 to 2013.

Name of folder: FLTF\026_Drainage

Names of data files:

QA_FLTF Drainage ClearTube Lysimeters.xls
QA_FLTF Drainage large lysimeters.xls